KV7 CHANNELS: STRUCTURE, PHYSIOLOGY AND PHARMACOLOGY

EDITED BY: Thomas Andrew Jepps, Vincenzo Barrese and Francesco Miceli
PUBLISHED IN: Frontiers in Physiology

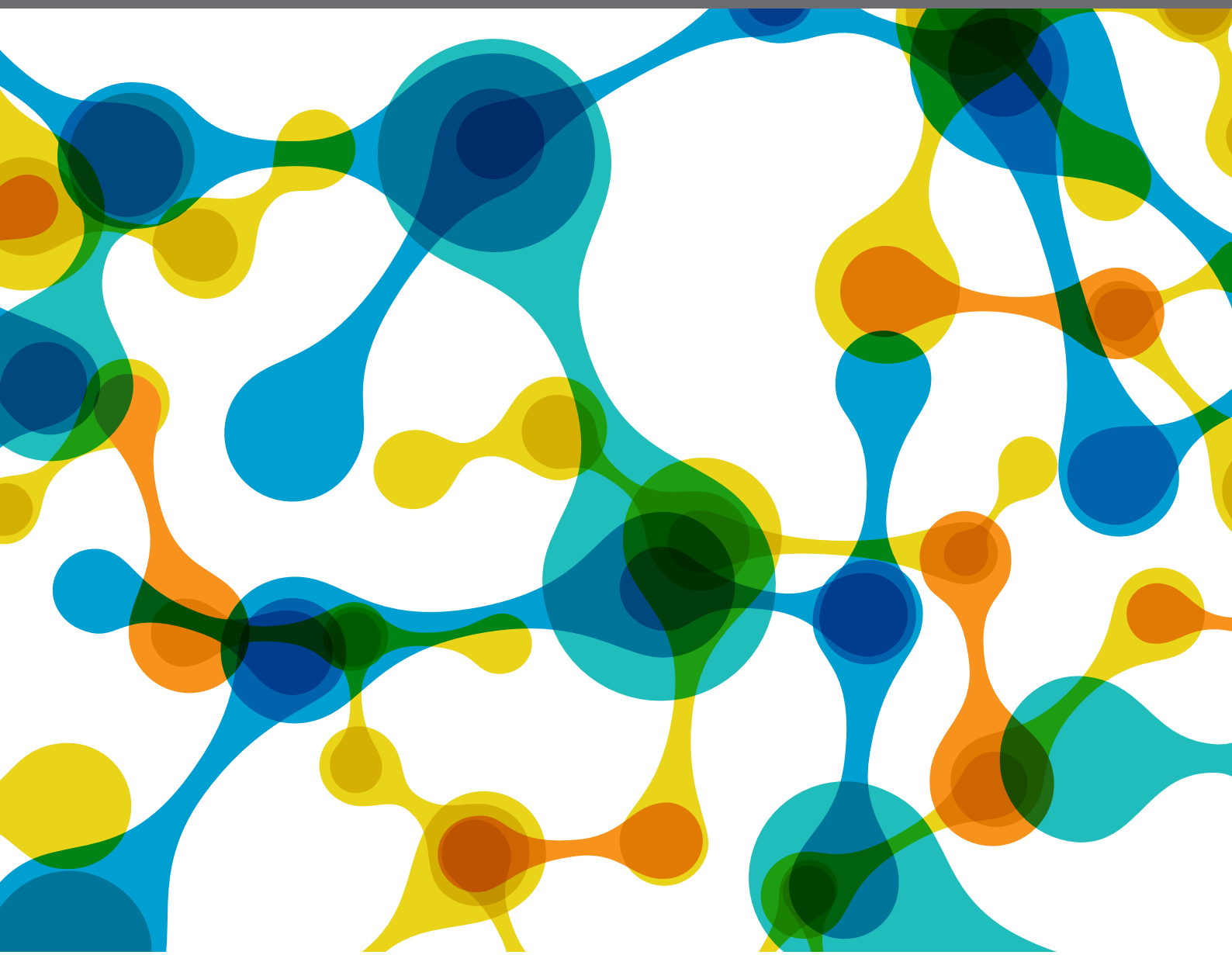

frontiers Research Topics

ISSN 1664-8714
ISBN 978-2-88966-914-1
DOI 10.3389/978-2-88966-914-1

About Frontiers

Frontiers is more than just an open-access publisher of scholarly articles: it is a pioneering approach to the world of academia, radically improving the way scholarly research is managed. The grand vision of Frontiers is a world where all people have an equal opportunity to seek, share and generate knowledge. Frontiers provides immediate and permanent online open access to all its publications, but this alone is not enough to realize our grand goals.

Frontiers Journal Series

The Frontiers Journal Series is a multi-tier and interdisciplinary set of open-access, online journals, promising a paradigm shift from the current review, selection and dissemination processes in academic publishing. All Frontiers journals are driven by researchers for researchers; therefore, they constitute a service to the scholarly community. At the same time, the Frontiers Journal Series operates on a revolutionary invention, the tiered publishing system, initially addressing specific communities of scholars, and gradually climbing up to broader public understanding, thus serving the interests of the lay society, too.

Dedication to Quality

Each Frontiers article is a landmark of the highest quality, thanks to genuinely collaborative interactions between authors and review editors, who include some of the world's best academicians. Research must be certified by peers before entering a stream of knowledge that may eventually reach the public - and shape society; therefore, Frontiers only applies the most rigorous and unbiased reviews.
Frontiers revolutionizes research publishing by freely delivering the most outstanding research, evaluated with no bias from both the academic and social point of view. By applying the most advanced information technologies, Frontiers is catapulting scholarly publishing into a new generation.

What are Frontiers Research Topics?

Frontiers Research Topics are very popular trademarks of the Frontiers Journals Series: they are collections of at least ten articles, all centered on a particular subject. With their unique mix of varied contributions from Original Research to Review Articles, Frontiers Research Topics unify the most influential researchers, the latest key findings and historical advances in a hot research area! Find out more on how to host your own Frontiers Research Topic or contribute to one as an author by contacting the Frontiers Editorial Office: frontiersin.org/about/contact

KV7 CHANNELS: STRUCTURE, PHYSIOLOGY AND PHARMACOLOGY

Topic Editors:
Thomas Andrew Jepps, University of Copenhagen, Denmark
Vincenzo Barrese, University of Naples Federico II, Italy
Francesco Miceli, University of Naples Federico II, Italy

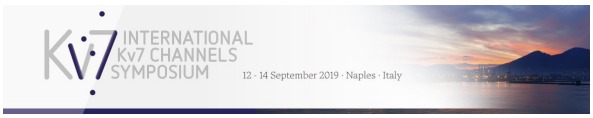

This Research Topic was in partnership with CAP Partner for the International Kv7 Channels Symposium held in Naples, Italy on September 2019.

Citation: Jepps, T. A., Barrese, V., Miceli, F., eds. (2021). Kv7 Channels: Structure, Physiology and Pharmacology. Lausanne: Frontiers Media SA.
doi: 10.3389/978-2-88966-914-1

Table of Contents

frontiers in Physiology

EDITORIAL
published: 16 April 2021
doi: 10.3389/fphys.2021.679317

Editorial: Kv7 Channels: Structure, Physiology, and Pharmacology

Thomas A. Jepps[1]*, *Vincenzo Barrese*[2]* and *Francesco Miceli*[2]*

[1] Vascular Biology Group, Department of Biomedical Sciences, University of Copenhagen, Copenhagen, Denmark,
[2] Department of Neuroscience, Reproductive Sciences and Dentistry, University of Naples Federico II, Naples, Italy

Keywords: Kv7 channels, KCNQ channel, physiology, pharmacology, ion channels

Editorial on the Research Topic

Kv7 Channels: Structure, Physiology, and Pharmacology

The Kv7 family of voltage-gated potassium (K^+) channels consists of five members (Kv7.1-7.5) encoded for by the KCNQ1-5 genes, respectively. Kv7 channels assemble as tetramers of identical or compatible α subunits, with each α subunit consisting of six transmembrane segments (S1–S6) and cytoplasmic N- and C-termini. The transmembrane segments between S1 and S4 form the voltage-sensing domain (VSD), where the S4 segment is crucial for channel gating as it contains positively charged arginines (Rs), each separated by non-polar residues. The S5 and S6 segments and the interconnecting loop participate to the formation of the pore domain (PD). Kv7 channels are characterized by a long intracellular C-terminus, containing domains necessary for tetramerization and involved in binding and transductional activity by critical regulators, such as phosphatidylinositol 4,5-bisphosphate (PIP2), calmodulin (CaM), syntaxin, A-kinase-anchoring proteins and proteinkinase C, and ankyrin-G (Barrese et al., 2018).

Kv7 channels produce currents that are voltage-activated, slowly activating and non-inactivating, which were first recorded in bullfrog sympathetic neurons (Brown and Adams, 1980). At this time, the molecular identity of the channels was unknown, so the K^+ current was termed the "M-current," which derives from the observation that muscarinic acetylcholine receptor agonist, muscarine, inhibited this voltage-sensitive K^+ current (Brown and Adams, 1980). The muscarinic acetylcholine receptors are coupled to Gq proteins, and it is now known that activation of other Gq protein-coupled receptors will also inhibit the M-current by depleting the levels of PIP_2 in the membrane (Marrion, 1997; Suh and Hille, 2002; Ford et al., 2003; Zhang et al., 2003). Kv7 channels, unlike other Kv channels, are highly sensitive to PIP_2, which acts as a cofactor that mediates coupling of the VSD with the PD. Thus, without PIP_2, membrane depolarization does not cause pore opening (Delmas and Brown, 2005; Zaydman et al., 2013).

Several years later, Kv7.1 (KCNQ1) expression was first identified in the heart (Barhanin et al., 1996; Sanguinetti et al., 1996), where it is responsible for the slowly activating delayed rectifier K^+ current "I_{Ks}." Mutations in KCNQ1 (or its ancillary subunit, KCNE1) cause a large number of hereditary arrhythmias that are manifest as a prolongation of the QT interval in electrocardiograms (LQT1 syndrome: Wang et al., 1996; Herbert et al., 2002). In 1998, KCNQ2 and KCNQ3 (encoding Kv7.2 and Kv7.3 proteins, respectively) were cloned, and mutations in these genes were associated to a form of epilepsy called Benign Familial Neonatal Convulsions (BFNC: Biervert et al., 1998; Charlier et al., 1998; Singh et al., 1998). Wang et al. (1998) demonstrated that the kinetic properties of the Kv7.2/7.3 heteromeric channel resembled closely those of the native M-current, which was also inhibited by muscarine. Later, Kv7.4 (KCNQ4) was identified on the basal membrane of the outer hair cells of the inner ear and auditory nerves, with mutations to the channel associated with autosomal dominant deafness (DFNA2; Kubisch et al., 1999; Kharkovets et al., 2000, 2006; Søgaard et al., 2001). Finally, Kv7.5 (KCNQ5) was identified as a molecular correlate of the M-current by forming

OPEN ACCESS

Edited by:
Christoph Fahlke, Julich-Forschungszentrum, Helmholtz-Verband Deutscher Forschungszentren (HZ), Germany

Reviewed by:
Marcus Schewe, University of Kiel, Germany

***Correspondence:**
Thomas A. Jepps
tjepps@sund.ku.dk
Vincenzo Barrese
vincenzo.barrese@unina.it
Francesco Miceli
frmiceli@unina.it

Specialty section:
This article was submitted to Membrane Physiology and Membrane Biophysics, a section of the journal Frontiers in Physiology

Received: *11 March 2021*
Accepted: *25 March 2021*
Published: *16 April 2021*

Citation:
Jepps TA, Barrese V and Miceli F (2021) Editorial: Kv7 Channels: Structure, Physiology, and Pharmacology. Front. Physiol. 12:679317. doi: 10.3389/fphys.2021.679317

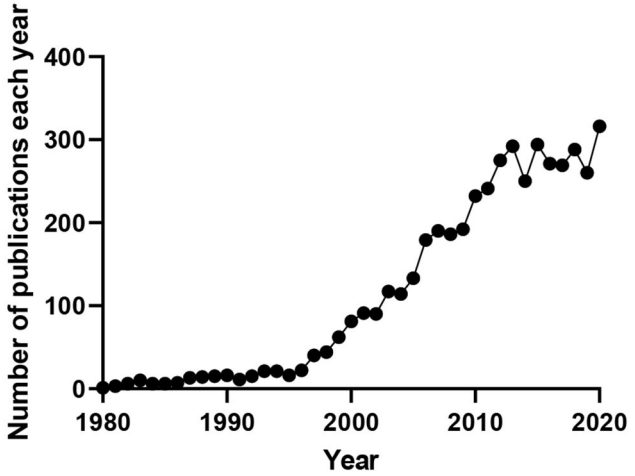

FIGURE 1 | Number of publications produced per year containing the terms "M-current," "KCNQ(X)," or "Kv7(.X)." Data obtained from www.pubmed.ncbi.nlm.nih.gov.

heteromultimers with Kv7.3 (Lerche et al., 2000; Schroeder et al., 2000; Shah et al., 2002).

Many cell types throughout the body depend functionally on Kv7 channel expression, with mutations to these channels, or their ancillary subunits, underling multiple diseases. Research interest in these channels continues to grow as their involvement in disease and potential as therapeutic targets becomes more apparent (**Figure 1**).

With such a large and continuously growing interest in Kv7 channel research, a special Research Topic in Frontiers in Physiology was created following the International Kv7 Channels Symposium in Naples, Italy, 2019. This Research Topic has collected 17 articles, including seven original research papers, three mini-reviews, and seven full reviews from prominent scientists in the field. The collection of papers in this Research Topic expands the current knowledge on the structure, pathophysiology, and pharmacology of Kv7 channels.

KV7 CHANNEL REGULATION

Kv7 channels are voltage-gated channels and Wang et al. summarize the most recent knowledge on Kv7.1 assembly, kinetics of activation and inactivation, voltage-sensor pore coupling, and regulation by KCNE subunits as well as other signaling molecules. As well as being voltage-dependent, several endogenous small molecules can modulate Kv7 channel activity. The study by Greenwood and Stott builds on previous work showing G-protein βγ subunits are obligatory for Kv7.4 channel activity. In particular, Gβ3 was shown to be necessary for Kv7 activity in rat renal vascular smooth muscle cells. Larsson et al. review the regulation of Kv7 channels by Polyunsaturated Fatty Acids (PUFAs). In particular, PUFAs increase the current and produce a leftward shift in the voltage-dependence through both direct and indirect mechanisms. CaM is often regarded an essential auxiliary subunit of Kv7 channels that modulates function. The work by Zhuang and Yan identifies structural determinants that are necessary for CaM and PIP_2 regulation. Their work shows that the third EF hand (EF3) of CaM is required for the calcium-dependent regulation of Kv7.4 activation, and that the S2–S3 loop of Kv7.4 is essential for the regulation mediated by CaM. Tran et al. described two variants of the CaM-binding Helix A of Kv7.2 channels in two patients with developmental and epileptic encephalopathy (DEE). Functional studies revealed that these two variants suppressed channel current density and impaired CaM and PIP_2 regulation, a result consistent with the severe DEE phenotype associated with these mutations. Interestingly, the novel Kv7.2/7.3 channel-selective opener, SF0034, rescued current amplitudes of the mutated channels suggesting a potential therapy for KCNQ2 encephalopathy.

Abbott reviews our current perception of Kv7 channels as simply voltage-dependent channels, questioning whether they should be considered ligand-gated channels that are also sensitive to voltage in certain cell types. The review presents our current knowledge on the regulation of Kv7 channels by voltage, KCNE subunits, PIP_2, and CaM, as well as neurotransmitters such as GABA and GABA-related endogenous metabolites β-hydroxybutyric acid (BHB) and γ-amino-β-hydroxybutyric acid (GABOB). Van der Horst et al. discuss another voltage-independent regulatory mechanism in their review focusing on the complex regulation of Kv7 channels following cAMP-activation in multiple cell types.

PHARMACOLOGICAL TARGETING OF KV7 CHANNELS IN NEUROLOGICAL DISEASES

Hoshi discusses the molecular mechanisms controlling suppression of the M-current in neurones, the relevance of lipid metabolism as well as the potential therapeutic implications in epilepsy and contribution of these mechanisms to the anti-seizure effect of valproic acid. These findings, along with those highlighted in the Abbott review about the direct binding of BHB to Kv7.3 channels, validate the therapeutic potential of Kv7 channel activation in epilepsy, as also demonstrated by the Miceli study. Miceli et al. describe the first missense loss-of-function (LoF) pathogenic variant within the S4 segment of Kv7.3, identified in three individuals with BFNE. Functional studies revealed that homomeric Kv7.3 M240R channels were not functional, whereas heteromeric channels incorporating wild type Kv7.2, wild type Kv7.3, and Kv7.3 M240R subunits (at cDNA ratio of 1:0.5:0.5, respectively), a stoichiometry reproducing the genetic combination occurring in the affected family members, displayed a depolarizing shift in activation gating. Interestingly, the functional deficit caused by both mutations could be restored partially by the pharmacological activation of Kv7 current. In particular, the application of BHB, a ketone body generated during the ketogenic diet (KD), reversed channel dysfunction induced by the mutation in Kv7.3, thus providing the rationale for the use of KD in patients carrying LoF variants in Kv7.2 or Kv7.3.

Mutations in KCNQ2 and KCNQ3 have more recently been associated with DEE (Weckhuysen et al., 2012). The clinical heterogeneity described in patients carrying mutations in Kv7.2 and Kv7.3 cannot be explained only with the severity of channel dysfunction, as the degree of developmental delay does not completely correlate with the frequency or severity of seizures. The review by Dirkx et al. discusses that Kv7 channels might have a crucial role beyond the control of neuronal firing. In particular, the differential expression and function of Kv7 channels during development might regulate fundamental steps such as differentiation, proliferation, and synaptogenesis that, if altered, profoundly modify brain structure and function. However, the heterogenous phenotype found in many epileptic patients might be explained with the close relationship and reciprocal influence between neuronal excitability, structural alterations, and neuronal plasticity. Baculis et al. review the current knowledge regarding the activity-dependent regulation of Kv7 channels at the synaptic level, and their contribution to intrinsic and synaptic plasticity. Such evidence also provides the molecular basis for the role of Kv7 channels in cognition and behavior, and further interesting insight into the association of KCNQ2 and KCNQ3 variants with developmental disorders and intellectual disability.

Robust evidence generated in the past two decades have convincingly expanded the spectrum of pathophysiological roles of Kv7 channels beyond epilepsy. These data have been the basis for novel therapeutic approaches for the treatment of several neurological diseases. Vigil et al. review the studies investigating the efficacy of Kv7 modulators in stroke, traumatic brain injury, drug addiction and mood disorders, and highlight the pharmacodynamic and pharmacokinetic issues (such as subunit selectivity and brain-specific delivery) that should be addressed to obtain more effective therapeutic treatments for these diseases.

KV7 CHANNELS CAN NO LONGER BE REGARDED AS "CARDIAC" AND "NEURONAL" CHANNELS

Since they were first discovered in neurones and cardiac myocytes, Kv7 channels are often termed the "cardiac" Kv7 channel (Kv7.1) and the "neuronal" Kv7 channels (Kv7.2-7.5). However, Kv7 channels are now recognized to play important physiological roles in many cell types, highlighted by several papers in this Research Topic. Kv7 channels are key determinants of vascular smooth muscle contractility. The study by Brueggemann et al. suggests a Kv7.4:Kv7.5 stoichiometry of 2:2, with alternating Kv7.4 and Kv7.5 α-subunits as the predominating channel in rat mesenteric artery smooth muscle cells. As mentioned previously, the study by Greenwood and Stott investigates the βγ subunit regulation of Kv7 channels in rat renal arteries. Ma et al. investigate the interactive regulation of the Kv7 and large-conductance Ca^{2+}-sensitive K^+ (BK) channels in rat arteries, showing that in adult arteries the functional impact of Kv7 channels increases after blocking BK channels. This study also showed aged-related changes in Kv7 channel activity, with blockade of BK channels having no effect on Kv7 channel activity in arteries from young rats. Keeping within the vascular wall, Baldwin et al. provide the first evidence of Kv7.4 and Kv7.5 channels within rat mesenteric endothelial cells and found they were involved in nitric oxide release in these vessels. Kv7 channels are expressed in a variety of non-vascular smooth muscle, and the review by Malysz and Petkov highlights the expression and functional role of Kv7 channels in urinary bladder smooth muscle. Mondejar-Parreño et al. review the impact of Kv7 channels on multiple aspects of pulmonary physiology. In their review, the role of Kv7 channels in several pulmonary diseases is discussed, as well as the therapeutic potential of targeting these channels.

CONCLUSION

This Research Topic underscores the important physiological roles and pharmacological potential of Kv7 channels in multiple tissues. The papers in this Research Topic highlight the complexities of the Kv7 voltage- and ligand-gated potassium channels, and that there is still much to discover about the myriad of cell-dependent physiological roles for these channels.

AUTHOR CONTRIBUTIONS

All authors listed have made a substantial, direct and intellectual contribution to the work, and approved it for publication.

FUNDING

The present work was supported by the Italian Ministry for University and Research (PRIN 2017YH3SXK) to FM and a Lundbeck Foundation grant (R323-2018-3674) to TAJ.

REFERENCES

Barhanin, J., Lesage, F., Guillemare, E., Fink, M., Lazdunski, M., and Romey, G. (1996). KvLQT1 and IsK (minK) proteins associate to form the IKS cardiac potassium current. *Nature* 384, 78–80. doi: 10.1038/384078a0

Barrese, V., Stott, J. B., and Greenwood, I. A. (2018). KCNQ-Encoded potassium channels as therapeutic targets. *Annu. Rev. Pharmacol. Toxicol.* 58, 625–648. doi: 10.1146/annurev-pharmtox-010617-052912

Biervert, C., Schroeder, B. C., Kubisch, C., Berkovic, S. F., Propping, P., Jentsch, T. J., et al. (1998). A potassium channel mutation in neonatal human epilepsy. *Science* 279, 403–406. doi: 10.1126/science.279.5349.403

Brown, D. A., and Adams, P. R. (1980). Muscarinic suppression of a novel voltage-sensitive K+ current in a vertebrate neurone. *Nature* 283, 673–676. doi: 10.1038/283673a0

Charlier, C., Singh, N. A., Ryan, S. G., Lewis, T. B., Reus, B. E., Leach, R. J., et al. (1998). A pore mutation in a novel KQT-like potassium channel gene in an idiopathic epilepsy family. *Nat. Genet.* 18, 53–55. doi: 10.1038/ng0198-53

Delmas, P., and Brown, D. A. (2005). Pathways modulating neural KCNQ/M (Kv7) potassium channels. *Nat. Rev. Neurosci.* 6, 850–862. doi: 10.1038/nrn1785

Ford, C. P., Stemkowski, P. L., Light, P. E., and Smith, P. A. (2003). Experiments to test the role of phosphatidylinositol 4,5-bisphosphate in

neurotransmitter-induced M-channel closure in bullfrog sympathetic neurons. *J. Neurosci.* 23, 4931–4941. doi: 10.1523/JNEUROSCI.23-12-04931.2003

Herbert, E., Trusz-Gluza, M., Moric, E., Smiłowska-Dzielicka, E., Mazurek, U., and Wilczok, T. (2002). KCNQ1 gene mutations and the respective genotype-phenotype correlations in the long QT syndrome. *Med. Sci. Monit.* 8:RA240-8.

Kharkovets, T., Dedek, K., Maier, H., Schweizer, M., Khimich, D., Nouvian, R., et al. (2006). Mice with altered KCNQ4 K+ channels implicate sensory outer hair cells in human progressive deafness. *EMBO J.* 25, 642–652. doi: 10.1038/sj.emboj.7600951

Kharkovets, T., Hardelin, J. P., Safieddine, S., Schweizer, M., El-Amraoui, A., C., Petit, C., et al. (2000). KCNQ4, a K+ channel mutated in a form of dominant deafness, is expressed in the inner ear and the central auditory pathway. *Proc. Natl. Acad. Sci. U.S.A.* 97, 4333–4338. doi: 10.1073/pnas.97.8.4333

Kubisch, C., Schroeder, B. C., Friedrich, T., Lütjohann, B., El-Amraoui, A., Marlin, S., et al. (1999). KCNQ4, a novel potassium channel expressed in sensory outer hair cells, is mutated in dominant deafness. *Cell* 96, 437–446. doi: 10.1016/S0092-8674(00)80556-5

Lerche, C., Scherer, C. R., Seebohm, G., Derst, C., Wei, A. D., Busch, A. E., et al. (2000). Molecular cloning and functional expression of KCNQ5, a potassium channel subunit that may contribute to neuronal M-current diversity. *J. Biol. Chem.* 275, 22395–22400. doi: 10.1074/jbc.M002378200

Marrion, N. V. (1997). Control of M-current. *Annu. Rev. Physiol.* 59, 483–504. doi: 10.1146/annurev.physiol.59.1.483

Sanguinetti, M. C., Curran, M. E., Zou, A., Shen, J., Spector, P. S., Atkinson, D. L., et al. (1996). Coassembly of K(V)LQT1 and minK (IsK) proteins to form cardiac I(Ks) potassium channel. *Nature* 384, 80–83. doi: 10.1038/384080a0

Schroeder, B. C., Hechenberger, M., Weinreich, F., Kubisch, C., and Jentsch, T. J. (2000). KCNQ5, a novel potassium channel broadly expressed in brain, mediates M-type currents. *J. Biol. Chem.* 275, 24089–24095. doi: 10.1074/jbc.M003245200

Shah, M. M., Mistry, M., Marsh, S. J., Brown, D. A., and Delmas, P. (2002). Molecular correlates of the M-current in cultured rat hippocampal neurons. *J. Physiol.* 544, 29–37. doi: 10.1113/jphysiol.2002.028571

Singh, N. A., Charlier, C., Stauffer, D., DuPont, B. R., Leach, R. J., Melis, R., et al. (1998). A novel potassium channel gene, KCNQ2, is mutated in an inherited epilepsy of newborns. *Nat. Genet.* 18, 25–29. doi: 10.1038/ng0198-25

Søgaard, R., Ljungstrøm, T., Pedersen, K. A., Olesen, S. P., and Jensen, B. S. (2001). KCNQ4 channels expressed in mammalian cells: functional characteristics and pharmacology. *Am. J. Physiol. Cell Physiol.* 280, C859–C866. doi: 10.1152/ajpcell.2001.280.4.C859

Suh, B.-C., and Hille, B. (2002). Recovery from muscarinic modulation of M current channels requires phosphatidylinositol 4,5-bisphosphate synthesis. *Neuron* 35, 507–520. doi: 10.1016/S0896-6273(02)00790-0

Wang, H. S., Pan, Z., Shi, W., Brown, B. S., Wymore, R. S., Cohen, I. S., et al. (1998). KCNQ2 and KCNQ3 potassium channel subunits: molecular correlates of the M-channel. *Science* 282, 1890–1893. doi: 10.1126/science.282.5395.1890

Wang, Q., Curran, M. E., Splawski, I., Burn, T. C., Millholland, J. M., VanRaay, T. J., et al. (1996). Positional cloning of a novel potassium channel gene: KVLQT1 mutations cause cardiac arrhythmias. *Nat. Genet.* 12, 17–23. doi: 10.1038/ng0196-17

Weckhuysen, S., Mandelstam, S., Suls, A., Audenaert, D., Deconinck, T., Claes, L. R. F., et al. (2012). KCNQ2 encephalopathy: emerging phenotype of a neonatal epileptic encephalopathy. *Ann. Neurol.* 71, 15–25. doi: 10.1002/ana.22644

Zaydman, M. A., Silva, J. R., Delaloye, K., Li, Y., Liang, H., Larsson, H. P., et al. (2013). Kv7.1 ion channels require a lipid to couple voltage sensing to pore opening. *Proc. Natl. Acad. Sci. U.S.A.* 110, 13180–13185. doi: 10.1073/pnas.1305167110

Zhang, H., Craciun, L. C., Mirshahi, T., Rohács, T., Lopes, C. M. B., Jin, T., et al. (2003). PIP(2) activates KCNQ channels, and its hydrolysis underlies receptor-mediated inhibition of M currents. *Neuron* 37, 963–975. doi: 10.1016/S0896-6273(03)00125-9

Conflict of Interest: The authors declare that the research was conducted in the absence of any commercial or financial relationships that could be construed as a potential conflict of interest.

frontiers in Physiology

ORIGINAL RESEARCH
published: 14 January 2020
doi: 10.3389/fphys.2019.01573

The Gβ1 and Gβ3 Subunits Differentially Regulate Rat Vascular Kv7 Channels

*Iain A. Greenwood and Jennifer B. Stott**

Vascular Biology Research Centre, Institute of Molecular and Clinical Sciences, St George's University of London, London, United Kingdom

Within the vasculature Kv7 channels are key regulators of basal tone and contribute to a variety of receptor mediated vasorelaxants. The Kv7.4 isoform, abundant within the vasculature, is key to these processes and was recently shown to have an obligatory requirement of G-protein βγ subunits for its voltage dependent activity. There is an increasing appreciation that with 5 Gβ subunits and 12 Gγ subunits described in mammalian cells that different $G\beta_x\gamma_x$ combinations can confer selectivity in Gβγ effector stimulation. Therefore, we aimed to characterize the Gβ subunit(s) which basally regulate Kv7.4 channels and native vascular Kv7 channels. In Chinese Hamster Ovary cells overexpressing Kv7.4 and different Gβx subunits only Gβ1, Gβ3, and Gβ5 enhanced Kv7.4 currents, increasing the activation kinetics and negatively shifting the voltage dependence of activation. In isolated rat renal artery myocytes, proximity ligation assay detected an interaction of Kv7.4 with Gβ1 and Gβ3 subunits, but not other isoforms. Morpholino directed knockdown of Gβ1 in rat renal arteries did not alter Kv7 dependent currents but reduced Kv7.4 protein expression. Knockdown of Gβ3 in rat renal arteries resulted in decreased basal K^+ currents which were not sensitive to pharmacological inhibition of Kv7 channels. These studies implicate the Gβ1 subunit in the synthesis or stability of Kv7.4 proteins, whilst revealing that the Gβ3 isoform is responsible for the basal activity of Kv7 channels in native rat renal myocytes. These findings demonstrate that different Gβ subunits have important individual roles in ion channel regulation.

Keywords: G protein βγ subunits, Kv7 channels, vascular smooth muscle, G protein signaling, potassium channel

OPEN ACCESS

Edited by:
Thomas Andrew Jepps, University of Copenhagen, Denmark

Reviewed by:
Rían Manville, University of Brighton, United Kingdom
Sarah B. Withers, The University of Manchester, United Kingdom
Bill McIntire, University of Virginia, United States

***Correspondence:**
Jennifer B. Stott
jstott@sgul.ac.uk

Specialty section:
This article was submitted to Membrane Physiology and Membrane Biophysics, a section of the journal Frontiers in Physiology

Received: *01 November 2019*
Accepted: *16 December 2019*
Published: *14 January 2020*

Citation:
Greenwood IA and Stott JB (2020) The Gβ1 and Gβ3 Subunits Differentially Regulate Rat Vascular Kv7 Channels. Front. Physiol. 10:1573. doi: 10.3389/fphys.2019.01573

INTRODUCTION

The Kv7 family of voltage gated potassium channels are crucial regulators of membrane excitability (Haick and Byron, 2016; Barrese et al., 2018). Within the vasculature this role extends itself to regulating cell contractility where the activity of these channels subdues the activity of voltage gated calcium channels and thus the entry of Ca^{2+}– the primary contractile stimulus. This has been evidenced in several vessel types where pharmacological blockade of Kv7 channels results in increased contractility of vessels in *ex vivo* preparations (Chadha et al., 2012; Lee et al., 2015; Stott et al., 2015), and reduced renal blood flow *in vivo* (Salomonsson et al., 2015). Of the 5 Kv7 isoforms (Kv7.1–Kv7.5), the Kv7.4 channel has been most implicated in the regulation of vascular reactivity – molecular knockdown of this isoform increases vessel contractility whilst decreasing the ability to respond to vasodilators (Chadha et al., 2012, 2014; Stott et al., 2016, 2018), and it

is Kv7.4 expression which is reduced in hypertensive animal models (Jepps et al., 2011). Due to their importance in vascular reactivity, uncovering mechanisms which govern native vascular Kv7 channel activity has been of key interest and recently G protein βγ subunits (Gβγ) were shown to be crucial regulators of basal Kv7 channel activity (Stott et al., 2015). These two strongly bound proteins were originally identified as components of heterotrimeric G proteins, which couple to G protein-coupled receptors (GPCR). However, Gβγ subunits were acknowledged to be important signaling mediators with the discovery that muscarinic acetylcholine induced hyperpolarization of cardiomyocytes occurred via Gβγ-mediated activation of the K_{ACh} channel (Kir3.1/3.4) (Logothetis et al., 1987). Subsequently it has been shown that Gβγ regulate other ion channels [CaV_2 (Herlitze et al., 1996), TRPM3 (Badheka et al., 2017; Dembla et al., 2017; Quallo et al., 2017)] as well as numerous enzymes (e.g., adenylyl cyclase, PI-3 Kinase (Federman et al., 1992; Stephens et al., 1994; Ford et al., 1998).

Proximity ligation assays (PLA) studies with Kv7.4 and Gβ antibodies revealed a high level of channel-Gβγ interaction in unstimulated smooth muscle cells and structurally different inhibitors of Gβγ effector sites (e.g., gallein, M119K, GRK2i) attenuated heterologously expressed Kv7.4 channels and smooth muscle Kv7 currents in the absence of receptor stimulation (Stott et al., 2015). These findings revealed that Kv7.4 is constitutively regulated by an obligatory interaction with Gβγ. However, there are 5 Gβ (1–5) and 12 Gγ (1–5, 7–13) subunits described in mammals, and subunits display specificity in forming dimer pairs with the $G\beta_x\gamma_x$ composition known to alter GPCR behavior and effector coupling (Macrez-Lepretre et al., 1997; Bayewitch et al., 1998a,b; McIntire et al., 2001; Khan et al., 2015). Moreover, there are preferential associations for GPCR-ion channel couplings e.g., Gβγ inhibition of N-type calcium channels after α2-adrenoceptor stimulation is more effective when the receptor is coupled with Gβ1 or Gβ2 (Mahmoud et al., 2012), whilst β1-adrenoceptor coupling to Kir3.2 displays a preference for Gβ5 containing dimers (Robillard et al., 2000). We aimed to determine if a specific Gβ subunit was responsible for the basal regulation of Kv7.4 in native arterial smooth muscle cells and ascertain the effect of the five different Gβ isoforms on heterologously expressed Kv7.4. Our data reveal a striking difference between different Gβ isoforms that impacts on vascular responsiveness.

RESULTS

Stott et al. (2015) showed that intracellular perfusion of heterogeneous Gβγ subunits isolated from bovine brain enhances heterologously expressed Kv7.4 currents, produces a leftward shift in the voltage dependence of activation and reduces the rate of activation of these currents. These findings were replicated in CHO cells transiently transfected with Kv7.4, where intracellular perfusion with 250 ng/ml of Gβγ subunits significantly increased voltage dependent currents compared with control (**Figure 1**). Gβ1–4 show a high degree of homology, whereas Gβ5 is the most structurally distinct Gβ subunit. To determine the effect of individual Gβ subunits from the structurally similar Gβ1–4 group

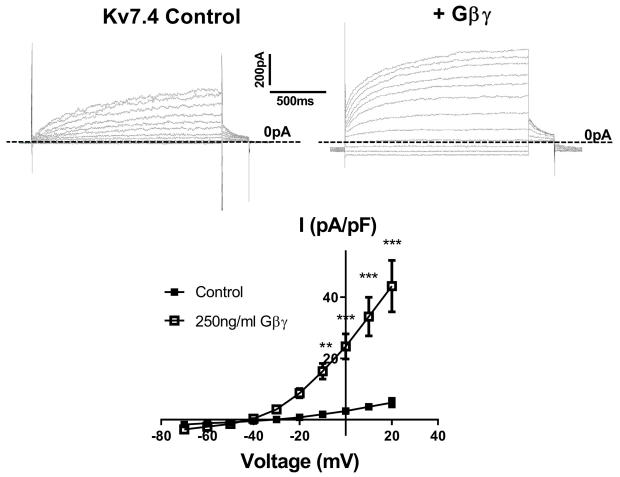

FIGURE 1 | Gβγ enhances Kv7.4 currents in CHO expression system. Top panels show representative traces of currents generated in cells expressing Kv7.4 either with the control intracellular solution (left) or with 250 ng/ml Gβγ purified from bovine brain (right). Zero current is indicated by the dashed line. Mean IV relationship of Kv7.4 currents in control (n = 7) or with 250 ng/ml Gβγ (n = 4) is shown in bottom panel. Data was analyzed by Bonferroni *post hoc* test following a two-way ANOVA. $p < 0.01$ is denoted (**) and $p < 0.005$ is denoted (***).

on Kv7.4 currents, we examined the effect each of these subunits on heterologously expressed Kv7.4 channels. Chinese Hamster Ovary (CHO) cells transfected with both Kv7.4 and Gβ1 or Gβ3 plasmids significantly increased K^+ currents compared to cells expressing Kv7.4 and the empty vector [e.g., 12.4 ± 1.6 pA/pF to 27.9 ± 7.7 (Gβ1) and 22.5 ± 4.2 (Gβ3) at 40 mV] (**Figure 2**). For both Gβ subunits this effect on Kv7.4 was accompanied by a leftward shift in the voltage dependence of activation [from −2.3 mV to −9.1 mV (Gβ1) and −5.9 mV (Gβ3)] (**Figure 2D**) and an increase in the rate of activation of the currents over a range of voltages [from 576 ± 45.4 ms to 316.7 ± 53.7 ms (Gβ1) and 310 ± 49.2 ms (Gβ3) at 40 mV] (**Figure 2E**). These effects on kinetics are analogous to the effect of Gβγ subunits isolated from bovine brain on Kv7.4 (Stott et al., 2015). In contrast, neither Gβ2 nor Gβ4 affected heterologously expressed Kv7.4 currents [11.9 ± 3.8 pA/pF (Gβ2) and 14.4 ± 5.7 pA/pF (Gβ4) at 40 mV] (**Figures 3A,B**). Interestingly, however, the structurally distinct Gβ5 also significantly enhanced Kv7.4 currents (26.3 ± 6.8 pA/pF at 40 mV), produced a leftward shift in the voltage dependence of activation (−8.1 mV) and increased the rate of activation of the currents (319 ± 34 ms) (**Figures 3C–F**).

To uncover the Gβx subunit(s) responsible for the basal activity of the native vascular Kv7 channel, we first examined the expression of the three Gβ isoforms which enhanced Kv7.4 currents – Gβ1, 3, and 5. Immunofluorescence performed on isolated rat renal artery myocytes showed strong expression of both Gβ1 and 3 in the cytosolic and sub-membranous regions (**Figures 4A,B**). Interestingly, expression of Gβ5 was confined to the nucleus of these cells (**Figure 4C**). To ascertain which subunits interacted with Kv7.4 in rat renal myocytes we further undertook a series of PLA studies. It has been shown that proteins

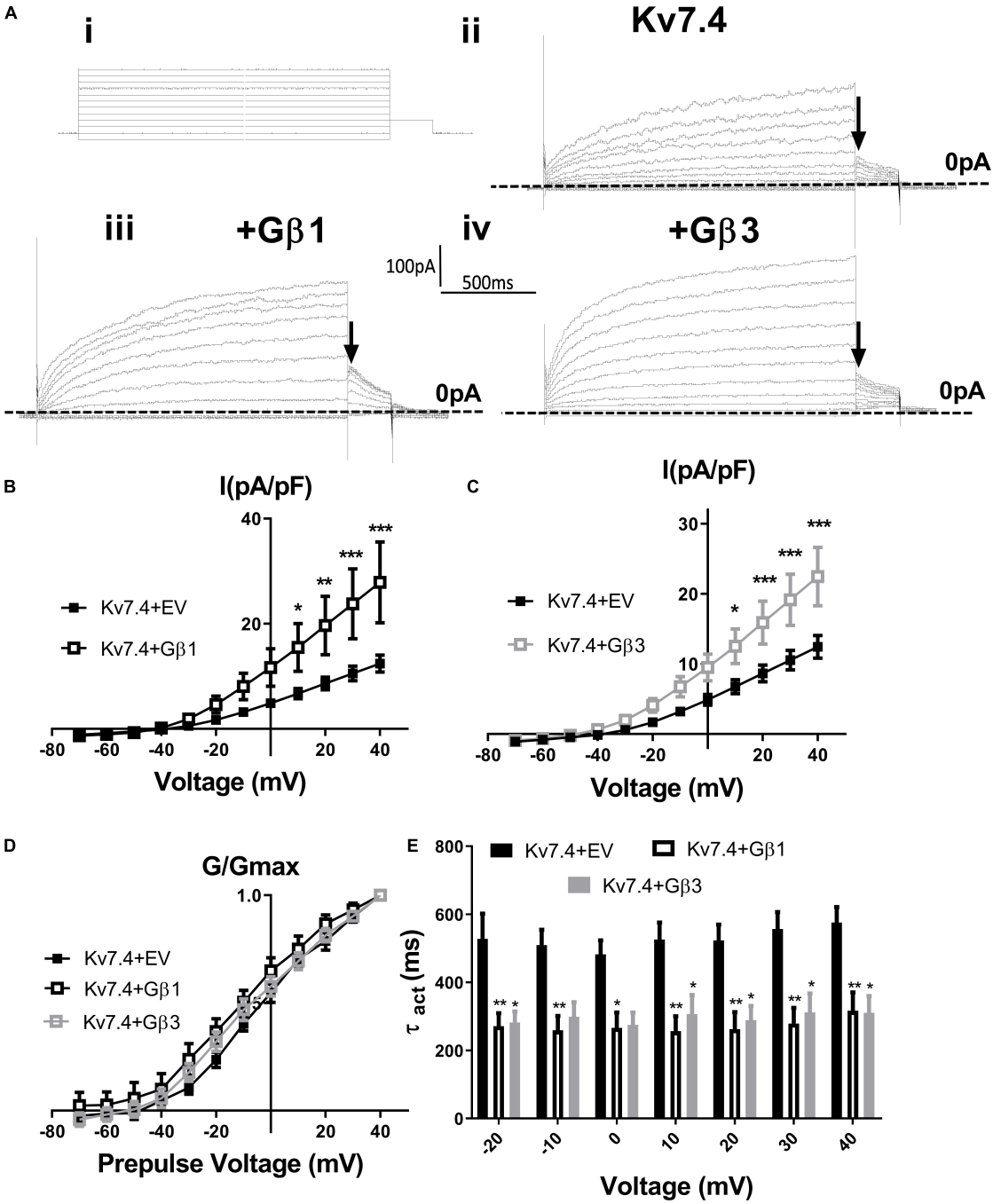

FIGURE 2 | Gβ1 and Gβ3 positively modulate Kv7.4 currents. **(Ai)** Diagram of voltage step protocol used to examine IV relationships. **(Aii–iv)** Representative traces of currents generated in cells expressing Kv7.4 with an empty vector (EV) (ii), Gβ1 (iii) or Gβ3 (iv). Zero current is indicated by the dashed line and point used for determination of voltage dependence of activation is indicated by the arrow. Mean data is shown in panel **(B)** (Gβ1, $n = 14$) and panel **(C)** (Gβ3, $n = 13$). **(D)** Voltage dependence of activation to determine V1/2 of Kv7.4 with EV (−2.4 ± 2.3 mV), Gβ1 (−9.12 ± 3.9 mV), and Gβ3 (−5.9 ± 3.3 mV). **(E)** Time dependence of activation of Kv7.4 currents when expressed with EV, Gβ1, and Gβ3 from −20 mV to 40 mV. Data was analyzed by Bonferroni *post hoc* test following a two-way ANOVA. $p < 0.05$ is denoted (*), $p < 0.01$ is denoted (**) and $p < 0.005$ is denoted (***).

can influence ion channels from distances ≤200 nm (Tajada et al., 2017), and PLA detects protein-protein interactions well within this range at ≤40 nm. PLA was performed in rat renal artery myocytes either in control or after treatment with 50 μmol/L gallein. Gallein disrupts Gβγ interactions and so was used as a pharmacological control in determining positive interactions. PLA punctae detected for the combinations of both Kv7.4-Gβ1 (8.2 ± 0.8 puncta/cell) and Kv7.4-Gβ3 (18.7 ± 2 puncta/cell)

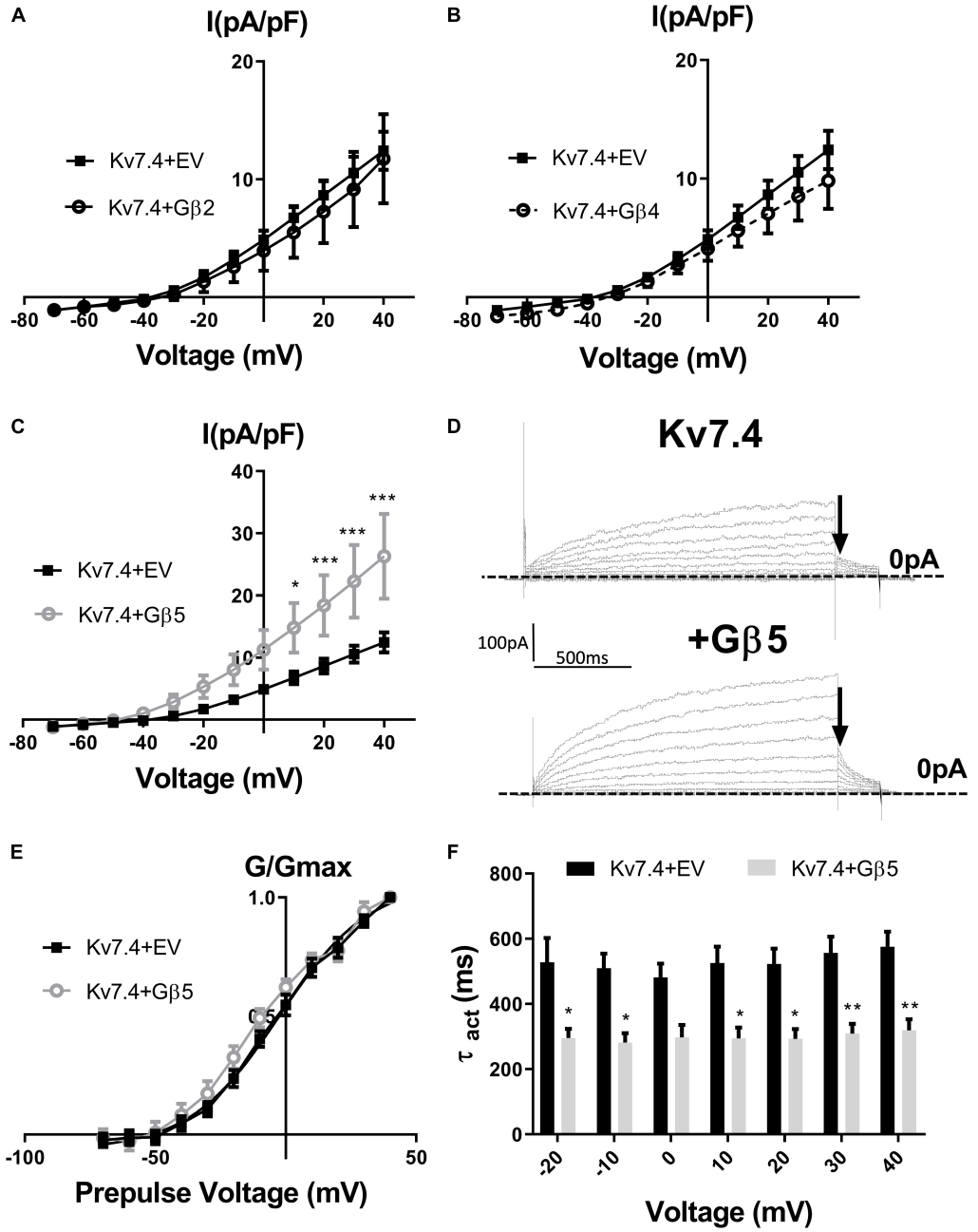

FIGURE 3 | Gβ2, Gβ4, and Gβ5 effects on Kv7.4 currents. IV relationships of Kv7.4 currents in empty vector (EV) or when co-transfected with Gβ2 (**A**, $n = 12$), Gβ4 (**B**, $n = 10$) or Gβ5 (**C**, $n = 12$). **(D)** Representative traces of currents cells expression Kv7.4 + EV (upper panel) or with Gβ5 (lower panel). Zero current is indicated by the dashed line and point used for determination of voltage dependence of activation is indicated by the arrow. **(E)** Voltage dependence of activation curves to determine V1/2 of Kv7.4 with EV (−2.4 ± 2.3 mV) and Gβ5 (−8.1 ± 3 mV). **(F)** Time dependence of activation of Kv7.4 currents when expressed with EV or Gβ5 from −20 mV to 40 mV. Data was analyzed by Bonferroni *post hoc* test following a two-way ANOVA. $p < 0.05$ is denoted (*), $p < 0.01$ is denoted (**), and $p < 0.005$ is denoted (***).

which were significantly reduced by gallein treatment [change to 3.8 ± 0.4 (Gβ1) and 8.8 ± 1.8 (Gβ3) puncta/cell] (**Figure 5**). PLA experiments with Kv7.4-Gβ5 PLA antibody combinations did not detect any gallein sensitive PLA puncta (2.7 ± 0.8 puncta/cell to 2.0 ± 0.4 puncta/cell) (**Figure 5**). These data reveal an association of Kv7.4 with Gβ1 and Gβ3 in vascular smooth muscle cells.

In order to assess the role of Gβ1 and Gβ3 on native vascular Kv7 currents, we performed morpholino directed knockdown of each subunit and examined the Kv7 currents by electrophysiology. Control cells produced K^+ currents which had a modest sensitivity to the Kv7 channel blocker linopirdine (10 μmol/L) with currents at +40 mV being reduced from

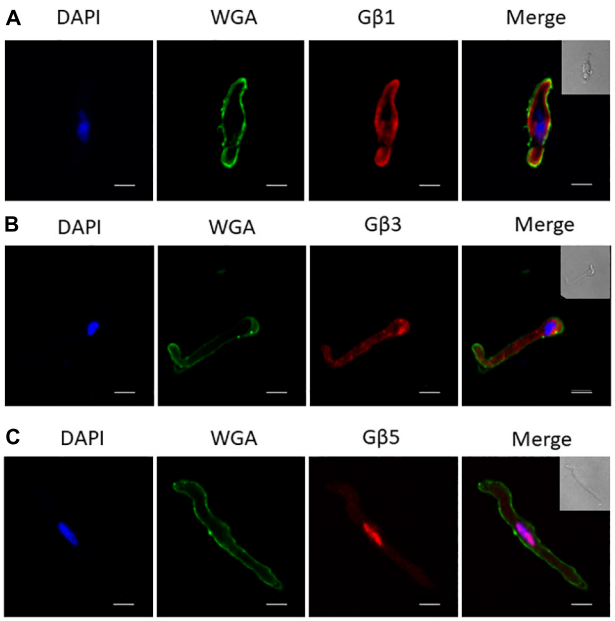

FIGURE 4 | Immunofluorescence of specific Gβ subunits in rat renal artery myocytes. Representative images showing staining in isolated rat renal artery myocytes of Gβ1 **(A)**, Gβ3 **(B)**, and Gβ5 **(C)**, all in red pseudocolour. Nuclear staining by DAPI is shown in blue pseudocolour, while membrane staining by Wheat Germ Agglutinin (WGA) is shown in green pseudocolour. Scale bar: 10 μm.

7.2 ± 0.8 pA/pF to 4.2 ± 0.4 pA/pF (**Figure 6A**). Gβ1 morpholino knockdown cells produced K^+ currents of the same magnitude as control (6.41 ± 1 pA/pF at 40 mV), whereas K^+ currents in Gβ3 morpholino knockdown cells were significantly reduced (3.8 ± 0.7 pA/pF at 40 mV) (**Figure 6B**). Kv7 inhibition with 10 μmol/L linopirdine significantly reduced K^+ currents in Gβ1 cells (from 6.41 ± 1 pA/pF to 3.2 ± 0.6 pA/pF at 40 mV) (**Figure 7A**). Immunofluorescence confirmed that Gβ1 morpholino knockdown reduced Gβ1 expression (**Figure 7B**), and did not affect Gβ3 expression (**Figure 7C**). However, total Kv7.4 abundance was also reduced in Gβ1 knockdown cells (**Figure 7D**). In cells treated with Gβ3 morpholino, 10 μmol/L linopirdine had no significant effect on K^+ currents (from 3.8 ± 0.7 pA/pF to 2.8 ± 0.4 pA/pF at 40 mV) (**Figure 8A**). Immunofluorescence confirmed knockdown of Gβ3 (**Figure 8B**), whilst no effects on Gβ1 or Kv7.4 expression was seen (**Figures 8C,D**).

DISCUSSION

Several ion channels have now been shown to be regulated by Gβγ subunits revealing the importance of Gβγ subunit-channel regulation in different physiological processes. However, with the increasing recognition of the importance of individual $G\beta_x\gamma_x$ combinations in conferring selectivity in effector regulation, defining these properties is a new frontier in Gβγ research. This study demonstrates for the first time the importance of individual Gβ subunits on Kv7.4 channel function. We show that Kv7.4 channel activity can be regulated by several Gβ isoforms in a cell expression system (Gβ1, 3, and 5), but that in native vascular myocytes specific roles for different subunits are described. Gβ1 subunits appear to regulate the synthesis or stability of Kv7.4, whereas Gβ3 regulate basal channel activity in rat renal artery myocytes.

Gβγ Specificity

With 5 Gβ (1–5) and 12 Gγ (1–5, 7–13) subtypes expressed in mammals, a growing body of evidence has demonstrated specific functions for different subunits, but it remains an oft overlooked aspect of Gβγ regulation. Gβ subunits are highly homologous and between Gβ1, 2, 3, and 4 there are 79–90% sequence similarities (Khan et al., 2013). Gβ5 is the least homologous and shows 51–52% homology when compared to all other subtypes. However, different subunits clearly exert different regulations and here we show specificity in the Gβ isoforms which can regulate Kv7.4 and native vascular Kv7 channels. Only Gβ1, 3, and 5 mirrored the effect on Kv7.4 currents previously reported for purified Gβγ (i.e., increased current amplitude, leftward shift in voltage dependence of activation and increased rate of activation) (Stott et al., 2015). Gβ2 and 4 were without effect. Of the 3 Gβ isoforms that enhanced Kv7.4 channels, only Gβ1 and 3 interacted with Kv7.4 in a gallein-dependent manner in renal artery myocytes. Moreover, only Gβ3 knockdown impaired native Kv7 channel currents analogous to treatment with gallein reported previously (Stott et al., 2015). It is interesting that although Gβ1 enhanced Kv7.4 currents in an overexpression system, knockdown of Gβ1 had no effect on Kv7 currents in renal artery myocytes even though there is a decrease in Kv7.4 protein in these cells. It is likely that the reduction in Kv7.4 is not severe enough to affect overall current density in the acute knockdown protocol over 48 h that we performed. However, our findings clearly indicate that Gβ1 regulates the expression of Kv7.4 at some level (discussed in detail below). Overall the results from our over-expression and native studies suggest that even though Gβ1 can regulate Kv7.4 currents, in myocytes that role is played by Gβ3 and this could indicate that Gβ3 is the preferential regulator of Kv7.4.

Another consideration is that native Kv7 channels present in rat renal artery myocytes could well be a hetero-tetramer with Kv7.5 subunits (Brueggemann et al., 2014; Chadha et al., 2014), and currents produced by these hetero-tetramers are also enhanced with application of Gβγ isolated from bovine brain (unpublished data). It is unclear if differential regulation by different Gβ seen here for Kv7.4 would also apply to the Kv7.4/7.5 channel although it seems likely. It is also known that vascular Kv7 channels undergo regulation by other molecules e.g., KCNE subunits (Jepps et al., 2015). It is possible that in the native system where such complexities exist, these different factors contribute to the Gβ regulation of the channel. Further studies will investigate how different regulators and channel compositions alter Gβ subunit regulation, but it is clear from our study is that Gβ3 basally regulates the native Kv7 current in renal artery myocytes. This is of interest in the area of the vascular biology of hypertension, where a polymorphism in Gβ3 has been associated with a hypertensive phenotype (Semplicini et al., 2015). This

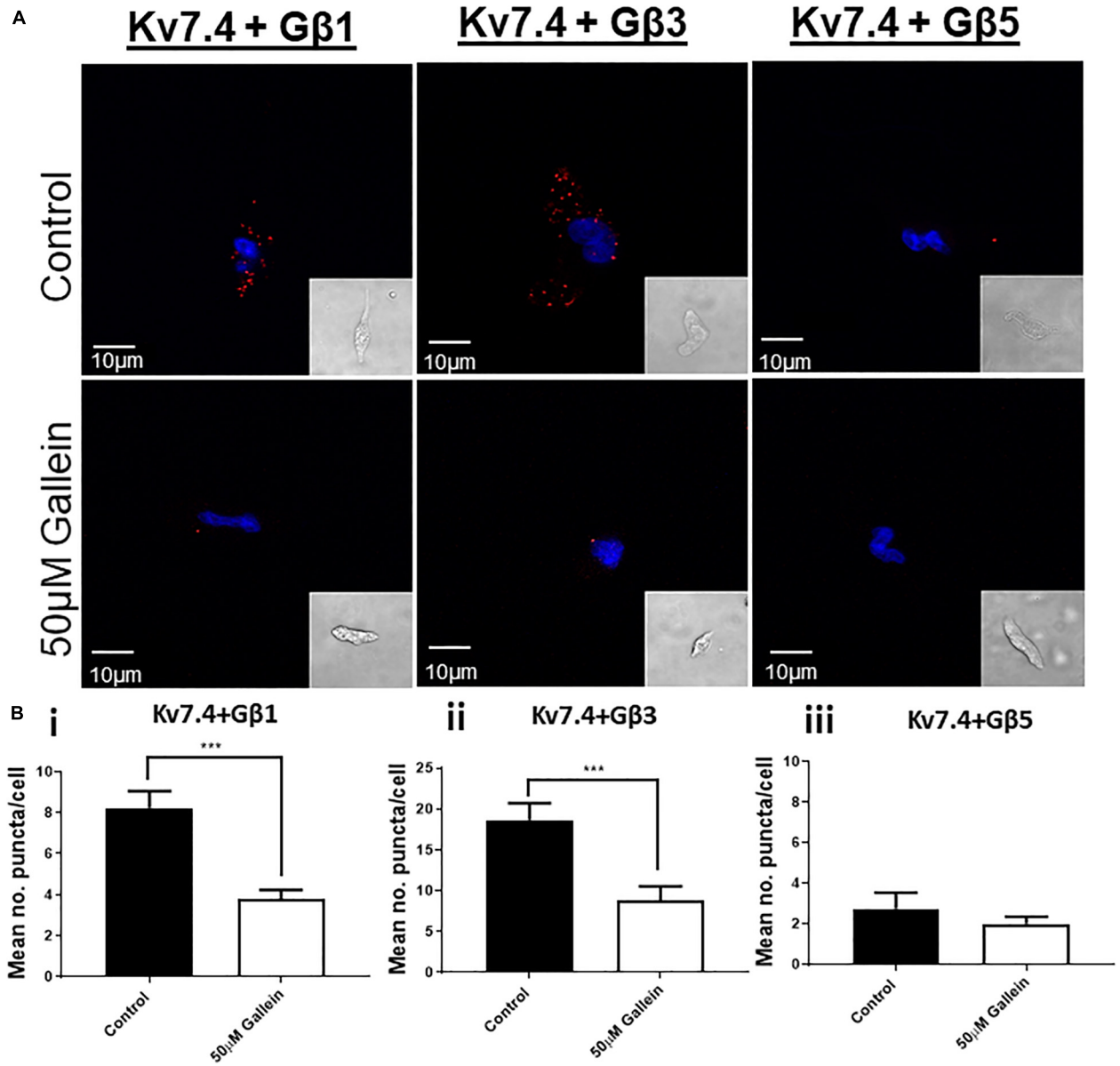

FIGURE 5 | Proximity Ligation Assay detection of Kv7.4 interactions with specific Gβ subunits. **(A)** Representative images of renal artery myocytes investigated for interactions between Kv7.4 and Gβ1, Gβ3 or Gβ5 in control (upper panels) or after treatment with 50 μmol/L gallein (lower panels). **(B)** Mean data of number of PLA puncta/cell before and after 50 μmol/L gallein treatment for Kv7.4- Gβ1 (i, n = 30–31, N = 5), Kv7.4- Gβ3 (ii, n = 15–33, N = 3–4), and Kv7.4- Gβ1 (iii, n = 11–12, N = 2). "n" = number of cells and "N" = number of animals. Scale bars represent 10 μm. PLA data was analyzed by one-way ANOVA with Bonferroni *post hoc* analysis where $p < 0.005$ is denoted (***).

polymorphism produces a truncated version of the Gβ3 protein, but it remains to be seen how this might regulate Kv7.4 or native vascular Kv7 channels. Finally, the role of Gβ5 remains unclear as we did not find this to be associated with Kv7.4 in rat renal artery myocytes, but it is possible that this may be an important regulator of Kv7.4 channels in other cell types.

It is important to note that our study has not investigated the role of Gγ in Kv7.4 channel regulation and this could well be an important determinant as described recently for Kir channels (Tabak et al., 2019). Certainly, in overexpression studies the Gγ natively expressed in these cells could be a determinant in the behavior of the Gβ subunits expressed. Subunits have been shown to exhibit preferences in forming $G\beta_x\gamma_x$ dimers (Pronin and Gautam, 1992; Schmidt et al., 1992; Dupre et al., 2009) whereas Gβ5 is thought to preferentially couple not to Gγ, but to a Regulator of G protein Signaling (RGS7) (Cabrera et al., 1998). There have also been differing reports about the coupling of Gβ3, with some reports showing that it can function without Gγ (Schmidt et al., 1992; Dingus et al., 2005; Poon et al., 2009). This is likely due to differences in experimental methods used, but

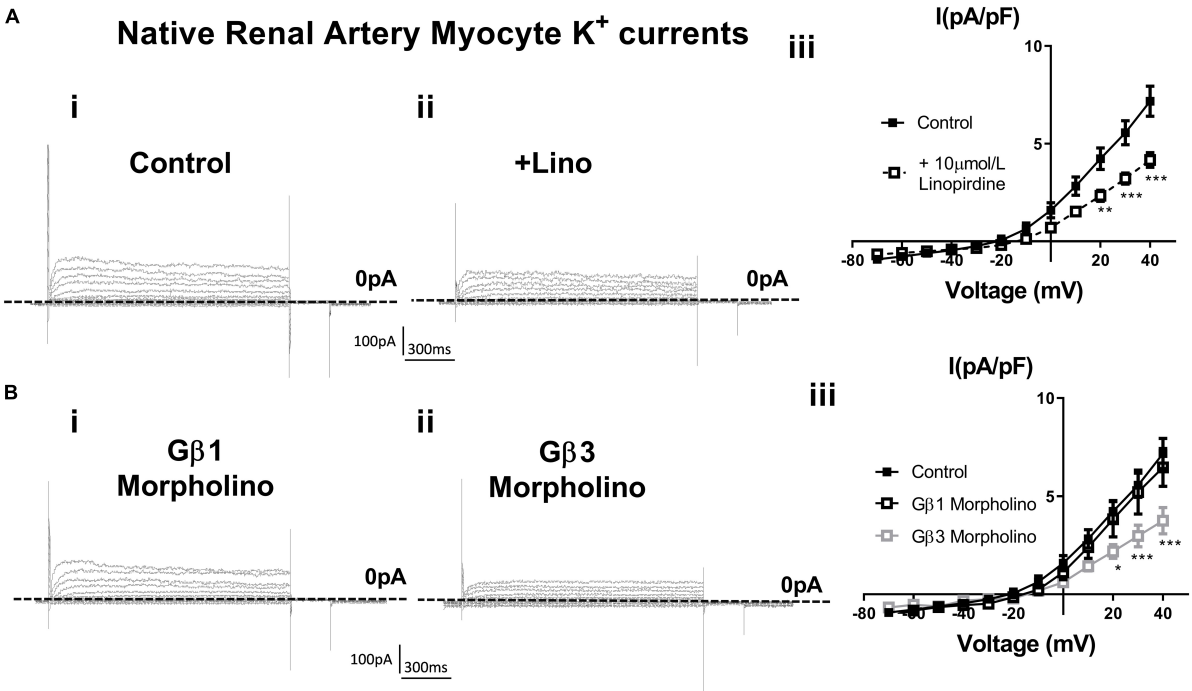

FIGURE 6 | K^+ currents in renal artery myocytes – effects of linopirdine and β1 or β3 morpholino. **(A)** Representative images of whole cell K^+ currents recorded in rat renal artery myocytes in control (i) or in the presence of 10 μm/L linopirdine (ii), and mean data [iii, $n = 17$ $N = 4$ (control), $n = 9$ $N = 4$ (linopirdine)]. Zero current is indicated by the dashed line. **(B)** Representative images of whole cell K^+ currents recorded in rat renal artery myocytes after morpholino knockdown of Gβ1 (i) or Gβ3 (ii) and mean data [iii, $n = 10$ $N = 4$ (Gβ1), $n = 8$ $N = 4$ (Gβ3)]. Zero current is indicated by the dashed line. "*n*" = number of cells and "*N*" = number of animals. Data was analyzed by Bonferroni *post hoc* test following a two-way ANOVA. $p < 0.05$ is denoted (*), $p < 0.01$ is denoted (**), and $p < 0.005$ is denoted (***).

what is clear is that what can theoretically interact *in vitro* may not be what actually occurs *in situ*. Gγ subunits are much more diverse, and some have argued that the diversity in Gβγ signaling is due to the Gγ in the dimer, rather than the Gβ. However our studies are complemented by work in native cells and we clearly show definitive roles for Gβ1 and 3 here and we demonstrate that disabling this subunit affects Kv7 channels. However, further studies will begin to examine the role of Gγ in these processes.

Gβγ in Trafficking

We describe here that knockdown of Gβ1 decreases Kv7.4 abundance in renal artery myocytes. This was an unexpected finding from a control experiment, but displays another different facet of Gβ regulation. As discussed above, the decrease in Kv7.4 was not severe enough to affect Kv7 current density, but it is possible that a longer period of knockdown would give more information on this relationship. Knockout of Gβ1 has been shown to be embryonic or perinatally lethal so this is not possible (Okae and Iwakura, 2010). However, these findings are supported by previous findings where Gβ1 regulate protein expression – knockdown increases Gβ4 expression (Hwang et al., 2005) and also alters Kir expression levels (Zylbergold et al., 2014). As it stands it is impossible to know at what level Gβ1 regulates Kv7.4 expression in myocytes without a much more detailed investigation into Kv7.4 protein synthesis and stability in these cells, but insights from previous work shows us that Gβγ can variously be involved in transcription, translation, trafficking and degradation of proteins and their genes (Khan et al., 2016). Knockdown studies have also demonstrated that Gβ subunits are involved in the expression of Gγ subunits – Gβ1 knockdown results in decreased Gγ5 expression, whilst Gγ2, 5, and 12 were decreased by Gβ2 knockdown (Hwang et al., 2005) – but this may be not be a direct regulatory effect but due to a result of removing the binding partners of these Gγ subunits ceases their production.

These findings underlie how the identity of the Gβ subunit is crucial for different aspects of ion channel regulation. That we demonstrate that two closely related Gβ subunits have two different regulatory capacities for Kv7.4 channels in the vasculature is quite striking, and is important in changing the way we think about Gβγ regulation. This work is significant in the growing move away from viewing Gβγ as homogenous dimer pairs to viewing these subunits as complex, disparate entities with specific regulatory responsibilities within cells.

MATERIALS AND METHODS

Ethical Approval

All experiments were performed in accordance with the United Kingdom Animals (Scientific Procedures) Act 1986.

Cell Culture

Chinese Hamster Ovary (CHO) cells were maintained in Dulbecco's modified Eagle's medium – high glucose

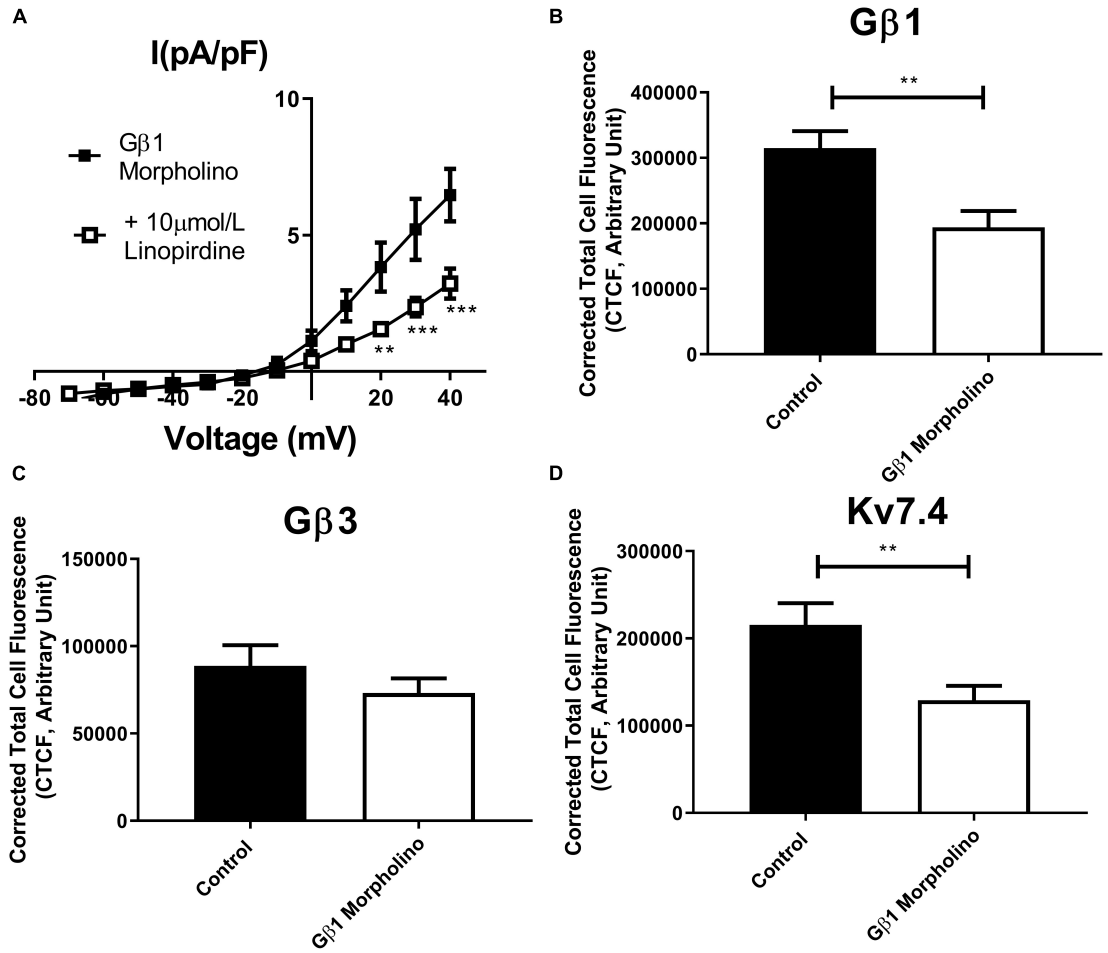

FIGURE 7 | Gβ1 knockdown effects on renal artery myocytes. **(A)** Mean data of whole cell K^+ currents recorded in rat renal artery myocytes in Gβ1 morpholino in control (n = 10, N = 4) or in the presence of 10 μm/L linopirdine (n = 8, N = 4). Mean fluorescence intensity of **(B)** Gβ1 (n = 20–22, N = 4) **(C)** Gβ3 (n = 15, N = 3) or **(D)** Kv7.4 (n = 14, N = 3) in renal artery myocytes in control morpholino or Gβ1 morpholino. "n" = number of cells and "N" = number of animals. Electrophysiology data was analyzed by Bonferroni *post hoc* test following a two-way ANOVA. IF data was analyzed by one-way ANOVA with Bonferroni *post hoc* analysis. $p < 0.01$ is denoted (**) and $p < 0.005$ is denoted (***).

solution supplemented with 10% fetal bovine serum and 1% penicillin/streptomycin in an incubator with 5% CO_2. Cells were split into six well plates for transfection for electrophysiology experiments. Cells were transfected with Kv7.4 and either Gβ1–5 or an empty vector (EV). Plasmids were mixed with Lipofectamine 2000 in Opti-MEM for 20 min before being added to cells. A total of 3 μg of plasmid was transfected in a 1:1 ratio for 24 h. Cells were briefly trypsinised on the day of experiments and plated on 13 mm coverslips in media at room temperature for 30 min and were then stored in the fridge for use within 8 h.

Animals

Male Wistar rats (175–225 g, Charles River United Kingdom) were kept in a 12 h light/dark cycle with free access to food and water. Animals were culled on the day of experiment by Schedule 1 cervical dislocation. Renal arteries (RA) were dissected of adherent fat and connective tissue and stored on ice in a physiological saline solution (PSS) containing (in mmol/L); 4.5 KCl, 120 NaCl, 1.2 $MgSO_4.7H_2O$, 1.2 $NaH_2PO4.2H_2O$, 25 $NaHCO_3$.5 D-Glucose, and 1.25 $CaCl_2$.

Morpholino Knockdown

To study the role of Gβ1 and Gβ3 in native Kv7 currents, knockdown in RA was performed by transfection with morpholino nucleotides as described in vessels previously (Stott et al., 2018). Gβ1 and Gβ3 morpholino nucleotides and mismatched control nucleotides (5 μmol/L, Genetools) were mixed with Lipofectamine 2000 (Life Technologies, United Kingdom) in Opti-MEM and left at room temperature for 2 h. RA were transfected with this mix in Dulbecco's modified eagle's medium F-12 with 1% penicillin/streptomycin at 37°C for 48 h.

Cell Isolation

Freshly dissected renal arteries were used for isolation of individual myocytes for proximity ligation assay, whereas vessels

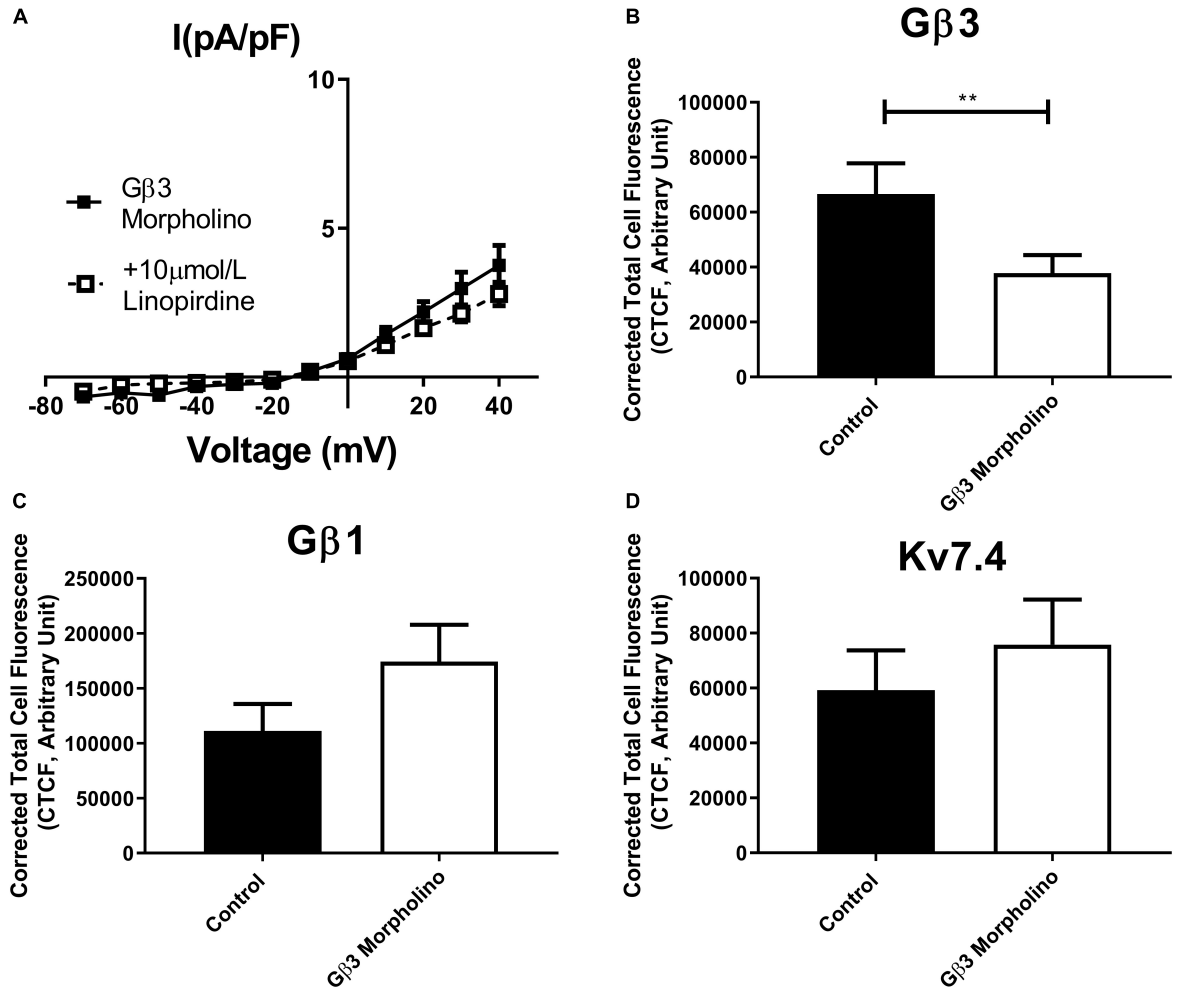

FIGURE 8 | Gβ3 knockdown effects on renal artery myocytes. **(A)** Mean data of whole cell K^+ currents recorded in rat renal artery myocytes in Gβ3 morpholino in control (n = 8, N = 4) or in the presence of 10 μm/L linopirdine (n = 5, N = 4). Mean fluorescence intensity of **(B)** Gβ3 (n = 20–23, N = 4) **(C)** Gβ1 (n = 20–21, N = 4) or **(D)** Kv7.4 (n = 15, N = 3) in renal artery myocytes in control morpholino or Gβ3 morpholino. "n" = number of cells and "N" = number of animals. Electrophysiology data was analyzed by Bonferroni *post hoc* test following a two-way ANOVA. IF data was analyzed by one-way ANOVA with Bonferroni *post hoc* analysis. $p < 0.01$ is denoted (**).

incubated in control or morpholino for 48 h were used for electrophysiology. Vessels were bathed for 10 min in a nominally Ca^{2+} free solution (in mmol/L: 6 KCl, 120 NaCl, 1.2 MgCl2, 12 D-glucose and 10 HEPES, pH 7.4 with NaOH). Vessels were then incubated at 37°C for 20 (incubated) or 23 (fresh) min in Ca^{2+} free solution containing in mg/ml: 1.5 collagenase, 0.75 thermolysin, 1 trypsin inhibitor and 1 bovine serum albumin (all Sigma Aldrich, United Kingdom). Vessels were then washed in Ca^{2+} free solution for 10 min and then triturated to liberate myocytes. The cell solution was plated on 13 mm coverslips in a 24 well plate and supplemented with an equivalent volume of 2.5 mmol/L Ca^{2+} solution to allow the cells to adhere.

Immunofluorescence

Freshly isolated myocytes from renal arteries from vessels transfected with control or Gβ1 and Gβ3 morpholino were prepared as above. Cells were fixed with 3% PFA on ice for 20 min and stored in PBS at 4°C. Cells were treated with 0.1 mol/L glycine for 5 min and then incubated in blocking solution (PBS containing 0.1% Triton X-100 and 1% bovine serum albumin) for 1 h at RT before being incubated overnight at 4°C with the following primary antibodies: (i) rabbit anti-Kv7.4 antibody (dilution 1:100, Abcam, Cambridge, United Kingdom); (ii) rabbit anti-Gβ1 (dilution 1:100, Genetex, #GTX114442); mouse anti-Gβ3 (dilution 1:100, Abnova #H00002784-MO1) (iii) rabbit anti- Gβ5 (dilution 1:200, Abcam, #ab185206). Samples were then washed with PBS and incubated for 1 h with donkey anti-rabbit or donkey anti-mouse secondary antibodies conjugated to Alexa Fluor 568, respectively (dilution 1:100, Thermo-Fisher, Paisley, United Kingdom). All antibodies were diluted in blocking solution. Subsequently, samples were washed with PBS and mounted using VECTASHIELD Antifade Medium containing DAPI for nuclei counterstaining (Vector Laboratories, Peterborough, United Kingdom). Coverslips were

analyzed using a Zeiss LSM 510 Meta argon/krypton laser scanning confocal microscope (Carl Zeiss, Jena, Germany). Corrected total cell fluorescence (CTCF) was calculated using ImageJ software as elsewhere described (Burgess et al., 2010).

Proximity Ligation Assay

Freshly isolated cells were used as described above. 1 mL of solution containing 2.5 mmol/L $CaCl_2$ was added to each well and cells were placed in an incubator (37°C, 5% CO_2) for 30 min to equilibrate. Cells then underwent treatment: 50 μmol/L gallein or DMSO control (30 min). Gallein was used as a pharmacological control for identifying positive interactions with Gβx subunits, and only interactions which were sensitive to gallein were considered as true interactions. Coverslips were immediately fixed with 3% PFA on ice for 20 min and stored in PBS at 4°C. For the proximity ligation assay, cells were permeablised with 0.01% Triton X-100 for 5 min. The Duolink *in situ* PLA detection kit (Sigma-Aldrich, United Kingdom) was used to detect single molecule interactions for Kv7.4 (anti-mouse (N43/6, RRID:AB_2131828, UC Davis/NIH NeuroMab Facility) or anti-rabbit (Abcam, Cambridge, United Kingdom) and G protein β subunits; anti-Gβ1 (rabbit, Genetex, #GTX114442), anti-Gβ2 (rabbit, Cusabio, #CSB-PA009604ESR2HU), anti-Gβ3 (mouse, Abnova #H00002784-MO1), and anti-Gβ5 (rabbit, Abcam, #ab185206). Experiments were performed as per manufacturer's instructions; primary antibodies were incubated at 1:200 overnight at 4°C. Red fluorescent oligonucleotides produced as the end product of the procedure were visualized using a Zeiss Confocal LSM 510. Images were analyzed using ImageJ software using the particle detector tool. The number of puncta per cell was calculated as the average of two mid sections in each cell.

Electrophysiology

All current recordings were made using Axopatch 200B amplifier (Axon Instruments) at room temperature. Whole –cell electrical signals were generated and digitized at 1 kHz using a Digidata 1322A hosted by a PC running pClamp 9.0 software (Molecular Devices). For recordings cells were placed in an external solution containing (in mmol/L); 140 NaCl, 4 KCl, 2 $CaCl_2$, 1 $MgCl_2$, and 10 HEPES. Patch pipettes with a resistance of 4–12 MΩ were filled with a pipette solution containing (in mmol/L); 110 K gluconate, 30 KCl, 0.5 $MgCl_2$, 5 HEPES, and 0.5 EGTA. Cells were held at −60 mV and currents amplitude was monitored by application of a test pulse to 40 mV every 20 s. To generate current-voltage relationships a voltage step protocol was used from a holding potential of −60 mV testing a range of voltages from −70 to 40 mV in 10 mv increments at 15 s intervals.

Reagents

Gβ1 plasmid was kindly gifted by Dr. Kim Jonas. Gβ2–5 were purchased from Addgene (catalog nos. 36113, 36114, 54469, and 54470). Gallein and linopirdine were obtained from Tocris (Bristol, United Kingdom). Gβγ subunits isolated from bovine brain were purchased from Merck Millipore.

Statistics

All values are expressed as mean ± SEM. All statistical analyses and non-linear regression curve fitting were performed with GraphPad Prism 7 software. In experiments which utilize native rat myocytes "n" represents the number of cells analyzed and "N" represents the number of subjects. Analyzes of immunofluorescence data were performed by Student's *t*-test, and Proximity Ligation Assay data by one-way ANOVA multiple comparisons test with Bonferroni *post hoc* analysis. Analyses of electrophysiological data used two-way ANOVA with Bonferroni *post hoc* analysis. Differences were considered significant at $p < 0.05$.

DATA AVAILABILITY STATEMENT

The datasets generated for this study are available on request to the corresponding author.

ETHICS STATEMENT

The animal study was reviewed and approved by the St George's University of London Animal Ethics Committee.

AUTHOR CONTRIBUTIONS

JS undertook the research, analyzed and interpreted the data, and wrote the manuscript. JS and IG designed and funded the data and revised the manuscript. Both authors read and finally approved the manuscript.

FUNDING

This work was funded by a British Heart Foundation award (PG/15/97/31862) to JS and IG.

REFERENCES

Badheka, D., Yudin, Y., Borbiro, I., Hartle, C. M., Yazici, A., Mirshahi, T., et al. (2017). Inhibition of Transient Receptor Potential Melastatin 3 ion channels by G-protein βγ subunits. *Elife* 6:e26147. doi: 10.7554/eLife.26147

Barrese, V., Stott, J. B., and Greenwood, I. A. (2018). KCNQ-encoded potassium channels as therapeutic targets. *Annu. Rev. Pharmacol. Toxicol.* 58, 625–648. doi: 10.1146/annurev-pharmtox-010617-052912

Bayewitch, M. L., Avidor-Reiss, T., Levy, R., Pfeuffer, T., Nevo, I., Simonds, W. F., et al. (1998a). Differential modulation of adenylyl cyclases I and II by various G beta subunits. *J. Biol. Chem.* 273, 2273–2276. doi: 10.1074/jbc.273.4.2273

Bayewitch, M. L., Avidor-Reiss, T., Levy, R., Pfeuffer, T., Nevo, I., Simonds, W. F., et al. (1998b). Inhibition of adenylyl cyclase isoforms V and VI by various Gbetagamma subunits. *FASEB J.* 12, 1019–1025. doi: 10.1096/fasebj.12.11.1019

Brueggemann, L. I., Mackie, A. R., Cribbs, L. L., Freda, J., Tripathi, A., Majetschak, M., et al. (2014). Differential protein kinase C-dependent modulation of Kv7.4 and Kv7.5 subunits of vascular Kv7 channels. *J. Biol. Chem.* 289, 2099–2111. doi: 10.1074/jbc.M113.527820

Burgess, A., Vigneron, S., Brioudes, E., Labbe, J. C., Lorca, T., and Castro, A. (2010). Loss of human Greatwell results in G2 arrest and multiple mitotic defects due to deregulation of the cycli B-Cdc/PP2A balance. *Proc. Natl. Acad. Sci. U.S.A.* 107, 12564–12569. doi: 10.1073/pnas.0914191107

Cabrera, J. L., de Freitas, F., Satpaev, D. K., and Slepak, V. Z. (1998). Identification of the Gbeta5-RGS7 protein complex in the retina. *Biochem. Biophys. Res. Commun.* 249, 898–902. doi: 10.1006/bbrc.1998.9218

Chadha, P. S., Jepps, T. A., Carr, G., Stott, J. B., Zhu, H. L., Cole, W. C., et al. (2014). Contribution of Kv7.4/Kv7.5 heteromers to intrinsic and calcitonin gene-related peptide-induced cerebral reactivity. *Arterioscler. Thromb. Vasc. Biol.* 34, 887–893. doi: 10.1161/ATVBAHA.114.303405

Chadha, P. S., Zunke, F., Zhu, H. L., Davis, A. J., Jepps, T. A., Olesen, S. P., et al. (2012). Reduced KCNQ4-encoded voltage-dependent potassium channel activity underlies impaired β-adrenoceptor-mediated relaxation of renal arteries in hypertension. *Hypertension* 59, 877–884. doi: 10.1161/hypertensionaha.111.187427

Dembla, S., Behrendt, M., Mohr, F., Goecke, C., Sondermann, J., and Schneider, F. M. (2017). Anti-nociceptive action of peripheral mu-opiod receptors by G-beta-gamma protein-mediated inhibition of TRPM3 channels. *Elife* 6:e26280. doi: 10.7554/eLife.26280

Dingus, J., Wells, C. A., Campbell, L., Cleator, J. H., Robinson, K., and Hildebrandt, J. D. (2005). G Protein betagamma dimer formation: Gbeta and Ggamma differentially determine efficiency of in vitro dimer formation. *Biochemistry* 44, 11885–11890.

Dupre, D. J., Robitaille, M., Rebois, R. V., and Hebert, T. E. (2009). The role of Gbetagamma subunits in the organisation, assembly and function of GPCR signalling complexes. *Annu. Rev. Pharmacol. Toxicol.* 49, 31–56. doi: 10.1146/annurev-pharmtox-061008-103038

Federman, A. D., Conklin, B. R., Schrader, K. A., Reed, R. R., and Bourne, H. R. (1992). Hormonal stimulation of adenylyl cyclase through G_i-protein beta gamma subunits. *Nature* 356, 159–161. doi: 10.1038/356159a0

Ford, C. E., Skiba, N. P., Bae, H., Daaka, Y., Reuveny, E., Shekter, L. R., et al. (1998). Molecular basis for interactions of G protein betagamma subunits with effectors. *Science* 280, 1271–1274. doi: 10.1126/science.280.5367.1271

Haick, J. M., and Byron, K. L. (2016). Novel treatment strategies for smooth muscle disorders: targeting Kv7 potassium channels. *Pharmacol. Ther.* 165, 14–25. doi: 10.1016/j.pharmthera.2016.05.002

Herlitze, S., Garcia, D. E., Mackie, K., Hille, B., Scheuer, T., and Catterall, W. A. (1996). Modulation of Ca2+ channels by G-protein beta gamma subunits. *Nature* 380, 258–262. doi: 10.1038/380258a0

Hwang, J. I., Choi, S., Fraser, I. D., Chang, M. S., and Simon, M. I. (2005). Silencing the expression of multiple Gbeta-subunits eliminates signalling mediated by all four families of G proteins. *Proc. Natl. Acad. Sci. U.S.A.* 102, 9493–9498. doi: 10.1073/pnas.0503503102

Jepps, T. A., Carr, G., Lundegaard, P. R., Olesen, S. P., and Greenwood, I. A. (2015). Fundamental role for the KCNE4 ancillary subunit in Kv7.4 regulation of arterial tone. *J. Physiol.* 593, 5324–5340. doi: 10.1113/JP271286

Jepps, T. A., Chadha, P. S., Davis, A. J., Harhun, M. I., Cockerill, G. W., Olesen, S. P., et al. (2011). Downregulation of Kv7.4 channel activity in primary and secondary hypertension. *Circulation* 124, 602–611. doi: 10.1161/CIRCULATIONAHA.111.032136

Khan, S. M., Min, A., Gora, S., Houranieh, G. M., Campden, R., Robitaille, M., et al. (2015). Gβ4γ1 as a modulator of M3 muscarinic receptor signalling and novel roles of Gβ1 subunits in the modulation of cellular signalling. *Cell. Signal.* 27, 1597–1608. doi: 10.1016/j.cellsig.2015.04.007

Khan, S. M., Sleno, R., Gora, S., Zylbergold, P., Laverdure, J. P., Labbe, J. C., et al. (2013). The expanding roles of Gβγ subunits in G protein-coupled receptor signalling and drug action. *Pharmacol. Rev.* 65, 545–577. doi: 10.1124/pr.111.005603

Khan, S. M., Sung, J. Y., and Hebert, T. E. (2016). Gβγ subunits – different spaces, different faces. *Pharmacol. Res.* 111, 434–441. doi: 10.1016/j.phrs.2016.06.026

Lee, S., Yang, Y., Tanner, M. A., Li, M., and Hill, M. A. (2015). Heterogeneity in Kv7 channel function in the cerebral and coronary circulation. *Microcirculation* 22, 109–121. doi: 10.1111/micc.12183

Logothetis, D. E., Kurachi, Y., Galper, J., Neer, E. J., and Clapham, D. E. (1987). The beta gamma subunits of GTP-binding proteins activate the muscarinic K+ channel in the heart. *Nature* 325, 321–326. doi: 10.1038/325321a0

Macrez-Lepretre, N., Kalkbrenner, F., Morel, J. L., Schultz, G., and Mironneau, J. (1997). G protein heterotrimer Galpha13beta1gamma3 couples the angiotensin AT1A receptor to increases in cytoplasmic Ca2+ in rat portal vein myocytes. *J. Biol. Chem.* 272, 10095–10102. doi: 10.1074/jbc.272.15.10095

Mahmoud, S., Yun, J. K., and Ruiz-Velasco, V. (2012). Gβ2 and Gβ4 participate in the opiod and adrenergic receptor-mediated Ca2+ channel modulation in rat sympathetic neurons. *J. Physiol.* 590, 4673–4689. doi: 10.1113/jphysiol.2012.237644

McIntire, W. E., MacCleery, G., and Garrison, J. C. (2001). The G protein beta subunit is a determinant in the coupling of Gs to the beta 1-adrenergic and A2a adenosine receptors. *J. Biol. Chem.* 276, 15801–15809. doi: 10.1074/jbc.m011233200

Okae, H., and Iwakura, Y. (2010). Neural tube defects and impaired neural progenitor cell proliferation in Gbeta1-deficient mice. *Dev. Dyn.* 239, 1089–1101. doi: 10.1002/dvdy.22256

Poon, L. S., Chan, A. S., and Wong, Y. H. (2009). Gbeta3 forms distinct dimers with specific Ggamma subunits and preferentially activates the β3 isoform of phospholipase C. *Cell. Signal.* 21, 737–744. doi: 10.1016/j.cellsig.2009.01.018

Pronin, A. N., and Gautam, N. (1992). Interaction between G-protein beta and gamma subunit types is selective. *Proc. Natl. Acad. Sci. U.S.A.* 89, 6220–6224. doi: 10.1073/pnas.89.13.6220

Quallo, T., Alkhatib, O., Gentry, C., Andersson, D. A., and Bevan, S. (2017). G protein βγ subunits inhibit TRPM3 ion channels in sensory neurons. *Elife* 6:e26138. doi: 10.7554/eLife.26138

Robillard, L., Ethier, N., Lachance, M., and Hebert, T. E. (2000). Gbetagamma subunit combinations differentially modulate receptor and effector coupling in vivo. *Cell. Signal.* 12, 673–682. doi: 10.1016/s0898-6568(00)00118-2

Salomonsson, M., Brasen, J. C., Braunstein, T. H., Hagelgvist, P., Holstein-Rathlou, N. H., and Sorensen, C. M. (2015). Kv7.4 channels participate in the control of rodent renal vascular resting tone. *Acta Physiol. (Oxf.)* 214, 402–414. doi: 10.1111/apha.12525

Schmidt, C. J., Thomas, T. C., Levine, M. A., and Neer, E. J. (1992). Specificity of G protein beta and gamma subunit interaction. *J. Biol. Chem.* 267, 13807–13810.

Semplicini, A., Grandi, T., Sandona, C., Cattelan, A., and Ceolotto, G. (2015). G-protein β3-subunit gene C825T polymorphism and cardiovascular risk: an updated review. *High Blood Press. Cardiovasc. Prev.* 22, 225–232. doi: 10.1007/s40292-015-0093-4

Stephens, L., Smrcka, A., Cooke, F. T., Jackson, T. R., Sternweis, P. C., and Hawkins, P. T. (1994). A novel phosphoinositide 3 kinase activity in myeloid-derived cells is activated by G protein beta gamma subunits. *Cell* 77, 83–93. doi: 10.1016/0092-8674(94)90237-2

Stott, J. B., Barrese, V., and Greenwood, I. A. (2016). Kv7 channel activation underpins EPAC-dependent relaxations of rat arteries. *Arterioscler. Thromb. Vasc. Biol.* 36, 2404–2415.

Stott, J. B., Barrese, V., Suresh, M., Masoodi, S., and Greenwood, I. A. (2018). Investigating the role of G Protein βγ in Kv7-dependent relaxations of the rat vasculature. *Arterioscler. Thromb. Vasc. Biol.* 38, 2091–2102. doi: 10.1161/ATVBAHA.118.311360

Stott, J. B., Povstyan, O. V., Carr, G., Barrese, V., and Greenwood, I. A. (2015). G-protein βγ subunits are positive regulators of Kv7.4 and native vascular Kv7 channel activity. *Proc. Natl. Acad. Sci. U.S.A.* 112, 6497–6502. doi: 10.1073/pnas.1418605112

Tabak, G., Keren-Raifman, T., Kahanovitch, U., and Dascal, N. (2019). Mutual action by Gγ and Gβ for optimal activation of GIRK channels in a channel subunit-specific manner. *Sci. Rep.* 9:508. doi: 10.1038/s41598-018-36833-y

Tajada, S., Moreno, C. M., O'Dwyer, S., Woods, S., Sato, D., Navedo, M. F., et al. (2017). Distance constraints on activation of TRPV4 channels by AKAP150-bound PKCα in arterial myocytes. *J. Gen. Physiol.* 149, 639–659. doi: 10.1085/jgp.201611709

Zylbergold, P., Sleno, R., Khan, S. M., Jacobi, A. M., Belhke, M. A., and Hebert, T. E. (2014). Kir3 channel ontogeny – the role of Gβγ subunits in channel assembly and trafficking. *Front. Cell. Neurosci.* 8:108. doi: 10.3389/fncel.2014.00108

Conflict of Interest: The authors declare that the research was conducted in the absence of any commercial or financial relationships that could be construed as a potential conflict of interest.

The handling Editor declared past co-authorship with one of the authors IG.

frontiers in Physiology

MINI REVIEW
published: 25 May 2020
doi: 10.3389/fphys.2020.00513

M-Current Suppression, Seizures and Lipid Metabolism: A Potential Link Between Neuronal Kv7 Channel Regulation and Dietary Therapies for Epilepsy

Naoto Hoshi[1,2]*

[1] Department of Pharmaceutical Sciences, University of California, Irvine, Irvine, CA, United States, [2] Department of Physiology and Biophysics, University of California, Irvine, Irvine, CA, United States

Neuronal Kv7 channel generates a low voltage-activated potassium current known as the M-current. The M-current can be suppressed by various neurotransmitters that activate Gq-coupled receptors. Because the M-current stabilizes membrane potential at the resting membrane potential, its suppression transiently increase neuronal excitability. However, its physiological and pathological roles *in vivo* is not well understood to date. This review summarizes the molecular mechanism underlying M-current suppression, and why it remained elusive for many years. I also summarize how regulation of neuronal Kv7 channel contributes to anti-seizure action of valproic acid through inhibition of palmitoylation of a Kv7 channel binding protein, and discuss about a potential link with anti-seizure mechanisms of medium chain triglyceride ketogenic diet.

Keywords: Kv7 channel, regulation – physiological, valproic acid, epilepsy, medium chain fatty, palmitoylation

OPEN ACCESS

Edited by:
Francesco Miceli,
University of Naples Federico II, Italy

Reviewed by:
Maria Virginia Soldovieri,
University of Molise, Italy
Enrique Soto,
Meritorious Autonomous University of Puebla, Mexico

***Correspondence:**
Naoto Hoshi
nhoshi@uci.edu

Specialty section:
This article was submitted to Membrane Physiology and Membrane Biophysics, a section of the journal Frontiers in Physiology

Received: *17 March 2020*
Accepted: *27 April 2020*
Published: *25 May 2020*

Citation:
Hoshi N (2020) M-Current Suppression, Seizures and Lipid Metabolism: A Potential Link Between Neuronal Kv7 Channel Regulation and Dietary Therapies for Epilepsy. Front. Physiol. 11:513. doi: 10.3389/fphys.2020.00513

INTRODUCTION

The M-current is a low voltage-activated potassium current generated by combination of neuronal KCNQ/Kv7 subunits (Kv7.2, 7.3, 7.4, and 7.5; Jentsch, 2000; Delmas and Brown, 2005; Greene and Hoshi, 2017). Since the activation threshold of neuronal Kv7 channels is near the resting membrane potential, activation of this channel strongly antagonizes membrane depolarization, and neuronal firing. Several neurotransmitters and hormones suppress neuronal Kv7 channel activity via Gq-coupled GPCRs, a phenomenon commonly known as M-current suppression, which diminishes its negative regulation, and creates temporal increase in neuronal firings (Delmas and Brown, 2005). Because M-current suppression causes drastic increase in neuronal excitability, M-current suppression has been considered to have a significant impact on central nervous functions. However, because there were no tools to prevent M-current suppression until very recently, physiological and pathological roles of M-current suppression *in vivo* are not well understood. Since this is a special issue for Kv7 channels covering various aspects, this review will focus on M-current suppression and its contribution to anti-seizure action of valproic acid.

MOLECULAR MECHANISM OF M-CURRENT SUPPRESSION

Despite its clear physiological effects on neuronal excitability, elucidating molecular mechanism underlying M-current suppression took many years. The first proposed candidate was a protein

kinase C (PKC)-mediated mechanism, where activation of PKC by phorbol esters can suppress M-current (Higashida and Brown, 1986). It seemed to be a plausible mechanism because Gq-coupled receptors activate phospholipase C (PLC), which then activates PKC. However, follow up studies from several labs showed that PKC inhibitors do not disrupt M-current suppression, which undermined this mechanism (Bosma and Hille, 1989; Shapiro et al., 2000; Stemkowski et al., 2002).

A next proposed mechanism was by intracellular calcium. Treatments that rise intracellular calcium has been shown to suppress the M-current (Yu et al., 1994; Selyanko and Brown, 1996; Cruzblanca et al., 1998). In addition, calmodulin, a calcium sensing protein, was identified as an auxiliary subunit for Kv7 channels (Wen and Levitan, 2002; Yus-Najera et al., 2002). Furthermore, co-expression of the calcium insensitive mutant calmodulin diminished calcium-induced M-current suppression (Gamper and Shapiro, 2003). These studies clearly demonstrate that intracellular calcium can suppress the M-current and mediates M-current suppression induced by some receptors. However, inhibiting calcium responses failed to disrupt M-current suppression induced by m1 muscarinic receptors (Shapiro et al., 2000) or by purinergic ATP receptor (Stemkowski et al., 2002), which suggests that this is not the universal mechanism.

Next candidate mechanism involves phosphatydilinositol-4,5-bisphosphate (PIP2). Phosphoinositides are minor acidic phospholipids with an inositol sugar head (Falkenburger et al., 2010). Depending on the positions and numbers of phosphorylation of the inositol sugar head, phosphoionsitides show distinct physiological functions on various biological processes ranging from endocytosis, cell growth, to membrane protein regulation at various membrane compartments (Suh and Hille, 2008). PIP2 is the lipid substrate for PLC, but it is also an essential co-factor for various transporters and ion channels (Falkenburger et al., 2010). Kv7 channel family is one example of these proteins, and cannot transduce potassium ion without PIP2 binding (Suh and Hille, 2008; Sun and MacKinnon, 2020). Since PIP2 is consumed by PLC upon Gq-coupled receptor activation, depletion of PIP2 can generate M-current suppression (Suh and Hille, 2002; Zhang et al., 2003). In addition, enzymatic increase in PIP2 concentration at the plasma membrane can partially disrupt M-current suppression, which supports the PIP2 depletion hypothesis (Suh et al., 2006). However, this also raises a question: if PIP2 is an essential co-factor for many ion channels and transporters, how can PIP2 regulate M-current without having off-target side effects?

Soon after this discovery, a related but distinct pathway was found involving a scaffold protein, AKAP79/150 (79 human/150 rodent). AKAP79/150 is a scaffold protein that anchors protein kinase A (PKA), PKC, protein phosphatase 2B (PP2B/calcineurin) and calmodulin, and has identified as a Kv7.2 binding protein (Hoshi et al., 2003). AKAP79/150 locates at the inner surface of the plasma membrane through PIP2 binding and attached fatty acid by protein palmitoylation (Dell'Acqua et al., 1998; Wong and Scott, 2004; Keith et al., 2012). It has been shown that activation of muscarinic acetylcholine receptor requires Kv7.2 channel anchored PKC via AKAP79/150 for M-current suppression (Hoshi et al., 2003; Hoshi et al., 2005; Kosenko et al., 2012). The identified pathway is summarized as follows (**Figures 1A,B**; Kosenko et al., 2012): activation of Gq-coupled receptor activates AKAP79/150 anchored PKC and phosphorylates Kv7.2 subunits. PKC phosphorylates target serine residues of Kv7.2 subunits including one located at the calmodulin binding site. Phosphorylation of the conserved serine residue at the calmodulin binding site interferes with calmodulin binding, which leads to a change in CaM-Kv7 configuration that reduces the affinity of Kv7.2 subunit toward PIP2. Thus, Kv7 channel activity is suppressed. This Kv7.2-AKAP79/150-calmodulin complex also provides a molecular mechanism illustrating calcium-induced M-current suppression. Namely, calcium-bound calmodulin changes CaM-Kv7.2 configuration and reduces affinity of Kv7.2 to PIP2 (**Figure 1C**; Kosenko and Hoshi, 2013). Together, Kv7.2 channel complex integrates distinct signals to decrease in sensitivity of Kv7 channel toward PIP2, which leads to M-current suppression. This mechanism explains how a ubiquitous cofactor, PIP2, can selectively regulates Kv7 channels.

The Kv7.2-AKAP79/150-PKC protein complex not only provided insights as to how distinct stimuli suppress the M-current, but it also explains why PKC inhibitors could not disrupt M-current suppression in past studies. It revealed that AKAP79/150 binding to PKC protects PKC molecules from commonly used PKC inhibitors (Hoshi et al., 2010). In summary, PIP2 is an important regulator of Kv7 channel activity. Reduction of PIP2 level or sensitivity of Kv7 channel to PIP2 can reversibly induce M-current suppression.

INHIBITION OF S-PALMITOYLATION OF AKAP79/150 CONTRIBUTES TO ANTI-SEIZURE EFFECTS OF VALPROIC ACID THROUGH Kv7.2 CHANNELS

Valproic acid is a branched short chain fatty acid, and is one of the most commonly prescribed anti-epileptic drugs used for many decades (Perucca, 2002). Various mechanisms have been proposed to explain its anti-seizure effects such as enhancement of inactivation of sodium channel, increase in GABA content in the brain, changing fatty acid metabolism, and inhibition of HDAC (Perucca, 2002; Silva et al., 2008). However, the exact mechanism of action is not well understood to date. Recently, multi-day treatment with valproic acid has been shown to disrupt M-current suppression, which contributes to its anti-seizure action *in vivo* (Kay et al., 2015). In this mechanism, valproic acid inhibits a subset of protein palmitoylation in the brain including AKAP79/150. Because palmitoylation of AKAPa79/150 is required for phosphorylation of Kv7.2 subunit by AKAP79/150-anchored PKC, deficient palmitoylation preserves the M-current from suppressive neurotransmitters during seizures, which prevents aggravation of seizures (Kay et al., 2015; **Figure 2A**). A follow-up study using Kv7.2 mutant knock-in mice that lack the target PKC acceptor serine, Kv7.2(S559A), showed no further anti-seizure effect

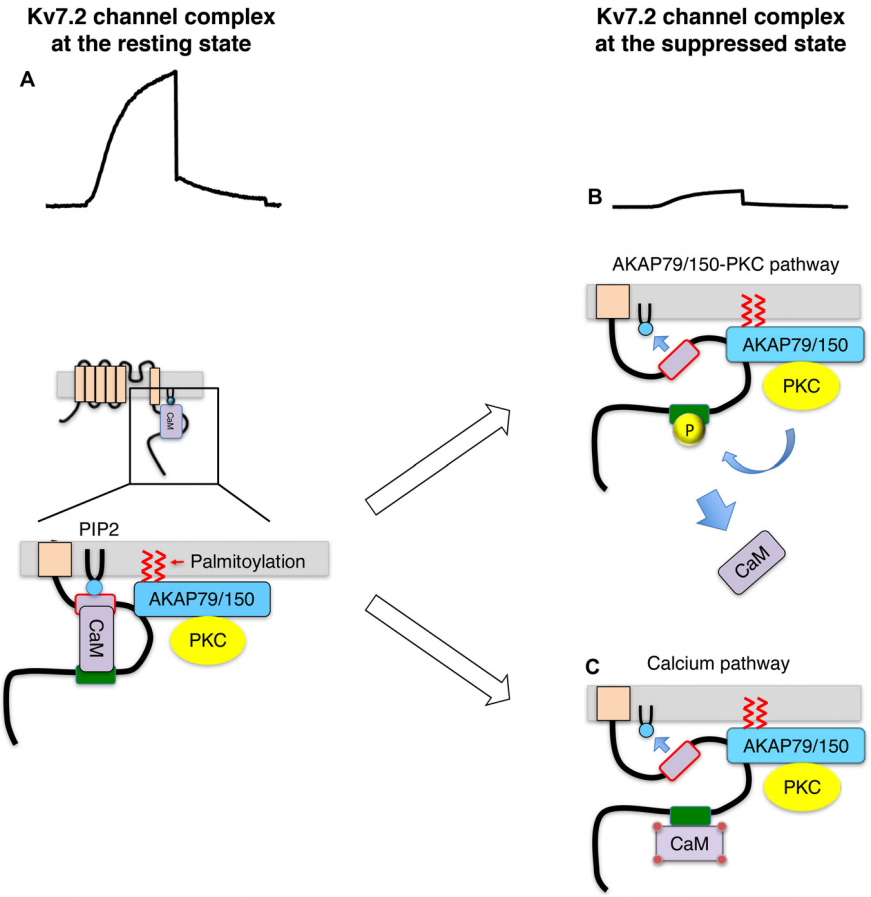

FIGURE 1 | Summary of Kv7.2 channel protein complex and its changes during M-current suppression, modified from ref (Kosenko et al., 2012). **(A)** Kv7.2 channel complex at the resting state. **(B)** Suppressed Kv7.2 channel through AKAP79/150-PKC pathway. Kv7.2 subunit is phosphorylated by AKAP79/150 anchored PKC when Gq-coupled receptors are activated. Phosphorylated Kv7.2 subunits release CaM, which reduces PIP2 binding to Kv7.2 subunit reducing functioning channels. **(C)** Suppressed Kv7.2 channel through intracellular calcium. Some Gq-coupled receptors suppress M-current via increase in intracellular calcium. Calcium-bound CaM changes configuration of Kv7.2 binding, which reduces PIP2 binding to Kv7.2 subunit.

of valproic acid treatment (Greene et al., 2018), which confirmed that valproic acid acts on the AKAP79/150-PKC-Kv7.2 pathway. This study also suggests that neuronal Kv7 channel is the major effector for non-acute anti-seizure action of valproic acid treatment.

REGULATION OF AKAP79/150 PALMITOYLATION AND FAT METABOLISM IN NEURON

S-Palmitoylation is a posttranslational modification that attaches long-chain fatty acids (C14,16,and 18), predominantly palmitic acid (C16), to cysteine residues through a thioester bond (Linder and Deschenes, 2007). Palmitoylation of proteins facilitates membrane localization at various membrane compartments. For the plasma membrane, protein palmitoylation facilitates its localization at the lipid raft, signaling hot spot (Linder and Deschenes, 2007). S-palmitoylation is characterized by cycles of palmitoylation and de-palmitoylation of the same protein molecules in response to cellular stimuli, which distinct itself from other one-time lipid modifications such as myristoylation (Linder and Deschenes, 2007). S-palmitoylation is mediated by DHHC palmitoyl acyltransferases utilizing long fatty acid-CoA as substrates (Fukata and Fukata, 2010). Among 23 members of DHHC enzymes, DHHC2 has been shown to mediate palmitoylation of AKPA79/150 (Woolfrey et al., 2015). Palmitoylation of AKAP79/150 at dendrites in neurons are regulated by neuronal activities, which correlates well with glutaminergic synaptic strength (Keith et al., 2012). Stimuli that cause long-term potentiation of synapses increase palmitoylation of AKAP79/150, while stimuli that cause long-term depression of synapses enhance de-palmitoylation. These findings suggest that palmitoylation of AKAP79/150 is in a dynamic equilibrium, which requires constant supply of palmitoyl-CoA.

Despite the fact that 60% of brain weight is lipid, neurons have a surprisingly low capacity for lipid metabolism including beta-oxidation in mitochondria or lipid synthesis (Belanger et al., 2011; Schonfeld and Reiser, 2013; Bruce et al., 2017; Romano et al., 2017). In addition, acyl-CoA in neurons is maintain at

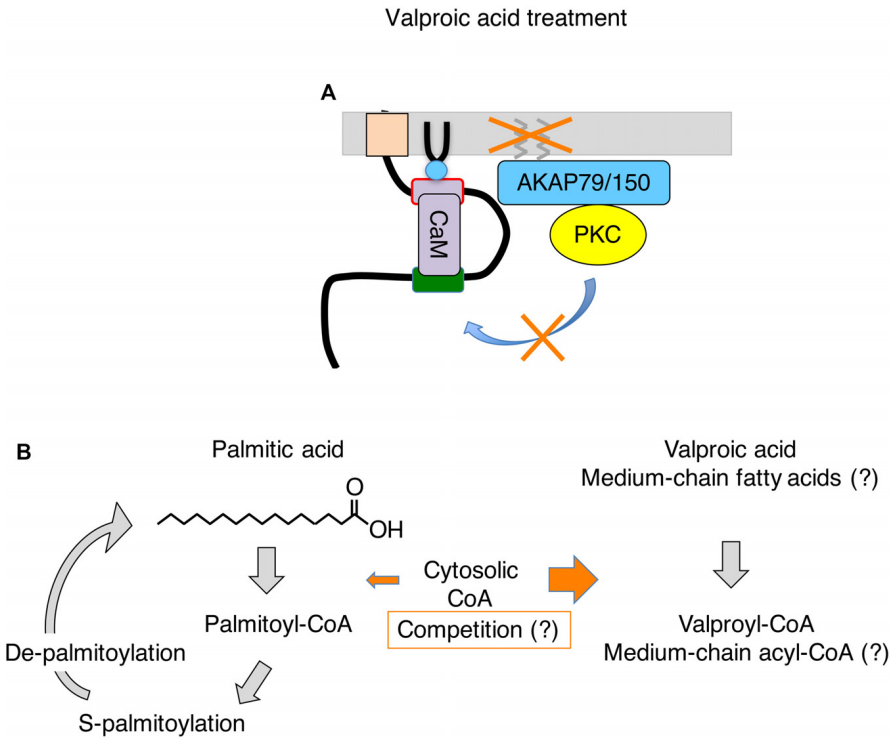

FIGURE 2 | Summary of events induced by valproic acid treatment on Kv7.2 channel complex. **(A)** Valproic acid treatment inhibits S-palmitoylation of AKAP79/150. Palmitoylation-deficient AKAP79/150 cannot mediate PKC phosphorylation of Kv7.2 subunit, which preserves M-current during seizures. **(B)** Summary of S-palmitoylation cycle and a potential action of valproic acid in this process. Valproic acid treatment may deplete free cytosolic CoA and interfere with generation of palmitoyl-CoA. A similar mechanism may be applicable to MCT therapy. See text for detail.

very low concentration, otherwise leads to neurodegeneration (Ellis et al., 2013). This low capacity of processing lipids in neurons implies that substrates for lipid processes including membrane synthesis or palmitoylation must be supplied directly and promptly from the cerebrospinal fluid or surrounding astrocytes rather than synthesized inside the neurons (Belanger et al., 2011). Increasing evidence suggests that neuron-astrocyte metabolic coupling plays an important role for supplying fatty acids, and removing excess lipid from neurons (Belanger et al., 2011; Ioannou et al., 2019). Therefore, if valproic acid changes substrate supplies such as palmitic acid, it would have drastic effects on neurons, which suggests that the site of action for valproic acid can be metabolically active non-neuronal cells such as astrocytes.

CROSSROAD FOR S-PALMITOYLATION, VALPROIC ACID AND MEDIUM CHAIN FATTY ACIDS

Valproic acid has various pharmacological effects, as mentioned earlier, and conditions that complicate pinning down its mechanism of action. For instance, the optimal therapeutic serum concentration of valproic acid is 300 to 700 μM (Perucca, 2002), which is significantly higher than other therapeutic compounds that function as ligands at a sub-micromolar range. Even though a concentration of valproic acid in the cerebrospinal fluid is 10 ∼ 30% of those in the serum (Loscher and Nau, 1983), valproic acid is most likely not a high-affinity ligand for target proteins. In addition, there are several processes where valproic acid can interfere with palmitoylation without acting as an enzyme inhibitor.

One potential mechanism is interference with coenzyme A (CoA) conjugation with long-chain fatty acids in the cytoplasm. Because valproic acid is a fatty acid, it is conjugated to CoA for processing. It is known that the cytosolic CoA is used for lipid synthesis, membrane trafficking and protein modification, and its concentration in mammalian cells is between 20–140 μM, while mitochondrial CoA, which is involved in energy production, is 2–5 mM (Leonardi et al., 2005). It has been shown that valproic acid can deplete free CoA and interfere with lipid metabolism including beta oxidation (Silva et al., 2008). In addition, *in vitro* study shows that valproic acid inhibits long fatty acid acyl transferase in brain microsomes by reducing palmitoyl-CoA (Bazinet et al., 2006). Therefore, high occupancy of CoA by valproic acid may interfere with supply of palmitoyl-CoA.

On the other hand, decreasing the palmitoyl-CoA pool in neurons may be achieved by conditions unrelated to valproic acid. Similar scenarios discussed above may be applied to shorter fatty acids that are not suitable as a substrate for palmitoylation. Dietary therapies known as ketogenic diet have been used to treat drug refractory epilepsy. These diets are composed of a high

fat diet, reduced carbohydrate intake, and induction of ketosis (Warren et al., 2018). A modern improvement of ketogenic diet was addition of medium chain fatty triglycerides (MCT) in the therapy, which are rich in octanoic acid (C8), and decanoic acid (C10). MCT was originally added to the regimen because they are more ketogenic than long chain triglycerides (Huttenlocher et al., 1971). However, it has been shown that both octanoic acid (Wlaz et al., 2012), and decanoic acid (Chang et al., 2016) have anti-seizure effects without inducing ketosis. In addition, it has been shown that MCT diet can raise serum concentration of octanoic acid to 300 μM and decanoic acid to 100 μM (Haidukewych et al., 1982), which is above concentration of cytosolic CoA and similar to the therapeutic concentration of valproic acid. Furthermore, triheptanoin, a triglyceride contains three heptanoates (C7), also has anti-seizure effects (Borges and Sonnewald, 2012), which generates three heptanoyl-CoA per compound. These pieces of emerging evidence suggest that medium chain fatty acids themselves are anticonvulsants. Various hypotheses are proposed as a mechanism for anti-seizure effects of these medium chain fatty acids ranging from changing energy production, neurotransmitter balance and ion channel activities (Warren et al., 2018). However, I would like to point out that carbon numbers of these anticonvulsant medium chain fatty acids (C7-C10) are outside of the acceptable carbon length of S-acyltransferase (C12-C18) that mediate protein palmitoylation (Rana et al., 2018). If these medium chain fatty acids can dominate cytosolic acyl-CoA pool and reduce palmitoyl-CoA, it would suppress palmitoylation of AKAP79/150 and have a similar outcome achieved by valproic acid. Only difference would be that medium chain fatty acids can be metabolized in various cells other than hepatocytes.

Based on the discussion above, the purpose of the ketogenic diet therapy for anti-epileptic treatment may not be creating a ketosis, but may be producing shorter fatty acids, which changes palmitoylation profiles in neurons. In summary, identification of palmitoylation as a contribution factor for anti-seizure action of valproic acid provides a prototypical mechanism for linking lipid metabolism and anti-seizure action. Further studies are required to determine whether MCT ketogenic therapy induce similar changes in palmitoylation profile of neuronal proteins.

AUTHOR CONTRIBUTIONS

The author confirms being the sole contributor of this work and has approved it for publication.

REFERENCES

Bazinet, R. P., Weis, M. T., Rapoport, S. I., and Rosenberger, T. A. (2006). Valproic acid selectively inhibits conversion of arachidonic acid to arachidonoyl-CoA by brain microsomal long-chain fatty acyl-CoA synthetases: relevance to bipolar disorder. *Psychopharmacology (Berl)* 184, 122–129. doi: 10.1007/s00213-005-0272-4

Belanger, M., Allaman, I., and Magistretti, P. J. (2011). Brain energy metabolism: focus on astrocyte-neuron metabolic cooperation. *Cell Metab.* 14, 724–738. doi: 10.1016/j.cmet.2011.08.016

Borges, K., and Sonnewald, U. (2012). Triheptanoin–a medium chain triglyceride with odd chain fatty acids: a new anaplerotic anticonvulsant treatment? *Epilepsy Res.* 100, 239–244. doi: 10.1016/j.eplepsyres.2011.05.023

Bosma, M. M., and Hille, B. (1989). Protein kinase C is not necessary for peptide-induced suppression of M current or for desensitization of the peptide receptors. *Proc. Natl. Acad. Sci. U.S.A.* 86, 2943–2947. doi: 10.1073/pnas.86.8.2943

Bruce, K. D., Zsombok, A., and Eckel, R. H. (2017). Lipid processing in the brain: a key regulator of systemic metabolism. *Front. Endocrinol.* 8:60. doi: 10.3389/fendo.2017.00060

Chang, P., Augustin, K., Boddum, K., Williams, S., Sun, M., Terschak, J. A., et al. (2016). Seizure control by decanoic acid through direct AMPA receptor inhibition. *Brain* 139, 431–443. doi: 10.1093/brain/awv325

Cruzblanca, H., Koh, D. S., and Hille, B. (1998). Bradykinin inhibits M current via phospholipase C and Ca2+ release from IP3-sensitive Ca2+ stores in rat sympathetic neurons. *Proc. Natl. Acad. Sci. U.S.A.* 95, 7151–7156. doi: 10.1073/pnas.95.12.7151

Dell'Acqua, M. L., Faux, M. C., Thorburn, J., Thorburn, A., and Scott, J. D. (1998). Membrane-targeting sequences on AKAP79 bind phosphatidylinositol-4, 5-bisphosphate. *EMBO J.* 17, 2246–2260. doi: 10.1093/emboj/17.8.2246

Delmas, P., and Brown, D. A. (2005). Pathways modulating neural KCNQ/M (Kv7) potassium channels. *Nat. Rev. Neurosci.* 6, 850–862. doi: 10.1038/nrn1785

Ellis, J. M., Wong, G. W., and Wolfgang, M. J. (2013). Acyl coenzyme A thioesterase 7 regulates neuronal fatty acid metabolism to prevent neurotoxicity. *Mol. Cell. Biol.* 33, 1869–1882. doi: 10.1128/MCB.01548-12

Falkenburger, B. H., Jensen, J. B., Dickson, E. J., Suh, B. C., and Hille, B. (2010). Phosphoinositides: lipid regulators of membrane proteins. *J. Physiol.* 588, 3179–3185. doi: 10.1113/jphysiol.2010.192153

Fukata, Y., and Fukata, M. (2010). Protein palmitoylation in neuronal development and synaptic plasticity. *Nat. Rev. Neurosci.* 11, 161–175. doi: 10.1038/nrn2788

Gamper, N., and Shapiro, M. S. (2003). Calmodulin mediates Ca2+-dependent modulation of M-type K+ channels. *J. Gen. Physiol.* 122, 17–31. doi: 10.1085/jgp.200208783

Greene, D. L., and Hoshi, N. (2017). Modulation of Kv7 channels and excitability in the brain. *Cell. Mol. Life Sci.* 74, 495–508. doi: 10.1007/s00018-016-2359-y

Greene, D. L., Kosenko, A., and Hoshi, N. (2018). Attenuating M-current suppression in vivo by a mutant Kcnq2 gene knock-in reduces seizure burden and prevents status epilepticus-induced neuronal death and epileptogenesis. *Epilepsia* 59, 1908–1918. doi: 10.1111/epi.14541

Haidukewych, D., Forsythe, W. I., and Sills, M. (1982). Monitoring octanoic and decanoic acids in plasma from children with intractable epilepsy treated with medium-chain triglyceride diet. *Clin. Chem.* 28, 642–645. doi: 10.1093/clinchem/28.4.642

Higashida, H., and Brown, D. A. (1986). Two polyphosphatidylinositide metabolites control two K+ currents in a neuronal cell. *Nature* 323, 333–335. doi: 10.1038/323333a0

Hoshi, N., Langeberg, L. K., Gould, C. M., Newton, A. C., and Scott, J. D. (2010). Interaction with AKAP79 modifies the cellular pharmacology of PKC. *Mol. Cell* 37, 541–550. doi: 10.1016/j.molcel.2010.01.014

Hoshi, N., Langeberg, L. K., and Scott, J. D. (2005). Distinct enzyme combinations in AKAP signalling complexes permit functional diversity. *Nat. Cell Biol.* 7, 1066–1073. doi: 10.1038/ncb1315

Hoshi, N., Zhang, J. S., Omaki, M., Takeuchi, T., Yokoyama, S., Wanaverbecq, N., et al. (2003). AKAP150 signaling complex promotes suppression of the M-current by muscarinic agonists. *Nat. Neurosci.* 6, 564–571. doi: 10.1038/nn1062

Huttenlocher, P. R., Wilbourn, A. J., and Signore, J. M. (1971). Medium-chain triglycerides as a therapy for intractable childhood epilepsy. *Neurology* 21, 1097–1103. doi: 10.1212/WNL.21.11.1097

Ioannou, M. S., Jackson, J., Sheu, S. H., Chang, C. L., Weigel, A. V., Liu, H., et al. (2019). Neuron-astrocyte metabolic coupling protects against activity-induced fatty acid toxicity. *Cell* 177:e1514. doi: 10.1016/j.cell.2019.04.001

Jentsch, T. J. (2000). Neuronal KCNQ potassium channels: physiology and role in disease. *Nat. Rev. Neurosci.* 1, 21–30. doi: 10.1038/35036198

Kay, H. Y., Greene, D. L., Kang, S., Kosenko, A., and Hoshi, N. (2015). M-current preservation contributes to anticonvulsant effects of valproic acid. *J. Clin. Invest.* 125, 3904–3914. doi: 10.1172/JCI79727

Keith, D. J., Sanderson, J. L., Gibson, E. S., Woolfrey, K. M., Robertson, H. R., Olszewski, K., et al. (2012). Palmitoylation of A-kinase anchoring protein 79/150 regulates dendritic endosomal targeting and synaptic plasticity mechanisms. *J. Neurosci.* 32, 7119–7136. doi: 10.1523/JNEUROSCI.0784-12.2012

Kosenko, A., and Hoshi, N. (2013). A change in configuration of the calmodulin-KCNQ channel complex underlies Ca2+-dependent modulation of KCNQ channel activity. *PLoS One* 8:e82290. doi: 10.1371/journal.pone.0082290

Kosenko, A., Kang, S., Smith, I. M., Greene, D. L., Langeberg, L. K., Scott, J. D., et al. (2012). Coordinated signal integration at the M-type potassium channel upon muscarinic stimulation. *EMBO J.* 31, 3147–3156. doi: 10.1038/emboj.2012.156

Leonardi, R., Zhang, Y. M., Rock, C. O., and Jackowski, S. (2005). Coenzyme A: back in action. *Prog. Lipid Res.* 44, 125–153. doi: 10.1016/j.plipres.2005.04.001

Linder, M. E., and Deschenes, R. J. (2007). Palmitoylation: policing protein stability and traffic. *Nat. Rev. Mol. Cell Biol.* 8, 74–84. doi: 10.1038/nrm2084

Loscher, W., and Nau, H. (1983). Distribution of valproic acid and its metabolites in various brain areas of dogs and rats after acute and prolonged treatment. *J. Pharmacol. Exp. Ther.* 226, 845–854.

Perucca, E. (2002). Pharmacological and therapeutic properties of valproate: a summary after 35 years of clinical experience. *CNS Drugs* 16, 695–714. doi: 10.2165/00023210-200216100-00004

Rana, M. S., Kumar, P., Lee, C. J., Verardi, R., Rajashankar, K. R., and Banerjee, A. (2018). Fatty acyl recognition and transfer by an integral membrane S-acyltransferase. *Science* 359:eaao6326. doi: 10.1126/science.aao6326

Romano, A., Koczwara, J. B., Gallelli, C. A., Vergara, D., Micioni Di Bonaventura, M. V., Gaetani, S., et al. (2017). Fats for thoughts: an update on brain fatty acid metabolism. *Int. J. Biochem. Cell Biol.* 84, 40–45. doi: 10.1016/j.biocel.2016.12.015

Schonfeld, P., and Reiser, G. (2013). Why does brain metabolism not favor burning of fatty acids to provide energy? Reflections on disadvantages of the use of free fatty acids as fuel for brain. *J. Cereb. Blood Flow Metab.* 33, 1493–1499. doi: 10.1038/jcbfm.2013.128

Selyanko, A. A., and Brown, D. A. (1996). Regulation of M-type potassium channels in mammalian sympathetic neurons: action of intracellular calcium on single channel currents. *Neuropharmacology* 35, 933–947. doi: 10.1016/0028-3908(96)00135-9

Shapiro, M. S., Roche, J. P., Kaftan, E. J., Cruzblanca, H., Mackie, K., and Hille, B. (2000). Reconstitution of muscarinic modulation of the KCNQ2/KCNQ3 K(+) channels that underlie the neuronal M current. *J. Neurosci.* 20, 1710–1721. doi: 10.1523/JNEUROSCI.20-05-01710.2000

Silva, M. F., Aires, C. C., Luis, P. B., Ruiter, J. P., Ijlst, L., Duran, M., et al. (2008). Valproic acid metabolism and its effects on mitochondrial fatty acid oxidation: a review. *J. Inherit. Metab. Dis.* 31, 205–216. doi: 10.1007/s10545-008-0841-x

Stemkowski, P. L., Tse, F. W., Peuckmann, V., Ford, C. P., Colmers, W. F., and Smith, P. A. (2002). ATP-inhibition of M current in frog sympathetic neurons involves phospholipase C but not Ins P(3), Ca(2+), PKC, or Ras. *J. Neurophysiol.* 88, 277–288. doi: 10.1152/jn.2002.88.1.277

Suh, B. C., and Hille, B. (2002). Recovery from muscarinic modulation of M current channels requires phosphatidylinositol 4,5-bisphosphate synthesis. *Neuron* 35, 507–520. doi: 10.1016/S0896-6273(02)00790-0

Suh, B. C., and Hille, B. (2008). PIP2 is a necessary cofactor for ion channel function: how and why? *Annu. Rev. Biophys.* 37, 175–195. doi: 10.1146/annurev.biophys.37.032807.125859

Suh, B. C., Inoue, T., Meyer, T., and Hille, B. (2006). Rapid chemically induced changes of PtdIns(4,5)P2 gate KCNQ ion channels. *Science* 314, 1454–1457. doi: 10.1126/science.1131163

Sun, J., and MacKinnon, R. (2020). Structural basis of human KCNQ1 modulation and gating. *Cell* 180, 340–347.e9. doi: 10.1016/j.cell.2019.12.003

Warren, E. C., Walker, M. C., and Williams, R. S. B. (2018). All you need is fats-for seizure control: using amoeba to advance epilepsy research. *Front. Cell. Neurosci.* 12:199. doi: 10.3389/fncel.2018.00199

Wen, H., and Levitan, I. B. (2002). Calmodulin is an auxiliary subunit of KCNQ2/3 potassium channels. *J. Neurosci.* 22, 7991–8001. doi: 10.1523/JNEUROSCI.22-18-07991.2002

Wlaz, P., Socala, K., Nieoczym, D., Luszczki, J. J., Zarnowska, I., Zarnowski, T., et al. (2012). Anticonvulsant profile of caprylic acid, a main constituent of the medium-chain triglyceride (MCT) ketogenic diet, in mice. *Neuropharmacology* 62, 1882–1889. doi: 10.1016/j.neuropharm.2011.12.015

Wong, W., and Scott, J. D. (2004). AKAP signalling complexes: focal points in space and time. *Na.t Rev. Mol. Cell Biol.* 5, 959–970. doi: 10.1038/nrm1527

Woolfrey, K. M., Sanderson, J. L., and Dell'acqua, M. L. (2015). The palmitoyl acyltransferase DHHC2 regulates recycling endosome exocytosis and synaptic potentiation through palmitoylation of AKAP79/150. *J. Neurosci.* 35, 442–456. doi: 10.1523/JNEUROSCI.2243-14.2015

Yu, S. P., O'malley, D. M., and Adams, P. R. (1994). Regulation of M current by intracellular calcium in bullfrog sympathetic ganglion neurons. *J. Neurosci.* 14, 3487–3499. doi: 10.1523/JNEUROSCI.14-06-03487.1994

Yus-Najera, E., Santana-Castro, I., and Villarroel, A. (2002). The identification and characterization of a noncontinuous calmodulin-binding site in noninactivating voltage-dependent KCNQ potassium channels. *J. Biol. Chem.* 277, 28545–28553. doi: 10.1074/jbc.M204130200

Zhang, H., Craciun, L. C., Mirshahi, T., Rohacs, T., Lopes, C. M., Jin, T., et al. (2003). PIP(2) activates KCNQ channels, and its hydrolysis underlies receptor-mediated inhibition of M currents. *Neuron* 37, 963–975. doi: 10.1016/S0896-6273(03)00125-9

Conflict of Interest: The author declares that the research was conducted in the absence of any commercial or financial relationships that could be construed as a potential conflict of interest.

frontiers in Physiology

REVIEW
published: 04 June 2020
doi: 10.3389/fphys.2020.00504

Gating and Regulation of KCNQ1 and KCNQ1 + KCNE1 Channel Complexes

*Yundi Wang, Jodene Eldstrom and David Fedida**

Department of Anesthesiology, Pharmacology & Therapeutics, The University of British Columbia, Vancouver, BC, Canada

The IKs channel complex is formed by the co-assembly of Kv7.1 (KCNQ1), a voltage-gated potassium channel, with its β-subunit, KCNE1 and the association of numerous accessory regulatory molecules such as PIP2, calmodulin, and yotiao. As a result, the IKs potassium current shows kinetic and regulatory flexibility, which not only allows IKs to fulfill physiological roles as disparate as cardiac repolarization and the maintenance of endolymph K^+ homeostasis, but also to cause significant disease when it malfunctions. Here, we review new areas of understanding in the assembly, kinetics of activation and inactivation, voltage-sensor pore coupling, unitary events and regulation of this important ion channel complex, all of which have been given further impetus by the recent solution of cryo-EM structural representations of KCNQ1 alone and KCNQ1+KCNE3. Recently, the stoichiometric ratio of KCNE1 to KCNQ1 subunits has been confirmed to be variable up to a ratio of 4:4, rather than fixed at 2:4, and we will review the results and new methodologies that support this conclusion. Significant advances have been made in understanding differences between KCNQ1 and IKs gating using voltage clamp fluorimetry and mutational analysis to illuminate voltage sensor activation and inactivation, and the relationship between voltage sensor translation and pore domain opening. We now understand that the KCNQ1 pore can open with different permeabilities and conductance when the voltage sensor is in partially or fully activated positions, and the ability to make robust single channel recordings from IKs channels has also revealed the complicated pore subconductance architecture during these opening steps, during inactivation, and regulation by 1−4 associated KCNE1 subunits. Experiments placing mutations into individual voltage sensors to drastically change voltage dependence or prevent their movement altogether have demonstrated that the activation of KCNQ1 alone and IKs can best be explained using allosteric models of channel gating. Finally, we discuss how the intrinsic gating properties of KCNQ1 and IKs are highly modulated through the impact of intracellular signaling molecules and co-factors such as PIP2, protein kinase A, calmodulin and ATP, all of which modulate IKs current kinetics and contribute to diverse IKs channel complex function.

Keywords: KCNE1, KCNQ1, IKs, activation gating, calmodulin, single channels, PKA

Abbreviations: G-V, conductance-voltage relationship; IKs, delayed cardiac rectifier K^+ current; I-V, current-voltage relationship; *k*, slope factor; LQTS, long QT syndrome; $V_{1/2}$, voltage at half-maximal activation or inactivation; VCF, voltage clamp fluorimetry; VSD, voltage sensor domain; WT, wild type.

OPEN ACCESS

Edited by:
Francesco Miceli,
University of Naples Federico II, Italy

Reviewed by:
Bernard Attali,
Tel Aviv University, Israel
Alain J. Labro,
University of Antwerp, Belgium

***Correspondence:**
David Fedida
david.fedida@ubc.ca

Specialty section:
This article was submitted to Membrane Physiology and Membrane Biophysics, a section of the journal Frontiers in Physiology

Received: *17 March 2020*
Accepted: *24 April 2020*
Published: *04 June 2020*

Citation:
Wang Y, Eldstrom J and Fedida D (2020) Gating and Regulation of KCNQ1 and KCNQ1 + KCNE1 Channel Complexes. Front. Physiol. 11:504. doi: 10.3389/fphys.2020.00504

THE WORLD OF Kv7.1 AND ITS ACCESSORY SUBUNITS

Potassium ion channels are categorized structurally and functionally into four major classes; calcium-activated, inward rectifying, tandem two-pore domain, and voltage-gated potassium (Kv) channels, and are known to play an essential role in cell signaling in both excitable and non-excitable cells. Within the Kv7 channel family, which belongs to the voltage-gated potassium channels class, the tetrameric voltage-gated KCNQ potassium channel subfamily is comprised of five known isoforms, Kv7.1−7.5 (KCNQ1-5). Recent research has improved our understanding of the gating and regulatory mechanisms of the first isoform, Kv7.1, commonly referred to as KCNQ1, alone and in complex with its regulatory subunit KCNE1. While reviews published about 5 years ago have dealt with these topics in detail, in this review we aim to incorporate recent experiments and new insights that allow us to refine the conceptual framework established by these authors (Zaydman and Cui, 2014; Liin et al., 2015; Nakajo and Kubo, 2015; Cui, 2016).

Expression of KCNQ1 has been detected throughout the body including in the heart, inner ear, pancreas, kidney, colon and intestine, stomach, and thyroid gland (Robbins, 2001; Liin et al., 2015; Nakajo and Kubo, 2015; Cui, 2016). When expressed alone, KCNQ1 produces a fast activating and deactivating current (**Figure 1**) which undergoes a mostly hidden inactivation, revealed as a hook in the tail current (Sanguinetti et al., 1996; Pusch et al., 1998; Tristani-Firouzi and Sanguinetti, 1998; Hou et al., 2017). The inactivation is quite apparent when KCNQ1 is expressed in mammalian cells (Meisel et al., 2018; Westhoff et al., 2019), but much less apparent when expressed in oocytes (Hou et al., 2017). This fast activating and deactivating KCNQ1 current has a very low conductance (**Figure 1B**; Yang and Sigworth, 1998; Hou et al., 2017), but has yet to be positively identified with any endogenous current(s) in the body (Abbott, 2014). Unlike other members of the KCNQ channel subfamily, KCNQ1 has been reported to associate with all five single transmembrane domain KCNE β-subunits, KCNE1-5, which modify channel kinetics to a greater or lesser extent (Barhanin et al., 1996; Melman et al., 2002b; Eldstrom and Fedida, 2011). The sometimes dramatic modulation of KCNQ1 kinetics by specific KCNE subunits, and the expression of different KCNE subunits in various tissues to a large degree underlie the diverse physiological roles that KCNQ1 plays throughout the body (Sanguinetti, 2000). KCNE1 co-expression with KCNQ1 increases current expression and greatly slows activation and deactivation kinetics. Both KCNE2 and KCNE3 in combination with KCNQ1 induce constitutively open channels not only across, but also beyond both ends of the physiological voltage range, with KCNE3 producing currents with much larger current amplitudes (Schroeder et al., 2000b). KCNE4 and KCNE5 on the other hand have an inhibitory effect when combined with KCNQ1 and decrease current amplitude under physiological conditions (Schroeder et al., 2000a; Angelo et al., 2002; Grunnet et al., 2002).

As well as the KCNEs, KCNQ1 is also regulated by several other molecules including PIP2, ATP, calmodulin (CaM) and PKA (Loussouarn et al., 2003; Matavel and Lopes, 2009; Zaydman et al., 2013; Thompson et al., 2017) which in turn further increase the flexibility of current complexes and contribute to their importance throughout body systems. KCNE1 confers significant changes on KCNQ1 tetramer properties via a variable complex stoichiometry, and modulation of biophysical mechanisms underlying voltage gating, such as voltage sensor domain (VSD) activation, pore domain (PD) opening and VSD-PD coupling as well as mechanisms of inactivation. In addition, the roles that other modulator proteins can have at the structural interface between KCNQ1 VSD activation and the time course of PD gating further contributes to the known diversity of IKs behavior. By understanding gating mechanisms both in the presence and absence of KCNE1 we can begin to better understand the physiology of the channel complex and the pathophysiology of the various diseases associated with IKs, and also perhaps eventually develop better therapeutic treatments for patients suffering from consequential arrhythmia syndromes.

KCNE1 MODULATION OF KCNQ1 KINETICS IN HEALTH AND DISEASE

How KCNQ1 and its accessory subunit KCNE1 traffic and assemble to form complexes with unique physiological roles is still a subject of some debate. Overall, two main theories for trafficking and assembly exist, one involves KCNE1 and KCNQ1 trafficking separately, KCNE1 by a vesicular route and KCNQ1 trafficking by an endoplasmic reticulum or sarcoplasmic reticulum route (Poulsen and Klaerke, 2007; Jiang et al., 2017; Kaur et al., 2020). Once at the plasma membrane the two subunits then assemble. In this case, it has also been suggested that KCNE1 can dissociate from KCNQ1 and be replaced by either new KCNE1 or KCNE2, the latter of which has been shown to traffic independently to the cell surface (Jiang et al., 2009). Alternatively, assembly of KCNE1 and KCNQ1 occurs early during biogenesis, perhaps in the endoplasmic reticulum, following which the complex traffics together to the plasma membrane (Krumerman et al., 2004; Chandrasekhar et al., 2006), likely through the endoplasmic reticulum − plasma membrane junction and driven by KCNQ1 (Oliveras et al., 2020).

The impact of KCNE1 co-assembly on KCNQ1 is the most studied and best understood of the accessory subunits. KCNE1 co-expression depolarizes the voltage dependence of activation (G-V) of KCNQ1 by about +50 mV, slows activation 1000-fold, and delays deactivation kinetics (Sanguinetti et al., 1996), as shown in **Figure 1**. A fully saturated 4:4 octameric complex of KCNE1 and KCNQ1 (EQ in **Figure 1A**) has the slowest activation kinetics compared with KCNQ1 alone (**Figure 1B**) and the most positive half-activation potential (G-V $V_{1/2}$, **Figure 1E**). KCNE1 increases the macroscopic current by increasing the underlying single-channel conductance and stabilizing the open pore (Werry et al., 2013; **Figure 1A**, upper panels, note different current scaling), while eliminating the inactivation seen in KCNQ1 channels (Tristani-Firouzi and Sanguinetti, 1998; Hou et al., 2017; Meisel et al., 2018; **Figures 1A,B**). These pore effects of KCNE1 are accompanied by changes in the Rb^+/K^+ selectivity (Pusch et al., 2000; Zaydman et al., 2014) and in

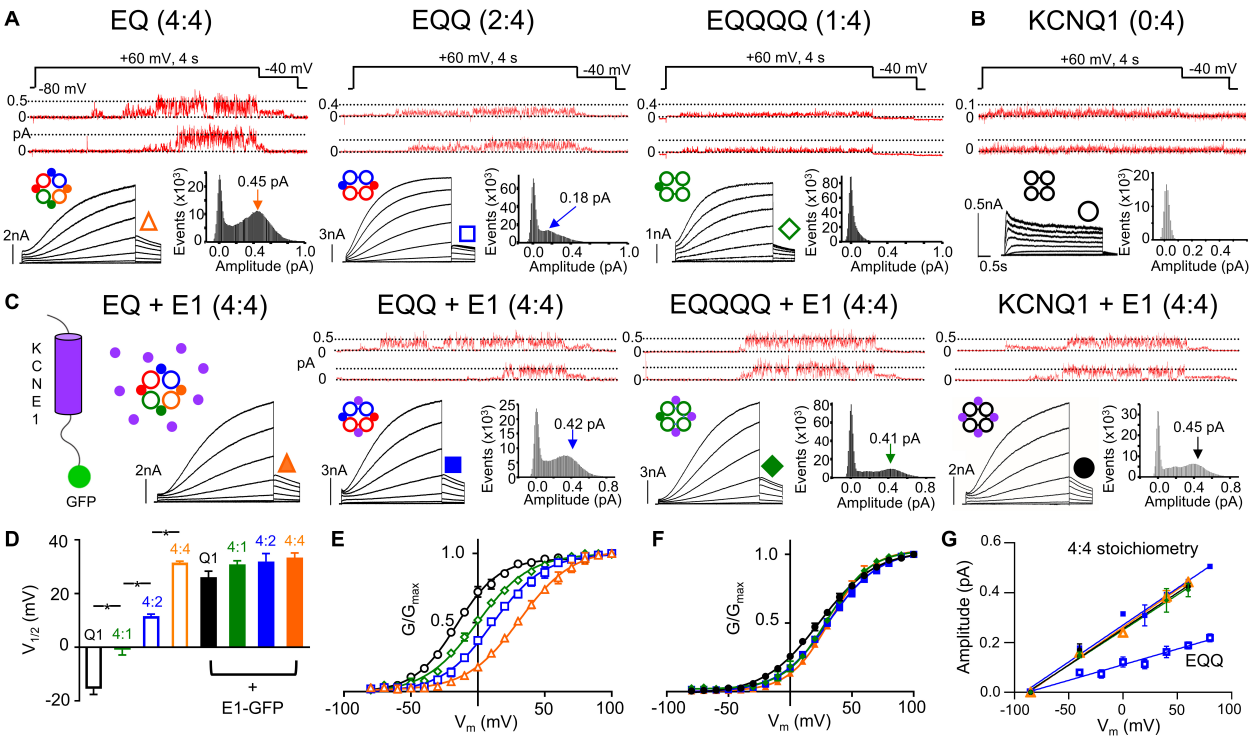

FIGURE 1 | IKs channel gating depends on the stoichiometric ratio of KCNE1:KCNQ1. Representative single channel (above) and whole cell currents (below) with single channel all-points amplitude histograms of active sweeps (lower right) are shown for EQ (orange), EQQ (blue), EQQQQ (green), and KCNQ1 (black) expressed alone **(A–B)** or in combination with wild-type KCNE1-GFP (**C**, all panels). The predicted stoichiometry of KCNE1:KCNQ1 in each case is shown above. Arrows on histograms indicate the peak of the major Gaussian fit. Whole cell protocol: 4 s pulses from –80 mV to between –80 and +100 mV, followed by a repolarizing step to –40 mV for 1 s. Single channel protocol: 4 s pulses from –60 mV (–80 mV for EQQQQ) to +60 mV for 4 s, repolarized to –40 mV for 0.75 s. In A-C, topologies of expected channel Q1 and E1 complexes indicated as large hollow and small filled circles, respectively. **(D)** $V_{1/2}$ of activation (n = 3–11; *$p < 0.05$) as indicated. Mean G-V plots from peak tail currents: KCNQ1 (black), EQQQQ (green), EQQ (blue), and EQ (orange) expressed alone **(E)** and in the presence of KCNE1 (**F**; filled symbols). **(G)** Slope conductance for each construct showing peak open amplitudes in the presence of KCNE1 (4:4 stoichiometry, EQ, EQQ, EQQQQ and KCNQ1 in the presence of KCNE1) and EQQ alone. Conductance not measured for EQQQQ or KCNQ1 alone. All error bars in this and other figures denote mean ± SE. Figure adapted from Murray et al. (2016), **Figures 1–3**. Reproduced with permission of CC-BY 4.0.

the pharmacological effects of various drugs (Busch et al., 1997; Abitbol et al., 1999; Yu et al., 2013; Wrobel et al., 2016; Hou et al., 2019; Wang et al., 2020) and fatty acid analogs (Larsson et al., 2018; Liin et al., 2018).

Functionally, the co-assembly of KCNE1 with KCNQ1 reproduces most of the characteristics of the delayed rectifier potassium current, IKs, in the heart, although the occurrence of mutations in the other KCNE subunits (2−5) in clinical cases of LQTS (Eldstrom and Fedida, 2011) and lone atrial fibrillation (Olesen et al., 2014) indicate that the full exposition of IKs likely requires a more complete understanding of the contributions of KCNE subunits other than KCNE1 to the channel complex. IKs together with IKr, the hERG channel, and possible accessory subunits of its own (Abbott et al., 1999) form the main repolarizing currents of the cardiac action potential (Barhanin et al., 1996; Wang et al., 1996; Sanguinetti et al., 1996). Specifically, IKs has been reported to create a "repolarization reserve" at fast heart rates, when channels can open and current summates between beats to generate a large repolarizing current which shortens the action potential and facilitates diastolic filling of the ventricles. As KCNE1 delays activation to such a large degree, the open probability of the channel reaches only about 0.2 after 4 s at room temperature (Werry et al., 2013), which suggests that IKs channels remain 99.6% closed during the normal heartbeat (Ruscic et al., 2013) and limits their major contribution to action potential repolarization to sympathetic activation during times of stress.

Due to the critical role of IKs in heart rhythm regulation, unsurprisingly, many mutations in KCNQ1 and KCNEs have been functionally linked to life-threatening long and short QT syndromes as well as atrial fibrillation (Wang et al., 1996; Chen Y. H. et al., 2003; Moss and Kass, 2005; Olesen et al., 2014; Steffensen et al., 2015; Peng et al., 2017). IKs current has, however, also been reported in the inner ear where it plays an important role in maintaining endolymph K^+ homeostasis. The flow of potassium ions into hair cells within the cochlea depolarizes them and results in downstream hearing transduction to the brain. Some homozygous mutations in KCNE1 have been found to cause Jervell and Lange-Nielson syndrome (JLNS), a LQT syndrome with deafness (citealpBR61; Chouabe et al., 1997). Interestingly, other homozygous LQT mutations do not seem to be associated with deafness (Jackson et al., 2014).

STRUCTURAL PROPERTIES OF KCNQ1

The KCNQ1 α subunit like that of nearly all other Kv channel is comprised of six transmembrane segments, S1-S6 (Lee et al., 2009), and together four KCNQ1 monomers co-assemble as a tetramer to form the KCNQ1 channel. Transmembrane helices S1-S4 form the VSD with the S5-S6 helices forming the pore domain (PD) of the channel in a domain-swapped manner that is the VSD of one domain regulates the PD of the adjacent subunit (Long et al., 2005a; Sun and MacKinnon, 2017). The S4 segment of KCNQ1 contains a net total charge of +3 which arises from positively charged arginine residues, and this is unlike other Kv channels which contain two extra gating charges. During gating, salt bridges between a conserved glutamate (E160) in S2, and positive charges in S4 (R228) present at rest, are broken and reformed with R231 and R237 (see below section on Electromechanical Coupling) as the S4 moves outward (Cui, 2016). Aqueous clefts allow extracellular or intracellular accessibility to most of these charges at rest and during channel activation as the gating charges in the S4 segment sense and move in response to changes in transmembrane voltage. The PD on the other hand contains an ion selectivity filter made up of a series of highly conserved amino acids in potassium channels, GYGDXX. In addition to the six transmembrane segments which make up the VSD and PD, the KCNQ1 monomer also contains four intracellular helices. In order to open the pore of the KCNQ1 tetramer, alone, or in complex with KCNE1, the VSD must activate, and this means that upon membrane depolarization the S4 segment moves extracellularly with some degree of rotation to transfer charges across the electric field from the inside to the outside across a charge transfer center (Tao et al., 2010). How the four VSDs within the tetramer act, whether independently, or together to open the channel pore is controversial, but it is generally understood that this translation of the S4 segment is first transferred to the S4-S5 linker. In response to this movement in the linker, the cytoplasmic lower halves of the S6 segment, which normally form a barrier to ion passage, pull apart which leads to pore opening (reviewed in Labro and Snyders, 2012). Potassium ions can then enter the selectivity filter and dehydrate, transiting the filter in coordination with backbone carbonyl oxygen atoms, along what is referred to as a "low resistance pathway" for efficient conduction of potassium ions (Doyle et al., 1998).

CO-ASSEMBLY OF KCNQ1 WITH KCNE1

The subunit assembly ratio of KCNE1 to KCNQ1 has been a matter of debate over the past several years, with some groups reporting a fixed KCNE1:KCNQ1 ratio of 2:4 and others reporting a variable stoichiometry between 1:4 and 4:4 depending on the concentration of KCNE1. In biochemical studies involving subunit counting and also in fluorescence photobleaching, the suggestion is that the stoichiometry is fixed at 2:4 (Chen H. et al., 2003; Morin and Kobertz, 2008; Plant et al., 2014). However, there are also suggestions that the number of KCNE1 subunits bound to KCNQ1 can be variable, based on the fact that the gating of KCNQ1 is dependent on the expression level of KCNE1 (Cui et al., 1994; Wang et al., 1998; Yu et al., 2013), the pharmacological properties (Yu et al., 2013) and other single subunit counting experiments which support a variable stoichiometry of up to 4:4 (Nakajo et al., 2010). Recent experiments using linked constructs of KCNE1 and KCNQ1 which force the stoichiometry of KCNE1 to KCNQ1 from between 1:4 to 4:4 (**Figure 1**) have definitively established the ability of the two proteins to assemble in different stoichiometries (Nakajo et al., 2010; Murray et al., 2016). Current activation becomes progressively slower as more KCNE1 subunits are added into the KCNQ1 ion channel tetramer compared with KCNQ1 alone (**Figure 1A**, right to left panels). Changes in macroscopic channel kinetics show the G-V curve of IKs becoming progressively depolarized with more KCNE1 subunits in the IKs complex (**Figures 1D,E**), and increased single channel conductance and latency to first opening in 4:4 compared with 1:4, 2:4, and 0:4 complexes (Murray et al., 2016; Hou et al., 2017; **Figure 1A**, upper panels). Co-expression of KCNE1 along with the fixed 2:4 and 1:4 constructs leads to incorporation of the free KCNE1 into spare sites in the channel complex and recapitulation of the whole cell and single channel kinetics, G-V curve and conductance of the 4:4 fully saturated heteromeric channel (**Figures 1C–G**). The use of targeted unnatural amino acid expression to incorporate different numbers of cross-linkable KCNE1 subunits into IKs complexes and predictably change the UV-induced current decay rate provides further strong support for the variable stoichiometry model of KCNQ1 and KCNE1 assembly (Murray et al., 2016; Westhoff et al., 2017). Interestingly, in support of these conclusions, the recent cryo-EM structure of KCNQ1+KCNE3 was captured in a 4:4 stoichiometry (Sun and MacKinnon, 2020).

Having established the potential for different numbers of KCNE1 forming complexes with KCNQ1 in oocytes and mammalian cell expression systems, the stoichiometry of association is by no means as clear physiologically in different mammals, including humans. The half-activation voltage and deactivation rates for IKs vary between dog, guinea-pig and rabbit (Chinn, 1993; Liu and Antzelevitch, 1995; Lei and Brown, 1996), all mammals used to model human cardiac electrophysiology, which suggests the possibility that different species have different KCNQ1:KCNE1 stoichiometries underlying their IKs. In human myocytes (Bosch et al., 1998; Virag et al., 2001) the kinetics, and in iPSC-CM the drug sensitivity to ML277 suggests an unsaturated ratio of 2:4 KCNE1:KCNQ1 (Yu et al., 2013), although the maturity and uniformity of iPS cells is generally not yet fully understood (Pourrier and Fedida, 2020). As well, different primary sequences for the KCNE1 subunits may contribute to the different physiological expression and kinetics of IKs in different species. An understanding of the stoichiometry of IKs is extremely important, as determining the exact numbers of regulatory subunits impacts the efficacy of pharmacological drugs, which has consequences for the treatment of cardiac arrhythmic disorders associated with mutations in KCNQ1 and KCNE1. Most activators of the IKs channel complex such as stilbenes, ML277, L-364,373 and zinc pyrithione, with the exception of mefenamic acid (Abitbol et al., 1999;

Doolan et al., 2002; Magyar et al., 2006; Wang et al., 2020), phenylboronic acid (Mruk and Kobertz, 2009), and some polyunsaturated fatty acids (Larsson et al., 2018; Liin et al., 2018; Bohannon et al., 2020) are reported to have limited efficacy on both partially and fully saturated IKs complexes (Yu et al., 2013). Post-translational modification of KCNQ1 during β-adrenergic stimulation is also stoichiometrically graded with a response to cyclic adenosine monophosphate (cAMP) requiring at least one KCNE1 (Thompson et al., 2018b). A variable stoichiometry model for IKs therefore allows for great flexibility in the modulation of KCNQ1 kinetics and the IKs current.

EVOLUTION OF ACTIVATION MODELS FOR KCNQ1 AND IKs

Mechanistically, our understanding of the gating properties of voltage-dependent potassium channels such as KCNQ1 and IKs originates from analyses carried out on *Shaker* channels and the squid axon. The Markov state models used to simulate the activation of KCNQ1 and KCNQ1+KCNE1 channels, and to understand VSD involvement in pore opening, originate in the Eyring rate theory models of Eyring et al. (1949); Hodgkin and Huxley (1952). The basic assumptions of their model for the squid axon potassium channel included the idea of four identical and independent gating particles that, if positively charged, would cross the electric field from the interior of the axon to the outside before the channel could open. This led to a five-state sequential gating scheme comprising four closed states and an open state, many key features of which are still relevant almost 70 years later, not least because the cloning of potassium channels has revealed a tetrameric structure of VSDs that fits neatly into the Hodgkin-Huxley model scheme (Jan and Jan, 1989). In voltage-dependent *Shaker* channels it is generally accepted that, like in the original Hodgkin and Huxley model, the delay seen in *Shaker* channel activation requires that more than one VSD transition must occur before channel opening, and thus that all four identical VSDs must undergo independent conformational changes when the channel is closed. Unlike the original model, each VSD in the case of *Shaker* channels is preferred to undergo two independent conformational changes (resting to intermediate to activated) before the VSD becomes activated (Zagotta et al., 1994). Once all four VSDs are activated, the channel undergoes a final or multiple concerted transition(s) (Schoppa and Sigworth, 1998; Ledwell and Aldrich, 1999) from closed to open. This final transition(s) is required because channel opening after the activation delay is slower than predicted from a strict Hodgkin-Huxley model, and this makes the overall activation scheme cooperative as the opening transition depends on the state of all four subunits, which implies interaction between them (Sigworth, 1994; Zagotta et al., 1994; Horrigan et al., 1999).

These concepts from squid axon and *Shaker* potassium channels were first adapted into KCNQ1 and IKs channels by Silva and Rudy (2005). The activation delay observed suggests that the VSDs of KCNQ1 and IKs, much like those of *Shaker*, must also undergo at least two transitions during VSD activation, prior to PD opening. As such, both initial KCNQ1 and IKs models assumed a scheme where four VSDs transition independently through two conformational changes prior to full activation, and then undergo a single concerted step to allow PD opening. To simulate slow activation in IKs, the first VSD transition in the KCNQ1 model from resting to intermediate states was slowed. Both the second VSD transition rate as well as the transition between the first and second open state were further modified to be rapid. Together, these modifications ensured that more channels would remain in the resting state for a longer time and slow IKs activation. Experimentally, a delay in KCNQ1 deactivation was also seen, suggesting the presence of multiple open states between the inactivated state and the last closed state for the KCNQ1 gating model. In KCNQ1 and IKs this leads to models with 15 closed states, and different open states, and in the case of KCNQ1 alone, an inactivated state. Five open states were introduced for KCNQ1 alone, and two for IKs to account in part for activation delay and for multi-exponential deactivation kinetics. The Silva and Rudy IKs gating model was later briefly modified in 2013 to account for single channel conductance behaviors seen in IKs (Werry et al., 2013). In this model, four VSDs are postulated to independently undergo the first transition following which a sub-conducting level may be reached after at least one VSD undergoes a second independent transition to a fully activated conformation.

ADVANCED EXPERIMENTAL METHODS GIVE NEW INSIGHT INTO ACTIVATION MODELS

The Silva and Rudy models, like the Hodgkin and Huxley models, are classical in the sense that data from direct interrogation of VSD movement, either gating current measurements, or VCF, and from single channel measurements were not available at the time that the models were developed. In the past decade, however, data from VCF and other techniques has been collected that has improved our understanding of the underlying molecular events during KCNQ1 and IKs activation. Cysteine accessibility was initially used to show that KCNE1 and KCNE3 stabilized VSDs in the resting or active conformations, respectively, via alteration of the voltage sensor equilibrium to favor specific states (Nakajo and Kubo, 2007; Rocheleau and Kobertz, 2008). As a more direct means to follow voltage sensor movement, VCF tracks changes in emission from fluorophores attached to the extracellular end of the S4 segment as its environment changes during voltage sensing (Mannuzzu et al., 1996), and while the signals from different fluorophores can vary, it has generally been shown to give a reliable measure of S4 displacement in a variety of Kv channels (Larsson et al., 1996; Cha and Bezanilla, 1997; Claydon and Fedida, 2007; Horne et al., 2010). Gating currents provide a quantitative measure of net charge displacement during channel activation, and have supported the corresponding VCF studies in KCNQ1 alone (Ruscic et al., 2013; Barro-Soria et al., 2014). Pore dynamics and the existence of subconductance states were inferred some years ago from noise analysis and multi-channel patches (Romey et al., 1997; Sesti and Goldstein, 1998; Yang and Sigworth, 1998), but an accurate measure of IKs conductance

and the ratio of KCNQ1 to IKs conductance remained elusive until the single channel kinetics were characterized more recently (Werry et al., 2013; Murray et al., 2016) and the detailed subconductance architecture of IKs channels during activation was revealed in wild-type channels, and in LQTS disease mutants (Eldstrom et al., 2015).

VOLTAGE SENSOR FLUORESCENCE FROM KCNQ1 ALONE

Fluorescence-voltage (F-V) relationships for KCNQ1 and IKs have usually been obtained after removal of extracellular cysteines in the S3 and S6 domains, and the mutation and labeling of G219C in the S3-S4 linker with Alexa Fluor 488 C_5-Maleimide (Alexa488) (Osteen et al., 2010; Barro-Soria et al., 2014; Hou et al., 2017; Westhoff et al., 2019). The C214A/G219C/C331A construct shows a $V_{1/2}$ of ionic current activation that is ∼10 mV hyperpolarized to WT, but otherwise has unchanged current kinetics. Tetramethyl rhodamine (TMR) has also been used as a fluorophore, as have other locations in the S3-S4 loop, K218, and V221. A comparative study showed that these give similar, but not identical F-V relationships, with TMR exhibiting a fluorescence quenching upon depolarization, and the Alexa488 at 221C site giving the most hyperpolarized F-V relationship (Barro-Soria et al., 2014). Examples of Alexa488 fluorescence from KCNQ1 alone are shown in **Figure 2A**, along with ion currents. There is general consensus that when expressed without KCNE1 the fluorescence waveforms and the fluorescence-voltage relationship (F-V, representing VSD movement) of KCNQ1 overlap quite well with the time course of current activation and better with the G-V (representing pore opening) curves, respectively (**Figure 2C**, black symbols) (Osteen et al., 2010; Nakajo and Kubo, 2014). This overlap suggests that each VSD movement contributes in a 1:1 ratio to channel conductance (Osteen et al., 2010). In support of this conclusion that KCNQ1 channels can open when only a single VSD is activated, using the mutant I268A KCNQ1 channel, Ma et al. reported a larger than expected voltage-independent constitutive current in resting channels, which was explained by the authors as spontaneous transitions between closed and open states of the channel in the absence of any VSD movement (Ma et al., 2011). Similarly, in the mutant L353K KCNQ1 channel which locks the PD open – thus also creating a constitutive current – the VSDs are still capable of visiting a fully resting conformation (Zaydman et al., 2014). In other words, much like the mutant I268A KCNQ1 channel, the mutant L353K channel suggested that PD opening is possible with less than four, and perhaps zero activated VSDs.

Based on these experiments, a 15-state allosteric Markov gating scheme which allows PD opening and channel subconductance states even before the activation of a single VSD, was put forward to explain KCNQ1 gating (Osteen et al., 2010). No distinction was made between a model where all four VSDs moved in concert to allow PD opening, and one where VSDs moved independently, and the PD transitioned to the fully open state through subconductance levels. Although this model predicted PD opening when only one VSD was activated, and simulated experimental data well, the presence of a second voltage sensor step was not directly addressed, rather the model suggested that a second subunit movement occurred that represented pore opening to larger sublevels with each voltage sensor activated. The presence of two VSD steps during KCNQ1 channel activation as suggested in *Shaker* and IKs (Zagotta et al., 1994; Silva and Rudy, 2005) was addressed in subsequent experiments. Two fluorescence components were observed for KCNQ1 alone and interpreted to mean that the VSDs each underwent two transitions during activation as originally suggested by Silva and Rudy and analyzed in more detail in mutational studies (Wu et al., 2010; Nakajo and Kubo, 2014; Zaydman et al., 2014). Constitutive currents through both a pair of charge-reversing mutations that arrested the VSDs in either intermediate E160R/R231E (E1R/R2E) or activated E160R/R237E (E1R/R4E) states, showed that channel opening could occur when zero to four VSDs were in either intermediate or activated states. Combined with the concept that the channel can also open when all four VSDs are in the ground resting state, a 30-state allosteric model was proposed, where the VSD could either be in resting, intermediate or activated states and the PD could either be closed or open. Allosteric coupling between the voltage sensor and PD was also further decomposed in this model

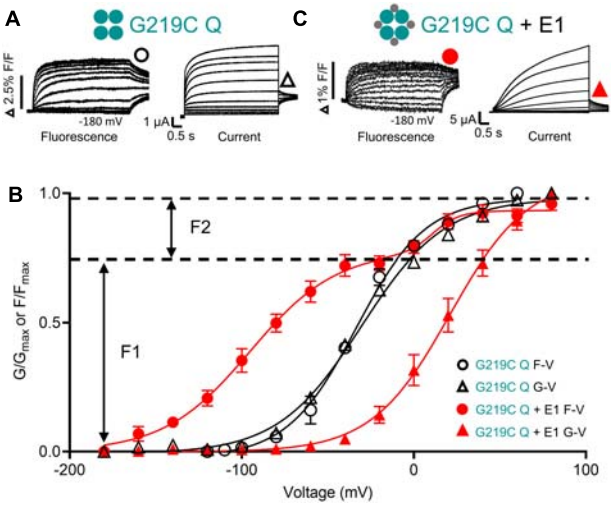

FIGURE 2 | Voltage sensor movement (F-V) and pore opening (G-V) of KCNQ1 in the absence and presence of KCNE1. Fluorescence (left) and current recordings (right) are shown for G219C-KCNQ1 in the absence (G219C Q) **(A)** and presence of KCNE1 (G219C Q + E1) **(B)**. Expected channel Q1 and E1 complex topologies shown as large and small filled circles, respectively. A three-step protocol was used for current and fluorescence: 4 s pre-pulses to –140 mV (not shown), followed by 5 s steps to potentials between +80 and –180 mV, with a final repolarization step to –40 mV for 1 s. **(C)** Mean G–V and F–V plots obtained in the absence (G219C Q F-V: black circles; G219C Q G-V: black triangles) and presence of KCNE1 (G219C Q + E1 F-V: red circles; G219C Q + E1 G-V: red triangles). The G219C Q + E1 F-V was fit with a double Boltzmann function to obtain F1 and F2 components. Other F-V and G-V curves were fit with a single Boltzmann function. Fluorescence and current data were replotted from Westhoff et al. (2019), Figure 8 with permission.

to its elementary components, "k" which represents PD opening and VSD activation and, "θ" which represents VSD-PD coupling.

KCNQ1 VOLTAGE SENSOR FLUORESCENCE IN THE PRESENCE OF KCNE1

There is a clear consensus that independent voltage sensor movement is allosterically coupled to PD opening in KCNQ1 channels expressed alone. When KCNQ1 is co-expressed with KCNE1, understanding activation has proven more complex. What is generally accepted in all studies is that KCNE1 dramatically increases the voltage separation between the voltage sensor fluorescence F-V and the G-V, and the fluorescence signal itself is clearly divided into two activating components, F1 and F2 (Osteen et al., 2010, 2012; Barro-Soria et al., 2014; Nakajo and Kubo, 2014; Zaydman et al., 2014; Westhoff et al., 2019). The $V_{1/2}$ of the F1 component, which comprises about 2/3 of the fluorescence signal, is hyperpolarized to close to −100 mV in the presence of KCNE1, while the $V_{1/2}$ of the F2 component is at ∼+20 mV, close the $V_{1/2}$ of the G-V which is depolarized 40−50 mV in the presence of KCNE1 (**Figures 2B,C**). Gating charge movement shows a similar hyperpolarization when KCNQ1 is co-expressed with KCNE1, overlaying the voltage dependence of F1 and confirming that the hyperpolarized F1-V represents S4 displacement (Barro-Soria et al., 2014). It has not yet been possible to resolve gating currents that correlate with the F2 movement, and this is attributed to the slow time course of F2-dependent charge movement. However, external MTSET modification of cysteine residues placed near the top of S4 show two-step modification with depolarizations to 0 mV or above, and thus support the idea of two VSD movements during IKs activation (Barro-Soria et al., 2014). The position of the F1-V at much more negative potentials than the G-V suggests independent movement of VSDs to an intermediate state from which they do not open in the presence of KCNE1 (Zaydman et al., 2014). The voltage dependence of the second voltage sensor fluorescence component, F2, is aligned with the G-V and thus more closely associated with the activated state of the voltage sensor and pore opening.

As well as the steady-state changes, KCNE1 imposes a discordance between the time course of current and fluorescence signals, which together with the F-V to G-V separation, implies that KCNE1 induces a requirement for movement of multiple voltage sensors before channel opening (Osteen et al., 2010; Barro-Soria et al., 2014). A similar sequential gating scheme to that proposed by Silva and Rudy requiring all four VSDs to be activated prior to PD opening, with a single open state was favored. The overlap of the F2 component of the F-V curve with the G-V suggested that a concerted activation step involving all four VSDs from the intermediate to activated state occurred, after which the channel opened. In other words, the F2 component represented PD opening. This is similar to cooperative gating schemes described for *Shaker* channels, and early IKs models (Silva and Rudy, 2005) which also invoked a concerted VSD step prior to channel opening. Other groups have explained the presence of F1 and F2 components in the F-V and the wide separation of the F1-V and the G-V in KCNQ1+KCNE1 with a model that not only includes two state transitions for the VSDs, but also assumes independent VSD movement (Zaydman et al., 2014). Although constitutive currents are seen in the KCNQ1 charge reversal (E1R/R2E and E1R/R4E) mutants (which arrested VSDs in the intermediate and activated states, respectively), when these mutants are co-expressed with KCNE1, the E1R/R2E IKs currents are eliminated whereas the E1R/R4E IKs currents increase 10-fold. The absence of E1R/R2E IKs currents suggest that in the presence of KCNE1, the PD cannot open when VSDs are in the intermediate state but can open when 0−4 VSDs are in the activated state. Thus, the second fluorescence step is equated with VSD transitions and not PD opening. From these experiments intermediate-open (IO) states were omitted from the 30-state KCNQ1 model, to generate a model for IKs where at least one VSD must be activated for the PD to open regardless of the state of the other VSDs (Zaydman et al., 2014).

VSD MUTANTS PROVE USEFUL

Several groups have directly addressed the question of a requirement for all voltage sensors to move for the PD to open by using voltage sensor mutations to change the voltage-dependence of VSD movement, or prevent it altogether. R231W and L353K stabilize the channel in the open state and R243W stabilizes the channel in the closed state in the presence of KCNE1, and when mutant KCNQ1 subunits in KCNQ1 concatenated tetramers were co-expressed with KCNE1, a linear relationship between the shift in the voltage dependence of activation and the number of mutated subunits was observed (Meisel et al., 2012). This suggested that each subunit contributed incrementally to channel gating, and that much like KCNQ1 alone, the KCNQ1/KCNE1 channel complex could open when 0−4 VSDs were activated. Mutant cycle analysis of these constructs revealed very low values of inter-subunit free energy coupling values, which is more consistent with weak allosteric gating transitions than conformational changes comprising large and cooperative quaternary rearrangements, and supports the conclusion that a concerted cooperative activation step is not required. Consistent with the results from the R243W mutant in KCNQ1, macroscopic IKs currents were also seen in the depolarizing KCNE1 mutant, F57W, in one, two or four KCNE1 subunits concatenated with KCNQ1 subunits, and the voltage-dependence of activation was progressively depolarized as the number of F57W subunits in IKs complexes was increased. As well, decreased conductance levels were seen in both whole cell and single channel recordings with increasing numbers of mutated subunits (Westhoff et al., 2019), rather like that seen when R243W was expressed in three of four subunits (Meisel et al., 2012).

A more extreme mutation is E160R, thought to prevent S4 translation altogether, rather than just shift the voltage dependence to very positive potentials (Zaydman et al., 2014). Recent experiments have conclusively established that VSDs containing this mutation are essentially held in a ground resting

state by the electrostatic repulsion between E160R and R228 (**Figure 3A**; Westhoff et al., 2019): G229C residues which are buried at rest and can normally be modified by extracellular MTS reagents in wild-type subunits upon activation, cannot be labeled and so remain buried in E160R VSDs despite large depolarizations; G219C residues in E160R VSDs cannot be labeled upon depolarization by Alexa488 or do not undergo environmental change during applied depolarizations and so no change in fluorescence is detected; and E160R-containing subunits are correctly assembled into tetrameric channels as shown by introduced TEA sensitivity. Consistent with the R234W and F57W experiments, after introducing the E160R mutant in one or two, but not four concatenated KCNQ1 subunits, subjectively normal macroscopic IKs currents are observed (**Figure 3B**), although activation kinetics are changed as the G-V $V_{1/2}$ is depolarized and the slope is decreased (**Figures 3C,D**). Similarly, in the presence of KCNE1, the E160R mutation in 1−3 subunits gives whole cell currents with depolarized $V_{1/2}$s of activation, decreased activation delays (**Figures 3E,F**) and decreased conductance levels in both whole cell and single channel recordings as more E160R subunits are incorporated into tetramers (Westhoff et al., 2019). Taken together, these results all suggest that a final cooperative concerted voltage sensor transition is not required during the activation process for either KCNQ1 channels (Osteen et al., 2010; Westhoff et al., 2019) or complexes of KCNQ1 and KCNE1 (Meisel et al., 2012; Zaydman et al., 2014; Westhoff et al., 2019). The channel PD can open at rest, when a single voltage sensor reaches an intermediate activated state in KCNQ1 channels, and when it reaches the fully activated state in KCNQ1+KCNE1 channels. However, there are penalties incurred when less than four VSDs activate and these include a greater energy barrier to opening as suggested by the progressive depolarizing displacement of the $V_{1/2}$ of the G-V, and reduction in the single channel conductance (Meisel et al., 2012; Westhoff et al., 2019).

A CONSENSUS BETWEEN ALLOSTERIC MODELS OF KCNQ1 AND IKs ACTIVATION GATING

A number of different non-cooperative allosteric models have been proposed for the activation gating and PD opening of KCNQ1 and KCNQ1+KCNE1 channel complexes. As noted earlier, models of only KCNQ1 (Osteen et al., 2010) and KCNQ1±KCNE1 (Zaydman et al., 2014; Westhoff et al., 2019) support the activation of single independent VSDs with allosteric coupling to opening of the PD (see below). These are analogous to activation gating models proposed for the related BK and HCN channels which suggest that with each successive VSD activation, the probability of PD opening increases multiplied by an allosteric factor "L" raised to the power of the number of activated subunits (Horrigan et al., 1999; Altomare et al., 2001; Flynn and Zagotta, 2018). In support of these non-concerted models, machine learning methodology applied to atomistic modeling of IKs is able to simulate most aspects of activation gating, including two-step voltage sensor displacement, I-V relationships and subconductance states – in this case determined by the pore energy profile (Ramasubramanian and Rudy, 2018). Modeling also demonstrates that restraining the movement of one, two and three VSDs, does not affect the ability of channels to conduct current in the manner demonstrated experimentally (Meisel et al., 2012; Westhoff et al., 2019), which supports non-concerted coupling between VSDs and the PD. In these simulations KCNQ1/KCNE1 was found to open to prominent subconductance levels. Subconductance was least when KCNQ1 lacked KCNE1 accessory subunits, and the addition of KCNE1 allowed access to progressively larger subconductance states, which effectively reproduced experimental recordings of IKs single channels from fixed channel complexes of differing numbers of KCNE1 subunits (**Figure 1**; Murray et al., 2016).

VOLTAGE SENSOR DOMAIN – PORE DOMAIN (VSD−PD) COUPLING

This topic has been well reviewed previously and we would encourage readers to consult representative reviews for a broader, more detailed historical coverage (Blunck and Batulan, 2012; Vardanyan and Pongs, 2012; Barros et al., 2019). Here, we will update VSD-PD coupling focused on KCNQ1, considering newer data, particularly from fluorescence (Zaydman et al., 2013; Barro-Soria et al., 2017; Hou et al., 2017, 2019, 2020), single channel recordings (Werry et al., 2013; Hou et al., 2017; Thompson et al., 2017; Westhoff et al., 2019) and recently published cryo-EM structures of KCNQ1 (Sun and MacKinnon, 2017, 2020).

ELECTROMECHANICAL COUPLING

The process of linking the movement of the VSD to pore opening is termed electromechanical coupling. In domain-swapped Kv channels this is accomplished through the S4-S5 linker (S4-S5L) and specific interactions with the C-terminal domain of S6 (**Figure 4**). Coupling of the VSD and PD can be disrupted by specific mutations or interventions in both of these regions in KCNQ1 and IKs (Choveau et al., 2011; Labro et al., 2011; Ma et al., 2011), and indeed residues in these two locations appear to co-evolve with one another in Kv channels (Lee et al., 2009). Our understanding of how these disparate portions of the channel work together to effect channel opening upon depolarization was greatly facilitated by the publication of the first crystal structure of a domain swapped Kv channel by the MacKinnon lab in Long et al. (2005b). The structure showed the helical S4-S5 linker sitting on a splayed C-terminal portion of the S6 domain. The diameter of the inner vestibule indicates that this is an open conformation of the PD, and as there are no closed-state structures of Kv channels, many studies have hypothesized ways in which S4-S5L can open the closed pore, playing the role of lever or bolt (Blunck and Batulan, 2012; Chowdhury and Chanda, 2012; Barros et al., 2019). In the first case the S4 must drag on the S4-S5L, which sits as a cuff at the helical bundle formed by the four S6 domains crossing one another, and

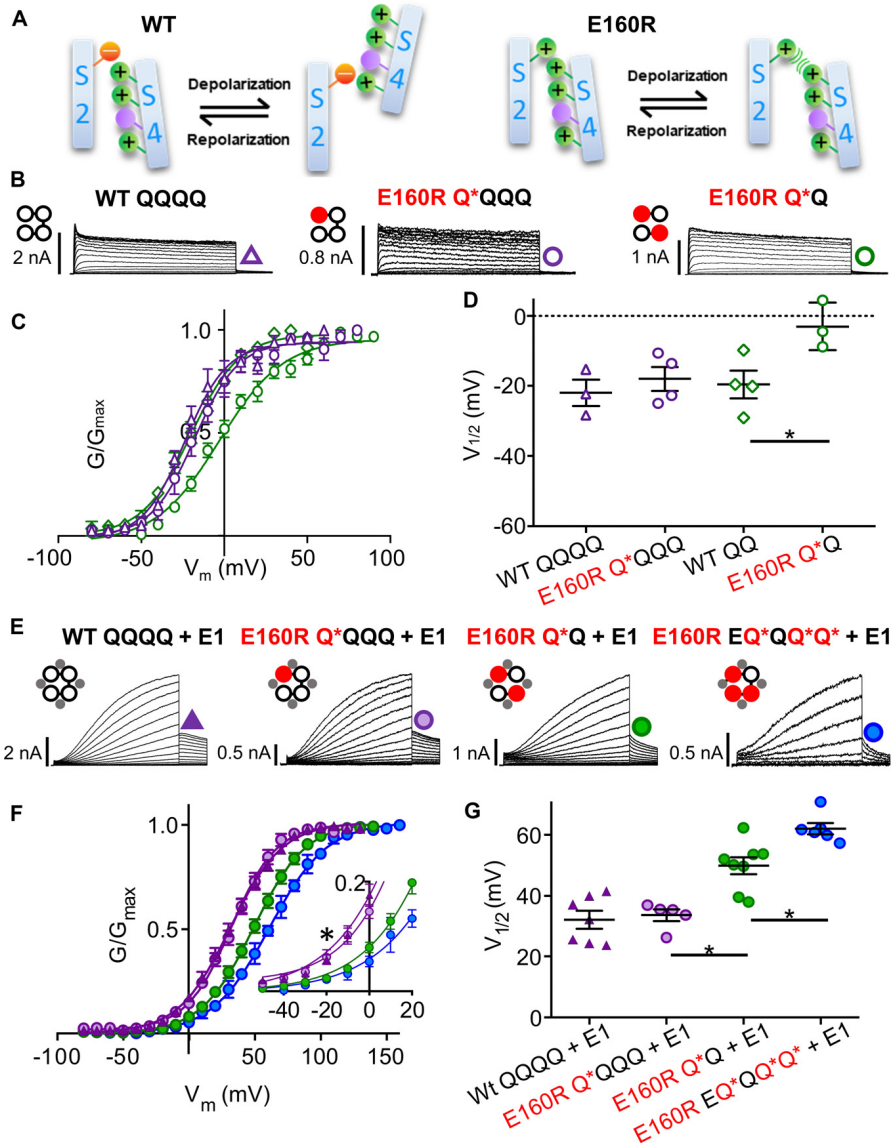

FIGURE 3 | Functional currents from KCNQ1 and KCNQ1 + KCNE1 channel complexes with one, two or three E160R mutations **(A)** Cartoons representing possible charge interactions between WT S2 and S4 TMDs during activation and deactivation (left) and E160R mutants when VSD movement is impeded by charge repulsion (right). Channel topology configurations of WT Q1 (black) and E160R mutant (red) subunits, with E1 (gray) are shown adjacent to current traces **(B,E)**. Black lines represent tethers between subunits. Currents were obtained using the same protocol as in **Figures 1B–D**. In the absence of KCNE1. Currents **(B)**, mean G-V **(C)**, and summary $V_{1/2}$ of activation **(D)** for KCNQ1 complexes containing zero (WT QQQQ: purple triangles; WT QQ: green diamonds), one (E160R Q*QQQ; purple circles) or two (E160R Q*Q; green circles) E160R mutant subunits (n = 3–4; *p < 0.05). **(E–G)** In the presence of KCNE1. Currents **(E)**, mean G-V **(F)** $V_{1/2}$ of activation **(G)** for Q1 + E1 complexes containing zero (WT QQQQ; purple triangles), one (E160R Q*QQQ; purple circles), two (E160R Q*Q; green circles) or three (E160R EQ*QQ*Q*; blue circles) E160R subunits (n = 5–8; *p < 0.05). (**E**, Inset) Expanded view of G-V plots between –50 and +20 mV (*p < 0.05). Figure adapted from Westhoff et al. (2019), **Figures 1**, **3**.

cause the S5 domains to pull the S6 domains apart. In the second case the S4-S5L is theorized to act like a bolt to hold the S6 domains together to constrict the PD, akin to the ligand/receptor model (Choveau et al., 2012), where the removal of the bolt or ligand (S4-S5L) allows the S6 domain to passively open. The mechanism utilized depends on the intrinsic property of the pore, whether it is more stable in the closed state (*Shaker*, Kv1.2) or more stable in the open state (KCNQ1, HCN2) reviewed in Chowdhury and Chanda (2012), Vardanyan and Pongs (2012). A significant number of VSD and PD mutations give rise to a constitutive component of KCNQ1 current and form part of the evidence that places it in the latter group. In addition, KCNQ1 lacks the glycine hinge and the PVP motif in the bundle crossing (Seebohm et al., 2006; Labro and Snyders, 2012) found in several other Kv channel S6 domains which creates a kink in the helix to

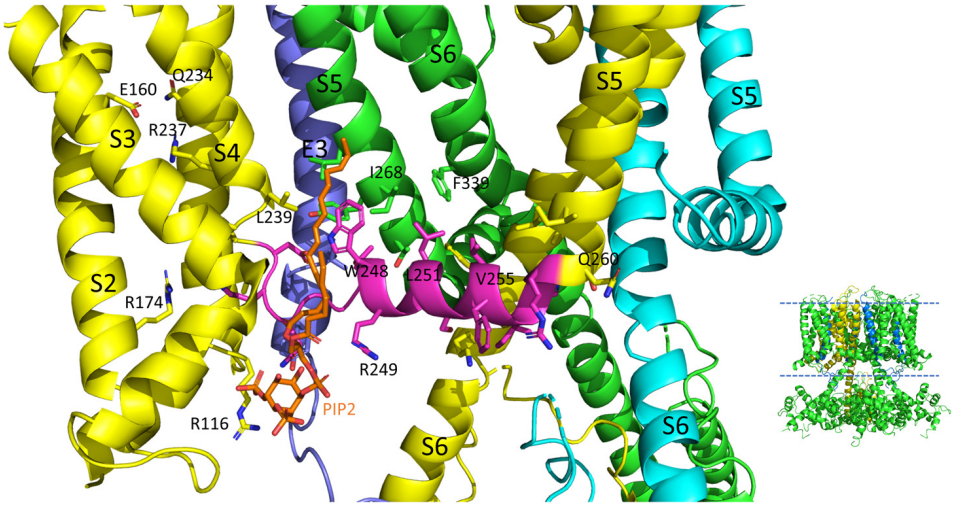

FIGURE 4 | S4-S5L interactions of the PIP2 bound hKCNQ1/KCNE3/CaM structure. Each of three subunits of the tetramer is shown in a different color. The S4-S5L of the yellow subunit is shown in magenta for emphasis. Side chains of residues of the S4-S5L and residues within 4Å of these are shown, in addition to E160, R237 and Q234 in the yellow subunit to emphasize the activated state of the VSD. Only some of the more visible side chains are labeled but all residues appearing to interact with the linker include: R116, R174, I198, L239, H240, V241, Q260, E261, L262, and I263 (yellow subunit); E261, Y267, I268, and L271 (green subunit); none (cyan subunit); L75 and Y79 (KCNE3); PIP2. CaM and most of the intracellular portions (illustrated in inset to right), as well as the VSD of the cyan subunit, a third entire subunit and all but one KCNE3 (dark blue) have been removed for clarity. Image made from pdb 6V01 (Sun and MacKinnon, 2020) using PyMOL software (The PyMOL Molecular Graphics System, Version 2.2.3 Schrödinger, LLC).

make up the narrowest region of intrinsically stable closed pores (Blunck and Batulan, 2012).

BEYOND THE MECHANICS, PIP2 IS ESSENTIAL FOR VSD-PD COUPLING

On top of the fundamental mechanical steps, the process of KCNQ1 channel opening is highly regulated. PIP2 depletion is known to decrease IKs channel currents (Loussouarn et al., 2003; Zhang et al., 2003; Park et al., 2005) but this depletion does not prevent S4 movement, as robust fluorescence recordings are still possible (Zaydman et al., 2013; Barro-Soria et al., 2017) and so it was concluded that the loss of PIP2 was uncoupling VSD movement from opening of the pore. Molecular dynamics simulation and other experimental results have mapped the binding site of PIP2 to residues in the S2-S3 and S4-S5L and the cytoplasmic end of the S6, placing PIP2 in a location in which it can interact with both the VSD and PD and thus affect VSD-PD coupling (Thomas et al., 2011; Zaydman et al., 2013; Eckey et al., 2014). In support of these data and conclusions, a cryo-EM structure with PIP2 bound (**Figure 4**) shows where the lipid is located near positive charges in the N-terminal domain (R116) and S2-S3L (R181, K183, R195, and K197) but also L239 in S4, Q244, W248 and R249 in the S4-S5L as well as K87 of KCNE3.

Mutations that prevent pore closure, and show instantaneous currents during step potential changes are either insensitive to PIP2 depletion (e.g., KCNQ1-L353K; Zaydman et al., 2013) or lose their voltage-dependent component (KCNQ1-I268A; Barro-Soria et al., 2017). An activated pore does appear to reduce some of the energy required to move the voltage sensor as long as coupling is intact. Not having to open the pore in the case of the uncoupled mutant V254M (middle of the S4-S5L, **Figure 4**) also appears to shift the F-V to slightly more negative potentials, though this was not the case with other uncoupled mutants closer to the PD (Hou et al., 2020).

Molecular dynamic simulations and an NMR structure have shown that KCNE1 sits in the lipid-filled cleft between two adjacent VSDs and the PD, probably not particularly dissimilar to where KCNE3 is found in cryo-EM structures (**Figures 4, 5**; Sun and MacKinnon, 2020), and based on this positioning is well placed to affect VSD-PD coupling. Consistent with this, mutations in the S4-S5L of KCNQ1 alone such as L251A, V255W, H258A and T247A, have produced similar changes to the activation waveform and G-V as those seen when KCNE1 is present in the complex (Labro et al., 2011). In the presence of KCNE1, the channel complex has also been shown to become more sensitive to PIP2 as a significantly lower concentration of exogenous PIP2 was required to prevent rundown upon excision of membrane patches.

In the last few years the published Cryo-EM structures of KCNQ1 (Sun and MacKinnon, 2017, 2020) have proven very useful in the interpretation of functional data. To date, all the published structures have activated VSDs (E160 is interacting with Q234 and R237, **Figure 4**) with the PD either uncoupled from the VSD due to a lack of PIP2, or a PIP2- containing structure in which the intracellular gate is open or opening but the filter is too narrow to coordinate a dehydrated potassium ion (Sun and MacKinnon, 2020). Whether there are more steps in the activation pathway that have not been transmitted to the selectivity filter or whether this is a feature of the KCNQ1 pore is at present unknown. The structure of human KCNQ1 with

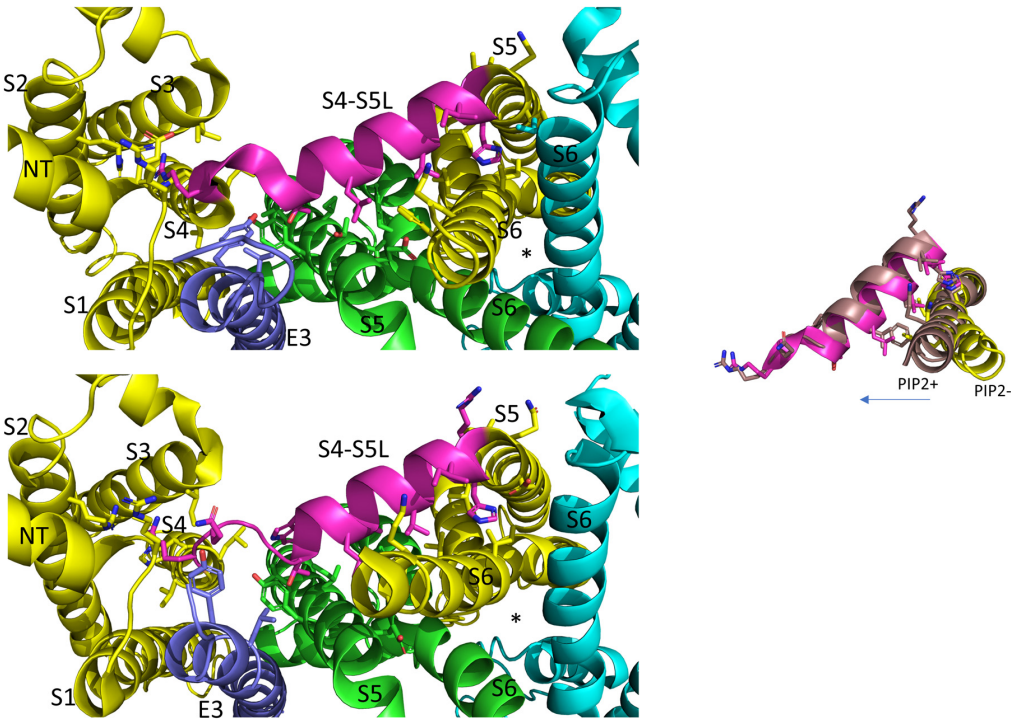

FIGURE 5 | In the PIP2 bound state the KCNQ1 S4-S5L appears to have pivoted out and S6 has expanded into the space vacated. View is from below. Each of three subunits of the tetramer is shown in a different color. The S4-S5L of the yellow subunit is shown in magenta for emphasis. The PIP2-free structure of hKCNQ1/CaM/KCNE3 is on top (6V00) and the PIP2-bound structure is on the bottom (6V01). The asterisks indicate the location of the inner vestibule. Most of the intracellular portions and transmembrane regions of the other subunits have been removed for clarity. Inset: overlay of just the linker and the covalently linked S6 subunit, in PIP2 bound and unbound states highlighting changes related to PD opening. Arrow points in direction of expansion. Image made from pdbs 6V01 and 6V00 (Sun and MacKinnon, 2020) using PyMOL software (The PyMOL Molecular Graphics System, Version 2.2.3 Schrödinger, LLC).

calmodulin (CaM) and KCNE3 created in the absence of PIP2 shows the S4-S5L to have a less structured N-terminal portion (**Figure 5**, upper panel) than the Kv1.2 S4-S5L, which is all helical. In addition, the linker itself is angled away from S6 which decreases the interaction between these two domains. In the presence of PIP2, several changes were noted and these include: the S6 domains are more splayed open, with the diameter at the putative S6 gate (S349) opening to >3.5 Å; the region after the S6 TMD becomes helical and makes continuous the S6 and HA domains; the interaction between the S2-S3L and CaM is lost and CaM is now reoriented 180 degrees toward the central axis of the channel complex. It is tempting to speculate that perhaps PIP2 is required in the coupling process to displace CaM so that the C-terminus can reorient itself for channel opening (**Figures 5**, **6**).

Comparing the charge pairing, with respect to E160 in the VSD, it appears that the same state has been captured in all of the human KCNQ1 structures (Sun and MacKinnon, 2020), with the E160 residue interacting with both Q234 and R237, which would, depending upon the pore conformation correspond with AC (where AC represents a state where the VSD is in the activated state and the pore is closed) (Zaydman et al., 2014) in the case of 6V00 when PIP2 is absent, or activated-open (AO) perhaps in 6V01 when PIP2 is present. In the cryo-EM structures, rearrangement of the interactions of the S4-S5L show it shifting outward, making room for its covalently linked S6 to splay open (**Figure 5**). The linker no longer makes contact with the neighboring S6 at V355 a residue previously implicated in the coupling process (Choveau et al., 2011) and mutations all along the bottom of S6 have been shown to affect activation, changing voltage dependence and kinetics (Boulet et al., 2007), highlighting the importance of this region as the channel gate (**Figure 5**). How the channel might reorient as it returns through the intermediate closed and then to the resting state, and how KCNE1 might influence this process will have to await new structures being solved. Until then, experiments utilizing peptides (Choveau et al., 2011), state specific mutations and molecular dynamics will continue to be used to obtain further insight into pore opening processes (Zaydman and Cui, 2014; Hou et al., 2017, 2019, 2020).

IKs PORE OPENINGS SHOW MULTIPLE CONDUCTANCE LEVELS

Even in the absence of single channel recordings it was clear that the openings of IKs were different from most other Kv channels (Yang and Sigworth, 1998). Not only did early data from macropatches suggest a high frequency flicker behavior, but in multi-channel patches sub-conductance behavior was observed. What is the origin of subconductance behavior? It has been proposed that if the pore enters heteromeric states that

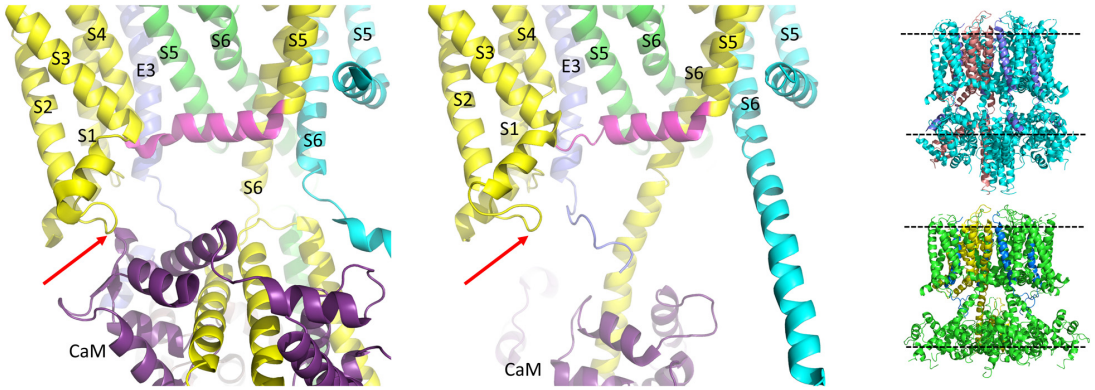

FIGURE 6 | CaM unbinds from the S2-S3L in the PIP2 bound structure of hKCNQ1/KCNE3/CaM. Each of three subunits of the tetramer is shown in a different color. The S4-S5L of the yellow subunit is shown in magenta for emphasis. Only one CaM molecule is shown in the PIP2-free structure on the left (6V00) and the PIP2-bound structure in the middle panel (6V01) and most of the intracellular portions (illustrated in insets to right), as well as the VSD of the cyan subunit, a third entire subunit and all but one KCNE3 have been removed for clarity. Red arrow points to CaM interaction site on the S2-S3L. Image made from pdb 6V00 and 6V01 (Sun and MacKinnon, 2020) using PyMOL software (The PyMOL Molecular Graphics System, Version 2.2.3 Schrödinger, LLC).

are sub-conducting and a late step in activation were relatively slow, then sublevels would be evident at all membrane potentials (Chapman et al., 1997) as is observed in IKs (Werry et al., 2013) and mutant Kv1.2 channels (Chapman et al., 1997; Chapman and VanDongen, 2005). IKs activation/opening could be slow for many potential reasons: (1) The movement of S4 is slow due to charge paucity (3 arginines compared to 7 positive charges in *Shaker*); (2) KCNE1 causes steric hindrance to the late movements of the VSD (i.e. the F2 component, Nakajo and Kubo, 2014), or the S4-S5L as KCNE3 is in direct interaction with the linker in the Cryo-EM structures and data suggest that the location of KCNE1 will not be significantly different (Melman et al., 2001, 2002a, 2004; Barro-Soria et al., 2017); (3) the nature of the S4-S5L, in that it is not all helical but possesses a loop connecting to the S4 domain (**Figure 5**; Sun and MacKinnon, 2017, 2020); (4) the dependence on PIP2 binding for coupling; (5) a requirement for structural rearrangement of the C-terminal domain and CaM reorientation (**Figure 6**). Whether it is all or some of these reasons or even additional factors, IKs clearly opens very slowly with currents failing to saturate even on depolarization for 100 s (Pusch et al., 2000). In addition, as discussed earlier, IKs appears relatively unique in another respect, the ability of the pore to open when only an individual VSD in the tetramer has activated (**Figure 3**; Westhoff et al., 2019), creating another mechanism for subconductance behavior.

Multiple subconductance states and opening levels makes the assignment of a single conductance value for the IKs channel difficult, as noted by Yang and Sigworth, as conductance values will be dominated by the higher sub-conductance states due to the generally higher probability of occupancy of these states at potentials where single channel currents are measured (Yang and Sigworth, 1998). Initially, as was historically typical, single channel data were analyzed using the half-amplitude criterion to assign open levels (Werry et al., 2013), but subsequently sub-conductance levels for IKs have been assigned using a 3/2 rule that was derived from analysis of 26 types of ion channels for assigning multiple conductance states to channels (Pollard et al., 1994). From patches with a well-defined Gaussian distribution and clear peak for the main opening level (see all points histogram for EQ in **Figure 1A**), which did not appear to be affected by filtering, whether at 200 or 1000 Hz, the remaining sub-conductance states were calculated based on the 3/2 rule (Werry et al., 2013; Murray et al., 2016; Thompson et al., 2017). In support of a 3/2 division, longer lived subconductance occupancies were clearly observed at the predicted levels. Single channels showing prominent subconductance behavior have subsequently been obtained from LQT1 mutants of KCNQ1 (Eldstrom et al., 2015), different stoichiometric ratios of KCNE1 to KCNQ1 (**Figure 1A**; Murray et al., 2016), during exposure to cAMP or mefenamic acid (Thompson et al., 2017, 2018a; Wang et al., 2020), and as a result of individual VSD movement (Westhoff et al., 2019). All these studies observed that subconductance behavior tended to be more stable at the onset of activity upon depolarization when it is more likely that not all VSDs are activated. Single channels have also been recorded from KCNQ1 in the absence of KCNE1 (**Figure 1B**; Hou et al., 2017). In this situation conductance of KCNQ1 alone is too small to analyze for subconductance behavior, but in the absence of KCNE1 coupling appears to be fairly tight as the F-V and G-V all but overlap (Osteen et al., 2010), and thus subconductance openings might not be a frequent occurrence in KCNQ1 alone.

When VSDs are stabilized in the activated state via charge reversal between the S2 domain and the S4 domain, E160R/R237E (Hou et al., 2017) or through gain of function mutations (S209F; Werry et al., 2013), or phosphorylation-dependent enhanced activation (Thompson et al., 2017, 2018a), higher sub-conductance levels are more predominant, but in all these instances a fast flickering of channel behavior during bursts is seen (**Figures 1A–C**). This may reflect the transient occupancy of a closed state not in the activation pathway (Werry et al., 2013), or a pore block that is as yet undefined. For KCNQ1 alone, the fast flicker process is reduced in high Rb^+ solutions,

which may be part of the reason that these currents through KCNQ1 are bigger than with K^+ solutions (Pusch et al., 2000). Once KCNQ1 pairs with KCNE1, the pore architecture appears to be different and Rb^+ is no longer as permeable. This is also true of ML277-bound KCNQ1, and may be related to ML277 preventing inactivation of the homomer (Xu et al., 2015), as there is a strong link between inactivation and Rb^+ permeability for KCNQ1 (Seebohm et al., 2003). Interestingly, IKs carrying the atrial fibrillation-linked mutation (AF) S140G in KCNQ1, has an increased Rb^+ permeability compared with wild-type IKs (Peng et al., 2017). A potential mechanism is suggested by recently published structures where both the region of the S1 domain containing S140 and the N-terminal domain of KCNEs approach the N-terminal portion of the filter helix.

INACTIVATION OF KCNQ1

Unlike IKs which appears not to undergo inactivation, KCNQ1 alone has been suggested to undergo two inactivation processes. A fast inactivation phase is sometimes seen after the initial current activation, but is most clearly revealed and studied as a transient increase in conductance after membrane repolarization to potentials which exceed −50 mV (Pusch, 1998; Hou et al., 2017; Meisel et al., 2018). An additional voltage-dependent slow inactivation phase has also been reported primarily in mutant KCNQ1 channels including the LQTs-associated mutations S338W (S339 in hKCNQ1) and L273F (Gibor et al., 2007; Hou et al., 2017; Meisel et al., 2018). Although various molecular mechanisms for inactivation have been proposed, the two KCNQ1 inactivation processes are in contrast to the classical N-, C- and U-type mechanisms of inactivation.

Fast N-type inactivation, often referred to using the analogy of a "ball-and-chain" mechanism, was originally proposed for sodium channel inactivation, and later for potassium channels, and involves a charged amino-terminal intracellular peptide domain which swings in after channel activation and occludes the PD to prevent ion conduction (Armstrong et al., 1973; Hoshi et al., 1990, 1991; MacKinnon et al., 1993; Aldrich, 2001; Gebauer et al., 2004). In *Shaker* channels, a single independently acting inactivation particle has been found to be both necessary and sufficient for pore occlusion and prevention of ion conduction (MacKinnon et al., 1993; Zhou et al., 2001). However, the lack of a N-terminal ball structure in KCNQ1 suggests that the channel does not undergo N-type inactivation. C-type inactivation, on the other hand involves conformational changes in the selectivity filter in the outer pore region (Hoshi et al., 1990; Baukrowitz and Yellen, 1996; Cuello et al., 2010) with other hallmarks including inhibition by high external K^+ (Lopez-Barneo et al., 1993), as in the case of hERG channels (Baukrowitz and Yellen, 1995; Wang et al., 1997). Whether these conformational changes in the selectivity filter result in pore constriction or subtle pore dilation is presently not understood. The lack of dependence on extracellular K^+ for both the fast and slow inactivation processes, and the acceleration of slow inactivation in the presence of high external K^+ (Meisel et al., 2018) suggests that KCNQ1 perhaps also does not undergo C-type inactivation (Pusch et al., 1998). Alternatively, it can be argued that KCNQ1 inactivation shares some similarities with C-type inactivation as slow inactivation has been shown to involve conformational changes in the outer carbonyl ring of the selectivity filter (Gibor et al., 2007). Discussed in greater detail later on, selectivity differences for Rb^+ and K^+ also differ between KCNQ1 which undergoes inactivation, and IKs which does not undergo inactivation (Pusch, 1998; Pusch et al., 2000; Seebohm et al., 2003). Lastly, U-type inactivation implicated in Kv1.5, Kv2.1, and Kv3.1 channels is the least understood of the potassium channel inactivation mechanisms (Klemic et al., 2001; Kurata et al., 2002; Kurata and Fedida, 2006; Cheng et al., 2010, 2011). The term U-type inactivation originates from the U-shaped inactivation-voltage curve which defines an inactivation process that is more complete at intermediate membrane voltages than at more positive potentials. The N-terminus and residues in the S3-S4 and S5-S6 linker have all been shown to play a role in U-type inactivation (Kurata et al., 2002; Cheng et al., 2010, 2011), but with fast inactivation only evident at particular times and potentials, again, U-type inactivation does not seem to underlie inactivation of KCNQ1 (Pusch et al., 1998).

To explain the initial fast inactivation in KCNQ1, a model which consisted of at least two distinct open states with voltage-independent transitions between the last open state and a non-conducting inactivated state was proposed (Pusch et al., 1998). KCNE1 was thought to either slow or prevent the transition to the last open state from which inactivation occurs. The presence of at least two open states was later independently confirmed using intracellular Na^+ block. The first open state, accessed when the channels are briefly opened, displayed relative insensitivity to intracellular Na^+ block. A stronger more sensitive block by Na^+ was reported after the channel was depolarized for a longer interval, thereby driving the KCNQ1 channel into a second open state (Pusch et al., 2001). On the basis of at least two open states, a model which accounted for KCNQ1's high Rb^+/K^+ conductance ratio was proposed as a rapid equilibrium process (flicker) between a flicker-open and flicker-closed state (Pusch et al., 2000). At high Rb^+ concentrations, the flicker-open state was favored over the flicker-closed state with the flickering rate slowed. A positive correlation between the extent of inactivation and Rb^+/K^+ conductance ratio was later used to explain inactivation in terms of flicker states (Seebohm et al., 2003). Inactivation was proposed to result when the flicker rate between the second flicker-closed and second flicker-open state was faster than that for the first flicker-closed and first flicker-open state suggesting that the two open states had different Rb^+/K^+ conductance ratios. As the association of KCNE1 decreases the Rb^+/K^+ conductance ratio, inactivation is therefore also abolished.

A recent reinterpretation of inactivation in KCNQ1 channels, is based on an activation model with two open states, and is also cognizant of changes in Rb^+/K^+ conductance ratio (Hou et al., 2017). As each KCNQ1 channel contains four VSDs, the original 30 state full activation gating scheme discussed previously can be simplified into a six-state scheme where the VSD undergoes resting to intermediate, and then to activated transitions, while the PD can open when the VSD is in any state. In prior work,

KCNQ1 was found to open initially into the IO state (where IO represents a state where the VSD is in the intermediate state and the pore is open) and then transition to an AO state (activated-open) (Zaydman et al., 2014). However, when the channel is in the AO state, VSD-pore coupling is less efficient and as such, pore opening requires higher voltages than in the IO state. Thus, when channels transition from the IO to the AO state in KCNQ1 during depolarizations to positive potentials, the total current will be reduced over the time spent depolarized, resulting in a process that imitates inactivation, and a "hook" in the tail current upon repolarization as channels return from AO to higher open probability IO states and subsequently close (Hou et al., 2017). Suppression of the IO and AO states by the KCNQ1 mutants F351A and S338F, unsurprisingly also eliminated inactivation.

This novel mechanism for inactivation, due to different mechanisms of VSD-pore coupling which occur in the IO and AO states, also explains why the co-assembly of KCNQ1 with KCNE1 abolishes inactivation. As mentioned previously, since co-assembly with KCNE1 eliminates the IO state, inactivation which arises from transitions between the IO and AO state are therefore also eliminated. As alluded to by the authors, though, this model likely does not account for the second slow inactivation phase seen in numerous KCNQ1 mutant channels. The L273F KCNQ1 mutant has been reported to exhibit both fast and slow inactivation (Gibor et al., 2007; Hou et al., 2017; Meisel et al., 2018) and the incorporation of the L273F mutant into increasing numbers of KCNQ1 subunits incrementally stabilizes a second inactivated state by progressively slowing down the inactivation recovery kinetics (Meisel et al., 2018). From this work Meisel and colleagues proposed that slow inactivation gating of mutant KCNQ1 channels likely occurs through an allosteric mechanism. Presently, it is not well understood if this slow inactivation is only seen in mutant KCNQ1 channels. If this slow inactivation is seen in WT KCNQ1 channels, how this allosteric mechanism fits into the presently understood mechanisms for KCNQ1 activation gating and fast inactivation also remains to be determined.

MODULATORS OF KCNQ1 AND IKs

The kinetics of KCNQ1 are not only affected by co-assembly with KCNE1, but also by modulation induced by several intracellular signaling molecules and co-factors such as calmodulin (CaM), ATP, and protein kinase A (PKA). **Figure 7** graphically summarizes the signaling pathway for β-adrenergic enhancement of IKs (right panel) as well as the binding sites (left lower panel) and impact of these intracellular proteins on IKs (top tables).

CaM MODULATES CURRENT AMPLITUDE AND ASSEMBLY

One of the first pieces of evidence that calcium and potentially calcium binding proteins could modulate IKs was the sensitivity of the current to calcium in guinea pig cardiomyocytes (Tohse, 1990). Calmodulin (CaM), a highly conserved calcium binding protein has been recognized as a key modulator of various channels such as Cav1.2 and Nav1.5 all of which are involved in the regulation of the cardiac action potential (Sorensen et al., 2013). As mutations in CaM, KCNQ1 and KCNE1 have all been linked to LQTS, it is not surprising that CaM plays a diverse role in both IKs assembly and gating. Using metal affinity chromatography, CaM was first found to co-purify with a 6xHis-tagged C-terminus portion of KCNQ1 (Ghosh et al., 2006). Binding of CaM to the C-terminus portion of KCNQ1 was later confirmed using immunoprecipitation in both the presence and absence of Ca^{2+} (Shamgar et al., 2006) as well as structurally using x-ray crystallographic data (Dvir et al., 2014). This C-terminus structure was also further confirmed in the recent cryo-EM structure of KCNQ1 (Sun and MacKinnon, 2017). Specifically, CaM was found to bind to the two proximal cytosolic helices (helices A and B) in a 1:1 ratio of KCNQ1 to CaM. In addition to this C-terminal binding site, however, the cryo-EM structure also revealed a novel CaM binding site located at the S2-S3 loop of the VSD (**Figure 6**) not present in the original crystallographic structural representation which did not contain the transmembrane domains of the channel (Sachyani et al., 2014; Sun and MacKinnon, 2017, 2020). Thus, by interacting with both the VSDs at the S2-S3 loop and helices A and B (**Figure 7**, left panel), CaM was recently proposed to provide a potential link between the VSD and PD. In support of this hypothesis, PIP2, previously found to be critical in VSD-PD coupling has been shown to compete with CaM for binding at helix B at specifically residues K526 and K527 (Tobelaim et al., 2017). As such, CaM, much like PIP2, may also act to stabilize the channel in its open state.

Beyond this recent discovery that CaM may play a role in VSD-PD coupling, classically, CaM has more consistently been reported to be important for channel assembly (Ghosh et al., 2006; Shamgar et al., 2006; Sachyani et al., 2014). Point mutations in helix A (1375D) and helix B (V516D) which altered CaM binding have been shown to reduce protein expression and decrease current density suggesting that CaM may be required for proper channel assembly, folding and tetramerization (Haitin et al., 2008; Sachyani et al., 2014). In addition, KCNQ1 has also been reported to traffic to the cell surface in a process dependent on Ca^{2+} and CaM. Jiang et al. have shown that, following Angiotensin II type 1 receptor (AT1R)-mediated KCNQ1 trafficking, the channel may then combine with KCNE1 which in turn increases IKs current amplitude (Jiang et al., 2017). The Ca^{2+}-insensitive CaM mutant, CaM_{1234}, however, was shown to prevent AT1R stimulation from increasing IKs current density, suggesting that CaM not only plays a role in channel assembly and tetramerization but also in trafficking.

Electrophysiological studies have also provided consistent evidence supporting the important roles calcium and CaM play in enhancing both KCNQ1 and IKs current. Increasing intracellular Ca^{2+} concentrations has been found to enhance KCNQ1 current amplitude (Shamgar et al., 2006). Consistent with this, chelation of Ca^{2+} by BAPTA has been reported to decrease KCNQ1 current amplitude (Ghosh et al., 2006) with the previously reported increase in current amplitude following administration of intracellular Ca^{2+} (Shamgar et al., 2006)

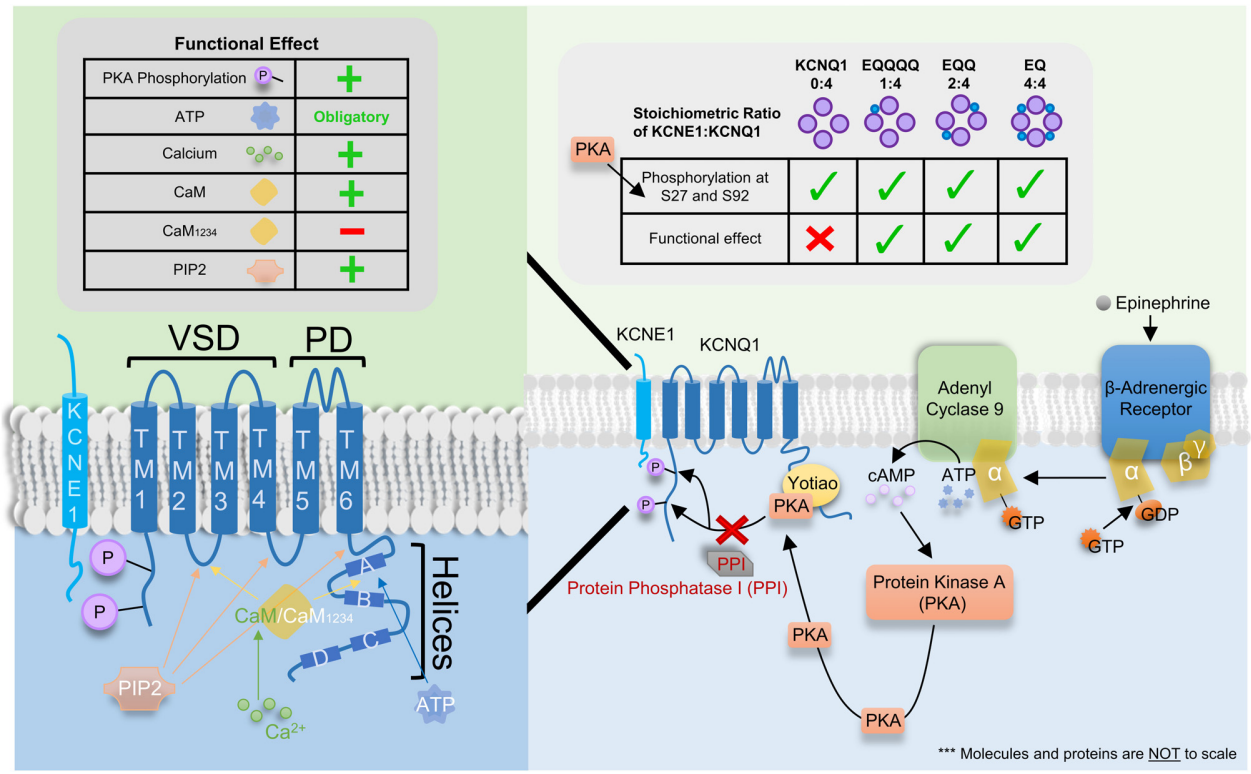

FIGURE 7 | Binding site, signaling pathway and functional effect of various intracellular signaling molecules and co-factors on IKs. Left Table: Functional effect of protein kinase A (PKA) phosphorylation, ATP, Ca^{2+}, CaM, CaM_{1234}, and PIP2 on IKs where "+" and "–" denotes a stimulatory and inhibitory effect, respectively. "Obligatory" indicates ATP is required for channel conductance. Left panel: Cartoon of the single transmembrane β-subunit KCNE1 and the α-subunit KCNQ1. KCNQ1 consists of 6 transmembrane domains (TM1-4 and TM5-6 form the voltage sensor and pore domain, respectively) and 4 helices (A–D). Four KCNQ1 subunits come together to form the channel with 1-4 KCNE1 subunits. Binding sites for ATP, CaM/CaM_{1234} and PIP2 as well as sites of PKA phosphorylation are depicted using colored arrows (for binding sites) or directly on KCNQ1 (for PKA phosphorylation). Ca^{2+} is known to bind to CaM but not CaM_{1234} however, Ca^{2+} may modulate the channel by binding and interacting with other proteins and/or other locations on the IKs channel complex which are presently unknown. Right Table: The impact of KCNE1:KCNQ1 stoichiometry on the phosphorylation of residues S27 and S92 by PKA and the consequent functional effect. Checkmarks indicate PKA phosphorylation occurs or a functional effect is seen on the respective stoichiometrically fixed KCNE1:KCNQ1 complex (EQ, EQQ, EQQQQ, and KCNQ1). The "X" indicates a functional effect is not seen despite PKA phosphorylation of KCNQ1. Right panel: Signaling pathway for β-adrenergic enhancement of IKs current through PKA phosphorylation.

possibly explained by the ability of CaM to relieve KCNQ1 inactivation in a Ca^{2+} dependent manner (Ghosh et al., 2006). In the presence of KCNE1, the role of CaM in enhancing current amplitude is preserved. Both the co-assembly with CaM_{1234} (Sachyani et al., 2014) and bath application of the CaM antagonist W7 (Shamgar et al., 2006) have been reported to decrease IKs current amplitude. Interestingly, CaM_{12} but not CaM_{34} was also shown to decrease IKs current amplitude, suggesting that not only is CaM able to modulate IKs, but its modulation is highly dependent on Ca^{2+}, and specifically where Ca^{2+} binds in the KCNE1-KCNQ1-CaM complex (Sachyani et al., 2014). From a cell signaling point of view, the stimulatory action of CaM has been shown to be modulated by calcium/calmodulin-dependent protein kinase II (CaMKII). Intracellular application of the CaMKII inhibitor, autocamtide-2 as well as another inhibitor, KN-93, reduced IKs current amplitude. KN-93 preincubation was also able to prevent any stimulatory action of intracellular CaM administration suggesting that CaMKII may act to turn off CaM enhancement of IKs (Xie et al., 2015). However, more studies to confirm and uncover the full signaling pathway of CaM mediated IKs enhancement and channel assembly are still needed.

ATP IS ESSENTIAL FOR CHANNEL OPENING

Several studies have demonstrated that the removal of ATP decreases or completely abolishes IKs activity, with current rescued by the reintroduction of ATP (Loussouarn et al., 2003). Using photo-crosslinking, the phosphates of ATP were suggested to electrostatically interact with a cluster of basic residues (R380, K393, and R397), whereas the nucleoside moieties of ATP were suggested to interact with hydrophobic aromatic residues such as W379 in the helix A to helix B region downstream from the S6 segment (Li et al., 2013; **Figure 7**, left panel). Functional studies have indicated that, although both W379S and the double mutant R380S/R397W abolish KCNQ1 currents, F-V signals are still present and are identical to that of WT KCNQ1, which

indicates that ATP binding is not required for VSD movement. Moreover, in a prior study, PIP2, known to be essential for VSD-PD coupling, was found to hyperpolarize the F-V curve of a constitutively open KCNQ1 mutant, L353K (Zaydman et al., 2013). This shift was abolished in the absence of PIP2, but removal of ATP sites in the background of L353K did not eliminate the displacement of the F-V curve, suggesting that ATP is perhaps not involved in VSD-PD coupling (Li et al., 2013). These results suggest that ATP plays a role in PD opening through interactions with the KCNQ1 C-terminus, but other ATP binding sites may exist which could in the future reveal a role for ATP in either VSD movement and/or VSD-PD coupling.

β-ADRENERGIC ENHANCEMENT OF CURRENT THROUGH PKA PHOSPHORYLATION

Under stressful conditions, circulating sympathetic hormones such as epinephrine bind to and activate G-protein coupled β-adrenergic receptors leading to the release of the α-subunit of the G-protein (Terrenoire et al., 2005; **Figure 7**, right panel). This α-subunit in turn activates adenyl cyclase 9 which leads to an increase in the intracellular levels of cAMP. The binding of cAMP then activates protein kinase A (PKA), which phosphorylates the C-terminus of KCNQ1 in the presence of Yotiao (Marx et al., 2002). Specifically, PKA phosphorylation has previously been described to occur at residues S27 and S92 (Marx et al., 2002; Lopes et al., 2007; Lundby et al., 2013). Although KCNQ1 alone has been found to be largely unresponsive to the functional transduction of PKA phosphorylation (Kurokawa et al., 2003), the phosphorylation of the N-terminus of KCNQ1 in the presence of KCNE1 produces a left-shift in the voltage dependence of activation, a slowing of deactivation kinetics and an increase in current amplitude (Dilly et al., 2004; Terrenoire et al., 2005). Together these changes in kinetics increase repolarizing current and shorten the cardiac action potential to allow sufficient time for ventricular filling. PKA-mediated phosphorylation is later removed by protein phosphatase 1. cAMP is degraded by the cAMP-specific phosphodiesterase, PDE4D3.

Using linked constructs which fix the KCNE1:KCNQ1 stoichiometry at different ratios (Murray et al., 2016), the hyperpolarizing shift in the voltage dependence of activation following cAMP exposure was progressively increased with increasingly saturated IKs complexes: the more KCNE1 in the complex, the greater the hyperpolarization, which showed that not only is the action of cAMP on IKs stoichiometrically dependent, but also that only one KCNE1 subunit is required for a basal response of the IKs complex to cAMP (Thompson et al., 2018b). In support of this latter finding, shortening of the first latency to opening in the presence of cAMP was seen in IKs constructs with KCNE1:KCNQ1 ratios of 1:4 and 2:4, similar to that seen in fully saturated IKs complexes. Using a phosphomimetic KCNQ1 mutant, this shortening of the first latency following cAMP treatment seen in WT channels was reduced but not completely abolished in the mutant S27D channel, indicating that this residue is only partly responsible for the shortening of first latency seen post-cAMP (Thompson et al., 2018a). Although phosphorylation of residue S27 plays a partial role in shortening of the first latency, it appears to be largely responsible for cAMP mediated changes in open probability. The double phosphomimic mutant S27D/S92D on the other hand completely abolished any changes in first latency, single-channel conductance and subconductance distribution as a result of cAMP exposure. Mechanistically, these effects of phosphorylation are largely mediated by enhancement of VSD activation, allowing the channel to open more frequently, quicker, and to higher sublevels, as mutant channels with fixed-activated VSDs showed little further response to cAMP (Thompson et al., 2017).

CONCLUSION

The KCNQ1 channel current is highly modulated by co-assembly with a wide range of accessory molecules and proteins, some of which have been reviewed here. Of most significance is the modulation of KCNQ1 by its β-subunit, KCNE1. Through the use of linked constructs which fix the ratio of KCNE1 to KCNQ1, the stoichiometry of association has been definitively shown to be variable between 1:4 to 4:4. Despite this, discussions surrounding the stoichiometry of KCNE1 and KCNQ1 remain relevant, not only as the KCNE1:KCNQ1 ratio in humans is presently unknown, but also because the stoichiometry of the IKs channel complex influences the efficacy of various therapeutic drugs and the action of accessory molecules such as CaM and ATP, and β-adrenergic enhancement of IKs via PKA phosphorylation.

The co-assembly of KCNE1 with KCNQ1, apart from changing the response to accessory molecules, also alters channel kinetic properties such as activation and deactivation, increasing conductance, and eliminating both the fast and slow inactivation seen in KCNQ1 channels. Recent experiments have suggested that these changes are mediated without fundamental changes in the allosteric coupling of voltage sensors to the pore activation gate, and although allosteric gating of KCNQ1 channels is generally accepted, much work still remains to be done in order to fully understand gating of KCNQ1 in association with its accessory subunits.

Molecular dynamics and docking simulations in combination with the recent cryo-EM structures of KCNQ1+CaM and KCNQ1+KCNE3+CaM have given many structure-function insights into the binding of various accessory molecules – notably, PIP2 which is essential for VSD-PD coupling, and CaM which plays a wide range of roles including in channel assembly and as an activator. Still, the exact binding location of the full KCNE1 subunit within the KCNQ1 tetramer remains uncertain. Given the many actions of KCNE1 and the physiological importance of the IKs channel, cryo-EM structures of KCNQ1+KCNE1 in both the presence and, where possible, the absence of essential accessory molecules such as CaM, PIP2 and ATP is probably the next major step needed to gain a more robust understanding of how KCNE1 is able to dramatically modulate the channel properties of KCNQ1.

AUTHOR CONTRIBUTIONS

All authors contributed equally to the writing and editing of this manuscript.

FUNDING

This research was funded by the Natural Sciences and Engineering Research Council of Canada (Grant #RGPIN-2016-05422), the Canadian Institutes of Health Research (#PJT-156181), and the Heart and Stroke Foundation of Canada (#G17-0018392) grants to DF. YW holds a Canadian Institutes of Health Research – Frederick Banting and Charles Best Canada Graduate Scholarship.

ACKNOWLEDGMENTS

We would like to thank Dr. Emely Thompson for her assistance in drafting figures.

REFERENCES

Abbott, G. W. (2014). Biology of the KCNQ1 potassium channel. *New J. Sci.* 2014, 1–26. doi: 10.1155/2014/237431

Abbott, G. W., Sesti, F., Splawski, I., Buck, M. E., Lehmann, W. H., Timothy, K. W., et al. (1999). MiRP1 forms I Kr potassium channels with HERG and is associated with cardiac arrhythmia. *Cell* 97, 175–187. doi: 10.1016/s0092-8674(00)80728-x

Abitbol, I., Peretz, A., Lerche, C., Busch, A. E., and Attali, B. (1999). Stilbenes and fenamates rescue the loss of I KS channel function induced by an LQT5 mutation and other IsK mutants. *EMBO J.* 18, 4137–4148. doi: 10.1093/emboj/18.15.4137

Aldrich, R. W. (2001). Fifty years of inactivation. *Nature* 411, 643–644. doi: 10.1038/35079705

Altomare, C., Bucchi, A., Camatini, E., Baruscotti, M., Viscomi, C., Moroni, A., et al. (2001). Integrated allosteric model of voltage gating of HCN channels. *J. Gen. Physiol.* 117, 519–532. doi: 10.1085/jgp.117.6.519

Angelo, K., Jespersen, T., Grunnet, M., Nielsen, M. S., Klaerke, D. A., and Olesen, S. P. (2002). KCNE5 induces time- and voltage-dependent modulation of the KCNQ1 current. *Biophys. J.* 83, 1997–2006. doi: 10.1016/s0006-3495(02)73961-1

Armstrong, C. M., Bezanilla, F., and Rojas, E. (1973). Destruction of sodium conductance inactivation in squid axons perfused with pronase. *J. Gen. Physiol.* 62, 375–391. doi: 10.1085/jgp.62.4.375

Barhanin, J., Lesage, F., Guillemare, E., Fink, M., Lazdunski, M., and Romey, G. (1996). K v LQT1 and IsK (minK) proteins associate to form the I Ks cardiac potassium current. *Nature* 384, 78–80. doi: 10.1038/384078a0

Barros, F., Pardo, L. A., Dominguez, P., Sierra, L. M., and de la Pena, P. (2019). New structures and gating of voltage-dependent potassium (Kv) channels and their relatives: a multi-domain and dynamic question. *Int. J. Mol. Sci.* 20:248. doi: 10.3390/ijms20020248

Barro-Soria, R., Ramentol, R., Liin, S. I., Perez, M. E., Kass, R. S., and Larsson, H. P. (2017). KCNE1 and KCNE3 modulate KCNQ1 channels by affecting different gating transitions. *Proc. Natl. Acad. Sci. U.S.A.* 114, E7367–E7376. doi: 10.1073/pnas.1710335114

Barro-Soria, R., Rebolledo, S., Liin, S. I., Perez, M. E., Sampson, K. J., Kass, R. S., et al. (2014). KCNE1 divides the voltage sensor movement in KCNQ1/KCNE1 channels into two steps. *Nat. Commun.* 5:3750. doi: 10.1038/ncomms4750

Baukrowitz, T., and Yellen, G. (1995). Modulation of K + current by frequency and external [K +]: a tale of two inactivation mechanisms. *Neuron* 15, 951–960. doi: 10.1016/0896-6273(95)90185-x

Baukrowitz, T., and Yellen, G. (1996). Use-dependent blockers and exit rate of the last ion from the multi-ion pore of a K + channel. *Science* 271, 653–656. doi: 10.1126/science.271.5249.653

Blunck, R., and Batulan, Z. (2012). Mechanism of electromechanical coupling in voltage-gated potassium channels. *Front. Pharmacol.* 3:166. doi: 10.3389/fphar.2012.00166

Bohannon, B. M., Wu, X., Wu, X., Perez, M. E., Liin, S. I, and Larsson, H. P. (2020). Polyunsaturated fatty acids produce a range of activators for heterogeneous IKs channel dysfunction. *J. Gen. Physiol.* 152:e201912396. doi: 10.1085/jgp.201912396

Bosch, R. F., Gaspo, R., Busch, A. E., Lang, H. J., Li, G. R., and Nattel, S. (1998). Effects of the chromanol 293B, a selective blocker of the slow, component of the delayed rectifier K+ current, on repolarization in human and guinea pig ventricular myocytes. *Cardiovasc. Res.* 38, 441–450. doi: 10.1016/s0008-6363(98)00021-2

Boulet, I. R., Labro, A. J., Raes, A. L., and Snyders, D. J. (2007). Role of the S6 C-terminus in KCNQ1 channel gating. *J. Physiol.* 585, 325–337. doi: 10.1113/jphysiol.2007.145813

Busch, A. E., Busch, G. L., Ford, E., Suessbrich, H., Lang, H. J., Greger, R., et al. (1997). The role of the IsK protein in the specific pharmacological properties of the IKs channel complex. *Br. J. Pharmacol.* 122, 187–189.

Cha, A., and Bezanilla, F. (1997). Characterizing voltage-dependent conformational changes in the Shaker K + channel with fluorescence. *Neuron* 19, 1127–1140. doi: 10.1016/s0896-6273(00)80403-1

Chandrasekhar, K. D., Bas, T., and Kobertz, W. R. (2006). KCNE1 subunits require co-assembly with K+ channels for efficient trafficking and cell surface expression. *J. Biol. Chem.* 281, 40015–40023. doi: 10.1074/jbc.m604398200

Chapman, M. L., and VanDongen, A. M. J. (2005). K channel subconductance levels result from heteromeric pore conformations. *J. Gen. Physiol.* 126, 87–103. doi: 10.1085/jgp.200509253

Chapman, M. L., VanDongen, H. M. A., and VanDongen, A. M. J. (1997). Activation-dependent subconductance levels in the drk1 K channel suggest a subunit basis for ion permeation and gating. *Biophys. J.* 72, 708–719. doi: 10.1016/s0006-3495(97)78707-1

Chen, H., Kim, L. A., Rajan, S., Xu, S., and Goldstein, S. A. (2003). Charybdotoxin binding in the I(Ks) pore demonstrates two MinK subunits in each channel complex. *Neuron* 40, 15–23. doi: 10.1016/s0896-6273(03)00570-1

Chen, Y. H., Xu, S. J., Bendahhou, S., Wang, X. L., Wang, Y., Xu, W. Y., et al. (2003). KCNQ1 gain-of-function mutation in familial atrial fibrillation. *Science* 299, 251–254. doi: 10.1126/science.1077771

Cheng, Y. M., Azer, J., Niven, C. M., Mafi, P., Allard, C. R., Qi, J., et al. (2011). Molecular determinants of U-type inactivation in Kv2.1 channels. *Biophys. J.* 101, 651–661. doi: 10.1016/j.bpj.2011.06.025

Cheng, Y. M., Fedida, D., and Kehl, S. J. (2010). Kinetic analysis of the effects of H+ or Ni2+ on Kv1.5 current shows that both ions enhance slow inactivation and induce resting inactivation. *J. Physiol.* 15, 3011–3030. doi: 10.1113/jphysiol.2010.191544

Chinn, K. (1993). Two delayed rectifiers in guinea pig ventricular myocytes distinguished by tail current kinetics. *J. Pharmacol. Exp. Ther.* 264, 553–560.

Chouabe, C., Neyroud, N., Guicheney, P., Lazdunski, M., Romey, G., and Barhanin, J. (1997). Properties of KvLQT1 K + channel mutations in Romano-Ward and Jervell and Lange-Nielsen inherited cardiac arrhythmias. *EMBO J.* 16, 5472–5479. doi: 10.1093/emboj/16.17.5472

Choveau, F. S., Abderemane-Ali, F., Coyan, F. C., Es-Salah-Lamoureux, Z., Baro, I., and Loussouarn, G. (2012). Opposite effects of the S4-S5 linker and PIP(2) on voltage-gated channel function: KCNQ1/KCNE1 and Other channels. *Front. Pharmacol.* 3:125. doi: 10.3389/fphar.2012.00125

Choveau, F. S., Rodriguez, N., Abderemane Ali, F., Labro, A. J., Rose, T., Dahimene, S., et al. (2011). KCNQ1 channels voltage dependence through a voltage-dependent binding of the S4-S5 linker to the pore domain. *J. Biol. Chem.* 286, 707–716. doi: 10.1074/jbc.M110.146324

Chowdhury, S., and Chanda, B. (2012). Perspectives on: conformational coupling in ion channels: thermodynamics of electromechanical coupling in voltage-gated ion channels. *J. Gen. Physiol.* 140, 613–623. doi: 10.1085/jgp.201210840

Claydon, T. W., and Fedida, D. (2007). Voltage clamp fluorimetry studies of mammalian voltage-gated K(+) channel gating. *Biochem. Soc. Trans.* 35, 1080–1082. doi: 10.1042/bst0351080

Cuello, L. G., Jogini, V., Cortes, D. M., and Perozo, E. (2010). Structural mechanism of C-type inactivation in K(+) channels. *Nature* 466, 203–208. doi: 10.1038/nature09153

Cui, J. (2016). Voltage-dependent gating: novel insights from KCNQ1 channels. *Biophys. J.* 110, 14–25. doi: 10.1016/j.bpj.2015.11.023

Cui, J., Kline, R. P., Pennefather, P., and Cohen, I. S. (1994). Gating of I sK expressed in *Xenopus oocytes* depends on the amount of mRNA injected. *J. Gen. Physiol.* 104, 87–105. doi: 10.1085/jgp.104.1.87

Dilly, K. W., Kurokawa, J., Terrenoire, C., Reiken, S., Lederer, W. J., Marks, A. R., et al. (2004). Overexpression of beta2-adrenergic receptors cAMP-dependent protein kinase phosphorylates and modulates slow delayed rectifier potassium channels expressed in murine heart: evidence for receptor/channel co-localization. *J. Biol. Chem.* 279, 40778–40787. doi: 10.1074/jbc.m406010200

Doolan, G. K., Panchal, R. G., Fonnes, E. L., Clarke, A. L., Williams, D. A., and Petrou, S. (2002). Fatty acid augmentation of the cardiac slowly activating delayed rectifier current (I Ks) is conferred by hminK. *FASEB J.* 16, NIL57–NIL71.

Doyle, D. A., Cabral, J. M., Pfuetzner, R. A., Kuo, A. L., Gulbis, J. M., Cohen, S. L., et al. (1998). The structure of the potassium channel: molecular basis of K + conduction and selectivity. *Science* 280, 69–77. doi: 10.1126/science.280.5360.69

Dvir, M., Strulovich, R., Sachyani, D., Ben-Tal Cohen, I., Haitin, Y., Dessauer, C., et al. (2014). Long QT mutations at the interface between KCNQ1 helix C and KCNE1 disrupt I(KS) regulation by PKA and PIP(2). *J. Cell Sci.* 127, 3943–3955. doi: 10.1242/jcs.147033

Eckey, K., Wrobel, E., Strutz-Seebohm, N., Pott, L., Schmitt, N., and Seebohm, G. (2014). Novel Kv7.1-phosphatidylinositol 4,5-bisphosphate interaction sites uncovered by charge neutralization scanning. *J. Biol. Chem.* 289, 22749–22758. doi: 10.1074/jbc.M114.589796

Eldstrom, J., and Fedida, D. (2011). The voltage-gated channel accessory protein KCNE2: multiple ion channel partners, multiple ways to long QT syndrome. *Expert Rev. Mol. Med.* 13:e38. doi: 10.1017/S1462399411002092

Eldstrom, J., Wang, Z., Werry, D., Wong, N., and Fedida, D. (2015). Microscopic mechanisms for long QT syndrome type 1 revealed by single-channel analysis of I(Ks) with S3 domain mutations in KCNQ1. *Heart Rhythm.* 12, 386–394. doi: 10.1016/j.hrthm.2014.10.029

Eyring, H., Lumry, R., and Woodbury, J. W. (1949). Some applications of modern rate theory to physiological systems. *Record Chem. Prog.* 100, 100–114.

Flynn, G. E., and Zagotta, W. N. (2018). Insights into the molecular mechanism for hyperpolarization-dependent activation of HCN channels. *Proc. Natl. Acad. Sci. U.S.A.* 115, E8086–E8095. doi: 10.1073/pnas.1805596115

Gebauer, M., Isbrandt, D., Sauter, K., Callsen, B., Nolting, A., Pongs, O., et al. (2004). N-type inactivation features of Kv4.2 channel gating. *Biophys. J.* 86, 210–223. doi: 10.1016/s0006-3495(04)74097-7

Ghosh, S., Nunziato, D. A., and Pitt, G. S. (2006). KCNQ1 assembly and function is blocked by long-QT syndrome mutations that disrupt interaction with calmodulin. *Circ. Res.* 98, 1048–1054. doi: 10.1161/01.res.0000218863.44140.f2

Gibor, G., Yakubovich, D., Rosenhouse-Dantsker, A., Peretz, A., Schottelndreier, H., Seebohm, G., et al. (2007). An inactivation gate in the selectivity filter of KCNQ1 potassium channels. *Biophys. J.* 93, 4159–4172. doi: 10.1529/biophysj.107.107987

Grunnet, M., Jespersen, T., Rasmussen, H. B., Ljungstrom, T., Jorgensen, N. K., Olesen, S. P., et al. (2002). KCNE4 is an inhibitory subunit to the KCNQ1 channel. *J. Physiol.* 542, 119–130. doi: 10.1113/jphysiol.2002.017301

Haitin, Y., Yisharel, I., Malka, E., Shamgar, L., Schottelndreier, H., Peretz, A., et al. (2008). S1 constrains S4 in the voltage sensor domain of Kv7.1 K+ channels. *PLoS One.* 3:e1935. doi: 10.1371/journal.pone.0001935

Hodgkin, A. L., and Huxley, A. F. (1952). A quantitative description of membrane current and its application to conduction and excitation in nerve. *J. Physiol.* 117, 500–544. doi: 10.1113/jphysiol.1952.sp004764

Horne, A. J., Peters, C. J., Claydon, T. W., and Fedida, D. (2010). Fast and slow voltage sensor rearrangements during activation gating in Kv1.2 channels detected using tetramethylrhodamine fluorescence. *J. Gen. Physiol.* 136, 83–99. doi: 10.1085/jgp.201010413

Horrigan, F. T., Cui, J. M., and Aldrich, R. W. (1999). Allosteric voltage gating of potassium channels I - mSlo ionic currents in the absence of Ca 2+. *J. Gen. Physiol.* 114, 277–304. doi: 10.1085/jgp.114.2.277

Hoshi, T., Zagotta, W. N., and Aldrich, R. W. (1990). Biophysical and molecular mechanisms of Shaker potassium channel inactivation. *Science* 250, 533–538. doi: 10.1126/science.2122519

Hoshi, T., Zagotta, W. N., and Aldrich, R. W. (1991). Two types of inactivation in Shaker K + channels: effects of alterations in the carboxy-terminal region. *Neuron* 7, 547–556. doi: 10.1016/0896-6273(91)90367-9

Hou, P., Eldstrom, J., Shi, J., Zhong, L., McFarland, K., Gao, Y., et al. (2017). Inactivation of KCNQ1 potassium channels reveals dynamic coupling between voltage sensing and pore opening. *Nat. Commun.* 8:1730. doi: 10.1038/s41467-017-01911-8

Hou, P., Kang, P. W., Kongmeneck, A. D., Yang, N. D., Liu, Y., Shi, J., et al. (2020). Two-stage electro-mechanical coupling of a KV channel in voltage-dependent activation. *Nat. Commun.* 11:676. doi: 10.1038/s41467-020-14406-w

Hou, P., Shi, J., White, K. M., Gao, Y., and Cui, J. (2019). ML277 specifically enhances the fully activated open state of KCNQ1 by modulating VSD-pore coupling. *Elife* 8:e48576. doi: 10.7554/eLife.48576

Jackson, H. A., McIntosh, S., Whittome, B., Asuri, S., Casey, B., Kerr, C., et al. (2014). LQTS in Northern BC: homozygosity for KCNQ1 V205M presents with a more severe cardiac phenotype but with minimal impact on auditory function. *Clin. Genet.* 86, 85–90. doi: 10.1111/cge.12235

Jan, L. Y., and Jan, Y. N. (1989). Voltage-sensitive ion channels. *Cell* 56, 13–25.

Jervell, A., and Lange-Nielsen, F. (1957). Congenital deaf-mutism, functional heart disease with prolongation of the Q-T interval and sudden death. *Am. Heart J.* 54, 59–68. doi: 10.1016/0002-8703(57)90079-0

Jiang, M., Wang, Y., and Tseng, G. N. (2017). Adult ventricular myocytes segregate KCNQ1 and KCNE1 to keep the IKs amplitude in check until when larger IKs is needed. *Circ. Arrhythm. Electrophysiol.* 10:e005084. doi: 10.1161/CIRCEP.117.005084

Jiang, M., Xu, X., Wang, Y., Toyoda, F., Liu, X. S., Zhang, M., et al. (2009). Dynamic partnership between KCNQ1 and KCNE1 and influence on cardiac IKs current amplitude by KCNE2. *J. Biol. Chem.* 284, 16452–16462. doi: 10.1074/jbc.M808262200

Kaur, S., Bernas, T., Wilson, Z., Schultz, T., Jiang, M., and Tseng, G. N. (2020). How do KCNQ1 and KCNE1 assemble to form the slow-delayed-rectifier (IKs) channels in adult ventricular mocytes (AVMs)? *Biophys. J.* 118:268a. doi: 10.1016/j.bpj.2019.11.1546

Klemic, K. G., Kirsch, G. E., and Jones, S. W. (2001). U-type inactivation of Kv3.1 and Shaker potassium channels. *Biophys. J.* 81, 814–826. doi: 10.1016/s0006-3495(01)75743-8

Krumerman, A., Gao, X., Bian, J. S., Melman, Y. F., Kagan, A., and McDonald, T. V. (2004). An LQT mutant minK alters KvLQT1 trafficking. *Am. J. Physiol. Cell Physiol.* 286, C1453–C1463.

Kurata, H. T., and Fedida, D. (2006). A structural interpretation of voltage-gated potassium channel inactivation. *Prog. Biophys. Mol. Biol.* 92, 185–208. doi: 10.1016/j.pbiomolbio.2005.10.001

Kurata, H. T., Soon, G. S., Eldstrom, J. R., Lu, G. W. K., Steele, D. F., and Fedida, D. (2002). Amino-terminal determinants of U-type inactivation of voltage-gated K + channels. *J. Biol. Chem.* 277, 29045–29053. doi: 10.1074/jbc.m111470200

Kurokawa, J., Chen, L., and Kass, R. S. (2003). Requirement of subunit expression for cAMP-mediated regulation of a heart potassium channel. *Proc. Natl. Acad. Sci. U.S.A.* 100, 2122–2127. doi: 10.1073/pnas.0434935100

Labro, A. J., Boulet, I. R., Choveau, F. S., Mayeur, E., Bruyns, T., Loussouarn, G., et al. (2011). The S4-S5 linker of KCNQ1 channels forms a structural scaffold with the S6 segment controlling gate closure. *J. Biol. Chem.* 286, 717–725. doi: 10.1074/jbc.M110.146977

Labro, A. J., and Snyders, D. J. (2012). Being flexible: the voltage-controllable activation gate of kv channels. *Front. Pharmacol.* 3:168. doi: 10.3389/fphar.2012.00168

Larsson, H. P., Baker, O. S., Dhillon, D. S., and Isacoff, E. Y. (1996). Transmembrane movement of the Shaker K + Channel S4. *Neuron* 16, 387–397. doi: 10.1016/s0896-6273(00)80056-2

Larsson, J. E., Larsson, H. P., and Liin, S. I. (2018). KCNE1 tunes the sensitivity of KV7.1 to polyunsaturated fatty acids by moving turret residues close to the binding site. *Elife* 7:e37257. doi: 10.7554/eLife.37257

Ledwell, J. L., and Aldrich, R. W. (1999). Mutations in the S4 region isolate the final voltage-dependent cooperative step in potassium channel activation. *J. Gen. Physiol.* 113, 389–414. doi: 10.1085/jgp.113.3.389

Lee, S. Y., Banerjee, A., and MacKinnon, R. (2009). Two separate interfaces between the voltage sensor and pore are required for the function of voltage-dependent K(+) channels. *PLoS Biol.* 7:e47. doi: 10.1371/journal.pbio.1000047

Lei, M., and Brown, H. F. (1996). Two components of the delayed rectifier potassium current. IK, in rabbit sino-atrial node cells. *Exp. Physiol.* 81, 725–741. doi: 10.1113/expphysiol.1996.sp003972

Li, Y., Gao, J., Lu, Z., McFarland, K., Shi, J., Bock, K., et al. (2013). Intracellular ATP binding is required to activate the slowly activating K+ channel I(Ks). *Proc. Natl. Acad. Sci. U.S.A.* 110, 18922–18927. doi: 10.1073/pnas.1315649110

Liin, S. I., Barro-Soria, R., and Larsson, H. P. (2015). The KCNQ1 channel – remarkable flexibility in gating allows for functional versatility. *J. Physiol.* 593, 2605–2615. doi: 10.1113/jphysiol.2014.287607

Liin, S. I., Yazdi, S., Ramentol, R., Barro-Soria, R., and Larsson, H. P. (2018). Mechanisms underlying the dual effect of polyunsaturated fatty acid analogs on Kv7.1. *Cell Rep.* 24, 2908–2918. doi: 10.1016/j.celrep.2018.08.031

Liu, D. W., and Antzelevitch, C. (1995). Characteristics of the delayed rectifier current (I Kr and I Ks) in canine ventricular epicardial, midmyocardial, and endocardial myocytes: a weaker I Ks contributes to the longer action potential of the M cell. *Circ. Res.* 76, 351–365. doi: 10.1161/01.res.76.3.351

Long, S. B., Campbell, E. B., and MacKinnon, R. (2005a). Crystal structure of a mammalian voltage-dependent Shaker family K + channel. *Science* 309, 897–903. doi: 10.1126/science.1116269

Long, S. B., Campbell, E. B., and Mackinnon, R. (2005b). Voltage sensor of Kv1.2: structural basis of electromechanical coupling. *Science* 309, 903–908. doi: 10.1126/science.1116270

Lopes, C. M., Remon, J. I., Matavel, A., Sui, J. L., Keselman, I., Medei, E., et al. (2007). Protein kinase a modulates PLC-dependent regulation and PIP2-sensitivity of K+ channels. *Channels* 1, 124–134. doi: 10.4161/chan.4322

Lopez-Barneo, J., Hoshi, T., Heinemann, S. H., and Aldrich, R. W. (1993). Effects of external cations and mutations in the pore region on C-type inactivation of Shaker potassium channels. *Receptors Channels* 1, 61–71.

Loussouarn, G., Park, K. H., Bellocq, C., Baro, I., Charpentier, F., and Escande, D. (2003). Phosphatidylinositol-4,5-bisphosphate, PIP2, controls KCNQ1/KCNE1 voltage-gated potassium channels: a functional homology between voltage-gated and inward rectifier K+ channels. *EMBO J.* 22, 5412–5421. doi: 10.1093/emboj/cdg526

Lundby, A., Andersen, M. N., Steffensen, A. B., Horn, H., Kelstrup, C. D., Francavilla, C., et al. (2013). In vivo phosphoproteomics analysis reveals the cardiac targets of beta-adrenergic receptor signaling. *Sci. Signal.* 6:rs11. doi: 10.1126/scisignal.2003506

Ma, L. J., Ohmert, I., and Vardanyan, V. (2011). Allosteric features of KCNQ1 gating revealed by alanine scanning mutagenesis. *Biophys. J.* 100, 885–894. doi: 10.1016/j.bpj.2010.12.3726

MacKinnon, R., Aldrich, R. W., and Lee, A. W. (1993). Functional stoichiometry of Shaker potassium channel inactivation. *Science* 262, 757–759. doi: 10.1126/science.7694359

Magyar, J., Horvath, B., Banyasz, T., Szentandrassy, N., Birinyi, P., Varro, A., et al. (2006). L-364,373 fails to activate the slow delayed rectifier K+ current in canine ventricular cardiomyocytes. *Naunyn Schmiedebergs Arch. Pharmacol.* 373, 85–89.

Mannuzzu, L. M., Moronne, M. M., and Isacoff, E. Y. (1996). Direct physical measurement of conformational rearrangement underlying potassium channel gating. *Science* 271, 213–216. doi: 10.1126/science.271.5246.213

Marx, S. O., Kurokawa, J., Reiken, S., Motoike, H., D'Armiento, J., Marks, A. R., et al. (2002). Requirement of a macromolecular signaling complex for beta adrenergic receptor modulation of the KCNQ1-KCNE1 potassium channel. *Science* 295, 496–499. doi: 10.1126/science.1066843

Matavel, A., and Lopes, C. M. (2009). PKC activation and PIP(2) depletion underlie biphasic regulation of IKs by Gq-coupled receptors. *J. Mol. Cell. Cardiol.* 46, 704–712. doi: 10.1016/j.yjmcc.2009.02.006

Meisel, E., Dvir, M., Haitin, Y., Giladi, M., Peretz, A., and Attali, B. (2012). KCNQ1 channels do not undergo concerted but sequential gating transitions in both the absence and the presence of KCNE1 protein. *J. Biol. Chem.* 287, 34212–34224. doi: 10.1074/jbc.m112.364901

Meisel, E., Tobelaim, W., Dvir, M., Haitin, Y., Peretz, A., and Attali, B. (2018). Inactivation gating of Kv7.1 channels does not involve concerted cooperative subunit interactions. *Channels* 12, 89–99. doi: 10.1080/19336950.2018.1441649

Melman, Y. F., Domänech, A., De la Luna, S., and McDonald, T. V. (2001). Structural determinants of KvLQT1 control by the KCNE family of proteins. *J. Biol. Chem.* 276, 6439–6444. doi: 10.1074/jbc.m010713200

Melman, Y. F., Krumerman, A., and McDonald, T. V. (2002a). A single transmembrane site in the KCNE-encoded proteins controls the specificity of KvLQT1 channel gating. *J. Biol. Chem.* 277, 25187–25194. doi: 10.1074/jbc.m200564200

Melman, Y. F., Krummerman, A., and McDonald, T. V. (2002b). KCNE regulation of KvLQT1 channels: structure-function correlates. *Trends Cardiovasc. Med.* 12, 182–187. doi: 10.1016/s1050-1738(02)00158-5

Melman, Y. F., Um, S. Y., Krumerman, A., Kagan, A., and McDonald, T. V. (2004). KCNE1 binds to the KCNQ1 pore to regulate potassium channel activity. *Neuron* 42, 927–937. doi: 10.1016/j.neuron.2004.06.001

Morin, T. J., and Kobertz, W. R. (2008). Counting membrane-embedded KCNE beta-subunits in functioning K+ channel complexes. *Proc. Natl. Acad. Sci. U.S.A.* 105, 1478–1482. doi: 10.1073/pnas.0710366105

Moss, A. J., and Kass, R. S. (2005). Long QT syndrome: from channels to cardiac arrhythmias. *J. Clin. Invest.* 115, 2018–2024. doi: 10.1172/jci25537

Mruk, K., and Kobertz, W. R. (2009). Discovery of a novel activator of KCNQ1-KCNE1 K channel complexes. *PLoS One* 4:e4236. doi: 10.1371/journal.pone.0004236

Murray, C. I., Westhoff, M., Eldstrom, J., Thompson, E., Emes, R., and Fedida, D. (2016). Unnatural amino acid photo-crosslinking of the channel complex demonstrates a KCNE1:KCNQ1 stoichiometry of up to 4:4. *Elife* 5:e11815. doi: 10.7554/eLife.11815

Nakajo, K., and Kubo, Y. (2007). KCNE1 and KCNE3 stabilize and/or slow voltage sensing S4 segment of KCNQ1 channel. *J. Gen. Physiol.* 130, 269–281. doi: 10.1085/jgp.200709805

Nakajo, K., and Kubo, Y. (2014). Steric hindrance between S4 and S5 of the KCNQ1/KCNE1 channel hampers pore opening. *Nat. Commun.* 5:4100. doi: 10.1038/ncomms5100

Nakajo, K., and Kubo, Y. (2015). KCNQ1 channel modulation by KCNE proteins via the voltage-sensing domain. *J. Physiol.* 593, 2617–2625. doi: 10.1113/jphysiol.2014.287672

Nakajo, K., Ulbrich, M. H., Kubo, Y., and Isacoff, E. Y. (2010). Stoichiometry of the KCNQ1-KCNE1 ion channel complex. *Proc. Natl. Acad. Sci. U.S.A.* 107, 18862–18867. doi: 10.1073/pnas.1010354107

Olesen, M. S., Nielsen, M. W., Haunso, S., and Svendsen, J. H. (2014). Atrial fibrillation: the role of common and rare genetic variants. *Eur. J. Hum. Genet.* 22, 297–306. doi: 10.1038/ejhg.2013.139

Oliveras, A., Serrano-Novillo, C., Moreno, C., de la Cruz, A., Valenzuela, C., Soeller, C., et al. (2020). The unconventional biogenesis of Kv7.1-KCNE1 complexes. *Sci. Adv.* 6:eaay4472. doi: 10.1126/sciadv.aay4472

Osteen, J. D., Barro-Soria, R., Robey, S., Sampson, K. J., Kass, R. S., and Larsson, H. P. (2012). Allosteric gating mechanism underlies the flexible gating of KCNQ1 potassium channels. *Proc. Natl. Acad. Sci. U. S. A.* 109, 7103–7108. doi: 10.1073/pnas.1201582109

Osteen, J. D., Gonzalez, C., Sampson, K. J., Iyer, V., Rebolledo, S., Larsson, H. P., et al. (2010). KCNE1 alters the voltage sensor movements necessary to open the KCNQ1 channel gate. *Proc. Natl. Acad. Sci. U. S. A.* 107, 22710–22715. doi: 10.1073/pnas.1016300108

Park, K. H., Piron, J., Dahimene, S., Merot, J., Baro, I., Escande, D., et al. (2005). Impaired KCNQ1-KCNE1 and phosphatidylinositol-4,5-bisphosphate interaction underlies the long QT syndrome. *Circ. Res.* 96, 730–739. doi: 10.1161/01.res.0000161451.04649.a8

Peng, G., Barro-Soria, R., Sampson, K. J., Larsson, H. P., and Kass, R. S. (2017). Gating mechanisms underlying deactivation slowing by two KCNQ1 atrial fibrillation mutations. *Sci. Rep.* 7:45911. doi: 10.1038/srep45911

Plant, L. D., Xiong, D., Dai, H., and Goldstein, S. A. (2014). Individual IKs channels at the surface of mammalian cells contain two KCNE1 accessory subunits. *Proc. Natl. Acad. Sci. U.S.A.* 111, E1438–E1446. doi: 10.1073/pnas.1323548111

Pollard, J. R., Arispe, N., Rojas, E., and Pollard, H. B. (1994). A geometric sequence which accurately describes allowed multiple conductance levels of ion channels – the 3-Halves (3/2)-Rule. *J. Gen. Physiol.* 104, A32–A33.

Poulsen, A. N., and Klaerke, D. A. (2007). The KCNE1 beta-subunit exerts a transient effect on the KCNQ1 K+ channel. *Biochem. Biophys. Res. Commun.* 363, 133–139. doi: 10.1016/j.bbrc.2007.08.146

Pourrier, M., and Fedida, D. (2020). The emergence of human induced pluripotent stem cell-derived cardiomyocytes (hiPSC-CMs) as a platform to model arrhythmogenic diseases. *Int. J. Mol. Sci.* 21:657. doi: 10.3390/ijms21020657

Pusch, M. (1998). Increase of the single-channel conductance of KvLQT1 potassium channels induced by the association with minK. *Pflugers Archiv.* 437, 172–174.

Pusch, M., Bertorello, L., and Conti, F. (2000). Gating and flickery block differentially affected by rubidium in homomeric KCNQ1 and heteromeric KCNQ1/KCNE1 potassium channels. *Biophys. J.* 78, 211–226.

Pusch, M., Ferrera, L., and Friedrich, T. (2001). Two open states and rate-limiting gating steps revealed by intracellular Na+ block of human KCNQ1 and KCNQ1/KCNE1 K+ channels. *J. Physiol.* 533, 135–143.

Pusch, M., Magrassi, R., Wollnik, B., and Conti, F. (1998). Activation and inactivation of homomeric KvLQT1 potassium channels. *Biophys. J.* 75, 785–792.

Ramasubramanian, S., and Rudy, Y. (2018). The structural basis of IKs Ion-channel activation: mechanistic insights from molecular simulations. *Biophys. J.* 114, 2584–2594. doi: 10.1016/j.bpj.2018.04.023

Robbins, J. (2001). KCNQ potassium channels: physiology, pathophysiology, and pharmacology. *Pharmacol. Ther.* 90, 1–19.

Rocheleau, J. M., and Kobertz, W. R. (2008). KCNE peptides differently affect voltage sensor equilibrium and equilibration rates in KCNQ1 K+ channels. *J. Gen. Physiol.* 131, 59–68.

Romey, G., Attali, B., Chouabe, C., Abitbol, I., Guillemare, E., Barhanin, J., et al. (1997). Molecular mechanism and functional significance of the MinK control of the KvLQT1 channel activity. *J. Biol. Chem.* 272, 16713–16716.

Ruscic, K. J., Miceli, F., Villalba-Galea, C. A., Dai, H., Mishina, Y., Bezanilla, F., et al. (2013). IKs channels open slowly because KCNE1 accessory subunits slow the movement of S4 voltage sensors in KCNQ1 pore-forming subunits. *Proc. Natl. Acad. Sci. U.S.A.* 110, E559–E566. doi: 10.1073/pnas.1222616110

Sachyani, D., Dvir, M., Strulovich, R., Tria, G., Tobelaim, W., Peretz, A., et al. (2014). Structural basis of a Kv7.1 potassium channel gating module: studies of the intracellular c-terminal domain in complex with calmodulin. *Structure* 22, 1582–1594.

Sanguinetti, M. C. (2000). Maximal function of minimal K + channel subunits. *Trends Pharmacol. Sci.* 21, 199–201.

Sanguinetti, M. C., Curran, M. E., Zou, A., Shen, J., Spector, P. S., Atkinson, D. L., et al. (1996). Coassembly of K v LQT1 and minK (IsK) proteins to form cardiac I Ks potassium channel. *Nature* 384, 80–83.

Schoppa, N. E., and Sigworth, F. J. (1998). Activation of Shaker potassium channels III. An activation gating model for wild-type and V2 mutant channels. *J. Gen. Physiol.* 111, 313–342.

Schroeder, B. C., Hechenberger, M., Weinreich, F., Kubisch, C., and Jentsch, T. J. (2000a). KCNQ5, a novel potassium channel broadly expressed in brain, mediates M-type currents. *J. Biol. Chem.* 275, 24089–24095.

Schroeder, B. C., Waldegger, S., Fehr, S., Bleich, M., Warth, R., Greger, R., et al. (2000b). A constitutively open potassium channel formed by KCNQ1 and KCNE3. *Nature* 403, 196–199.

Seebohm, G., Sanguinetti, M. C., and Pusch, M. (2003). Tight coupling of rubidium conductance and inactivation in human KCNQ1 potassium channels. *J. Physiol.* 552, 369–378.

Seebohm, G., Strutz-Seebohm, N., Ureche, O. N., Baltaev, R., Lampert, A., Kornichuk, G., et al. (2006). Differential roles of S6 domain hinges in the gating of KCNQ potassium channels. *Biophys. J.* 90, 2235–2244.

Sesti, F., and Goldstein, S. A. N. (1998). Single-channel characteristics of wild-type I Ks channels and channels formed with two minK mutants that cause long QT syndrome. *J. Gen. Physiol.* 112, 651–663.

Shamgar, L., Ma, L. J., Schmitt, N., Haitin, Y., Peretz, A., Wiener, R., et al. (2006). Calmodulin is essential for cardiac I-KS channel gating and assembly - Impaired function in long-QT mutations. *Circ. Res.* 98, 1055–1063.

Sigworth, F. J. (1994). Voltage gating of ion channels. *Q. Rev. Biophys.* 27, 1–40.

Silva, J., and Rudy, Y. (2005). Subunit interaction determines IKs participation in cardiac repolarization and repolarization reserve. *Circulation* 112, 1384–1391.

Sorensen, A. B., Sondergaard, M. T., and Overgaard, M. T. (2013). Calmodulin in a heartbeat. *FEBS J.* 280, 5511–5532. doi: 10.1111/febs.12337

Steffensen, A. B., Refsgaard, L., Andersen, M. N., Vallet, C., Mujezinovic, A., Haunso, S., et al. (2015). IKs gain- and loss-of-function in early-onset lone atrial fibrillation. *J. Cardiovasc. Electrophysiol.* 26, 715–723. doi: 10.1111/jce.12666

Sun, J., and MacKinnon, R. (2017). Cryo-EM structure of a KCNQ1/CaM complex reveals insights into congenital long QT syndrome. *Cell* 169, 1042–1050.e9. doi: 10.1016/j.cell.2017.05.019

Sun, J., and MacKinnon, R. (2020). Structural basis of human KCNQ1 modulation and gating. *Cell* 180, 340–347.e9. doi: 10.1016/j.cell.2019.12.003

Tao, X., Lee, A., Limapichat, W., Dougherty, D. A., and MacKinnon, R. (2010). A gating charge transfer center in voltage sensors. *Science* 328, 67–73. doi: 10.1126/science.1185954

Terrenoire, C., Clancy, C. E., Cormier, J. W., Sampson, K. J., and Kass, R. S. (2005). Autonomic control of cardiac action potentials: role of potassium channel kinetics in response to sympathetic stimulation. *Circ. Res.* 96, e25–e34.

Thomas, A. M., Harmer, S. C., Khambra, T., and Tinker, A. (2011). Characterization of a binding site for anionic phospholipids on KCNQ1. *J. Biol. Chem.* 286, 2088–2100. doi: 10.1074/jbc.M110.153551

Thompson, E., Eldstrom, J., and Fedida, D. (2018a). Single channel kinetic analysis of the cAMP effect on IKs mutants, S209F and S27D/S92D. *Channels* 12, 276–283. doi: 10.1080/19336950.2018.1499369

Thompson, E., Eldstrom, J., Westhoff, M., McAfee, D., Balse, E., and Fedida, D. (2017). cAMP-dependent regulation of IKs single-channel kinetics. *J. Gen. Physiol.* 149, 781–798. doi: 10.1085/jgp.201611734

Thompson, E., Eldstrom, J., Westhoff, M., McAfee, D., and Fedida, D. (2018b). The IKs channel response to cAMP is modulated by the KCNE1:KCNQ1 stoichiometry. *Biophys. J.* 115, 1731–1740. doi: 10.1016/j.bpj.2018.09.018

Tobelaim, W. S., Dvir, M., Lebel, G., Cui, M., Buki, T., Peretz, A., et al. (2017). Competition of calcified calmodulin N lobe and PIP2 to an LQT mutation site in Kv7.1 channel. *Proc. Natl. Acad. Sci. U.S.A.* 114, E869–E878. doi: 10.1073/pnas.1612622114

Tohse, N. (1990). Calcium-sensitive delayed rectifier potassium current in guinea pig ventricular cells. *Am. J. Physiol.* 258, H1200–H1206.

Tristani-Firouzi, M., and Sanguinetti, M. C. (1998). Voltage-dependent inactivation of the human K + channel KvLQT1 is eliminated by association with minimal K + channel (minK) subunits. *J. Physiol.* 510, 37–45.

Vardanyan, V., and Pongs, O. (2012). Coupling of voltage-sensors to the channel pore: a comparative view. *Front. Pharmacol.* 3:145. doi: 10.3389/fphar.2012.00145

Virag, L., Iost, N., Opincariu, M., Szolnoky, J., Szecsi, J., Bogats, G., et al. (2001). The slow component of the delayed rectifier potassium current in undiseased human ventricular myocytes. *Cardiovasc. Res.* 49, 790–797.

Wang, Q., Curran, M. E., Splawski, I., Burn, T. C., Millholland, J. M., VanRaay, T. J., et al. (1996). Positional cloning of a novel potassium channel gene: KVLQT1 mutations cause cardiac arrhythmias. *Nat. Genet.* 12, 17–23.

Wang, S. M., Liu, S. G., Morales, M. J., Strauss, H. C., and Rasmusson, R. L. (1997). A quantitative analysis of the activation and inactivation kinetics of HERG expressed in Xenopus oocytes. *J. Physiol.* 502, 45–60.

Wang, W. Y., Xia, J., and Kass, R. S. (1998). MinK-KvLQT1 fusion proteins, evidence for multiple stoichiometries of the assembled I sK channel. *J. Biol. Chem.* 273, 34069–34074.

Wang, Y., Eldstrom, J., and Fedida, D. (2020). The I Ks Ion channel activator mefenamic acid requires KCNE1 and modulates channel gating in a subunit-dependent manner. *Mol. Pharmacol.* 97, 132–144. doi: 10.1124/mol.119.117952

Werry, D., Eldstrom, J., Wang, Z., and Fedida, D. (2013). Single-channel basis for the slow activation of the repolarizing cardiac potassium current. I(Ks). *Proc. Natl. Acad. Sci. U.S.A.* 110, E996–E1005. doi: 10.1073/pnas.1214875110

Westhoff, M., Eldstrom, J., Murray, C. I., Thompson, E., and Fedida, D. (2019). I Ks ion-channel pore conductance can result from individual voltage sensor movements. *Proc. Natl. Acad. Sci. U.S.A.* 116, 7879–7888. doi: 10.1073/pnas.1811623116

Westhoff, M., Murray, C. I., Eldstrom, J., and Fedida, D. (2017). Photo-cross-linking of IKs demonstrates state-dependent interactions between KCNE1 and KCNQ1. *Biophys. J.* 113, 415–425. doi: 10.1016/j.bpj.2017.06.005

Wrobel, E., Rothenberg, I., Krisp, C., Hundt, F., Fraenzel, B., Eckey, K., et al. (2016). KCNE1 induces fenestration in the Kv7.1/KCNE1 channel complex that

allows for highly specific pharmacological targeting. *Nat. Commun.* 7:12795. doi: 10.1038/ncomms12795

Wu, D., Delaloye, K., Zaydman, M. A., Nekouzadeh, A., Rudy, Y., and Cui, J. (2010). State-dependent electrostatic interactions of S4 arginines with E1 in S2 during Kv7.1 activation. *J. Gen. Physiol.* 135, 595–606. doi: 10.1085/jgp.201010408

Xie, Y., Ding, W. G., and Matsuura, H. (2015). Ca2+/calmodulin potentiates I Ks in sinoatrial node cells by activating Ca2+/calmodulin-dependent protein kinase II. *Pflugers Arch.* 467, 241–251. doi: 10.1007/s00424-014-1507-1

Xu, Y., Wang, Y., Zhang, M., Jiang, M., Rosenhouse-Dantsker, A., Wassenaar, T., et al. (2015). Probing binding sites and mechanisms of action of an I(Ks) activator by computations and experiments. *Biophys. J.* 108, 62–75. doi: 10.1016/j.bpj.2014.10.059

Yang, Y. S., and Sigworth, F. J. (1998). Single-channel properties of I Ks potassium channels. *J. Gen. Physiol.* 112, 665–678.

Yu, H., Lin, Z., Mattmann, M. E., Zou, B., Terrenoire, C., Zhang, H., et al. (2013). Dynamic subunit stoichiometry confers a progressive continuum of pharmacological sensitivity by KCNQ potassium channels. *Proc. Natl. Acad. Sci. U.S.A.* 110, 8732–8737. doi: 10.1073/pnas.1300684110

Zagotta, W. N., Hoshi, T., and Aldrich, R. W. (1994). Shaker potassium channel gating. III: evaluation of kinetic models for activation. *J. Gen. Physiol.* 103, 321–362.

Zaydman, M. A., and Cui, J. (2014). PIP2 regulation of KCNQ channels: biophysical and molecular mechanisms for lipid modulation of voltage-dependent gating. *Front. Physiol.* 5:195. doi: 10.3389/fphys.2014.00195

Zaydman, M. A., Kasimova, M. A., McFarland, K., Beller, Z., Hou, P., Kinser, H. E., et al. (2014). Domain-domain interactions determine the gating, permeation, pharmacology, and subunit modulation of the IKs ion channel. *Elife.* 3:e03606. doi: 10.7554/eLife.03606

Zaydman, M. A., Silva, J. R., Delaloye, K., Li, Y., Liang, H., Larsson, H. P., et al. (2013). Kv7.1 ion channels require a lipid to couple voltage sensing to pore opening. *Proc. Natl. Acad. Sci. U.S.A.* 110, 13180–13185. doi: 10.1073/pnas.1305167110

Zhang, H., Craciun, L. C., Mirshahi, T., Rohacs, T., Lopes, C. M., Jin, T., et al. (2003). PIP(2) activates KCNQ channels, and its hydrolysis underlies receptor-mediated inhibition of M currents. *Neuron* 37, 963–975.

Zhou, M., Morais-Cabral, J. H., Mann, S., and MacKinnon, R. (2001). Potassium channel receptor site for the inactivation gate and quaternary amine inhibitors. *Nature* 411, 657–661.

Conflict of Interest: The authors declare that the research was conducted in the absence of any commercial or financial relationships that could be construed as a potential conflict of interest.

frontiers in Physiology

MINI REVIEW
published: 11 June 2020
doi: 10.3389/fphys.2020.00641

Polyunsaturated Fatty Acids as Modulators of K_V7 Channels

Johan E. Larsson‡, Damon J. A. Frampton‡ and Sara I. Liin†*

Department of Biomedical and Clinical Sciences, Linköping University, Linköping, Sweden

Voltage-gated potassium channels of the K_V7 family are expressed in many tissues. The physiological importance of K_V7 channels is evident from specific forms of disorders linked to dysfunctional K_V7 channels, including variants of epilepsy, cardiac arrhythmia and hearing impairment. Thus, understanding how K_V7 channels are regulated in the body is of great interest. This Mini Review focuses on the effects of polyunsaturated fatty acids (PUFAs) on K_V7 channel activity and possible underlying mechanisms of action. By summarizing reported effects of PUFAs on K_V7 channels and native K_V7-mediated currents, we conclude that the generally observed effect is a PUFA-induced increase in current amplitude. The increase in current is commonly associated with a shift in the voltage-dependence of channel opening and in some cases with increased maximum conductance. Auxiliary KCNE subunits, which associate with K_V7 channels in certain tissues, may influence PUFA effects, though findings are conflicting. Both direct and indirect activating PUFA effects have been described, direct effects having been most extensively studied on $K_V7.1$. The negative charge of the PUFA head-group has been identified as critical for electrostatic interaction with conserved positively charged amino acids in transmembrane segments 4 and 6. Additionally, the localization of double bonds in the PUFA tail tunes the apparent affinity of PUFAs to $K_V7.1$. Indirect effects include those mediated by PUFA metabolites. Indirect inhibitory effects involve K_V7 channel degradation and re-distribution from lipid rafts. Understanding how PUFAs regulate K_V7 channels may provide insight into physiological regulation of K_V7 channels and bring forth new therapeutic strategies.

Keywords: docosahexaenoic acid, KCNE, KCNQ, K_V7, lipid, polyunsaturated fatty acid, voltage-gated potassium channel

OPEN ACCESS

Edited by:
Thomas Andrew Jepps, University of Copenhagen, Denmark

Reviewed by:
Jennifer Beth Stott, St George's, University of London, United Kingdom
Xavier Gasull, University of Barcelona, Spain
Anna Wiktorowska-Owczarek, Medical University of Lodz, Poland

***Correspondence:**
Sara I. Liin
sara.liin@liu.se

†ORCID:
Sara I. Liin
orcid.org/0000-0001-8493-0114

‡*These authors share first authorship*

Specialty section:
This article was submitted to Membrane Physiology and Membrane Biophysics, a section of the journal Frontiers in Physiology

Received: *18 March 2020*
Accepted: *20 May 2020*
Published: *11 June 2020*

Citation:
Larsson JE, Frampton DJA and Liin SI (2020) Polyunsaturated Fatty Acids as Modulators of K_V7 Channels. Front. Physiol. 11:641. doi: 10.3389/fphys.2020.00641

INTRODUCTION

It is well established that lipids can influence the function of voltage-gated ion channels and their organization in the membrane (Dart, 2010; Elinder and Liin, 2017). Specific members within the K_V7 family of voltage-gated potassium channels have been under intense study, owing to their physiological regulation by the phospholipid PIP_2 (phosphatidylinositol 4,5-bisphosphate; reviewed in Zaydman and Cui, 2014; Taylor and Sanders, 2017). However, several years of studies have revealed that unesterified, so called free fatty acids, may also regulate K_V7 channel function. Polyunsaturated fatty acids (PUFAs) in particular have emerged as interesting K_V7 modulators. This Mini Review will provide a brief essential background on K_V7 channels and PUFAs, followed

by a summary of our present understanding of PUFAs as K_V7 channel modulators and potential future developments.

PHYSIOLOGICAL ROLE AND GENERAL ARCHITECTURE OF K_V7 CHANNELS

The K_V7 family of voltage-gated potassium channels, of which there are five different isoforms, termed $K_V7.1$ to $K_V7.5$, are encoded by the *KCNQ* genes. The tissue distribution of K_V7 subtypes varies, and the channels serve different physiological roles (**Figure 1A**). $K_V7.1$ (in complex with the auxiliary KCNE1 protein, see further details below) is most famous for generating the slow current I_{Ks} in cardiomyocytes, important for cardiac repolarization (Barhanin et al., 1996; Sanguinetti et al., 1996), while also maintaining the ionic balance of endolymph in the inner ear (Neyroud et al., 1997). Heteromers of $K_V7.2$ and $K_V7.3$ generate the neuronal M-current (I_M) important for stabilizing the negative resting membrane potential of neurons and thereby regulating excitability (Wang et al., 1998; Cooper et al., 2000). $K_V7.4$ also contributes to maintaining the ionic balance of endolymph (Kubisch et al., 1999; Kharkovets et al., 2000), as well as contributing to the negative membrane potential in smooth muscle cells at rest (Jepps et al., 2011; Chadha et al., 2014; Jepps et al., 2015). $K_V7.5$ is suggested to form heteromers with other neuronal and smooth muscle K_V7 subtypes and contribute to their function in these tissues (Lerche et al., 2000; Chadha et al., 2014). Because of their important role in physiology, dysfunctional K_V7 channels are often linked to disorders characterized by abnormal potassium ion conductance, including cardiac arrhythmia, hearing impairment, epilepsy, pain, and hypertension (Barrese et al., 2018). For a more extensive overview of expression and physiological and pathological implications of K_V7 channels, we recommend recent reviews on this topic (Barrese et al., 2018; Miceli et al., 2018).

Each *KCNQ* gene encodes one K_V7 subunit, composed of six transmembrane segments (helices, referred to as S1–S6) and intracellular *N* and *C* termini (Jentsch, 2000). Four such K_V7 subunits assemble into functional tetrameric K_V7 channels, which can be either homomeric or heteromeric (Schwake et al., 2003; Schwake et al., 2006). A cryogenic electron microscopy structure of $K_V7.1$ visualizes how transmembrane segments S5–S6 of all four subunits form the central pore domain, whereas S1 to S4 of each subunit form the peripheral voltage-sensing domains (**Figure 1B**; Sun and MacKinnon, 2017). The determined structure reveals a domain swapped architecture, meaning that the voltage-sensing domain of one subunit lies adjacent to the pore-forming segments of its neighboring subunit (Sun and MacKinnon, 2017). Conserved, positively charged arginines in S4 of the voltage-sensing domain act as the primary voltage-sensing residues in K_V7 channels (Panaghie and Abbott, 2007; Miceli et al., 2008). Under hyperpolarized conditions, S4 is in a "downwards," internal, conformation, and the gate (located in the internal part of S6) of the central ion conducting pore is closed (Cui, 2016). Upon depolarization, S4 moves via intermediate conformations to an "upwards," external, conformation (Barro-Soria et al., 2014; Zaydman et al., 2014; Taylor et al., 2020), which triggers opening of the S6 gate and potassium conductance through the pore (Cui, 2016; Hou et al., 2020). Endogenous or exogenous ligands and auxiliary proteins may interact with and modulate the activity of K_V7 channels by altering S4 movement, gate opening, or the coupling between the two. For instance, auxiliary KCNE subunits (KCNE1-5) interact with K_V7 channels to modulate their expression and biophysical properties (Abbott, 2016; Barrese et al., 2018). Several studies assign the single-transmembrane segment of KCNE subunits to a space between neighboring voltage-sensing domains (see **Figure 1B** for putative KCNE localization; e.g., Chung et al., 2009; Xu et al., 2013; Sun and MacKinnon, 2020).

STRUCTURE AND PROPERTIES OF PUFAs

Polyunsaturated fatty acids are naturally occurring lipids known to modulate the activity of numerous voltage-gated ion channels (reviewed in Elinder and Liin, 2017). PUFA characteristics include a carboxylic acid "head-group" and an unbranched, aliphatic hydrocarbon "tail" with at least two double bonds in *cis* geometry (**Figure 1C**). The carboxyl head-group is either uncharged or negatively charged, depending on the protonation status (**Figure 1C**). The pKa value of carboxyl heads of PUFAs in proximity of ion channels approaches 7.4 (Hamilton, 1998; Liin et al., 2015), and so approximately 50% of PUFA head-groups are expected to be deprotonated and negatively charged at physiological pH. The *cis* double bonds allow polyunsaturated tails to bend and explore geometries that are not possible in the absence of *cis* double bonds (Feller, 2008; Yazdi et al., 2016). PUFAs are typically described according to the number of carbons and double bonds in the tail or their omega classification. **Figure 1C** shows the structure of docosahexaenoic acid (DHA), which has 22 carbons and 6 double bonds in its tail (22:6) and is an omega-3 PUFA (i.e., the first double bond is at the 3rd carbon from the methyl end). Examples of other physiologically relevant PUFAs that can be obtained via diet or synthesized from other essential fatty acids in the human body are arachidonic acid (AA, 20:4, omega-6), linoleic acid (LA, 18:2, omega-6), alpha-linolenic acid (ALA, 18:3, omega-3), and eicosapentaenoic acid (EPA, 20:5, omega-3). Reported physiological levels of PUFAs in plasma, serum, or cerebrospinal fluid are around 10–50 μM, but may reach higher levels during, for instance, excessive dietary PUFA intake (Conquer and Holub, 1998; Fraser et al., 2003; Brouwer et al., 2006).

REPORTED PUFA EFFECTS ON K_V7 CHANNELS AND CURRENTS

Table 1 summarizes reported PUFA effects on heterologously expressed K_V7 channels and isolated native currents generated by K_V7 channels. Notably, PUFA effects have thus far only been studied on $K_V7.1$–$K_V7.3$. A majority of studies have explored the acute effects of extracellular application of AA, ALA, DHA, EPA, or LA. These effects are achieved within the range of

A

	$K_V7.1$	$K_V7.1$/KCNE1	$K_V7.2/7.3$	$K_V7.4$	$K_V7.5$
Expression (selected examples)	Widely expressed in different tissues	Heart and ear	Nervous system	Ear and smooth musculature	Nervous system and smooth musculature
Physiological role (selected examples)	Big variation depending on KCNE co-expression. E.g. $K_V7.1$/KCNE3 is important for potassium recycling in intestinal epithelium	Generates the slow current I_{Ks} in cardiac tissue and maintains ionic balance of endolymph	Generates the neuronal M-current that stabilizes negative resting membrane potential	Maintains ionic balance of endolymph and contributes to negative membrane potential in smooth muscle cells	Contributes to neuronal M-current and contributes to negative membrane potential in smooth muscle cells

B

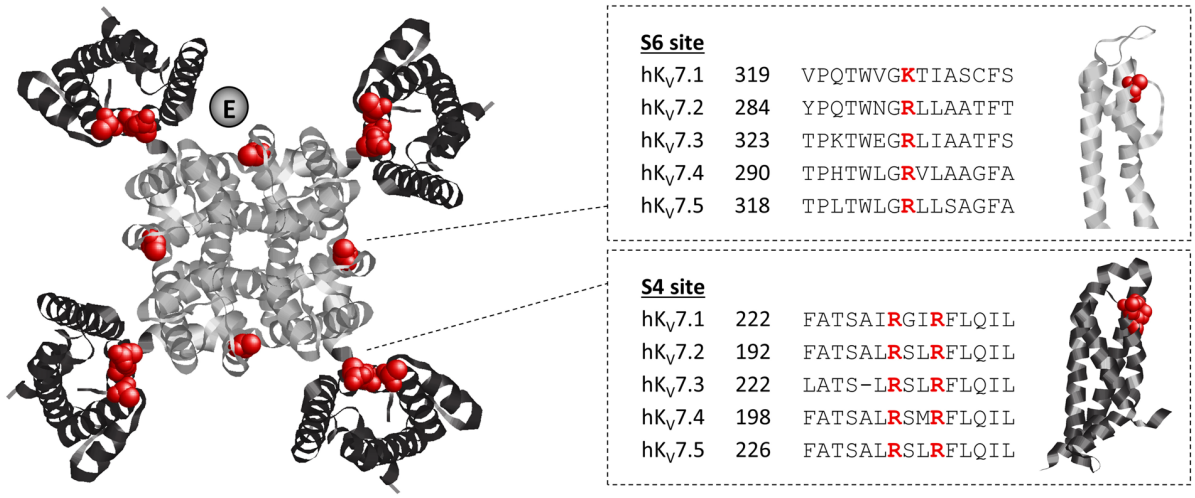

C

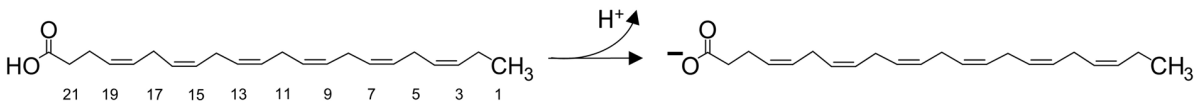

D

PUFA effects	$K_V7.1$	$K_V7.1$/KCNE1	$K_V7.2/7.3$	$K_V7.4$	$K_V7.5$
ΔI_{Amp}	↑ / —	↑ / —	↑	nd	nd
ΔV_{50}	← / —	← / → / —	←	nd	nd
ΔG_{max}	—	↑ / —	—	nd	nd

FIGURE 1 | Overview of K_V7 channel and PUFA molecular structures, and typified PUFA effects. **(A)** Schematic overview of K_V7 subtype expression and functional role. Note that these are examples, as some K_V7 subtypes have widespread expression and function. **(B)** Top view of $K_V7.1$ (PDB: 5VMS) with central pore domain in gray and peripheral voltage-sensing domains in black. Putative localization of KCNE at one $K_V7.1$ channel subunit is indicated [each subunit may accommodate one KCNE subunit (Sun and MacKinnon, 2020)]. Experimentally identified positively charged residues important for PUFA effects in $K_V7.1$ (Liin et al., 2018) are highlighted in red. Sequence alignment of the S6 site (important for G_{max} effect) and S4 site (important for V_{50} effect) of all K_V7 isoforms are provided along with a side view of relevant channel domain. **(C)** Structure of the PUFA DHA, which has a carboxyl head linked to a 22-carbon long aliphatic tail with six *cis* double bonds. Deprotonation of the carboxyl head occurs at pH exceeding the pKa of the head-group, this endows DHA with a single negative charge. **(D)** Schematic overview of PUFA effect on current amplitude (I_{Amp}), mid-point of the $G(V)$ curve (V_{50}), and maximum conductance (G_{max}) on indicated K_V7 subtypes. Please refer to **Table 1** for further details. nd denotes not determined.

minutes after PUFA application. The most consistently observed PUFA effect on heterologously expressed K_V7 channels is an increased current amplitude at a range of negative voltages, an effect reported for several PUFAs tested on $K_V7.1$ and heteromeric $K_V7.2/7.3$ channels (**Table 1**). Several studies report a PUFA-induced shift in the conductance *versus* voltage [$G(V)$] curve toward more negative voltages (described as negative shift in V_{50} in **Table 1**; Liin et al., 2015; Moreno et al., 2015; Liin et al., 2016a). Additionally, PUFAs may increase the maximum conductance observed at the most positive voltages (described

TABLE 1 | Summary of reported PUFA effects on indicated K_V7 channels/currents.

Channel/current	Experimental system	PUFA	Time perspective	Main effect(s) reported†	References
Heterologous expression:					
$hK_V7.1$	*Xenopus* oocytes	DHA, EPA	Acute	Faster activation kinetics *~5% at + 100 mV by 20 μM EPA*	Doolan et al., 2002
$hK_V7.1$	*Xenopus* oocytes	DHA, EPA	Acute	Increased current amplitude Negative shift in V_{50} *-9 to -14 mV by 70 μM DHA or EPA*	Liin et al., 2015
$hK_V7.1$	COS7	EPA	Acute	(No effect by 20 μM EPA)	Moreno et al., 2015
$hK_V7.1$/KCNE1	*Xenopus* oocytes	DHA, EPA	Acute	Increased current amplitude *29% at + 40 mV by 20 μM DHA* Slowed activation kinetics *~73% at + 100 mV by 20 μM EPA*	Doolan et al., 2002
$hK_V7.1$/KCNE1	COS7	DHA, EPA	Acute	Increased current amplitude *83% at + 60 mV by 20 μM DHA* *37% at + 60 mV by 20 μM EPA* Negative shift in V_{50} *-9 mV by 20 μM EPA*	Moreno et al., 2015
$hK_V7.1$/KCNE1	COS7	DHA, EPA	Prolonged	Negative or positive shift in V_{50} *-8 mV by 20 μM DHA* *+ 10 mV by 20 μM EPA*	Moreno et al., 2015
$hK_V7.1$/KCNE1	*Xenopus* oocytes	DHA	Acute	(No effect by 70 μM DHA)	Liin et al., 2015
$hK_V7.1$/KCNE1	*Xenopus* oocytes	LA, DHA	Acute	Increased current amplitude and G_{max} *~70% in G_{max} by 20 μM DHA*	Bohannon et al., 2020
$hK_V7.2/7.3$	*Xenopus* oocytes	ALA, DHA, EPA	Acute	Increased current amplitude Negative shift in V_{50} *-7 to -11 mV by 70 μM ALA, DHA, or EPA*	Liin et al., 2016a
$hK_V7.2/7.3$/KCNE1	*Xenopus* oocytes	DHA	Acute	Increased current amplitude Negative shift in V_{50} *-8 mV by 70 μM DHA*	Liin et al., 2016a
$hK_V7.2/7.3$/KCNE2	*Xenopus* oocytes	DHA	Acute	Increased current amplitude Negative shift in V_{50} *-5 mV by 70 μM DHA*	Liin et al., 2016a
Native current:					
I_{Ks}	Guinea pig ventricular cardiomyocytes	DHA	Acute	Increased current amplitude *38% at + 20 mV by 10 μM DHA* Accelerated deactivation *19% at -40 mV by 10 μM DHA*	Moreno et al., 2015
I_M	Rodent neuroblastoma cells	AA, DHA	Acute	Biphasic effects (both decreased and increased current amplitude) *observed for 5–50 μM PUFA*	Behe et al., 1992
I_M	Bullfrog sympathetic neurons	AA	Acute	Increased current amplitude *~30–60% by 5–100 μM AA*	Villarroel, 1993, 1994; Yu, 1995

†*Effects may vary between tested PUFAs (in such cases, most prominent effects have been listed and quantitative examples are provided in italic). AA denotes arachidonic acid, ALA denotes linolenic acid, LA denotes linoleic acid, DHA denotes docosahexaenoic acid, EPA denotes eicosapentaenoic acid. Acute effects indicate effects observed within minutes. Prolonged effects indicate effects observed within hours to days. V_{50} denotes the mid-point of the G(V) curve and is used to report on changes in the voltage dependence of channel opening. G_{max} denotes the top of the G(V) curve and is used to report on changes in the maximum conductance. COS7 is a fibroblast cell line derived from the African green monkey C. aethiops.*

as increase in G_{max} in **Table 1**; Bohannon et al., 2020). Both the shift in V_{50} and increase in G_{max} may contribute to the overall increase in current amplitude at different voltages. For clarity, we will refer to the three effects as "increase in current amplitude," "shift in V_{50}," and "increase in G_{max}." **Figure 1D** schematically illustrates PUFA effects on each of these parameters on different K_V7 subtypes, whereas **Table 1** reflects the complexity of effects and highlights examples of reported effects at specific PUFA concentrations. Typically, PUFA concentrations of 7 μM or higher are required to induce significant effects. Note that PUFA effects on current amplitude have typically been quantified at relatively depolarized voltages, which may not be physiologically relevant. However, because PUFAs generally also shift V_{50} toward negative voltages, the relative increase in current amplitude is larger at less depolarized voltages. Although studies rarely quantify PUFA effects in a more physiologically relevant voltage range, a prominent increase in current amplitude at less depolarized voltages is observed in several studies (Doolan et al., 2002; Liin et al., 2015; Moreno et al., 2015; Liin et al., 2016a).

In addition, PUFA effects on opening and closing kinetics have been described (Doolan et al., 2002; Moreno et al., 2015). However, effects on kinetics appear complex, with a range of described effects varying from PUFA to PUFA (Doolan et al., 2002; Moreno et al., 2015). Moreover, prolonged PUFA exposure over several days triggers a plethora of convoluted effects resulting in either negative *or* positive shift in V_{50}, depending on PUFA (Moreno et al., 2015).

Reported PUFA effects on native K_V7 currents largely agree with effects on heterologously expressed K_V7 channels (**Table 1**). In a majority of guinea pig ventricular cardiomyocytes, acute application of DHA increases I_{Ks} amplitude (presumably generated by $K_V7.1$/KCNE1 channels; Moreno et al., 2015). However, in a subset of cardiomyocytes DHA instead decreases I_{Ks} amplitude (Moreno et al., 2015). Several studies observe increases in I_M amplitude induced by AA or DHA in bullfrog sympathetic neurons (which presumably is generated by $K_V7.2/7.3$ channels; Villarroel, 1993, 1994; Yu, 1995).

IMPACT OF KCNE SUBUNITS ON PUFA EFFECTS

Because KCNE subunits associate with K_V7 channels in multiple tissues, evaluating the impact of KCNE co-expression on PUFA effects is of interest. Auxiliary subunits have been shown to affect the response of other K_V channels to PUFAs. For instance, DHA, or AA augmentation of the Slo1 channel is potentiated or enabled, respectively, when the channel is co-expressed with specific β subunits (Sun et al., 2007; Hoshi et al., 2013a). Furthermore, AA modulation of K_V4 channel inactivation kinetics is only observed if $K_V4.2$ or $K_V4.3$ are co-expressed with their KChIP subunit (Holmqvist et al., 2001). We found that neither KCNE1 nor KCNE2 co-expression with $K_V7.2/7.3$ affected the ability of DHA to shift V_{50} of $K_V7.2/7.3$ (Liin et al., 2016a). However, the occurrence and physiological relevance of complexes formed by $K_V7.2/7.3$ and KCNE subunits remains questionable at present. Conflicting results are found regarding the impact of KCNE1 co-expression with $K_V7.1$ on PUFA effects (**Table 1** and **Figure 1D**). Doolan et al. (2002) report that KCNE1 is required for DHA-mediated effects on $K_V7.1$ current amplitude, as they find that 20 μM of DHA increases the current amplitude of $K_V7.1$/KCNE1, but not $K_V7.1$. By comparison, 20 μM of EPA slowed activation kinetics for $K_V7.1$/KCNE1 without affecting current amplitude (Doolan et al., 2002). In contrast, we report that DHA at concentrations of 7 μM or higher shifts V_{50} of $K_V7.1$ toward negative voltages and that the presence of KCNE1 largely abolishes this V_{50} effect (Liin et al., 2015; Bohannon et al., 2020). However, we observe a DHA-induced increase in $K_V7.1$/KCNE1 current amplitude and G_{max} (Bohannon et al., 2020). A third study, by Moreno and colleagues, reports that 20 μM of DHA or EPA increases $K_V7.1$/KCNE1 current amplitude and shifts V_{50} of $K_V7.1$/KCNE1 toward negative voltages (Moreno et al., 2015). However, no EPA effect is observed on $K_V7.1$ alone (Moreno et al., 2015). The reason for these conflicting findings is not clear. One contributing factor may be the use of different expression systems (*Xenopus* oocytes *versus* mammalian COS7 cells). As previously remarked (Valenzuela, 2016), higher PUFA concentrations may be required in experiments with *Xenopus* oocytes than for mammalian cells to induce comparable effects. Another aspect to consider may be the method of PUFA application. We note larger DHA effects on current amplitude upon constant DHA perfusion compared to a single DHA application (Liin et al., 2015; Bohannon et al., 2020). Both Doolan *et al.,* and Moreno *et al.,* describe results employing PUFA perfusion.

PUFA PROPERTIES IMPORTANT FOR K_V7 EFFECTS

Previous studies have shown that PUFAs may interact directly with diverse ion channels to modulate their activity (Elinder and Liin, 2017). Moreno et al. (2015) concluded that the concurrent increase in $K_V7.1$/KCNE1 current amplitude and negative shift in V_{50} implicate an effect on channel gating as the primary mechanism. We made the same observation in our initial work (Liin et al., 2015). In subsequent work we have since explored this possibility utilizing PUFA analogs, site-directed mutagenesis, and pH manipulation.

We find that a negatively charged PUFA head-group is critical to the shift in V_{50} of $K_V7.1$ and $K_V7.2/7.3$ toward negative voltages. Fully deprotonated PUFAs (promoted by an alkaline extracellular solution) cause larger negative V_{50} shifts (Liin et al., 2015; Larsson et al., 2018; Bohannon et al., 2019). Protonated PUFAs and uncharged PUFA analogs (PUFA methyl esters) are unable to shift V_{50} (Liin et al., 2015, 2016a). Positively charged PUFA analogs (PUFA amines) instead shift V_{50} toward more positive voltages (Liin et al., 2015, 2016a; Larsson et al., 2018). This set of experiments implies an electrostatic mechanism of action underlying PUFA effects on V_{50}, and shows that the magnitude of this electrostatic effect is determined by the protonation status of the PUFA head-group. Notably, we observe clear activating effects by PUFAs on $K_V7.1$/KCNE1 (comparable to those on $K_V7.1$ alone) during experimental conditions that promote PUFA deprotonation (Liin et al., 2015; Larsson et al., 2018). This suggests that the lack of PUFA effects on $K_V7.1$/KCNE1 in our hands is because of KCNE1-induced protonation of the PUFA head-group. Moreover, these findings suggest that provided the head-group of a given PUFA analog has a low pKa value (and thus is deprotonated at physiological pH) said PUFA analog can be utilized to achieve greater effects on $K_V7.1$ alone at physiological pH while simultaneously retaining activating effects on $K_V7.1$/KCNE1 at physiological pH.

The PUFA head-group is not the sole determinant of the magnitude of PUFA effects. The first indication of this came from studies by Doolan et al. (2002) and Moreno et al. (2015) both of which show DHA induces overall greater effects on $K_V7.1$/KCNE1 than EPA does. This is in agreement with our comparison of 16 PUFAs with different tail properties, in which we find that PUFAs with double bonds proximal to the head-group have a higher apparent affinity to $K_V7.1$/KCNE1, compared with PUFAs with more distal double bonds (Bohannon et al., 2019). In contrast, there was either no or weak correlation

between tail length or number of double tail bonds and $K_V7.1$/KCNE1 effects (Bohannon et al., 2019). The proximal localization of double bonds relative to the head-group of DHA may contribute to the relatively greater effect, when compared to EPA at specific concentrations. The mechanistic basis for why proximal double bonds enhance PUFA interaction with $K_V7.1$ remains unknown, but may be related to flexibility in the hydrocarbon tail. Studies of PUFA interaction with the Slo1-β1 BK channel suggest that bending at specific carbons distally in the hydrocarbon tail are required for interaction with the channel (Tian et al., 2016). Speculatively, greater bending capabilities close to the head-group may be required for high affinity binding of PUFAs to $K_V7.1$.

PROPOSED DIRECT PUFA SITES OF ACTION IN K_V7

Polyunsaturated fatty acid analogs with lower head-group pKa values have been instrumental in determining the mechanism of action of PUFAs on $K_V7.1$. PUFA analogs with glycine or taurine head-groups have estimated pKa values that are 1 and 5.5 units lower than that of carboxyl head-groups, respectively, (Bohannon et al., 2020), and are examples of PUFA analogs with exaggerated acute effects on V_{50} of both $K_V7.1$ and $K_V7.1$/KCNE1 at physiological pH (Liin et al., 2015). In experiments utilizing DHA-glycine (DHA-Gly) or AA-taurine (N-AT), we have shown that PUFA analogs interact with S4 to shift V_{50}. This is observed in voltage-clamp fluorometry experiments that track S4 movement as a PUFA-induced shift in S4 movement toward negative voltages (Liin et al., 2015, 2016b). Individual mutations of the two top arginines in S4 of $K_V7.1$ into uncharged glutamines (R228Q and R231Q) either reduce or abrogate entirely the ability of PUFAs to shift V_{50} of $K_V7.1$ and $K_V7.1$/KCNE1 (Liin et al., 2015, 2018). These findings suggest that electrostatic interaction between the negative PUFA head-group and these positively charged arginines in S4 facilitates the upward S4 movement, which contributes to the PUFA effect on V_{50} (illustrated as "S4 site" in **Figure 1B**).

Although charge-neutralizing mutation of S4 arginines removes the V_{50} effect of PUFAs, an increase in G_{max} of $K_V7.1$ and $K_V7.1$/KCNE1 is still observed (Liin et al., 2018). This increase in G_{max} is also electrostatic in nature, as it is abolished following mutation of a lysine at the top of S6 into an uncharged glutamine (Liin et al., 2018). Experiments combined with molecular dynamics simulations suggest that electrostatic interaction between the negative PUFA head-group and the positively charged lysine at position 326 of S6 (illustrated as "S6 site" in **Figure 1B**) triggers conformational changes in the ion-conducting pore in and near the selectivity filter. These conformational changes appear to promote potassium ion conductance in a way that contributes to the PUFA effect on G_{max}. Altogether, these findings suggest that PUFAs have at least two independent sites of electrostatic action in $K_V7.1$ channels. Similar sites have been suggested for $K_V7.2$ and, to some extent, $K_V7.3$ (Larsson et al., 2020).

PROPOSED INDIRECT PUFA EFFECTS ON K_V7

Besides direct effects, PUFAs may influence K_V7 channels through other mechanisms, including altering bilayer organization and properties or generating active PUFA metabolites. Indication of additional pathways of PUFA modulation of K_V7 channels comes from prolonged exposure (48 h) of $K_V7.1$/KCNE1 channels to DHA or EPA (Moreno et al., 2015). For instance, prolonged DHA or EPA exposure reduces total $K_V7.1$ protein levels in COS7 cells, presumably by inducing protein degradation (Moreno et al., 2015). Prolonged exposure also triggers spatial redistribution of $K_V7.1$/KCNE1 in the membrane, presumably by disruption of lipid rafts (Moreno et al., 2015). It has been speculated that mechanical properties of the membrane (such as thickness and stiffness) may contribute to altered $K_V7.1$/KCNE1 behavior in different membrane microdomains (Moreno et al., 2015). Given that PUFAs regulate other ion channels through modulating the mechanical properties of membranes (Boland and Drzewiecki, 2008), the possible contributions of such indirect PUFA effects on K_V7 channels in different microdomains warrants further studies.

Regarding the influence of active metabolites, AA is central in oxygenase-driven metabolic pathways that generate leukotrienes and prostaglandins (Shimizu and Wolfe, 1990). Treatment of bullfrog sympathetic neurons with an inhibitor of the lipoxygenase pathway reduces I_M and prevents AA-mediated increases in I_M amplitude (Villarroel, 1993; Yu, 1995), presumably by impeding downstream AA metabolites that modulate I_M effects (Yu, 1995). These findings highlight the multifaceted nature of PUFA signaling and the challenges of dissecting underlying mechanisms in more complex cellular systems and longer time scales.

FUTURE DIRECTIONS

Several studies report that micromolar concentrations of PUFAs increase $K_V7.1$-7.3 currents and have provided insights into mechanisms of how acute and prolonged PUFA exposure impacts K_V7 channels. However, there are still several open questions. For instance:

(i) Given the conservation among K_V7 channels of charged residues identified to be crucial to PUFA effects (**Figure 1B**), are the effects and underlying mechanisms of action conserved among all K_V7 isoforms?

(ii) What is the physiological relevance of PUFA effects reported on heterologously expressed K_V7 channels? PUFA have been reported to alter cardiac and neuronal excitability [e.g., by shortening action potential duration and QT interval, and increasing the threshold for action potential firing (e.g., Leaf et al., 2003; Boland and Drzewiecki, 2008; DeGiorgio and Taha, 2016; Liin et al., 2016a; Skarsfeldt et al., 2020)], and vascular tone [by promoting vascular smooth muscle relaxation (e.g., Hoshi et al., 2013b; Limbu et al., 2018)]. However, as PUFAs act

on many types of channels, the extent of Kv7 contribution to such general effects remain to be determined.

(iii) Can a mechanistic understanding of PUFA modulation of K_V7 channels open up new therapeutic avenues? For instance, how viable is modulation of circulating PUFA levels for the tuning of neuronal and cardiac excitability, and what are the prospects of PUFA analogs as pharmacological K_V7 channel activators?

To conclude, PUFAs modulate the activity of K_V7 channels through a range of mechanisms. Studies of heterologously expressed K_V7 channels have revealed important insights into mechanisms underlying K_V7 channel activation via direct PUFA-channel interactions. However, several aspects of PUFA modulation of K_V7 channels remain unclear and require further studies. This is particularly true for comprehending the compounded results of both direct and indirect PUFA effects in differing time scales and cellular systems.

AUTHOR CONTRIBUTIONS

All authors designed the study and wrote the manuscript.

FUNDING

This project has received funding from the European Research Council (ERC) under the European Union's Horizon 2020 research and innovation program (grant agreement No. 850622).

ACKNOWLEDGMENTS

We thank Dr. H. Peter Larsson, University of Miami, and Dr. Fredrik Elinder, Linköping University, for comments on the manuscript.

REFERENCES

Abbott, G. W. (2016). "Chapter 1 - The KCNE family of ion channel regulatory subunits," *Ion Channels in Health and Disease*. G. S. Pitt (Boston, MA: Academic Press), 1–24. doi: 10.1016/b978-0-12-802002-9.00001-7

Barhanin, J., Lesage, F., Guillemare, E., Fink, M., Lazdunski, M., and Romey, G. (1996). K(V)LQT1 and lsK (minK) proteins associate to form the I(Ks) cardiac potassium current. *Nature* 384, 78–80. doi: 10.1038/384078a0

Barrese, V., Stott, J. B., and Greenwood, I. A. (2018). KCNQ-Encoded potassium channels as therapeutic targets. *Annu. Rev. Pharmacol. Toxicol.* 58, 625–648. doi: 10.1146/annurev-pharmtox-010617-052912

Barro-Soria, R., Rebolledo, S., Liin, S. I., Perez, M. E., Sampson, K. J., Kass, R. S., et al. (2014). KCNE1 divides the voltage sensor movement in KCNQ1/KCNE1 channels into two steps. *Nat. Commun.* 5:3750. doi: 10.1038/ncomms4750

Behe, P., Sandmeier, K., and Meves, H. (1992). The effect of arachidonic acid on the M current of NG108-15 neuroblastoma x glioma hybrid cells. *Pflugers. Arch.* 422, 120–128. doi: 10.1007/bf00370411

Bohannon, B. M., Perez, M. E., Liin, S. I., and Larsson, H. P. (2019). omega-6 and omega-9 polyunsaturated fatty acids with double bonds near the carboxyl head have the highest affinity and largest effects on the cardiac IK s potassium channel. *Acta Physiol. (Oxf)* 225:e13186. doi: 10.1111/apha.13186

Bohannon, B. M., Wu, X., Wu, X., Perez, M. E., Liin, S. I., and Larsson, H. P. (2020). Polyunsaturated fatty acids produce a range of activators for heterogeneous IKs channel dysfunction. *J. Gen. Physiol.* 152:e201912396.

Boland, L. M., and Drzewiecki, M. M. (2008). Polyunsaturated fatty acid modulation of voltage-gated ion channels. *Cell Biochem. Biophys.* 52, 59–84. doi: 10.1007/s12013-008-9027-2

Brouwer, I. A., Zock, P. L., Camm, A. J., Bocker, D., Hauer, R. N., Wever, E. F., et al. (2006). Effect of fish oil on ventricular tachyarrhythmia and death in patients with implantable cardioverter defibrillators: the study on omega-3 fatty acids and ventricular arrhythmia (SOFA) randomized trial. *JAMA* 295, 2613–2619.

Chadha, P. S., Jepps, T. A., Carr, G., Stott, J. B., Zhu, H. L., Cole, W. C., et al. (2014). Contribution of kv7.4/kv7.5 heteromers to intrinsic and calcitonin gene-related peptide-induced cerebral reactivity. *Arterioscler. Thromb. Vasc. Biol.* 34, 887–893. doi: 10.1161/atvbaha.114.303405

Chung, D. Y., Chan, P. J., Bankston, J. R., Yang, L., Liu, G., Marx, S. O., et al. (2009). Location of KCNE1 relative to KCNQ1 in the I(KS) potassium channel by disulfide cross-linking of substituted cysteines. *Proc. Natl. Acad. Sci. U.S.A.* 106, 743–748. doi: 10.1073/pnas.0811897106

Conquer, J. A., and Holub, B. J. (1998). Effect of supplementation with different doses of DHA on the levels of circulating DHA as non-esterified fatty acid in subjects of Asian Indian background. *J. Lipid Res.* 39, 286–292.

Cooper, E. C., Aldape, K. D., Abosch, A., Barbaro, N. M., Berger, M. S., Peacock, W. S., et al. (2000). Colocalization and coassembly of two human brain M-type potassium channel subunits that are mutated in epilepsy. *Proc. Natl. Acad. Sci. U.S.A.* 97, 4914–4919. doi: 10.1073/pnas.090092797

Cui, J. (2016). Voltage-dependent gating: novel Insights from KCNQ1 Channels. *Biophys. J.* 110, 14–25. doi: 10.1016/j.bpj.2015.11.023

Dart, C. (2010). Lipid microdomains and the regulation of ion channel function. *J. Physiol.* 588, 3169–3178. doi: 10.1113/jphysiol.2010.191585

DeGiorgio, C. M., and Taha, A. Y. (2016). Omega-3 fatty acids (-3 fatty acids) in epilepsy: animal models and human clinical trials. *Exp. Rev. Neurother.* 16, 1141–1145. doi: 10.1080/14737175.2016.1226135

Doolan, G. K., Panchal, R. G., Fonnes, E. L., Clarke, A. L., Williams, D. A., and Petrou, S. (2002). Fatty acid augmentation of the cardiac slowly activating delayed rectifier current (IKs) is conferred by hminK. *FASEB J.* 16, 1662–1664. doi: 10.1096/fj.02-0084fje

Elinder, F., and Liin, S. I. (2017). Actions and mechanisms of polyunsaturated fatty acids on voltage-gated ion channels. *Front. Physiol.* 8:43. doi: 10.3389/fphys.2017.00043

Feller, S. E. (2008). Acyl chain conformations in phospholipid bilayers: a comparative study of docosahexaenoic acid and saturated fatty acids. *Chem. Phys. Lipids* 153, 76–80. doi: 10.1016/j.chemphyslip.2008.02.013

Fraser, D. D., Whiting, S., Andrew, R. D., Macdonald, E. A., Musa-Veloso, K., and Cunnane, S. C. (2003). Elevated polyunsaturated fatty acids in blood serum obtained from children on the ketogenic diet. *Neurology* 60, 1026–1029. doi: 10.1212/01.wnl.0000049974.74242.c6

Hamilton, J. A. (1998). Fatty acid transport: difficult or easy? *J. Lipid Res.* 39, 467–481.

Holmqvist, M. H., Cao, J., Knoppers, M. H., Jurman, M. E., Distefano, P. S., Rhodes, K. J., et al. (2001). Kinetic modulation of Kv4-mediated A-current by Arachidonic Acid is dependent on potassium channel interacting proteins. *J. Neurosci.* 21, 4154–4161. doi: 10.1523/jneurosci.21-12-04154.2001

Hoshi, T., Tian, Y., Xu, R., Heinemann, S. H., and Hou, S. (2013a). Mechanism of the modulation of BK potassium channel complexes with different auxiliary subunit compositions by the omega-3 fatty acid DHA. *Proc. Natl. Acad. Sci. U.S.A.* 110, 4822–4827. doi: 10.1073/pnas.1222003110

Hoshi, T., Wissuwa, B., Tian, Y., Tajima, N., Xu, R., Bauer, M., et al. (2013b). Omega-3 fatty acids lower blood pressure by directly activating large-conductance Ca2+-dependent K+ channels. *Proc. Natl. Acad. Sci. U.S.A.* 110, 4816–4821. doi: 10.1073/pnas.1221997110

Hou, P., Kang, P. W., Kongmeneck, A. D., Yang, N. D., Liu, Y., Shi, J., et al. (2020). Two-stage electro-mechanical coupling of a KV channel in voltage-dependent activation. *Nat. Commun.* 11, 676.

Jentsch, T. J. (2000). Neuronal KCNQ potassium channels: physiology and role in disease. *Nat. Rev. Neurosci.* 1, 21–30. doi: 10.1038/35036198

Jepps, T. A., Carr, G., Lundegaard, P. R., Olesen, S. P., and Greenwood, I. A. (2015). Fundamental role for the KCNE4 ancillary subunit in Kv7.4 regulation of arterial tone. *J. Physiol.* 593, 5325–5340. doi: 10.1113/jp271286

Jepps, T. A., Chadha, P. S., Davis, A. J., Harhun, M. I., Cockerill, G. W., Olesen, S. P., et al. (2011). Downregulation of Kv7.4 channel activity in primary and

secondary hypertension. *Circulation* 124, 602–611. doi: 10.1161/circulationaha.111.032136

Kharkovets, T., Hardelin, J. P., Safieddine, S., Schweizer, M., El-Amraoui, A., Petit, C., et al. (2000). KCNQ4, a K+ channel mutated in a form of dominant deafness, is expressed in the inner ear and the central auditory pathway. *Proc. Natl. Acad. Sci. U.S.A.* 97, 4333–4338. doi: 10.1073/pnas.97.8.4333

Kubisch, C., Schroeder, B. C., Friedrich, T., Lutjohann, B., El-Amraoui, A., Marlin, S., et al. (1999). KCNQ4, a novel potassium channel expressed in sensory outer hair cells, is mutated in dominant deafness. *Cell* 96, 437–446. doi: 10.1016/s0092-8674(00)80556-5

Larsson, J. E., Karlsson, U., Wu, X., and Liin, S. I. (2020). Combining endocannabinoids with retigabine for enhanced M-channel effect and improved KV7 subtype selectivity. *J. Gen. Physiol.* 152:e202012576.

Larsson, J. E., Larsson, H. P., and Liin, S. I. (2018). KCNE1 tunes the sensitivity of KV7.1 to polyunsaturated fatty acids by moving turret residues close to the binding site. *Elife* 7:e37257.

Leaf, A., Xiao, Y. F., Kang, J. X., and Billman, G. E. (2003). Prevention of sudden cardiac death by n-3 polyunsaturated fatty acids. *Pharmacol. Ther.* 98, 355–377. doi: 10.1016/s0163-7258(03)00039-1

Lerche, C., Scherer, C. R., Seebohm, G., Derst, C., Wei, A. D., Busch, A. E., et al. (2000). Molecular cloning and functional expression of KCNQ5, a potassium channel subunit that may contribute to neuronal M-current diversity. *J. Biol. Chem.* 275, 22395–22400. doi: 10.1074/jbc.m002378200

Liin, S. I., Karlsson, U., Bentzen, B. H., Schmitt, N., and Elinder, F. (2016a). Polyunsaturated fatty acids are potent openers of human M-channels expressed in *Xenopus laevis* oocytes. *Acta Physiol. (Oxf)* 218, 28–37.

Liin, S. I., Larsson, J. E., Barro-Soria, R., Bentzen, B. H., and Larsson, H. P. (2016b). Fatty acid analogue N-arachidonoyl taurine restores function of IKs channels with diverse long QT mutations. *Elife* 5:e20272.

Liin, S. I., Silvera Ejneby, M., Barro-Soria, R., Skarsfeldt, M. A., Larsson, J. E., Starck Harlin, F., et al. (2015). Polyunsaturated fatty acid analogs act antiarrhythmically on the cardiac IKs channel. *Proc. Natl. Acad. Sci. U.S.A.* 112, 5714–5719. doi: 10.1073/pnas.1503488112

Liin, S. I., Yazdi, S., Ramentol, R., Barro-Soria, R., and Larsson, H. P. (2018). Mechanisms underlying the dual effect of polyunsaturated fatty acid analogs on Kv7.1. *Cell Rep.* 24, 2908–2918. doi: 10.1016/j.celrep.2018.08.031

Limbu, R., Cottrell, G. S., and McNeish, A. J. (2018). Characterisation of the vasodilation effects of DHA and EPA, n-3 PUFAs (fish oils), in rat aorta and mesenteric resistance arteries. *PLoS one* 13:e0192484. doi: 10.1371/journal.pone.0192484

Miceli, F., Soldovieri, M. V., Ambrosino, P., Manocchio, L., Mosca, I., and Taglialatela, M. (2018). Pharmacological targeting of neuronal Kv7.2/3 channels: a focus on chemotypes and receptor sites. *Curr. Med. Chem.* 25, 2637–2660. doi: 10.2174/0929867324666171012122852

Miceli, F., Soldovieri, M. V., Hernandez, C. C., Shapiro, M. S., Annunziato, L., and Taglialatela, M. (2008). Gating consequences of charge neutralization of arginine residues in the S4 segment of K(v)7.2, an epilepsy-linked K+ channel subunit. *Biophys. J.* 95, 2254–2264. doi: 10.1529/biophysj.107.128371

Moreno, C., de la Cruz, A., Oliveras, A., Kharche, S. R., Guizy, M., Comes, N., et al. (2015). Marine n-3 PUFAs modulate IKs gating, channel expression, and location in membrane microdomains. *Cardiovasc. Res.* 105, 223–232. doi: 10.1093/cvr/cvu250

Neyroud, N., Tesson, F., Denjoy, I., Leibovici, M., Donger, C., Barhanin, J., et al. (1997). A novel mutation in the potassium channel gene KVLQT1 causes the Jervell and Lange-Nielsen cardioauditory syndrome. *Nat. Genet.* 15, 186–189. doi: 10.1038/ng0297-186

Panaghie, G., and Abbott, G. W. (2007). The role of S4 charges in voltage-dependent and voltage-independent KCNQ1 potassium channel complexes. *J. Gen. Physiol.* 129, 121–133. doi: 10.1085/jgp.200609612

Sanguinetti, M. C., Curran, M. E., Zou, A., Shen, J., Spector, P. S., Atkinson, D. L., et al. (1996). Coassembly of K(V)LQT1 and minK (IsK) proteins to form cardiac I(Ks) potassium channel. *Nature* 384, 80–83. doi: 10.1038/384080a0

Schwake, M., Athanasiadu, D., Beimgraben, C., Blanz, J., Beck, C., Jentsch, T. J., et al. (2006). Structural determinants of M-type KCNQ (Kv7) K+ channel assembly. *J. Neurosci.* 26, 3757–3766. doi: 10.1523/jneurosci.5017-05.2006

Schwake, M., Jentsch, T. J., and Friedrich, T. (2003). A carboxy-terminal domain determines the subunit specificity of KCNQ K+ channel assembly. *EMBO Rep.* 4, 76–81. doi: 10.1038/sj.embor.embor715

Shimizu, T., and Wolfe, L. S. (1990). Arachidonic acid cascade and signal transduction. *J. Neurochem.* 55, 1–15. doi: 10.1111/j.1471-4159.1990.tb08813.x

Skarsfeldt, M. A., Liin, S. I., Larsson, H. P., and Bentzen, B. H. (2020). Polyunsaturated fatty acid-derived IKs channel activators shorten the QT interval ex-vivo and in-vivo. *Acta Physiol. (Oxf)* e13471. doi: 10.1111/apha.13471

Sun, J., and MacKinnon, R. (2017). Cryo-EM Structure of a KCNQ1/CaM complex reveals insights into congenital long QT syndrome. *Cell* 169, 1042–1050.

Sun, J., and MacKinnon, R. (2020). Structural basis of human KCNQ1 modulation and gating. *Cell* 180, 340–347.

Sun, X., Zhou, D., Zhang, P., Moczydlowski, E. G., and Haddad, G. G. (2007). Beta-subunit-dependent modulation of hSlo BK current by arachidonic acid. *J. Neurophysiol.* 97, 62–69. doi: 10.1152/jn.00700.2006

Taylor, K. C., Kang, P. W., Hou, P., Yang, N. D., Kuenze, G., Smith, J. A., et al. (2020). Structure and physiological function of the human KCNQ1 channel voltage sensor intermediate state. *Elife* 9:e53901.

Taylor, K. C., and Sanders, C. R. (2017). Regulation of KCNQ/Kv7 family voltage-gated K(+) channels by lipids. *Biochim. Biophys. Acta Biomembr.* 1859, 586–597. doi: 10.1016/j.bbamem.2016.10.023

Tian, Y., Aursnes, M., Hansen, T. V., Tungen, J. E., Galpin, J. D., Leisle, L., et al. (2016). Atomic determinants of BK channel activation by polyunsaturated fatty acids. *Proc. Natl. Acad. Sci. U.S.A.* 113, 13905–13910. doi: 10.1073/pnas.1615562113

Valenzuela, C. (2016). M-channels and n-3 polyunsaturated fatty acids: role in pain and epilepsy. *Acta Physiol. (Oxf)* 218, 7–9.

Villarroel, A. (1993). Suppression of neuronal potassium A-current by arachidonic acid. *FEBS Lett.* 335, 184–188. doi: 10.1016/0014-5793(93)80726-b

Villarroel, A. (1994). On the role of arachidonic acid in M-current modulation by muscarine in bullfrog sympathetic neurons. *J. Neurosci.* 14(11 Pt 2), 7053–7066. doi: 10.1523/jneurosci.14-11-07053.1994

Wang, H. S., Pan, Z., Shi, W., Brown, B. S., Wymore, R. S., Cohen, I. S., et al. (1998). KCNQ2 and KCNQ3 potassium channel subunits: molecular correlates of the M-channel. *Science* 282, 1890–1893. doi: 10.1126/science.282.5395.1890

Xu, Y., Wang, Y., Meng, X. Y., Zhang, M., Jiang, M., Cui, M., et al. (2013). Building KCNQ1/KCNE1 channel models and probing their interactions by molecular-dynamics simulations. *Biophys. J.* 105, 2461–2473. doi: 10.1016/j.bpj.2013.09.058

Yazdi, S., Stein, M., Elinder, F., Andersson, M., and Lindahl, E. (2016). The molecular basis of polyunsaturated fatty acid interactions with the shaker voltage-gated potassium channel. *PLoS Comput. Biol.* 12:e1004704. doi: 10.1371/journal.pcbi.1004704

Yu, S. P. (1995). Roles of arachidonic acid, lipoxygenases and phosphatases in calcium-dependent modulation of M-current in bullfrog sympathetic neurons. *J. Physiol.* 487, 797–811. doi: 10.1113/jphysiol.1995.sp020919

Zaydman, M. A., and Cui, J. (2014). PIP2 regulation of KCNQ channels: biophysical and molecular mechanisms for lipid modulation of voltage-dependent gating. *Front. Physiol.* 5:195. doi: 10.3389/fphys.2014.00195

Zaydman, M. A., Kasimova, M. A., McFarland, K., Beller, Z., Hou, P., Kinser, H. E., et al. (2014). Domain-domain interactions determine the gating, permeation, pharmacology, and subunit modulation of the IKs ion channel. *Elife* 3:e03606.

Conflict of Interest: A patent application (#62/032,739) including a description of the interaction of charged lipophilic compounds with the $K_V7.1$ channel has been submitted by the University of Miami with SL identified as one of the inventors.

The remaining authors declare that the research was conducted in the absence of any commercial or financial relationships that could be construed as a potential conflict of interest.

frontiers in Physiology

REVIEW
published: 19 June 2020
doi: 10.3389/fphys.2020.00688

Pharmacological Manipulation of K_V7 Channels as a New Therapeutic Tool for Multiple Brain Disorders

*Fabio A. Vigil, Chase M. Carver and Mark S. Shapiro**

Department of Cellular and Integrative Physiology, University of Texas Health San Antonio, San Antonio, TX, United States

K_V7 ("M-type," KCNQ) K^+ currents, play dominant roles in controlling neuronal excitability. They act as a "brake" against hyperexcitable states in the central and peripheral nervous systems. Pharmacological augmentation of M current has been developed for controlling epileptic seizures, although current pharmacological tools are uneven in practical usefulness. Lately, however, M-current "opener" compounds have been suggested to be efficacious in preventing brain damage after multiple types of insults/diseases, such as stroke, traumatic brain injury, drug addiction and mood disorders. In this review, we will discuss what is known to date on these efforts and identify gaps in our knowledge regarding the link between M current and therapeutic potential for these disorders. We will outline the preclinical experiments that are yet to be performed to demonstrate the likelihood of success of this approach in human trials. Finally, we also address multiple pharmacological tools available to manipulate different K_V7 subunits and the relevant evidence for translational application in the clinical use for disorders of the central nervous system and multiple types of brain insults. We feel there to be great potential for manipulation of K_V7 channels as a novel therapeutic mode of intervention in the clinic, and that the paucity of existing therapies obligates us to perform further research, so that patients can soon benefit from such therapeutic approaches.

Keywords: K_V7, potassium channels, stroke, traumatic brain injury, drug addiction, anxiety, bipolar disorder

OPEN ACCESS

Edited by:
Francesco Miceli,
University of Naples Federico II, Italy

Reviewed by:
Edward C. Cooper,
Baylor College of Medicine,
United States
Naoto Hoshi,
University of California, Irvine,
United States

****Correspondence:***
Mark S. Shapiro
shapirom@uthscsa.edu

Specialty section:
This article was submitted to Membrane Physiology and Membrane Biophysics, a section of the journal Frontiers in Physiology

Received: *21 April 2020*
Accepted: *27 May 2020*
Published: *19 June 2020*

Citation:
Vigil FA, Carver CM and Shapiro MS (2020) Pharmacological Manipulation of K_V7 Channels as a New Therapeutic Tool for Multiple Brain Disorders. Front. Physiol. 11:688. doi: 10.3389/fphys.2020.00688

INTRODUCTION

K_V7 channels, also known as M-type, or KCNQ channels, are low-threshold voltage gated K^+ channels first described almost 40 years ago as underlying the cholinergic slow excitatory post-synaptic potential in sympathetic neurons (Brown and Adams, 1980; Constanti and Brown, 1981). K_V7 channels can be composed of homo- or heterotetrameric assembly of $K_V7.1$-$K_V7.5$ subunits; however, only $K_V7.2$-5 are expressed in the nervous system (Jentsch, 2000). In a wide variety of central and peripheral neurons, M-channels play a significant role in controlling active and passive discharge properties, including action potential threshold, resting membrane potential, spike afterhyperpolarization (AHPs), and shunting conductance (Jones et al., 1995; Yue and Yaari, 2004; Peters et al., 2005; Shah et al., 2008). Consistent with that role, channels composed of $K_V7.2$ and 7.3 in varying composition are mainly localized in brain to the axon initial segment (Cooper et al., 2001; Pan et al., 2006; Rasmussen et al., 2007), adjacent to the Na_V channels that generate action potentials. Since M channels deactivate slowly, they contribute to AHP currents

(Tzingounis and Nicoll, 2008). Excessive K_v7-channel suppression or channel dysfunction often leads to seizures or other epileptic syndromes (Biervert et al., 1998; Singh et al., 1998; Ambrosino et al., 2015; Miceli et al., 2015; Greene and Hoshi, 2017), leading to the idea that proper M-channel function acts as a "brake" to prevent excess hyperexcitability (Maljevic et al., 2008; Soldovieri et al., 2011), by accumulated M-current activation increasing the threshold for firing (Peters et al., 2005; Tzingounis and Nicoll, 2008) and increasing the interspike interval (Lawrence et al., 2006).

M current is so named for its discovery as a K^+ conductance suppressed by stimulation of muscarinic acetylcholine receptors in sympathetic ganglia neurons (Brown et al., 1995). In those cells, the action is via $G_{q/11}$-mediated activation of phospholipase C, which hydrolyzes phosphatidylinositol-4,5-bisphospate (PIP_2), reducing its abundance in the membrane (Haley et al., 1998; Suh and Hille, 2005), and by activation of protein kinase C (Hoshi et al., 2003). Since PIP_2 binding is required for M-channel opening (Zhang et al., 2003; Li et al., 2005; Suh et al., 2006; Sun and MacKinnon, 2020), its depletion reduces M-current amplitudes in a voltage-independent manner (Shapiro et al., 2000; Nakajo and Kubo, 2005; Choveau et al., 2018). However, in those same neurons, other $G_{q/11}$-coupled receptors suppress M current via release of Ca^{2+} from IP_3-gated stores, loading of Ca^{2+} into calmodulin (Gamper and Shapiro, 2003; Winks et al., 2005; Zaika et al., 2007) and changes in configuration of CaM molecules bound to the proximal carboxy terminus of $K_v7.1$-7.5 subunits (Yus-Najera et al., 2002; Haitin and Attali, 2008) in varying configurations (Haitin and Attali, 2008; Kosenko and Hoshi, 2013; Strulovich et al., 2016; Sun and MacKinnon, 2017; Chang et al., 2018; Archer et al., 2019).

Pharmacological manipulation of M current has been studied extensively as a therapeutic option for epilepsy (Kapetanovic et al., 1995; Rostock et al., 1996; Armand et al., 1999; Miceli et al., 2008; Amabile and Vasudevan, 2013; Splinter, 2013) and for analgesia (Blackburn-Munro and Jensen, 2003; Munro and Dalby-Brown, 2007; Szelenyi, 2013; Hayashi et al., 2014; Abd-Elsayed et al., 2015; Zheng et al., 2015; Busserolles et al., 2016; Wang and Li, 2016; Du et al., 2018; Li et al., 2019). Retigabine (RTG) was developed some 20 years ago as an anti-epileptic drug that acts by augmenting M current (Main et al., 2000; Rundfeldt and Netzer, 2000; Tatulian and Brown, 2003; Wuttke et al., 2005) and is widely used in research labs. Retigabine induces a hyperpolarizing shift of $K_v7.2$-5 channel activation (but not $K_v7.1$), resulting in current enhancement at potentials positive to −80 mV (Tatulian et al., 2001). However, although FDA-approved, its long-term side-effects (e.g., dilation of smooth muscle, blue tinting to skin over time) has led to its withdrawal from the market. Recently, however, a plethora of more selective "next-generation" M channel-targeting compounds have been developed. That may make manipulation of M current a modality used for myriad of brain disorders and insults, besides as anti-convulsants. In this review we will explore some of the possible new therapeutic uses of pharmacological M-current manipulation in treating brain dysfunction.

M CURRENT AND NEUROVASCULAR INJURIES

Two research groups first explored the role of M current during metabolic stress induced by oxygen and glucose deprivation (OGD) using cell culture models. They observed RTG-induced enhancement of M current to significantly reduce neuronal death in organotypic cultures of hippocampal slices subjected to 30 min of OGD, whereas M-current block with XE991 (Zaczek et al., 1998) resulted in increased neuronal death (Boscia et al., 2006; Gamper et al., 2006). Similar observations were reported by Barrese et al. (2015), using rat caudate brain slices. All these groups observed that OGD-induced damage was reduced by pharmacological M-current augmentation. Therefore, it seemed possible that pharmacological M-current enhancement could reduce brain damage after a stroke. Indeed, our group showed M-current augmentation to be neuroprotective after occlusive stroke. M-current augmentation strongly reduced stroke-induced neuronal death, the maladaptive immune response, and locomotor deficits (Bierbower et al., 2015). In a rat model, RTG treatment impaired stroke-induced increases in blood brain barrier (BBB) permeability, opening of tight junctions from microvascular endothelial cells, and cerebral infarct area (Zhao et al., 2018). An evident connection between stroke and the previous OGD models is that both involve cellular metabolic stress.

More recently, Vigil et al. (2020) also showed pharmacological M-current augmentation to prevent brain damage after traumatic brain injury (TBI). With only one *i.p.* injection of RTG 30 min post-injury, we observed significant reductions in post-traumatic seizures and seizure susceptibility, cellular energetic demand, the maladaptive inflammatory/immune response, breakdown of the BBB, and cell death (Vigil et al., 2020). Thus, we believe that prevention of initial TBI-induced hyperexcitability, even before a post-traumatic seizure can occur, severely hampered the damaging TBI-induced cascade of events. Interestingly, an increase in $K_v7.2$ expression in TBI-subjected animals treated with RTG was observed in cortical and dentate gyrus hippocampal cells up to 6 days after TBI, although this transcriptional up-regulation is likely not to last much longer than 10 days (Carver et al., 2020; Vigil et al., 2020). As RTG has a half-life of 2 h in animals (Valeant Pharmaceuticals), it is reasonable to assume that M-current augmentation facilitated a later increase in $K_v7.2$ transcription in neurons that survive the insult. This elevated expression of the *kcnq2* gene could represent a second longer-term therapeutic window, as one could take advantage of the increased expression of $K_v7.2$ channels to maximize the effects of therapeutic treatment. Recently, acute RTG administration was also reported to improve pain and motor neuron recovery after spinal-cord injury (SCI). Wu et al. (2020) observed RTG treatment to be effective up to 3 days after SCI if local delivery of RTG was performed by a pump implant.

Based on the above, a reasonable hypothesis is that pharmacological M-current augmentation reduces neuronal firing after TBI, SCI and, stroke, and as in the OGD model, reduces cellular energy demand. Therefore, reducing Na^+/K^+ ATPase activity, osmotic unbalance, and cell lysis.

This hypothesis is summarized in **Figure 1**. However, we are only beginning to use *in vivo* models to confirm the cause of cell death after post-traumatic seizures. Moreover, the various elements of the injury-induced cascade of events are likely to further cross-activate each other resulting in the secondary injury often observed in TBI (Beez et al., 2017; Simon et al., 2017), SCI (Ahuja et al., 2017), and stroke (Hemphill et al., 2015; Beez et al., 2017). By initially preventing this cascade of events at the start, M-current augmentation should have long-lasting beneficial effects in these neurovascular injury events (**Figure 1**).

The secondary effects of TBI can be observed in epileptogenesis in which the injury converts a healthy brain into a brain in which synchronous neuronal activity and seizures are more likely to occur. Traumatic brain injury is responsible for 20% of symptomatic epilepsies and 5–6% of all epilepsy (Garga and Lowenstein, 2006). Higher risk of post-traumatic epilepsy may persist for up to a decade after an initial TBI, but an indeterminate latent period can last between months and years without any presentation of overt seizures (Frey, 2003; Christensen et al., 2009; Lowenstein, 2009). Hence, prior to seizure presentation, TBI must induce pathophysiological changes in the brain that increase seizure susceptibility and epileptogenesis. Post-traumatic epileptogenesis entails a wide scope of regulatory plasticity from many different ion channels, including $GABA_A$ receptors, HCN channels, and K_v7 channels, which often provide inhibitory opposition in response to neuronal hyperexcitability. However, both excitatory and inhibitory circuit reorganizations after TBI lead to maladaptive synaptic connectivity, contributing to epileptogenesis (Hunt et al., 2013). Due to the capacity of M-channel openers to act as an inhibitory force to the brain during susceptible periods of the post-traumatic cascade, they could provide control, and possibly prevention, of TBI-induced epilepsy.

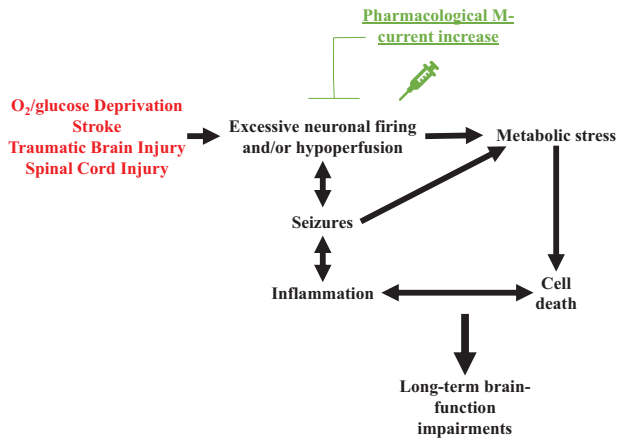

FIGURE 1 | Schematic representation of the over-arching hypothesis proposed to explain the therapeutic effects of pharmacological M-current augmentation after O_2/glucose deprivation, stroke, traumatic brain injury and spinal cord injury. These neurovascular insults all share brain hypoperfusion and/or excessive neuronal firing, leading to cellular metabolic stress, cell lysis.Cell death hyper-activates the immune system of the brain, increasing insult-related inflammation. If uncontrolled,this hyper-inflammation may result in further cell death, creating a deleterious cycle of positive feedback between these events. Insult-induced excessive neuronal firing also promotes seizures, which further increase cellular metabolic stress and enhanced inflammatory responses, facilitating the occurrence of more seizures. Acute pharmacological M-current increase post-insult stops this cascade of events by reducing the initial increased cellular energy demand.

Another role played by K_v7 channels, specifically $K_v7.4$ and $K_v7.5$, are as regulators of excitability in blood vessels smooth muscle (Yeung et al., 2008; Joshi et al., 2009). Thus, it is possible that part of the beneficial effect of M-current augmentation might be ascribed to an acute increase in blood flow that would lead to a greater supply of glucose and O_2 to support metabolic demands. However, the dilation of bladder smooth muscle, leading to urinary incontinence, has been suggested to be due to RTG actions on afferent nerve activity, rather than direct regulation of bladder myocyte contraction (Tykocki et al., 2019). In TBI and stroke models, increases in BBB permeability and infarct area were reduced by RTG treatment (Zhao et al., 2018; Vigil et al., 2020). Zhao et al. (2018) suggest that RTG may reduce BBB permeability by inhibition of injury-induced increase in expression of protein kinase C delta (PKCδ) and of the extracellular matrix proteinases, MMP-2 and MMP-9. Phosphorylation by PKCδ activates MMP-2/9, which degrades tight junction-associated proteins of cerebral vascular endothelial cells, resulting in increased BBB permeability. How RTG treatment reduces injury-induced expression of MMP-2/9 and PKCδ is unknown. Additionally, more experiments measuring brain blood flow and BBB permeability at different time points after injury in animals treated with RTG are still necessary to further investigate this matter.

An additional confound to consider is that RTG seems to affect other ion channels besides K_v7 channels. Retigabine at 10 μM concentration reduces $K_v2.1$ current by ∼20% and at 100 μM, RTG inhibits ∼80% of $K_v2.1$ current (Stas et al., 2016). Retigabine at 10 μM also reduces current throughout L-type voltage-gated Ca^{2+} channels by >50% (Mani et al., 2013). Experimental evidence shows that RTG also acts on $GABA_A$ receptors at concentrations above 10 μM (Treven et al., 2015). Inhibition of these channels may also play a role in the aforementioned therapeutic effects. For treatment of epilepsy in patients, the mean free average plasma concentrations of RTG is approximately 0.83 μM and maximum mean free plasma concentrations (Cmax) is approximately 1 μM (Gunthorpe et al., 2012). Hence, if the same doses are used for treatment of other diseases/injuries, off-target effects are likely to be avoided.

M CURRENT AND DRUG ADDICTION

Alcohol Addiction

One of the first demonstrations of the relationship between M current and drugs of abuse centers on alcohol addiction. Moore et al. (1990) showed that M current from hippocampal CA1 pyramidal neurons was inhibited by ethanol. In that same year, M current was recorded for the first time in ventral

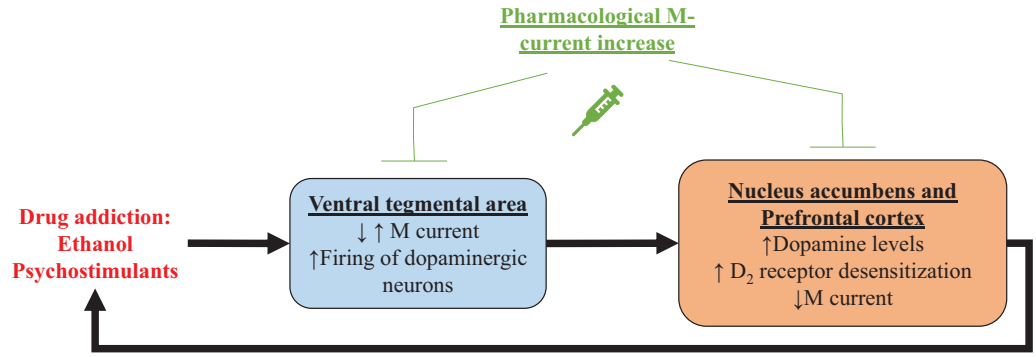

FIGURE 2 | Shown is a proposed mechanism by which drug addiction may involve M current. Psychostimulant-induced increase in dopamine levels within the ventral tegmental area (VTA)could correlate with decreased M current in dopaminergic neurons, and/or increased M current in GABAergic neurons. In either case, increase firing of dopaminergic neurons in the ventral tegmental area releases more dopamine in the nucleus accumbens and the prefrontal cortex, inducing reward. Prolonged increases in dopamine levels result in desensitization of dopamine receptors. Concomitantly, M current is reduced in nucleus accumbens and prefrontal cortex, possibly caused by dopamine receptor desensitization.All of these addiction-induced alterations lead to increased drug intake, creating a deleterious cycle, which can be broken by pharmacological M-current increases in all of these brain regions.

tegmental area (VTA) neurons (Lacey et al., 1990), a region that plays a key role in reward, mood and drug addiction (Di Chiara and Imperato, 1988; Lammel et al., 2012; Morales and Pickel, 2012), including to alcohol (Gessa et al., 1985; Rodd-Henricks et al., 2000). Koyama et al. (2007) showed that ethanol increases spontaneous firing frequency and suppresses M current in VTA dopaminergic neurons, with a correlation between the two actions. Ethanol seems to inhibit $K_v7.2/7.3$ heteromers by a PIP_2-related mechanism (Kim et al., 2019). Ethanol has also been shown to reduce $K_v7.2$ trafficking to the membrane in neurons of the nucleus accumbens (NAc; McGuier et al., 2016), a region that is heavily innervated by the VTA and fundamental for reward and drug addiction (Weiss et al., 1993; Robinson and Berridge, 2003; Morales and Pickel, 2012). Retigabine injection, either systemically or into the NAc, significantly reduced voluntary ethanol consumption in rats, without any significant effect in sucrose or water consumption, whereas injection of XE991 increased it (Knapp et al., 2014; McGuier et al., 2016, 2018). Finally, systemic treatment with the $K_v7.2$ and $K_v7.4$ opener, ML213 (Yu et al., 2010), also reduced ethanol intake in rats (McGuier et al., 2018). Taken together, this evidence suggests regulation of M current to be linked to alcoholism, and that M-current augmentation may represent a mode of therapeutic intervention to treat alcoholism disease (**Figure 2**).

Psychostimulant Addiction

Pharmacological M-current augmentation has also been tested as a treatment for addiction to the psychostimulants, cocaine, methylphenidate (Ritalin) and phencyclidine (PCP) in rat models (Hansen et al., 2007). Retigabine injection was shown to significantly reduce cocaine, methylphenidate and PCP-induced locomotor activity and c-Fos expression in the NAc and the primary motor cortex. Retigabine treatment also impaired methylphenidate-induced overflow of dopamine in the striatum (Hansen et al., 2007). More recently, Parrilla-Carrero et al. (2018) showed that training to self-administer cocaine reduced spike frequency adaptation (SFA) and AHPs in a subpopulation of prelimbic prefrontal cortex (PL-PFC) neurons. This increase in excitability was resistant to extinction training and enhanced by a cued reinstatement test. These neurons also show decreased M current amplitudes and reduced sensitivity to dopamine. *Ex vivo* treatment with RTG restored the SFA and AHPs of these PL-PFC neurons. Moreover, RTG injection directly into the PL-PFC was shown to reduce reinstatement-induced drug-seeking behavior (Parrilla-Carrero et al., 2018), a model of relapse in rodents. Psychostimulants are known to increase dopamine levels in the brain, resulting in desensitization of D_2 receptors (D_2Rs; Volkow et al., 2010; Juarez and Han, 2016). Experiments with heterologously expressed dopamine D_2R and $K_v7.1$-7.4 channels revealed D_2R stimulation to increase M current in a mechanism involving G proteins of the $G_{o/i}$ subtype (Ljungstrom et al., 2003). Hence, it is possible that the decrease of M-current amplitudes observed with psychostimulants is related to desensitization of D_2Rs, involving diminished D_2R facilitation of K_v7 channel opening (**Figure 2**). This hypothesis could explain the hyperexcitability observed in VTA and PL-PFC. Reduction in membrane levels of K_v7 channels could also play a role in psychostimulant-induced reduction of M current amplitudes.

In brief, addiction to both ethanol and psychostimulants seem to result in reduced M-current expression and/or amplitudes, and this reduction may be related to enhanced drug-seeking behavior (**Figure 2**). Indeed, pharmacological M-current augmentation has shown beneficial effects in a number of addiction models. We believe the VTA to be an ideal target for the use of pharmacological M-current augmentation as a novel treatment for addiction, although we do not yet know if the mechanism of action would be due to changes in the excitability of VTA dopaminergic neurons, GABAergic neurons, or both. Ventral tegmental area projections are the main source of dopamine in all the brain regions mentioned above (Ikemoto, 2007; Ferreira et al., 2008; Hosp et al., 2011; Morales and Pickel,

2012; Han et al., 2017). Even though RTG injection into the VTA does reduce ethanol consumption (McGuier et al., 2018), for example, intra-VTA injections are not of course feasible clinically. Nonetheless, the unique composition of K_v7 channels in the VTA could represent a therapeutic opportunity. Ventral tegmental area expresses high levels of neuronal $K_v7.4$ subunits (Li et al., 2017), compared to neurons from other regions in the brain, in which $K_v7.4$ has little to no expression (Kharkovets et al., 2000; Saganich et al., 2001; Greene and Hoshi, 2017). This could allow for the use of drugs that specifically target $K_v7.4$, such as fasudil (Li et al., 2017), as a treatment for addiction. However, continuous pharmacological M-current augmentation through $K_v7.4$ channels is likely to induce hearing and blood pressure problems (Kharkovets et al., 2000; Kharkovets et al., 2006; Yeung et al., 2008; Joshi et al., 2009). Thus, more preclinical studies are necessary for pharmacological M-current augmentation to be used as a treatment for drug addiction.

M CURRENT AND MOOD DISORDERS

Depression

The VTA also plays a major role in mood disorders such as depression (Nestler and Carlezon, 2006; **Figure 3**), a widespread chronic illness characterized by low mood, lack of energy, sadness, and anhedonia (Cui, 2015). Pharmacological M-current augmentation, either systemically or in the VTA, reduces depression-like behavior in the social defeat depression mouse model, measured by different depression paradigms (Friedman et al., 2016). Additionally, intra-VTA viral vector transfection of $K_v7.3$ channels also reduced depression like behavior, as did anterograde expression of $K_v7.3$ in the NAc via intra-VTA injections of viral vector (Friedman et al., 2016). Li et al. (2017) observed that systemic pharmacological augmentation of $K_v7.4$ channels with fasudil also reduced depression-like behavior and excitability of VTA neurons in the social defeat depression mice model.

Bipolar Disorder

Bipolar disorder is a severe chronic mood dysfunction that is characterized by oscillation between episodes of depression and of mania (American Psychiatric Association, 2013). During manic episodes, patients experience euphoria, hyperactivity, and high levels of risk-taking behavior (American Psychiatric Association, 2013). In rodents, manic episodes can be modeled by injection of amphetamine (AMPH), combined with the benzodiazepine, chlordiazepoxide (CDP). The combination of these drugs induces hyperactivity and this phenotype can be examined with drugs used for treating bipolar disorder in the clinic, such as lithium (Dencker et al., 2008; Redrobe and Nielsen, 2009). M-current augmentation has also displayed beneficial effects in rodent models of mania (**Figure 3**). Studies have found that administration of RTG 30 min before testing impaired AMPH + CDP-induced hyperactivity with no effects on basal locomotor activity (Dencker et al., 2008). Redrobe and Nielsen (2009) observed that enhancement of M current with ICA-27243, which selectively augments currents from $K_v7.2/7.3$ channels, also reduced AMPH + CDP-induced hyperactivity. On the other hand, enhancement of $K_v7.4$-7.5 currents by BMS-204352 did not have significant anti-manic effects. Further studies using the AMPH + CDP model showed RTG to reduce the AMPH + CDP-induced increase in cellular metabolic demand in the thalamus, striatum and retrosplenial cortex (Kristensen et al., 2012). Furthermore, intravenous injection of RTG was shown to reduce AMPH-induced locomotor activity, neuronal firing in the VTA, and dopamine release in the NAc, whereas XE991 had the opposite effect (Sotty et al., 2009). Retigabine was also shown to

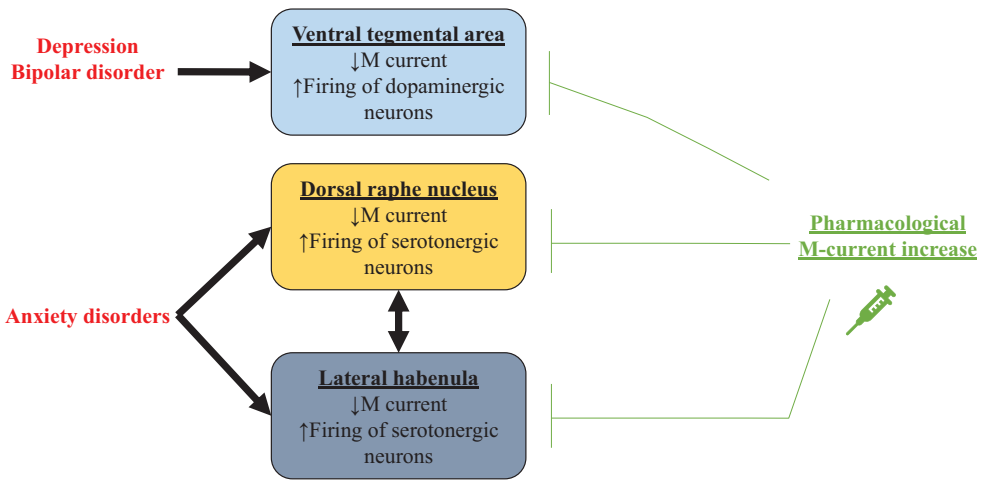

FIGURE 3 | Schematic representation showing how decreased M current could be related to mood disorders. In depression and bipolar disorder, impaired M current in dopaminergic neurons of the ventral tegmental area (VTA) results in excessive firing. For anxiety disorders, M current is decreased in serotonergic neurons of the dorsal raphe nucleus and the lateral habenula. Pharmacological M-current increase in these regions could thus be used as a therapeutic tool for treating these mood disorders.

impair sensitization after multiple AMPH injections in rodents (Dencker and Husum, 2010).

A new genetic dimension involves glycogen synthase kinase 3 beta (GSK3β), which is best known for intra-nuclear re-phosphorylation of the transcription factor, nuclear factor of activated T-lymphocytes (NFAT), which despite its name, is ubiquitous in brain and critical to synaptic plasticity (Graef et al., 1999). Retigabine was found to increase phosphorylation of GSK3β in hippocampus and in the pre-frontal cortex (Kristensen et al., 2012). Such phosphorylation of GSK3β at serine 9 reduces kinase activity, similar to the effect of standard anti-manic agents, such as lithium (Stambolic et al., 1996; De Sarno et al., 2002). Using *in vitro* studies, GSK3β was seen to phosphorylate $K_v7.2$ subunits, suppressing M current and lithium impairs this phosphorylation, rescuing M current (Borsotto et al., 2007). This relationship could offer a plausible novel target for the treatment of bipolar disorder.

Valproic acid (VPA) is an anti-epileptic agent commonly used in the clinic as a mood stabilizer for treatment of patients with bipolar disorder (Chiu et al., 2013; Cipriani et al., 2013). Using *in vitro* and *in vivo* mice models, part of the antiepileptic effect of VPA was shown to be due to inhibition of muscarinic-induced suppression of M current and to be dependent of $K_v7.2$ phosphorylation at S558 (Kay et al., 2015; Greene et al., 2018). It is possible that the beneficial effect of VPA as a mood stabilizer may also be related to drug-induced M-current increases. Nonetheless, VPA has various mechanism of action that are not related to M current (Tomson et al., 2016; Collins-Yoder and Lowell, 2017). Therefore, a direct link between VPA-induced facilitation of M current and its effect as a mood stabilizer remains to be proven.

In humans, associations between bipolar disorder and single nucleotide polymorphisms (SNPs) in the *kcnq2* gene have been found (Borsotto et al., 2007; Judy et al., 2013). These SNPs disturb the interaction of $K_v7.2$ with ankyrin G (Borsotto et al., 2007) and protein phosphatase 2A (Judy et al., 2013), which could impair channel assembly and dephosphorylation, respectively. Finally, bipolar patients have decrease methylation of exon 11 in the *kcnq3* gene, resulting in lower expression of $K_v7.3$ (Kaminsky et al., 2015).

Anxiety

Both BMS-204352 and RTG have anxiolytic-like effects in the zero-maze and marble-burying rodent paradigms. Those effects were blocked by XE991 without any observed motor alterations, supporting pharmacological M-current enhancement as an anxiolytic treatment (Korsgaard et al., 2005). Anxiolytic-like dose-dependent effects of RTG were also observed in the conditioned emotional-response paradigm (Munro et al., 2007). As proposed by Hansen et al. (2008), the anxiolytic-like effects of BMS-204352, observed by Korsgaard et al. (2005), suggest $K_v7.4$ and 7.5 to play an important role in anxiety. Immunostaining experiments show $K_v7.4$ channels to be highly expressed in serotonergic neurons of the dorsal raphe nucleus (DRN; Hansen et al., 2008; Zhao et al., 2017), a region of the brain known to play a central role in anxiety regulation (Graeff et al., 1997; Lowry et al., 2008). For example, increased activity of serotonergic neurons from the DRN are observed in rodent models of induced anxiety (Maier and Watkins, 2005). The excitability of serotonergic neurons from the DRN can be manipulated by pharmacological and genetic manipulation of $K_v7.4$ (Zhao et al., 2017). Hence, pharmacological M-current augmentation may have anxiolytic effects due to an increase in M current composed of $K_v7.4$ homomers in serotonergic DRN neurons, resulting in reduced firing (**Figure 3**). Corroborating with this hypothesis, pharmacological M-current augmentation has been shown to reduce preoperative anxiety of human patients (Yadav et al., 2017). M current in the lateral habenula (LHb) also seems to play a role in anxiety disorders. Hyperexcitability in LHb was observed in a mouse model of ethanol withdrawal, concomitant with reduced M current, specifically from $K_v7.2$ and 7.3. Additionally, infusion of RTG in the LHb impaired ethanol withdrawal-induced anxiety behavior (Kang et al., 2017). Curiously, intra-LHb injection of SB242084, an antagonist of the serotonin receptor 5-HT_{2C}, also reduced ethanol withdrawal-induced anxiety behavior and increased $K_v7.2$ and 7.3 membrane protein levels (Fu et al., 2020). Serotonin 5-HT_{2C} receptors are coupled to $G_{q/11}$ and therefore activate phospholipase C (Martin et al., 2014), which could modulate M current. But how these events could affect K_v7 channel membrane levels remains to be understood.

The evidence presented in this section highlight the promise of pharmacological M-current augmentation to be an effective treatment for multiple mood disorders, with different specificities of brain regions and channel subunits among the disorders. M-current regulation of dopaminergic VTA neurons may play a major role in depression and bipolar disorders (**Figure 3**). The VTA is an interesting therapeutic target due to its peculiarly high expression of $K_v7.4$ compared to other brain regions (Kharkovets et al., 2000; Saganich et al., 2001; Greene and Hoshi, 2017). Nevertheless, brain-specific drug delivery would presently be necessary to avoid peripherical effects (Kharkovets et al., 2000; Kharkovets et al., 2006; Yeung et al., 2008; Joshi et al., 2009). High expression of $K_v7.4$ channels can also be found in the DRN, where it is a potential therapeutic target for anxiety disorders, although for such disorders, augmentation of $K_v7.2$ and 7.3 in the LHb may also be necessary/beneficial. It is important to remember that the LHb and the raphe nuclei have reciprocal innervations between each other (Vertes et al., 1999; Yang et al., 2008; Metzger et al., 2017; Zhang et al., 2018). Moreover, M current might even be important in the etiology of bipolar and anxiety disorders (Borsotto et al., 2007; Judy et al., 2013; Kaminsky et al., 2015; Kang et al., 2017; Fu et al., 2020). It is likely that in both disorders, regulation of M-current by serotonergic and dopaminergic receptors (Ljungstrom et al., 2003; Fu et al., 2020) is disturbed by disease-induced alterations in these neurotransmitters and their receptors.

CONCLUSION

Currently pharmacological M-current manipulation is only approved by the FDA for treatment of epilepsy, although as mentioned above, RTG is off the market and its predecessor,

flupertine (Szelenyi, 2013), has unacceptable liver toxicity (Puls et al., 2011; Michel et al., 2012). However, the plethora of "next-generation" M-channel openers (Miceli et al., 2018), of which many were highlighted at the recent International K_v7 symposium in Naples, Italy in 2019, show great translational promise. Animal research indicates M current to be a therapeutic target for multiple brain disorders, including those with no current treatments, such as TBI and psychostimulant addiction. *But which compound should be tested first for these?* RTG has a clinical history as an adjunctive treatment for epilepsy (Brodie et al., 2010; Tompson et al., 2013). Thus, repurposing RTG could represent the fastest way to the clinic, as it is already FDA-approved (in oral, but not injectable, form) and is the compound most incorporated into preclinical research involving M-channel augmentation. However, the prolonged use of RTG entails adverse side effects, such as reversible skin discoloration, retinal pigmentation abnormalities, cognitive changes, and urinary incontinence (Beacher et al., 2015; Zaugg et al., 2017). The discoloration effects are largely due to the properties of the dimerized compound that may be mitigated in more recent derivatives of RTG that have yet to undergo clinical trials. It has been suggested that other side effects may also be reduced by identifying RTG-derivatives that are more potent and selective for $K_v7.2/7.3$ channels (Grunnet et al., 2014; Kumar et al., 2016). Another benefit of selectivity for $K_v7.2/7.3$ has been suggested in the treatment of tinnitus involving M-current dependent plasticity in the dorsal cochlear nucleus (Li et al., 2013; Kalappa et al., 2015). As previously mentioned, RTG also has dose-dependent side effects on $K_v2.1$ (Stas et al., 2016), L-type voltage-gated Ca^{2+} channels (Mani et al., 2013), and $GABA_A$ receptors (Treven et al., 2015). In addition, newer insights suggest that GABA interacts with, and activates, certain K_v7 subtypes due to a conserved binding pocket (Manville and Abbott, 2018, 2020). Thus, the use of more potent and specific M-channel compounds, as well as alternative strategies to regulate M-channel transcription, need to be further explored.

Much is still unknown about how M current is involved in the variety of neurological diseases mentioned in this review. Even basic preclinical tests remain to be performed for most of them. For example, for the new RTG-derivatives the minimum and maximum effective doses and possible side effects of long-term use are unknown. In neurovascular injuries, the necessity of one or only a few doses of treatment after the injury should eliminate the risks associated with long-term use of a drug. Since mood disorders are chronic diseases, the clinical use of pharmacological M-current augmentation necessitates prolonged use, presenting an extra challenge. It is also necessary to start investigating brain-specific delivery of M-current modulators. Addiction is a case that remains a bigger challenge. In rodent models, M current has been described to reduce both drug intake and relapse-like drug seeking behavior. Translating this to the clinic, M-current augmentation might be useful for treatment of an active drug user and/or to reduce relapse of a patient that is no longer using the drug. Both possibilities can only be truly tested in clinical trials. Pharmacological M-current augmentation is likely to be a therapeutic tool for a spectrum of pathological situations, as discussed here. However, there is still a long road ahead until clinical trials establish the true value of this mode of therapeutic intervention.

AUTHOR CONTRIBUTIONS

All authors wrote the manuscript.

FUNDING

This work was supported by the U.S. Department of Defense CDMRP grant W81XWH-15-1-0284 (MS), National Institutes of Health grant R01 159040 (MS), American Heart Association post-doctoral fellowship 20POST35180050 (FV), and the Morrison Trust of San Antonio (MS).

REFERENCES

Abd-Elsayed, A. A., Ikeda, R., Jia, Z., Ling, J., Zuo, X., Li, M., et al. (2015). KCNQ channels in nociceptive cold-sensing trigeminal ganglion neurons as therapeutic targets for treating orofacial cold hyperalgesia. *Mol. Pain* 11:45.

Ahuja, C. S., Wilson, J. R., Nori, S., Kotter, M. R. N., Druschel, C., Curt, A., et al. (2017). Traumatic spinal cord injury. *Nat. Rev. Dis. Primers* 3:17018.

Amabile, C. M., and Vasudevan, A. (2013). Ezogabine: a novel antiepileptic for adjunctive treatment of partial-onset seizures. *Pharmacotherapy* 33, 187–194. doi: 10.1002/phar.1185

Ambrosino, P., Alaimo, A., Bartollino, S., Manocchio, L., De Maria, M., Mosca, I., et al. (2015). Epilepsy-causing mutations in $K_v7.2$ C-terminus affect binding and functional modulation by calmodulin. *Biochim. Biophys. Acta* 1852, 1856–1866. doi: 10.1016/j.bbadis.2015.06.012

American Psychiatric Association (2013). *Diagnostic and Statistical Manual of Mental Disorders*, 5th Edn. Washington, DC: American Psychiatric Association.

Archer, C. R., Enslow, B. T., Taylor, A. B., De la Rosa, V., Bhattacharya, A., and Shapiro, M. S. (2019). A mutually induced conformational fit underlies Ca2+-directed interactions between calmodulin and the proximal C terminus of KCNQ4 K+ channels. *J. Biol. Chem.* 294, 6094–6112. doi: 10.1074/jbc.ra118.006857

Armand, V., Rundfeldt, C., and Heinemann, U. (1999). Effects of retigabine (D-23129) on different patterns of epileptiform activity induced by 4-aminopyridine in rat entorhinal cortex hippocampal slices. *Naunyn Schmiedebergs Arch. Pharmacol.* 359, 33–39. doi: 10.1007/pl00005320

Barrese, V., Taglialatela, M., Greenwood, I. A., and Davidson, C. (2015). Protective role of K_v7 channels in oxygen and glucose deprivation-induced damage in rat caudate brain slices. *J. Cereb. Blood Flow Metab.* 35, 1593–1600. doi: 10.1038/jcbfm.2015.83

Beacher, N. G., Brodie, M. J., and Goodall, C. (2015). A case report: retigabine induced oral mucosal dyspigmentation of the hard palate. *BMC Oral Health* 15:122. doi: 10.1186/s12903-015-0102-y

Beez, T., Steiger, H. J., and Etminan, N. (2017). Pharmacological targeting of secondary brain damage following ischemic or hemorrhagic stroke, traumatic brain injury, and bacterial meningitis - a systematic review and meta-analysis. *BMC Neurol.* 17:209. doi: 10.1186/s12883-017-0994-z

Bierbower, S. M., Choveau, F. S., Lechleiter, J. D., and Shapiro, M. S. (2015). Augmentation of M-type (KCNQ) potassium channels as a novel strategy to reduce stroke-induced brain injury. *J. Neurosci.* 35, 2101–2111. doi: 10.1523/jneurosci.3805-14.2015

Biervert, C., Schroeder, B. C., Kubisch, C., Berkovic, S. F., Propping, P., Jentsch, T. J., et al. (1998). A potassium channel mutation in

neonatal human epilepsy. *Science* 279, 403–406. doi: 10.1126/science.279.5349.403

Blackburn-Munro, G., and Jensen, B. S. (2003). The anticonvulsant retigabine attenuates nociceptive behaviours in rat models of persistent and neuropathic pain. *Eur. J. Pharmacol* 460, 109–116. doi: 10.1016/s0014-2999(02)02924-2

Borsotto, M., Cavarec, L., Bouillot, M., Romey, G., Macciardi, F., Delaye, A., et al. (2007). PP2A-Bgamma subunit and KCNQ2 K+ channels in bipolar disorder. *Pharmacogenomics J.* 7, 123–132. doi: 10.1038/sj.tpj.6500400

Boscia, F., Annunziato, L., and Taglialatela, M. (2006). Retigabine and flupirtine exert neuroprotective actions in organotypic hippocampal cultures. *Neuropharmacology* 51, 283–294. doi: 10.1016/j.neuropharm.2006.03.024

Brodie, M. J., Lerche, H., Gil-Nagel, A., Elger, C., Hall, S., Shin, P., et al. (2010). Efficacy and safety of adjunctive ezogabine (retigabine) in refractory partial epilepsy. *Neurology* 75, 1817–1824. doi: 10.1212/wnl.0b013e3181fd6170

Brown, D. A., and Adams, P. R. (1980). Muscarinic suppression of a novel voltage-sensitive K+ current in a vertebrate neurone. *Nature* 283, 673–676. doi: 10.1038/283673a0

Brown, D. A., Buckley, N. J., Caulfield, M. P., Duffy, S. M., Jones, S., Lamas, J. A., et al. (1995). "Coupling of muscarinic acetylcholine receptors to neural ion channels: closure of K+ channels," in *Molecular Mechanisms of Muscarinic Acetylcholine Receptor Function*, ed. J. Wess (Austin, TX: RG Lanes Co), 165–182.

Busserolles, J., Tsantoulas, C., Eschalier, A., and Lopez Garcia, J. A. (2016). Potassium channels in neuropathic pain: advances, challenges, and emerging ideas. *Pain* 157(Suppl. 1), S7–S14.

Carver, C. M., Hastings, S. D., Cook, M. E., and Shapiro, M. S. (2020). Functional responses of the hippocampus to hyperexcitability depend on directed, neuron-specific KCNQ2 K+ channel plasticity. *Hippocampus* 30, 435–455. doi: 10.1002/hipo.23163

Chang, A., Abderemane-Ali, F., Hura, G. L., Rossen, N. D., Gate, R. E., and Minor, D. L. Jr. (2018). A calmodulin C-lobe Ca2+-dependent switch governs K_v7 channel function. *Neuron* 97, 836.e6–852.e6.

Chiu, C. T., Wang, Z., Hunsberger, J. G., and Chuang, D. M. (2013). Therapeutic potential of mood stabilizers lithium and valproic acid: beyond bipolar disorder. *Pharmacol. Rev.* 65, 105–142. doi: 10.1124/pr.111.005512

Choveau, F., de la Rosa, V., Bierbower, S. M., Hernandez, C. C., and Shapiro, M. S. (2018). Phosphatidylinositol 4,5-bisphosphate (PIP2) regulates KCNQ3 K+ channels through multiple sites of action. *J. Biol. Chem.* 293, 19411–19428. doi: 10.1074/jbc.ra118.005401

Christensen, J., Pedersen, M. G., Pedersen, C. B., Sidenius, P., Olsen, J., and Vestergaard, M. (2009). Long-term risk of epilepsy after traumatic brain injury in children and young adults: a population-based cohort study. *Lancet* 373, 1105–1110. doi: 10.1016/s0140-6736(09)60214-2

Cipriani, A., Reid, K., Young, A. H., Macritchie, K., and Geddes, J. (2013). Valproic acid, valproate and divalproex in the maintenance treatment of bipolar disorder. *Cochrane Database Syst. Rev.* 2013:CD003196.

Collins-Yoder, A., and Lowell, J. (2017). Valproic acid: special considerations and targeted monitoring. *J. Neurosci. Nurs.* 49, 56–61. doi: 10.1097/jnn.0000000000000259

Constanti, A., and Brown, D. A. (1981). M-Currents in voltage-clamped mammalian sympathetic neurones. *Neurosci. Lett.* 24, 289–294. doi: 10.1016/0304-3940(81)90173-7

Cooper, E. C., Harrington, E., Jan, Y. N., and Jan, L. Y. (2001). M channel KCNQ2 subunits are localized to key sites for control of neuronal network oscillations and synchronization in mouse brain. *J. Neurosci.* 21, 9529–9540. doi: 10.1523/jneurosci.21-24-09529.2001

Cui, R. (2015). Editorial: a systematic review of depression. *Curr. Neuropharmacol.* 13:480. doi: 10.2174/1570159x1304150831123535

De Sarno, P., Li, X., and Jope, R. S. (2002). Regulation of Akt and glycogen synthase kinase-3 beta phosphorylation by sodium valproate and lithium. *Neuropharmacology* 43, 1158–1164. doi: 10.1016/s0028-3908(02)00215-0

Dencker, D., Dias, R., Pedersen, M. L., and Husum, H. (2008). Effect of the new antiepileptic drug retigabine in a rodent model of mania. *Epilepsy Behav.* 12, 49–53. doi: 10.1016/j.yebeh.2007.09.023

Dencker, D., and Husum, H. (2010). Antimanic efficacy of retigabine in a proposed mouse model of bipolar disorder. *Behav. Brain Res.* 207, 78–83. doi: 10.1016/j.bbr.2009.09.040

Di Chiara, G., and Imperato, A. (1988). Drugs abused by humans preferentially increase synaptic dopamine concentrations in the mesolimbic system of freely moving rats. *Proc. Natl. Acad. Sci. U.S.A.* 85, 5274–5278. doi: 10.1073/pnas.85.14.5274

Du, X., Gao, H., Jaffe, D., Zhang, H., and Gamper, N. (2018). M-type K+ channels in peripheral nociceptive pathways. *Br. J. Pharmacol.* 175, 2158–2172. doi: 10.1111/bph.13978

Ferreira, J. G., Del-Fava, F., Hasue, R. H., and Shammah-Lagnado, S. J. (2008). Organization of ventral tegmental area projections to the ventral tegmental area-nigral complex in the rat. *Neuroscience* 153, 196–213. doi: 10.1016/j.neuroscience.2008.02.003

Frey, L. C. (2003). Epidemiology of posttraumatic epilepsy: a critical review. *Epilepsia* 44, 11–17. doi: 10.1046/j.1528-1157.44.s10.4.x

Friedman, A. K., Juarez, B., Ku, S. M., Zhang, H., Calizo, R. C., Walsh, J. J., et al. (2016). KCNQ channel openers reverse depressive symptoms via an active resilience mechanism. *Nat. Commun.* 7:11671.

Fu, R., Mei, Q., Shiwalkar, N., Zuo, W., Zhang, H., Gregor, D., et al. (2020). Anxiety during alcohol withdrawal involves 5-HT2C receptors and M-channels in the lateral habenula. *Neuropharmacology* 163:107863. doi: 10.1016/j.neuropharm.2019.107863

Gamper, N., and Shapiro, M. S. (2003). Calmodulin mediates Ca2+-dependent modulation of M-type K+ channels. *J. Gen. Physiol.* 122, 17–31. doi: 10.1085/jgp.200208783

Gamper, N., Zaika, O., Li, Y., Martin, P., Hernandez, C. C., Perez, M. R., et al. (2006). Oxidative modification of M-type K+ channels as a mechanism of cytoprotective neuronal silencing. *EMBO J.* 25, 4996–5004. doi: 10.1038/sj.emboj.7601374

Garga, N., and Lowenstein, D. H. (2006). Posttraumatic epilepsy: a major problem in desperate need of major advances. *Epilepsy Curr.* 6, 1–5. doi: 10.1111/j.1535-7511.2005.00083.x

Gessa, G. L., Muntoni, F., Collu, M., Vargiu, L., and Mereu, G. (1985). Low doses of ethanol activate dopaminergic neurons in the ventral tegmental area. *Brain Res.* 348, 201–203. doi: 10.1016/0006-8993(85)90381-6

Graef, I. A., Mermelstein, P. G., Stankunas, K., Neilson, J. R., Deisseroth, K., Tsien, R. W., et al. (1999). L-type calcium channels and GSK-3 regulate the activity of NF-ATc4 in hippocampal neurons. *Nature* 401, 703–708. doi: 10.1038/44378

Graeff, F. G., Viana, M. B., and Mora, P. O. (1997). Dual role of 5-HT in defense and anxiety. *Neurosci. Biobehav. Rev.* 21, 791–799. doi: 10.1016/s0149-7634(96)00059-0

Greene, D. L., and Hoshi, N. (2017). Modulation of K_v7 channels and excitability in the brain. *Cell Mol. Life. Sci.* 74, 495–508. doi: 10.1007/s00018-016-2359-y

Greene, D. L., Kosenko, A., and Hoshi, N. (2018). Attenuating M-current suppression in vivo by a mutant Kcnq2 gene knock-in reduces seizure burden and prevents status epilepticus-induced neuronal death and epileptogenesis. *Epilepsia* 59, 1908–1918. doi: 10.1111/epi.14541

Grunnet, M., Strobaek, D., Hougaard, C., and Christophersen, P. (2014). K_v7 channels as targets for anti-epileptic and psychiatric drug-development. *Eur. J. Pharmacol.* 726, 133–137. doi: 10.1016/j.ejphar.2014.01.017

Gunthorpe, M. J., Large, C. H., and Sankar, R. (2012). The mechanism of action of retigabine (ezogabine), a first-in-class K+ channel opener for the treatment of epilepsy. *Epilepsia* 53, 412–424. doi: 10.1111/j.1528-1167.2011.03365.x

Haitin, Y., and Attali, B. (2008). The C-terminus of K_v7 channels: a multifunctional module. *J. Physiol.* 586, 1803–1810. doi: 10.1113/jphysiol.2007.149187

Haley, J. E., Abogadie, F. C., Delmas, P., Dayrell, M., Vallis, Y., Milligan, G., et al. (1998). The alpha subunit of Gq contributes to muscarinic inhibition of the M- type potassium current in sympathetic neurons. *J. Neurosci.* 18, 4521–4531. doi: 10.1523/jneurosci.18-12-04521.1998

Han, X., Jing, M. Y., Zhao, T. Y., Wu, N., Song, R., and Li, J. (2017). Role of dopamine projections from ventral tegmental area to nucleus accumbens and medial prefrontal cortex in reinforcement behaviors assessed using optogenetic manipulation. *Metab. Brain Dis.* 32, 1491–1502. doi: 10.1007/s11011-017-0023-3

Hansen, H. H., Andreasen, J. T., Weikop, P., Mirza, N., Scheel-Kruger, J., and Mikkelsen, J. D. (2007). The neuronal KCNQ channel opener retigabine inhibits locomotor activity and reduces forebrain excitatory responses to

the psychostimulants cocaine, methylphenidate and phencyclidine. *Eur. J. Pharmacol.* 570, 77–88. doi: 10.1016/j.ejphar.2007.05.029

Hansen, H. H., Waroux, O., Seutin, V., Jentsch, T. J., Aznar, S., and Mikkelsen, J. D. (2008). K_v7 channels: interaction with dopaminergic and serotonergic neurotransmission in the CNS. *J. Physiol.* 586, 1823–1832. doi: 10.1113/jphysiol.2007.149450

Hayashi, H., Iwata, M., Tsuchimori, N., and Matsumoto, T. (2014). Activation of peripheral KCNQ channels attenuates inflammatory pain. *Mol. Pain* 10:15.

Hemphill, J. C. III, Greenberg, S. M., Anderson, C. S., Becker, K., Bendok, B. R., Cushman, M., et al. (2015). Guidelines for the management of spontaneous intracerebral hemorrhage: a guideline for healthcare professionals from the american heart association/american stroke association. *Stroke* 46, 2032–2060. doi: 10.1161/str.0000000000000069

Hoshi, N., Zhang, J. S., Omaki, M., Takeuchi, T., Yokoyama, S., Wanaverbecq, N., et al. (2003). AKAP150 signaling complex promotes suppression of the M-current by muscarinic agonists. *Nat. Neurosci.* 6, 564–571. doi: 10.1038/nn1062

Hosp, J. A., Pekanovic, A., Rioult-Pedotti, M. S., and Luft, A. R. (2011). Dopaminergic projections from midbrain to primary motor cortex mediate motor skill learning. *J. Neurosci.* 31, 2481–2487. doi: 10.1523/jneurosci.5411-10.2011

Hunt, R. F., Boychuk, J. A., and Smith, B. N. (2013). Neural circuit mechanisms of post-traumatic epilepsy. *Front. Cell Neurosci.* 7:89. doi: 10.3389/fncel.2013.00089

Ikemoto, S. (2007). Dopamine reward circuitry: two projection systems from the ventral midbrain to the nucleus accumbens-olfactory tubercle complex. *Brain Res. Rev.* 56, 27–78. doi: 10.1016/j.brainresrev.2007.05.004

Jentsch, T. J. (2000). Neuronal KCNQ potassium channels: physiology and role in disease. *Nat. Rev. Neurosci.* 1, 21–30. doi: 10.1038/35036198

Jones, S., Brown, D. A., Milligan, G., Willer, E., Buckley, N. J., and Caulfield, M. P. (1995). Bradykinin excites rat sympathetic neurons by inhibition of M current through a mechanism involving B2 receptors and Gαq/11. *Neuron* 14, 399–405. doi: 10.1016/0896-6273(95)90295-3

Joshi, S., Sedivy, V., Hodyc, D., Herget, J., and Gurney, A. M. (2009). KCNQ modulators reveal a key role for KCNQ potassium channels in regulating the tone of rat pulmonary artery smooth muscle. *J. Pharmacol. Exp. Ther.* 329, 368–376. doi: 10.1124/jpet.108.147785

Juarez, B., and Han, M. H. (2016). Diversity of dopaminergic neural circuits in response to drug exposure. *Neuropsychopharmacology* 41, 2424–2446. doi: 10.1038/npp.2016.32

Judy, J. T., Seifuddin, F., Pirooznia, M., Mahon, P. B., Jancic, D., Goes, F. S., et al. (2013). Converging evidence for epistasis between ANK3 and potassium channel gene KCNQ2 in bipolar disorder. *Front. Genet.* 4:87. doi: 10.3389/fgene.2013.00087

Kalappa, B. I., Soh, H., Duignan, K. M., Furuya, T., Edwards, S., Tzingounis, A. V., et al. (2015). Potent KCNQ2/3-specific channel activator suppresses in vivo epileptic activity and prevents the development of tinnitus. *J. Neurosci.* 35, 8829–8842. doi: 10.1523/jneurosci.5176-14.2015

Kaminsky, Z., Jones, I., Verma, R., Saleh, L., Trivedi, H., Guintivano, J., et al. (2015). DNA methylation and expression of KCNQ3 in bipolar disorder. *Bipolar Disord.* 17, 150–159. doi: 10.1111/bdi.12230

Kang, S., Li, J., Zuo, W., Fu, R., Gregor, D., Krnjevic, K., et al. (2017). Ethanol withdrawal drives anxiety-related behaviors by reducing M-type potassium channel activity in the lateral habenula. *Neuropsychopharmacology* 42, 1813–1824. doi: 10.1038/npp.2017.68

Kapetanovic, I. M., Yonekawa, W. D., and Kupferberg, H. J. (1995). The effects of D-23129, a new experimental anticonvulsant drug, on neurotransmitter amino acids in the rat hippocampus in vitro. *Epilepsy Res.* 22, 167–173. doi: 10.1016/0920-1211(95)00050-x

Kay, H. Y., Greene, D. L., Kang, S., Kosenko, A., and Hoshi, N. (2015). M-current preservation contributes to anticonvulsant effects of valproic acid. *J. Clin. Invest.* 125, 3904–3914. doi: 10.1172/jci79727

Kharkovets, T., Dedek, K., Maier, H., Schweizer, M., Khimich, D., Nouvian, R., et al. (2006). Mice with altered KCNQ4 K+ channels implicate sensory outer hair cells in human progressive deafness. *EMBO J.* 25, 642–652. doi: 10.1038/sj.emboj.7600951

Kharkovets, T., Hardelin, J. P., Safieddine, S., Schweizer, M., El-Amraoui, A., Petit, C., et al. (2000). KCNQ4, a K+ channel mutated in a form of dominant deafness, is expressed in the inner ear and the central auditory pathway. *Proc. Natl. Acad. Sci. U.S.A.* 97, 4333–4338. doi: 10.1073/pnas.97.8.4333

Kim, K. W., Kim, K., Lee, H., and Suh, B. C. (2019). Ethanol elevates excitability of superior cervical ganglion neurons by inhibiting K_v7 channels in a cell type-specific and PI(4,5)P2-dependent manner. *Int. J. Mol. Sci.* 20:4419. doi: 10.3390/ijms20184419

Knapp, C. M., O'Malley, M., Datta, S., and Ciraulo, D. A. (2014). The K_v7 potassium channel activator retigabine decreases alcohol consumption in rats. *Am. J. Drug Alcohol Abuse* 40, 244–250. doi: 10.3109/00952990.2014.892951

Korsgaard, M. P., Hartz, B. P., Brown, W. D., Ahring, P. K., Strobaek, D., and Mirza, N. R. (2005). Anxiolytic effects of Maxipost (BMS-204352) and retigabine via activation of neuronal K_v7 channels. *J. Pharmacol. Exp. Ther.* 314, 282–292. doi: 10.1124/jpet.105.083923

Kosenko, A., and Hoshi, N. (2013). A change in configuration of the calmodulin-KCNQ channel complex underlies Ca2+-dependent modulation of KCNQ channel activity. *PLoS One* 8:e82290. doi: 10.1371/journal.pone.0082290

Koyama, S., Brodie, M. S., and Appel, S. B. (2007). Ethanol inhibition of m-current and ethanol-induced direct excitation of ventral tegmental area dopamine neurons. *J. Neurophysiol.* 97, 1977–1985. doi: 10.1152/jn.00270.2006

Kristensen, L. V., Sandager-Nielsen, K., and Hansen, H. H. (2012). K(v) 7 (KCNQ) channel openers normalize central 2-deoxyglucose uptake in a mouse model of mania and increase prefrontal cortical and hippocampal serine-9 phosphorylation levels of GSK3beta. *J. Neurochem.* 121, 373–382. doi: 10.1111/j.1471-4159.2012.07704.x

Kumar, M., Reed, N., Liu, R., Aizenman, E., Wipf, P., and Tzounopoulos, T. (2016). Synthesis and evaluation of potent KCNQ2/3-specific channel activators. *Mol. Pharmacol.* 89, 667–677. doi: 10.1124/mol.115.103200

Lacey, M. G., Calabresi, P., and North, R. A. (1990). Muscarine depolarizes rat substantia nigra zona compacta and ventral tegmental neurons in vitro through M1-like receptors. *J. Pharmacol. Exp. Ther.* 253, 395–400.

Lammel, S., Lim, B. K., Ran, C., Huang, K. W., Betley, M. J., Tye, K. M., et al. (2012). Input-specific control of reward and aversion in the ventral tegmental area. *Nature* 491, 212–217. doi: 10.1038/nature11527

Lawrence, J. J., Saraga, F., Churchill, J. F., Statland, J. M., Travis, K. E., Skinner, F. K., et al. (2006). Somatodendritic K_v7/KCNQ/M channels control interspike interval in hippocampal interneurons. *J. Neurosci.* 26, 12325–12338. doi: 10.1523/jneurosci.3521-06.2006

Li, L., Li, J., Zuo, Y., Dang, D., Frost, J. A., and Yang, Q. (2019). Activation of KCNQ channels prevents paclitaxel-induced peripheral neuropathy and associated neuropathic pain. *J. Pain* 20, 528–539. doi: 10.1016/j.jpain.2018.11.001

Li, L., Sun, H., Ding, J., Niu, C., Su, M., Zhang, L., et al. (2017). Selective targeting of M-type potassium K_v 7.4 channels demonstrates their key role in the regulation of dopaminergic neuronal excitability and depression-like behaviour. *Br. J. Pharmacol.* 174, 4277–4294. doi: 10.1111/bph.14026

Li, S., Choi, V., and Tzounopoulos, T. (2013). Pathogenic plasticity of $K_v7.2/3$ channel activity is essential for the induction of tinnitus. *Proc. Natl. Acad. Sci. U.S.A.* 110, 9980–9985. doi: 10.1073/pnas.1302770110

Li, Y., Gamper, N., Hilgemann, D. W., and Shapiro, M. S. (2005). Regulation of K_v7 (KCNQ) K+ channel open probability by phosphatidylinositol (4,5)-bisphosphate. *J. Neurosci.* 25, 9825–9835. doi: 10.1523/jneurosci.2597-05.2005

Ljungstrom, T., Grunnet, M., Jensen, B. S., and Olesen, S. P. (2003). Functional coupling between heterologously expressed dopamine D(2) receptors and KCNQ channels. *Pflugers Arch.* 446, 684–694. doi: 10.1007/s00424-003-1111-2

Lowenstein, D. H. (2009). Epilepsy after head injury: an overview. *Epilepsia* 50(Suppl. 2), 4–9. doi: 10.1111/j.1528-1167.2008.02004.x

Lowry, C. A., Hale, M. W., Evans, A. K., Heerkens, J., Staub, D. R., Gasser, P. J., et al. (2008). Serotonergic systems, anxiety, and affective disorder: focus on the dorsomedial part of the dorsal raphe nucleus. *Ann. N. Y. Acad. Sci.* 1148, 86–94.

Maier, S. F., and Watkins, L. R. (2005). Stressor controllability and learned helplessness: the roles of the dorsal raphe nucleus, serotonin, and corticotropin-releasing factor. *Neurosci. Biobehav. Rev.* 29, 829–841. doi: 10.1016/j.neubiorev.2005.03.021

Main, M. J., Cryan, J. E., Dupere, J. R., Cox, B., Clare, J. J., and Burbidge, S. A. (2000). Modulation of KCNQ2/3 potassium channels by the novel anticonvulsant retigabine. *Mol. Pharmacol.* 58, 253–262. doi: 10.1124/mol.58.2.253

Maljevic, S., Wuttke, T. V., and Lerche, H. (2008). Nervous system K_v7 disorders: breakdown of a subthreshold brake. *J. Physiol.* 586, 1791–1801. doi: 10.1113/jphysiol.2008.150656

Mani, B. K., O'Dowd, J., Kumar, L., Brueggemann, L. I., Ross, M., and Byron, K. L. (2013). Vascular KCNQ (K_v7) potassium channels as common signaling intermediates and therapeutic targets in cerebral vasospasm. *J. Cardiovasc. Pharmacol.* 61, 51–62. doi: 10.1097/fjc.0b013e3182771708

Manville, R. W., and Abbott, G. W. (2018). Gabapentin is a potent activator of KCNQ3 and KCNQ5 potassium channels. *Mol. Pharmacol.* 94, 1155–1163. doi: 10.1124/mol.118.112953

Manville, R. W., and Abbott, G. W. (2020). Potassium channels act as chemosensors for solute transporters. *Commun. Biol.* 3:90.

Martin, C. B., Hamon, M., Lanfumey, L., and Mongeau, R. (2014). Controversies on the role of 5-HT(2C) receptors in the mechanisms of action of antidepressant drugs. *Neurosci. Biobehav. Rev.* 42, 208–223. doi: 10.1016/j.neubiorev.2014.03.001

McGuier, N. S., Griffin, W. C. III, Gass, J. T., Padula, A. E., Chesler, E. J., and Mulholland, P. J. (2016). K_v7 channels in the nucleus accumbens are altered by chronic drinking and are targets for reducing alcohol consumption. *Addict. Biol.* 21, 1097–1112. doi: 10.1111/adb.12279

McGuier, N. S., Rinker, J. A., Cannady, R., Fulmer, D. B., Jones, S. R., Hoffman, M., et al. (2018). Identification and validation of midbrain Kcnq4 regulation of heavy alcohol consumption in rodents. *Neuropharmacology* 138, 10–19. doi: 10.1016/j.neuropharm.2018.05.020

Metzger, M., Bueno, D., and Lima, L. B. (2017). The lateral habenula and the serotonergic system. *Pharmacol. Biochem. Behav.* 162, 22–28. doi: 10.1016/j.pbb.2017.05.007

Miceli, F., Soldovieri, M. V., Ambrosino, P., Manocchio, L., Mosca, I., and Taglialatela, M. (2018). Pharmacological targeting of neuronal $K_v7.2/3$ channels: a focus on chemotypes and receptor sites. *Curr. Med. Chem.* 25, 2637–2660. doi: 10.2174/0929867324666171012122852

Miceli, F., Soldovieri, M. V., Martire, M., and Taglialatela, M. (2008). Molecular pharmacology and therapeutic potential of neuronal K_v7-modulating drugs. *Curr. Opin. Pharmacol.* 8, 65–74. doi: 10.1016/j.coph.2007.10.003

Miceli, F., Striano, P., Soldovieri, M. V., Fontana, A., Nardello, R., Robbiano, A., et al. (2015). A novel KCNQ3 mutation in familial epilepsy with focal seizures and intellectual disability. *Epilepsia* 56, e15–e20. doi: 10.1111/epi.12887

Michel, M. C., Radziszewski, P., Falconer, C., Marschall-Kehrel, D., and Blot, K. (2012). Unexpected frequent hepatotoxicity of a prescription drug, flupirtine, marketed for about 30 years. *Br. J. Clin. Pharmacol.* 73, 821–825. doi: 10.1111/j.1365-2125.2011.04138.x

Moore, S. D., Madamba, S. G., and Siggins, G. R. (1990). Ethanol diminishes a voltage-dependent K+ current, the M-current, in CA1 hippocampal pyramidal neurons in vitro. *Brain Res.* 516, 222–228. doi: 10.1016/0006-8993(90)90922-x

Morales, M., and Pickel, V. M. (2012). Insights to drug addiction derived from ultrastructural views of the mesocorticolimbic system. *Ann. N. Y. Acad. Sci.* 1248, 71–88. doi: 10.1111/j.1749-6632.2011.06299.x

Munro, G., and Dalby-Brown, W. (2007). K_v7 (KCNQ) channel modulators and neuropathic pain. *J. Med. Chem.* 50, 2576–2582. doi: 10.1021/jm060989l

Munro, G., Erichsen, H. K., and Mirza, N. R. (2007). Pharmacological comparison of anticonvulsant drugs in animal models of persistent pain and anxiety. *Neuropharmacology* 53, 609–618. doi: 10.1016/j.neuropharm.2007.07.002

Nakajo, K., and Kubo, Y. (2005). Protein kinase C shifts the voltage dependence of KCNQ/M channels expressed in *Xenopus oocytes*. *J. Physiol.* 569, 59–74. doi: 10.1113/jphysiol.2005.094995

Nestler, E. J., and Carlezon, W. A. Jr. (2006). The mesolimbic dopamine reward circuit in depression. *Biol. Psychiatry* 59, 1151–1159. doi: 10.1016/j.biopsych.2005.09.018

Pan, Z., Kao, T., Horvath, Z., Lemos, J., Sul, J. Y., Cranstoun, S. D., et al. (2006). A common ankyrin-G-based mechanism retains KCNQ and NaV channels at electrically active domains of the axon. *J. Neurosci.* 26, 2599–2613. doi: 10.1523/jneurosci.4314-05.2006

Parrilla-Carrero, J., Buchta, W. C., Goswamee, P., Culver, O., McKendrick, G., Harlan, B., et al. (2018). Restoration of K_v7 channel-mediated inhibition reduces cued-reinstatement of cocaine seeking. *J. Neurosci.* 38, 4212–4229. doi: 10.1523/jneurosci.2767-17.2018

Peters, H. C., Hu, H., Pongs, O., Storm, J. F., and Isbrandt, D. (2005). Conditional transgenic suppression of M channels in mouse brain reveals functions in neuronal excitability, resonance and behavior. *Nat. Neurosci.* 8, 51–60. doi: 10.1038/nn1375

Puls, F., Agne, C., Klein, F., Koch, M., Rifai, K., Manns, M. P., et al. (2011). Pathology of flupirtine-induced liver injury: a histological and clinical study of six cases. *Virchows Arch.* 458, 709–716. doi: 10.1007/s00428-011-1087-9

Rasmussen, H. B., Frokjaer-Jensen, C., Jensen, C. S., Jensen, H. S., Jorgensen, N. K., Misonou, H., et al. (2007). Requirement of subunit co-assembly and ankyrin-G for M-channel localization at the axon initial segment. *J. Cell Sci.* 120, 953–963. doi: 10.1242/jcs.03396

Redrobe, J. P., and Nielsen, A. N. (2009). Effects of neuronal K_v7 potassium channel activators on hyperactivity in a rodent model of mania. *Behav. Brain Res.* 198, 481–485. doi: 10.1016/j.bbr.2008.12.027

Robinson, T. E., and Berridge, K. C. (2003). Addiction. *Annu. Rev. Psychol.* 54, 25–53.

Rodd-Henricks, Z. A., McKinzie, D. L., Crile, R. S., Murphy, J. M., and McBride, W. J. (2000). Regional heterogeneity for the intracranial self-administration of ethanol within the ventral tegmental area of female Wistar rats. *Psychopharmacology* 149, 217–224. doi: 10.1007/s002139900347

Rostock, A., Tober, C., Rundfeldt, C., Bartsch, R., Engel, J., Polymeropoulos, E. E., et al. (1996). D-23129: a new anticonvulsant with a broad spectrum activity in animal models of epileptic seizures. *Epilepsy Res.* 23, 211–223. doi: 10.1016/0920-1211(95)00101-8

Rundfeldt, C., and Netzer, R. (2000). The novel anticonvulsant retigabine activates M-currents in Chinese hamster ovary-cells tranfected with human KCNQ2/3 subunits. *Neurosci. Lett.* 282, 73–76. doi: 10.1016/s0304-3940(00)00866-1

Saganich, M. J., Machado, E., and Rudy, B. (2001). Differential expression of genes encoding subthreshold-operating voltage-gated K+ channels in brain. *J. Neurosci.* 21, 4609–4624. doi: 10.1523/jneurosci.21-13-04609.2001

Shah, M. M., Migliore, M., Valencia, I., Cooper, E. C., and Brown, D. A. (2008). Functional significance of axonal K_v7 channels in hippocampal pyramidal neurons. *Proc. Natl. Acad. Sci. U.S.A.* 105, 7869–7874. doi: 10.1073/pnas.0802805105

Shapiro, M. S., Roche, J. P., Kaftan, E. J., Cruzblanca, H., Mackie, K., and Hille, B. (2000). Reconstitution of muscarinic modulation of the KCNQ2/KCNQ3 K+ channels that underlie the neuronal M current. *J. Neurosci.* 20, 1710–1721. doi: 10.1523/jneurosci.20-05-01710.2000

Simon, D. W., McGeachy, M. J., Bayir, H., Clark, R. S., Loane, D. J., and Kochanek, P. M. (2017). The far-reaching scope of neuroinflammation after traumatic brain injury. *Nat. Rev. Neurol.* 13, 171–191. doi: 10.1038/nrneurol.2017.13

Singh, N. A., Charlier, C., Stauffer, D., DuPont, B. R., Leach, R. J., Melis, R., et al. (1998). A novel potassium channel gene, KCNQ2, is mutated in an inherited epilepsy of newborns. *Nat. Genet.* 18, 25–29. doi: 10.1038/ng0198-25

Soldovieri, M. V., Miceli, F., and Taglialatela, M. (2011). Driving with no brakes: molecular pathophysiology of K_v7 potassium channels. *Physiology* 26, 365–376. doi: 10.1152/physiol.00009.2011

Sotty, F., Damgaard, T., Montezinho, L. P., Mork, A., Olsen, C. K., Bundgaard, C., et al. (2009). Antipsychotic-like effect of retigabine [N-(2-Amino-4-(fluorobenzylamino)-phenyl)carbamic acid ester], a KCNQ potassium channel opener, via modulation of mesolimbic dopaminergic neurotransmission. *J. Pharmacol. Exp. Ther.* 328, 951–962. doi: 10.1124/jpet.108.146944

Splinter, M. Y. (2013). Efficacy of retigabine in adjunctive treatment of partial onset seizures in adults. *J. Cent. Nerv. Syst. Dis.* 5, 31–41.

Stambolic, V., Ruel, L., and Woodgett, J. R. (1996). Lithium inhibits glycogen synthase kinase-3 activity and mimics wingless signalling in intact cells. *Curr. Biol.* 6, 1664–1668.

Stas, J. I., Bocksteins, E., Jensen, C. S., Schmitt, N., and Snyders, D. J. (2016). The anticonvulsant retigabine suppresses neuronal K_v2-mediated currents. *Sci. Rep.* 6:35080.

Strulovich, R., Tobelaim, W. S., Attali, B., and Hirsch, J. A. (2016). Structural insights into the M-channel proximal C-terminus/calmodulin complex. *Biochemistry* 55, 5353–5365. doi: 10.1021/acs.biochem.6b00477

Suh, B.-C., and Hille, B. (2005). Regulation of ion channels by phosphatidylinositol 4,5-bisphosphate. *Curr. Opin. Neurobiol.* 15, 370–378. doi: 10.1016/j.conb.2005.05.005

Suh, B. C., Inoue, T., Meyer, T., and Hille, B. (2006). Rapid chemically induced changes of PtdIns(4,5)P2 gate KCNQ ion channels. *Science* 314, 1454–1457. doi: 10.1126/science.1131163

Sun, J., and MacKinnon, R. (2017). Cryo-EM structure of a KCNQ1/CaM complex reveals insights into congenital long-QT syndrome. *Cell* 169, 1042.e9–1050.e9.

Sun, J., and MacKinnon, R. (2020). Structural basis of human KCNQ1 modulation and gating. *Cell* 180, 340.e9–347.e9.

Szelenyi, I. (2013). Flupirtine, a re-discovered drug, revisited. *Inflamm. Res.* 62, 251–258. doi: 10.1007/s00011-013-0592-5

Tatulian, L., and Brown, D. A. (2003). Effect of the KCNQ potassium channel opener retigabine on single KCNQ2/3 channels expressed in CHO cells. *J. Physiol.* 549, 57–63. doi: 10.1113/jphysiol.2003.039842

Tatulian, L., Delmas, P., Abogadie, F. C., and Brown, D. A. (2001). Activation of expressed KCNQ potassium currents and native neuronal M-type potassium currents by the anti-convulsant drug retigabine. *J. Neurosci.* 21, 5535–5545. doi: 10.1523/jneurosci.21-15-05535.2001

Tompson, D. J., Crean, C. S., Reeve, R., and Berry, N. S. (2013). Efficacy and tolerability exposure-response relationship of retigabine (ezogabine) immediate-release tablets in patients with partial-onset seizures. *Clin. Ther.* 35, 1174.e4–1185.e4.

Tomson, T., Battino, D., and Perucca, E. (2016). Valproic acid after five decades of use in epilepsy: time to reconsider the indications of a time-honoured drug. *Lancet Neurol.* 15, 210–218. doi: 10.1016/s1474-4422(15)00314-2

Treven, M., Koenig, X., Assadpour, E., Gantumur, E., Meyer, C., Hilber, K., et al. (2015). The anticonvulsant retigabine is a subtype selective modulator of GABAA receptors. *Epilepsia* 56, 647–657. doi: 10.1111/epi.12950

Tykocki, N. R., Heppner, T. J., Dalsgaard, T., Bonev, A. D., and Nelson, M. T. (2019). The K_v 7 channel activator retigabine suppresses mouse urinary bladder afferent nerve activity without affecting detrusor smooth muscle K(+) channel currents. *J. Physiol.* 597, 935–950. doi: 10.1113/jp277021

Tzingounis, A. V., and Nicoll, R. A. (2008). Contribution of KCNQ2 and KCNQ3 to the medium and slow afterhyperpolarization currents. *Proc. Natl. Acad. Sci. U.S.A.* 105, 19974–19979. doi: 10.1073/pnas.0810535105

Vertes, R. P., Fortin, W. J., and Crane, A. M. (1999). Projections of the median raphe nucleus in the rat. *J. Comp. Neurol.* 407, 555–582. doi: 10.1002/(sici)1096-9861(19990517)407:4<555::aid-cne7>3.0.co;2-e

Vigil, F. A., Bozdemir, E., Bugay, V., Chun, S. H., Hobbs, M., Sanchez, I., et al. (2020). Prevention of brain damage after traumatic brain injury by pharmacological enhancement of KCNQ (K_v7, "M-type") K(+) currents in neurons. *J. Cereb. Blood Flow Metab.* 40, 1256–1273. doi: 10.1177/0271678X19857818

Volkow, N. D., Wang, G. J., Fowler, J. S., Tomasi, D., Telang, F., and Baler, R. (2010). Addiction: decreased reward sensitivity and increased expectation sensitivity conspire to overwhelm the brain's control circuit. *Bioessays* 32, 748–755. doi: 10.1002/bies.201000042

Wang, J. J., and Li, Y. (2016). KCNQ potassium channels in sensory system and neural circuits. *Acta Pharmacol. Sin.* 37, 25–33. doi: 10.1038/aps.2015.131

Weiss, F., Lorang, M. T., Bloom, F. E., and Koob, G. F. (1993). Oral alcohol self-administration stimulates dopamine release in the rat nucleus accumbens: genetic and motivational determinants. *J. Pharmacol. Exp. Ther.* 267, 250–258.

Winks, J. S., Hughes, S., Filippov, A. K., Tatulian, L., Abogadie, F. C., Brown, D. A., et al. (2005). Relationship between membrane phosphatidylinositol-4,5-bisphosphate and receptor-mediated inhibition of native neuronal M channels. *J. Neurosci.* 25, 3400–3413. doi: 10.1523/jneurosci.3231-04.2005

Wu, Z., Li, L., Xie, F., Xu, G., Dang, D., and Yang, Q. (2020). Enhancing KCNQ channel activity improves neurobehavioral recovery after spinal cord injury. *J. Pharmacol. Exp. Ther.* 373, 72–80. doi: 10.1124/jpet.119.264010

Wuttke, T. V., Seebohm, G., Bail, S., Maljevic, S., and Lerche, H. (2005). The new anticonvulsant retigabine favors voltage-dependent opening of the Kv7.2 (KCNQ2) channel by binding to its activation gate. *Mol. Pharmacol.* 67, 1009–1017. doi: 10.1124/mol.104.010793

Yadav, G., Jain, G., and Singh, M. (2017). Role of flupirtine in reducing preoperative anxiety of patients undergoing craniotomy procedure. *Saudi J. Anaesth.* 11, 158–162.

Yang, L. M., Hu, B., Xia, Y. H., Zhang, B. L., and Zhao, H. (2008). Lateral habenula lesions improve the behavioral response in depressed rats via increasing the serotonin level in dorsal raphe nucleus. *Behav. Brain Res.* 188, 84–90. doi: 10.1016/j.bbr.2007.10.022

Yeung, S., Schwake, M., Pucovsky, V., and Greenwood, I. (2008). Bimodal effects of the Kv7 channel activator retigabine on vascular K+ currents. *Br. J. Pharmacol.* 155, 62–72. doi: 10.1038/bjp.2008.231

Yu, H., Wu, M., Hopkins, C., Engers, J., Townsend, S., Lindsley, C., et al. (2010). "A small molecule activator of KCNQ2 and KCNQ4 channels," in *Proceedings of the Probe Reports from the NIH Molecular Libraries Program*, (Bethesda, MD: National Center for Biotechnology Information).

Yue, C., and Yaari, Y. (2004). KCNQ/M channels control spike afterdepolarization and burst generation in hippocampal neurons. *J. Neurosci.* 24, 4614–4624. doi: 10.1523/jneurosci.0765-04.2004

Yus-Najera, E., Santana-Castro, I., and Villarroel, A. (2002). The identification and characterization of a non-continuous calmodulin binding site in non-inactivating voltage-dependent KCNQ potassium channels. *J. Biol. Chem.* 24:24.

Zaczek, R., Chorvat, R. J., Saye, J. A., Pierdomenico, M. E., Maciag, C. M., Logue, A. R., et al. (1998). Two new potent neurotransmitter release enhancers, 10,10-bis(4- pyridinylmethyl)-9(10H)-anthracenone and 10,10-bis(2-fluoro-4- pyridinylmethyl)-9(10H)-anthracenone: comparison to linopirdine. *J. Pharmacol. Exp. Ther.* 285, 724–730.

Zaika, O., Tolstykh, G. P., Jaffe, D. B., and Shapiro, M. S. (2007). Inositol triphosphate-mediated Ca2+ signals direct purinergic P2Y-receptor regulation of neuronal ion channels. *J. Neurosci.* 27, 8914–8926. doi: 10.1523/jneurosci.1739-07.2007

Zaugg, B. E., Bell, J. E., Taylor, K. Y., and Bernstein, P. S. (2017). Ezogabine (Potiga) maculopathy. *Retin. Cases Brief. Rep.* 11, 38–43. doi: 10.1097/icb.0000000000000283

Zhang, H., Craciun, L. C., Mirshahi, T., Rohacs, T., Lopes, C. M., Jin, T., et al. (2003). PIP2 activates KCNQ channels, and its hydrolysis underlies receptor-mediated inhibition of M currents. *Neuron* 37, 963–975. doi: 10.1016/s0896-6273(03)00125-9

Zhang, H., Li, K., Chen, H. S., Gao, S. Q., Xia, Z. X., Zhang, J. T., et al. (2018). Dorsal raphe projection inhibits the excitatory inputs on lateral habenula and alleviates depressive behaviors in rats. *Brain Struct. Funct.* 223, 2243–2258. doi: 10.1007/s00429-018-1623-3

Zhao, C., Su, M., Wang, Y., Li, X., Zhang, Y., Du, X., et al. (2017). Selective modulation of K+ Channel Kv7.4 significantly affects the excitability of DRN 5-HT neurons. *Front. Cell Neurosci.* 11:405. doi: 10.3389/fncel.2017.00405

Zhao, Y. J., Nai, Y., Li, S. Y., and Zheng, Y. H. (2018). Retigabine protects the blood-brain barrier by regulating tight junctions between cerebral vascular endothelial cells in cerebral ischemia-reperfusion rats. *Eur. Rev. Med. Pharmacol. Sci.* 22, 8509–8518.

Zheng, Y., Xu, H., Zhan, L., Zhou, X., Chen, X., and Gao, Z. (2015). Activation of peripheral KCNQ channels relieves gout pain. *Pain* 156, 1025–1035.

Conflict of Interest: The authors have submitted a pending US patent for the use of K_v7 channel openers as a novel therapy for traumatic brain injury, held in the name of Advanced Neuroresearch Therapeutics, LLC.

frontiers in Physiology

REVIEW
published: 23 June 2020
doi: 10.3389/fphys.2020.00583

KCNQs: Ligand- and Voltage-Gated Potassium Channels

*Geoffrey W. Abbott**

Bioelectricity Laboratory, Department of Physiology and Biophysics, School of Medicine, University of California, Irvine, Irvine, CA, United States

Voltage-gated potassium (Kv) channels in the KCNQ (Kv7) family are essential features of a broad range of excitable and non-excitable cell types and are found in organisms ranging from *Hydra vulgaris* to *Homo sapiens*. Although they are firmly in the superfamily of S4 domain-bearing voltage-sensing ion channels, KCNQ channels are highly sensitive to a range of endogenous and exogenous small molecules that act directly on the pore, the voltage-sensing domain, or the interface between the two. The focus of this review is regulation of KCNQs by direct binding of neurotransmitters and metabolites from both animals and plants and the role of the latter in the effects of plants consumed for food and as traditional folk medicines. The conceptual question arises: Are KCNQs voltage-gated channels that are also sensitive to ligands or ligand-gated channels that are also sensitive to voltage?

Keywords: epilepsy, GABA, herbal medicine, hypertension, KCNE, KCNQ2, KCNQ3, KCNQ5

OPEN ACCESS

Edited by:
Francesco Miceli,
University of Naples Federico II, Italy

Reviewed by:
Luis A. Pardo,
Max Planck Institute for Experimental Medicine, Germany
Yang Li,
Shanghai Institute of Materia Medica, Chinese Academy of Sciences, China

***Correspondence:**
Geoffrey W. Abbott
abbottg@uci.edu

Specialty section:
This article was submitted to Membrane Physiology and Membrane Biophysics, a section of the journal Frontiers in Physiology

Received: *25 March 2020*
Accepted: *11 May 2020*
Published: *23 June 2020*

Citation:
Abbott GW (2020) KCNQs: Ligand- and Voltage-Gated Potassium Channels. Front. Physiol. 11:583. doi: 10.3389/fphys.2020.00583

INTRODUCTION

Ion channels provide aqueous conduits across cell membranes that allow transmembrane movement of aqueous ions down their electrochemical gradient and across the hydrophobic interior of the lipid bilayer. Although this process is not active transport, it can achieve rates approaching the diffusion limit and also ion selectivity ratios as high as 100:1 even for K^+ over the smaller but similarly charged Na^+ (Hille et al., 1999). Ion channels can be categorized using various approaches, such as by their primary sequence (there are many different ion channel gene families organized by sequence similarity), ion selectivity (e.g., K^+ versus Na^+) or how they are opened (e.g., by voltage changes or by ligands). Voltage-gated ion channels are best known for their roles in excitable cell processes, including skeletal and cardiac muscle contraction and nervous signaling, functions that demand they respond to changes in membrane potential by opening to allow ion movement that shapes the action potentials in these tissues. Some voltage-gated ion channels also serve vital functions in non-excitable tissues, including in polarized epithelial cells.

Many voltage-gated channels also respond to ligands. It was previously recognized, before the molecular correlates of channels were even identified, that many native voltage-dependent currents are sensitive to small molecules. Indeed, before molecular cloning, pharmacology was the primary method for identifying specific currents. These cases most often involve block of a specific ion channel and consequent inhibition of its current in a process separate from the normal gating processes of the channel or, in some circumstances, augmenting the existing gating

processes of the channel, e.g., augmentation of voltage-gated sodium channel inactivation by anti-arrhythmic/analgesic drugs (Viswanathan et al., 2001). However, more recently, we are beginning to understand that some voltage-gated ion channels either require specific endogenous small molecules for their activity or are highly sensitive to a range of endogenous and exogenous small molecules that augment their activity at a given membrane potential. The focus of this review is the KCNQ (Kv7) subfamily of voltage-gated potassium (Kv) channels and the mechanisms of their activation by a range of ligands.

KCNQ CHANNEL ARCHITECTURE

Voltage-gated potassium (Kv) channels, including the KCNQs, possess four repeating units, each of which is a separate gene product. The channel forms as a tetramer of KCNQ α subunits. Each unit contains six transmembrane segments with segments 1–4 (S1–S4) forming one voltage sensing domain (VSD) and S5,S6 contributing from each unit to form one quarter of an interlocking pore structure (**Figures 1A,B**) (Papazian et al., 1987; Tempel et al., 1987; MacKinnon, 1991; Doyle et al., 1998; Long et al., 2005a).

The VSD is the defining feature of voltage-gated ion channels; each VSD contains a transmembrane helix (S4) endowed with periodic basic residues that sense membrane potential (Catterall, 1995). The flexible VSD can, therefore, shift position relative to the membrane electric field in response to membrane potential changes (**Figures 1C,D**). This conformational shift is transmitted to the pore module via an intracellular linker region, termed the S4–S5 linker in voltage-gated potassium (Kv channels) and other interactions between elements of the pore module and S4 (Bezanilla and Perozo, 2003). Transmembrane segments S1 and S2 within the VSD contain acidic residues that shield or stabilize S4 as it transitions to its activated state upon membrane depolarization (Cuello et al., 2004; DeCaen et al., 2009). Thus, voltage-dependent ion channel gating is electromechanically coupled to the plasma membrane potential (**Figure 1D**; Long et al., 2005b).

In KCNQ and other K^+ channels, selectivity over, e.g., Na^+ ions is achieved by backbone carbonyl oxygen atoms of glycine residues in the canonical GYGD K^+ selectivity filter motif. This forms a pseudo-hydration shell that accommodates K^+ perfectly but is too large to properly coordinate Na^+. Diffusion of K^+ ions through the K^+ channel pore requires binding and unbinding of ions to the pore elements (Ranganathan et al., 1996; Doyle et al., 1998; Zhou and MacKinnon, 2003).

Similar to other ion channels, some KCNQ α subunit assemblies also form complexes with one or more non-pore-forming, ancillary subunits (McCrossan and Abbott, 2004; Panaghie and Abbott, 2006; Pongs and Schwarz, 2010). This includes the KCNE subfamily of single-transmembrane domain ancillary subunits (**Figure 1C**). Each KCNE isoform can regulate more than one type of Kv α subunit (McCrossan and Abbott, 2004), and some Kv α subunit types can each be regulated by more than one KCNE subunit isoform. For example, all five human KCNE isoforms can regulate KCNQ1. The varied functional outcomes of these assemblies permit KCNQ1 to serve a wide variety of functions in both excitable cells, such as ventricular cardiomyocytes, and in non-excitable cells such as gastric and thyroid epithelial cells (Abbott, 2014).

REGULATION OF KCNQ CHANNEL ACTIVATION BY VOLTAGE, PIP_2 AND Ca^{2+}

There are five known human *KCNQ* genes in the 40-member Kv α subunit gene family (Abbott, 2014). KCNQ1 is highly studied because of its association with human disease, variety of roles in physiology, and broad functional repertoire. KCNQ2–5 are also highly studied for their roles in the brain (primarily KCNQ2, 3, and 5) (Biervert et al., 1998; Singh et al., 1998; Wang et al., 1998; Tzingounis et al., 2010; Klinger et al., 2011), vasculature (KCNQ4, 5) (Yeung et al., 2007), and auditory epithelium and auditory neurons (KCNQ4) (Kubisch et al., 1999). All the homomeric and heteromeric α subunit-only KCNQ channels studied have been found to be highly sensitive to phosphatidylinositol 4,5-bisphosphate (PIP_2). Specifically, unlike some other Kv channels that undergo more subtle modulation by PIP_2, KCNQ channels require interaction with PIP_2 to pass current (Zaydman et al., 2013). This is because PIP_2 acts as a cofactor that mediates coupling of the KCNQ VSD with its pore module. Thus, without PIP_2, VSD activation in response to membrane depolarization does not itself cause pore opening (Zaydman et al., 2013).

This is one example of how we can consider KCNQ channel gating to be ligand- as well as voltage-dependent in much the same way as we consider Ca^{2+}-activated K^+ channels, such as BK, to be both Ca^{2+}- and voltage-activated. Interestingly, as for KCNQ channels, BK channel activation is often cast as voltage-initiated but modulated by steady-state intracellular [Ca^2+]. Yet, in one study designed to mimic physiological conditions, ligand-gating by Ca^{2+} was found to be rate-limiting for BK channel function. It was concluded that BK channels in native systems function primarily as ligand-gated ion channels, activated by intracellular Ca^{2+} (Berkefeld and Fakler, 2013). The Ca^{2+} binding sites on BK channels required for activation are located intracellularly in the Ca^{2+} bowl, located in the C-terminus of the RCK2 domain, and in the RCK1 domain (Lee and Cui, 2010).

For many Kv channels, activation is modeled as a linear process, in which VSD activation must occur before pore opening. In the case of KCNQ channels and, incidentally, also for voltage activation of BK channels, coupling between the VSD and pore module is probably better represented by an allosteric model rather than a linear process. In the allosteric model, the pore is capable of opening without VSD activation, but VSD activation increases the likelihood of pore opening (Zaydman and Cui, 2014). Studies of KCNQ1 have shown that pore opening does not require activation of all four VSDs (Osteen et al., 2012). In addition, we found that, despite the pore of a KCNQ1 mutant (F340W) (in complexes with KCNE1) being locked open, voltage-sensitive inactivation that required S4 movement still occurred, providing additional evidence for non-linear coupling (Panaghie et al., 2008).

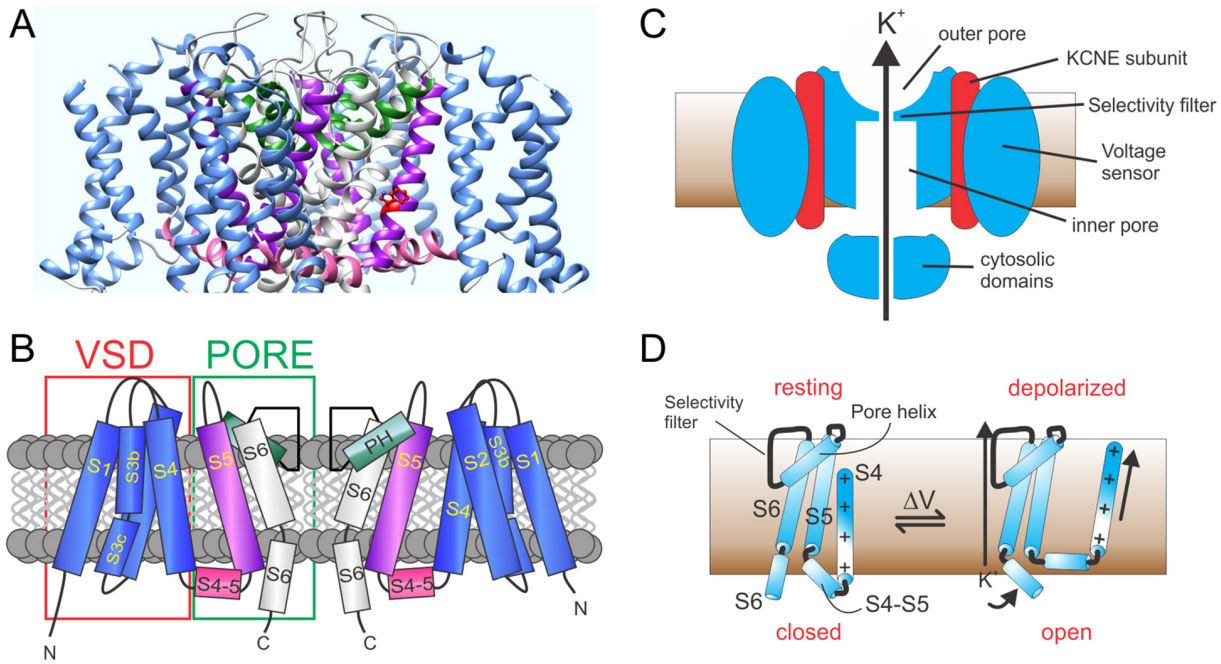

FIGURE 1 | KCNQ channel architecture. **(A)** KCNQ1–KCNQ3 chimeric structural model based on cryo-EM structure of *Xenopus* KCNQ1 (Sun and MacKinnon, 2017). **(B)** Schematic showing membrane topology; domain coloring as above. VSD, voltage sensing domain; PH, pore helix. **(C)** Section through KCNQ1–KCNE complex showing main features. **(D)** Cartoon of voltage gating depicting the S4–S6 portions of a Kv α subunit monomer and the types of conformational shifts that may occur upon membrane depolarization.

It is likely that PIP_2 is required for allosteric coupling between the activated VSD and the open pore based on studies in KCNQ1 (Zaydman et al., 2013), KCNQ2, and KCNQ3 (Choveau et al., 2018). PIP_2 probably does not open the pore directly; i.e., effects of coupling alone can explain its obligate role in KCNQ channel opening (Zaydman et al., 2013), but one can still consider KCNQ gating as ligand-dependent as without PIP_2 the voltage-dependent gating process cannot occur.

PIP_2 regulation of KCNQs is thought to serve an essential role in control of cellular excitability in tissues expressing KCNQs. For example, PIP_2 depletion via activation of muscarinic acetylcholine receptors is thought to be a major mechanism for the excitatory action of acetylcholine. By depleting PIP_2, neuronal M-current (generated primarily by KCNQ2–KCNQ3 heteromers) is inhibited, favoring neuronal depolarization and increased action potential frequency. As KCNQ2–KCNQ3 heteromers are located in key positions, such as the axon initial segment and in nodes of Ranvier, they can act as gatekeepers for action potential propagation (Brown and Adams, 1980; Klinger et al., 2011).

Various structure–function studies have provided a picture of the likely sites at which PIP_2 binds and/or acts allosterically on KCNQ channels to exert its strong influence on channel activation. The sites that coordinate functionally relevant interactions of PIP_2 are clustered in or near the S2–S3 and S4–S5 linkers and at or near the junction between S6 and the C-terminal domain (Kim et al., 2017; Choveau et al., 2018) (**Figures 2A,B**). This clustering makes perfect sense for the proposed role of PIP_2 in coordinating bidirectional coupling between the VSD and the pore.

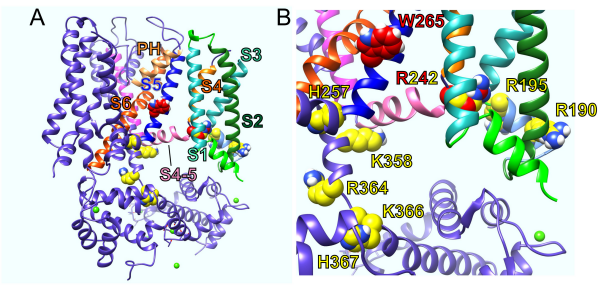

FIGURE 2 | KCNQ residues influential in effects of PIP_2, GABA, and metabolites. **(A)** KCNQ1–KCNQ3 chimeric structural model showing residues important for effects of PIP_2 (yellow) and GABA and metabolites (red). PH, pore helix. **(B)** Close-up of residues in A with human KCNQ3 residue numbering.

KCNQ channels are also sensitive to Ca^{2+} by virtue of calmodulin (CaM), which is an essential ancillary subunit for KCNQ channels (Gamper et al., 2005; Ghosh et al., 2006; Shamgar et al., 2006). CaM binds to the proximal C-terminus of KCNQ1 and is thought to compete with PIP_2 to stabilize the KCNQ1 open state; this also occurs in physiological relevant complexes in which KCNQ1-CaM co-assembles with the KCNE1 ancillary subunit to form I_{Ks} complexes (see below) (Tobelaim et al., 2017).

It is thought that increases in cytosolic Ca^{2+} can compensate for receptor-mediated depletion of PIP_2 via an interaction between the calcified N lobe of CaM and the KCNQ1 proximal C-terminus (at Helix B) that mimics or substitutes for the KCNQ1-PIP_2 interaction to curtail I_{Ks} current inhibition (Tobelaim et al., 2017). Increased cytosolic Ca^{2+} and consequent CaM calcification may also alter the manner in which CaM binds to KCNQ channels based on experiments with KCNQ2 such that calcified CaM displaces PIP_2 by altering the binding site and channel affinity for PIP_2 (Kosenko and Hoshi, 2013). Thus, KCNQ channel gating is also Ca^{2+}-sensitive, with Ca^{2+} binding to calmodulin displacing and/or substituting for PIP_2 to favor opening at more negative membrane potentials. Interestingly, CaM is also required for KCNQ2 exit from the endoplasmic reticulum, and this also, therefore, ensures that even KCNQ2 trafficking is ligand (Ca^{2+})-dependent (Alaimo et al., 2009).

REGULATION OF KCNQ CHANNEL ACTIVATION BY KCNE SUBUNITS

Channels formed by KCNQ1 in complexes with the single transmembrane domain KCNE1 ancillary subunit are essential in the heart and auditory system. The most striking result of KCNQ1–KCNE1 co-assembly is that KCNE1 greatly slows KCNQ1 activation (Yang et al., 1997; Sesti and Goldstein, 1998). Among the mechanistic models proposed for this effect, some suggest that KCNE1 slows S4 movement (Nakajo and Kubo, 2007; Ruscic et al., 2013), and others support direct slowing of KCNQ1 pore opening by KCNE1 (Rocheleau et al., 2006) or that KCNE1 imposes the need for movement of multiple voltage sensors before KCNQ1 channels open unlike what is thought to be the case for homomeric KCNQ1 (Osteen et al., 2010, 2012).

To modulate KCNQ1 in this manner, KCNE1 probably lies in a groove close to both the pore module and VSD (**Figure 3**). Essential for ventricular repolarization and for endolymph secretion in the inner ear, KCNQ1–KCNE1 channels also require PIP_2 for activation and are a hundredfold more sensitive to PIP_2 than are homomeric KCNQ1 channels. The proposed binding site for PIP_2 abuts regions considered important for KCNE1 regulation of KCNQ1, helping to explain the considerable influence of KCNE1 on KCNQ1 PIP_2 sensitivity (Li et al., 2011).

KCNQ1 can be converted to a constitutively open channel exhibiting relatively little voltage dependence across the physiological voltage range by forming heteromeric complexes with either KCNE2 (in gastric parietal cells) or KCNE3 (in intestinal epithelium) (Lee et al., 2000; Schroeder et al., 2000; Tinel et al., 2000; Roepke et al., 2006). To perform their function in gastric glands, i.e., provide a K^+ efflux pathway from parietal cells to supply the gastric H^+/K^+-ATPase with luminal K^+ ions so that it can secrete protons into the stomach lumen, KCNQ1–KCNE2 channels must exhibit two properties. First, they must stay open and non-inactivated at weakly negative voltages (probably largely between −40 and −20 mV in parietal cells); second, they must continue to function efficiently while withstanding the highly acidic extracellular environment of the gastric pits (pH 2–3).

The constitutive activation is probably achieved by KCNE2 favoring the activated conformation of the VSD, a phenomenon that has been studied in much greater detail for KCNQ1–KCNE3 channels because their greater macroscopic currents facilitate electrophysiological and mutagenesis-based structure function studies (Abbott, 2015, 2016). Homomeric KCNQ1 channels are inhibited by extracellular H^+ ions, manifested as a positive shift in the voltage dependence of activation and slower activation. KCNQ1–KCNE2 current, in contrast, is augmented by low extracellular pH. This property is endowed by the KCNE2 extracellular N-terminus and neighboring region of the transmembrane domain and is not a general property of constitutively open KCNQ1 channels because KCNQ1–KCNE3 channels are largely voltage-independent (see below) yet insensitive to pH (Heitzmann et al., 2004, 2007).

Unlike KCNE2, KCNE3 permits KCNQ1 to pass macroscopic outward currents at levels equivalent to or greater than those generated by homomeric KCNQ1 (Schroeder et al., 2000). KCNE3 favors constitutive activation of KCNQ1 by locking the voltage sensor in its activated conformation rather than by directly locking the pore open independent of the voltage sensor (Nakajo and Kubo, 2007; Panaghie and Abbott, 2007). The McDonald lab discovered that residues in the KCNE3 transmembrane domain are essential for KCNQ1–KCNE3 constitutive activation (Melman et al., 2001, 2002). We subsequently identified additional KCNE3 residues at the membrane-proximal region of the extracellular portion of KCNE3 (D54, D55), which interact with KCNQ1–S4 as part of the constitutive activation process (Choi and Abbott, 2010). It is not yet entirely clear how PIP_2 regulates gating of constitutively active KCNQ1–KCNE2 or KCNQ1–KCNE3 channels, but co-assembly of KCNQ1 with KCNE3 protects the channel from the inhibition observed for homomeric KCNQ1 upon sphingomyelinase removal of lipid head groups from the plasma membrane (Choi and Abbott, 2010). Furthermore, in recent cryo-electron microscopy–resolved structures in the presence and absence of PIP_2, KCNE3 appeared to be locking open the voltage sensor as we previously concluded (Panaghie and Abbott, 2007), but in the absence of PIP_2, the pore still appeared to be closed (Sun and MacKinnon, 2020). Further electrophysiological analyses are necessary to confirm these findings, but it appears that even KCNQ1–KCNE3 channels require PIP_2 for VSD-pore coupling and pore opening, at least in the conditions used for structural analysis.

ACTIVATION OF KCNQ CHANNELS BY DIRECT BINDING OF NEUROTRANSMITTERS AND METABOLITES

Neuronal KCNQ channels (KCNQ2-5 isoforms) each contain a conserved Trp residue in their S5 segment that confers sensitivity to the anticonvulsant, retigabine (Tatulian et al., 2001; Schenzer et al., 2005). Binding of retigabine to KCNQ2–5 isoforms negative-shifts their voltage dependence of activation. At a

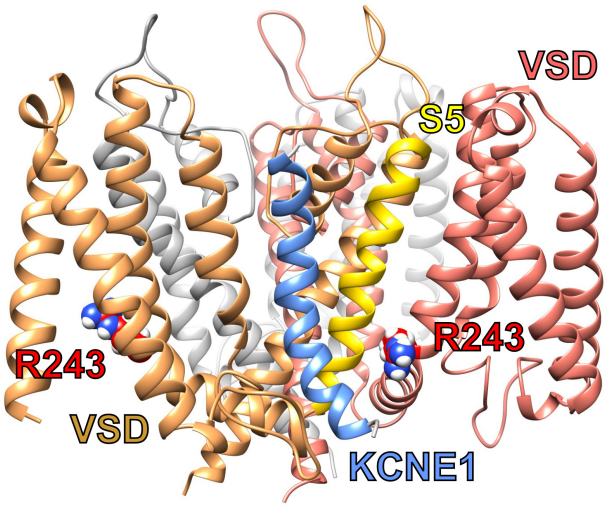

FIGURE 3 | Predicted structure of KCNQ1-KCNE1 complex. KCNQ1–KCNE1 structural model showing predicted position of KCNE1 (blue between two KCNQ1 subunits (sand and salmon) and close to S5 (yellow) and R243 (red) or one subunit. Plotted from model coordinates made available in Kang et al. (2008).

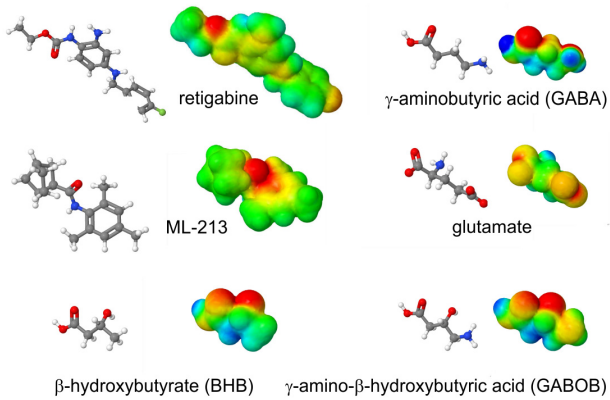

FIGURE 4 | Structures and calculated electrostatic surface potentials of KCNQ activators. Structures and calculated electrostatic surface potentials of KCNQ activators as indicated; red = negative, blue = positive extremes. Plotted using Jmol.

given voltage, wash-in of retigabine increases KCNQ2–5 current without the need to change the voltage. Thus, although KCNQ channels are highly voltage-sensitive, they can be "activated" at a given voltage by a ligand (retigabine) that requires (and likely binds to) the S5 Trp (W265 in KCNQ3, for example). KCNQ3 is the most highly retigabine-sensitive KCNQ channel, but KCNQ2, 4, and 5 each also respond. KCNQ1 is not activated by retigabine because KCNQ1 lacks the S5 Trp (Schroder et al., 2001).

The S5 Trp is thought to favor binding of (and is certainly required for activation by) molecules such as retigabine because they contain a negative electrostatic surface potential centered on a carbonyl group (Kim et al., 2015) (**Figure 4**). The S5 Trp has been conserved in evolution for about 600 million years and is present in the neuronal KCNQ-type channels of essentially all deuterostomes and also some of the Cnidaria but absent in protostomes (the genomes of which contain a KCNQ channel that lacks the S5 Trp) (Manville et al., 2018) (**Figures 5A,B**). Hypothesizing that the S5 Trp is conserved to bind an endogenous ligand, we began looking for ligands with similar chemical properties to retigabine. This led to the discovery that γ-aminobutyric acid (GABA), which also

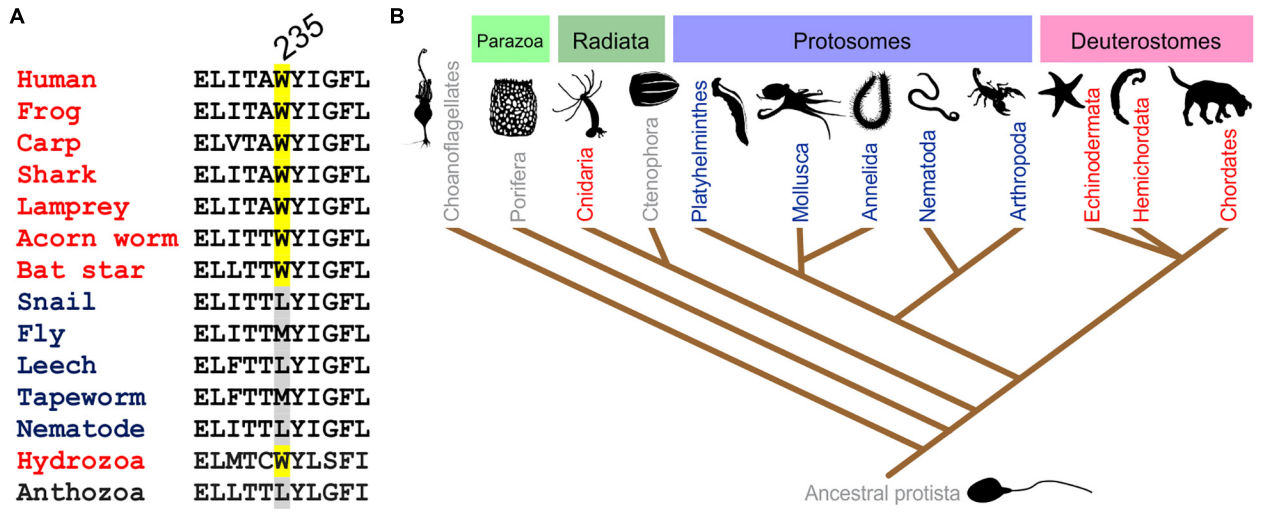

FIGURE 5 | Conservation of the KCNQ5 S5 Trp. **(A)** Sequence alignment of the GABA-binding S5 Trp-containing portion of KCNQ5 or the closest ortholog in various organisms. Adapted with permission from Manville et al., 2018. **(B)** Evolutionary relationships of organisms showing representation of KCNQ channels in major animal clades. Red, organisms contain multiple KCNQs, including one or more with the GABA-binding S5 Trp; blue, one KCNQ, lacking the GABA-binding S5 Trp; gray, no KCNQ. From Manville et al. (2018) used with permission.

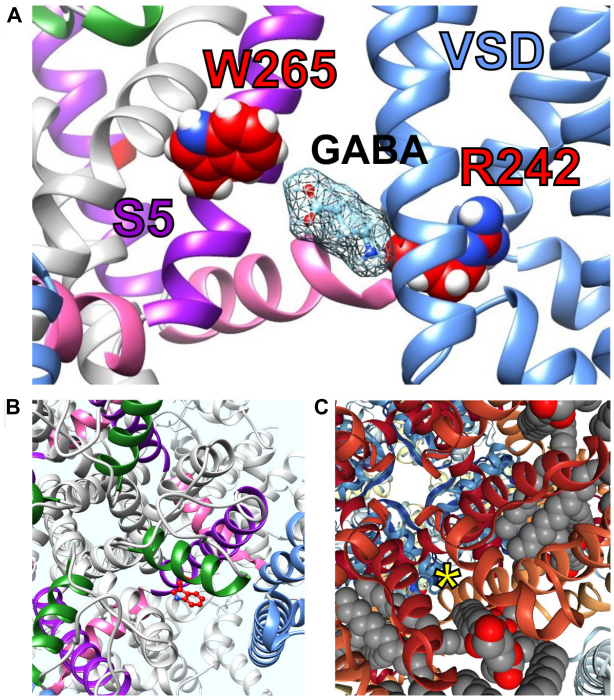

FIGURE 6 | Predicted KCNQ GABA binding site and accessibility. **(A)** SwissDock prediction of GABA binding pose in KCNQ3. VSD, voltage sending domain. **(B)** Extracellular view of KCNQ3-W265 (red) showing possibility access site from outside the cell. Purple, S5; blue, VSD, pink, S4, S5 linker; green pore helix. From Manville et al. (2018) used with permission. **(C)** Similar view as in panel B, but in the Kv1.2–Kv2.1 "paddle-chimera" structure (Long et al., 2007) showing S5 accessibility (*) despite lipid presence (lipids shown in gray/red). Adapted from Manville et al. (2018) with permission.

possesses a carbonyl group with associated predicted negative electrostatic surface potential (**Figure 4**), binds directly and S5-Trp dependently (**Figure 6A**) to KCNQ2, 3, 4, and 5, but not KCNQ1 (which lacks the S5 Trp) (Manville et al., 2018).

An arginine situated between the voltage-sensing S4 segment and the intracellular linker region that connects S4 to S5 (S4–S5 linker) is also required for GABA binding (Manville et al., 2019) (**Figure 6A**). This dependence, together with docking studies, suggest a surprisingly deep binding site for GABA, but the site appears to be accessible from the extracellular side (**Figures 6B,C**). The S4–S5 linker arginine (R242 in KCNQ3) is also in the region that coordinates binding and/or the functional effects of PIP_2 (Kim et al., 2017). However, activation of KCNQ2/3 by GABA was unaffected by depletion of PIP_2, either by activation of muscarinic acetylcholine receptors or by wortmannin application (Manville et al., 2018). It is, therefore, possible that GABA works differently from retigabine in that it may not be as dependent on PIP_2 for coupling of the VSD to the pore for activation or perhaps helps replace PIP_2 in this role. Interestingly, the S4–S5 linker arginine residue important for PIP_2 effects on KCNQs, (i.e., KCNQ3–R242, KCNQ5–R212) is also required for GABA effects and, specifically, for binding. We know this because, unlike the large majority of studies examining Kv channel pharmacology, which rely solely on functional effects to infer binding, we directly quantified binding of tritiated GABA to wild-type versus R212A–KCNQ5 (Manville et al., 2019). Given the dual role of this residue in binding of GABA and probably PIP_2, it is difficult to ascertain the role of PIP_2 in coordinating GABA effects by mutation of this residue. Future studies could involve more comprehensive depletion of PIP_2 and then application of GABA followed by quantification of binding and functional effects. The K_d for GABA binding to KCNQ3 expressed in *Xenopus* oocytes is 126 nM (Manville et al., 2018), which is close to the tonic GABA level in the brain, reported at 160 nM (Santhakumar et al., 2006; Lee et al., 2010). This could mean that neuronal KCNQ channels are equipped to sense changes in tonic GABA levels.

Electrophysiological recordings of cloned channels in *Xenopus* oocytes and CHO cells and endogenous M-current in PC12 cells and mouse dorsal root ganglia (DRG) neurons showed that KCNQ3 and 5, but not KCNQ2 or 4, are "activated" by sub-micromolar to micromolar levels of GABA, making these channels more sensitive than many canonical GABA receptors. GABA negative-shifts the voltage dependence of KCNQ3 and KCNQ5 activation and also that of heteromeric KCNQ2/3 channels, the main molecular correlate of neuronal M-current. At a given voltage (e.g., −60 mV), wash-in of GABA is observed as an increase in activity with immediate onset that peaks at roughly 3 min. Thus, at a constant voltage, KCNQ channels possessing the S5 Trp can be "ligand-activated" by GABA in much the same way as canonical $GABA_A$ receptors (albeit without inactivation or desensitization as is observed for $GABA_A$ receptors) (Manville et al., 2018).

As GABA is the primary inhibitory neurotransmitter in metazoans, its activation of neuronal KCNQ channels makes physiologic sense, at least in broad terms; i.e., activation of M-current in a neuron tends to reduce excitability of that neuron. The structurally related excitatory neurotransmitter, glutamate, lacks the predicted surface negative surface potential and does not activate KCNQ2/3 channels even at millimolar concentrations (Manville et al., 2018). In addition, mutation of the S5 Trp to a leucine removes the ability of GABA to activate KCNQ2/3 channels and also greatly reduces GABA binding (quantified using tritiated GABA radioligand binding studies in *Xenopus* oocytes expressing KCNQ2/3) (Manville et al., 2018). The inhibitory neurotransmitter, glycine, which does not exhibit a strong surface negative electrostatic potential coupled to a carbonyl group, also did not activate KCNQ2/3 even at millimolar concentrations. However, modification of glycine to add these properties, e.g., by adding specific types of fluorophenyl ring, enabled glycine derivatives to bind to and selectively activate different KCNQ channel isoforms (Manville and Abbott, 2019b).

GABA binds directly to the pore module of KCNQ2-5 α subunits yet only activates channels containing KCNQ3 or KCNQ5. Together with the binding data described above, this suggests that the S5 Trp is required for binding but that other thus-far unidentified residues can influence whether binding leads to activation. What could be the physiological purpose, if any, of GABA binding to specific KCNQ subunits but not opening them? One possibility is that this is so that other

gating modifiers can influence whether GABA binding leads to activation in a context-specific manner (see section on interaction with solute transporters below). Another potential explanation is that GABA binding to channels that it does not activate exerts effects because it influences whether other active ligands can enter the GABA binding pocket on KCNQ channels. Yet another possibility is that binding of GABA to, e.g., KCNQ2 when in KCNQ2/3 heteromers does contribute to activation or modulates activation.

Aside from GABA, related endogenous metabolites β-hydroxybutyric acid (BHB) and γ-amino-β-hydroxybutyric acid (GABOB) also activate KCNQ3, KCNQ5, and KCNQ2/3, and they also require the S5 Trp (Manville et al., 2018, 2020). GABOB and BHB each also exhibit predicted negative electrostatic surface potential centered on a carbonyl group (**Figure 4**). GABOB is present endogenously in mammalian brain (Hayashi, 1959) and has also been utilized as an anticonvulsant drug outside the United States although it is low potency and more effective when used together with another anticonvulsant (Chemello et al., 1980; Swiss Pharmaceutical Society, 2000). GABOB is a partial agonist of $GABA_B$ receptors and a $GABA_A$ receptor agonist, and we recently found that GABOB is a high-potency partial agonist of KCNQ2/3 channels. GABOB is capable of competing out retigabine, GABA, and BHB from the KCNQ channel GABA binding pocket, reducing their inhibitory effects on excitability both *in vitro* and *in vivo* (Manville et al., 2018, 2020).

BHB is among the first and most important ketone bodies produced when mammals fast or adopt a ketogenic diet. Induction of ketosis has shown promise as an anticonvulsant approach, particularly in children with refractory epilepsy. Although there are several hypotheses for the antiepileptic mechanism of ketosis, BHB levels have been positively correlated with the efficacy of this therapeutic approach (Gilbert et al., 2000). BHB can reach 4 mM in the serum of children on a ketogenic diet and 1 mM in the brain (Pan et al., 2000). BHB activates KCNQ2/3 channels with an EC_{50} of 1 μM; therefore, levels observed in children in ketosis are well within the potential therapeutic range if KCNQ2/3 activation is part of this action. BHB was highly effective as an acute anticonvulsant protective agent in the mouse pentylene tetrazole chemoconvulsant seizure assay, and co-administration of an excess of GABOB reduced the efficacy of BHB in this model (and also reduced BHB activation of KCNQ2/3 *in vitro*) (Manville et al., 2018, 2020). Given this evidence, it is feasible that neuronal KCNQ channels sense the balance between GABA, BHB, GABOB, and other endogenous metabolites to regulate neuronal excitability.

Results from voltage-clamp fluorometry experiments suggest that retigabine binding to the KCNQ3 pore module stabilizes both the open state of the pore module and the activated step of the VSD, resulting in greatly slowed channel closing or deactivation under basal PIP_2 conditions (Kim et al., 2017). However, when PIP_2 interaction with the channel was disrupted, either by mutation or by PIP_2 depletion, the communication between pore module and VSD was greatly disrupted. VSD conformation, as inferred by a greatly increased fluorescence signal from the PIP_2-disconnected VSD, was highly perturbed although the VSD appeared still able to respond to voltage, and its voltage dependence was still hyperpolarized by retigabine (Kim et al., 2017).

Voltage clamp fluorometry studies of GABA activation of KCNQs have, to our knowledge, thus far not been reported. However, ionic permeability series experiments demonstrated that the relative permeability of Na^+ and Cs^+ compared to that of K^+ is increased by GABA activation of KCNQ3 and KCNQ5 channels but not by binding to KCNQ2 or KCNQ4 channels (which does not result in activation). This suggests that GABA binding to KCNQ3 and KCNQ5 induces a conformational change in the pore module that is not observed upon solely voltage-dependent activation in the absence of GABA (Manville and Abbott, 2020b). GABA activation of KCNQs can be observed as a negative shift in the voltage dependence of activation when plotting an I/V relationship or at a given voltage as an increase in current upon GABA wash-in. Combined with the evidence of a novel pore conformation upon GABA binding only when activation follows, GABA potentiation of KCNQ channel current can be viewed as a ligand-gating process, albeit in a channel that is also sensitive to voltage, analogous to the situation in BK channels with Ca^{2+} and voltage.

ACTIVATION OF KCNQ CHANNELS BY DIRECT BINDING OF PLANT METABOLITES

Several plant metabolites are now known to bind in a similar location to GABA within KCNQ channels but with some notable differences discussed below. In some cases, KCNQ activation by plant compounds provides a plausible molecular mechanistic basis for the purported benefits of certain botanical folk medicines.

Cilantro (*Coriandrum sativum*) probably originated in Iran (Batmanglij, 2018) and grows wild throughout Western Asia and Southern Europe. Cilantro has been consumed by humans for thousands of years; it was likely cultivated by the Ancient Egyptians and was discovered in the early Neolithic archeological site in Nahal Hemar Cave in Israel (Cumo, 2013). Cilantro and culantro (*Eryngium foetidum*), which has a similar but stronger taste than cilantro, have been used as traditional folk medicines in regions including Central and South America and the Caribbean (**Figure 7A**). The plants are used to treat a wide variety of disorders, including seizures (culantro is also referred to as fitweed) (Simon and Singh, 1986), and for their purported analgesic, anti-diabetic, and anti-inflammatory properties (Sahib et al., 2013). Each of these species contains several fatty aldehydes that give them the striking citrus-like cilantro/culantro smell and taste.

A 1:100 dilution of aqueous solution obtained by evaporating off the methanol from a methanolic extract of cilantro leaf activated KCNQ2/3 channels expressed in *Xenopus* oocytes by negatively shifting the voltage dependence of activation. Screening of nine compounds previously found by others to

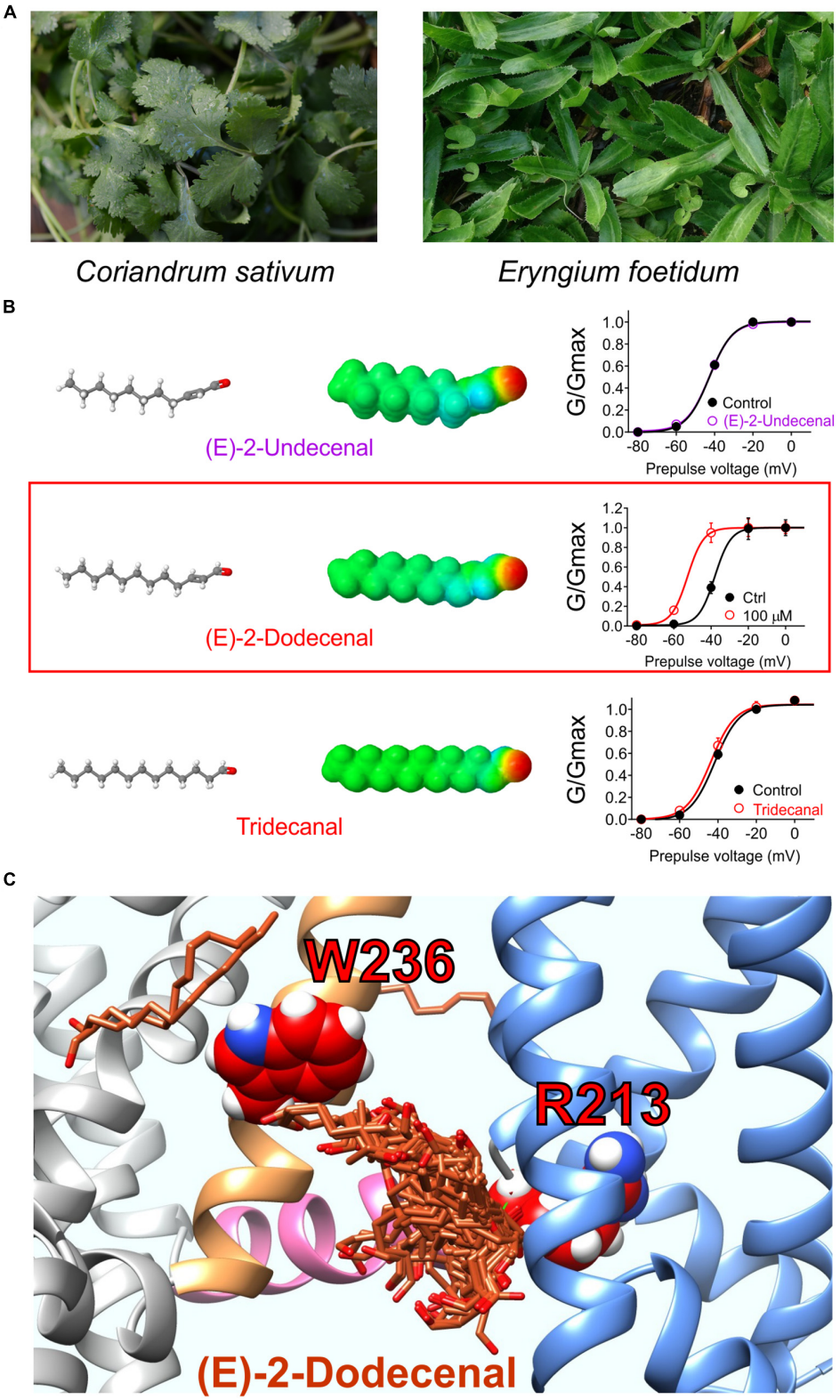

FIGURE 7 | Molecular basis for cilantro anticonvulsant effects. **(A)** Images of cilantro (left) and culantro (right). Required photo permissions: https://creativecommons.org/licenses/by/2.0/; https://commons.wikimedia.org/wiki/File:Culantro_(Eryngium_foetidum)_6.jpg. **(B)** Left, structures and Jmol surface electrostatic potential plots of three structurally similar fatty aldehydes; right, their corresponding effects on KCNQ2/3 G/V relationships (quantified from tail currents). Adapted from Manville and Abbott (2019a) with permission. **(C)** SwissDock prediction of E-2-dodecenal binding poses in KCNQ2. Blue, VSD; sand, S5; pink, S4, S5 linker.

be the most highly represented compounds in methanolic cilantro leaf extracts revealed a single compound that activated KCNQ2/3. The compound, E-2-dodecenal, activated KCNQ2 and KCNQ5 preferentially with lesser effects on KCNQ1 and KCNQ4 and no effect on KCNQ3, and KCNQ2/3 channels were highly sensitive (EC_{50} of 60 nM). E-2-dodecenal, also known as eryngial, is a fatty aldehyde; other fatty aldehydes with one more or one less carbon did not activate KCNQ2/3 even at millimolar quantities, indicating surprising selectivity among these compounds (Manville and Abbott, 2019a) (**Figure 7B**). E-2-dodecenal exhibits a predicted carbonyl-centered negative electrostatic surface potential and was predicted by SwissDock (Grosdidier et al., 2011a,b) docking studies to bind in a pocket near the KCNQ2–W236 residue in S5 but closer to KCNQ2–R213, which, unlike the S5 Trp, is present in the entire KCNQ family (hence, KCNQ1 was also activated by E-2-dodecenal). KCNQ2–R213 lies at the hinge between S4 in the VSD and the S4–S5 linker region. Consistent with docking studies (**Figure 7C**), in mutagenesis studies, the S5 Trp and the S4–S5 Arg were both required for E-2-dodecenal effects in KCNQ2/3 channels; in KCNQ1, the S4–S5 Arg (R243) was influential but not essential, and it was more important in KCNQ1–KCNE1 channels. This suggests that the requirement for the S5 Trp and the S4–S5 Arg for binding/activation of small molecules are context-dependent and that some molecules may well bind in this same pocket but with different molecular requirements and to different residues. In mouse PTZ-induced seizure studies, E-2-dodecenal was similarly effective at delaying seizures (Manville and Abbott, 2019a) as cilantro extract in a prior study of PTZ-induced seizures in rats (Karami et al., 2015). The findings were consistent with E-2-dodecenal activation of KCNQ2/3 channels contributing significantly to the known anticonvulsant effects of cilantro and culantro.

Interestingly, a loss-of-function variant of the S4–S5 Arg in human KCNQ2 (R213W) associates with both benign familial neonatal convulsions (Sadewa et al., 2008; Miceli et al., 2013) and the much more severe epileptic encephalopathy (Sadewa et al., 2008; Miceli et al., 2013; Milh et al., 2015). Further, the loss-of-function human KCNQ2–R213N variant is linked to epileptic encephalopathy in a two-generation pedigree in which various family members exhibited asymmetric quadriplegia, lifelong myokomia, and/or tonic-clonic seizures (Weckhuysen et al., 2012; Miceli et al., 2013; Orhan et al., 2014), further emphasizing the importance of this residue in KCNQ2 gating and in epilepsy. R213 lies in a BFNE and epileptic encephalopathy mutation hotspot that stretches from the S4-proximal S4–S5 linker to the extracellular end of S4; similar hotspots are present in S6 and the pore region (Zhang et al., 2020). In human KCNQ1, a mutation of the equivalent residue to histidine (R243H) reduces PIP_2 affinity and is associated with the cardiac arrhythmia, long QT syndrome (Park et al., 2005). Future analyses are required to determine whether compounds such as E-2-dodecenal can rescue epilepsy-associated KCNQ2–R213 or arrhythmia-associated KCNQ1–R243 mutant channels or if the mutation precludes binding and/or functional efficacy as we observed for KCNQ2–R213A.

The African shrub *Mallotus oppositifolius* (**Figure 8A**) is also used as a folk anticonvulsant (Igwe et al., 2016). Previously it was discovered that mallotoxin (a.k.a. rottlerin), a compound found in *Mallotus sp.*, hyperpolarizes the voltage dependence of KCNQ1 channel activation; however, it was at that time concluded to not modulate KCNQ2/3 channels (Matschke et al., 2016). An additional compound in *Mallotus oppositifolius*, 3-ethyl-2-hydroxy-2-cyclopenten-1-one, also activates KCNQ1 via R243 on the KCNQ1 S4–S5 linker (**Figures 8B,C**), but its effects do not synergize with those of mallotoxin to activate KCNQ1, and they may be unable to both bind in the same pocket (**Figure 8D**). Activation by *Mallotus* compounds of KCNQ1 alone and in complexes with KCNEs may contribute to its purported therapeutic effects in GI and cardiovascular disorders and diabetes given the known roles of KCNQ1 in these systems (De Silva et al., 2018; Manville and Abbott, 2018).

Unlike the prior study (Matschke et al., 2016), we found that mallotoxin and another compound within *Mallotus oppositifolius*, isovaleric acid (**Figure 8B**), each activate KCNQ2/3 channels. Mallotoxin and isovaleric acid preferentially activate KCNQ2 over KCNQ3 and appear able to both bind in the same GABA-binding pocket. Mallotoxin apparently binds closer to the S4–S5 Arg, explaining why it can also activate KCNQ1 (De Silva et al., 2018; Manville and Abbott, 2018). Isovaleric acid, which is also found in the commonly consumed herbal supplement valerian root, possesses the characteristic carbonyl-centered negative electrostatic surface potential, is predicted to bind closer to and requires the S5 Trp for activation and, hence, cannot activate KCNQ1 (**Figure 8E**). Mallotoxin and isovaleric acid are predicted to be able to bind simultaneously in the same binding pocket in KCNQ2/3 channels; accordingly, their activating (and anticonulvsant) effects synergize (**Figure 8F**) unlike those of MTX and CPT1 (**Figure 8D**) (De Silva et al., 2018; Manville and Abbott, 2018).

Consistent with docking and mutagenesis studies, GABOB (100 μM) was able to prevent isovaleric acid (500 μM) from activating KCNQ2, suggesting a common binding pocket. Interestingly, as isovaleric acid and mallotoxin preferentially activate KCNQ2, when combined with KCNQ3-preferring retigabine they were so effective that KCNQ2/3 channels were locked open even at −120 mV. *In vitro* studies suggested that combining lower doses of the three could be used as a therapeutic strategy to achieve effective KCNQ2/3 channel opening while minimizing some of the known retigabine-associated toxicity (Garin Shkolnik et al., 2014), but this triple combination has not yet been examined *in vivo* (Manville and Abbott, 2018).

In the vasculature, channels formed by KCNQ5 (Mackie et al., 2008; Yeung et al., 2008; Mani et al., 2009) alone and/or in complexes with KCNQ4 and the regulatory subunit KCNE4 (Jepps et al., 2011, 2015; Abbott and Jepps, 2016) are influential in setting vascular tone and as such are a potential target for blood pressure–lowering medications. Many botanical folk medicines are thought to help lower blood pressure and are used for this purpose currently. In some cases, this tradition is supported by preclinical and/or clinical evidence (Manville et al., 2019). In a study of 10 such botanical "hypotensive"

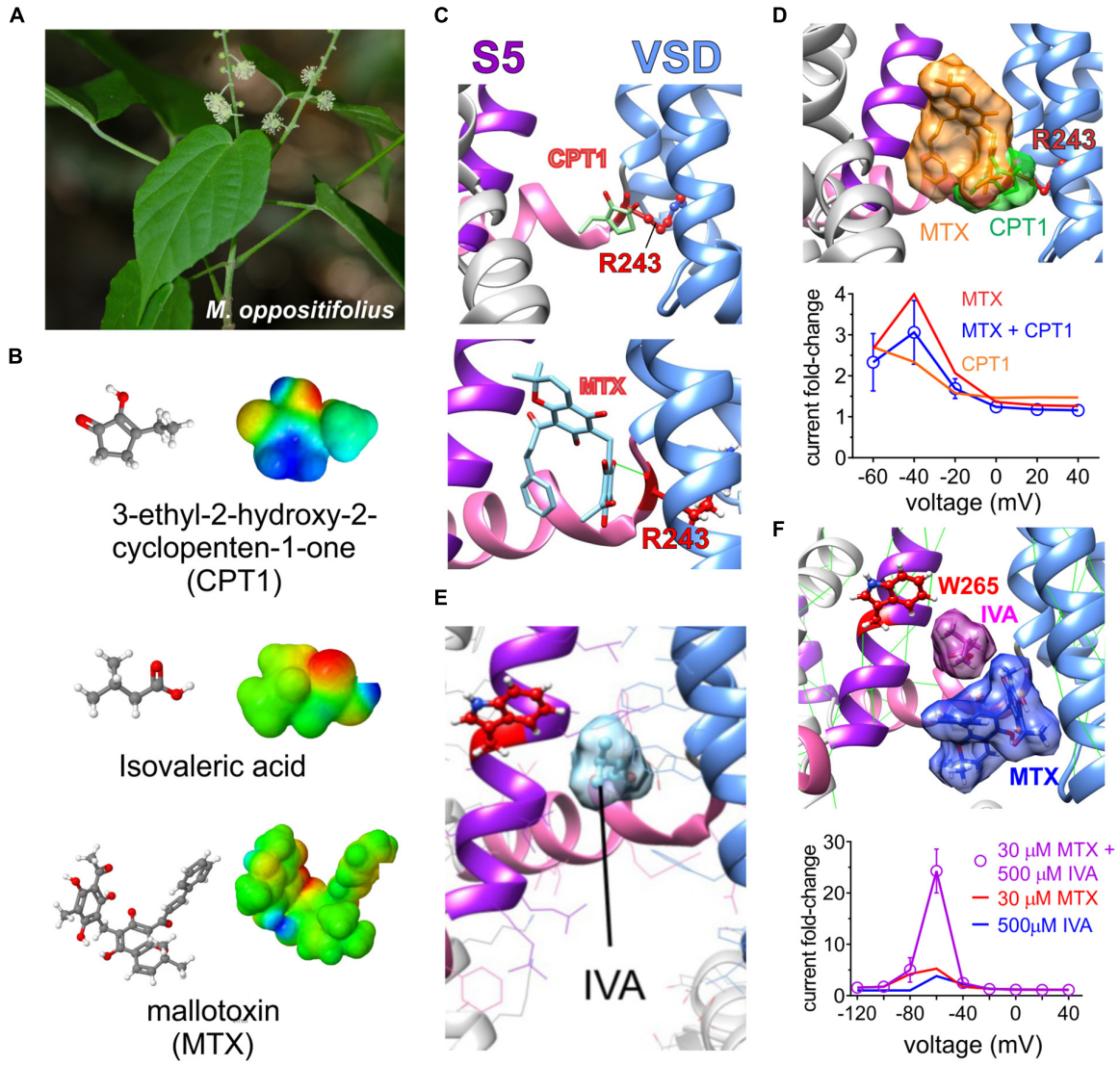

FIGURE 8 | Molecular basis for *Mallotus oppositifolius* anticonvulsant effects. Images from or adapted with permission from De Silva et al. (2018) and Manville and Abbott (2018). **(A)** Image of *Malloutus oppositifolius*. **(B)** Structures and Jmol surface electrostatic potential plots of three KCNQ-activating compounds from *Malloutus oppositifolius*. **(C)** Predicted binding sites of CPT1 and MTX within KCNQ1. VSD, voltage sensor. **(D)** Upper, predicted overlap of CPT1 and MTX binding sites that would prevent both occupying a single binding pocket in KCNQ1. Lower, Effects of CPT1 and MTX (100 μM) alone or together quantified as KCNQ1 current fold-change versus voltage, showing lack of synergy or summation. **(E)** Predicted binding site of isovaleric acid (IVA) within KCNQ2/3. Red, KCNQ2–W236, or KCNQ3–W265. **(F)** Upper, predicted neighboring binding poses of IVA and MTX binding sites that could allow both to occupy a single binding pocket in KCNQ2 or 3. Lower, Effects of IVA and MTX alone or together quantified as KCNQ2/3 current fold-change versus voltage, showing synergistic effects.

folk medicines, all 10 activated KCNQ5 channels and strikingly did not activate KCNQ2/3 channels, indicating some degree of isoform specificity. These included very commonly consumed plants, such as ginger, thyme, oregano, basil, marjoram, and fennel as well as herbal remedy staples, such as lavender, chamomile, and *Sophora* species uses in traditional Chinese medicine. Some of these plants have a surprisingly ancient and rich history with respect to their use by human species (**Figure 9A**; Manville et al., 2019).

One of the plants studied, the traditional Chinese medicine Ku shen (*Sophora flavescens*) (**Figure 9B**), contains a molecule, aloperine, which isoform-specifically activated KCNQ5 with an EC_{50} of 390 nM. Matrine and oxymatrine, also present in *S. flavescens* (**Figure 9C**), exerted mild activating effects that moderately augmented those of aloperine but did not synergize with it (Manville et al., 2019). Aloperine requires the S4–S5 linker arginine (KCNQ5–R212) for both binding to (as suggested by competition with tritiated GABA) and activation of KCNQ5 and was predicted to dock close to this residue (**Figure 9D**; Manville et al., 2019), which is also in or near the predicted PIP_2 binding site as discussed in the sections on PIP_2 and GABA above.

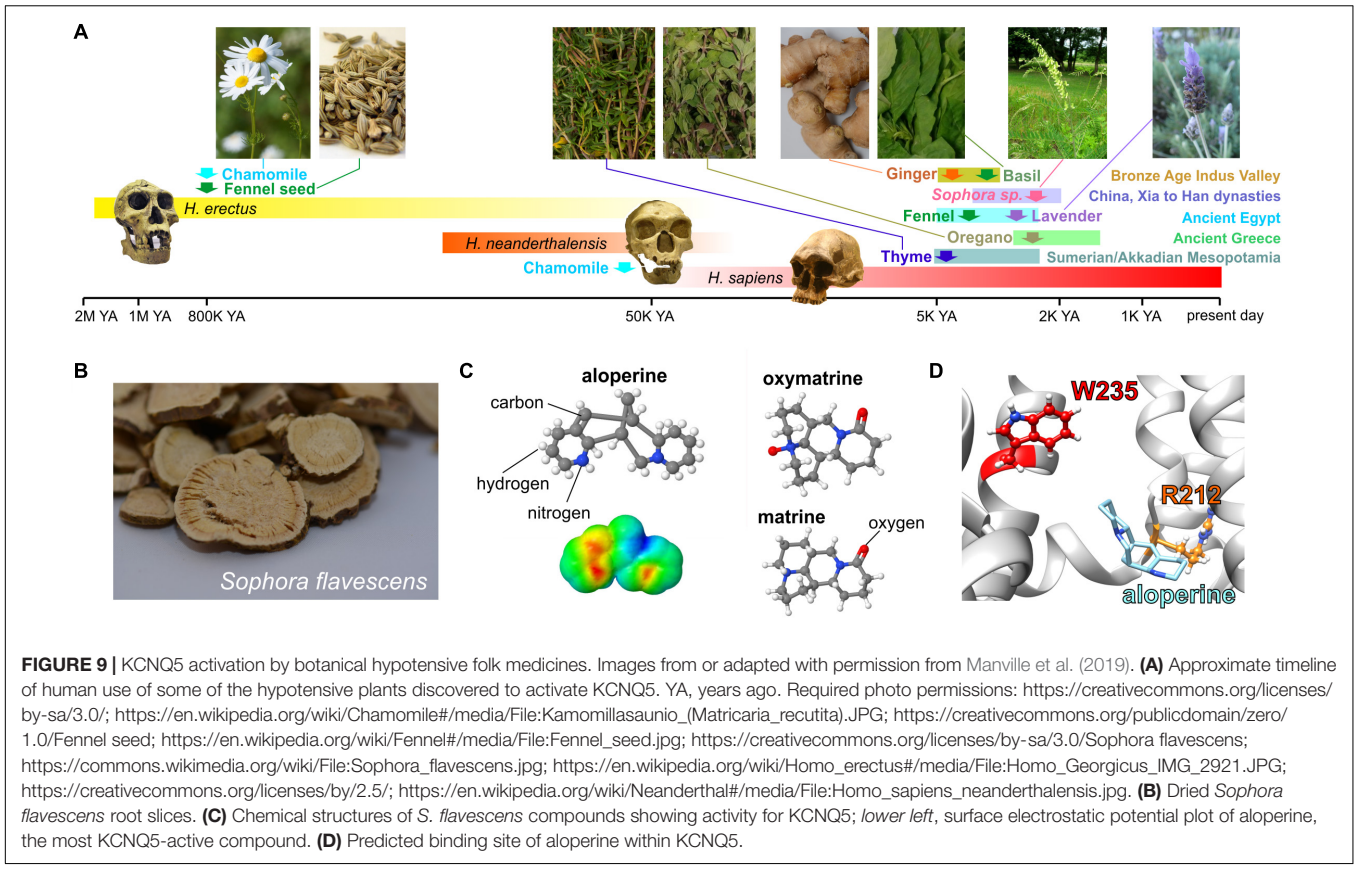

FIGURE 9 | KCNQ5 activation by botanical hypotensive folk medicines. Images from or adapted with permission from Manville et al. (2019). **(A)** Approximate timeline of human use of some of the hypotensive plants discovered to activate KCNQ5. YA, years ago. Required photo permissions: https://creativecommons.org/licenses/by-sa/3.0/; https://en.wikipedia.org/wiki/Chamomile#/media/File:Kamomillasaunio_(Matricaria_recutita).JPG; https://creativecommons.org/publicdomain/zero/1.0/Fennel seed; https://en.wikipedia.org/wiki/Fennel#/media/File:Fennel_seed.jpg; https://creativecommons.org/licenses/by-sa/3.0/Sophora flavescens; https://commons.wikimedia.org/wiki/File:Sophora_flavescens.jpg; https://en.wikipedia.org/wiki/Homo_erectus#/media/File:Homo_Georgicus_IMG_2921.JPG; https://creativecommons.org/licenses/by/2.5/; https://en.wikipedia.org/wiki/Neanderthal#/media/File:Homo_sapiens_neanderthalensis.jpg. **(B)** Dried *Sophora flavescens* root slices. **(C)** Chemical structures of *S. flavescens* compounds showing activity for KCNQ5; *lower left*, surface electrostatic potential plot of aloperine, the most KCNQ5-active compound. **(D)** Predicted binding site of aloperine within KCNQ5.

In sum, the above studies strongly suggest that KCNQ channels evolved a binding pocket accessible to neurotransmitters, plant metabolites, and other endogenous and exogenous compounds, many of which can activate KCNQ channels by inducing a novel pore conformation and/or altering coupling between the VSD and pore. Two models are proposed, one requiring PIP_2 and one not (**Figures 10A–D**). KCNQ isoform selectivity of the small molecules is varied. Retigabine, for example, activates KCNQ2–5 but not KCNQ1 (because it lacks the S5 Trp) (Schroder et al., 2001); conversely, aloperine is relatively KCNQ5-specific (Manville et al., 2019). Molecules such as aloperine and GABA bind to multiple KCNQ isoforms but only activate a subset; therefore, selectivity is often functional not physical (Manville et al., 2018, 2019). In addition, KCNQs are modulated by a range of different ancillary subunits that can dramatically alter the binding site, selectivity, and/or functional effects of small molecules and must be considered and, where possible, leveraged for increased specificity (Panaghie and Abbott, 2006). Finally, some small molecules, e.g., glycine derivatives that we engineered to activate KCNQs and which rely on the S4–S5 Arg, can exhibit isoform selectivity within the KCNQ family but also activate KCNA1 (but not KCNA2), Kv channels outside the KCNQ family that also bear the S4–S5 Arg (Manville and Abbott, 2020a). Indeed, GABA obviously activates canonical GABA receptors (in addition to KCNQs) (Schofield et al., 1987), and retigabine also activates GABA receptors (Treven et al., 2015). Thus, it is important to recognize that isoform selectivity within a channel family often does not guarantee selectivity in a broader sense—a challenge for drug development in this area.

CROSSTALK BETWEEN KCNQ-SOLUTE TRANSPORTER INTERACTIONS AND LIGAND GATING OF KCNQ CHANNELS

An interesting factor in regulation of KCNQs by small molecules, such as neurotransmitters, metabolites and PIP_2, is the ability of KCNQs to form reciprocally regulating macromolecular complexes with certain sodium-coupled solute transporters. Members of this class of transporters utilize the downhill sodium gradient from extracellular to intracellular compartments to provide energy powering the uphill transport of solutes, such as sugars, neurotransmitters, and ions, into cells. One such example is the sodium-coupled *myo*-inositol transporters (SMIT1 and SMIT2, encoded by *SLC5A3* and *SLC5A11*), each of which can co-assemble with various KCNQs (Abbott et al., 2014; Manville et al., 2017; Neverisky and Abbott, 2017). *Myo*-inositol is a cyclic polyol that is among the most important osmolytes in mammalian physiology (Berry, 2011). Especially important in the context of this review, it is also a substrate for production of signaling molecules, including phosphatidylinositol phosphates such as PIP_2 and can transport *myo*-inositol efficiently enough

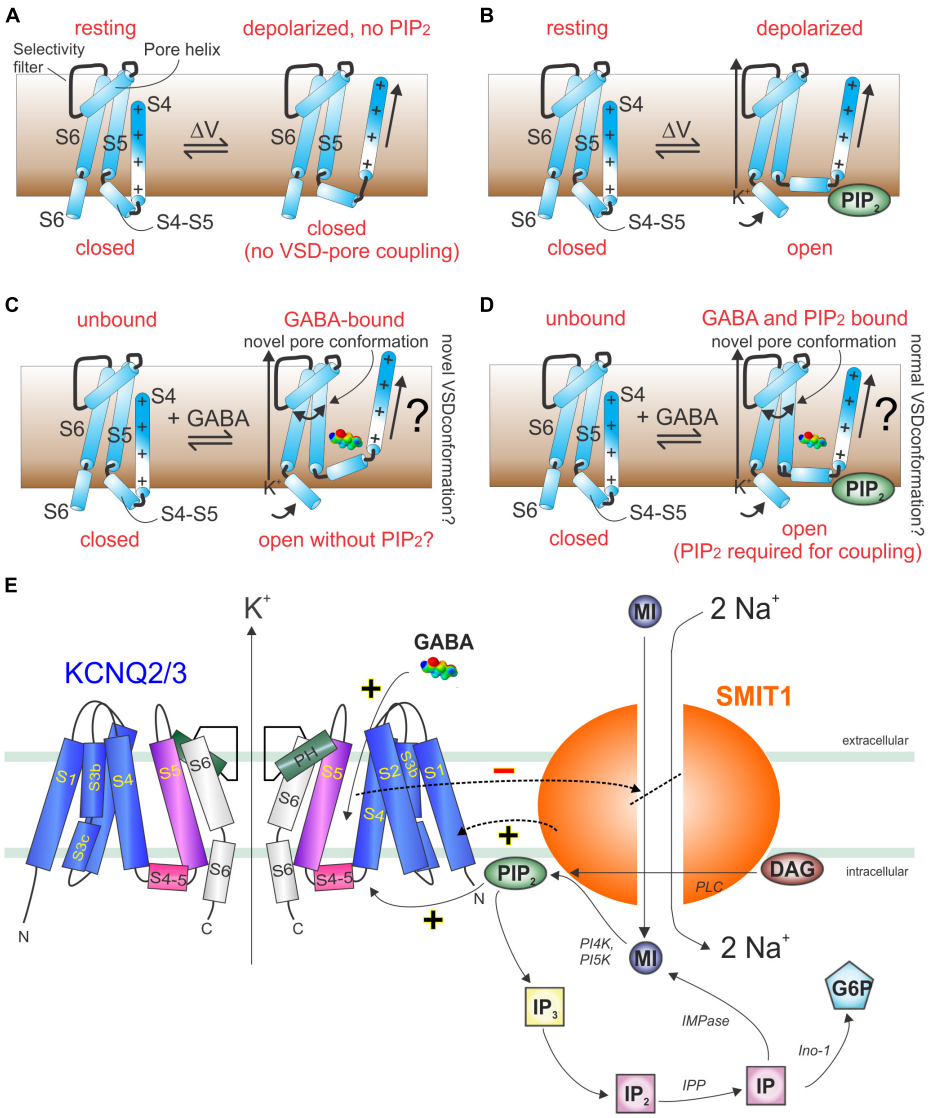

FIGURE 10 | Models of GABA and PIP_2 signaling in KCNQ and KCNQ2/3–SMIT1 complexes. **(A)** Cartoon showing lack of communication between the KCNQ VSD and pore in the absence of PIP_2. **(B)** Cartoon showing voltage-dependent activation of KCNQs in the presence of PIP2. **(C)** Cartoon showing hypothetical GABA-induced KCNQ activation in the absence of PIP_2. **(D)** Cartoon showing hypothetical GABA-induced KCNQ activation in the presence of PIP_2. **(E)** Cartoon of KCNQ2/3–SMIT1 interactions showing the functional consequences of physical interaction and modulation by small molecules. DAG, diacylglycerol; G6P, glucose-6-phosphate; IMPase, inositol monophosphatase; IP, inositol phosphate; inositol polyphosphatase 1-phosphatase; MI, *myo*-inositol; PI4K, phosphatidylinositol 4-kinase; *PI5K*, phosphatidylinositol-5 kinase; PLC, phospholipase C. From Manville and Abbott (2020b) with permission.

to increase local PIP_2 concentration and KCNQ-dependently couple osmotic potential to cellular excitability (Dai et al., 2016).

Myo-inositol levels in the cerebrospinal fluid (CSF) are tightly regulated. *Myo*-inositol is actively concentrated in the CSF from the blood, primarily across the choroid plexus epithelium, via basolateral uptake through SMIT1 (Spector and Lorenzo, 1975; Guo et al., 1997). SMIT1 is expressed at both the basolateral and apical membranes of the choroid plexus epithelium and can form complexes with KCNQ1–KCNE2 channels at the apical side (Abbott et al., 2014).

KCNQ1–KCNE2 channels inhibit SMIT1 transport activity, reducing *myo*-inositol uptake, when studied in *Xenopus* oocytes (Abbott et al., 2014). SMIT1 is likely sensitive to the conformation of KCNQ1–KCNE2, and the KCNE2 subunit is required for inhibition but requires KCNQ1 to be also be present. KCNQ1-specific inhibitors also inhibit co-assembled SMIT1 activity, suggesting that K^+ efflux through KCNQ1 helps SMIT1 bring in more substrate, but only when the KCNQ1 conformation is amenable. Apical KCNQ1–KCNE2-SMIT1 channel-transporter complexes may regulate CSF *myo*-inositol composition. Removal of KCNE2 from these complexes may, thus, result in too much *myo*-inositol being removed from the CSF, a hypothesis supported by the finding that *Kcne2*$^{-/-}$ mice have reduced CSF *myo*-inositol, which is associated with increased seizure

susceptibility that is corrected by *myo*-inositol mega-dosing (Abbott et al., 2014). We do not yet know why the reduction in CSF *myo*-inositol predisposes to seizures, but it is possible that it causes local imbalances in PIP_2 and other signaling molecules in a manner that adversely affects ion channel activity, including neuronal KCNQs (Dai et al., 2016; Neverisky and Abbott, 2017).

SMIT1 also physically couples (to the pore module) of KCNQ2 (Manville et al., 2017); SMIT1 and SMIT2 co-assemble with KCNQ2/3 complexes in nodes of Ranvier and axon initial segments in mouse and/or rat brain (Neverisky and Abbott, 2017). SMIT1 alters the pore conformation, gating kinetics, and pharmacology of KCNQ1, KCNQ1–KCNE1, KCNQ2, KCNQ3, and KCNQ2/3 channels (Manville et al., 2017). These effects, including hyperpolarization of KCNQ2/3 channel activation voltage dependence, can occur without the necessity for SMIT1 to be transporting *myo*-inositol; i.e., they occur because of direct physical interaction between SMIT1 and the channels listed (Manville et al., 2017). In addition, however, transport of *myo*-inositol through SMIT1 can increase the substrate for local PIP_2 production, which can also regulate the KCNQ2/3 channel indirectly (Dai et al., 2016; Neverisky and Abbott, 2017).

GABA and other small molecules that activate KCNQ2/3 channels inhibit co-assembled SMIT1 *myo*-inositol transport activity, both in mouse dorsal root ganglia and when co-expressed in *Xenopus* oocytes (Manville and Abbott, 2020b). This suggests a feedback loop in which GABA activation of KCNQ2/3 reduces the local substrate for PIP_2 and, thus, eventually inhibits KCNQ2/3, releasing inhibition of co-assembled SMIT1 (**Figure 10E**; Manville and Abbott, 2020b). Intriguingly, co-assembly of SMIT1 alters KCNQ isoform sensitivity to BHB, such that KCNQ2 is now activated and KCNQ3 not, whereas the reverse is true in the absence of SMIT1 (Manville and Abbott, 2020b). However, GABA isoform sensitivity remains the same. Thus, KCNQ channels act as chemosensors permitting co-assembled transporters to respond to small molecules to which they were previously insensitive (GABA, BHB, retigabine), and conversely, the co-assembled transporter tunes how KCNQs respond to these small molecules (Manville and Abbott, 2020b). When one considers that KCNQ2/3 channels also co-assemble with dopamine and glutamate transporters, the stage is potentially set for previously unexpected regulatory mechanisms, e.g., GABA controlling neuronal uptake of other neurotransmitters via direct binding to voltage-gated channel-transporter complexes (Manville and Abbott, 2019c).

CONCLUSION

The physiological importance of specific roles for the signaling mechanisms outlined in this review will become clearer when data are available for mice in which regulation of KCNQs by GABA and related metabolites are disrupted—studies that are ongoing in the author's laboratory. As discussed for BK channels, KCNQ channels should be considered as channels gated by both voltage and by ligands, and the preponderance of either mechanism is likely context-dependent, specific to a given cell type under specific voltages, ligand concentration ranges, and interacting regulatory proteins that influence all these factors.

As KCNQ channel open probability can be dramatically increased at a given voltage by direct binding of GABA, via induction of a pore conformation that is not observed in activated channels in the absence of GABA (using relative ion permeability as a readout of pore conformation) (Manville and Abbott, 2020b), in this context, the channel can be viewed as ligand-activated. Conversely, in the absence of GABA, KCNQs can open solely in response to membrane depolarization with the sizeable caveat that for this to occur, binding of a different ligand (PIP_2) near the S4–S5 linker is required to couple VSD movement to the pore module in a manner that actually results in pore opening (Kim et al., 2017).

AUTHOR CONTRIBUTIONS

GA wrote the manuscript and prepared the figures.

FUNDING

The author is grateful for financial support from the United States National Institutes of Health awards GM130377 and NS107671.

ACKNOWLEDGMENTS

The author thanks Dr. Rían W. Manville (University of Brighton, UK) for helpful discussions and for conducting many of the experiments reviewed in this article, Bo Abbott for lavender, ginger, cilantro, and *S. flavescens* root slice images, and Helen M. Abbott for many years of expert advice on plants.

REFERENCES

Abbott, G. W. (2014). Biology of the KCNQ1 potassium channel. *New J. Sci.* 2014:237431.

Abbott, G. W. (2015). The KCNE2 K(+) channel regulatory subunit: ubiquitous influence, complex pathobiology. *Gene* 569, 162–172. doi: 10.1016/j.gene.2015.06.061

Abbott, G. W. (2016). KCNE1 and KCNE3: the yin and yang of voltage-gated K(+) channel regulation. *Gene* 576, 1–13. doi: 10.1016/j.gene.2015.09.059

Abbott, G. W., and Jepps, T. A. (2016). Kcne4 deletion sex-dependently alters vascular reactivity. *J. Vasc. Res.* 53, 138–148. doi: 10.1159/000449060

Abbott, G. W., Tai, K. K., Neverisky, D. L., Hansler, A., Hu, Z., Roepke, T. K., et al. (2014). KCNQ1, KCNE2, and Na^+-coupled solute transporters form reciprocally regulating complexes that affect neuronal excitability. *Sci. Signal.* 7:ra22. doi: 10.1126/scisignal.2005025

Alaimo, A., Gomez-Posada, J. C., Aivar, P., Etxeberria, A., Rodriguez-Alfaro, J. A., Areso, P., et al. (2009). Calmodulin activation limits the rate of KCNQ2 K+ channel exit from the endoplasmic reticulum. *J. Biol. Chem.* 284, 20668–20675. doi: 10.1074/jbc.m109.019539

Batmanglij, N. (2018). *A Taste of Persia: An Introduction to Persian Cooking*. London: I.B.Tauris.

Berkefeld, H., and Fakler, B. (2013). Ligand-gating by Ca^{2+} is rate limiting for physiological operation of BK(Ca) channels. *J. Neurosci.* 33, 7358–7367. doi: 10.1523/jneurosci.5443-12.2013

Berry, G. T. (2011). Is prenatal myo-inositol deficiency a mechanism of CNS injury in galactosemia? *J. Inherit. Metab. Dis.* 34, 345–355. doi: 10.1007/s10545-010-9260-x

Bezanilla, F., and Perozo, E. (2003). The voltage sensor and the gate in ion channels. *Adv. Protein Chem.* 63, 211–241. doi: 10.1016/s0065-3233(03)63009-3

Biervert, C., Schroeder, B. C., Kubisch, C., Berkovic, S. F., Propping, P., Jentsch, T. J., et al. (1998). A potassium channel mutation in neonatal human epilepsy. *Science* 279, 403–406. doi: 10.1126/science.279.5349.403

Brown, D. A., and Adams, P. R. (1980). Muscarinic suppression of a novel voltage-sensitive K+ current in a vertebrate neurone. *Nature* 283, 673–676. doi: 10.1038/283673a0

Catterall, W. A. (1995). Structure and function of voltage-gated ion channels. *Annu. Rev. Biochem.* 64, 493–531. doi: 10.1146/annurev.bi.64.070195.002425

Chemello, R., Giaretta, D., Pellegrini, A., and Testa, G. (1980). [Effect of gamma-amino-beta-hydroxybutyric acid (GABHB) on experimentally-induced epileptic activity]. *Riv. Neurol.* 50, 253–268.

Choi, E., and Abbott, G. W. (2010). A shared mechanism for lipid- and beta-subunit-coordinated stabilization of the activated K+ channel voltage sensor. *FASEB J.* 24, 1518–1524. doi: 10.1096/fj.09-145219

Choveau, F. S., De La Rosa, V., Bierbower, S. M., Hernandez, C. C., and Shapiro, M. S. (2018). Phosphatidylinositol 4,5-bisphosphate (PIP2) regulates KCNQ3 K(+) channels by interacting with four cytoplasmic channel domains. *J. Biol. Chem.* 293, 19411–19428. doi: 10.1074/jbc.ra118.005401

Cuello, L. G., Cortes, D. M., and Perozo, E. (2004). Molecular architecture of the KvAP voltage-dependent K+ channel in a lipid bilayer. *Science* 306, 491–495. doi: 10.1126/science.1101373

Cumo, C. (2013). *Encyclopedia of Cultivated Plants: From Acacia to Zinnia*. Santa Barbara, CA: ABC-CLIO.

Dai, G., Yu, H., Kruse, M., Traynor-Kaplan, A., and Hille, B. (2016). Osmoregulatory inositol transporter SMIT1 modulates electrical activity by adjusting PI(4,5)P2 levels. *Proc. Natl. Acad. Sci. U.S.A.* 113, E3290–E3299.

De Silva, A. M., Manville, R. W., and Abbott, G. W. (2018). Deconstruction of an African folk medicine uncovers a novel molecular strategy for therapeutic potassium channel activation. *Sci. Adv.* 4:eaav0824. doi: 10.1126/sciadv.aav0824

DeCaen, P. G., Yarov-Yarovoy, V., Sharp, E. M., Scheuer, T., and Catterall, W. A. (2009). Sequential formation of ion pairs during activation of a sodium channel voltage sensor. *Proc. Natl. Acad. Sci. U.S.A.* 106, 22498–22503. doi: 10.1073/pnas.0912307106

Doyle, D. A., Morais Cabral, J., Pfuetzner, R. A., Kuo, A., Gulbis, J. M., Cohen, S. L., et al. (1998). The structure of the potassium channel: molecular basis of K+ conduction and selectivity. *Science* 280, 69–77. doi: 10.1126/science.280.5360.69

Gamper, N., Li, Y., and Shapiro, M. S. (2005). Structural requirements for differential sensitivity of KCNQ K^+ channels to modulation by Ca^{2+}/calmodulin. *Mol. Biol. Cell* 16, 3538–3551. doi: 10.1091/mbc.e04-09-0849

Garin Shkolnik, T., Feuerman, H., Didkovsky, E., Kaplan, I., Bergman, R., Pavlovsky, L., et al. (2014). Blue-gray mucocutaneous discoloration: a new adverse effect of ezogabine. *JAMA Dermatol.* 150, 984–989.

Ghosh, S., Nunziato, D. A., and Pitt, G. S. (2006). KCNQ1 assembly and function is blocked by long-QT syndrome mutations that disrupt interaction with calmodulin. *Circ. Res.* 98, 1048–1054. doi: 10.1161/01.res.0000218863.44140.f2

Gilbert, D. L., Pyzik, P. L., and Freeman, J. M. (2000). The ketogenic diet: seizure control correlates better with serum beta-hydroxybutyrate than with urine ketones. *J Child Neurol* 15, 787–790. doi: 10.1177/088307380001501203

Grosdidier, A., Zoete, V., and Michielin, O. (2011a). Fast docking using the CHARMM force field with EADock DSS. *J. Comput. Chem.* 32, 2149–2159. doi: 10.1002/jcc.21797

Grosdidier, A., Zoete, V., and Michielin, O. (2011b). SwissDock, a protein-small molecule docking web service based on EADock DSS. *Nucleic Acids Res.* 39, W270–W277.

Guo, W., Shimada, S., Tajiri, H., Yamauchi, A., Yamashita, T., Okada, S., et al. (1997). Developmental regulation of Na^+ / myo-inositol cotransporter gene expression. *Brain Res. Mol. Brain Res.* 51, 91–96. doi: 10.1016/s0169-328x(97)00220-9

Hayashi, T. (1959). The inhibitory action of beta-hydroxy-gamma-aminobutyric acid upon the seizure following stimulation of the motor cortex of the dog. *J. Physiol.* 145, 570–578. doi: 10.1113/jphysiol.1959.sp006163

Heitzmann, D., Grahammer, F., Von Hahn, T., Schmitt-Graff, A., Romeo, E., Nitschke, R., et al. (2004). Heteromeric KCNE2/KCNQ1 potassium channels in the luminal membrane of gastric parietal cells. *J. Physiol.* 561, 547–557. doi: 10.1113/jphysiol.2004.075168

Heitzmann, D., Koren, V., Wagner, M., Sterner, C., Reichold, M., Tegtmeier, I., et al. (2007). KCNE beta subunits determine pH sensitivity of KCNQ1 potassium channels. *Cell. Physiol. Biochem.* 19, 21–32. doi: 10.1159/000099189

Hille, B., Armstrong, C. M., and Mackinnon, R. (1999). Ion channels: from idea to reality. *Nat. Med.* 5, 1105–1109. doi: 10.1038/13415

Igwe, K. K., Madubuike, A. J., Otuokere, I. E., Amaku, F. J., and Chika, I. (2016). GC-MS analysis for structural identification and bioactive compounds in methanolic leaf extract of *Mallotus oppositifolius*. *Int. J. Sci. Res. Manage.* 4, 4123–4129.

Jepps, T. A., Carr, G., Lundegaard, P. R., Olesen, S. P., and Greenwood, I. A. (2015). Fundamental role for the KCNE4 ancillary subunit in Kv7.4 regulation of arterial tone. *J. Physiol.* 593, 5325–5340. doi: 10.1113/jp271286

Jepps, T. A., Chadha, P. S., Davis, A. J., Harhun, M. I., Cockerill, G. W., Olesen, S. P., et al. (2011). Downregulation of kv7.4 channel activity in primary and secondary hypertension. *Circulation* 124, 602–611. doi: 10.1161/circulationaha.111.032136

Kang, C., Tian, C., Sonnichsen, F. D., Smith, J. A., Meiler, J., George, A. L., et al. (2008). Structure of KCNE1 and implications for how it modulates the KCNQ1 potassium channel. *Biochemistry* 47, 7999–8006. doi: 10.1021/bi800875q

Karami, R., Hosseini, M., Mohammadpour, T., Ghorbani, A., Sadeghnia, H. R., Rakhshandeh, H., et al. (2015). Effects of hydroalcoholic extract of *Coriandrum sativum* on oxidative damage in pentylenetetrazole-induced seizures in rats. *Iran. J. Neurol.* 14, 59–66.

Kim, R. Y., Pless, S. A., and Kurata, H. T. (2017). PIP2 mediates functional coupling and pharmacology of neuronal KCNQ channels. *Proc. Natl. Acad. Sci. U.S.A.* 114, E9702–E9711.

Kim, R. Y., Yau, M. C., Galpin, J. D., Seebohm, G., Ahern, C. A., Pless, S. A., et al. (2015). Atomic basis for therapeutic activation of neuronal potassium channels. *Nat. Commun.* 6:8116.

Klinger, F., Gould, G., Boehm, S., and Shapiro, M. S. (2011). Distribution of M-channel subunits KCNQ2 and KCNQ3 in rat hippocampus. *Neuroimage* 58, 761–769. doi: 10.1016/j.neuroimage.2011.07.003

Kosenko, A., and Hoshi, N. (2013). A change in configuration of the calmodulin-KCNQ channel complex underlies Ca^{2+}-dependent modulation of KCNQ channel activity. *PLoS One* 8:e82290. doi: 10.1371/journal.pone.0082290

Kubisch, C., Schroeder, B. C., Friedrich, T., Lutjohann, B., El-Amraoui, A., Marlin, S., et al. (1999). KCNQ4, a novel potassium channel expressed in sensory outer hair cells, is mutated in dominant deafness. *Cell* 96, 437–446. doi: 10.1016/s0092-8674(00)80556-5

Lee, M. P., Ravenel, J. D., Hu, R. J., Lustig, L. R., Tomaselli, G., Berger, R. D., et al. (2000). Targeted disruption of the Kvlqt1 gene causes deafness and gastric hyperplasia in mice. *J. Clin. Invest.* 106, 1447–1455. doi: 10.1172/jci10897

Lee, S., Yoon, B. E., Berglund, K., Oh, S. J., Park, H., Shin, H. S., et al. (2010). Channel-mediated tonic GABA release from glia. *Science* 330, 790–796. doi: 10.1126/science.1184334

Lee, U. S., and Cui, J. (2010). BK channel activation: structural and functional insights. *Trends Neurosci.* 33, 415–423. doi: 10.1016/j.tins.2010.06.004

Li, Y., Zaydman, M. A., Wu, D., Shi, J., Guan, M., Virgin-Downey, B., et al. (2011). KCNE1 enhances phosphatidylinositol 4,5-bisphosphate (PIP2) sensitivity of IKs to modulate channel activity. *Proc. Natl. Acad. Sci. U.S.A.* 108, 9095–9100. doi: 10.1073/pnas.1100872108

Long, S. B., Campbell, E. B., and Mackinnon, R. (2005a). Crystal structure of a mammalian voltage-dependent Shaker family K+ channel. *Science* 309, 897–903. doi: 10.1126/science.1116269

Long, S. B., Campbell, E. B., and Mackinnon, R. (2005b). Voltage sensor of Kv1.2: structural basis of electromechanical coupling. *Science* 309, 903–908. doi: 10.1126/science.1116270

Long, S. B., Tao, X., Campbell, E. B., and Mackinnon, R. (2007). Atomic structure of a voltage-dependent K+ channel in a lipid membrane-like environment. *Nature* 450, 376–382. doi: 10.1038/nature06265

Mackie, A. R., Brueggemann, L. I., Henderson, K. K., Shiels, A. J., Cribbs, L. L., Scrogin, K. E., et al. (2008). Vascular KCNQ potassium channels as novel targets for the control of mesenteric artery constriction by vasopressin, based on studies in single cells, pressurized arteries, and *in vivo* measurements of mesenteric vascular resistance. *J. Pharmacol. Exp. Ther.* 325, 475–483. doi: 10.1124/jpet.107.135764

MacKinnon, R. (1991). Determination of the subunit stoichiometry of a voltage-activated potassium channel. *Nature* 350, 232–235. doi: 10.1038/350232a0

Mani, B. K., Brueggemann, L. I., Cribbs, L. L., and Byron, K. L. (2009). Opposite regulation of KCNQ5 and TRPC6 channels contributes to vasopressin-stimulated calcium spiking responses in A7r5 vascular smooth muscle cells. *Cell Calcium* 45, 400–411. doi: 10.1016/j.ceca.2009.01.004

Manville, R. W., and Abbott, G. W. (2018). Ancient and modern anticonvulsants act synergistically in a KCNQ potassium channel binding pocket. *Nat. Commun.* 9:3845.

Manville, R. W., and Abbott, G. W. (2019a). Cilantro leaf harbors a potent potassium channel-activating anticonvulsant. *FASEB J.* 33, 11349–11363.

Manville, R. W., and Abbott, G. W. (2019b). *In silico* re-engineering of a neurotransmitter to activate KCNQ potassium channels in an isoform-specific manner. *Commun. Biol.* 2:401.

Manville, R. W., and Abbott, G. W. (2019c). Teamwork: ion channels and transporters join forces in the brain. *Neuropharmacology* 161:107601. doi: 10.1016/j.neuropharm.2019.04.007

Manville, R. W., and Abbott, G. W. (2020a). Isoform-selective KCNA1 potassium channel openers built from glycine. *J. Pharmacol. Exp. Ther.* 373, 391–401. doi: 10.1124/jpet.119.264507

Manville, R. W., and Abbott, G. W. (2020b). Potassium channels act as chemosensors for solute transporters. *Commun. Biol.* 3:90.

Manville, R. W., Neverisky, D. L., and Abbott, G. W. (2017). SMIT1 modifies KCNQ channel function and pharmacology by physical interaction with the pore. *Biophys. J.* 113, 613–626. doi: 10.1016/j.bpj.2017.06.055

Manville, R. W., Papanikolaou, M., and Abbott, G. W. (2018). Direct neurotransmitter activation of voltage-gated potassium channels. *Nat. Commun.* 9:1847.

Manville, R. W., Papanikolaou, M., and Abbott, G. W. (2020). M-channel activation contributes to the anticonvulsant action of the ketone body beta-hydroxybutyrate. *J. Pharmacol. Exp. Ther.* 372, 148–156. doi: 10.1124/jpet.119.263350

Manville, R. W., Van Der Horst, J., Redford, K. E., Katz, B. B., Jepps, T. A., and Abbott, G. W. (2019). KCNQ5 activation is a unifying molecular mechanism shared by genetically and culturally diverse botanical hypotensive folk medicines. *Proc. Natl. Acad. Sci. U.S.A.* 116, 21236–21245. doi: 10.1073/pnas.1907511116

Matschke, V., Piccini, I., Schubert, J., Wrobel, E., Lang, F., Matschke, J., et al. (2016). The natural plant product rottlerin activates Kv7.1/KCNE1 channels. *Cell. Physiol. Biochem.* 40, 1549–1558. doi: 10.1159/000453205

McCrossan, Z. A., and Abbott, G. W. (2004). The MinK-related peptides. *Neuropharmacology* 47, 787–821. doi: 10.1016/j.neuropharm.2004.06.018

Melman, Y. F., Domenech, A., De La Luna, S., and Mcdonald, T. V. (2001). Structural determinants of KvLQT1 control by the KCNE family of proteins. *J. Biol. Chem.* 276, 6439–6444. doi: 10.1074/jbc.m010713200

Melman, Y. F., Krumerman, A., and Mcdonald, T. V. (2002). A single transmembrane site in the KCNE-encoded proteins controls the specificity of KvLQT1 channel gating. *J. Biol. Chem.* 277, 25187–25194. doi: 10.1074/jbc.m200564200

Miceli, F., Soldovieri, M. V., Ambrosino, P., Barrese, V., Migliore, M., Cilio, M. R., et al. (2013). Genotype-phenotype correlations in neonatal epilepsies caused by mutations in the voltage sensor of K(v)7.2 *potassium channel subunits*. *Proc. Natl. Acad. Sci. U.S.A.* 110, 4386–4391. doi: 10.1073/pnas.1216867110

Milh, M., Lacoste, C., Cacciagli, P., Abidi, A., Sutera-Sardo, J., Tzelepis, I., et al. (2015). Variable clinical expression in patients with mosaicism for KCNQ2 mutations. *Am. J. Med. Genet. A* 167A, 2314–2318. doi: 10.1002/ajmg.a.37152

Nakajo, K., and Kubo, Y. (2007). KCNE1 and KCNE3 stabilize and/or slow voltage sensing S4 segment of KCNQ1 channel. *J. Gen. Physiol.* 130, 269–281. doi: 10.1085/jgp.200709805

Neverisky, D. L., and Abbott, G. W. (2017). KCNQ-SMIT complex formation facilitates ion channel-solute transporter cross talk. *FASEB J.* 31, 2828–2838. doi: 10.1096/fj.201601334r

Orhan, G., Bock, M., Schepers, D., Ilina, E. I., Reichel, S. N., Loffler, H., et al. (2014). Dominant-negative effects of KCNQ2 mutations are associated with epileptic encephalopathy. *Ann. Neurol.* 75, 382–394.

Osteen, J. D., Barro-Soria, R., Robey, S., Sampson, K. J., Kass, R. S., and Larsson, H. P. (2012). Allosteric gating mechanism underlies the flexible gating of KCNQ1 potassium channels. *Proc. Natl. Acad. Sci. U.S.A.* 109, 7103–7108. doi: 10.1073/pnas.1201582109

Osteen, J. D., Gonzalez, C., Sampson, K. J., Iyer, V., Rebolledo, S., Larsson, H. P., et al. (2010). KCNE1 alters the voltage sensor movements necessary to open the KCNQ1 channel gate. *Proc. Natl. Acad. Sci. U.S.A.* 107, 22710–22715. doi: 10.1073/pnas.1016300108

Pan, J. W., Rothman, T. L., Behar, K. L., Stein, D. T., and Hetherington, H. P. (2000). Human brain beta-hydroxybutyrate and lactate increase in fasting-induced ketosis. *J. Cereb. Blood Flow Metab.* 20, 1502–1507. doi: 10.1097/00004647-200010000-00012

Panaghie, G., and Abbott, G. W. (2006). The impact of ancillary subunits on small-molecule interactions with voltage-gated potassium channels. *Curr. Pharm. Des.* 12, 2285–2302. doi: 10.2174/138161206777585175

Panaghie, G., and Abbott, G. W. (2007). The role of S4 charges in voltage-dependent and voltage-independent KCNQ1 potassium channel complexes. *J. Gen. Physiol.* 129, 121–133. doi: 10.1085/jgp.200609612

Panaghie, G., Purtell, K., Tai, K. K., and Abbott, G. W. (2008). Voltage-dependent C-type inactivation in a constitutively open K+ channel. *Biophys. J.* 95, 2759–2778. doi: 10.1529/biophysj.108.133678

Papazian, D. M., Schwarz, T. L., Tempel, B. L., Jan, Y. N., and Jan, L. Y. (1987). Cloning of genomic and complementary DNA from Shaker, a putative potassium channel gene from Drosophila. *Science* 237, 749–753. doi: 10.1126/science.2441470

Park, K. H., Piron, J., Dahimene, S., Merot, J., Baro, I., Escande, D., et al. (2005). Impaired KCNQ1-KCNE1 and phosphatidylinositol-4,5-bisphosphate interaction underlies the long QT syndrome. *Circ. Res.* 96, 730–739. doi: 10.1161/01.res.0000161451.04649.a8

Pongs, O., and Schwarz, J. R. (2010). Ancillary subunits associated with voltage-dependent K+ channels. *Physiol. Rev.* 90, 755–796. doi: 10.1152/physrev.00020.2009

Ranganathan, R., Lewis, J. H., and Mackinnon, R. (1996). Spatial localization of the K+ channel selectivity filter by mutant cycle-based structure analysis. *Neuron* 16, 131–139. doi: 10.1016/s0896-6273(00)80030-6

Rocheleau, J. M., Gage, S. D., and Kobertz, W. R. (2006). Secondary structure of a KCNE cytoplasmic domain. *J. Gen. Physiol.* 128, 721–729. doi: 10.1085/jgp.200609657

Roepke, T. K., Anantharam, A., Kirchhoff, P., Busque, S. M., Young, J. B., Geibel, J. P., et al. (2006). The KCNE2 potassium channel ancillary subunit is essential for gastric acid secretion. *J. Biol. Chem.* 281, 23740–23747. doi: 10.1074/jbc.m604155200

Ruscic, K. J., Miceli, F., Villalba-Galea, C. A., Dai, H., Mishina, Y., Bezanilla, F., et al. (2013). IKs channels open slowly because KCNE1 accessory subunits slow the movement of S4 voltage sensors in KCNQ1 pore-forming subunits. *Proc. Natl. Acad. Sci. U.S.A.* 110, E559–E566.

Sadewa, A. H., Sasongko, T. H., Gunadi, Lee, M. J., Daikoku, K., Yamamoto, A., et al. (2008). Germ-line mutation of KCNQ2, p.R213W, in a Japanese family with benign familial neonatal convulsion. *Pediatr. Int.* 50, 167–171. doi: 10.1111/j.1442-200x.2008.02539.x

Sahib, N. G., Anwar, F., Gilani, A. H., Hamid, A. A., Saari, N., and Alkharfy, K. M. (2013). Coriander (*Coriandrum sativum* L.): a potential source of high-value components for functional foods and nutraceuticals–a review. *Phytother. Res.* 27, 1439–1456.

Santhakumar, V., Hanchar, H. J., Wallner, M., Olsen, R. W., and Otis, T. S. (2006). Contributions of the GABAA receptor alpha6 subunit to phasic and tonic inhibition revealed by a naturally occurring polymorphism in the alpha6 gene. *J. Neurosci.* 26, 3357–3364. doi: 10.1523/jneurosci.4799-05.2006

Schenzer, A., Friedrich, T., Pusch, M., Saftig, P., Jentsch, T. J., Grotzinger, J., et al. (2005). Molecular determinants of KCNQ (Kv7) K+ channel sensitivity to the anticonvulsant retigabine. *J. Neurosci.* 25, 5051–5060. doi: 10.1523/jneurosci.0128-05.2005

Schofield, P. R., Darlison, M. G., Fujita, N., Burt, D. R., Stephenson, F. A., Rodriguez, H., et al. (1987). Sequence and functional expression of the GABA

A receptor shows a ligand-gated receptor super-family. *Nature* 328, 221–227. doi: 10.1038/328221a0

Schroder, R. L., Jespersen, T., Christophersen, P., Strobaek, D., Jensen, B. S., and Olesen, S. P. (2001). KCNQ4 channel activation by BMS-204352 and retigabine. *Neuropharmacology* 40, 888–898. doi: 10.1016/s0028-3908(01)00029-6

Schroeder, B. C., Waldegger, S., Fehr, S., Bleich, M., Warth, R., Greger, R., et al. (2000). A constitutively open potassium channel formed by KCNQ1 and KCNE3. *Nature* 403, 196–199. doi: 10.1038/35003200

Sesti, F., and Goldstein, S. A. (1998). Single-channel characteristics of wild-type IKs channels and channels formed with two minK mutants that cause long QT syndrome. *J. Gen. Physiol.* 112, 651–663. doi: 10.1085/jgp.112.6.651

Shamgar, L., Ma, L., Schmitt, N., Haitin, Y., Peretz, A., Wiener, R., et al. (2006). Calmodulin is essential for cardiac IKS channel gating and assembly: impaired function in long-QT mutations. *Circ. Res.* 98, 1055–1063. doi: 10.1161/01.res.0000218979.40770.69

Simon, O. R., and Singh, N. (1986). Demonstration of anticonvulsant properties of an aqueous extract of Spirit Weed (*Eryngium foetidum* L.). *West Indian Med. J.* 35, 121–125.

Singh, N. A., Charlier, C., Stauffer, D., Dupont, B. R., Leach, R. J., Melis, R., et al. (1998). A novel potassium channel gene. KCNQ2, is mutated in an inherited epilepsy of newborns. *Nat. Genet.* 18, 25–29. doi: 10.1038/ng0198-25

Spector, R., and Lorenzo, A. V. (1975). Myo-inositol transport in the central nervous system. *Am. J. Physiol.* 228, 1510–1518. doi: 10.1152/ajplegacy.1975.228.5.1510

Sun, J., and MacKinnon, R. (2017). Cryo-EM structure of a KCNQ1/CaM complex reveals insights into congenital long QT syndrome. *Cell* 169, 1042–1050.e9. doi: 10.1016/j.cell.2017.05.019

Sun, J., and MacKinnon, R. (2020). Structural basis of human KCNQ1 modulation and gating. *Cell* 180, 340–347.e9. doi: 10.1016/j.cell.2019.12.003

Swiss Pharmaceutical Society (2000). *Index Nominum 2000: International Drug Directory*. Didcot: Taylor & Francis.

Tatulian, L., Delmas, P., Abogadie, F. C., and Brown, D. A. (2001). Activation of expressed KCNQ potassium currents and native neuronal M-type potassium currents by the anti-convulsant drug retigabine. *J. Neurosci.* 21, 5535–5545. doi: 10.1523/jneurosci.21-15-05535.2001

Tempel, B. L., Papazian, D. M., Schwarz, T. L., Jan, Y. N., and Jan, L. Y. (1987). Sequence of a probable potassium channel component encoded at Shaker locus of Drosophila. *Science* 237, 770–775. doi: 10.1126/science.2441471

Tinel, N., Diochot, S., Borsotto, M., Lazdunski, M., and Barhanin, J. (2000). KCNE2 confers background current characteristics to the cardiac KCNQ1 potassium channel. *EMBO J.* 19, 6326–6330. doi: 10.1093/emboj/19.23.6326

Tobelaim, W. S., Dvir, M., Lebel, G., Cui, M., Buki, T., Peretz, A., et al. (2017). Competition of calcified calmodulin N lobe and PIP2 to an LQT mutation site in Kv7.1 channel. *Proc. Natl. Acad. Sci. U.S.A.* 114, E869–E878.

Treven, M., Koenig, X., Assadpour, E., Gantumur, E., Meyer, C., Hilber, K., et al. (2015). The anticonvulsant retigabine is a subtype selective modulator of GABAA receptors. *Epilepsia* 56, 647–657. doi: 10.1111/epi.12950

Tzingounis, A. V., Heidenreich, M., Kharkovets, T., Spitzmaul, G., Jensen, H. S., Nicoll, R. A., et al. (2010). The KCNQ5 potassium channel mediates a component of the afterhyperpolarization current in mouse hippocampus. *Proc. Natl. Acad. Sci. U.S.A.* 107, 10232–10237. doi: 10.1073/pnas.1004644107

Viswanathan, P. C., Bezzina, C. R., George, A. L. Jr., Roden, D. M., Wilde, A. A., and Balser, J. R. (2001). Gating-dependent mechanisms for flecainide action in SCN5A-linked arrhythmia syndromes. *Circulation* 104, 1200–1205. doi: 10.1161/hc3501.093797

Wang, H. S., Pan, Z., Shi, W., Brown, B. S., Wymore, R. S., Cohen, I. S., et al. (1998). KCNQ2 and KCNQ3 potassium channel subunits: molecular correlates of the M-channel. *Science* 282, 1890–1893. doi: 10.1126/science.282.5395.1890

Weckhuysen, S., Mandelstam, S., Suls, A., Audenaert, D., Deconinck, T., Claes, L. R., et al. (2012). KCNQ2 encephalopathy: emerging phenotype of a neonatal epileptic encephalopathy. *Ann. Neurol.* 71, 15–25. doi: 10.1002/ana.22644

Yang, W. P., Levesque, P. C., Little, W. A., Conder, M. L., Shalaby, F. Y., and Blanar, M. A. (1997). KvLQT1, a voltage-gated potassium channel responsible for human cardiac arrhythmias. *Proc. Natl. Acad. Sci. U.S.A.* 94, 4017–4021. doi: 10.1073/pnas.94.8.4017

Yeung, S., Schwake, M., Pucovsky, V., and Greenwood, I. (2008). Bimodal effects of the Kv7 channel activator retigabine on vascular K+ currents. *Br. J. Pharmacol.* 155, 62–72. doi: 10.1038/bjp.2008.231

Yeung, S. Y., Pucovsky, V., Moffatt, J. D., Saldanha, L., Schwake, M., Ohya, S., et al. (2007). Molecular expression and pharmacological identification of a role for K(v)7 channels in murine vascular reactivity. *Br. J. Pharmacol.* 151, 758–770. doi: 10.1038/sj.bjp.0707284

Zaydman, M. A., and Cui, J. (2014). PIP2 regulation of KCNQ channels: biophysical and molecular mechanisms for lipid modulation of voltage-dependent gating. *Front. Physiol.* 5:195. doi: 10.3389/fphys.2014.00195

Zaydman, M. A., Silva, J. R., Delaloye, K., Li, Y., Liang, H., Larsson, H. P., et al. (2013). Kv7.1 ion channels require a lipid to couple voltage sensing to pore opening. *Proc. Natl. Acad. Sci. U.S.A.* 110, 13180–13185. doi: 10.1073/pnas.1305167110

Zhang, J., Kim, E. C., Chen, C., Procko, E., Pant, S., Lam, K., et al. (2020). Identifying mutation hotspots reveals pathogenetic mechanisms of KCNQ2 epileptic encephalopathy. *Sci. Rep.* 10:4756.

Zhou, Y., and MacKinnon, R. (2003). The occupancy of ions in the K+ selectivity filter: charge balance and coupling of ion binding to a protein conformational change underlie high conduction rates. *J. Mol. Biol.* 333, 965–975. doi: 10.1016/j.jmb.2003.09.022

Conflict of Interest: The author declares that the research was conducted in the absence of any commercial or financial relationships that could be construed as a potential conflict of interest.

frontiers in Physiology

REVIEW
published: 26 June 2020
doi: 10.3389/fphys.2020.00634

Kv7 Channels in Lung Diseases

*Gema Mondejar-Parreño[1,2,3], Francisco Perez-Vizcaino[1,2,3] and Angel Cogolludo[1,2,3]**

[1]*Departamento de Farmacología y Toxicología, Facultad de Medicina, Universidad Complutense de Madrid, Madrid, Spain,* [2]*Ciber Enfermedades Respiratorias (Ciberes), Madrid, Spain,* [3]*Instituto de Investigación Sanitaria Gregorio Marañón (IISGM), Madrid, Spain*

Lung diseases constitute a global health concern causing disability. According to WHO in 2016, respiratory diseases accounted for 24% of world population mortality, the second cause of death after cardiovascular diseases. The Kv7 channels family is a group of voltage-dependent K^+ channels (Kv) encoded by *KCNQ* genes that are involved in various physiological functions in numerous cell types, especially, cardiac myocytes, smooth muscle cells, neurons, and epithelial cells. Kv7 channel α-subunits are regulated by KCNE1–5 ancillary β-subunits, which modulate several characteristics of Kv7 channels such as biophysical properties, cell-location, channel trafficking, and pharmacological sensitivity. Kv7 channels are mainly expressed in two large groups of lung tissues: pulmonary arteries (PAs) and bronchial tubes. In PA, Kv7 channels are expressed in pulmonary artery smooth muscle cells (PASMCs); while in the airway (trachea, bronchus, and bronchioles), Kv7 channels are expressed in airway smooth muscle cells (ASMCs), airway epithelial cells (AEPs), and vagal airway C-fibers (VACFs). The functional role of Kv7 channels may vary depending on the cell type. Several studies have demonstrated that the impairment of Kv7 channel has a strong impact on pulmonary physiology contributing to the pathophysiology of different respiratory diseases such as cystic fibrosis, asthma, chronic obstructive pulmonary disease, chronic coughing, lung cancer, and pulmonary hypertension. Kv7 channels are now recognized as playing relevant physiological roles in many tissues, which have encouraged the search for Kv7 channel modulators with potential therapeutic use in many diseases including those affecting the lung. Modulation of Kv7 channels has been proposed to provide beneficial effects in a number of lung conditions. Therefore, Kv7 channel openers/enhancers or drugs acting partly through these channels have been proposed as bronchodilators, expectorants, antitussives, chemotherapeutics and pulmonary vasodilators.

Keywords: Kv7 channels, KCNE, respiratory diseases, asthma, chronic obstructive pulmonary disease, pulmonary hypertension

OPEN ACCESS

Edited by:
Francesco Miceli,
University of Naples Federico II, Italy

Reviewed by:
Núria Comes,
University of Barcelona, Spain
Nikita Gamper,
University of Leeds, United Kingdom

****Correspondence:***
Angel Cogolludo
acogolludo@med.ucm.es

Specialty section:
This article was submitted to Membrane Physiology and Membrane Biophysics, a section of the journal Frontiers in Physiology

Received: *18 March 2020*
Accepted: *18 May 2020*
Published: *26 June 2020*

Citation:
Mondejar-Parreño G, Perez-Vizcaino F and Cogolludo A (2020) Kv7 Channels in Lung Diseases. Front. Physiol. 11:634. doi: 10.3389/fphys.2020.00634

LUNG DISEASES: ONE WORLD'S HEALTH CONCERN

Lung diseases constitute a global health concern causing severe physical limitations and premature death, and entails enormous costs associated with treatment, hospital-based and primary care (Tobin, 2005). Mortality from overall lung diseases is very striking according to data collected by the WHO in 2016, in which respiratory diseases account for 24% of world population mortality, the second cause of death after cardiovascular diseases (WHO Global Health Estimates, 2020). At the top of mortality rate within lung diseases, the 9% of the population dies of tuberculosis. Second and third positions include chronic obstructive pulmonary disease (COPD) and lower respiratory infections with 5.4 and 5.2%, respectively. These are followed by lung cancer (affecting trachea, bronchus, and lungs) with 3% and, lastly, asthma and other respiratory

diseases with a 0.7 and 0.6%, respectively (**Figure 1**). Most major respiratory diseases are avoidable and can be mitigated by reducing exposure to air pollution, toxic smoke of biomass fuel, tobacco smoke, and different allergens (Laumbach and Kipen, 2012). Additional factors, such as aging, genetic predisposition, nutritional status, obesity, physical inactivity, raised blood pressure, human immunodeficiency virus 1 infection (HIV-1), or other infections may influence the risk of developing lung diseases. Lung diseases can be classified into three main groups depending on the lung tissue involved. First, airways diseases including asthma, COPD, emphysema, cystic fibrosis, or bronchitis in which the bronchial tubes are narrowed or blocked and the transport of oxygen and other gases are affected (Athanazio, 2012). Second, lung tissue diseases which affect the structure of alveoli or the interstitium (Corvol et al., 2009), such as pneumonia, tuberculosis, pulmonary edema, acute respiratory distress syndrome, sarcoidosis, and pulmonary fibrosis, where the lungs are unable to expand fully (Dellaripa, 2018). The third group includes diseases affecting the pulmonary vessels, such as pulmonary hypertension characterized by vasoconstriction, vascular remodeling, inflammation, and thrombosis (Cummings and Bhalla, 2015). This last group of diseases may end up affecting heart function.

Coronavirus disease 2019 (COVID-19), caused by severe acute respiratory syndrome coronavirus 2 (SARS-CoV-2), has recently rapidly evolved into a global pandemic. To date, risk factors associated with admission to ICU and mortality include cardiovascular comorbidities while respiratory diseases paradoxically do not appear to increase the prevalence or severity of the viral infection (Halpin et al., 2020; Li et al., 2020).

Kv7 CHANNEL STRUCTURE AND REGULATION

The Kv7 channel family, is a group of voltage-dependent K^+ channels subfamily Q, which are involved in various physiological activities of numerous cell types, especially, cardiac myocytes, smooth muscle cells, neurons, and epithelial cells (Stott et al., 2014). The different Kv7 channels isoforms are encoded by *KCNQ1–5* genes located at chromosomal loci *11p15*, *20q13*, *8q24*, *1p34*, and *6q13*, respectively (Barrese et al., 2018). *KCNQ* genes encode for five Kv7 proteins, Kv7.1–Kv7.5 channels, comprising approximately 650–940 aminoacids. Each pore-forming α-subunit of Kv7 channels has six helices transmembrane domains (TM). The TM5 and TM6 are part of the pore while the TM4 constitutes the voltage-detection domain. Four α-subunits form the transmembrane pore assembling into a homo- or hetero-tetrameric channel (Taylor and Sanders, 2017). Kv7 channels can be regulated by potassium voltage-gated channel subfamily E regulatory subunits (KCNEs) ancillary subunits (KCNE1–5, also called minK-related peptides), which present a single transmembrane domain with 103–177 residues, encoded by the five *KCNE1–5* genes located at chromosomal loci *21q11*, *21q11*, *11q13*, *2q36*, and *Xq23*, respectively (Lundquist et al., 2006). These KCNE subunits modulate several features of Kv7 channels such as biophysical properties, cell localization, channel trafficking, and sensitivity to different drugs (Barrese et al., 2018).

Mutations in all five *KCNQ* and *KCNE* genes have been shown to underlie excitability hereditary disorders (Jentsch, 2000; Maljevic et al., 2010; Lehman et al., 2017; Barrese et al., 2018). Particularly, mutations affecting *KCNQ1* gene cause disorders related to cardiac electrical activity such as long-QT syndrome, short-QT syndrome, and atrial fibrillation leading to severe arrhythmias and sudden death (Li et al., 1998; Chen et al., 2003). *KCNQ2* and *KCNQ3* gene mutations have been identified in different epilepsy syndromes (Neubauer et al., 2008) and, moreover, *KCNQ3* gain-of-function variant have been related to autism and developmental disability (Sands et al., 2019). Kv7.4 channels expressed in the cochlea are essential for normal hearing, and *KCNQ4* mutations are linked to hearing loss (Kubisch et al., 1999; Jung et al., 2019). Lastly, mutations in the Kv7.5 channel encoded by *KCNQ5* gene cause epilepsy and intellectual disability (Lehman et al., 2017). Different mutations have also been found in all five *KCNE* genes, mainly related to cardiac arrhythmias (Splawski et al., 2000; Lundby et al., 2008; Ohno et al., 2009; Abbott, 2016).

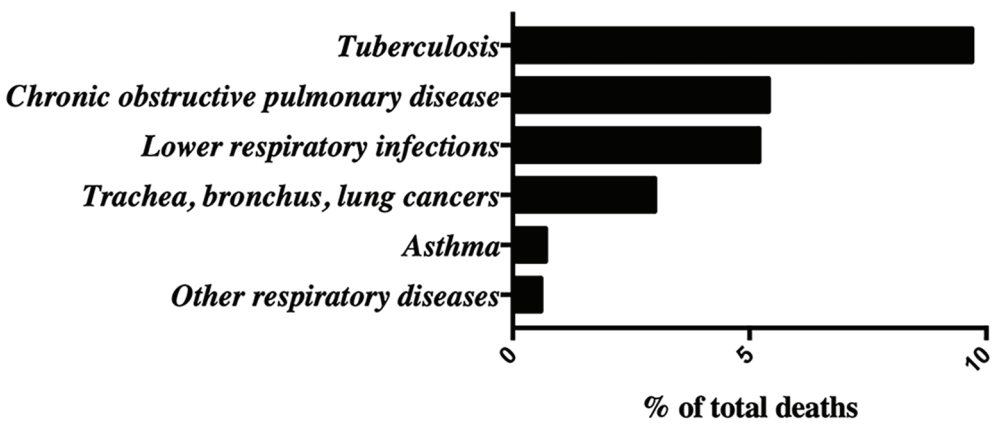

FIGURE 1 | Global lung diseases epidemiological data adapted from the *World Health Organization (WHO) Website*: Mortality rates in 2016 measured as % of total deaths.

Different combinations of Kv7 channels and KCNE subunits can be found depending on the cell type. Thus, there is a Kv7 channel isoform-specific expression playing different roles depending on tissue types (see section Kv7 Channel Expression in the Lung). Many KCNE subunits have been shown to modulate Kv7 channels α-subunits expressed in heterologous systems, providing a valuable experimental platform for elucidating structure-function relationships and mechanistic differences. Thus, all five KCNE proteins have been demonstrated to modulate Kv7.1 channels expressed in heterologous systems with diverse effects (Van Horn et al., 2011; Sun and MacKinnon, 2020). For instance, KCNE1 causes the Kv7.1 channel to activate at more positive voltages, slows its activation and deactivation, increases its conductance, and suppresses its inactivation (Sun and MacKinnon, 2020). While, KCNE2 and KCNE4 have inhibitory effects on Kv7.1 activity (Grunnet et al., 2002; Vanoye et al., 2009; Hu et al., 2019), KCNE3 stabilizes Kv7.1 channels voltage sensors (S4 segment) in an activated state turning the channel voltage-independent (Barro-Soria et al., 2015). Such a mechanism seems to require the participation of the signaling lipid phosphatidylinositol 4,5-bisphosphate (PIP_2) in non-excitable cells such as lung epithelial cells (Zhou et al., 2019; Sun and MacKinnon, 2020). Sun and MacKinnon have recently identified binding sites of PIP_2 on Kv7.1 channels present in the S0, the S2-S3 loop, and the S4-S5 linker, and proposed a model in which the conformational change following PIP_2 interaction would results in dilation of the pore's gate (Sun and MacKinnon, 2020). In addition, KCNE subunits regulate traffic and cell surface expression of Kv7.1 channels (Roura-Ferrer et al., 2010; Hu et al., 2019). The information about the regulation of Kv7.2 and Kv7.3 channels by KCNE subunits is more limited. In *Xenopus* oocytes, KCNE1 was found to slow Kv7.2/7.3 heteromer currents and decreased their magnitude (Yang et al., 1998). Likewise, KCNE2 was shown to accelerate the deactivation kinetics of Kv7.2 and Kv7.2/7.3 channels transiently expressed in COS cells (Tinel et al., 2000). Whereas, KCNE1, KCNE2, and especially KCNE4 and KCNE5 increased Kv7.4 currents, co-expression with KCNE3 led to a strong attenuation (Strutz-Seebohm et al., 2006; de Jong and Jepps, 2018). Moreover, KCNE4 was shown to co-localize with Kv7.4 channels, regulating its activity and membrane abundance in mesenteric arterial myocytes (Jepps et al., 2015). Finally, Kv7.5 channels were shown to be affected by KCNE1 and KCNE3, but not by other KCNE subunits in *Xenopus* oocytes and HEK-293 cells (Roura-Ferrer et al., 2009, 2012). Thus, while KCNE1 was shown to slow activation and increase Kv7.5 currents, KCNE3 drastically inhibited these currents (Roura-Ferrer et al., 2009, 2012).

The activity of Kv7 channels is modulated by G protein-coupled membrane receptors (GPCRs). Thus, activation of different GPCR have been shown to inhibit M-type (Kv7) currents, with a dominant participation of the G_q and G_{11} α-subunits (Caulfield et al., 1994; Haley et al., 1998; Delmas and Brown, 2005). For instance, in neurons, Kv7 activity is decreased by M_1 and M_3 muscarinic and H_1 histaminic receptors coupled to $G_{q/11}$ proteins through different signal transduction pathways, including depletion of PIP_2, activation of protein kinase C (PKC), or increased intracellular calcium (Delmas and Brown, 2005; Higashida et al., 2005; Taylor and Sanders, 2017; Barrese et al., 2018). In human airway smooth muscle cells, histamine was found to inhibit Kv7.5 channels though a PKC-dependent phosphorylation of Ser441 (Haick et al., 2017). On the other hand, it is well recognized that stimulation of β-adrenergic receptor increases the activity of different Kv7 channels in different tissues such as cardiac (Kv7.1), neuronal (Kv7.2/Kv7.3), and vascular (Kv7.4/Kv7.5 and Kv7.5) channels (Jentsch, 2000; Marx et al., 2002; Chadha et al., 2014; Mani et al., 2016; Barrese et al., 2018). Likewise, in human airway smooth muscle cells, Kv7.5 channels are robustly enhanced by activation of β-adrenoceptors *via* a mechanism involving cyclic adenosine monophosphate/protein kinase A (cAMP/PKA)-dependent phosphorylation (Brueggemann et al., 2018). This effect might be shared with other GPCRs but does not seem to account for Kv7.4 activation. The mechanism may involve increased membrane expression of Kv7 channels mediated by colchicine-sensitive microtubule disruption (Lindman et al., 2018). Kv7 channels are also regulated by GPCR-independent mediators activating soluble guanylate cyclase (sGC) such as nitric oxide (NO) (Mondejar-Parreño et al., 2019) and natriuretic peptide (Stott et al., 2015). The implications in respiratory diseases and drug therapy are discussed below.

In addition to regulation by KCNE β-subunits and GPCRs, Kv7 channels can be regulated by scaffolding proteins, sodium-coupled myo-inositol transporter (SMIT), lipids, microRNAs, and/or further signaling mechanisms as extensively reviewed elsewhere (Delmas and Brown, 2005; Zaydman and Cui, 2014; Taylor and Sanders, 2017; Barrese et al., 2018; Byron and Brueggemann, 2018).

Kv7 CHANNEL EXPRESSION IN THE LUNG

Kv7 channels are expressed mainly in pulmonary arteries (PAs) and in the bronchial tubes (**Figure 2**). In PA, Kv7 channels are expressed in pulmonary artery smooth muscle cells (PASMCs); while in the bronchial tubes (trachea, bronchus and bronchioles), Kv7 channels are expressed in airway smooth muscle cells (ASMCs), airway epithelial cells (AEPs) and vagal airway C-fibers (VACFs). The functional role of Kv7 channels may vary depending on the cell type. While most of the available studies have provided relevant information on the particular expression of α-subunits in these cell types, evidence for the expression of heteromeric Kv7 complexes or KCNE subunits is still very scarce.

Pulmonary Artery Smooth Muscle Cells

The expression of Kv7 channels in mice and rat PA has been demonstrated in several studies. Specifically, their expression is located in PASMC. In these cells, the expression of Kv7.1, Kv7.4, and Kv7.5 channels predominates; but Kv7.4 channels expression appears to be the most relevant. The expression of Kv7.2 and Kv7.3 channels in PASMCs is still controversial (Joshi et al., 2009; Morecroft et al., 2009; Chadha et al., 2012; Li et al., 2014a; Sedivy et al., 2015; Eid and Gurney, 2018; Mondejar-Parreño et al., 2018). The existence of Kv7.1/7.5 or Kv7.4/7.5 heteromeric

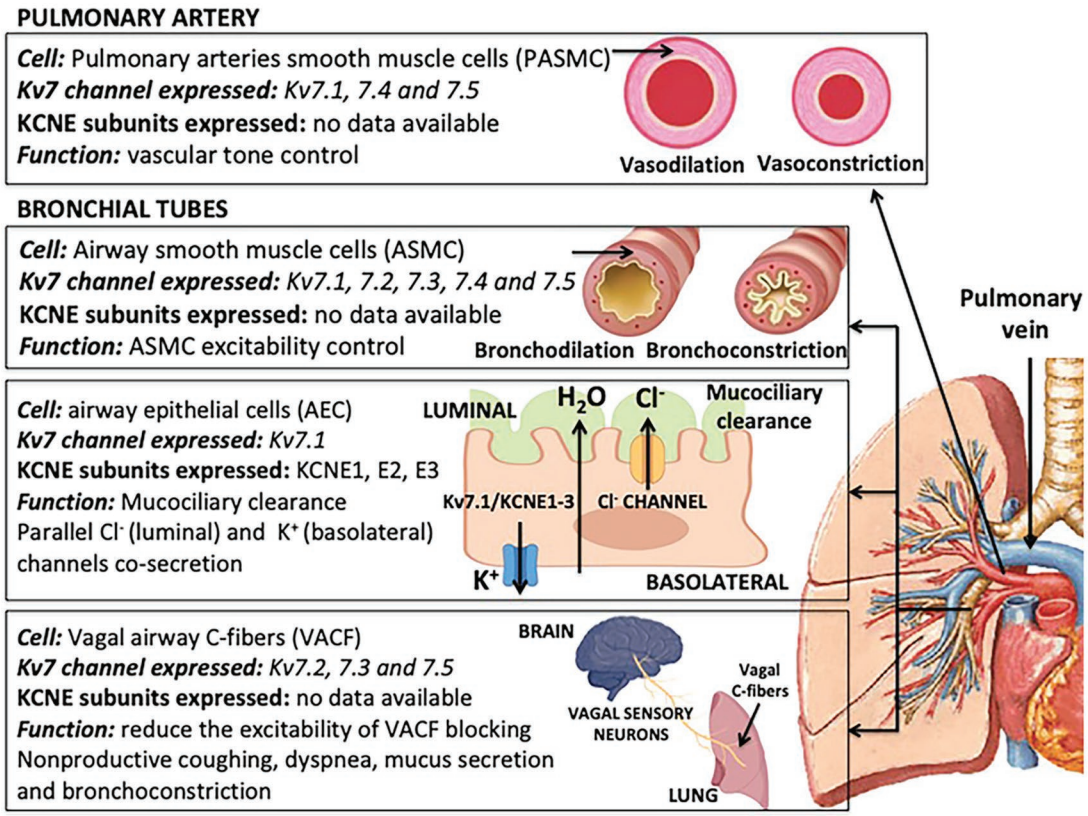

FIGURE 2 | Expression and functions of isoform-specific Kv7 channel and potassium voltage-gated channel subfamily E regulatory subunits (KCNE) ancillary subunit in lung cells.

complexes in vascular smooth muscle has been postulated on several studies (Chadha et al., 2014; Oliveras et al., 2014; Barrese et al., 2018). In particular, Kv7.4/7.5 heteromers have been proposed as the dominant functional vascular Kv7 channels, supported by electrophysiological data showing that Kv7 currents in freshly isolated vascular smooth muscle cells have phenotypes intermediate to the respective homomeric Kv7.4 and Kv7.5 channels (Brueggemann et al., 2014a; Chadha et al., 2014; Fosmo and Skraastad, 2017; Barrese et al., 2018). We have recently confirmed that Kv7.4/7.5 heteromeric complexes are also present in PASMC (authors' unpublished observations). Although, in other types of arteries, the expression of Kv7 channels has been located also in endothelial cells (Goodwill et al., 2016), whether this is also the case for pulmonary artery endothelial cells (PAECs) remains unknown. The main function of these channels is to regulate pulmonary vascular tone, due to their contribution to maintain the membrane potential (Em) of PASMC (Joshi et al., 2009; Sedivy et al., 2015; Mondejar-Parreño et al., 2018, 2019).

Airway Smooth Muscle Cells

There is some interspecies variability in the expression of Kv7 channel isoforms in the airways. Thus, ASMCs from guinea pigs were shown to express Kv7 channels with a relative abundance of *KCNQ2* > *KCNQ5* > *KCNQ4* > *KCNQ3* and, to a lesser extent, *KCNQ1* (Brueggemann et al., 2011). Comparatively, *KCNQ* mRNA expression in ASMC revealed a high expression of *KCNQ4* followed by a fainter expression of *KCNQ5* and *KCNQ1* transcripts (Brueggemann et al., 2014b). Studies in human tracheal muscle revealed abundant expression of *KCNQ1* relative to guinea pig, a modest expression of *KCNQ4* and *KCNQ5* and no detectable expression of *KCNQ2* or *KCNQ3* (Brueggemann et al., 2011). A further study showed that cultured human ASMCs express all *KCNQ* genes with a predominant relative abundance of *KCNQ5* mRNA followed by *KCNQ3* or *KCNQ4*, while *KCNQ2* and *KCNQ1* mRNA are expressed to a lesser extent (Brueggemann et al., 2018). These differences in the expression profile of Kv7 channels in human tissue could be due to phenotypic changes associated with cell culture. Measurements of Kv7 currents and functional studies assessing airway smooth muscle contractility in the bronchioles from different species have pointed to Kv7 channels as important players in maintaining, resting Em, and controlling ASMC excitability (Evseev et al., 2013; Brueggemann et al., 2014b, 2018).

Airway Epithelial Cells

Airway epithelial cells (AECs) predominates the expression of Kv7.1 channels, also named KvLQT1, along with the expression of KCNE1 and KCNE3 ancillary subunits (Mall et al., 2000;

Boucherot et al., 2001; Trinh et al., 2007; Preston et al., 2010; Frizzell and Hanrahan, 2012; Kroncke et al., 2016; Hynes and Harvey, 2019). Nevertheless, KCNE2 has also been found to be expressed in *Calu-3* cells, a model for human submucosal serous cells of the lung, where it has been suggested to regulate *KCNQ1* (Cowley and Linsdell, 2002a). Chloride (Cl^-) secretion in AEC is essential to mucociliary clearance and requires the co-activation of Cl^- channels in luminal membrane and, in parallel, of K^+ channels in the basolateral membrane which involves Kv7.1 channels (Frizzell and Hanrahan, 2012).

Vagal Airway C-Fibers

Using single-cell mRNA, Sun et al. have recently demonstrated that *KCNQ2*, *KCNQ3*, and *KCNQ5* are consistently expressed in mouse airway sensory afferent nerves and remarkably, the expression of *KCNQ3* mRNA was the most prevalent (Sun et al., 2019). Most vagal sensory nerves in the respiratory tract are nociceptive C-fibers. Increased VACF activity may contribute to the nonproductive coughing, dyspnea, parasympathetic reflex mucus secretion, and bronchoconstriction. Thus, it has been proposed that activation of Kv7 channels may reduce the vagal C-fibers excitability innervating the airways, and being useful to treat chronic cough.

Kv7 CHANNELS IN LUNG DISEASES

This section covers the potential pathophysiological role of Kv7 channels in different respiratory diseases such as cystic fibrosis, asthma, COPD, chronic coughing, lung cancer, and pulmonary hypertension.

Cystic Fibrosis

The airway surface liquid layer represents a key primary defense mechanism of mucociliary clearance, which crucially depends on the transport of chloride into the lumen of the airways, and the subsequent movement of water. Cl^- ion transport across the apical membrane is mainly driven by a cAMP-regulated Cl^- channel named cystic fibrosis transmembrane conductance regulator (CFTR) and by the calcium-activated Cl^- channels (CaCC) (Frizzell and Hanrahan, 2012; Bartoszewski et al., 2017). However, a possible overlap between these two pathways has also been proposed (Billet and Hanrahan, 2013). Cystic fibrosis is an autosomal recessive disease due to mutations in the gene encoding CFTR and characterized by alterations in the composition and volume of secreted luminal fluids. The CFTR is a member of the ATP-binding cassette (ABC) transporter superfamily known to function as an ion cannel that conducts chloride ions across epithelial cell membranes and is responsible for salt secretion in response to cAMP/PKA stimulation. Thus, mutations of the CFTR gene lead to defective cAMP-dependent Cl^- secretion and enhanced Na^+ absorption throughout the apical membrane of airway epithelia.

CFTR has been shown to influence both function and properties of other membrane channels, such as epithelial Na^+ channels, inward rectifying renal outer medullary K^+ channel (ROMK), outwardly rectifying Cl^- channels, and aquaporin 3 (Schwiebert et al., 1999). Cl^- secretion in AEC requires the parallel co-activation of Cl^- channels and K^+ channels, in the luminal surface and the basolateral membrane, respectively. Whereas Cl^- channels are required for Cl^- efflux to the luminal side of the AEC, K^+ channels are needed for K^+ recycling *via* the basolateral membrane (Boucherot et al., 2001; Bartoszewski et al., 2017). Kv7.1 channels have been shown to contribute to the basolateral cAMP-activated K^+ conductance in human airway epithelium (Mall et al., 1996, 2000; Bardou et al., 2009). This study also showed that the Kv7.1 channel inhibitor chromanol 293B inhibited Cl^- secretion suggesting an important role of these K^+ channels in maintaining cAMP-dependent Cl^- secretion in human airways. Since CFTR is a modulator of other ion channels, several studies have analyzed whether it controls the activity of Kv7.1 channels. Studies analyzing this issue have led to contradictory results. Thus, while initial studies suggested that CFTR could directly modulate Kv7.1 conductance (Cunningham et al., 1992; Loussouarn et al., 1996; Mall et al., 2000), this was not the case in other studies (Boucherot et al., 2001). Interestingly, using CFTR KO mice, Belfodil et al. (2003) found that cAMP-sensitive Kv7.1 currents were regulated by CFTR in renal distal but not in proximal tubule cells, suggesting that the possible modulation of Kv7.1 is unlikely to involve a direct interaction.

As stated above, human airway epithelia also express CaCC that are activated by extracellular nucleotides [adenosine triphosphate (ATP) and/or uracil triphosphate (UTP)] and other Ca^{2+}-increasing agonists. CaCC was shown to be preserved or enhanced in human and murine cystic fibrosis airways as a mechanism to compensate for the lack of CFTR (Clarke et al., 1994; Grubb et al., 1994). Since, CaCC-mediated Cl^- secretion appears to be preserved in cystic fibrosis its pharmacological stimulation has been suggested as a therapeutic tool for bypassing dysfunctional CFTR. Mall et al. demonstrated that activation of the cAMP pathway increased CaCC-mediated secretion in cystic fibrosis and, conversely, chromanol 293B, an inhibitor of cAMP-activated Kv7.1 channels was able to fully abolish nucleotide-activated Cl^- secretion (Mall et al., 2003). Hence, the authors proposed that activation of Kv7.1 channels, together with hSK4 K^+ channels, may improve Cl^- secretion *via* CaCC in human cystic fibrosis airway tissues (Mall et al., 2003). Altogether, these studies indicate the Kv7.1 channel activation may help to improve mucociliary clearance in cystic fibrosis airways.

Elevated levels of reactive oxygen species (ROS) lead to oxidative stress and DNA damage in several tissues providing a common pathological mechanism in all inflammatory lung diseases. Hydrogen peroxide (H_2O_2) has been proven to stimulate several components of the Cl^- secretion in the airway epithelia, including the cAMP-dependent activation of CFTR and the basolateral K^+ channels (Cowley and Linsdell, 2002b; Ivonnet et al., 2015). The basolateral K^+ conductance was abrogated by clofilium, a Kv7.1 channel inhibitor, suggesting a role for these channels in the H_2O_2-stimulated response (Cowley and Linsdell, 2002b; Ivonnet et al., 2015). In line with this, H_2O_2 has been reported to potently enhance Kv7 currents (Gamper et al., 2006; Kim et al., 2016). Activation of transmembrane adenylyl cyclase by H_2O_2 has been proposed as a triggering

mechanism for the cAMP-activated basolateral Kv7.1 current (Ivonnet et al., 2015). The stimulated anion secretion by ROS could act as a compensatory protective mechanism to keep the airways clear from damaging radicals and to hold acceptable airway surface liquid levels.

While the Kv7.1 channel is the member of the *KCNQ* family with the strongest evidence of its functional expression and physiological role in lung epithelial cells, others (*KCNQ3* and *KCNQ5*) have been detected in the apical or lateral membranes (Moser et al., 2008). In addition, mRNA transcripts for several KCNE accessory subunits (*KCNE2* and *KCNE3*) have been found in human airway Calu-3 cells (Cowley and Linsdell, 2002a). Kv7.1 channels expressed in *Xenopus* oocytes were shown to be activated by an increase in intracellular cAMP concentration, independently of co-expression with KCNE1 or KCNE3 ancillary subunits (Boucherot et al., 2001). On the other hand, Potet et al. demonstrated that recombinant Kv7.1/KCNE1 complexes expressed in *Cos-7* cells were totally insensitive to cAMP (Potet et al., 2001). The co-assembly of Kv7.1 with KCNE3 subunits markedly affects Kv7.1 channel properties (abolishing its voltage dependence) and has been proposed to form the cAMP-activated basolateral K^+ channels contributing to Cl^- secretion in colonic epithelial cells (Schroeder et al., 2000). Interestingly, Preston et al. evidenced that cAMP-stimulated Cl^- secretion across tracheal epithelia was severely reduced in *KCNE3*$^{(-/-)}$ mice (Preston et al., 2010). While the involvement of KCNE3 in airway secretion requires confirmation in future studies, the structural basis of the interaction of Kv7.1 with KCNE3 leading to a constitutive activation of Kv7.1 channel activity has been recently established (Kroncke et al., 2016; Sun and MacKinnon, 2020).

Asthma

Asthma is characterized by hyper-contractility of bronchial smooth muscle attributed to an increased concentration of different bronchoconstrictor agonists, or enhanced sensitivity to them, leading to aberrant narrowing of the airways (Penn, 2008). Acetylcholine, leukotriene D4, endothelin, and histamine represent the most relevant locally released bronchoconstrictor agonists that activate GPCR on ASMC, leading to increased cytosolic Ca^{2+} concentration and contraction (Jude et al., 2008; Penn, 2008). This together with the strong inflammation leads to an acute hypersensitivity to different air stimulants that produce ASMC bronchospasm and that, in the long term, promote smooth muscle proliferation and hypertrophy (Stott et al., 2014). Kv7 channels are considered negative regulators of ASMC contraction due to their major contribution to maintain negative Em negative, preventing L-type-Ca^{2+} channel activation and the subsequent bronchoconstriction (Brueggemann et al., 2011). Several members of the Kv7 family are expressed in ASMCs (Brueggemann et al., 2011; Bartoszewski et al., 2017). The relative abundance expression of the Kv7 members appears to differ depending on the location (trachea vs. bronchioles) and depending on the animal species as mentioned above (Brueggemann et al., 2011, 2014b; Evseev et al., 2013). Several studies have evidenced that bronchoconstrictor agonists negatively regulate the activity of Kv7 channels. Thus, methacholine, carbachol, or histamine reduce Kv7 currents in guinea pig, mouse, and rat ASMCs (Brueggemann et al., 2011, 2014; Haick et al., 2017). On the other hand, structurally unrelated Kv7 channel activators cause a concentration-dependent relaxation of small bronchioles (Brueggemann et al., 2014b) and tracheal rings (Evseev et al., 2013). Of note, *in vivo* administration of the Kv7 channel opener retigabine was proven to transiently reduce bronchoconstriction induced by methacholine in mice (Evseev et al., 2013).

Chronic administration of long-acting β_2-adrenergic receptor agonist elicits a time- and concentration-dependent relaxation of rat airways, with remarkable desensitization to short-term or with repeated treatments. Co-administration of retigabine plus the long-acting β_2-adrenergic receptor agonist formoterol was shown to cause a sustained reduction of methacholine-induced bronchoconstriction and reduced the desensitization observed with formoterol alone (Brueggemann et al., 2014b). These findings suggest that using a Kv7 channel enhancer together a β_2-adrenergic receptor agonist may improve bronchodilator therapy.

In addition to exaggerated bronchoconstriction, asthma is characterized by a chronic inflammatory response in the airways that is targeted primarily with inhaled corticosteroids. As stated in the previous section basolateral membrane K^+ channels play a key role in stimulating Cl^- transport across AEPs (Frizzell and Hanrahan, 2012). Unlike in cystic fibrosis, a decrease in airway mucus secretion ameliorates the symptomatology of asthma. Very recently, Hynes and Harvey have demonstrated that dexamethasone produces an inhibition of transepithelial chloride ion secretion though a rapid non-genomic inhibition of Kv7.1 channels and KCNN4 ($K_{Ca}3.1$) (Hynes and Harvey, 2019). Thus, it is plausible that down-regulation of Kv7.1 channel activity might contribute to the potential benefit of corticosteroids to reverse airway hypersecretion.

Chronic Obstructive Pulmonary Disease (COPD)

COPD is a progressive life-threatening lung disease characterized by airway obstruction due to inflammation of the small airways. The disease evolves with irreversible limitation of airflow, loss of lung function and severe acute exacerbations which significantly deteriorate the patient's quality of life (Barnes et al., 2003). β-adrenergic receptors (β-AR) agonists promote airway smooth muscle relaxation and are the drugs of choice for rescue from acute bronchoconstriction in asthma and COPD. A recent study has shown that the long-acting β-AR formoterol robustly enhanced Kv7 currents in human ASMCs (Brueggemann et al., 2018). Furthermore, these authors provided evidence that Kv7.5 is the predominant Kv7 α-subunit in human ASMCs and identified a PKA-dependent phosphorylation of S53 on the N-terminus of Kv7.5 channel subunits as a potential mechanism of activation following the stimulation of the βAR/cAMP pathway (Brueggemann et al., 2018).

The exposure to cigarette smoking is the principal cause of COPD (Salvi, 2014). Recently Sevilla-Montero et al. have analyzed the impact of cigarette smoke exposure on the pulmonary vasculature (Sevilla-Montero et al., 2019). Authors showed that cigarette smoke extract exposure had direct effects

on human fibroblasts and PASMCs, promoting a senescent phenotype which contributed to the secretion of inflammatory molecules and increase the proliferation of non-exposed cells. Furthermore, cigarette smoke extract exposure affected cell contractility attenuated the pulmonary vascular responses to Kv7 channel modulators and dysregulated the expression and activity of Kv7.4 channels. The results suggest that cigarette smoke may impair pulmonary vascular tone atleast in part through Kv7.4 downregulation (Sevilla-Montero et al., 2019).

A sequence polymorphism of the human *KCNE2* gene has been found to be associated with altered lung function (Soler-Artigas et al., 2011; Sabater-Lleal et al., 2014). The deletion of *KCNE2* reduced pulmonary expression of the Kv7.1 α-subunit suggesting the formation of pulmonary KCNQ1-KCNE2 complexes (Zhou et al., 2019). *KCNE2*$^{(-/-)}$ mice had reduced blood O_2, increased CO_2, increased pulmonary apoptosis, and increased inflammatory mediators TNF-α, IL-6, and leukocytes in bronchoalveolar lavage fluids (Zhou et al., 2019). These data indicated KCNE2 regulates *KCNQ1* in the lungs and is required for normal lung function.

Chronic Cough

Airway sensory afferent nerves are essential for triggering different reflex responses to potential injurious stimuli (Undem and Kollarik, 2005). Most vagal sensory afferent nerves which terminate in the respiratory tract are C-fibers (Undem and Kollarik, 2005). The excessive activity of VACF induces different symptoms associated with inflammatory lung diseases, such as nonproductive coughing, dyspnea, parasympathetic reflex mucus secretion and bronchoconstriction (Mazzone and Undem, 2016). Consequently, ion channels that regulate the excitability of C-fibers in the airways can be an attractive therapeutic target aimed at reducing the symptoms of various inflammatory diseases of the airways. Using single-cell mRNA analysis, Sun and collaborators have very recently shown that *KCNQ2*, *KCNQ3*, and *KCNQ5* are consistently expressed in mouse lung specific nodose neurons with *KCNQ3* being the most predominant (Sun et al., 2019). This study suggested that Kv7.3 channels are the major contributors to the Kv7-M current in the nodal neurons of the mouse lungs. The Kv7 channel activator retigabine increased the amplitude and accelerated the activation rate of the M-current, caused a prominent hyperpolarization, and suppressed the excitability of mouse nodose neurons. These effects were reversed or prevented in the presence of XE991, a Kv7 channel inhibitor. Remarkably, nebulized retigabine was found to attenuate cough evoked by inhalation of irritant gases (SO_2 and NH_3) in awake mice (Sun et al., 2019). Although future studies are needed to confirm their role in the regulation of C-fiber excitability of the airways in humans, these data indicate that Kv7.3 channels may provide a novel therapeutic target to reduce the conditions associated with pulmonary inflammatory diseases such as chronic coughing.

Non-small Cell Lung Cancer

K^+ channels regulate a number of processes of key relevance in cancer biology such as cell volume control, pH regulation, migration, proliferation, differentiation, apoptosis, and drug resistance (Rao et al., 2015; Prevarskaya et al., 2018; Haworth and Brackenbury, 2019; Serrano-Novillo et al., 2019). Thus, there is increasing evidence that K^+ channels play an important role in cancer; but a clear scenario is still far due to the plethora of K^+ channel isoforms and their diverse repertoire of effects. Notably, K^+ channels regulate cell cycle, but according to the channel isoform, its level of expression, the cell type, and the stage of differentiation the effects are diverse. For instance, Kv channels may exhibit proliferative or anti-proliferative roles, depending on the channel subtype and the phase of the cell cycle (Rao et al., 2015). Moreover changes in the phenotypes, signaling pathways, and pattern of expression of K^+ channels may be observed in cancer, which increases the complexity of K^+ channels regulation on cell viability. In addition to the well-characterized involvement of several Kv channels (most notably Kv1.1, Kv1.3, Kv1.5, Kv10.1, Kv10.2, and Kv11.1) in cancer (Rao et al., 2015), some members of the Kv7 family have also been suggested to participate in cell proliferation and cancer (Serrano-Novillo et al., 2019).

K^+ channels participate in tumor cell invasion and metastasis propagation *via* regulation of cell migration and growth (O'Grady and Lee, 2005; Schwab et al., 2008; Arcangeli et al., 2009; Prevarskaya et al., 2010). Indeed, inhibiting or silencing K^+ channels reduces the proliferation of cancer cells (Pancrazio et al., 1993; Jang et al., 2011). Kv7.1 channels have been highlighted in cell migration, proliferation, and repair of AECs (Trinh et al., 2007). In 2014, Girault and colleagues showed an increased expression (by 1.5- to 7-fold) of Kv7.1 channels in tumor lung adenocarcinoma samples, compared to non-neoplastic tissues from 17 of 26 patients (Girault et al., 2014). Authors found that the proliferation rates of lung adenocarcinoma cell monolayers were reduced by the Kv7.1 channel blockers clofilium and chromanol, or after silencing Kv7.1 channels using a specific siRNA. These data suggest that Kv7.1 channels could be a potential therapeutic target in lung cancer (Girault et al., 2014).

On the other hand, K^+ channels have also been implicated in both early and late stages of apoptosis. The decrease in cell volume is one of the earliest and necessary morphological changes observed in cells undergoing apoptosis. Active K^+ channels in the plasma membrane leads to K^+ and Cl^- outflow through K^+ and Cl^- channels, this generates an osmotic gradient leading to an outward water transport through aquaporins which results in a decrease in cell volume (Maeno et al., 2000). In later stages of apoptosis, the augmented intracellular K^+ concentration ($[K^+]_{int}$) suppresses caspase and nuclease activity and, conversely, the decreased $[K^+]_{int}$ caused by K^+ channel activation, promotes apoptosis (Burg et al., 2008). There is a wealth of literature supporting that the M- channel activators have a neuroprotective role *via* Kv7 activation and reduction of hyperactivity and, hence, suppression of glutamate excitotoxicity (Gamper et al., 2006; Bierbower et al., 2015; Vigil et al., 2020). It is likely that flupirtine would work the same way (Panchanathan et al., 2013; Li et al., 2014a). Nevertheless, its ability to inhibit cell viability has also been reported. Thus, Lee et al. showed that flupirtine exerted anti-proliferative effects in canine osteosarcoma cells by enhancing Kv7.5 function and arresting cells in the G_0/G_1 phases (Lee et al., 2014).

Similarly, retigabine was found to exhibit anti-proliferative effects in *C2C12* myoblasts (Iannotti et al., 2010).

Non-small-cell lung cancer (NSCLC) accounts for most cancer deaths. Aberrant activation of the epidermal growth factor receptor (EGFR) is involved in the pathogenesis and progression of several human cancers, including NSCLC (Melosky, 2014). Indeed, approximately 10–38% of NSCLC patients have EGFR gene mutations (Lin et al., 2014). EGFR tyrosine kinase inhibitors, such as Gefitinib have become standard first-line treatment for these patients (Cohen et al., 2003). However, acquired resistance represents a major limitation for drug efficacy. Cancer stem cells have self-renewal properties in various solid tumors, and play a key role in tumor growth and progression (Wang et al., 2013) and in therapy resistance (Steinbichler et al., 2018). A subset of cancer stem cells, termed the "side population" (SP), have elevated clonogenic potential and higher expression levels of ABC-transporters than main-population cells known as non-SP cells (Richard et al., 2013) and are considered to be responsible for anti-cancer drug resistance (Singh et al., 2010; Leon et al., 2016). Choi and colleagues have demonstrated a reduced mRNA expression of *KCNQ3* and *KCNQ5* in SP cells compared to non-SP cells (Choi et al., 2017). The treatment of flupirtine (a Kv7.2–7.5 channel enhancer) decreased the viability of SP and non-SP cells. In addition, the combination treatment of gefitinib plus flupirtine was more effective, compared to the individual treatment of both drugs, in decreasing the viability of both non-SP cells, and gefitinib-resistant SP cells. According to their results, the combination treatment of gefitinib plus flupirtine was proposed to reduce the viability of gefitinib-resistant cells through inhibition of the EGFR-Ras-Raf-ERK pathway *via* (Choi et al., 2017). These results suggest that the activation of Kv7.3 and Kv7.5 channels could play an important role in the induction of apoptosis in SP cells, either by participating in the decrease of the cellular volume necessary for apoptosis initiation; or by decreasing $[K^+]_{int}$, which results in the activation of caspases and nucleases.

Pulmonary Hypertension

Pulmonary hypertension is defined by an increase in mean pulmonary arterial pressure at rest, as assessed by right heart catheterization. Based on pathophysiological findings, clinical presentation, hemodynamic characteristics, and therapeutic considerations, pulmonary hypertension is categorized into five groups by WHO: pulmonary arterial hypertension (PAH), pulmonary hypertension due to left-sided heart disease, pulmonary hypertension due to lung disease or hypoxia, chronic thromboembolic pulmonary hypertension, and multifactorial pulmonary hypertension (Simonneau et al., 2019). PAH is characterized by excessive pulmonary vasoconstriction and progressive remodeling of the distal PAs, resulting in elevated pulmonary vascular resistance and, eventually, in right ventricular failure (McLaughlin et al., 2015). Reduced expression or function of K^+ channels (notably Kv1.5 and TASK-1 channels) in PASMCs results in a more depolarized Em, and is considered to contribute to the enhanced vasoconstriction and proliferation (Moudgil et al., 2006; Boucherat et al., 2015; Hayabuchi, 2017). In 2009, Joshi et al. demonstrated that Kv7 channel blockers, linopirdine, and XE991, inhibited the I_{KN} current in PASMCs and raised mean pulmonary arterial pressure (mPAP); while the Kv7 channel openers, retigabine and flupirtine, had the opposite effects (Joshi et al., 2009). Linopirdine can also increase mesenteric vascular resistance and systemic arterial pressure (Mackie et al., 2008). Functional expression of Kv7 channels in the pulmonary circulation was later confirmed by others (Morecroft et al., 2009; Eid and Gurney, 2018; Mondejar-Parreño et al., 2018). As in the systemic circulation, *KCNQ1* and especially *KCNQ4* and *KCNQ5* appear the most predominant *KCNQ* channels in the pulmonary circulation (Joshi et al., 2009; Morales-Cano et al., 2014; Sedivy et al., 2015; Mondejar-Parreño et al., 2018). The lack of selective drugs for the different Kv7 subunits hinders identification of the functional impact of individual Kv7 members (Barrese et al., 2018). Structurally related Kv7 enhancers such as retigabine and flupirtine (which activate all Kv7 isoforms except Kv7.1 channels) (Barrese et al., 2018) and zinc pyrithione (which activate all Kv7 members but Kv7.3) have been shown to induce pulmonary vasodilation (Joshi et al., 2009; Morecroft et al., 2009; Sedivy et al., 2015; Eid and Gurney, 2018; Mondejar-Parreño et al., 2018). In addition, drugs that block all Kv7 channels (i.e., linopirdine and XE991) are able to contract PAs previously primed (Chadha et al., 2012; Sedivy et al., 2015) or not (Joshi et al., 2009), whereas selective Kv7.1 blockers HMR1556, L768, L673, and JNJ39490282 (Barrese et al., 2018) have no contractile effects in PAs (Chadha et al., 2012). On the other hand, the application of R-L3, a compound purported to activate Kv7.1 channels, relaxed efficiently precontracted intrapulmonary arteries (Chadha et al., 2012; Mondejar-Parreño et al., 2018). These data suggest that even when Kv7.4 and Kv7.5 appear to be the most relevant Kv7 channels in controlling resting Em in PASMC, Kv7.1 channels are also functionally expressed.

The NO/cGMP pathway represents a key physiological signaling controlling tone in PAs, and drugs stimulating this pathway are used to treat PAH (Barnes and Liu, 1995), and drugs activating this pathway are used to treat pulmonary arterial hypertension. Recently, we have found that NO donors and riociguat, a stimulator of sGC used for the treatment of pulmonary arterial hypertension, enhance Kv7 current and induce membrane hyperpolarization in fresh isolated PASMCs contributing to pulmonary vasodilation (Mondejar-Parreño et al., 2019). Further, we identified Kv7.5 channels as a potential member of the Kv7 family targeted by these drugs.

The expression of Kv7 channels has been explored in several experimental models of pulmonary hypertension. While the hypoxic pulmonary vasoconstriction (HPV) reflects a physiological intrinsic property of PASMCs, which allows shifting blood flow from hypoxic to normoxic lung areas, coupling ventilation and perfusion, the chronic exposure to hypoxic air causes the pulmonary circulation to become hypertensive (Sylvester et al., 2012). Sedivy et al. found a significant loss of *KCNQ4* mRNA expression in PA from rats maintained for 3 days in a hypoxic environment, even when a significant reduction of the Kv7.4 protein expression could not be confirmed (Sedivy et al., 2015). On the other hand, the expression of *KCNQ1* and *KCNQ5* was unaffected. However, Li et al. reported that longer incubation on hypoxia (9 days) was associated with a downregulation of

KCNQ5 in the PAs (Li et al., 2014b). These authors also demonstrated that microRNA-190 (miR-190), whose expression is increased following the hypoxic exposure, directly targeted *KCNQ5*. This led the authors to propose the increased in miR-190 as a mechanism involved in the *KCNQ5* downregulation and enhanced vasoconstriction induced by hypoxia. In addition to the hypoxic pulmonary hypertension models, a slight reduction of *KCNQ5* expression has also been observed in rat lungs from monocrotaline-induced pulmonary hypertension (Morales-Cano et al., 2014). On the other hand, we found the expression of *KCNQ1*, *KCNQ4*, and *KCNQ5* mRNAs unaltered in lungs from Zucker rats, a model of type 2 diabetes, developing increased pulmonary arterial pressure, and right ventricular hypertrophy (Morales-Cano et al., 2019).

The potential impairment of *KCNQ* channels has been also explored in conditions associated with pulmonary hypertension. The HIV-1 infection is an established risk factor for PAH, although the pathological mechanisms underlying the development of HIV-related PAH remain unclear (Butrous, 2015). In a recent study using HIV-transgenic mice expressing seven of the nine HIV viral proteins and wild-type mice we observed that HIV mice had reduced lung expression of *KCNQ1* and *KCNQ5* channels (Mondejar-Parreño et al., 2018). By using vascular reactivity and patch-clamp experimental approaches we found decreased responses to the Kv7.1 channel activator L-364,373 but unaltered responses to retigabine (Mondejar-Parreño et al., 2018). These results suggest that Kv7 channels (especially Kv7.1) are impaired in mice expressing HIV-1 proteins.

Congenital diaphragmatic hernia is a rare congenital anomaly commonly associated with persistent pulmonary hypertension. A recent study showed that the expression of *KCNQ5*, but not that of *KCNQ1* or *KCNQ4*, was significantly downregulated at the mRNA and protein levels in rat lungs from nitrofen-induced congenital diaphragmatic hernia (Zimmer et al., 2017). Likewise, a markedly diminished *KCNQ5* expression was found in the pulmonary vasculature of congenital diaphragmatic hernia fetuses. Since Kv7.5 channels have shown to contribute to NO donors-induced pulmonary vasodilation (Mondejar-Parreño et al., 2019), its reduced availability in congenital diaphragmatic hernia could partly explain the poor therapeutic response to inhaled NO in these patients (Group (NINOS), 1997; Putnam et al., 2016).

Studies in experimental models have shown evidence that drugs activating Kv7 channels may be of benefit in the treatment of pulmonary hypertension with different etiologies (Morecroft et al., 2009; Sedivy et al., 2015). Morecroft et al. also demonstrated that flupirtine attenuated the development of chronic hypoxia-induced pulmonary hypertension in mice and reversed established pulmonary hypertension in mice that over-express the 5-HT transporter (SERT), apparently *via* Kv7 activation (Morecroft et al., 2009). In this study authors showed that the chronic treatment with flupirtine reduced mean right ventricle pressure (mRVP), pulmonary remodeling, and RV hypertrophy (RVH). More recently, Sedivy et al. confirmed the potential benefit of Kv7 channel openers showing the pulmonary antihypertensive effects of flupirtine in rats exposed to short-term (3–5 days) hypoxia (Sedivy et al., 2015). In line with this, we have found that retigabine-induced vasodilation is increased in PAs from pulmonary hypertensive animals and this is associated with an increased contribution of Kv7 channels to the net K^+ current present in pulmonary arterial myocytes (unpublished data from the author's laboratory).

Altogether, these findings suggest that Kv7 channels play a protective role in the pulmonary circulation limiting pulmonary vasoconstriction, and their activation may represent a promising therapeutic strategy in pulmonary hypertension.

Kv7 CHANNELS: NEW PHARMACOLOGICAL TARGETS IN RESPIRATORY DISEASES?

In addition to their well-established role in neural and cardiac tissue, studies over the last 20 decades have evidenced the expression and the plethora of cellular functions of Kv7 channels in numerous cell types. Thus, Kv7 channels are now recognized as playing relevant physiological roles in many tissues, which has encouraged the search for the therapeutic potential of Kv7 channel modulators in many diseases including those affected the lung. As stated in the previous section activation of Kv7 channels has been proposed to provide beneficial effects in a number of lung conditions. Therefore, Kv7 channel openers/enhancers or drugs acting partly through these channels could be proposed as bronchodilators, expectorants, antitussives, chemotherapeutics, and pulmonary vasodilators, as summarized below.

Flupirtine and retigabine are structurally related Kv7.2–7.5 channel activators. The discovery of Kv7 channels came later than the extensive use of flupirtine and retigabine as an analgesic and anticonvulsant, respectively, and whose mechanism of action was unknown until then (Schenzer et al., 2005). Retigabine has been shown to increase the open probability and cause a hyperpolarizing shift in the voltage dependence of activation of *KCNQ* channels by binding at the intracellular side of the pore-forming S5 helix around a key tryptophan (Trp) Trp236 in Kv7.2 and analogous residues in Kv7.3, 4, and 5 which is absent in Kv7.1 channels (Schenzer et al., 2005; Lange et al., 2009; Kim et al., 2015). Kim et al. have suggested that the retigabine interaction with this Trp residue depends largely on the formation of a hydrogen bond (Kim et al., 2015).

As the relevant role of Kv7 channels was discovered, the idea that these channels could constitute a new therapeutic strategy became more attractive, leading to investment in the development of new activators. The key residues for retigabine-binding have also been recognized to be also essential for the binding of other compounds such as S1 and BMS-204352; though these last drugs have a greater efficacy enhancing Kv7.4 and Kv7.5 isoforms rather than Kv7.2 or/and Kv7.3 channels (Dupuis et al., 2002; Bentzen et al., 2006). Zinc pyrithione activates the Kv7 channel by interacting with a binding site different to that of retigabine (Xiong et al., 2008). Hence, zinc pyrithione activates all Kv7 channels except for Kv7.3 channels, which is the most retigabine-sensitive. It is worth noting that the active compound in the action of zinc pyrithione on Kv7 channels is zinc, as

administration of free zinc also activates these channels by reducing their dependence on PIP_2 (Gao et al., 2017). The activity of ICA-27243, a drug more potent at activating Kv7.2/7.3 heteromeric channels than Kv7.4 homomeric channels or Kv7.3/7.5 heteromeric channels, is determined by a novel site inside the Kv7 channel voltage-detection domain (Wickenden et al., 2008; Blom et al., 2010). R-L3 is a benzodiazepine that activates Kv7.1 homomeric channels, but is considerably weaker when Kv7.1 is coexpressed with KCNE1 subunit, suggesting that R-L3 and KCNE1 subunits compete for the same interaction site on *KCNQ1* subunits (Salata et al., 1998).

Kv7 channels are currently new therapeutic targets in the field of lung diseases; consequently, there is still much to be learned about their physiological role, regulation, and possible impairment by pathological processes. The specific expression of certain Kv7 channel in different types of cells is of great pharmacological interest, since their selective modulation could provide beneficial therapeutic effects while avoiding the adverse effects associated with other isoforms (Stott et al., 2014). A clear example comes from the previous experience with retigabine and flupirtine, which have been used as analgesic and anticonvulsant, respectively, for many years but were withdrawn from the marked due to their adverse effects including the risk of serious liver injury, pigment changes in the retina and urinary retention (Herrmann et al., 1987; Brickel et al., 2012). While, as mentioned, both drugs activate Kv7.2–Kv7.5, they appear to display greater efficacy for Kv7.2 and Kv7.3 channels over Kv7.4 and Kv7.5 channels, which predominate in smooth muscle. Thus, it is expected that compounds selectively activate the Kv7.4 and/or the Kv7.5 subunit may be used in the treatment of vascular smooth muscle disorders with few neurological side effects. For instance, selective activation of Kv7.4 and Kv7.4/Kv7.5 channels (but not Kv7.1, Kv7.2, and Kv7.2/Kv7.3) has been implicated in the vasorelaxant effects of the Rho kinase inhibitor fasudil (Zhang et al., 2016). Thus, it is likely that, in addition to Rho kinase inhibition, activation of these channels may contribute to the beneficial effects of fasudil in cardiovascular conditions such as hypertension, vasospasm, stroke arteriosclerosis, pulmonary hypertension, and heart failure (Shi and Wei, 2013; Shimokawa and Satoh, 2015). Likewise, it is expected that selective Kv7.2 and Kv7.3 channel enhancers may be used to the treatment of neurological disorders with few adverse effects in smooth muscle cells (Stott et al., 2014; Barrese et al., 2018). Remarkably, Manville et al. have recently reported that the neurotransmitter γ-aminobutyric acid (GABA) and various metabolites (β-hydroxybutyric acid and γ-amino-β-hydroxybutyric acid) directly activate Kv7.3 and Kv7.5 but not Kv7.1, 2, and 4 (Manville et al., 2018). Manville and colleagues found that Trp residues in Kv7.3 (Trp265) and Kv7.5 (Trp270) were required for binding but not sufficient for GABA-induced activation. Thus, while Kv7.2 and Kv7.4 share analogous Trp residues and bind GABA, they are not activated by GABA (Manville and Abbott, 2018). Likewise, the synthetic GABA analog gabapentin, but not pregabalin, was also found to activate Kv7.3 and Kv7.5 (Manville and Abbott, 2018). Very recently, these authors have proposed a model in which the sodium-coupled myo-inositol transporter 1 (SMIT1) interacts with KCNQ2/3 and tunes the channel response to GABA and related metabolites (Manville and Abbott, 2020).

The search for Kv7 activators with a better safety profile than retigabine and flupirtine as well as the identification of novel potential therapeutic applications, has driven the development of a large number of compounds with Kv7 enhancing properties in the last decade (Jepps et al., 2013; Stott et al., 2014; Haick and Byron, 2016; Barrese et al., 2018).

Given the functional roles and ubiquitous expression of Kv7 channels in many tissues, drugs modulating Kv7 channels are presumed to cause off-target effects including alterations of the QT interval at the heart level, systemic hypotension, urinary retention or neuronal effects. This could be largely avoided by using localized drug delivery to the lungs by oral inhalation. Inhaled administration is the route of choice for many drugs (i.e., corticosteroids; anticholinegics, or β2-adrenergic receptor agonists) to treat respiratory diseases. Similarly, targeting lung Kv7 channels specifically using inhaled Kv7 activators may be an innovative approach for the treatment of COPD, cystic fibrosis, pulmonary hypertension, asthmatic events, lung cancer, bronchitis, and pulmonary edema.

Progress in the treatment of respiratory diseases is a global challenge because of its health and socio-economic implications. The optimal management and treatment of these diseases should be aimed at achieving adequate control of the disease, improving the quality of life of patients, and reducing hospitalizations and the enormous financial burden on healthcare systems. Targeting Kv7 channels in the treatment of lung disorders could be a promising therapeutic strategy. Here, we summarized the potential usefulness of Kv channel modulators in treating respiratory diseases.

Bronchodilators

Asthma and COPD are characterized by hyper-contraction of ASMC attributed to abnormally high concentrations of different bronchoconstrictor agonists and/or increased sensitivity to them, leading to pathological narrowing of the airways (Penn, 2008). K^+ channels are key regulators of Em in ASMC and their impairment causes membrane depolarization and bronchoconstriction (Hall, 2000). Among them, Kv7 channels contribute significantly to the negative resting Em in ASMC (Brueggemann et al., 2011). By acting on a different target, Kv7 channel openers offer the potential of being combined with standard bronchodilators such as β2-adrenergic receptor agonists and antimuscarinics as an adjuvant therapy to increase the efficacy or overcome desensitization (Brueggemann et al., 2014b).

Expectorants

The function of Kv7.1 together with KCNE1/E2/E3 subunits seems to play a key role in secretions in airway epithelial cells. The co-activation of Cl^- channels in the luminal surface and K^+ channels in the basolateral membrane in AEC is an essential requirement for Cl^- secretion (Frizzell and Hanrahan, 2012). The activation of Kv7.1 channels has an expectorant effect provoking or promoting the expulsion of accumulated bronchial secretions and the productive cough helping to airway clearance

(Mall et al., 2000; Al-Hazza et al., 2016; Kroncke et al., 2016; Hynes and Harvey, 2019). Kv7.1 channel openers or drugs that indirectly activate Kv7.1 channels might be beneficial in the treatment of bronchitis, COPD, cystic fibrosis and asthma (Boucherot et al., 2001; Athanazio, 2012; Hynes and Harvey, 2019).

Antitussives

Stimulation of airway C-fibers can be activated by inflammatory factors leading to the impulse to unproductive cough, dyspnea, mucus secretion and bronchoconstriction (Mazzone and Undem, 2016). Activation of Kv7.3 channels in VACF by retigabine has been shown to increase the M-current amplitude and to inhibit unproductive coughing (Sun et al., 2019). Thus, Kv7 activators could be useful as chronic coughing relievers in pulmonary inflammatory diseases.

Chemotherapy

Although, the role of Kv7 channel modulators as chemotherapy agents has been only barely studied, flupirtine has been shown to attenuate the resistance to gefitinib in a human lung cancer cell line (Choi et al., 2017). The anti-proliferative effect of flupirtine has also been proposed as potentially beneficial in other types of cancer (Lee et al., 2014). Additional studies are required to evaluate the potential of Kv7 channel activators with selectivity for particular isoforms as chemotherapy agents.

Pulmonary Vasodilators

K^+ channels are also key regulators of cellular Em in PASMCs, controlling the activity of voltage-dependent Ca^{2+} channels and, subsequently, pulmonary artery smooth muscle contraction. Pulmonary vascular tone is controlled by the interaction of different circulating or locally released vasoactive factors with vasoconstrictor or vasodilating properties. Acute modulation of the activity of K^+ channels has been extensively shown to contribute to the vascular effects of these vasoactive factors. Thus, different vasodilators such as nitric oxide, prostacyclin and calcitonin gene-related activate several K^+ channels and, conversely, vasoconstrictors as serotonin, angiotensin II, thromboxane A_2, noradrenaline and endothelin-1 have been shown to inhibit K^+ channels (Cogolludo et al., 2007; Stott et al., 2014). With such a crucial role in modulating and maintaining pulmonary arterial tone, changes in function and expression of K^+ channels during the development and pathogenesis of pulmonary hypertension results in aberrations of normal physiological functions. Consequently, K^+ channels openers are presumed to have a beneficial therapeutic effect, especially if their action can be directed to the pulmonary circulation (Gurney et al., 2010). Up to the present time, the availability of drugs modulating Kv7 channels has been relatively scarce. Advances in the understanding of the role of Kv7 channels in the pulmonary vasculature and the development of new selective drugs for these channels indicate that they may represent a useful therapeutic target for the treatment of pulmonary arterial hypertension. As detailed above, different studies have provided evidence that treatment with Kv7 channel activators such as flupirtine, retigabine, or fasudil is beneficial in different pulmonary hypertension models (Morecroft et al., 2009; Duong-Quy et al., 2013; Sedivy et al., 2015; Zhang and Wu, 2017). In addition, Kv7 channel activation has been shown to contribute to the pulmonary vasodilating effect induced by drugs approved for the pulmonary hypertension treatment such as nitric oxide or riociguat (Mondejar-Parreño et al., 2019).

CONCLUSIONS

In the last decade, a significant progress in the understanding of the role of Kv7 channels in lung physiology has been made. The recognition of the involvement of these channels in cellular functions of crucial relevance in the normal physiology of the lung, such as the control of water and salt transport across the epithelial cell membrane, the excitability of airway afferent nerves, and the regulation of airway and lung vascular smooth muscle tone, makes them attractive therapeutic targets in lung diseases. In this regard, deciphering the involvement and importance of specific Kv7 subunits in these cellular functions will lead to a significant advance that may constitute the basis for the therapeutic potential of selective Kv7 channel modulators in lung diseases.

AUTHOR CONTRIBUTIONS

GM-P, FP-V, and AC wrote the manuscript. All authors contributed to the article and approved the submitted version.

FUNDING

This work was funded by Ministerio de Economía y Competitividad grants (SAF2016-77222R to FP-V and AC), the Cardiovascular Medical Research and Education Fund (AC), Comunidad de Madrid (B2017/BMD-3727 to AC) and Ciber Enfermedades Respiratorias (Ciberes). GM-P is supported by a predoctoral CIBERES/Fundación Contra la Hipertensión Pulmonar-EMPATHY grant.

REFERENCES

Abbott, G. W. (2016). KCNE4 and KCNE5: K(+) channel regulation and cardiac arrhythmogenesis. *Gene* 593, 249–260. doi: 10.1016/j.gene.2016.07.069

Al-Hazza, A., Linley, J., Aziz, Q., Hunter, M., and Sandle, G. (2016). Upregulation of basolateral small conductance potassium channels (KCNQ1/KCNE3) in ulcerative colitis. *Biochem. Biophys. Res. Commun.* 470, 473–478. doi: 10.1016/j.bbrc.2015.12.086

Arcangeli, A., Crociani, O., Lastraioli, E., Masi, A., Pillozzi, S., and Becchetti, A. (2009). Targeting ion channels in cancer: a novel frontier in antineoplastic therapy. *Curr. Med. Chem.* 16, 66–93. doi: 10.2174/092986709787002835

Athanazio, R. (2012). Airway disease: similarities and differences between asthma, COPD and bronchiectasis. *Clinics* 67, 1335–1343. doi: 10.6061/clinics/2012(11)19

Bardou, O., Trinh, N. T. N., and Brochiero, E. (2009). Molecular diversity and function of K^+ channels in airway and alveolar epithelial cells. *Am. J. Phys. Lung Cell. Mol. Phys.* 296, L145–L155. doi: 10.1152/ajplung.90525.2008

Barnes, P. J., and Liu, S. F. (1995). Regulation of pulmonary vascular tone. *Pharmacol. Rev.* 47, 87–131.

Barnes, P. J., Shapiro, S. D., and Pauwels, R. A. (2003). Chronic obstructive pulmonary disease: molecular and cellularmechanisms. *Eur. Respir. J.* 22, 672–688. doi: 10.1183/09031936.03.00040703

Barrese, V., Stott, J. B., and Greenwood, I. A. (2018). KCNQ-encoded potassium channels as therapeutic targets. *Annu. Rev. Pharmacol. Toxicol.* 58, 625–648. doi: 10.1146/annurev-pharmtox-010617-052912

Barro-Soria, R., Perez, M. E., and Larsson, H. P. (2015). KCNE3 acts by promoting voltage sensor activation in KCNQ1. *Proc. Natl. Acad. Sci.* 112, E7286–E7292. doi: 10.1073/pnas.1516238112

Bartoszewski, R., Matalon, S., and Collawn, J. F. (2017). Ion channels of the lung and their role in disease pathogenesis. *Am. J. Phys. Lung Cell. Mol. Phys.* 313, L859–L872. doi: 10.1152/ajplung.00285.2017

Belfodil, R., Barrière, H., Rubera, I., Tauc, M., Poujeol, C., Bidet, M., et al. (2003). CFTR-dependent and -independent swelling-activated K^+ currents in primary cultures of mouse nephron. *Am. J. Physiol. Ren. Physiol.* 284, F812–F828. doi: 10.1152/ajprenal.00238.2002

Bentzen, B. H., Schmitt, N., Calloe, K., Dalby Brown, W., Grunnet, M., and Olesen, S.-P. (2006). The acrylamide (S)-1 differentially affects Kv7 (KCNQ) potassium channels. *Neuropharmacology* 51, 1068–1077. doi: 10.1016/j.neuropharm.2006.07.001

Bierbower, S. M., Choveau, F. S., Lechleiter, J. D., and Shapiro, M. S. (2015). Augmentation of M-type (KCNQ) potassium channels as a novel strategy to reduce stroke-induced brain injury. *J. Neurosci.* 35, 2101–2111. doi: 10.1523/JNEUROSCI.3805-14.2015

Billet, A., and Hanrahan, J. W. (2013). The secret life of CFTR as a calcium-activated chloride channel. *J. Physiol.* 591, 5273–5278. doi: 10.1113/jphysiol.2013.261909

Blom, S. M., Schmitt, N., and Jensen, H. S. (2010). Differential effects of ICA-27243 on cloned K(V)7 channels. *Pharmacology* 86, 174–181. doi: 10.1159/000317525

Boucherat, O., Chabot, S., Antigny, F., Perros, F., Provencher, S., and Bonnet, S. (2015). Potassium channels in pulmonary arterial hypertension. *Eur. Respir. J.* 46, 1167–1177. doi: 10.1183/13993003.00798-2015

Boucherot, A., Schreiber, R., and Kunzelmann, K. (2001). Regulation and properties of KCNQ1 (K(V)LQT1) and impact of the cystic fibrosis transmembrane conductance regulator. *J. Membr. Biol.* 182, 39–47. doi: 10.1007/s00232-001-0030-4

Brickel, N., Gandhi, P., VanLandingham, K., Hammond, J., and DeRossett, S. (2012). The urinary safety profile and secondary renal effects of retigabine (ezogabine): a first-in-class antiepileptic drug that targets KCNQ (K(v)7) potassium channels. *Epilepsia* 53, 606–612. doi: 10.1111/j.1528-1167.2012.03441.x

Brueggemann, L. I., Cribbs, L. L., Schwartz, J., Wang, M., Kouta, A., and Byron, K. L. (2018). Mechanisms of PKA-dependent potentiation of Kv7.5 channel activity in human airway smooth muscle cells. *Int. J. Mol. Sci.* 19:2223. doi: 10.3390/ijms19082223

Brueggemann, L. I., Haick, J. M., Cribbs, L. L., and Byron, K. L. (2014a). Differential activation of vascular smooth muscle Kv7.4, Kv7.5, and Kv7.4/7.5 channels by ML213 and ICA-069673. *Mol. Pharmacol.* 86, 330–341. doi: 10.1124/mol.114.093799

Brueggemann, L. I., Haick, J. M., Neuburg, S., Tate, S., Randhawa, D., Cribbs, L. L., et al. (2014b). KCNQ (Kv7) potassium channel activators as bronchodilators: combination with a β2-adrenergic agonist enhances relaxation of rat airways. *Am. J. Phys. Lung Cell. Mol. Phys.* 306, L476–L486. doi: 10.1152/ajplung.00253.2013

Brueggemann, L. I., Kakad, P. P., Love, R. B., Solway, J., Dowell, M. L., Cribbs, L. L., et al. (2011). Kv7 potassium channels in airway smooth muscle cells: signal transduction intermediates and pharmacological targets for bronchodilator therapy. *Am. J. Phys. Lung Cell. Mol. Phys.* 302, L120–L132. doi: 10.1152/ajplung.00194.2011

Burg, E. D., Remillard, C. V., and Yuan, J. X.-J. (2008). Potassium channels in the regulation of pulmonary artery smooth muscle cell proliferation and apoptosis: pharmacotherapeutic implications. *Br. J. Pharmacol.* 153, S99–S111. doi: 10.1038/sj.bjp.0707635

Butrous, G. (2015). Human immunodeficiency virus-associated pulmonary arterial hypertension: considerations for pulmonary vascular diseases in the developing world. *Circulation* 131, 1361–1370. doi: 10.1161/CIRCULATIONAHA.114.006978

Byron, K. L., and Brueggemann, L. I. (2018). Kv7 potassium channels as signal transduction intermediates in the control of microvascular tone. *Microcirculation* 25:e12419. doi: 10.1111/micc.12419

Caulfield, M. P., Jones, S., Vallis, Y., Buckley, N. J., Kim, G. D., Milligan, G., et al. (1994). Muscarinic M-current inhibition via G alpha q/11 and alpha-adrenoceptor inhibition of Ca^{2+} current via G alpha o in rat sympathetic neurones. *J. Physiol.* 477, 415–422. doi: 10.1113/jphysiol.1994.sp020203

Chadha, P. S., Jepps, T. A., Carr, G., Stott, J. B., Zhu, H.-L., Cole, W. C., et al. (2014). Contribution of kv7.4/kv7.5 heteromers to intrinsic and calcitonin gene-related peptide-induced cerebral reactivity. *Arterioscler. Thromb. Vasc. Biol.* 34, 887–893. doi: 10.1161/ATVBAHA.114.303405

Chadha, P. S., Zunke, F., Davis, A. J., Jepps, T. A., Linders, J. T. M., Schwake, M., et al. (2012). Pharmacological dissection of K(v)7.1 channels in systemic and pulmonary arteries. *Br. J. Pharmacol.* 166, 1377–1387. doi: 10.1111/j.1476-5381.2012.01863.x

Chen, Y.-H., Xu, S.-J., Bendahhou, S., Wang, X.-L., Wang, Y., Xu, W.-Y., et al. (2003). KCNQ1 gain-of-function mutation in familial atrial fibrillation. *Science* 299, 251–254. doi: 10.1126/science.1077771

Choi, S. Y., Kim, H.-R., Ryu, P. D., and Lee, S. Y. (2017). Regulation of voltage-gated potassium channels attenuates resistance of side-population cells to gefitinib in the human lung cancer cell line NCI-H460. *BMC Pharmacol. Toxicol.* 18:14. doi: 10.1186/s40360-017-0118-9

Clarke, L. L., Grubb, B. R., Yankaskas, J. R., Cotton, C. U., McKenzie, A., and Boucher, R. C. (1994). Relationship of a non-cystic fibrosis transmembrane conductance regulator-mediated chloride conductance to organ-level disease in Cftr(−/−) mice. *Proc. Natl. Acad. Sci.* 91, 479–483. doi: 10.1073/pnas.91.2.479

Cogolludo, A., Moreno, L., and Villamor, E. (2007). Mechanisms controlling vascular tone in pulmonary arterial hypertension: implications for vasodilator therapy. *Pharmacology* 79, 65–75. doi: 10.1159/000097754

Cohen, M. H., Williams, G. A., Sridhara, R., Chen, G., and Pazdur, R. (2003). FDA drug approval summary: gefitinib (ZD1839) (Iressa) tablets. *Oncologist* 8, 303–306. doi: 10.1634/theoncologist.8-4-303

Corvol, H., Flamein, F., Epaud, R., Clement, A., and Guillot, L. (2009). Lung alveolar epithelium and interstitial lung disease. *Int. J. Biochem. Cell Biol.* 41, 1643–1651. doi: 10.1016/j.biocel.2009.02.009

Cowley, E. A., and Linsdell, P. (2002a). Characterization of basolateral K^+ channels underlying anion secretion in the human airway cell line Calu-3. *J. Physiol.* 538, 747–757. doi: 10.1113/jphysiol.2001.013300

Cowley, E. A., and Linsdell, P. (2002b). Oxidant stress stimulates anion secretion from the human airway epithelial cell line Calu-3: implications for cystic fibrosis lung disease. *J. Physiol.* 543, 201–209. doi: 10.1113/jphysiol.2002.022400

Cummings, K. W., and Bhalla, S. (2015). Pulmonary vascular diseases. *Clin. Chest Med.* 36, 235–248. doi: 10.1016/j.ccm.2015.02.007

Cunningham, S. A., Worrell, R. T., Benos, D. J., and Frizzell, R. A. (1992). CAMP-stimulated ion currents in *Xenopus* oocytes expressing CFTR cRNA. *Am. J. Phys.* 262, C783–C788. doi: 10.1152/ajpcell.1992.262.3.C783

de Jong, I. E. M., and Jepps, T. A. (2018). Impaired Kv7 channel function in cerebral arteries of a tauopathy mouse model (rTg4510). *Phys. Rep.* 6:e13920. doi: 10.14814/phy2.13920

Dellaripa, P. F. (2018). Interstitial lung disease in the connective tissue diseases; a paradigm shift in diagnosis and treatment. *Clin. Immunol.* 186, 71–73. doi: 10.1016/j.clim.2017.09.015

Delmas, P., and Brown, D. A. (2005). Pathways modulating neural KCNQ/M (Kv7) potassium channels. *Nat. Rev. Neurosci.* 6, 850–862. doi: 10.1038/nrn1785

Duong-Quy, S., Bei, Y., Liu, Z., and Dinh-Xuan, A. T. (2013). Role of rho-kinase and its inhibitors in pulmonary hypertension. *Pharmacol. Ther.* 137, 352–364. doi: 10.1016/j.pharmthera.2012.12.003

Dupuis, D. S., Schrøder, R. L., Jespersen, T., Christensen, J. K., Christophersen, P., Jensen, B. S., et al. (2002). Activation of KCNQ5 channels stably expressed in HEK293 cells by BMS-204352. *Eur. J. Pharmacol.* 437, 129–137. doi: 10.1016/S0014-2999(02)01287-6

Eid, B. G., and Gurney, A. M. (2018). Zinc pyrithione activates K^+ channels and hyperpolarizes the membrane of rat pulmonary artery smooth muscle cells. *PLoS One* 13:e0192699. doi: 10.1371/journal.pone.0192699

Evseev, A. I., Semenov, I., Archer, C. R., Medina, J. L., Dube, P. H., Shapiro, M. S., et al. (2013). Functional effects of KCNQ K(+) channels in airway smooth muscle. *Front. Physiol.* 4:277. doi: 10.3389/fphys.2013.00277

Fosmo, A. L., and Skraastad, Ø. B. (2017). The Kv7 channel and cardiovascular risk factors. *Front. Cardiovasc. Med.* 4:75. doi: 10.3389/fcvm.2017.00075

Frizzell, R. A., and Hanrahan, J. W. (2012). Physiology of epithelial chloride and fluid secretion. *Cold Spring Harb. Perspect. Med.* 2:a009563. doi: 10.1101/cshperspect.a009563

Gamper, N., Zaika, O., Li, Y., Martin, P., Hernandez, C. C., Perez, M. R., et al. (2006). Oxidative modification of M-type K(+) channels as a mechanism of cytoprotective neuronal silencing. *EMBO J.* 25, 4996–5004. doi: 10.1038/sj.emboj.7601374

Gao, H., Boillat, A., Huang, D., Liang, C., Peers, C., and Gamper, N. (2017). Intracellular zinc activates KCNQ channels by reducing their dependence on phosphatidylinositol 4,5-bisphosphate. *Proc. Natl. Acad. Sci. U. S. A.* 114, E6410–E6419. doi: 10.1073/pnas.1620598114

Girault, A., Privé, A., Trinh, N. T. N., Bardou, O., Ferraro, P., Joubert, P., et al. (2014). Identification of KvLQT1 K^+ channels as new regulators of non-small cell lung cancer cell proliferation and migration. *Int. J. Oncol.* 44, 838–848. doi: 10.3892/ijo.2013.2228

Goodwill, A. G., Fu, L., Noblet, J. N., Casalini, E. D., Sassoon, D., Berwick, Z. C., et al. (2016). KV7 channels contribute to paracrine, but not metabolic or ischemic, regulation of coronary vascular reactivity in swine. *Am. J. Physiol. Heart Circ. Physiol.* 310, H693–H704. doi: 10.1152/ajpheart.00688.2015

Group (NINOS) (1997). Inhaled nitric oxide and hypoxic respiratory failure in infants with congenital diaphragmatic hernia. *Pediatrics* 99, 838–845. doi: 10.1542/peds.99.6.838

Grubb, B. R., Vick, R. N., and Boucher, R. C. (1994). Hyperabsorption of Na^+ and raised Ca(2+)-mediated Cl^- secretion in nasal epithelia of CF mice. *Am. J. Phys. Cell Phys.* 266, C1478–C1483. doi: 10.1152/ajpcell.1994.266.5.C1478

Grunnet, M., Jespersen, T., Rasmussen, H. B., Ljungstrøm, T., Jorgensen, N. K., Olesen, S.-P., et al. (2002). KCNE4 is an inhibitory subunit to the KCNQ1 channel. *J. Physiol.* 542, 119–130. doi: 10.1113/jphysiol.2002.017301

Gurney, A. M., Joshi, S., and Manoury, B. (2010). KCNQ potassium channels: new targets for pulmonary vasodilator drugs? *Adv. Exp. Med. Biol.* 661, 405–417. doi: 10.1007/978-1-60761-500-2_26

Haick, J. M., Brueggemann, L. I., Cribbs, L. L., Denning, M. F., Schwartz, J., and Byron, K. L. (2017). PKC-dependent regulation of Kv7.5 channels by the bronchoconstrictor histamine in human airway smooth muscle cells. *Am. J. Phys. Lung Cell. Mol. Phys.* 312, L822–L834. doi: 10.1152/ajplung.00567.2016

Haick, J. M., and Byron, K. L. (2016). Novel treatment strategies for smooth muscle disorders: targeting Kv7 potassium channels. *Pharmacol. Ther.* 165, 14–25. doi: 10.1016/j.pharmthera.2016.05.002

Haley, J. E., Abogadie, F. C., Delmas, P., Dayrell, M., Vallis, Y., Milligan, G., et al. (1998). The alpha subunit of Gq contributes to muscarinic inhibition of the M-type potassium current in sympathetic neurons. *J. Neurosci.* 18, 4521–4531. doi: 10.1523/JNEUROSCI.18-12-04521.1998

Hall, I. P. (2000). Second messengers, ion channels and pharmacology of airway smooth muscle. *Eur. Respir. J.* 15, 1120–1127. doi: 10.1034/j.1399-3003.2000.01523.x

Halpin, D. M. G., Faner, R., Sibila, O., Badia, J. R., and Agusti, A. (2020). Do chronic respiratory diseases or their treatment affect the risk of SARS-CoV-2 infection? *Lancet Respir. Med.* 5, 436–438. doi: 10.1016/S2213-2600(20)30167-3

Haworth, A. S., and Brackenbury, W. J. (2019). Emerging roles for multifunctional ion channel auxiliary subunits in cancer. *Cell Calcium* 80, 125–140. doi: 10.1016/j.ceca.2019.04.005

Hayabuchi, Y. (2017). The action of smooth muscle cell potassium channels in the pathology of pulmonary arterial hypertension. *Pediatr. Cardiol.* 38, 1–14. doi: 10.1007/s00246-016-1491-7

Herrmann, W. M., Kern, U., and Aigner, M. (1987). On the adverse reactions and efficacy of long-term treatment with flupirtine: preliminary results of an ongoing twelve-month study with 200 patients suffering from chronic pain states in arthrosis or arthritis. *Postgrad. Med. J.* 63, 87–103.

Higashida, H., Hoshi, N., Zhang, J.-S., Yokoyama, S., Hashii, M., Jin, D., et al. (2005). Protein kinase C bound with A-kinase anchoring protein is involved in muscarinic receptor-activated modulation of M-type KCNQ potassium channels. *Neurosci. Res.* 51, 231–234. doi: 10.1016/j.neures.2004.11.009

Hu, B., Zeng, W.-P., Li, X., Al-Sheikh, U., Chen, S.-Y., and Ding, J. (2019). A conserved arginine/lysine-based motif promotes ER export of KCNE1 and KCNE2 to regulate KCNQ1 channel activity. *Channels* 13, 483–497. doi: 10.1080/19336950.2019.1685626

Hynes, D., and Harvey, B. J. (2019). Dexamethasone reduces airway epithelial Cl^- secretion by rapid non-genomic inhibition of KCNQ1, KCNN4 and KATP K^+ channels. *Steroids* 151:108459. doi: 10.1016/j.steroids.2019.108459

Iannotti, F. A., Panza, E., Barrese, V., Viggiano, D., Soldovieri, M. V., and Taglialatela, M. (2010). Expression, localization, and pharmacological role of Kv7 potassium channels in skeletal muscle proliferation, differentiation, and survival after myotoxic insults. *J. Pharmacol. Exp. Ther.* 332, 811–820. doi: 10.1124/jpet.109.162800

Ivonnet, P., Salathe, M., and Conner, G. E. (2015). Hydrogen peroxide stimulation of CFTR reveals an Epac-mediated, soluble AC-dependent cAMP amplification pathway common to GPCR signalling. *Br. J. Pharmacol.* 172, 173–184. doi: 10.1111/bph.12934

Jang, S. H., Choi, S. Y., Ryu, P. D., and Lee, S. Y. (2011). Anti-proliferative effect of Kv1.3 blockers in A549 human lung adenocarcinoma in vitro and in vivo. *Eur. J. Pharmacol.* 651, 26–32. doi: 10.1016/j.ejphar.2010.10.066

Jentsch, T. J. (2000). Neuronal KCNQ potassium channels: physiology and role in disease. *Nat. Rev. Neurosci.* 1, 21–30. doi: 10.1038/35036198

Jepps, T. A., Carr, G., Lundegaard, P. R., Olesen, S.-P., and Greenwood, I. A. (2015). Fundamental role for the KCNE4 ancillary subunit in Kv7.4 regulation of arterial tone. *J. Physiol.* 593, 5325–5340. doi: 10.1113/JP271286

Jepps, T. A., Olesen, S. P., and Greenwood, I. A. (2013). One man's side effect is another man's therapeutic opportunity: targeting Kv7 channels in smooth muscle disorders. *Br. J. Pharmacol.* 168, 19–27. doi: 10.1111/j.1476-5381.2012.02133.x

Joshi, S., Sedivy, V., Hodyc, D., Herget, J., and Gurney, A. M. (2009). KCNQ modulators reveal a key role for KCNQ potassium channels in regulating the tone of rat pulmonary artery smooth muscle. *J. Pharmacol. Exp. Ther.* 329, 368–376. doi: 10.1124/jpet.108.147785

Jude, J. A., Wylam, M. E., Walseth, T. F., and Kannan, M. S. (2008). Calcium signaling in airway smooth muscle. *Proc. Am. Thorac. Soc.* 5, 15–22. doi: 10.1513/pats.200704-047VS

Jung, J., Lin, H., Koh, Y. I., Ryu, K., Lee, J. S., Rim, J. H., et al. (2019). Rare KCNQ4 variants found in public databases underlie impaired channel activity that may contribute to hearing impairment. *Exp. Mol. Med.* 51, 1–12. doi: 10.1038/s12276-019-0300-9

Kim, H.-J., Jeong, M.-H., Kim, K.-R., Jung, C.-Y., Lee, S.-Y., Kim, H., et al. (2016). Protein arginine methylation facilitates KCNQ channel-PIP2 interaction leading to seizure suppression. *Elife* 5:e17159. doi: 10.7554/eLife.17159

Kim, R. Y., Yau, M. C., Galpin, J. D., Seebohm, G., Ahern, C. A., Pless, S. A., et al. (2015). Atomic basis for therapeutic activation of neuronal potassium channels. *Nat. Commun.* 6:8116. doi: 10.1038/ncomms9116

Kroncke, B. M., Van Horn, W. D., Smith, J., Kang, C., Welch, R. C., Song, Y., et al. (2016). Structural basis for KCNE3 modulation of potassium recycling in epithelia. *Sci. Adv.* 2:e1501228. doi: 10.1126/sciadv.1501228

Kubisch, C., Schroeder, B. C., Friedrich, T., Lütjohann, B., El-Amraoui, A., Marlin, S., et al. (1999). KCNQ4, a novel potassium channel expressed in sensory outer hair cells, is mutated in dominant deafness. *Cell* 96, 437–446. doi: 10.1016/S0092-8674(00)80556-5

Lange, W., Geissendörfer, J., Schenzer, A., Grötzinger, J., Seebohm, G., Friedrich, T., et al. (2009). Refinement of the binding site and mode of action of the anticonvulsant retigabine on KCNQ K^+ channels. *Mol. Pharmacol.* 75, 272–280. doi: 10.1124/mol.108.052282

Laumbach, R. J., and Kipen, H. M. (2012). Respiratory health effects of air pollution: update on biomass smoke and traffic pollution. *J. Allergy Clin. Immunol.* 129, 3–13. doi: 10.1016/j.jaci.2011.11.021

Lee, B. H., Ryu, P. D., and Lee, S. Y. (2014). Serum starvation-induced voltage-gated potassium channel Kv7.5 expression and its regulation by Sp1 in canine osteosarcoma cells. *Int. J. Mol. Sci.* 15, 977–993. doi: 10.3390/ijms15010977

Lehman, A., Thouta, S., Mancini, G. M. S., Naidu, S., van Slegtenhorst, M., and McWalter, K. (2017). Loss-of-function and gain-of-function mutations in KCNQ5 cause intellectual disability or epileptic encephalopathy. *Am. J. Hum. Genet.* 101, 65–74. doi: 10.1016/j.ajhg.2017.05.016

Leon, G., MacDonagh, L., Finn, S. P., Cuffe, S., and Barr, M. P. (2016). Cancer stem cells in drug resistant lung cancer: targeting cell surface markers and signaling pathways. *Pharmacol. Ther.* 158, 71–90. doi: 10.1016/j.pharmthera.2015.12.001

Li, H., Chen, Q., Moss, A. J., Robinson, J., Goytia, V., Perry, J. C., et al. (1998). New mutations in the KVLQT1 potassium channel that cause long-QT syndrome. *Circulation* 97, 1264–1269. doi: 10.1161/01.CIR.97.13.1264

Li, C., Huang, P., Lu, Q., Zhou, M., Guo, L., and Xu, X. (2014a). KCNQ/Kv7 channel activator flupirtine protects against acute stress-induced impairments of spatial memory retrieval and hippocampal LTP in rats. *Neuroscience* 280, 19–30. doi: 10.1016/j.neuroscience.2014.09.009

Li, S.-S., Ran, Y.-J., Zhang, D.-D., Li, S.-Z., and Zhu, D. (2014b). MicroRNA-190 regulates hypoxic pulmonary vasoconstriction by targeting a voltage-gated

K^+ channel in arterial smooth muscle cells. *J. Cell. Biochem.* 115, 1196–1205. doi: 10.1002/jcb.24771

Li, X., Xu, S., Yu, M., Wang, K., Tao, Y., Zhou, Y., et al. (2020). Risk factors for severity and mortality in adult COVID-19 inpatients in Wuhan. *J. Allergy Clin. Immunol.* S0091-6749(20)30495-4. doi: 10.1016/j.jaci.2020.04.006

Lin, Y., Wang, X., and Jin, H. (2014). EGFR-TKI resistance in NSCLC patients: mechanisms and strategies. *Am. J. Cancer Res.* 4, 411–435.

Lindman, J., Khammy, M. M., Lundegaard, P. R., Aalkjær, C., and Jepps, T. A. (2018). Microtubule regulation of Kv7 channels orchestrates cAMP-mediated vasorelaxations in rat arterial smooth muscle. *Hypertension* 71, 336–345. doi: 10.1161/HYPERTENSIONAHA.117.10152

Loussouarn, G., Demolombe, S., Mohammad-Panah, R., Escande, D., and Baró, I. (1996). Expression of CFTR controls cAMP-dependent activation of epithelial K^+ currents. *Am. J. Phys.* 271, C1565–C1573. doi: 10.1152/ajpcell.1996.271.5.C1565

Lundby, A., Ravn, L. S., Svendsen, J. H., Hauns, S., Olesen, S.-P., and Schmitt, N. (2008). KCNE3 mutation V17M identified in a patient with lone atrial fibrillation. *Cell. Physiol. Biochem.* 21, 47–54. doi: 10.1159/000113746

Lundquist, A. L., Turner, C. L., Ballester, L. Y., and George, A. L. (2006). Expression and transcriptional control of human KCNE genes. *Genomics* 87, 119–128. doi: 10.1016/j.ygeno.2005.09.004

Mackie, A. R., Brueggemann, L. I., Henderson, K. K., Shiels, A. J., Cribbs, L. L., Scrogin, K. E., et al. (2008). Vascular KCNQ potassium channels as novel targets for the control of mesenteric artery constriction by vasopressin, based on studies in single cells, pressurized arteries, and in vivo measurements of mesenteric vascular resistance. *J. Pharmacol. Exp. Ther.* 325, 475–483. doi: 10.1124/jpet.107.135764

Maeno, E., Ishizaki, Y., Kanaseki, T., Hazama, A., and Okada, Y. (2000). Normotonic cell shrinkage because of disordered volume regulation is an early prerequisite to apoptosis. *Proc. Natl. Acad. Sci. U. S. A.* 97, 9487–9492. doi: 10.1073/pnas.140216197

Maljevic, S., Wuttke, T. V., Seebohm, G., and Lerche, H. (2010). KV7 channelopathies. *Arch. Eur. J. Physiol.* 460, 277–288. doi: 10.1007/s00424-010-0831-3

Mall, M., Gonska, T., Thomas, J., Schreiber, R., Seydewitz, H. H., Kuehr, J., et al. (2003). Modulation of Ca^{2+} activated Cl^- secretion by basolateral K^+ channels in human normal and cystic fibrosis airway epithelia. *Pediatr. Res.* 53, 608–618. doi: 10.1203/01.PDR.0000057204.51420.DC

Mall, M., Kunzelmann, K., Hipper, A., Busch, A. E., and Greger, R. (1996). CAMP stimulation of CFTR-expressing *Xenopus* oocytes activates a chromanol-inhibitable K^+ conductance. *Arch. Eur. J. Physiol.* 432, 516–522. doi: 10.1007/s004240050164

Mall, M., Wissner, A., Schreiber, R., Kuehr, J., Seydewitz, H. H., Brandis, M., et al. (2000). Role of K(V)LQT1 in cyclic adenosine monophosphate-mediated Cl(−) secretion in human airway epithelia. *Am. J. Respir. Cell Mol. Biol.* 23, 283–289. doi: 10.1165/ajrcmb.23.3.4060

Mani, B. K., Robakowski, C., Brueggemann, L. I., Cribbs, L. L., Tripathi, A., Majetschak, M., et al. (2016). Kv7.5 potassium channel subunits are the primary targets for PKA-dependent enhancement of vascular smooth muscle Kv7 currents. *Mol. Pharmacol.* 89, 323–334. doi: 10.1124/mol.115.101758

Manville, R. W., and Abbott, G. W. (2018). Gabapentin is a potent activator of KCNQ3 and KCNQ5 potassium channels. *Mol. Pharmacol.* 94, 1155–1163. doi: 10.1124/mol.118.112953

Manville, R. W., and Abbott, G. W. (2020). Potassium channels act as chemosensors for solute transporters. *Commun. Biol.* 3:90. doi: 10.1038/s42003-020-0820-9

Manville, R. W., Papanikolaou, M., and Abbott, G. W. (2018). Direct neurotransmitter activation of voltage-gated potassium channels. *Nat. Commun.* 9:1847. doi: 10.1038/s41467-018-04266-w

Marx, S. O., Kurokawa, J., Reiken, S., Motoike, H., D'Armiento, J., Marks, A. R., et al. (2002). Requirement of a macromolecular signaling complex for beta adrenergic receptor modulation of the KCNQ1-KCNE1 potassium channel. *Science* 295, 496–499. doi: 10.1126/science.1066843

Mazzone, S. B., and Undem, B. J. (2016). Vagal afferent innervation of the airways in health and disease. *Physiol. Rev.* 96, 975–1024. doi: 10.1152/physrev.00039.2015

McLaughlin, V. V., Shah, S. J., Souza, R., and Humbert, M. (2015). Management of pulmonary arterial hypertension. *J. Am. Coll. Cardiol.* 65, 1976–1997. doi: 10.1016/j.jacc.2015.03.540

Melosky, B. (2014). Review of EGFR TKIs in metastatic NSCLC, including ongoing trials. *Front. Oncol.* 4:244. doi: 10.3389/fonc.2014.00244

Mondejar-Parreño, G., Morales-Cano, D., Barreira, B., Callejo, M., Ruiz-Cabello, J., Moreno, L., et al. (2018). HIV transgene expression impairs K^+ channel function in the pulmonary vasculature. *Am. J. Phys. Lung Cell. Mol. Phys.* 315, L711–L723. doi: 10.1152/ajplung.00045.2018

Mondejar-Parreño, G., Moral-Sanz, J., Barreira, B., De la Cruz, A., Gonzalez, T., Callejo, M., et al. (2019). Activation of Kv7 channels as a novel mechanism for NO/cGMP-induced pulmonary vasodilation. *Br. J. Pharmacol.* 176, 2131–2145. doi: 10.1111/bph.14662

Morales-Cano, D., Callejo, M., Barreira, B., Mondejar-Parreño, G., Esquivel-Ruiz, S., Ramos, S., et al. (2019). Elevated pulmonary arterial pressure in Zucker diabetic fatty rats. *PLoS One* 14:e0211281. doi: 10.1371/journal.pone.0211281

Morales-Cano, D., Menendez, C., Moreno, E., Moral-Sanz, J., Barreira, B., Galindo, P., et al. (2014). The flavonoid quercetin reverses pulmonary hypertension in rats. *PLoS One* 9:e114492. doi: 10.1371/journal.pone.0114492

Morecroft, I., Murray, A., Nilsen, M., Gurney, A., and MacLean, M. (2009). Treatment with the Kv7 potassium channel activator flupirtine is beneficial in two independent mouse models of pulmonary hypertension. *Br. J. Pharmacol.* 157, 1241–1249. doi: 10.1111/j.1476-5381.2009.00283.x

Moser, S. L., Harron, S. A., Crack, J., Fawcett, J. P., and Cowley, E. A. (2008). Multiple KCNQ potassium channel subtypes mediate basal anion secretion from the human airway epithelial cell line Calu-3. *J. Membr. Biol.* 221, 153–163. doi: 10.1007/s00232-008-9093-9

Moudgil, R., Michelakis, E. D., and Archer, S. L. (2006). The role of K^+ channels in determining pulmonary vascular tone, oxygen sensing, cell proliferation, and apoptosis: implications in hypoxic pulmonary vasoconstriction and pulmonary arterial hypertension. *Microcirculation* 13, 615–632. doi: 10.1080/10739680600930222

Neubauer, B. A., Waldegger, S., Heinzinger, J., Hahn, A., Kurlemann, G., Fiedler, B., et al. (2008). KCNQ2 and KCNQ3 mutations contribute to different idiopathic epilepsy syndromes. *Neurology* 71, 177–183. doi: 10.1212/01.wnl.0000317090.92185.ec

O'Grady, S. M., and Lee, S. Y. (2005). Molecular diversity and function of voltage-gated (Kv) potassium channels in epithelial cells. *Int. J. Biochem. Cell Biol.* 37, 1578–1594. doi: 10.1016/j.biocel.2005.04.002

Ohno, S., Toyoda, F., Zankov, D. P., Yoshida, H., Makiyama, T., Tsuji, K., et al. (2009). Novel KCNE3 mutation reduces repolarizing potassium current and associated with long QT syndrome. *Hum. Mutat.* 30, 557–563. doi: 10.1002/humu.20834

Oliveras, A., Roura-Ferrer, M., Solé, L., de la Cruz, A., Prieto, A., Etxebarria, A., et al. (2014). Functional assembly of Kv7.1/Kv7.5 channels with emerging properties on vascular muscle physiology. *Arterioscler. Thromb. Vasc. Biol.* 34, 1522–1530. doi: 10.1161/ATVBAHA.114.303801

Panchanathan, E., Ramanathan, G., and Lakkakula, B. V. K. S. (2013). Effect of flupirtine on the growth and viability of U373 malignant glioma cells. *Cancer Biol. Med.* 10, 142–147. doi: 10.7497/j.issn.2095-3941.2013.03.004

Pancrazio, J. J., Tabbara, I. A., and Kim, Y. I. (1993). Voltage-activated K+ conductance and cell proliferation in small-cell lung cancer. *Anticancer Res.* 13, 1231–1234.

Penn, R. B. (2008). Embracing emerging paradigms of G protein-coupled receptor agonism and signaling to address airway smooth muscle pathobiology in asthma. *Naunyn Schmiedeberg's Arch. Pharmacol.* 378, 149–169. doi: 10.1007/s00210-008-0263-1

Potet, F., Scott, J. D., Mohammad-Panah, R., Escande, D., and Baró, I. (2001). AKAP proteins anchor cAMP-dependent protein kinase to KvLQT1/IsK channel complex. *Am. J. Physiol. Heart Circ. Physiol.* 280, H2038–H2045. doi: 10.1152/ajpheart.2001.280.5.H2038

Preston, P., Wartosch, L., Günzel, D., Fromm, M., Kongsuphol, P., Ousingsawat, J., et al. (2010). Disruption of the K^+ channel beta-subunit KCNE3 reveals an important role in intestinal and tracheal Cl^- transport. *J. Biol. Chem.* 285, 7165–7175. doi: 10.1074/jbc.M109.047829

Prevarskaya, N., Skryma, R., and Shuba, Y. (2010). Ion channels and the hallmarks of cancer. *Trends Mol. Med.* 16, 107–121. doi: 10.1016/j.molmed.2010.01.005

Prevarskaya, N., Skryma, R., and Shuba, Y. (2018). Ion channels in cancer: are cancer hallmarks oncochannelopathies? *Physiol. Rev.* 98, 559–621. doi: 10.1152/physrev.00044.2016

Putnam, L. R., Tsao, K., Morini, F., Lally, P. A., Miller, C. C., and Lally, K. P. (2016). Evaluation of variability in inhaled nitric oxide use and pulmonary hypertension in patients with congenital diaphragmatic hernia. *JAMA Pediatr.* 170, 1188–1194. doi: 10.1001/jamapediatrics.2016.2023

Rao, V. R., Perez-Neut, M., Kaja, S., and Gentile, S. (2015). Voltage-gated ion channels in cancer cell proliferation. *Cancer* 7, 849–875. doi: 10.3390/cancers7020813

Richard, V., Nair, M. G., Santhosh Kumar, T. R., and Pillai, M. R. (2013). Side population cells as prototype of chemoresistant, tumor-initiating cells. *Biomed. Res. Int.* 2013:517237. doi: 10.1155/2013/517237

Roura-Ferrer, M., Etxebarria, A., Solé, L., Oliveras, A., Comes, N., Villarroel, A., et al. (2009). Functional implications of KCNE subunit expression for the Kv7.5 (KCNQ5) channel. *Cell. Physiol. Biochem.* 24, 325–334. doi: 10.1159/000257425

Roura-Ferrer, M., Solé, L., Oliveras, A., Dahan, R., Bielanska, J., Villarroel, A., et al. (2010). Impact of KCNE subunits on KCNQ1 (Kv7.1) channel membrane surface targeting. *J. Cell. Physiol.* 225, 692–700. doi: 10.1002/jcp.22265

Roura-Ferrer, M., Solé, L., Oliveras, A., Villarroel, A., Comes, N., and Felipe, A. (2012). Targeting of Kv7.5 (KCNQ5)/KCNE channels to surface microdomains of cell membranes. *Muscle Nerve* 45, 48–54. doi: 10.1002/mus.22231

Sabater-Lleal, M., Mälarstig, A., Folkersen, L., Soler Artigas, M., Baldassarre, D., Kavousi, M., et al. (2014). Common genetic determinants of lung function, subclinical atherosclerosis and risk of coronary artery disease. *PLoS One* 9:e104082. doi: 10.1371/journal.pone.0104082

Salata, J. J., Jurkiewicz, N. K., Wang, J., Evans, B. E., Orme, H. T., and Sanguinetti, M. C. (1998). A novel benzodiazepine that activates cardiac slow delayed rectifier K^+ currents. *Mol. Pharmacol.* 54, 220–230. doi: 10.1124/mol.54.1.220

Salvi, S. (2014). Tobacco smoking and environmental risk factors for chronic obstructive pulmonary disease. *Clin. Chest Med.* 35, 17–27. doi: 10.1016/j.ccm.2013.09.011

Sands, T. T., Miceli, F., Lesca, G., Beck, A. E., Sadleir, L. G., Arrington, D. K., et al. (2019). Autism and developmental disability caused by KCNQ3 gain-of-function variants. *Ann. Neurol.* 86, 181–192. doi: 10.1002/ana.25522

Schenzer, A., Friedrich, T., Pusch, M., Saftig, P., Jentsch, T. J., Grötzinger, J., et al. (2005). Molecular determinants of KCNQ (Kv7) K^+ channel sensitivity to the anticonvulsant retigabine. *J. Neurosci.* 25, 5051–5060. doi: 10.1523/JNEUROSCI.0128-05.2005

Schroeder, B. C., Waldegger, S., Fehr, S., Bleich, M., Warth, R., Greger, R., et al. (2000). A constitutively open potassium channel formed by KCNQ1 and KCNE3. *Nature* 403, 196–199. doi: 10.1038/35003200

Schwab, A., Hanley, P., Fabian, A., and Stock, C. (2008). Potassium channels keep mobile cells on the go. *Physiology* 23, 212–220. doi: 10.1152/physiol.00003.2008

Schwiebert, E. M., Benos, D. J., Egan, M. E., Stutts, M. J., and Guggino, W. B. (1999). CFTR is a conductance regulator as well as a chloride channel. *Physiol. Rev.* 79, S145–S166. doi: 10.1152/physrev.1999.79.1.S145

Sedivy, V., Joshi, S., Ghaly, Y., Mizera, R., Zaloudikova, M., Brennan, S., et al. (2015). Role of Kv7 channels in responses of the pulmonary circulation to hypoxia. *Am. J. Phys. Lung Cell. Mol. Phys.* 308, L48–L57. doi: 10.1152/ajplung.00362.2013

Serrano-Novillo, C., Capera, J., Colomer-Molera, M., Condom, E., Ferreres, J. C., and Felipe, A. (2019). Implication of voltage-gated potassium channels in neoplastic cell proliferation. *Cancer* 11:287. doi: 10.3390/cancers11030287

Sevilla-Montero, J., Labrousse-Arias, D., Fernández-Pérez, C., Barreira, B., Mondejar-Parreño, G., Cogolludo, A., et al. (2019). Direct effects of cigarette smoke in pulmonary arterial cells alter vascular tone through arterial remodeling and Kv7.4 channel dysregulation. *BioRxiv* 555953. [Preprint]. doi: 10.1101/555953

Shi, J., and Wei, L. (2013). Rho kinases in cardiovascular physiology and pathophysiology: the effect of fasudil. *J. Cardiovasc. Pharmacol.* 62, 341–354. doi: 10.1097/FJC.0b013e3182a3718f

Shimokawa, H., and Satoh, K. (2015). 2015 ATVB plenary lecture: translational research on rho-kinase in cardiovascular medicine. *Arterioscler. Thromb. Vasc. Biol.* 35, 1756–1769. doi: 10.1161/ATVBAHA.115.305353

Simonneau, G., Montani, D., Celermajer, D. S., Denton, C. P., Gatzoulis, M. A., Krowka, M., et al. (2019). Haemodynamic definitions and updated clinical classification of pulmonary hypertension. *Eur. Respir. J.* 53:1801913. doi: 10.1183/13993003.01913-2018

Singh, A., Wu, H., Zhang, P., Happel, C., Ma, J., and Biswal, S. (2010). Expression of ABCG2 (BCRP) is regulated by Nrf2 in cancer cells that confers side population and chemoresistance phenotype. *Mol. Cancer Ther.* 9, 2365–2376. doi: 10.1158/1535-7163.MCT-10-0108

Soler Artigas, M., Loth, D. W., Wain, L. V., Gharib, S. A., Obeidat, M., Tang, W., et al. (2011). Genome-wide association and large-scale follow up identifies 16 new loci influencing lung function. *Nat. Genet.* 43, 1082–1090. doi: 10.1038/ng.941

Splawski, I., Shen, J., Timothy, K. W., Lehmann, M. H., Priori, S., Robinson, J. L., et al. (2000). Spectrum of mutations in long-QT syndrome genes. KVLQT1, HERG, SCN5A, KCNE1, and KCNE2. *Circulation* 102, 1178–1185. doi: 10.1161/01.CIR.102.10.1178

Steinbichler, T. B., Dudás, J., Skvortsov, S., Ganswindt, U., Riechelmann, H., and Skvortsova, I.-I. (2018). Therapy resistance mediated by cancer stem cells. *Semin. Cancer Biol.* 53, 156–167. doi: 10.1016/j.semcancer.2018.11.006

Stott, J. B., Barrese, V., Jepps, T. A., Leighton, E. V., and Greenwood, I. A. (2015). Contribution of Kv7 channels to natriuretic peptide mediated vasodilation in normal and hypertensive rats. *Hypertension* 65, 676–682. doi: 10.1161/HYPERTENSIONAHA.114.04373

Stott, J. B., Jepps, T. A., and Greenwood, I. A. (2014). KV7 potassium channels: a new therapeutic target in smooth muscle disorders. *Drug Discov. Today* 19, 413–424. doi: 10.1016/j.drudis.2013.12.003

Strutz-Seebohm, N., Seebohm, G., Fedorenko, O., Baltaev, R., Engel, J., Knirsch, M., et al. (2006). Functional coassembly of KCNQ4 with KCNE-beta-subunits in *Xenopus* oocytes. *Cell. Physiol. Biochem.* 18, 57–66. doi: 10.1159/000095158

Sun, H., Lin, A.-H., Ru, F., Patil, M. J., Meeker, S., Lee, L.-Y., et al. (2019). KCNQ/M-channels regulate mouse vagal bronchopulmonary C-fiber excitability and cough sensitivity. *JCI Insight* 4:e124467. doi: 10.1172/jci.insight.124467

Sun, J., and MacKinnon, R. (2020). Structural basis of human KCNQ1 modulation and gating. *Cell* 180, 340.e9–347.e9. doi: 10.1016/j.cell.2019.12.003

Sylvester, J. T., Shimoda, L. A., Aaronson, P. I., and Ward, J. P. T. (2012). Hypoxic pulmonary vasoconstriction. *Physiol. Rev.* 92, 367–520. doi: 10.1152/physrev.00041.2010

Taylor, K. C., and Sanders, C. R. (2017). Regulation of KCNQ/Kv7 family voltage-gated K^+ channels by lipids. *Biochim. Biophys. Acta Biomembr.* 1859, 586–597. doi: 10.1016/j.bbamem.2016.10.023

Tinel, N., Diochot, S., Lauritzen, I., Barhanin, J., Lazdunski, M., and Borsotto, M. (2000). M-type KCNQ2-KCNQ3 potassium channels are modulated by the KCNE2 subunit. *FEBS Lett.* 480, 137–141. doi: 10.1016/S0014-5793(00)01918-9

Tobin, M. J. (2005). Update in pulmonary diseases. *Ann. Intern. Med.* 142, 283–288. doi: 10.7326/0003-4819-142-4-200502150-00010

Trinh, N. T. N., Privé, A., Kheir, L., Bourret, J.-C., Hijazi, T., Amraei, M. G., et al. (2007). Involvement of KATP and KvLQT1 K^+ channels in EGF-stimulated alveolar epithelial cell repair processes. *Am. J. Phys. Lung Cell. Mol. Phys.* 293, L870–L882. doi: 10.1152/ajplung.00362.2006

Undem, B. J., and Kollarik, M. (2005). The role of vagal afferent nerves in chronic obstructive pulmonary disease. *Proc. Am. Thorac. Soc.* 2, 355–360. doi: 10.1513/pats.200504-033SR

Van Horn, W. D., Vanoye, C. G., and Sanders, C. R. (2011). Working model for the structural basis for KCNE1 modulation of the KCNQ1 potassium channel. *Curr. Opin. Struct. Biol.* 21, 283–291. doi: 10.1016/j.sbi.2011.01.001

Vanoye, C. G., Welch, R. C., Daniels, M. A., Manderfield, L. J., Tapper, A. R., and Sanders, C. R. (2009). Distinct subdomains of the KCNQ1 S6 segment determine channel modulation by different KCNE subunits. *J. Gen. Physiol.* 134, 207–217. doi: 10.1085/jgp.200910234

Vigil, F. A., Bozdemir, E., Bugay, V., Chun, S. H., Hobbs, M., Sanchez, I., et al. (2020). Prevention of brain damage after traumatic brain injury by pharmacological enhancement of KCNQ (Kv7, «M-type») K^+ currents in neurons. *J. Cereb. Blood Flow Metab.* 40, 1256–1273. doi: 10.1177/0271678X19857818

Wang, K., Zeng, J., Luo, L., Yang, J., Chen, J., Li, B., et al. (2013). Identification of a cancer stem cell-like side population in the HeLa human cervical carcinoma cell line. *Oncol. Lett.* 6, 1673–1680. doi: 10.3892/ol.2013.1607

WHO Global Health Estimates (2020). WHO; World Health Organization. Available at: http://www.who.int/healthinfo/global_burden_disease/en/ (Accessed March 1, 2020).

Wickenden, A. D., Krajewski, J. L., London, B., Wagoner, P. K., Wilson, W. A., Clark, S., et al. (2008). N-(6-chloro-pyridin-3-yl)-3,4-difluoro-benzamide (ICA-27243): a novel, selective KCNQ2/Q3 potassium channel activator. *Mol. Pharmacol.* 73, 977–986. doi: 10.1124/mol.107.043216

Xiong, Q., Sun, H., Zhang, Y., Nan, F., and Li, M. (2008). Combinatorial augmentation of voltage-gated KCNQ potassium channels by chemical openers. *Proc. Natl. Acad. Sci. U. S. A.* 105, 3128–3133. doi: 10.1073/pnas.0712256105

Yang, W. P., Levesque, P. C., Little, W. A., Conder, M. L., Ramakrishnan, P., Neubauer, M. G., et al. (1998). Functional expression of two KvLQT1-related potassium channels responsible for an inherited idiopathic epilepsy. *J. Biol. Chem.* 273, 19419–19423. doi: 10.1074/jbc.273.31.19419

Zaydman, M. A., and Cui, J. (2014). PIP2 regulation of KCNQ channels: biophysical and molecular mechanisms for lipid modulation of voltage-dependent gating. *Front. Physiol.* 5:195. doi: 10.3389/fphys.2014.00195

Zhang, X., An, H., Li, J., Zhang, Y., Liu, Y., Jia, Z., et al. (2016). Selective activation of vascular Kv7.4/Kv7.5 K^+ channels by fasudil contributes to its vasorelaxant effect. *Br. J. Pharmacol.* 173, 3480–3491. doi: 10.1111/bph.13639

Zhang, Y., and Wu, S. (2017). Effects of fasudil on pulmonary hypertension in clinical practice. *Pulm. Pharmacol. Ther.* 46, 54–63. doi: 10.1016/j.pupt.2017.08.002

Zhou, L., Köhncke, C., Hu, Z., Roepke, T. K., and Abbott, G. W. (2019). The KCNE2 potassium channel β subunit is required for normal lung function and resilience to ischemia and reperfusion injury. *FASEB J.* 33, 9762–9774. doi: 10.1096/fj.201802519R

Zimmer, J., Takahashi, T., Hofmann, A. D., and Puri, P. (2017). Downregulation of KCNQ5 expression in the rat pulmonary vasculature of nitrofen-induced congenital diaphragmatic hernia. *J. Pediatr. Surg.* 52, 702–705. doi: 10.1016/j.jpedsurg.2017.01.016

Conflict of Interest: The authors declare that the research was conducted in the absence of any commercial or financial relationships that could be construed as a potential conflict of interest.

frontiers in Physiology

REVIEW
published: 30 June 2020
doi: 10.3389/fphys.2020.00727

Cyclic AMP-Dependent Regulation of Kv7 Voltage-Gated Potassium Channels

*Jennifer van der Horst[1], Iain A. Greenwood[2] and Thomas A. Jepps[1]**

[1] Vascular Biology Group, Department of Biomedical Sciences, University of Copenhagen, Copenhagen, Denmark,
[2] Molecular and Clinical Sciences Institute, St. George's University of London, London, United Kingdom

Voltage-gated Kv7 potassium channels, encoded by *KCNQ* genes, have major physiological impacts cardiac myocytes, neurons, epithelial cells, and smooth muscle cells. Cyclic adenosine monophosphate (cAMP), a well-known intracellular secondary messenger, can activate numerous downstream effector proteins, generating downstream signaling pathways that regulate many functions in cells. A role for cAMP in ion channel regulation has been established, and recent findings show that cAMP signaling plays a role in Kv7 channel regulation. Although cAMP signaling is recognized to regulate Kv7 channels, the precise molecular mechanism behind the cAMP-dependent regulation of Kv7 channels is complex. This review will summarize recent research findings that support the mechanisms of cAMP-dependent regulation of Kv7 channels.

Keywords: Kv7 (KCNQ), cAMP, PKA, EPAC, physiology

OPEN ACCESS

Edited by:
Mark S. Shapiro, The University of Texas Health Science Center at San Antonio, United States

Reviewed by:
Naoto Hoshi, University of California, Irvine, United States
Maria Virginia Soldovieri, University of Molise, Italy

***Correspondence:**
Thomas A. Jepps
tjepps@sund.ku.dk

Specialty section:
This article was submitted to Membrane Physiology and Membrane Biophysics, a section of the journal Frontiers in Physiology

Received: *06 May 2020*
Accepted: *04 June 2020*
Published: *30 June 2020*

Citation:
van der Horst J, Greenwood IA and Jepps TA (2020) Cyclic AMP-Dependent Regulation of Kv7 Voltage-Gated Potassium Channels. Front. Physiol. 11:727. doi: 10.3389/fphys.2020.00727

cAMP-DEPENDENT SIGNALING

Regulators of cAMP: G Protein-Coupled Receptors

First discovered by Dr. Earl W. Sutherland in 1958 (Rall and Sutherland, 1958; Sutherland and Rall, 1958), cyclic adenosine monophosphate (cAMP) is well-recognized as an important intracellular secondary messenger molecule that can induce a cascade of events to influence cellular function (Patra and Brady, 2018). cAMP orchestrates numerous signal transduction pathways through the activation of several downstream effector proteins, resulting in a wide variety of cellular processes including gene transcription, cell growth and cell differentiation (Dumont et al., 1989; Sassone-Corsi, 1995; Mayr and Montminy, 2001; Sands and Palmer, 2008; Bacallao and Monje, 2015).

cAMP is created from ATP through the action of Adenylate cyclases (AC), of which there are nine membrane-bound isoforms (AC 1-9) and one soluble isoform (sASC). The characteristics of each isoform are summarized effectively in several reviews (Taussig and Gilman, 1995; Simonds, 1999; Hanoune and Defer, 2001; Sadana and Dessauer, 2009; Tresguerres et al., 2011; Halls and Cooper, 2017). Membrane-bound ACs are stimulated downstream of Gs-specific G protein-coupled receptor (GPCR) activation, while the sAC is insensitive to GPCR-dependent regulation (Braun and Dods, 1975; Braun et al., 1977; Forte et al., 1983). When a GPCR is activated by its extracellular ligand, it causes a conformational change in the receptor which activates the associated heteromeric G protein complex, consisting of an α, ß and γ subunit. Subsequently, the Gsα dissociates from the receptor and Gßγ subunits, activating AC and increasing cAMP

levels (see Pierce et al., 2002 for a detailed review of this signaling pathway). ACs can also be regulated by other intracellular signals, including Ca^{2+} and PKC (see Halls and Cooper, 2017 for a detailed review).

Phosphodiesterase's (PDEs) remain the only known route of cAMP degradation. The expression and localization of PDEs within a cell controls the magnitude and duration of cAMP-dependent events, as well as the compartmentalization and intracellular gradients of cAMP (Baillie, 2009). Thus, the expression and localization of PDEs in a cell contributes to the specificity of the cAMP-response following activation.

Effectors of cAMP: PKA and EPAC

cAMP mediates its effect by activation of effector proteins including protein kinase A (PKA), Epac (Exchange protein directly activated by cAMP), or cyclic nucleotide-gated channels (CNGCs) (Shabb, 2001; Bos, 2006; Biel and Michalakis, 2009). For many years it was believed that the effects of cAMP were mediated exclusively through the activation of intracellular PKA. PKA is a heterotetrameric holoenzyme consisting of two regulatory (R) subunits and two catalytic (C) subunits (Krebs and Beavo, 1979; Taylor et al., 2013; Turnham and Scott, 2016). There are two types of regulatory subunits, RI and RII, each consisting of two isoforms, RIα, RIβ, RIIα, RIIβ, each having different tissue expression, subcellular localization and cAMP binding affinity (Bechtel et al., 1977; Corbin et al., 1977, 1978; Zoller et al., 1979; Rannels and Corbin, 1980; Ringheim and Taylor, 1990; Taylor et al., 2012; Weigand et al., 2017). PKA that contains either RI or RII, form the two classes of PKA termed type I or type II, respectively. Binding of four cAMP molecules to each R subunit induces a conformational change and activates the kinase, resulting in the free catalytic subunits phosphorylating serine and threonine residues in specific substrate proteins (Welch et al., 2010).

Scaffolding proteins, such as A Kinase Anchoring Proteins (AKAPs; reviewed in Rubin, 1994; Scott et al., 2013; Dema et al., 2015) bind to the PKA-R subunits at the dimerization/docking domain at the N-terminus and targets PKA to specific subcellular locations to ensure specificity in signal transduction by placing PKA close to its appropriate substrate target, allowing compartmentalization of PKA (Scott et al., 1990; Carr et al., 1991; Bauman et al., 2006; Gold et al., 2006). AKAPs also bind other proteins such as protein kinase C and PDEs (Moleschi and Melacini, 2014). The AKAP family has more than 50 members and can be classified according to their binding specificity for the PKA-R subunits (Wong and Scott, 2004). The majority of the AKAPs bind to PKA-RII, however, several AKAPs bind to PKA-RI (Kinderman et al., 2006; Sarma et al., 2010). Only a few AKAPs have dual-specificity and can bind to both PKA-RI and PKA-RII, although with lower affinity for PKA-RI (Burns et al., 2003). This lower affinity for PKA-RI is due to the structural difference in the dimerization/docking domain in the N-terminal of RI (Huang et al., 1997; Gold et al., 2006). AKAPs are expressed in different tissues of the body and can facilitate tissue-specific signaling in many cells types including neurons (Glantz et al., 1992; Moita et al., 2002; Dell'Acqua et al., 2006), heart (Fink et al., 2001; Marx et al., 2002; Ruehr et al., 2004), and pancreas (Lester et al., 1997).

cAMP also activates Epac (Exchange protein directly activated by cAMP) (de Rooij et al., 1998; Kawasaki et al., 1998). Epac proteins, stimulated by cAMP binding, activate the Ras superfamily of small GTPases, Rap1 and Rap2. There are two known Epac proteins, Epac1 and Epac2, which are both present in almost all tissues but have different expression levels (Roscioni et al., 2008). Epac acts as guanine-nucleotide exchange factors and catalyzes the exchange of GDP for GTP on Rap1 and Rap2 with subsequent activation of these two GTPases (Cheng et al., 2008). This leads to activation of further downstream pathways, which will result in a variety of cellular functions, depending on specific tissue and cell type. In cardiac myocytes, for example, Epac plays a role in the cardiac Ca^{2+} regulation by increasing Ca^{2+} release from the sarcoplasmic reticulum (SR) via ryanodine receptor 2 (RyR2) and thereby effecting contraction (Fujita et al., 2017). Furthermore, a signaling pathway in which cAMP acts via Epac to modulate ion channel function has been identified (Renström et al., 1997; Kang et al., 2006; Stott et al., 2016). Additionally, Epac enhances the synaptic release of neurotransmitters following cAMP elevation in neurons (Shariati et al., 2016).

Cyclic nucleotide-gated channels (CNGCs) are also activated directly by cAMP signaling (Ludwig et al., 1998; Santoro et al., 1998). CNGCs are non-selective cation channels expressed in many tissues, including the heart, lung, kidney, pancreas, liver, spleen, testis and various neuronal systems (Kaupp and Seifert, 2002; Biel and Michalakis, 2007; Biel, 2009). CNGCs are activated by direct binding of cAMP or cGMP to the channel and activation of the channel results in the influx of extracellular cations causing depolarization of the cell membrane. One example of a CNGC is the hyperpolarization-activated and cyclic nucleotide–gated channels (HCN), which are expressed in the heart and the nervous system. These channels mainly conduct Na^+ and K^+ and are activated by a hyperpolarized membrane potential and stimulated by intracellular cyclic nucleotides. HCN channels are responsible for the "funny current" (I_f) in the heart and neurons, where they regulate pacemaker activity and neuronal firing (Difrancesco, 1986; DiFrancesco and Tortora, 1991; Moosmang et al., 1999; DiFrancesco, 2020).

KCNQ-ENCODED POTASSIUM CHANNELS

There are 12 sub-families of voltage-gated potassium channels (Kv1-Kv12), within which the Kv7 potassium channel family consists of five isoforms encoded by the *KCNQ1*-5 genes (Kv7.1-Kv7.5) (Robbins, 2001; Gutman et al., 2005). Like all Kv channels, Kv7 channels are voltage-sensing channels and open and close upon changes in transmembrane potential to selectively let K^+ ions pass through the channel. The Kv7 channels are comprised of four α-subunits, with each α-subunit consisting of six transmembrane (TM) spanning domains (S1-S6). S1-S4 form the voltage-sensing domain, while S5-S6 form the pore domain. Each α-subunit contains cytoplasmic amino

(N) – and carboxyl (C) – termini, which are essential for channel tetramerization and channel regulation (Barros et al., 2012). In the C-terminus of the channel, a coiled-coil sequence motif is the major determinant of channel assembly (Jenke et al., 2003; Schwake et al., 2003, 2006). Assembly of all four α-subunits placed in a cylindrical arrangement creates a pore through which the K^+ ions are conducted selectively (Heginbotham et al., 1992; Doyle et al., 1998). This assembly can be done with four identical α-subunits from the same Kv7 isoform to form homomeric channels, or by combining at least two types of α-subunits with other Kv7 isoforms to form heteromeric channels. Kv7.1 was thought to only form as a homotetrameric channel (Schwake et al., 2000); however, heterotetrameric assembly with Kv7.5 has been suggested (Oliveras et al., 2014). Kv7.3 homomers are weakly effective but form functional heterotetramers with Kv7.2 (Schroeder et al., 1998; Wang et al., 1998), Kv7.4 (Kubisch et al., 1999) and Kv7.5 (Schroeder et al., 2000a) subunits, and Kv7.4 heterotetramizes with Kv7.5 (Bal et al., 2008; Brueggemann et al., 2014b; Chadha et al., 2014; Jepps et al., 2015). Kv7 channels also interact with KCNE-encoded single transmembrane-spanning auxiliary protein subunits [KCNE1-5; also called MinK and MinK-related peptides (MiRPs)] that function as β or ancillary subunits (Abbott and Goldstein, 1998; McCrossan and Abbott, 2004; Abbott, 2016; Jepps, 2017). These KCNE proteins cannot form functional channels themselves but coassemble with Kv7 channels to modulate several functional properties of the channel, including membrane trafficking, voltage dependence, and kinetics of channel opening and closing (McCrossan and Abbott, 2004; Kanda and Abbott, 2012). Finally, Kv7 channels have a large cytoplasmic C-terminal composed of four segments (helix A-D) (Haitin and Attali, 2008; Xu et al., 2013; Barrese et al., 2018). In addition to coordinating channel tetramerization, several regulatory molecules interact with the C-terminal region to modulate Kv7 channel function, including calmodulin (CaM), phosphatidylinositol 4,5-biphosphate (PIP_2), protein kinase C (PKC), protein kinase A (PKA), A-kinase-anchoring protein (AKAP), ankyrin G (Ank-G) and Nedd4-2 (summarized by Haitin and Attali (2008) and Barrese et al., 2018).

This review will now focus on the mechanisms of cAMP-dependent regulation of Kv7 channels and explore a possible role for this mechanism for therapeutic targeting in diseases associated with Kv7 channel dysfunction.

cAMP REGULATION of Kv7 CHANNELS

Kv7.1

Kv7.1 channels are expressed in several tissues throughout the body including the heart, uterus, and epithelial cells of the inner ear, pancreas, airways, gastrointestinal tract and kidneys. In the heart, Kv7.1 associates with the ancillary subunit KCNE1 to constitute the channel responsible for the late repolarizing current termed I_{Ks} (Barhanin et al., 1996; Sanguinetti et al., 1996). Kv7.1 also associates with KCNE1 in the inner ear, where they regulate auditory function and pancreatic acinar cells where activation of the Kv7.1-KCNE1 channel provides the driving force for Cl^- secretion (Kim and Greger, 1999; Köttgen et al., 1999; Warth et al., 2002). In addition, Kv7.1 channels in the pancreatic ß-cells contribute to the regulation of insulin secretion, and loss of function mutations in the KCNQ1 gene leads to impaired ß-cell insulin secretion, which is associated with type 2 diabetes (Ullrich et al., 2005; Unoki et al., 2008; Yasuda et al., 2008; Yamagata et al., 2011; Liu et al., 2014; Torekov et al., 2014; Min Lee et al., 2017; Zhang et al., 2020). Furthermore, association of Kv7.1 with KCNE3 in epithelial tissues of the colon, small intestine and airways regulates the transport of water and salts (Schroeder et al., 2000b; Grahammer et al., 2001a,b; Vallon et al., 2005).

Kv7.1-KCNE1 channels have been studied extensively in cardiac myocytes where the channel is important for delayed cardiac repolarization and shapes action potential duration (Terrenoire et al., 2005). In addition, it is enhanced by sympathetic nerve activity through activation of β-adrenergic receptors (Bennett and Begenisch, 1987; Yazawa and Kameyama, 1990). Stimulation of the β-adrenergic receptor by noradrenaline released from the cardio-accelerator nerve causes an elevation of cAMP that increases I_{Ks} via PKA-dependent phosphorylation (Yazawa and Kameyama, 1990).

As mentioned previously, PKA actions are regulated by AKAPs, by positioning PKA and other cAMP-responsive enzymes in proximity to their substrates. In the heart, several AKAPs are expressed, including AKAP79/150 (human AKAP79/murine AKAP150), AKAP15/18δ and AKAP9. AKAP9, better known as yotiao, facilitates PKA-phosphorylation of serine 27 in the Kv7.1 N-terminus required for the proper functioning of the channel (Walsh et al., 1988; Walsh and Kass, 1991; Potet et al., 2001; Marx et al., 2002). Yotiao also associates with protein phosphatase 1 (PP1), phosphodiesterase (PDE) and AC to control I_{Ks} phosphorylation status (Terrenoire et al., 2009; Li et al., 2012). Yotiao binds directly to Kv7.1 C-terminus via a leucine zipper motif, an amino acid sequence in the C terminus of Kv7.1, and disruption of the complex by mutations in yotiao or KCNQ1 are associated with Long QT Syndrome (Kass et al., 2003; Fodstad et al., 2004; Chen et al., 2007). Besides acting as a scaffold protein, yotiao has a functional role that occurs after I_{Ks} phosphorylation. Studies revealed that cAMP-dependent activation of Kv7.1-KCNE1 depends not only on serine 27 phosphorylation but also requires the direct binding of yotiao to the Kv7.1 at the leucine zipper motif (Kurokawa et al., 2004; Chen et al., 2005; Chen and Kass, 2006). Furthermore, it was revealed that yotiao itself is a substrate for PKA phosphorylation and can be phosphorylated upon β adrenoceptor stimulation (Chen et al., 2005). Serine 43 was identified as target residue for PKA phosphorylation on yotiao, with mutations of this residue dampening cAMP effects on the I_{Ks} current, even though yotiao binding and phosphorylation of Kv7.1 channels were not affected. Taken together, these studies conclude that AKAP protein yotiao has a crucial and complex regulatory role on the cAMP-dependent activity of I_{Ks} channels (see **Figure 1A**).

Although PKA activation of Kv7.1 following β adrenergic stimulation can increase I_{Ks}, chronic β adrenergic stimulation downregulates the I_{Ks} response (Mona et al., 2014). Chronic

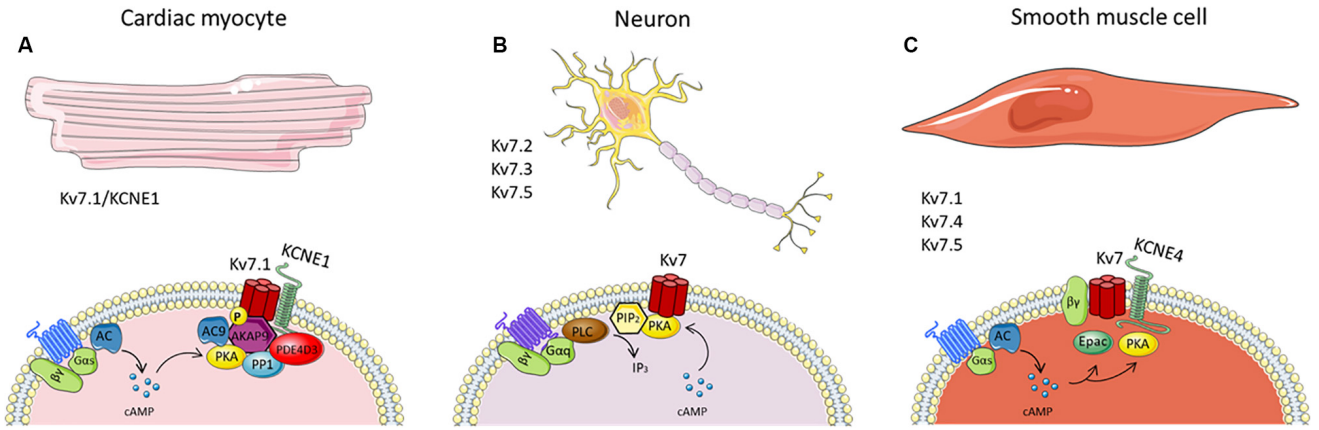

FIGURE 1 | Schematics of known cAMP-dependent Kv7 channel regulation in panel cardiac **(A)**, neurones **(B)** and smooth muscle cells **(C)**. The figure summarizes many of the known interaction partners involved in the cAMP-mediated regulation of Kv7 channels in the different cells types, thereby highlighting the heterogeneity of cAMP-Kv7 channel signaling. It should be noted that, although AKAP79/150 is associated with Kv7.2 channels, it has not been included in the figure since there is no evidence of its involvement in PKA phosphorylation of the channel.

β adrenergic stimulation led to a significant decrease in KCNE1 but not KCNQ1 mRNA expression in guinea pig cardiomyocytes. Furthermore, chronic *in vitro* and *in vivo* isoprenaline stimulation reduced KCNE1 protein expression and KCNE1 membrane expression in guinea pig cardiomyocytes. This effect was mediated via Epac1 and not PKA activation, leading to increased translocation of nuclear factor of activated T cell (NFAT), which was responsible for KCNE1 downregulation (Mona et al., 2014).

In the inner ear, cAMP activates Kv7.1-KCNE1 channels, which results in the secretion of K^+, necessary for normal hearing (Wang et al., 1996; Neyroud et al., 1997). However, the precise mechanisms underlying the cAMP-regulated increase in K^+ conductance in the inner ear are unclear (Sunose et al., 1997). In the intestine, cAMP enhances Kv7.1-KCNE3 currents and stimulates Cl^- secretion by hyperpolarizing the cell membrane and thereby amplifying the driving force for Cl^- exit through cystic fibrosis transmembrane conductance regulator Cl^- channels (Lohrmann et al., 1995; Diener et al., 1996; Suessbrich et al., 1996; Devor et al., 1997; Rufo et al., 1997; Schroeder et al., 2000b; Bajwa et al., 2007). An essential role for KCNE3 in cAMP-driven Cl^- secretion has been suggested from the observation that KCNE3 knockdown reduced cAMP-mediated Cl^- secretion across tracheal and intestinal epithelia without altering Kv7.1 expression (Preston et al., 2010) but the precise mechanism by which cAMP stimulates Kv7.1-KCNE3 channels in these cells is still unknown. Like for intestine epithelial cells, airway epithelial cells secrete Cl^- stimulated by the cAMP-signaling pathway, where blockade of Kv7.1 channels suppress the cAMP-mediated Cl^- secretion (Mall et al., 2000; Grahammer et al., 2001b; MacVinish et al., 2001; Cowley and Linsdell, 2002; Kim et al., 2007). However, the direct mechanism how cAMP mediates Kv7.1 channel activation responsible for Cl^- secretion needs to be further investigated. In pancreatic β-cells, Kv7.1 channels contribute to insulin secretion. Besides, a link between cAMP and insulin secretion has established (Malaisse and Malaisse-Lagae, 1984; Seino and Shibasaki, 2005). However, it remains to be determined if Kv7.1 channels play a role in this cAMP-dependent mechanism.

Modifiers of cAMP-Mediated Regulation of Kv7.1 Channels

Although the direct regulation of cAMP signaling on Kv7.1 channel activity is well described, several factors can modulate this interaction indirectly. For instance, Nicolas et al. (2008) determined that the PKA-dependent regulation of I_{Ks} was microtubule-dependent (Nicolas et al., 2008). Cytoskeletal microtubules are essential for proper trafficking of cardiac ion channels to the plasma membrane (Steele and Fedida, 2014), and although a physical interaction between Kv7.1 and the microtubule forming protein, β-tubulin, was shown, disruption of the microtubules did not modify the Kv7.1-KCNE1 channel membrane density or baseline currents in transfected COS-7 cells or cardiomyocytes. However, microtubule disruption decreased the I_{Ks} response to PKA-mediated stimulation. This was not due to altered channel phosphorylation, yotiao phosphorylation or the interaction between both proteins, suggesting that microtubules play an important role in the coupling of PKA-dependent Kv7.1 phosphorylation and its channel activation (Nicolas et al., 2008).

The effect of cAMP on the trafficking of Kv7.1 channels has also been investigated. PKA inhibition in Madin-Darby canine kidney (MDCK) cells reduces Kv7.1 channel membrane expression and increases intracellular accumulation of the Kv7.1 protein in late endosomes/lysosomes (Andersen et al., 2015). This suggests a role for PKA-mediated trafficking of Kv7.1 channels, although this was not a result of channel phosphorylation. A previous study by the same group found that two cAMP phosphorylation residues on Kv7.1, serine 27 and serine 92, were not crucial for trafficking Kv7.1 (Lundby et al., 2013). Instead the E3 ubiquitin ligase Nedd4-2 is required in this PKA-dependent

trafficking pathway (Andersen et al., 2015). Nedd4-2 is an ubiquitin-protein ligase that binds to ion channels containing a C-terminal proline-rich segment (PY motif) (Manning and Kumar, 2018). Among the Kv7 channels, Kv7.1 is the only isoform containing this sequence motif. Binding of Nedd4-2 to the C-terminal PY motif in Kv7.1 channels regulates the ubiquitylation of the channel and its internalization (Jespersen et al., 2007). Andersen et al. (2015) concluded that PKA regulated Nedd4-2-dependent trafficking of Kv7.1 but the precise mechanism how PKA influences Nedd4-2 needs to be determined (Andersen et al., 2015).

Kv7.2 and Kv7.3

Kv7.2 and Kv7.3 channels are widely expressed in neuronal tissues, where they form a heteromeric channel that generates the "M-current" (Brown and Adams, 1980; Wang et al., 1998; Wickenden et al., 2001; Roche et al., 2002; Shah et al., 2002). Kv7.5 channels are also a component of the M-channel in heteromeric formation with Kv7.3 (Lerche et al., 2000; Schroeder et al., 2000a; Tzingounis et al., 2010). The M-current in neurons maintains the negative resting membrane potential to limit neuronal firing and excitability (Marrion, 1997; Jentsch, 2000). M-currents are inhibited by Gq/11 coupled GPCRs such as muscarinic acetylcholine receptors M1, M3 and M5, or bradykinin B2 receptors. Stimulation of these receptors decreases M-current density resulting in depolarization, which subsequently increases neuronal excitability (Brown and Selyanko, 1985; Cruzblanca et al., 1998). It is well established that disruption of the M-current due to mutations in either *KCNQ2* or *KCNQ3* genes causes excessive neuronal excitability, leading to neuronal diseases, such as benign familial neonatal convulsions and epileptic encephalopathy (Biervert et al., 1998; Charlier et al., 1998; Singh et al., 1998; Jentsch, 2000; Castaldo et al., 2002; Borgatti et al., 2004; Weckhuysen et al., 2012, 2013).

Kv7.2/Kv7.3 currents in overexpressed *Xenopus* oocytes are enhanced by cAMP, which relies on PKA-mediated phosphorylation of serine 52 in the Kv7.2 N-terminus (Schroeder et al., 1998). Furthermore, Cooper et al. (2000) identified an interaction of Kv7.2 and PKA subunits in human brain samples by co-immunoprecipitation and affinity chromatography (Cooper et al., 2000). In addition, AKAP79/150 is associated with Kv7.2 channels (Hoshi et al., 2003, 2005; Zhang and Shapiro, 2012). Although the core AKAP79/150 complex contains PKA (Gold et al., 2006), it has not yet been determined whether AKAP70/150 facilitates PKA phosphorylation of Kv7.2 channel; however, AKAP79/150 is essential for the recruitment and phosphorylation of Kv7.2 channels by PKC (Hoshi et al., 2003; Higashida et al., 2005; Zhang and Shapiro, 2012).

Multiple other phosphorylation sites of Kv7.2/Kv7.3 channels have been identified using mass spectrometry. However, the responsible kinase for this phosphorylation remains elusive as not only PKA but also PKC and src tyrosine kinase can regulate Kv7.2/Kv7.3 channel phosphorylation (Gamper et al., 2003; Hoshi et al., 2003; Li et al., 2004; Surti et al., 2005). A recent study by Salzer et al. (2017) found 13 phosphorylation sites for human Kv7.2 using mass spectrometry, one already identified (serine 52) located at the N-terminus, whereas the remaining 12 were located in the C-terminus. Using *in vitro* phosphorylation assays the authors identified the protein kinases responsible for C-terminus Kv7.2 phosphorylation. Only two of the 12 residues (serine 438 and serine 455) were phosphorylated by PKA. Inhibition of PKA reduced Kv7.2 phosphorylation, which decreased channel sensitivity to PIP_2 depletion, thereby attenuating Kv7 channel regulation via M1 muscarinic receptors. Thus, phosphorylation of the Kv7.2 channel is necessary to maintain a reduced affinity for PIP_2 (Salzer et al., 2017; **Figure 1B**).

Kv7.5 channels are expressed in some regions of the brain, where they coassemble with Kv7.3 channels. Kv7.5/Kv7.3 channels show similar currents to the Kv7.2/Kv7.3 currents and are also inhibited by M1 muscarinic receptor activation (Schroeder et al., 2000a). Kv7.5 can be phosphorylated and stimulated by PKA on serine 53 on the N-terminus (Brueggemann et al., 2018); however, it is still unclear whether the heterotetrameric Kv7.3/Kv7.5 channel found in neurones are regulated in the same way by cAMP.

Kv7.4 and Kv7.5

Kv7.4 channels are expressed in the inner ear and auditory nerves (Kharkovets et al., 2000), the substantia nigra (Hansen et al., 2008), skeletal muscle cells (Iannotti et al., 2010), the mitochondria of cardiac myocytes (Testai et al., 2016) and in smooth muscle cells extensively (see Barrese et al., 2018 for a recent review of the smooth muscle literature). Kv7.5 channels are expressed in the brain, where they play a role in the regulation of neuronal excitability, and in skeletal and smooth muscle (Schroeder et al., 2000a; Roura-Ferrer et al., 2008; Iannotti et al., 2010; Haick and Byron, 2016).

In smooth muscle, there is evidence Kv7.4 and Kv7.5 channels exist as both homomers and heteromers (Brueggemann et al., 2011, 2014b; Chadha et al., 2014; Jepps et al., 2015). The first indication that smooth muscle Kv7 channels were activated by cAMP came from gastric smooth muscle cells. In these cells, β adrenoceptor stimulation with isoprenaline induced a current that resembled the neuronal M current, although at this time the molecular identity of the M current was still unknown (Sims et al., 1988).

In vascular smooth muscle, the use of pharmacological inhibitors and molecular interference has identified a role for Kv7 channels in receptor-mediated relaxations. The first identification was for β adrenoceptor-mediated vasodilatation in the renal vasculature (Chadha et al., 2012). Inhibition of Kv7 channels by XE991 or linopirdine and knockdown of Kv7.4 with *KCNQ4*-targeted small interfering RNA (siRNA), attenuated arterial relaxations to the β adrenoceptor agonist, isoprenaline (Chadha et al., 2012). More recent, experiments with morpholino-mediated suppression of Kv7.4 translation corroborated these findings (Stott et al., 2018). Furthermore, isoprenaline increased Kv7 currents in vascular smooth muscle cells isolated from rat arteries and in A7r5 cells (a rat aortic smooth muscle cell line) (Chadha et al., 2012; Stott et al., 2015; Mani et al., 2016; Brueggemann et al., 2018).

In hypertension, Kv7.4 protein expression is diminished causing reduced hyperpolarization and relaxation of the smooth muscle cells. Furthermore, in renal arteries from spontaneously

hypertensive rats, where Kv7.4 expression is reduced, receptor-mediated relaxations were diminished (Jepps et al., 2011; Chadha et al., 2012). Interestingly, in the cerebral arteries from hypertensive rats, there is no compromise of Kv7.4 channel expression and CGRP receptor-mediated relaxations are unaffected (Chadha et al., 2014).

Although targeting Kv7.4 in isolated vessels with siRNA- and morpholino-induced knockdown inhibits isoprenaline- and CGRP-induced relaxations (Chadha et al., 2014; Stott et al., 2018), there is evidence that Kv7.5 is required to elicit cAMP-dependent relaxations. In A7r5 cells, stimulation of β adrenoceptors and the downstream pathway enhanced the currents produced by Kv7.5 channels and heterotetrameric Kv7.4/Kv7.5 channels expressed exogenously, but not when homomeric Kv7.4 channels were expressed (Mani et al., 2016), suggesting cAMP-mediated regulation of Kv7.4 and Kv7.5 depends on the stoichiometry of the channel.

The precise Kv7 channel stoichiometry eliciting cAMP-dependent relaxations in vascular smooth muscle is still unknown. Kv7.4 channels are important for proper Kv7 channel function in arteries, highlighted by their downregulation in arteries from hypertensive animals, whereas both Kv7.4 and Kv7.5 may play a role in the cAMP-dependent activation. To further complicate this mechanism, KCNE4 co-assembles with Kv7.4 and Kv7.5 in vascular smooth muscle cells to alter the biophysical properties and cellular localization of these channels. Targeted knockdown of *Kcne4* in rat arteries depolarized the smooth muscle resting membrane potential and reduced vasorelaxations to Kv7 channel activators. Interestingly, in *Kcne4* knockout mice, only the males displayed attenuated Kv7 channel function, but both male and female *Kcne4* knockout mice had attenuated responses to isoprenaline. Given that *Kcne4* expression has been shown in several arterial beds, it could be facilitating the Kv7 channel-dependent cAMP relaxations (Jepps et al., 2015; Abbott and Jepps, 2016). The expression of KCNE4 in A7r5 cells is yet to be determined but including KCNE4 subunits in future studies investigating the cAMP-dependent Kv7.4/Kv7.5 channel activation could give valuable insight into this mechanism.

Both PKA and Epac enhance Kv7 channel activity in vascular smooth muscle (Khanamiri et al., 2013; Mani et al., 2016; Stott et al., 2016). Isoprenaline-mediated relaxations were attenuated by PKA inhibition in renal arteries, whilst the isoprenaline relaxations in mesenteric arteries were not affected (Stott et al., 2016). In the mesenteric artery, isoprenaline-induced linopirdine-sensitive relaxations were elicited through activation of Epac, which is present in both rat renal and mesenteric arteries, but more predominant in mesenteric arteries. With electrophysiology experiments, Kv7 currents were increased with direct Epac stimulation in smooth muscle cells isolated from renal and mesenteric arteries (Stott et al., 2016). These data highlight that cAMP-dependent stimulation of Kv7 channels in vascular smooth muscle is not only dependent on the Kv7 channel architecture but also the channel's association with downstream cAMP effector proteins, all of which are likely to be artery specific (see **Figure 1C**).

Kv7 channels are also expressed in airway smooth muscle cells (ASMCs) of rodents and humans. Pharmacological activators of Kv7 channels, including retigabine, flupirtine and S-1, relax airway smooth muscle cells from guinea pigs and human, and are important regulators of airway diameter (Brueggemann et al., 2012; Evseev et al., 2013). β2-adrenergic receptor agonists are commonly used for the treatment of asthma to relieve hyperconstriction of the airway (Cazzola et al., 2013), and are able to enhance Kv7 currents in ASMCs thereby inducing relaxation of rat airways (Brueggemann et al., 2014a). A later study by Brueggemann et al. (2018) revealed that β adrenoceptor stimulation activated the Kv7.5 channels in cultured human ASMCs, a response which was mediated by the PKA pathway (Brueggemann et al., 2018). This study identified serine 53 on the Kv7.5 N-terminus to be responsible for the increased Kv7.5 currents in response to cAMP elevation, which could be a common mechanism for β adrenoceptor/cAMP activation of Kv7.5 channels in vascular smooth muscle cells. Recent findings show that phosphorylation of serine 53 on the N-terminus of Kv7.5 increases its affinity for PIP_2, corresponding to enhanced channel activation (Brueggemann et al., 2020).

Kv7.4 and Kv7.5 are also expressed in the smooth muscle of the gastrointestinal tract (Ohya et al., 2002; Jepps et al., 2009; Ipavec et al., 2011; Adduci et al., 2013), bladder (Streng et al., 2004; Rode et al., 2010; Svalø et al., 2012, 2013; Afeli et al., 2013; Anderson et al., 2013), penis (Jepps et al., 2016) and uterus (McCallum et al., 2009) where important functional roles have been established. Whether Kv7 channels in these tissues are subjected to the same cAMP-dependent regulation as in vascular and airway smooth muscle remains to be determined. Given that, even within the vasculature, there are differences in the cAMP-dependent mechanisms that lead to Kv7 channel stimulation, the Kv7 channels in these smooth muscle tissues cannot be assumed to behave in the same way as has been described in airway and vascular smooth muscle. Future work should investigate how Kv7 channels are subjected to cAMP-dependent regulation in these tissues, which could lead to novel therapeutic strategies for the treatment of various smooth muscle disorders, such as constipation, preeclampsia, erectile dysfunction and incontinence.

Modifiers of cAMP-Mediated Regulation of Kv7.4 Channels

Gβγ subunits have a regulatory role on the modulation of Kv7.4 channels in vascular smooth muscle cells, which is Gβ subunit-specific (Stott et al., 2015, 2018; Greenwood and Stott, 2020). Gβγ subunit binding to Kv7.4 channels enhances the current in both HEK and CHO cells expressing Kv7.4, and in rat renal arterial smooth muscle cells. In addition, Gβγ subunit interaction is critical for the β adrenergic dependent activation of Kv7 channels in rat renal arteries, but not in rat mesenteric arteries. Contrarily, inhibition of Gβγ subunits attenuated the CGRP dependent relaxations in mesenteric arteries, but showed no effect on CGRP relaxation in cerebral arteries, highlighting the role of Gβγ in Kv7-dependent vasorelaxations to be artery specific and dependent on the vasorelaxant (Stott et al., 2018).

The microtubule network has also been implicated in the Kv7 channel-dependent cAMP-mediated relaxations in rat mesenteric and renal arteries (Lindman et al., 2018). Disruption of the microtubule network with colchicine increased the membrane expression of Kv7.4 channels, which enhanced membrane hyperpolarization, decreases in intracellular Ca^{2+} and vasorelaxation to isoprenaline and forskolin in a Kv7 channel-dependent manner, specifically (Lindman et al., 2018). Further work in this area is required to determine whether the microtubule network regulates cAMP signaling in smooth muscle cells.

CONCLUSION

The second messenger cAMP regulates Kv7 channel activity in many cell types, including cardiac myocytes, smooth muscle and neurons. However, cAMP-mediated regulation of Kv7 channels is complex and many aspects remain to be elucidated. Generation of cAMP results from stimulation of AC, of which 9 isoforms exist. Depending on the isoforms expressed in a cell type, extracellular signals through GPCR activation can be integrated differently. Identifying how different AC isoforms contribute to cAMP-dependent activation of Kv7 channels in different tissue types could lead to targeting of a particular isoform providing therapeutic benefits with fewer adverse effects. Furthermore, the recent discovery of Epac activation of Kv7.4/Kv7.5 channels in vascular smooth muscle adds more complexity to this pathway. Determining whether this cAMP/Epac pathway plays a role in the activation of other Kv7 channels will be necessary to fully understand the physiological impact of cAMP signaling through Kv7 channels. Finally, the importance of the KCNE subunits in the cAMP-dependent regulation of Kv7 channels has often been overlooked but is likely to have a substantial role. By better defining the cAMP regulation of Kv7 channels in different tissues, it may become possible to exploit subtle tissue-specific differences in the activation pathways in order to generate novel therapeutics.

AUTHOR CONTRIBUTIONS

All authors contributed to the drafting, revision and final approval of the manuscript.

FUNDING

TJ received funding from the Lundbeck Foundation (R307-2018-3674). JH received funding from the European Union's Horizon 2020 Research and Innovation Program under the Marie Skłodowska-Curie grant agreement No. 801199.

REFERENCES

Abbott, G. W. (2016). KCNE4 and KCNE5: K(+) channel regulation and cardiac arrhythmogenesis. *Gene* 593, 249–260. doi: 10.1016/j.gene.2016.07.069

Abbott, G. W., and Goldstein, S. A. (1998). A superfamily of small potassium channel subunits: form and function of the MinK-related peptides (MiRPs). *Q. Rev. Biophys.* 31, 357–398. doi: 10.1017/s0033583599003467

Abbott, G. W., and Jepps, T. A. (2016). Kcne4 deletion sex-dependently alters vascular reactivity. *J. Vasc. Res.* 53, 138–148. doi: 10.1159/000449060

Adduci, A., Martire, M., Taglialatela, M., Arena, V., Rizzo, G., Coco, C., et al. (2013). Expression and motor functional roles of voltage-dependent type 7 K+ channels in the human taenia coli. *Eur. J. Pharmacol.* 721, 12–20. doi: 10.1016/j.ejphar.2013.09.061

Afeli, S. A. Y., Malysz, J., and Petkov, G. V. (2013). Molecular expression and pharmacological evidence for a functional role of Kv7 channel subtypes in guinea pig urinary bladder smooth muscle. *PLoS One* 8:e75875. doi: 10.1371/journal.pone.0075875

Andersen, M. N., Hefting, L. L., Steffensen, A. B., Schmitt, N., Olesen, S.-P., Olsen, J. V., et al. (2015). Protein kinase A stimulates Kv7.1 surface expression by regulating Nedd4-2-dependent endocytic trafficking. *Am. J. Physiol. Cell Physiol.* 309, C693–C706.

Anderson, U. A., Carson, C., Johnston, L., Joshi, S., Gurney, A. M., and McCloskey, K. D. (2013). Functional expression of KCNQ (Kv7) channels in guinea pig bladder smooth muscle and their contribution to spontaneous activity. *Br. J. Pharmacol.* 169, 1290–1304. doi: 10.1111/bph.12210

Bacallao, K., and Monje, P. V. (2015). Requirement of cAMP signaling for Schwann cell differentiation restricts the onset of myelination. *PLoS One* 10:e0116948. doi: 10.1371/journal.pone.0116948

Baillie, G. S. (2009). Compartmentalized signalling: spatial regulation of cAMP by the action of compartmentalized phosphodiesterases. *FEBS J.* 276, 1790–1799. doi: 10.1111/j.1742-4658.2009.06926.x

Bajwa, P. J., Alioua, A., Lee, J. W., Straus, D. S., Toro, L., and Lytle, C. (2007). Fenofibrate inhibits intestinal Cl- secretion by blocking basolateral KCNQ1 K+ channels. *Am. J. Physiol. Liver Physiol.* 293, G1288–G1299.

Bal, M., Zhang, J., Zaika, O., Hernandez, C. C., and Shapiro, M. S. (2008). Homomeric and heteromeric assembly of KCNQ (Kv7) K+ channels assayed by total internal reflection fluorescence/fluorescence resonance energy transfer and patch clamp analysis. *J. Biol. Chem.* 283, 30668–30676. doi: 10.1074/jbc.m805216200

Barhanin, J., Lesage, F., Guillemare, E., Fink, M., Lazdunski, M., and Romey, G. (1996). KvLQT1 and IsK (minK) proteins associate to form the IKS cardiac potassium current. *Nature* 384, 78–80. doi: 10.1038/384078a0

Barrese, V., Stott, J. B., and Greenwood, I. A. (2018). KCNQ-encoded potassium channels as therapeutic targets. *Annu. Rev. Pharmacol. Toxicol.* 58, 625–648. doi: 10.1146/annurev-pharmtox-010617-052912

Barros, F., Dominguez, P., and de la Peña, P. (2012). Cytoplasmic domains and voltage-dependent potassium channel gating. *Front. Pharmacol.* 3:49. doi: 10.3389/fphar.2012.00049

Bauman, A. L., Soughayer, J., Nguyen, B. T., Willoughby, D., Carnegie, G. K., Wong, W., et al. (2006). Dynamic regulation of cAMP synthesis through anchored PKA-adenylyl cyclase V/VI complexes. *Mol. Cell* 23, 925–931. doi: 10.1016/j.molcel.2006.07.025

Bechtel, P. J., Beavo, J. A., and Krebs, E. G. (1977). Purification and characterization of catalytic subunit of skeletal muscle adenosine 3':5' monophosphate dependent protein kinase. *J. Biol. Chem.* 252, 2691–2697.

Bennett, P. B., and Begenisch, T. B. (1987). Catecholamines modulate the delayed rectifying potassium current (IK) in guinea pig ventricular myocytes. *Pflugers Arch.* 410, 217–219. doi: 10.1007/bf00581919

Biel, M. (2009). Cyclic nucleotide-regulated cation channels. *J. Biol. Chem.* 284, 9017–9021.

Biel, M., and Michalakis, S. (2007). Function and dysfunction of CNG channels: insights from channelopathies and mouse models. *Mol. Neurobiol.* 35, 266–277. doi: 10.1007/s12035-007-0025-y

Biel, M., and Michalakis, S. (2009). *Cyclic Nucleotide-Gated Channels. In CGMP: Generators, Effectors and Therapeutic Implications*. Berlin: Springer, 111–136.

Biervert, C., Schroeder, B. C., Kubisch, C., Berkovic, S. F., Propping, P., Jentsch, T. J., et al. (1998). A potassium channel mutation in neonatal human epilepsy. *Science* 279, 403–406. doi: 10.1126/science.279.5349.403

Borgatti, R., Zucca, C., Cavallini, A., Ferrario, M., Panzeri, C., Castaldo, P., et al. (2004). A novel mutation in KCNQ2-associated with BFNC, drug resistant epilepsy, and mental retardation. *Neurology* 63, 57–65. doi: 10.1212/01.wnl.0000132979.08394.6d

Bos, J. L. (2006). Epac proteins: multi-purpose cAMP targets. *Trends Biochem. Sci.* 31, 680–686. doi: 10.1016/j.tibs.2006.10.002

Braun, T., and Dods, R. F. (1975). Development of a Mn-2+-sensitive, 'soluble' adenylate cyclase in rat testis. *Proc. Natl. Acad. Sci. U.S.A.* 72, 1097–1101. doi: 10.1073/pnas.72.3.1097

Braun, T., Frank, H., Dods, R., and Sepsenwol, S. (1977). Mn2+-sensitive, soluble adenylate cyclase in rat testis. Differentiation from other testicular nucleotide cyclases. *Biochim. Biophys. Acta* 481, 227–235. doi: 10.1016/0005-2744(77)90155-3

Brown, D. A., and Adams, P. R. (1980). Muscarinic suppression of a novel voltage-sensitive K+ current in a vertebrate neurone [18]. *Nature* 283, 673–676. doi: 10.1038/283673a0

Brown, D. A., and Selyanko, A. A. (1985). Membrane currents underlying the cholinergic slow excitatory post-synaptic potential in the rat sympathetic ganglion. *J. Physiol.* 365, 365–387. doi: 10.1113/jphysiol.1985.sp015777

Brueggemann, L. I., Cribbs, L. L., and Byron, K. L. (2020). Structural determinants of Kv7.5 potassium channels that confer changes in phosphatidylinositol 4,5-bisphosphate (PIP2) affinity and signaling sensitivities in smooth muscle cells. *Mol. Pharmacol.* 97, 145–158. doi: 10.1124/mol.119.117192

Brueggemann, L. I., Cribbs, L. L., Schwartz, J., Wang, M., Kouta, A., and Byron, K. L. (2018). Mechanisms of PKA-dependent potentiation of Kv7.5 channel activity in human airway smooth muscle cells. *Int. J. Mol. Sci.* 19:2223. doi: 10.3390/ijms19082223

Brueggemann, L. I., Haick, J. M., Neuburg, S., Tate, S., Randhawa, D., Cribbs, L. L., et al. (2014a). KCNQ (Kv7) potassium channel activators as bronchodilators: combination with a β2-adrenergic agonist enhances relaxation of rat airways. *Am. J. Physiol. Lung Cell. Mol. Physiol.* 306, L476–L486.

Brueggemann, L. I., Kakad, P. P., Love, R. B., Solway, J., Dowell, M. L., Cribbs, L. L., et al. (2012). Kv7 potassium channels in airway smooth muscle cells: signal transduction intermediates and pharmacological targets for bronchodilator therapy. *Am. J. Physiol. Lung Cell. Mol. Physiol.* 302, L120–L132.

Brueggemann, L. I., Mackie, A. R., Cribbs, L. L., Freda, J., Tripathi, A., Majetschak, M., et al. (2014b). Differential protein kinase C-dependent modulation of Kv7.4 and Kv7.5 subunits of vascular Kv7 channels. *J. Biol. Chem.* 289, 2099–2111. doi: 10.1074/jbc.m113.527820

Brueggemann, L. I., Mackie, A. R., Martin, J. L., Cribbs, L. L., and Byron, K. L. (2011). Diclofenac distinguishes among homomeric and heteromeric potassium channels composed of KCNQ4 and KCNQ5 subunits. *Mol. Pharmacol.* 79, 10–23. doi: 10.1124/mol.110.067496

Burns, L. L., Canaves, J. M., Pennypacker, J. K., Blumenthal, D. K., and Taylor, S. S. (2003). Isoform specific differences in binding of a dual-specificity A-kinase anchoring protein to type I and type II regulatory subunits of PKA. *Biochemistry* 42, 5754–5763. doi: 10.1021/bi0265729

Carr, D. W., Stofko-Hahn, R. E., Fraser, I. D. C., Bishop, S. M., Acott, T. S., Brennan, R. G., et al. (1991). Interaction of the regulatory subunit (RII) of cAMP-dependent protein kinase with RII-anchoring proteins occurs through an amphipathic helix binding motif. *J. Biol. Chem.* 266, 14188–14192.

Castaldo, P., Giudice, E. M., del Coppola, G., Pascotto, A., Annunziato, L., and Taglialatela, M. (2002). Benign familial neonatal convulsions caused by altered gating of KCNQ2/KCNQ3 potassium channels. *J. Neurosci.* 22: RC199.

Cazzola, M., Page, C. P., Rogliani, P., and Matera, M. G. (2013). β2-agonist therapy in lung disease. *Am. J. Respir. Crit. Care Med.* 187, 690–696. doi: 10.1164/rccm.201209-1739pp

Chadha, P. S., Jepps, T. A., Carr, G., Stott, J. B., Zhu, H.-L., Cole, W. C., et al. (2014). Contribution of Kv7.4/Kv7.5 heteromers to intrinsic and calcitonin gene-related peptide-induced cerebral reactivity. *Arterioscler. Thromb. Vasc. Biol.* 34, 887–893. doi: 10.1161/atvbaha.114.303405

Chadha, P. S., Zunke, F., Zhu, H.-L., Davis, A. J., Jepps, T. A., Olesen, S. P., et al. (2012). Reduced KCNQ4-encoded voltage-dependent potassium channel activity underlies impaired β-adrenoceptor-mediated relaxation of renal arteries in hypertension. *Hypertension* 59, 877–884. doi: 10.1161/hypertensionaha.111.187427

Charlier, C., Singh, N. A., Ryan, S. G., Lewis, T. B., Reus, B. E., Leach, R. J., et al. (1998). A pore mutation in a novel KQT-like potassium channel gene in an idiopathic epilepsy family. *Nat. Genet.* 18, 53–55. doi: 10.1038/ng0198-53

Chen, L., and Kass, R. S. (2006). Dual roles of the A kinase-anchoring protein Yotiao in the modulation of a cardiac potassium channel: a passive adaptor versus an active regulator. *Eur. J. Cell Biol.* 85, 623–626. doi: 10.1016/j.ejcb.2006.03.002

Chen, L., Kurokawa, J., and Kass, R. S. (2005). Phosphorylation of the A-kinase-anchoring protein Yotiao contributes to protein kinase A regulation of a heart potassium channel. *J. Biol. Chem.* 280, 31347–31352. doi: 10.1074/jbc.m505191200

Chen, L., Marquardt, M. L., Tester, D. J., Sampson, K. J., Ackerman, M. J., and Kass, R. S. (2007). Mutation of an A-kinase-anchoring protein causes long-QT syndrome. *Proc. Natl. Acad. Sci. U.S.A.* 104, 20990–20995. doi: 10.1073/pnas.0710527105

Cheng, X., Ji, Z., Tsalkova, T., and Mei, F. (2008). Epac and PKA: a tale of two intracellular cAMP receptors. *Acta Biochim. Biophys. Sin.* 40, 651–662. doi: 10.1111/j.1745-7270.2008.00438.x

Cooper, E. C., Aldape, K. D., Abosch, A., Barbaro, N. M., Berger, M. S., Peacock, W. S., et al. (2000). Colocalization and coassembly of two human brain M-type potassium channel subunits that are mutated in epilepsy. *Proc. Natl. Acad. Sci. U.S.A.* 97, 4914–4919. doi: 10.1073/pnas.090092797

Corbin, J. D., Sugden, P. H., Lincoln, T. M., and Keely, S. L. (1977). Compartmentalization of adenosine 3':5' monophosphate and adenosine 3':5' monophosphate dependent protein kinase in heart tissue. *J. Biol. Chem.* 252, 3854–3861.

Corbin, J. D., Sugden, P. H., West, L., Flockhart, D. A., Lincoln, T. M., and McCarthy, D. (1978). Studies on the properties and mode of action of the purified regulatory subunit of bovine heart adenosine 3':5'-monophosphate-dependent protein kinase. *J. Biol. Chem.* 253, 3997–4003.

Cowley, E. A., and Linsdell, P. (2002). Characterizatin of basolateral K+ channels underlying anion secretion in the human airway cell line Calu-3. *J. Physiol.* 538, 747–757. doi: 10.1113/jphysiol.2001.013300

Cruzblanca, H., Koh, D. S., and Hille, B. (1998). Bradykinin inhibits M current via phospholipase C and Ca2+ release from IP3-sensitive Ca2+ stores in rat sympathetic neurons. *Proc. Natl. Acad. Sci. U.S.A.* 95, 7151–7156. doi: 10.1073/pnas.95.12.7151

Dell'Acqua, M. L., Smith, K. E., Gorski, J. A., Horne, E. A., Gibson, E. S., and Gomez, L. L. (2006). Regulation of neuronal PKA signaling through AKAP targeting dynamics. *Eur. J. Cell Biol.* 85, 627–633. doi: 10.1016/j.ejcb.2006.01.010

Dema, A., Perets, E., Schulz, M. S., Deák, V. A., and Klussmann, E. (2015). Pharmacological targeting of AKAP-directed compartmentalized cAMP signalling. *Cell. Signal.* 27, 2474–2487. doi: 10.1016/j.cellsig.2015.09.008

Devor, D. G., Singh, A. K., Gerlach, A. C., Frizzell, R. A., and Bridges, R. J. (1997). Inhibition of intestinal Cl- secretion by clotrimazole: Direct effect on basolateral membrane K+ channels. *Am. J. Physiol* 273, C531–C540.

Diener, M., Hug, F., Strabel, D., and Scharrer, E. (1996). Cyclic AMP-dependent regulation of K+ transport in the rat distal colon. *Br. J. Pharmacol.* 118, 1477–1487. doi: 10.1111/j.1476-5381.1996.tb15563.x

Difrancesco, D. (1986). Characterization of single pacemaker channels in cardiac sino-atrial node cells. *Nature* 324, 470–473. doi: 10.1038/324470a0

DiFrancesco, D. (2020). A brief history of pacemaking. *Front. Physiol.* 10:1599. doi: 10.3389/fphys.2019.01599

DiFrancesco, D., and Tortora, P. (1991). Direct activation of cardiac pacemaker channels by intracellular cyclic AMP. *Nature* 351, 145–147. doi: 10.1038/351145a0

Doyle, D. A., Morais Cabral, J., Pfuetzner, R. A., Kuo, A., Gulbis, J. M., Cohen, S. L., et al. (1998). The structure of the potassium channel: molecular basis of K+ conduction and selectivity. *Science* 280, 69–77. doi: 10.1126/science.280.5360.69

Dumont, J. E., Jauniaux, J. C., and Roger, P. P. (1989). The cyclic AMP-mediated stimulation of cell proliferation. *Trends Biochem. Sci.* 14, 67–71. doi: 10.1016/0968-0004(89)90046-7

Evseev, A. I., Semenov, I., Archer, C. R., Medina, J. L., Dube, P. H., Shapiro, M. S., et al. (2013). Functional effects of KCNQ K(+) channels in airway smooth muscle. *Front. Physiol.* 4:277. doi: 10.3389/fphys.2013.00277

Fink, M. A., Zakhary, D. R., Mackey, J. A., Desnoyer, R. W., Apperson-Hansen, C., Damron, D. S., et al. (2001). AKAP-mediated targeting of protein kinase A regulates contractility in cardiac myocytes. *Circ. Res.* 88, 291–297. doi: 10.1161/01.res.88.3.291

Fodstad, H., Swan, H., Laitinen, P., Piippo, K., Paavonen, K., Viitasalo, M., et al. (2004). Four potassium channel mutations account for 73% of the genetic spectrum underlying long−QT syndrome (LQTS) and provide evidence for a strong founder effect in Finland. *Ann. Med.* 36, 53–63. doi: 10.1080/17431380410032689

Forte, L. R., Bylund, D. B., and Zahler, W. L. (1983). Forskolin does not activate sperm adenylate cyclase. *Mol. Pharmacol.* 24, 42–47.

Fujita, T., Umemura, M., Yokoyama, U., Okumura, S., and Ishikawa, Y. (2017). The role of Epac in the heart. *Cell. Mol. Life Sci.* 74, 591–606. doi: 10.1007/s00018-016-2336-5

Gamper, N., Stockand, J. D., and Shapiro, M. S. (2003). Subunit-specific modulation of KCNQ potassium channels by Src tyrosine kinase. *J. Neurosci.* 23, 84–95. doi: 10.1523/jneurosci.23-01-00084.2003

Glantz, S. B., Amat, J. A., and Rubin, C. S. (1992). cAMP signaling in neurons: patterns of neuronal expression and intracellular localization for a novel protein, AKAP 150, that anchors the regulatory subunit of cAMP-dependent protein kinase IIβ. *Mol. Biol. Cell* 3, 1215–1228. doi: 10.1091/mbc.3.11.1215

Gold, M. G., Lygren, B., Dokurno, P., Hoshi, N., McConnachie, G., Taskén, K., et al. (2006). Molecular basis of AKAP specificity for PKA regulatory subunits. *Mol. Cell* 24, 383–395. doi: 10.1016/j.molcel.2006.09.006

Grahammer, F., Herling, A. W., Lang, H. J., Schmitt-Gräff, A., Wittekindt, O. H., Nitschke, R., et al. (2001a). The cardiac K+ channel KCNQ1 is essential for gastric acid secretion. *Gastroenterology* 120, 1363–1371. doi: 10.1053/gast.2001.24053

Grahammer, F., Warth, R., Barhanin, J., Bleich, M., and Hug, M. J. (2001b). The small conductance K+ channel, KCNQ1. Expression, function, and subunit composition in murine trachea. *J. Biol. Chem.* 276, 42268–42275. doi: 10.1074/jbc.m105014200

Greenwood, I. A., and Stott, J. B. (2020). The Gβ1 and Gβ3 subunits differentially regulate rat vascular Kv7 channels. *Front. Physiol.* 10:1573. doi: 10.3389/fphys.2019.01573

Gutman, G. A., Chandy, K. G., Grissmer, S., Lazdunski, M., McKinnon, D., Pardo, L. A., et al. (2005). International union of pharmacology. LIII. Nomenclature and molecular relationships of voltage-gated potassium channels. *Pharmacol. Rev.* 57, 473–508. doi: 10.1124/pr.57.4.10

Haick, J. M., and Byron, K. L. (2016). Novel treatment strategies for smooth muscle disorders: targeting Kv7 potassium channels. *Pharmacol. Ther.* 165, 14–25. doi: 10.1016/j.pharmthera.2016.05.002

Haitin, Y., and Attali, B. (2008). The C-terminus of Kv7 channels: a multifunctional module. *J. Physiol.* 586, 1803–1810. doi: 10.1113/jphysiol.2007.149187

Halls, M. L., and Cooper, D. M. F. (2017). Adenylyl cyclase signalling complexes – pharmacological challenges and opportunities. *Pharmacol. Ther.* 172, 171–180. doi: 10.1016/j.pharmthera.2017.01.001

Hanoune, J., and Defer, N. (2001). Regulation and role of adenylyl cyclase isoforms. *Annu. Rev. Pharmacol. Toxicol.* 41, 145–174.

Hansen, H. H., Waroux, O., Seutin, V., Jentsch, T. J., Aznar, S., and Mikkelsen, J. D. (2008). Kv7 channels: Interaction with dopaminergic and serotonergic neurotransmission in the CNS. *J. Physiol.* 586, 1823–1832. doi: 10.1113/jphysiol.2007.149450

Heginbotham, L., Abramson, T., and MacKinnon, R. (1992). A functional connection between the pores of distantly related ion channels as revealed by mutant K+ channels. *Science* 258, 1152–1155. doi: 10.1126/science.1279807

Higashida, H., Hoshi, N., Zhang, J.-S., Yokoyama, S., Hashii, M., Jin, D., et al. (2005). Protein kinase C bound with A-kinase anchoring protein is involved in muscarinic receptor-activated modulation of M-type KCNQ potassium channels. *Neurosci. Res.* 51, 231–234. doi: 10.1016/j.neures.2004.11.009

Hoshi, N., Langeberg, L. K., and Scott, J. D. (2005). Distinct enzyme combinations in AKAP signalling complexes permit functional diversity. *Nat. Cell Biol.* 7, 1066–1073. doi: 10.1038/ncb1315

Hoshi, N., Zhang, J.-S., Omaki, M., Takeuchi, T., Yokoyama, S., Wanaverbecq, N., et al. (2003). AKAP150 signaling complex promotes suppression of the M-current by muscarinic agonists. *Nat. Neurosci.* 6, 564–571. doi: 10.1038/nn1062

Huang, L. J. S., Durick, K., Weiner, J. A., Chun, J., and Taylor, S. S. (1997). Identification of a novel protein kinase A anchoring protein that binds both type I and type II regulatory subunits. *J. Biol. Chem.* 272, 8057–8064. doi: 10.1074/jbc.272.12.8057

Iannotti, F. A., Panza, E., Barrese, V., Viggiano, D., Soldovieri, M. V., and Taglialatela, M. (2010). Expression, localization, and pharmacological role of Kv7 potassium channels in skeletal muscle proliferation, differentiation, and survival after myotoxic insults. *J. Pharmacol. Exp. Ther.* 332, 811–820. doi: 10.1124/jpet.109.162800

Ipavec, V., Martire, M., Barrese, V., Taglialatela, M., and Currò, D. (2011). KV7 channels regulate muscle tone and nonadrenergic noncholinergic relaxation of the rat gastric fundus. *Pharmacol. Res.* 64, 397–409. doi: 10.1016/j.phrs.2011.06.016

Jenke, M., Sánchez, A., Monje, F., Stühmer, W., Weseloh, R. M., and Pardo, L. A. (2003). C-terminal domains implicated in the functional surface expression of potassium channels. *EMBO J.* 22, 395–403. doi: 10.1093/emboj/cdg035

Jentsch, T. J. (2000). Neuronal KCNQ potassium channels:physislogy and role in disease. *Nat. Rev. Neurosci.* 1, 21–30. doi: 10.1038/35036198

Jepps, T. A. (2017). Unravelling the complexities of vascular smooth muscle ion channels: fine tuning of activity by ancillary subunits. *Pharmacol. Ther.* 178, 57–66. doi: 10.1016/j.pharmthera.2017.03.010

Jepps, T. A., Carr, G., Lundegaard, P. R., Olesen, S.-P., and Greenwood, I. A. (2015). Fundamental role for the KCNE4 ancillary subunit in Kv7.4 regulation of arterial tone. *J. Physiol.* 593, 5325–5340. doi: 10.1113/jp271286

Jepps, T. A., Chadha, P. S., Davis, A. J., Harhun, M. I., Cockerill, G. W., Olesen, S. P., et al. (2011). Downregulation of Kv7.4 channel activity in primary and secondary hypertension. *Circulation* 124, 602–611.

Jepps, T. A., Greenwood, I. A., Moffatt, J. D., Sanders, K. M., and Ohya, S. (2009). Molecular and functional characterization of Kv7 K+ channel in murine gastrointestinal smooth muscles. *Am. J. Physiol. Gastrointest. Liver Physiol.* 297, G107–G115.

Jepps, T. A., Olesen, S. P., Greenwood, I. A., and Dalsgaard, T. (2016). Molecular and functional characterization of Kv7 channels in penile arteries and corpus cavernosum of healthy and metabolic syndrome rats. *Br. J. Pharmacol.* 173, 1478–1490. doi: 10.1111/bph.13444

Jespersen, T., Membrez, M., Nicolas, C., Pitard, B., Staub, O., Olesen, S., et al. (2007). The KCNQ1 potassium channel is down-regulated by ubiquitylating enzymes of the Nedd4/Nedd4-like family. *Cardiovasc. Res.* 74, 64–74. doi: 10.1016/j.cardiores.2007.01.008

Kanda, V. A., and Abbott, G. W. (2012). KCNE regulation of K(+) channel trafficking – a sisyphean task? *Front. Physiol.* 3:231. doi: 10.3389/fphys.2012.00231

Kang, G., Chepurny, O. G., Malester, B., Rindler, M. J., Rehmann, H., Bos, J. L., et al. (2006). cAMP sensor Epac as a determinant of ATP-sensitive potassium channel activity in human pancreatic β cells and rat INS-1 cells. *J. Physiol.* 573, 595–609. doi: 10.1113/jphysiol.2006.107391

Kass, R. S., Kurokawa, J., Marx, S. O., and Marks, A. R. (2003). Leucine/isoleucine zipper coordination of ion channel macromolecular signaling complexes in the heart. Roles in inherited arrhythmias. *Trends Cardiovasc. Med.* 13, 52–56. doi: 10.1016/s1050-1738(02)00211-6

Kaupp, U. B., and Seifert, R. (2002). Cyclic nucleotide-gated ion channels. *Physiol. Rev.* 82, 769–824.

Kawasaki, H., Springett, G. M., Mochizuki, N., Toki, S., Nakaya, M., Matsuda, M., et al. (1998). A family of cAMP-binding proteins that directly activate Rap1. *Science* 282, 2275–2279. doi: 10.1126/science.282.5397.2275

Khanamiri, S., Soltysinska, E., Jepps, T. A., Bentzen, B. H., Chadha, P. S., Schmitt, N., et al. (2013). Contribution of Kv7 channels to basal coronary flow and active response to ischemia. *Hypertens* 62, 1090–1097. doi: 10.1161/hypertensionaha.113.01244

Kharkovets, T., Hardelin, J. P., Safieddine, S., Schweizer, M., El-Amraoui, A., Petit, C., et al. (2000). KCNQ4, a K+ channel mutated in a form of dominant deafness,

is expressed in the inner ear and the central auditory pathway. *Proc. Natl. Acad. Sci. U.S.A.* 97, 4333–4338. doi: 10.1073/pnas.97.8.4333

Kim, J. K., Yoo, H. Y., Kim, S. J., Hwang, Y.-S., Han, J., Kim, J. A., et al. (2007). Effects of sevoflurane on the cAMP-induced short-circuit current in mouse tracheal epithelium and recombinant Cl- (CFTR) and K+ (KCNQ1) channels†. *Br. J. Anaesth.* 99, 245–251. doi: 10.1093/bja/aem123

Kim, S. J., and Greger, R. (1999). Voltage-dependent, slowly activating K+ current (I(Ks)) and its augmentation by carbachol in rat pancreatic acini. *Pflugers Arch. Eur. J. Physiol.* 438, 604–611. doi: 10.1007/s004240051083

Kinderman, F. S., Kim, C., Daake, S., von Ma, Y., Pham, B. Q., Spraggon, G., et al. (2006). A dynamic mechanism for AKAP binding to RII isoforms of cAMP-dependent protein kinase. *Mol. Cell* 24, 397–408. doi: 10.1016/j.molcel.2006.09.015

Köttgen, M., Hoefer, A., Kim, S. J., Beschorner, U., Schreiber, R., Hug, M. J., et al. (1999). Carbachol activates a K+ channel of very small conductance in the basolateral membrane of rat pancreatic acinar cells. *Pflugers Arch.* 438, 597–603. doi: 10.1007/s004240051082

Krebs, E. G., and Beavo, J. A. (1979). Phosphorylation-dephosphorylation of enzymes. *Annu. Rev. Biochem.* 48, 923–959. doi: 10.1146/annurev.bi.48.070179.004423

Kubisch, C., Schroeder, B. C., Friedrich, T., Lütjohann, B., El-Amraoui, A., Marlin, S., et al. (1999). KCNQ4, a novel potassium channel expressed in sensory outer hair cells, is mutated in dominant deafness. *Cell* 96, 437–446. doi: 10.1016/s0092-8674(00)80556-5

Kurokawa, J., Motoike, H. K., Rao, J., and Kass, R. S. (2004). Regulatory actions of the A-kinase anchoring protein Yotiao on a heart potassium channel downstream of PKA phosphorylation. *Proc. Natl. Acad. Sci. U.S.A.* 101, 16374–16378. doi: 10.1073/pnas.0405583101

Lerche, C., Scherer, C. R., Seebohm, G., Derst, C., Wei, A. D., Busch, A. E., et al. (2000). Molecular cloning and functional expression of KCNQ5, a potassium channel subunit that may contribute to neuronal M-current diversity. *J. Biol. Chem.* 275, 22395–22400. doi: 10.1074/jbc.m002378200

Lester, L. B., Langeberg, L. K., and Scott, J. D. (1997). Anchoring of protein kinase A facilitates hormone-mediated insulin secretion. *Proc. Natl. Acad. Sci. U.S.A.* 94, 14942–14947. doi: 10.1073/pnas.94.26.14942

Li, Y., Chen, L., Kass, R. S., and Dessauer, C. W. (2012). The A-kinase anchoring protein yotiao facilitates complex formation between adenylyl cyclase type 9 and the IKs potassium channel in heart. *J. Biol. Chem.* 287, 29815–29824. doi: 10.1074/jbc.m112.380568

Li, Y., Langlais, P., Gamper, N., Liu, F., and Shapiro, M. S. (2004). Dual phosphorylations underlie modulation of unitary KCNQ K+ channels by Src tyrosine kinase. *J. Biol. Chem.* 279, 45399–45407. doi: 10.1074/jbc.m408410200

Lindman, J., Khammy, M. M., Lundegaard, P. R., Aalkjær, C., and Jepps, T. A. (2018). Microtubule regulation of Kv7 channels orchestrates cAMP-mediated vasorelaxations in rat arterial smooth muscle. *Hypertension* 71, 336–345. doi: 10.1161/hypertensionaha.117.10152

Liu, L., Wang, F., Lu, H., Ren, X., and Zou, J. (2014). Chromanol 293B, an inhibitor of KCNQ1 channels, enhances glucose-stimulated insulin secretion and increases glucagon-like peptide-1 level in mice. *Islets* 6:e962386. doi: 10.4161/19382014.2014.962386

Lohrmann, E., Burhoff, I., Nitschke, R. B., Lang, H. J., Mania, D., Englert, H. C., et al. (1995). A new class of inhibitors of cAMP-mediated Cl- secretion in rabbit colon, acting by the reduction of cAMP-activated K+ conductance. *Pflügers Arch. Eur. J. Physiol.* 429, 517–530. doi: 10.1007/bf00704157

Ludwig, A., Zong, X., Jeglitsch, M., Hofmann, F., and Biel, M. (1998). A family of hyperpolarization-activated mammalian cation channels. *Nature* 393, 587–591. doi: 10.1038/31255

Lundby, A., Andersen, M. N., Steffensen, A. B., Horn, H., Kelstrup, C. D., Francavilla, C., et al. (2013). In vivo phosphoproteomics analysis reveals the cardiac targets of beta-adrenergic receptor signaling. *Sci. Signal.* 6:rs11. doi: 10.1126/scisignal.2003506

MacVinish, L. J., Guo, Y., Dixon, A. K., Murrell-Lagnado, R. D., and Cuthbert, A. W. (2001). Xe991 reveals differences in K(+) channels regulating chloride secretion in murine airway and colonic epithelium. *Mol. Pharmacol.* 60, 753–760.

Malaisse, W. J., and Malaisse-Lagae, F. (1984). The role of cyclic AMP in insulin release. *Experientia* 40, 1068–1075. doi: 10.1007/bf01971453

Mall, M., Wissner, A., Schreiber, R., Kuehr, J., Seydewitz, H. H., Brandis, M., et al. (2000). Role of K(v)LQT1 in cyclic adenosine monophosphate-mediated Cl-secretion in human airway epithelia. *Am. J. Respir. Cell Mol. Biol.* 23, 283–289. doi: 10.1165/ajrcmb.23.3.4060

Mani, B. K., Robakowski, C., Brueggemann, L. I., Cribbs, L. L., Tripathi, A., Majetschak, M., et al. (2016). Kv7.5 potassium channel subunits are the primary targets for PKA-dependent enhancement of vascular smooth muscle Kv7 currents. *Mol. Pharmacol.* 89, 323–334. doi: 10.1124/mol.115.101758

Manning, J. A., and Kumar, S. (2018). Physiological functions of Nedd4-2: lessons from knockout mouse models. *Trends Biochem. Sci.* 43, 635–647. doi: 10.1016/j.tibs.2018.06.004

Marrion, N. V. (1997). Control of M-current. *Annu. Rev. Physiol.* 59, 483–504.

Marx, S. O., Kurokawa, J., Reiken, S., Motoike, H., D'Armiento, J., Marks, A. R., et al. (2002). Requirement of a macromolecular signaling complex for beta adrenergic receptor modulation of the KCNQ1-KCNE1 potassium channel. *Science* 295, 496–499. doi: 10.1126/science.1066843

Mayr, B., and Montminy, M. (2001). Transcriptional regulation by the phosphorylation-dependent factor CREB. *Nat. Rev. Mol. Cell Biol.* 2, 599–609. doi: 10.1038/35085068

McCallum, L. A., Greenwood, I. A., and Tribe, R. M. (2009). Expression and function of Kv7 channels in murine myometrium throughout oestrous cycle. *Pflugers Arch. Eur. J. Physiol.* 457, 1111–1120. doi: 10.1007/s00424-008-0567-5

McCrossan, Z. A., and Abbott, G. W. (2004). The MinK-related peptides. *Neuropharmacology* 47, 787–821. doi: 10.1016/j.neuropharm.2004.06.018

Min Lee, S., Baik, J., Nguyen, D., Nguyen, V., Liu, S., Hu, Z., et al. (2017). *Kcne2* deletion impairs insulin secretion and causes type 2 diabetes mellitus. *FASEB J.* 31, 2674–2685. doi: 10.1096/fj.201601347

Moita, M. A. P., Lamprecht, R., Nader, K., and LeDoux, J. E. (2002). A-kinase anchoring proteins in amygdala are involved in auditory fear memory. *Nat. Neurosci.* 5, 837–838. doi: 10.1038/nn901

Moleschi, K., and Melacini, G. (2014). Signaling at crossroads: the dialogue between PDEs and PKA is spoken in multiple languages. *Biophys. J.* 107, 1259–1260. doi: 10.1016/j.bpj.2014.07.051

Mona, A., Xiao-Yan, Q., Ling, X., Balazs, O., Artavazd, T., Xiaobin, L., et al. (2014). Exchange protein directly activated by cAMP mediates slow delayed-rectifier current remodeling by sustained β-adrenergic activation in guinea pig hearts. *Circ. Res.* 114, 993–1003. doi: 10.1161/circresaha.113.302982

Moosmang, S., Biel, M., Hofmann, F., and Ludwig, A. (1999). Differential distribution of four hyperpolarization-activated cation channels in mouse brain. *Biol. Chem.* 380, 975–980. doi: 10.1515/bc.1999.121

Neyroud, N., Tesson, F., Denjoy, I., Leibovici, M., Donger, C., Barhanin, J., et al. (1997). A novel mutation in the potassium channel gene KVLQT1 causes the Jervell and Lange-Nielsen cardioauditory syndrome. *Nat. Genet.* 15, 186–189. doi: 10.1038/ng0297-186

Nicolas, C. S., Park, K.-H., Harchi, A., El Camonis, J., Kass, R. S., Escande, D., et al. (2008). IKs response to protein kinase A-dependent KCNQ1 phosphorylation requires direct interaction with microtubules. *Cardiovasc. Res.* 79, 427–435. doi: 10.1093/cvr/cvn085

Ohya, S., Asakura, K., Muraki, K., Watanabe, M., and Imaizumi, Y. (2002). Molecular and functional characterization of ERG, KCNQ, and KCNE subtypes in rat stomach smooth muscle. *Am. J. Physiol. Gastrointest. Liver Physiol.* 282, G277–G287.

Oliveras, A., Roura-Ferrer, M., Solé, L., La Cruz, A., De Prieto, A., Etxebarria, A., et al. (2014). Functional assembly of Kv7.1/Kv7.5 channels with emerging properties on vascular muscle physiology. *Arterioscler. Thromb. Vasc. Biol.* 34, 1522–1530.

Patra, C., and Brady, M. F. (2018). *Biochemistry, cAMP*. Treasure Island,FL: StatPearls.

Pierce, K. L., Premont, R. T., and Lefkowitz, R. J. (2002). Seven-transmembrane receptors. *Nat. Rev. Mol. Cell Biol.* 3, 639–650.

Potet, F., Scott, J. D., Mohammad-Panah, R., Escande, D., and Baró, I. (2001). AKAP proteins anchor cAMP-dependent protein kinase to KvLQT1/IsK channel complex. *Am. J. Physiol. Circ. Physiol.* 280, H2038–H2045.

Preston, P., Wartosch, L., Günzel, D., Fromm, M., Kongsuphol, P., Ousingsawat, J., et al. (2010). Disruption of the K+ channel beta-subunit KCNE3 reveals

an important role in intestinal and tracheal Cl- transport. *J. Biol. Chem.* 285, 7165–7175. doi: 10.1074/jbc.m109.047829

Rall, T. W., and Sutherland, E. W. (1958). Formation of a cyclic adenine ribonucleotide by tissue particles. *J. Biol. Chem.* 232, 1065–1076.

Rannels, S. R., and Corbin, J. D. (1980). Studies of functional domains of the regulatory subunit from cAMP-dependent protein kinase isozyme I. *J. Cyclic Nucleotide Res.* 6, 201–215.

Renström, E., Eliasson, L., and Rorsman, P. (1997). Protein kinase A-dependent and -independent stimulation of exocytosis by cAMP in mouse pancreatic B-cells. *J. Physiol.* 502(Pt 1), 105–118. doi: 10.1111/j.1469-7793.1997.105bl.x

Ringheim, G. E., and Taylor, S. S. (1990). Dissecting the domain structure of the regulatory subunit of cAMP-dependent protein kinase I and elucidating the role of MgATP. *J. Biol. Chem.* 265, 4800–4808.

Robbins, J. (2001). KCNQ potassium channels: physiology, pathophysiology, and pharmacology. *Pharmacol. Ther.* 90, 1–19. doi: 10.1016/s0163-7258(01)00116-4

Roche, J. P., Westenbroek, R., Sorom, A. J., Hille, B., Mackie, K., and Shapiro, M. S. (2002). Antibodies and a cysteine-modifying reagent show correspondence of M current in neurons to KCNQ2 and KCNQ3 K + channels. *Br. J. Pharmacol.* 137, 1173–1186. doi: 10.1038/sj.bjp.0704989

Rode, F., Svaløø, J., Sheykhzade, M., and Rønn, L. C. B. (2010). Functional effects of the KCNQ modulators retigabine and XE991 in the rat urinary bladder. *Eur. J. Pharmacol.* 638, 121–127. doi: 10.1016/j.ejphar.2010.03.050

de Rooij, J., Zwartkruis, F. J. T., Verheijen, M. H. G., Cool, R. H., Nijman, S. M. B., Wittinghofer, A., et al. (1998). Epac is a Rap1 guanine-nucleotide-exchange factor directly activated by cyclic AMP. *Nature* 396, 474–477. doi: 10.1038/24884

Roscioni, S. S., Elzinga, C. R. S., and Schmidt, M. (2008). Epac: effectors and biological functions. *Naunyn. Schmiedebergs. Arch. Pharmacol.* 377, 345–357. doi: 10.1007/s00210-007-0246-7

Roura-Ferrer, M., Solé, L., Martínez-Mármol, R., Villalonga, N., and Felipe, A. (2008). Skeletal muscle Kv7 (KCNQ) channels in myoblast differentiation and proliferation. *Biochem. Biophys. Res. Commun.* 369, 1094–1097. doi: 10.1016/j.bbrc.2008.02.152

Rubin, C. S. (1994). A kinase anchor proteins and the intracellular targeting of signals carried by cyclic AMP. *Biochim. Biophys. Acta* 1224, 467–479.

Ruehr, M. L., Russell, M. A., and Bond, M. (2004). A-kinase anchoring protein targeting of protein kinase A in the heart. *J. Mol. Cell. Cardiol.* 37, 653–665. doi: 10.1016/j.yjmcc.2004.04.017

Rufo, P. A., Merlin, D., Riegler, M., Ferguson-Maltzman, M. H., Dickinson, B. L., Brugnara, C., et al. (1997). The antifungal antibiotic, clotrimazole, inhibits chloride secretion by human intestinal T84 cells via blockade of distinct basolateral K+ conductances: demonstration of efficacy in the intact rabbit colon and in an in vivo mouse model of cholera. *J. Clin. Invest.* 100, 3111–3120. doi: 10.1172/jci119866

Sadana, R., and Dessauer, C. W. (2009). Physiological roles for G protein-regulated adenylyl cyclase isoforms: insights from knockout and overexpression studies. *Neurosignals.* 17, 5–22. doi: 10.1159/000166277

Salzer, I., Erdem, F. A., Chen, W.-Q., Heo, S., Koenig, X., Schicker, K. W., et al. (2017). Phosphorylation regulates the sensitivity of voltage-gated Kv7.2 channels towards phosphatidylinositol-4,5-bisphosphate. *J. Physiol.* 595, 759–776. doi: 10.1113/jp273274

Sands, W. A., and Palmer, T. M. (2008). Regulating gene transcription in response to cyclic AMP elevation. *Cell. Signal.* 20, 460–466. doi: 10.1016/j.cellsig.2007.10.005

Sanguinetti, M. C., Curran, M. E., Zou, A., Shen, J., Specter, P. S., Atkinson, D. L., et al. (1996). Coassembly of KVLQT1 and minK (IsK) proteins to form cardiac IKS potassium channel. *Nature* 384, 80–83. doi: 10.1038/384080a0

Santoro, B., Liu, D. T., Yao, H., Bartsch, D., Kandel, E. R., Siegelbaum, S. A., et al. (1998). Identification of a gene encoding a hyperpolarization-activated pacemaker channel of brain. *Cell* 93, 717–729. doi: 10.1016/s0092-8674(00)81434-8

Sarma, G. N., Kinderman, F. S., Kim, C., Daake, S., von Chen, L., Wang, B. C., et al. (2010). Structure of D-AKAP2:PKA RI complex: insights into AKAP specificity and selectivity. *Structure* 18, 155–166. doi: 10.1016/j.str.2009.12.012

Sassone-Corsi, P. (1995). Transcription factors responsive to cAMP. *Annu. Rev. Cell Dev. Biol.* 11, 355–377. doi: 10.1146/annurev.cb.11.110195.002035

Schroeder, B. C., Hechenberger, M., Weinreich, F., Kubisch, C., and Jentsch, T. J. (2000a). KCNQ5, a novel potassium channel broadly expressed in brain, mediates M-type currents. *J. Biol. Chem.* 275, 24089–24095. doi: 10.1074/jbc.m003245200

Schroeder, B. C., Kubisch, C., Stein, V., and Jentsch, T. J. (1998). Moderate loss of function of cyclic-AMP-modulated KCNQ2/KCNQ3 K+ channels causes epilepsy. *Nature* 396, 687–690. doi: 10.1038/25367

Schroeder, B. C., Waldegger, S., Fehr, S., Bleich, M., Warth, R., Greger, R., et al. (2000b). A constitutively open potassium channel formed by KCNQ1 and KCNE3. *Nature* 403, 196–199. doi: 10.1038/35003200

Schwake, M., Athanasiadu, D., Beimgraben, C., Blanz, J., Beck, C., Jentsch, T. J., et al. (2006). Structural determinants of M-type KCNQ (Kv7) K+ channel assembly. *J. Neurosci.* 26, 3757–3766. doi: 10.1523/jneurosci.5017-05.2006

Schwake, M., Jentsch, T. J., and Friedrich, T. (2003). A carboxy-terminal domain determines the subunit specificity of KCNQ K+ channel assembly. *EMBO Rep.* 4, 76–81. doi: 10.1038/sj.embor.embor715

Schwake, M., Pusch, M., Kharkovets, T., and Jentsch, T. J. (2000). Surface expression and single channel properties of KCNQ2/KCNQ3, M-type K+ channels involved in epilepsy. *J. Biol. Chem.* 275, 13343–13348. doi: 10.1074/jbc.275.18.13343

Scott, J. D., Dessauer, C. W., and Taskén, K. (2013). Creating order from chaos: cellular regulation by kinase anchoring. *Annu. Rev. Pharmacol. Toxicol.* 53, 187–210. doi: 10.1146/annurev-pharmtox-011112-140204

Scott, J. D., Stofko, R. E., McDonald, J. R., Comer, J. D., Vitalis, E. A., and Mangili, J. A. (1990). Type II regulatory subunit dimerization determines the subcellular localization of the cAMP-dependent protein kinase. *J. Biol. Chem.* 265, 21561–21566.

Seino, S., and Shibasaki, T. (2005). PKA-dependent and PKA-independent pathways for cAMP-regulated exocytosis. *Physiol. Rev.* 85, 1303–1342. doi: 10.1152/physrev.00001.2005

Shabb, J. B. (2001). Physiological substrates of cAMP-dependent protein kinase. *Chem. Rev.* 101, 2381–2411.

Shah, M. M., Mistry, M., Marsh, S. J., Brown, D. A., and Delmas, P. (2002). Molecular correlates of the M-current in cultured rat hippocampal neurons. *J. Physiol.* 544, 29–37. doi: 10.1113/jphysiol.2002.028571

Shariati, B., Thompson, E. L., Nicol, G. D., and Vasko, M. R. (2016). Epac activation sensitizes rat sensory neurons through activation of Ras. *Mol. Cell. Neurosci.* 70, 54–67. doi: 10.1016/j.mcn.2015.11.005

Simonds, W. F. (1999). G protein regulation of adenylate cyclase. *Trends Pharmacol. Sci.* 20, 66–73. doi: 10.1016/s0165-6147(99)01307-3

Sims, S. M., Singer, J.J., and Walsh, J. V. Jr. (1988). Antagonistic adrenergic-muscarinic regulation of M current in smooth muscle cells. *Science* 239, 190–193.

Singh, N. A., Charlier, C., Stauffer, D., DuPont, B. R., Leach, R. J., Melis, R., et al. (1998). A novel potassium channel gene, KCNQ2, is mutated in an inherited epilepsy of newborns. *Nat. Genet.* 18, 25–29. doi: 10.1038/ng0198-25

Steele, D. F., and Fedida, D. (2014). Cytoskeletal roles in cardiac ion channel expression. *Biochim. Biophys. Acta Biomembr.* 1838, 665–673. doi: 10.1016/j.bbamem.2013.05.001

Stott, J. B., Barrese, V., and Greenwood, I. A. (2016). Kv7 channel activation underpins EPAC-dependent relaxations of rat arteries. *Arterioscler. Thromb. Vasc. Biol.* 36, 2404–2411. doi: 10.1161/atvbaha.116.308517

Stott, J. B., Barrese, V., Suresh, M., Masoodi, S., and Greenwood, I. A. (2018). Investigating the role of G protein βγ in Kv7-dependent relaxations of the rat vasculature. *Arterioscler. Thromb. Vasc. Biol.* 38, 2091–2102. doi: 10.1161/atvbaha.118.311360

Stott, J. B., Povstyan, O. V., Carr, G., Barrese, V., and Greenwood, I. A. (2015). G-protein βγ subunits are positive regulators of Kv7.4 and native vascular Kv7 channel activity. *Proc. Natl. Acad. Sci. U.S.A.* 112, 6497–6502. doi: 10.1073/pnas.1418605112

Streng, T., Christoph, T., and Andersson, K. E. (2004). Urodynamic effects of the K+ channel (KCNQ) opener retigabine in freely moving, conscious rats. *J. Urol.* 172, 2054–2058. doi: 10.1097/01.ju.0000138155.33749.f4

Suessbrich, H., Bleich, M., Ecke, D., Rizzo, M., Waldegger, S., Lang, F., et al. (1996). Specific blockade of slowly activating I(sK) channels by chromanols - Impact on the role of I(sK) channels in epithelial. *FEBS Lett.* 396, 271–275. doi: 10.1016/0014-5793(96)01113-1

Sunose, H., Liu, J., and Marcus, D. C. (1997). cAMP increases K+ secretion via activation of apical IsK/KvLQT1 channels in strial marginal cells. *Hear. Res.* 114, 107–116. doi: 10.1016/s0378-5955(97)00152-4

Surti, T. S., Huang, L., Jan, Y. N., Jan, L. Y., and Cooper, E. C. (2005). Identification by mass spectrometry and functional characterization of two phosphorylation sites of KCNQ2/KCNQ3 channels. *Proc. Natl. Acad. Sci. U.S.A.* 102, 17828–17833. doi: 10.1073/pnas.0509122102

Sutherland, E. W., and Rall, T. W. (1958). Fractionation and characterization of a cyclic adenine ribonucleotide formed by tissue particles. *J. Biol. Chem.* 232, 1077–1091.

Svalø, J., Bille, M., Parameswaran Theepakaran, N., Sheykhzade, M., Nordling, J., and Bouchelouche, P. (2013). Bladder contractility is modulated by Kv7 channels in pig detrusor. *Eur. J. Pharmacol.* 715, 312–320. doi: 10.1016/j.ejphar.2013.05.005

Svalø, J., Hansen, H. H., Rønn, L. C. B., Sheykhzade, M., Munro, G., and Rode, F. (2012). Kv7 positive modulators reduce detrusor overactivity and increase bladder capacity in rats. *Basic Clin. Pharmacol. Toxicol.* 110, 145–153. doi: 10.1111/j.1742-7843.2011.00765.x

Taussig, R., and Gilman, A. G. (1995). Mammalian membrane-bound adenylyl cyclases. *J. Biol. Chem.* 270, 1–4. doi: 10.1074/jbc.270.1.1

Taylor, S. S., Ilouz, R., Zhang, P., and Kornev, A. P. (2012). Assembly of allosteric macromolecular switches: lessons from PKA. *Nat. Rev. Mol. Cell Biol.* 13, 646–658. doi: 10.1038/nrm3432

Taylor, S. S., Zhang, P., Steichen, J. M., Keshwani, M. M., and Kornev, A. P. (2013). PKA: lessons learned after twenty years. *Biochim. Biophys. Acta* 1834, 1271–1278. doi: 10.1016/j.bbapap.2013.03.007

Terrenoire, C., Clancy, C. E., Cormier, J. W., Sampson, K. J., and Kass, R. S. (2005). Autonomic control of cardiac action potentials. *Circ. Res.* 96, e25–e34.

Terrenoire, C., Houslay, M. D., Baillie, G. S., and Kass, R. S. (2009). The cardiac I_{Ks} potassium channel macromolecular complex includes the phosphodiesterase PDE4D3. *J. Biol. Chem.* 284, 9140–9146. doi: 10.1074/jbc.m805366200

Testai, L., Barrese, V., Soldovieri, M. V., Ambrosino, P., Martelli, A., Vinciguerra, I., et al. (2016). Expression and function of Kv7.4 channels in rat cardiac mitochondria: possible targets for cardioprotection. *Cardiovasc. Res.* 110, 40–50. doi: 10.1093/cvr/cvv281

Torekov, S. S., Iepsen, E., Christiansen, M., Linneberg, A., Pedersen, O., Holst, J. J., et al. (2014). KCNQ1 long QT syndrome patients have hyperinsulinemia and symptomatic hypoglycemia. *Diabetes* 63, 1315–1325. doi: 10.2337/db13-1454

Tresguerres, M., Levin, L. R., and Buck, J. (2011). Intracellular cAMP signaling by soluble adenylyl cyclase. *Kidney Int.* 79, 1277–1288. doi: 10.1038/ki.2011.95

Turnham, R. E., and Scott, J. D. (2016). Protein kinase A catalytic subunit isoform PRKACA. History, function and physiology. *Gene* 577, 101–108. doi: 10.1016/j.gene.2015.11.052

Tzingounis, A. V., Heidenreich, M., Kharkovets, T., Spitzmaul, G., Jensen, H. S., Nicoll, R. A., et al. (2010). The KCNQ5 potassium channel mediates a component of the afterhyperpolarization current in mouse hippocampus. *Proc. Natl. Acad. Sci. U.S.A.* 107, 10232–10237. doi: 10.1073/pnas.1004644107

Ullrich, S., Su, J., Ranta, F., Wittekindt, O. H., Ris, F., Rösler, M., et al. (2005). Effects of IKs channel inhibitors in insulin-secreting INS-1 cells. *Pflugers Arch. Eur. J. Physiol.* 451, 428–436. doi: 10.1007/s00424-005-1479-2

Unoki, H., Takahashi, A., Kawaguchi, T., Hara, K., Horikoshi, M., Andersen, G., et al. (2008). SNPs in KCNQ1 are associated with susceptibility to type 2 diabetes in East Asian and European populations. *Nat. Genet.* 40, 1098–1102. doi: 10.1038/ng.208

Vallon, V., Grahammer, F., Volkl, H., Sandu, C. D., Richter, K., Rexhepaj, R., et al. (2005). KCNQ1-dependent transport in renal and gastrointestinal epithelia. *Proc. Natl. Acad. Sci. U.S.A.* 102, 17864–17869. doi: 10.1073/pnas.0505860102

Walsh, K. B., and Kass, R. S. (1991). Distinct voltage-dependent regulation of a heart-delayed IK by protein kinases A and C. *Am. J. Physiol.* 261, C1081–C1090.

Walsh, K. B., Kass, R. S., Reiken, S., Motoike, H., D'Armiento, J., Marks, A. R., et al. (1988). Regulation of a heart potassium channel by protein kinase A and C. *Science* 242, 67–69. doi: 10.1126/science.2845575

Wang, H. S., Pan, Z., Shi, W., Brown, B. S., Wymore, R. S., Cohen, I. S., et al. (1998). KCNQ2 and KCNQ3 potassium channel subunits: molecular correlates of the M-channel. *Science* 282, 1890–1893. doi: 10.1126/science.282.5395.1890

Wang, Q., Curran, M. E., Splawski, I., Burn, T. C., Millholland, J. M., VanRaay, T. J., et al. (1996). Positional cloning of a novel potassium channel gene: KVLQT1 mutations cause cardiac arrhythmias. *Nat. Genet.* 12, 17–23. doi: 10.1038/ng0196-17

Warth, R., Garcia Alzamora, M., Kim, J., Zdebik, A., Nitschke, R., Bleich, M., et al. (2002). The role of KCNQ1/KCNE1 K+ channels in intestine and pancreas: lessons from the KCNE1 knockout mouse. *Pflügers Arch. Eur. J. Physiol.* 443, 822–828. doi: 10.1007/s00424-001-0751-3

Weckhuysen, S., Ivanovic, V., Hendrickx, R., Coster, R., Van Hjalgrim, H., Møller, R. S., et al. (2013). Extending the KCNQ2 encephalopathy spectrum: clinical and neuroimaging findings in 17 patients. *Neurology* 81, 1697–1703. doi: 10.1212/01.wnl.0000435296.72400.a1

Weckhuysen, S., Mandelstam, S., Suls, A., Audenaert, D., Deconinck, T., Claes, L. R. F., et al. (2012). KCNQ2 encephalopathy: emerging phenotype of a neonatal epileptic encephalopathy. *Ann. Neurol.* 71, 15–25. doi: 10.1002/ana.22644

Weigand, I., Ronchi, C. L., Rizk-Rabin, M., Dalmazi, G., Di Wild, V., Bathon, K., et al. (2017). Differential expression of the protein kinase A subunits in normal adrenal glands and adrenocortical adenomas. *Sci. Rep.* 7:49.

Welch, E. J., Jones, B. W., and Scott, J. D. (2010). Network with the AKAPs context-dependent regulation of anchored enzymes. *Mol. Interv.* 10, 86–97. doi: 10.1124/mi.10.2.6

Wickenden, A. D., Zou, A., Wagoner, P. K., and Jegla, T. (2001). Characterization of KCNQ5/Q3 potassium channels expressed in mammalian cells. *Br. J. Pharmacol.* 132, 381–384. doi: 10.1038/sj.bjp.0703861

Wong, W., and Scott, J. D. (2004). AKAP signalling complexes: Focal points in space and time. *Nat. Rev. Mol. Cell Biol.* 5, 959–970. doi: 10.1038/nrm1527

Xu, Q., Chang, A., Tolia, A., and Minor, D. L. (2013). Structure of a Ca2+/CaM:Kv7.4 (KCNQ4) B-helix complex provides insight into M current modulation. *J. Mol. Biol.* 425, 378–394. doi: 10.1016/j.jmb.2012.11.023

Yamagata, K., Senokuchi, T., Lu, M., Takemoto, M., Fazlul Karim, M., Go, C., et al. (2011). Voltage-gated K+ channel KCNQ1 regulates insulin secretion in MIN6 β-cell line. *Biochem. Biophys. Res. Commun.* 407, 620–625. doi: 10.1016/j.bbrc.2011.03.083

Yasuda, K., Miyake, K., Horikawa, Y., Hara, K., Osawa, H., Furuta, H., et al. (2008). Variants in KCNQ1 are associated with susceptibility to type 2 diabetes mellitus. *Nat. Genet.* 40, 1092–1097.

Yazawa, K., and Kameyama, M. (1990). Mechanism of receptor-mediated modulation of the delayed outward potassium current in guinea-pig ventricular myocytes. *J. Physiol.* 421, 135–150. doi: 10.1113/jphysiol.1990.sp017937

Zhang, J., Juhl, C. R., Hylten-Cavallius, L., Salling-Olsen, M., Linneberg, A., Holst, J. J., et al. (2020). Gain-of-function mutation in the voltage-gated potassium channel gene KCNQ1 and glucose-stimulated hypoinsulinemia – case report. *BMC Endocr. Disord.* 20:38. doi: 10.1186/s12902-020-0513-x

Zhang, J., and Shapiro, M. S. (2012). Activity-dependent transcriptional regulation of M-type (Kv7) K+ channels by AKAP79/150-mediated NFAT actions. *Neuron* 76, 1133–1146. doi: 10.1016/j.neuron.2012.10.019

Zoller, M. J., Kerlavage, A. R., and Taylor, S. S. (1979). Structural comparisons of cAMP-dependent protein kinases I and II from porcine skeletal muscle. *J. Biol. Chem.* 254, 2408–2412.

Conflict of Interest: The authors declare that the research was conducted in the absence of any commercial or financial relationships that could be construed as a potential conflict of interest.

frontiers in Physiology

ORIGINAL RESEARCH
published: 12 August 2020
doi: 10.3389/fphys.2020.00992

Heteromeric Channels Formed From Alternating Kv7.4 and Kv7.5 α-Subunits Display Biophysical, Regulatory, and Pharmacological Characteristics of Smooth Muscle M-Currents

*Lyubov I. Brueggemann[1], Leanne L. Cribbs[2] and Kenneth L. Byron[1]**

[1] Department of Molecular Pharmacology and Neuroscience, Loyola University Chicago, Maywood, IL, United States,
[2] Department of Cell and Molecular Physiology, Loyola University Chicago, Maywood, IL, United States

OPEN ACCESS

Edited by:
Francesco Miceli,
University of Naples Federico II, Italy

Reviewed by:
Angel Cogolludo,
Complutense University of Madrid, Spain
Harley Takatsuna Kurata,
University of Alberta, Canada

***Correspondence:**
Kenneth L. Byron
kbyron@luc.edu

Specialty section:
This article was submitted to Membrane Physiology and Membrane Biophysics, a section of the journal Frontiers in Physiology

Received: 16 March 2020
Accepted: 21 July 2020
Published: 12 August 2020

Citation:
Brueggemann LI, Cribbs LL and Byron KL (2020) Heteromeric Channels Formed From Alternating Kv7.4 and Kv7.5 α-Subunits Display Biophysical, Regulatory, and Pharmacological Characteristics of Smooth Muscle M-Currents. Front. Physiol. 11:992. doi: 10.3389/fphys.2020.00992

Smooth muscle cells of the vasculature, viscera, and lungs generally express multiple α-subunits of the Kv7 voltage-gated potassium channel family, with increasing evidence that both Kv7.4 and Kv7.5 can conduct "M-currents" that are functionally important for the regulation of smooth muscle contractility. Although expression systems demonstrate that functional channels can form as homomeric tetramers of either Kv7.4 or Kv7.5 α-subunits, there is evidence that heteromeric channel complexes, containing some combination of Kv7.4 and Kv7.5 α-subunits, may represent the predominant configuration natively expressed in some arterial myocytes, such as rat mesenteric artery smooth muscle cells (MASMCs). Our previous work has suggested that Kv7.4/Kv7.5 heteromers can be distinguished from Kv7.4 or Kv7.5 homomers based on their biophysical, regulatory, and pharmacological characteristics, but it remains to be determined how Kv7.4 and Kv7.5 α-subunits combine to produce these distinct characteristics. In the present study, we constructed concatenated dimers or tetramers of Kv7.4 and Kv7.5 α-subunits and expressed them in a smooth muscle cell line to determine if a particular α-subunit configuration can exhibit the features previously reported for natively expressed Kv7 currents in MASMCs. Several unique characteristics of native smooth muscle M-currents were reproduced under conditions that constrain channel formation to a Kv7.4:Kv7.5 stoichiometry of 2:2, with alternating Kv7.4 and Kv7.5 α-subunits within a tetrameric structure. Although other subunit arrangements/combinations are not ruled out, the findings provide new insights into the oligomerization of α-subunits and the ways in which Kv7.4/Kv7.5 subunit assembly can affect smooth muscle signal transduction and pharmacological responses to Kv7 channel modulating drugs.

Keywords: smooth muscle, Kv7.4, Kv7.5, α-subunit stoichiometry, M-current

INTRODUCTION

There are five pore-forming α-subunits (Kv7.1–Kv7.5) in the Kv7 family of voltage-gated potassium channels, each encoded by a single gene (*KCNQ1–KCNQ5*). In smooth muscle cells from various tissues, Kv7.4 and Kv7.5 have been implicated as the predominant contributors to native "M-currents," the name given to the outwardly rectifying Kv7 currents in neurons, which were discovered based on their regulation by muscarinic acetylcholine receptor activation, and subsequently found to be regulated by multiple other G protein-coupled receptor types (Delmas and Brown, 2005). M-currents in smooth muscle cells have also demonstrated regulation by muscarinic acetylcholine receptor activation (Sims et al., 1985; Brueggemann et al., 2012), as well as other smooth muscle contractile and relaxant signal transduction pathways (Byron and Brueggemann, 2018b).

It is widely accepted that functional Kv7 channels form as tetramers of α-subunits. In cellular expression systems, overexpression of either Kv7.4 or Kv7.5 results in functional channels, presumably homomeric tetramers of Kv7.4 or Kv7.5 α-subunits, respectively. However, M-currents through these Kv7.4 and Kv7.5 homomeric channels have distinguishing features. More specifically, we found that Kv7.5 expressed alone yielded M-currents with a more negative $V_{0.5}$ (−44 mV), compared with Kv7.4 expressed alone (−31 mV) (Brueggemann et al., 2011). In addition, Kv7.5 currents were strongly influenced by cellular signaling pathways—enhanced in amplitude by activation of cyclic adenosine monophosphate (cAMP)/protein kinase A (PKA) signaling, and inhibited by protein kinase C (PKC) signaling, whereas Kv7.4 currents were insensitive to these signaling pathways (Brueggemann et al., 2014b; Mani et al., 2016). Finally, a cyclooxygenase-2 inhibitor, diclofenac, induced a rapid and robust inhibition of Kv7.5 currents, but robustly enhanced the M-currents derived from expression of Kv7.4 alone (Brueggemann et al., 2011).

Exogenous *co-expression* of Kv7.4 with Kv7.5 could theoretically result in a mix of homomeric Kv7.4 and Kv7.5 channels, along with heteromeric tetramers that have a combination of both Kv7.4 and Kv7.5 α-subunits. Previous research, using a smooth muscle cell (A7r5 cell) expression system, revealed that M-currents in A7r5 cells co-expressing Kv7.4 with Kv7.5 had another distinct profile, with electrophysiological and pharmacological characteristics that could not be ascribed to a mix of Kv7.4 and Kv7.5 homomers (Brueggemann et al., 2011, 2014a,b; Mani et al., 2016). Co-expression of Kv7.4 and Kv7.5 yielded a voltage-dependent conductance that was well fit by a single Boltzmann function, with an intermediate $V_{0.5}$ (−38 mV) (Brueggemann et al., 2011). The currents displayed partial responsiveness to cAMP/PKA or PKC-dependent regulation (Mani et al., 2016), and a slow moderate inhibition by diclofenac, likely reflecting M-currents generated predominantly by heteromeric Kv7.4/Kv7.5 channels. Notably, native M-currents in mesenteric artery smooth muscle cells (MASMCs), which express both Kv7.4 and Kv7.5, had electrophysiological and pharmacological characteristics that differed from those of Kv7.4 or Kv7.5 homomeric channels, more closely resembling the exogenously co-expressed Kv7.4/Kv7.5 profile.

We sought to determine what form of heteromeric Kv7.4/Kv7.5 tetramers would confer the M-current profile observed in cells that co-express Kv7.4 and Kv7.5. To more effectively control the α-subunit stoichiometry, we constructed concatenated dimers or tetramers of Kv7.4 and Kv7.5 α-subunits and expressed them in A7r5 cells. The resulting M-currents provide new insights into how the oligomerization of α-subunits can influence the biophysical and regulatory characteristics of heteromeric Kv7.4/Kv7.5 channels in smooth muscle cells.

MATERIALS AND METHODS

Constructs

KCNQ5 cDNA encoding FLAG-tagged human Kv7.5 (accession number: AF202977), was a generous gift from Dr. T. Jentsch at the Max-Delbrück-Centrum for Molecular Medicine (Berlin, Germany), and human KCNQ4 (accession number: AF105202) was a generous gift from Dr. Ian Wood at the University of Leeds, Leeds, United Kingdom. Both cDNAs were subcloned into pIRES vectors (pIRES-FLAG-Q5, pIRES-Q4, respectively).

For construction of a Kv7.4-Kv7.5 (Q4–Q5) concatenated dimer vector, polymerase chain reaction (PCR) was used to link pIRES-Q4 to the 5′-end of FLAG-Q5, using primers to introduce *Bsm*BI-*Xho*I termini, targeting the 5′-end of FLAG-Q5 with pIRES-FLAG-Q5 as the template for PCR. The resulting product was inserted into the *Bsm*BI (nt 2040)-*Xho*I (vector) sites of pIRES-Q4. Finally, the *Bsr*GI (nt 343)-*Bsr*GI (vector) fragment of pIRES-FLAG-Q5 was inserted into the same sites of the partial construct resulting in pIRES-Q4-FLAG-Q5 (Q4–Q5).

To construct the reverse concatenated dimer, Kv7.5-Kv7.4 (Q5–Q4), the stop codon in the pIRES-FLAG-Q5 expression clone was eliminated by point mutation TAA to TAC. Polymerase chain reaction primers were used to amplify the first 270 nucleotides of Q4, adding an in-frame *Eco*RI site with the forward primer, using pIRES-Q4 as the template. The PCR product was joined to the 3′-end of pIRES-FLAG-Q5 at the in-frame *Eco*RI site, and lastly, the remaining portion of Q4 added using *Bsm*BI (nt 2014)-*Bam*HI (vector site).

A tetramer of four concatenated Kv7 subunits in the arrangement "Q5–Q4–Q5–Q4" was constructed by assembling the Kv7 dimers (each cloned into pIRES-2-EGFP) as follows. First, a silent point mutation introduced an *Eco*RV site in the Q5–Q4 dimer, creating "(Q5 + RV)–Q4." An in-frame junction linker was created by PCR against the N-terminus of (Q5 + RV)–Q4, introducing 5′ *Bsm*BI and 3′ *Bam*HI, and the PCR product was cloned into Q5–Q4–*Bsm*BI-*Bam*HI (vector). Finally, the Q5–Q4–(Q5 + RV) partial construct was excised from the cloning vector using *Sna*BI (vector)-*Eco*RV, and inserted into the same sites of (Q5 + RV)–Q4 to create "Q5–Q4–Q5–Q4."

QuikChange Lightning Site-Directed Mutagenesis Kit (Agilent Technologies) was used for point mutations. Polymerase chain reaction utilized Platinum II Hot Start PCR Master Mix (Invitrogen). All junctions were sequenced to confirm open

reading frames, and all constructs are depicted schematically in **Supplementary Figure S1**.

Cell Culture

A7r5 cells, an embryonic rat aortic smooth muscle cell line (Kimes and Brandt, 1976), were originally obtained from the ATCC (Byron and Taylor, 1993). A7r5 cells were cultured as described previously (Byron and Taylor, 1993). Kv7 constructs (described in section "Constructs") were introduced into subcultured A7r5 cells by transient transfection with Lipofectamine 3000® transfection reagent according to the manufacturer's protocol. A7r5 cells expressing the Kv7 constructs described in section "Constructs" were used for electrophysiological studies 7–14 days after transfection. No antibiotic resistance selection marker was utilized, but rather cells were selected based on the detection of EGFP fluorescence (EGFP was co-expressed via the bi-cistronic expression vector). The relatively long time (7–14 days) after transfection is intended to address the potential mismatch between overexpressed channels and natively expressed receptor signaling pathways. Previous studies have suggested that robust currents through exogenously expressed Kv7.5 channels in A7r5 cells are initially relatively insensitive to regulation by activation of natively expressed vasopressin receptors, but the signaling capacity adjusts with time after transfection, stabilizing in a week to 10 days to produce regulatory responses similar to those observed with natively expressed Kv7.5 (Byron and Brueggemann, 2018a).

Electrophysiology

We recorded whole cell M-currents using a perforated patch configuration under voltage-clamp conditions. Note that M-currents through exogenously expressed Kv7 channels are approximately 100-fold greater in amplitude than the M-currents recorded through natively expressed Kv7.5 in A7r5 cells (Brueggemann et al., 2009, 2011); the contributions of native Kv7.5 currents to the recordings were therefore deemed negligible. All experiments were conducted at room temperature (20°C) with continuous perfusion of bath solution as described previously (Brueggemann et al., 2007). The standard bath solution contained (in mM): 5 KCl, 130 NaCl, 10 HEPES, 2 $CaCl_2$, 1.2 $MgCl_2$, 5 glucose, pH 7.3. Standard internal (pipette) solution contained (in mM): 110 K gluconate, 30 KCl, 5 HEPES, 1 K_2EGTA, pH 7.2. Osmolality was adjusted to 270 mOsm/l with D-glucose. Amphotericin B (120 μg/ml) in the internal solution was used for membrane patch perforation. An Axopatch 200B amplifier, under control of PCLAMP10 software, was used to generate voltage-clamp command voltages. Series resistances after amphotericin perforation were 8–15 MΩ and were compensated by 60%. Whole-cell currents were digitized at 2 kHz and filtered at 1 kHz, respectively. Prior to treatments, stable M-currents were recorded under control conditions for at least 15 min. M-currents were recorded using a 5 s voltage step protocol from a −74 mV holding potential to test potentials ranging from −124 to −6 mV, followed by a 1 s step to −120 mV (values were corrected for liquid junction potential offline). The instantaneous tail current amplitude (estimated from exponential fit of current deactivation measured at −120 mV) was converted to conductance according to the equation: $G = I_{tail}/(-120 - E_K)$, where I_{tail} is the instantaneous tail current amplitude, −120 mV is the tail current step potential and E_K is the reversal potential for potassium (−86 mV). The resulting conductance plots, recorded in untreated (control) or treated cells, were fitted to a Boltzmann distribution: $G(V) = G_{max}/[1 + \exp(V_{0.5} - V)/k]$, where G is conductance, G_{max} is a maximal conductance, $V_{0.5}$ is the voltage of half-maximal activation and k is the slope factor.

Statistical Analysis

Data were analyzed using SigmaPlot (Systat Software, Inc., San Jose, CA, United States). Data are expressed as mean ± standard error of the mean (SEM). Sample size for each group was not pre-determined, but instead was based on effect size and intrinsic variability within each group under the recording and treatment conditions that were applied. Because of variations in expression levels and cell sizes, current amplitudes for individual cell I–V curves were normalized to the current amplitude achieved with a voltage step to −6 mV under control conditions; all statistical comparisons were performed on normalized data. Two-tailed paired Student's *t*-tests were used to compare parameters measured before and after treatments. For comparisons between two independent groups, two-tailed *t*-tests were used. Differences among multiple treatment groups were assessed by analysis of variance (ANOVA) followed by a Holm−Sidak *post hoc* test. Differences were considered statistically significant with P values ≤ 0.05. All groups were included in multiple groups ANOVA testing with no exceptions and results from all performed intergroup comparisons are reported irrespective of outcome.

RESULTS

Kv7.4–Kv7.5 (Q4–Q5) Dimers

To intentionally generate M-currents specifically from Kv7.4/Kv7.5 heteromers, we constructed an expression vector (Q4–Q5) designed to produce a concatenated dimer, with the N-terminus of Kv7.5 tethered to the C-terminus of Kv7.4, with the expectation that the expressed dimer pairs would assemble to form tetrameric channels containing two Kv7.4 α-subunits and two Kv7.5 α-subunits. Expression of this construct in A7r5 cells resulted in M-currents similar to those previously recorded when Kv7.4 and Kv7.5 were co-expressed via separate vectors in A7r5 cells, with an outwardly rectifying current-voltage profile, but with a significantly more negative $V_{0.5}$ of approximately −48 mV [**Figure 1**; $V_{0.5}$ was ∼−40 mV when Kv7.4 and Kv7.5 were co-expressed (Brueggemann et al., 2011, 2014b)].

We then tested treatments previously found to distinguish among Kv7.4 homomers, Kv7.5 homomers, and Kv7.4/Kv7.5 heteromers. Neither a robust cAMP/PKA-activating stimulus [combination of the adenylyl cyclase activator, forskolin (10 μM) with a cAMP phosphodiesterase inhibitor, isobutylmethylxanthine (IBMX, 500 μM)], nor a more physiological cAMP/PKA-activating stimulus (the β-adrenergic receptor agonist, isoproterenol, 1 μM), had any significant effect on M-currents via channels formed from Q4–Q5 dimers

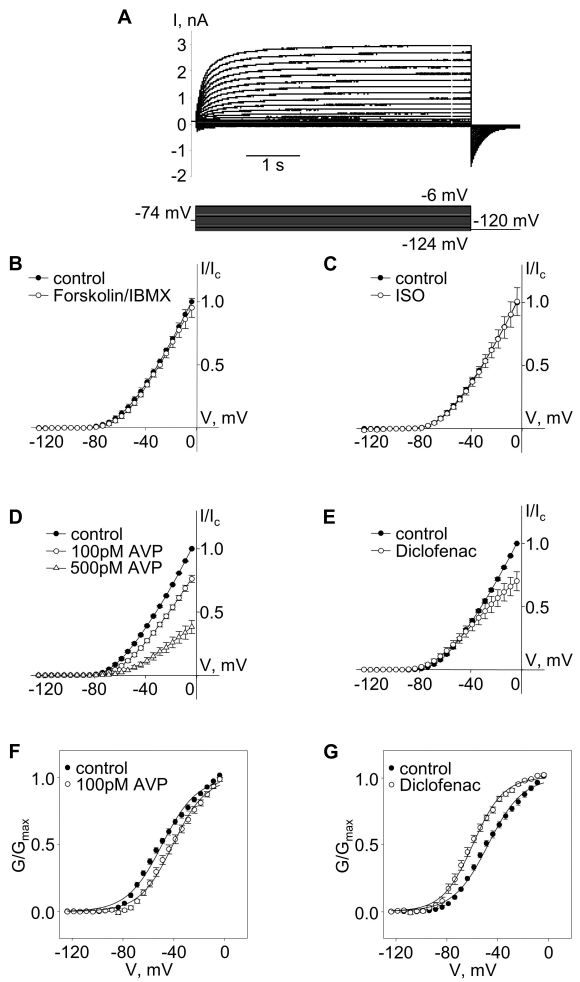

FIGURE 1 | M-currents through channels formed from Kv7.4–7.5 (Q4–Q5) dimers were insensitive to cAMP/PKA activation but were sensitive to AVP and diclofenac. **(A)** Representative superimposed raw current traces recorded from a cell expressing Q4–Q5 dimers subjected to a series of voltage steps applied from a holding voltage of −74 mV to test potentials ranging from −124 to −6 mV, followed by a step back to −120 mV. **(B–E)** Average normalized current–voltage (I–V) relationships in A7r5 cells expressing Q4–Q5 dimers, before (closed circles) and during application of **(B)** 10 μM forskolin in combination with 500 μM IBMX (Forskolin/IBMX for 15 min, open circles, $n = 4$), **(C)** 1 μM isoproterenol (ISO for 15 min, open circles, $n = 4$), **(D)** AVP (100 pM AVP for 15 min, open circles, followed by 500 pM AVP for 15 min open triangles, $n = 4$), **(E)** diclofenac [100 μM for 15 min, open circles, $n = 4$, **(D)**]. **(F,G)** Mean fractional conductance plots calculated from tail currents measured before (closed circles) and during application of **(F)** 100 pM AVP (open circles, $n = 4$) or **(G)** 100 μM diclofenac (open circles, $n = 4$) fitted to the Boltzmann distribution.

(**Figures 1B,C**; effects of treatments on current amplitude were assessed based on differences between currents measured following a voltage step to −20 mV under control conditions (before treatment) and following treatment for 10 min, using a paired Student's *t*-test). In contrast, treatment with arginine–vasopressin (AVP, 100 pM, 500 pM, a PKC-activating stimulus) induced a significant concentration-dependent suppression of the current amplitude (∼25% decrease, on average, at −20 mV with 100 pM AVP, $P = 0.005$ based on a paired Student's *t*-test, $n = 4$). The suppression of the current amplitude by 100 pM AVP was associated with a significant positive shift of the conductance plot (∼9 mV on average, $P = 0.007$, $n = 4$, **Figures 1D,F**; effects of treatments on voltage-dependence of activation were assessed based on differences between $V_{0.5}$ measured under control conditions (before treatment) and following treatment for 10 min, using a paired Student's *t*-test). Diclofenac (100 μM), was previously found to block Kv7.5 homomers, but to robustly enhance Kv7.4 homomers. The same treatment induced a very modest suppression of Q4–Q5 currents at voltages between −40 and 0 mV (**Figure 1E**). This effect of 100 μM diclofenac was associated with an approximately 12 mV negative shift of the Q4–Q5 voltage dependence of activation (a significant change in $V_{0.5}$, based on a paired Student's *t*-test, $P = 0.022$, $n = 4$, **Figure 1G**), similar to its previously reported effect on M-currents in A7r5 cells that co-expressed Kv7.4 and Kv7.5 (Brueggemann et al., 2011).

Kv7.5–Kv7.4 (Q5–Q4) Dimers

A cAMP/PKA-dependent enhancement of currents through Kv7.5 channels (and to a lesser extent though heteromeric Kv7.4/Kv7.5 channels) was previously attributed to phosphorylation of a serine residue (S53) found on the cytosolic N-terminal segment of the Kv7.5 α-subunit (but absent on Kv7.4, which, when expressed alone, was insensitive to cAMP/PKA-activating stimuli) (Brueggemann et al., 2018, 2020). The results shown in **Figures 1B,C** suggest that, unlike previous recordings of M-currents through co-expressed Kv7.4 and Kv7.5, M-currents through channels formed from Q4–Q5 dimers were completely insensitive to cAMP/PKA-activating stimuli. We considered that perhaps the tethering of the Kv7.5 N-terminus to the C-terminus of Kv7.4 in channels formed by the Q4–Q5 dimers might constrain the position of the S53 site and hence render the channels insensitive or unresponsive to regulation by PKA.

We constructed an expression vector for concatenated Q5–Q4 dimers, with α-subunits assembled in the opposite order to free up the Kv7.5 N-terminus S53 site (in this case the C-terminus of Kv7.5 was tethered to the N-terminus of Kv7.4). Expression of the Q5–Q4 dimer construct yielded M-currents with a $V_{0.5}$ of ∼−47 mV, similar to Q4–Q5, but in this case the currents were modestly, but significantly, enhanced by forskolin/IBMX treatment, and tended to be slightly enhanced in the presence of isoproterenol, though that effect was not significant. The effects of AVP and diclofenac were similar to what was observed for Q4–Q5 dimers, both in terms of suppression of current amplitude and the opposite shifts in voltage dependence (**Figure 2**).

Kv7.5–Kv7.4–Kv7.5–Kv7.4 (Q5–Q4–Q5–Q4) Tetramers

The Q5–Q4 dimer expression yielded M-currents with several characteristics that matched previous measurements of M-current in A7r5 cells co-expressing Kv7.4 and Kv7.5,

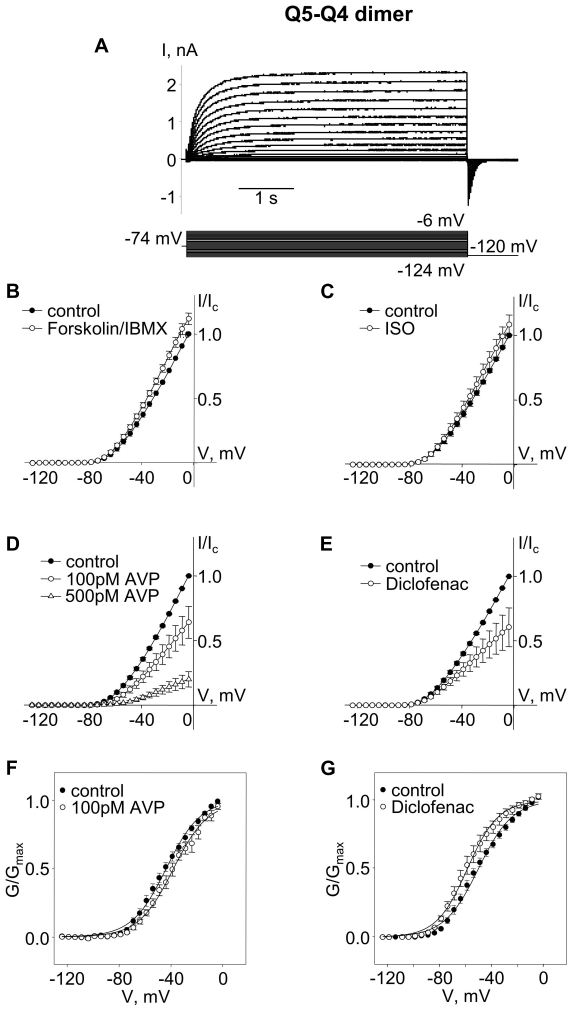

FIGURE 2 | M-currents through channels formed from Kv7.5–7.4 (Q5–Q4) dimers were sensitive to cAMP/PKA activation and sensitive to AVP and diclofenac. **(A)** Representative superimposed raw current traces recorded from a cell expressing Q5–Q4 dimers subjected to a series of voltage steps applied from a holding voltage of −74 mV to test potentials ranging from −124 to −6 mV, followed by a step back to −120 mV. **(B–E)** Average normalized current–voltage (I–V) relationships of Q5–Q4 dimer before (closed circles) and during application of 10 μM forskolin in combination with 500 μM IBMX [Forskolin/IBMX for 15 min, open circles, n = 6, **(B)**], 1 μM isoproterenol [ISO for 15 min, open circles, n = 4, **(C)**], AVP [100 pM AVP for 15 min, open circles, followed by 500 pM AVP for 15 min open triangles, *n* = 5, **(D)**], diclofenac [100 μM for 15 min, open circles, *n* = 4, **(E)**]. **(F,G)** Mean fractional conductance plots calculated from tail currents measured before (closed circles) and during application of 100 pM AVP [open circles, *n* = 5, **(F)**] or 100 μM diclofenac [open circles, *n* = 4, **(G)**] fitted to the Boltzmann distribution.

supporting a likely tetramer stoichiometry of two Kv7.4 and two Kv7.5. Although the dimers might be expected to assemble in a head-to-tail format with alternating α-subunits (e.g., Q4–Q5–Q4–Q5), we could not rule out a side-by-side assembly, such that like α-subunits are adjacent (e.g., Q4–Q4–Q5–Q5). To force an alternating α-subunit assembly, we made an expression vector for a tetrameric concatemer of Q5–Q4–Q5–Q4. Expression of this Q5–Q4–Q5–Q4 construct in A7r5 cells resulted in M-currents (**Figure 3A**) that resembled those from the Q5–Q4 dimers in terms of $V_{0.5}$ (∼−51 mV) and responses to forskolin/IBMX or isoproterenol (**Figures 3B,C**). These M-currents were slightly less sensitive to AVP, with an insignificant suppression of current amplitude or shift in $V_{0.5}$ by 100 pM AVP, but a significant suppression of current amplitude by 500 pM AVP (**Figures 3D,F**). Diclofenac did not significantly alter the current amplitude, but there was still a ∼12 mV mean negative shift in the $V_{0.5}$ of Q5–Q4–Q5–Q4 M-currents in the presence of diclofenac [**Figures 3E,G**, p = 0.022 (Student's paired t-test), n = 6].

M-Current Comparisons Among Kv7.4/Kv7.5 Heteromers From Co-expression, Dimer Expression, or Tetramer Expression

cAMP/PKA-Activating Stimuli

We compared the enhancing effects of forskolin/IBMX (**Figure 4A**) or isoproterenol (**Figure 4B**) on M-currents in A7r5 cells expressing Q4–Q5 dimers, Q5–Q4 dimers, or Q5–Q4–Q5–Q4 tetramers to M-currents measured in A7r5 cells co-expressing Kv7.4 and Kv7.5 (Q4 + Q5, based on data from results originally reported in Mani et al., 2016). Channels that formed from Q4–Q5 dimers were unresponsive to either the more robust cAMP/PKA-activating stimulus (forskolin/IBMX), or to isoproterenol (in both cases, significantly less responsive than channels formed from co-expressed Kv7.4 and Kv7.5). Expression of the reverse dimer (Q5–Q4) and the Q5–Q4–Q5–Q4 constructs produced M-currents that responded to forskolin/IBMX like the co-expressed Kv7.4/Kv7.5 M-currents, but they were slightly less sensitive to isoproterenol.

AVP and Diclofenac Effects on M-Current Amplitude

Arginine–vasopressin induced a similar concentration-dependent suppression of current amplitude in heteromeric Kv7.4/Kv7.5 channels regardless of whether they formed by co-expression of the individual α-subunits or by expression of Q4–Q5 dimers, Q5–Q4 dimers, or Q5–Q4–Q5–Q4 tetramers (**Figure 5A**). Diclofenac reduced M-current amplitude at −20 mV in cells co-expressing Kv7.4 and Kv7.5, though there was considerable variability in the extent of the effect, with some cells unaffected and others with robust suppression of the M-currents (**Figure 5B**, Q4 + Q5, black bar, based on results from Brueggemann et al., 2011). Cells expressing Q4–Q5 or Q5–Q4 dimers displayed a somewhat more uniform modest suppression of M-currents by diclofenac (**Figure 5B**, red and blue bars, respectively), with a mean response that did not differ significantly from the Kv7.4 and Kv7.5 co-expressing cells (Q4 + Q5). The tetrameric Q5–Q4–Q5–Q4 construct was significantly less affected by diclofenac in terms of its M-current amplitude at −20 mV (**Figure 5B**, green bar).

Voltage-Dependence of Activation

The voltages of half-maximal activation ($V_{0.5}$) of Kv7.4/Kv7.5 heteromers formed by co-expressed individual Kv7.4 and Kv7.5

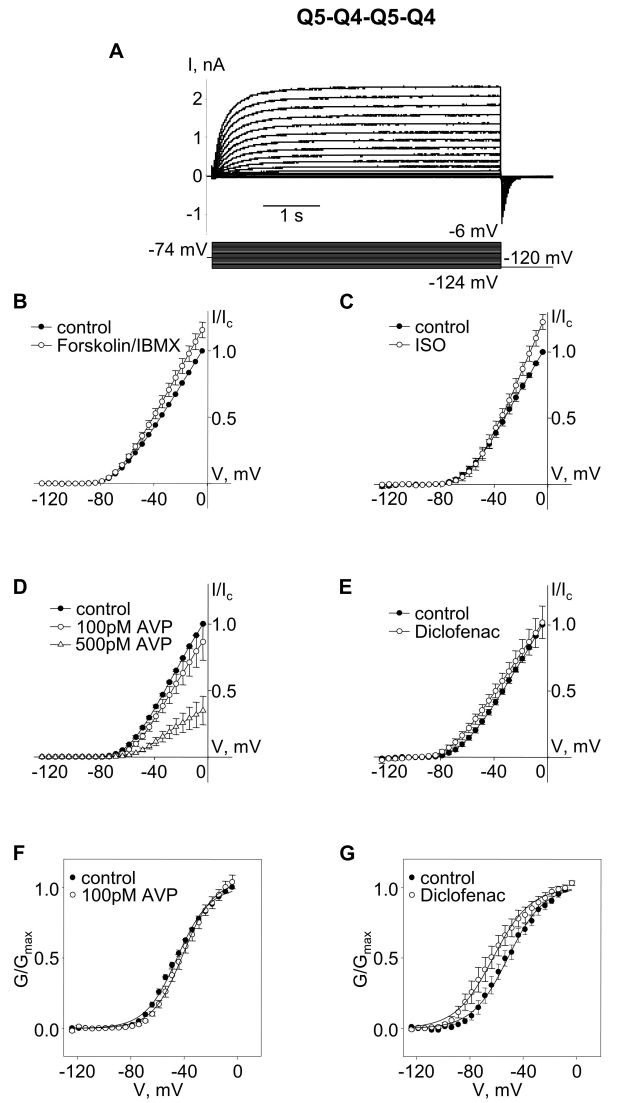

FIGURE 3 | M-currents through channels formed from concatenated Kv7.5–7.4–7.5–7.4 (Q5–Q4–Q5–Q4) tetramers were sensitive to cAMP/PKA activation and diclofenac, and sensitive to 500 pM AVP. **(A)** Representative superimposed raw current traces recorded from a cell expressing Q5–Q4–Q5–Q4 tetramers subjected to a series of voltage steps applied from a holding voltage of −74 mV to test potentials ranging from −124 to −6 mV, followed by a step back to −120 mV. **(B–E)** Average normalized current–voltage (I–V) relationships of concatenated Q5–Q4–Q5–Q4 before (closed circles) and during application of 10 μM forskolin in combination with 500 μM IBMX [Forskolin/IBMX for 15 min, open circles, *n* = 6, **(B)**], 1 μM isoproterenol [ISO for 15 min, open circles, *n* = 4, **(C)**], AVP [100 pM AVP for 15 min, open circles, followed by 500 pM AVP for 15 min open triangles, *n* = 5, **(D)**], diclofenac [100 μM for 15 min, open circles, *n* = 6, **(E)**]. **(F,G)** Mean fractional conductance plots calculated from tail currents measured before (closed circles) and during application of 100 pM AVP [open circles, *n* = 5, **(F)**] or 100 μM diclofenac [open circles, *n* = 6, **(G)**] fitted to the Boltzmann distribution.

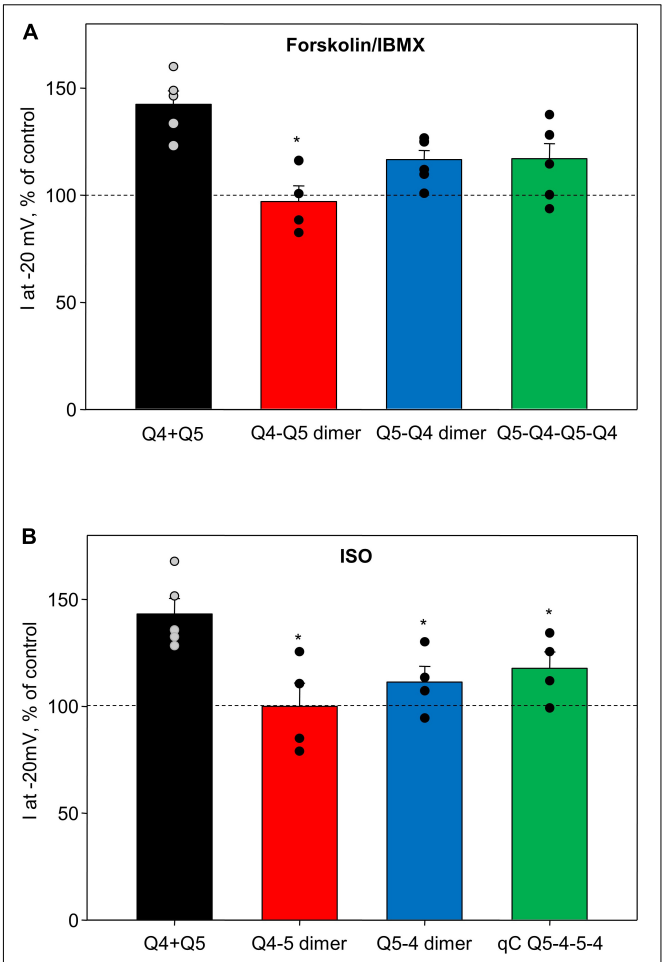

FIGURE 4 | Summary of forskolin/IBMX and isoproterenol-induced increase in current amplitude of Q4–Q5 dimers, Q5–Q4 dimers, and Q5–Q4–Q5–Q4 tetramers, in comparison with M-currents through channels formed from co-expressed individual Kv7.4 and Kv7.5 α-subunits (Q4 + Q5). **(A)** Summarized bar graph of forskolin/IBMX (10 and 500 μM, respectively) -induced current enhancement through co-expressed individual Kv7.4 and Kv7.5 channels (Q4 + Q5, black, *n* = 5), Q4–Q5 dimer (red, *n* = 4), Q5–Q4 dimers (blue, *n* = 6), and Q5–Q4–Q5–Q4 tetramers (green, *n* = 6), measured at −20 mV. *Significant difference from co-expressed individual Kv7.4 and Kv7.5 channels (*P* = 0.002, One Way ANOVA). **(B)** Summarized bar graph of isoproterenol (1 μM)-induced current enhancement through co-expressed individual Kv7.4 and Kv7.5 channels (Q4 + Q5, black, *n* = 5), Q4–Q5 dimer (red, *n* = 4), Q5–Q4 dimers (blue, *n* = 4), and Q5–Q4–Q5–Q4 tetramer (green, *n* = 4), measured at −20 mV. *Significant difference from co-expressed individual Kv7.4 and Kv7.5 channels (*P* = 0.015, One Way ANOVA). Dashed lines indicate control current level.

α-subunits (Q4 + Q5, based on results from Brueggemann et al., 2011, 2014b; Mani et al., 2016), Q4–Q5 dimers, Q5–Q4 dimers, and Q5–Q4–Q5–Q4 tetramers are compared in **Figure 6A**.

The dimeric and tetrameric constructs all formed channels that activate at significantly more negative voltages (**Figure 6A**, red, blue, and green bars), compared with channels formed as a result of co-expression of the individual α-subunits (**Figure 6A**, black bar). However, the effects of 100 pM AVP and diclofenac on $V_{0.5}$ were not significantly different among channels formed from co-expressed or concatenated constructs: AVP induced a positive shift of $V_{0.5}$, ranging from ∼4 to 9 mV (**Figure 6Bi**), while diclofenac (100 μM) induced a negative shift that tended

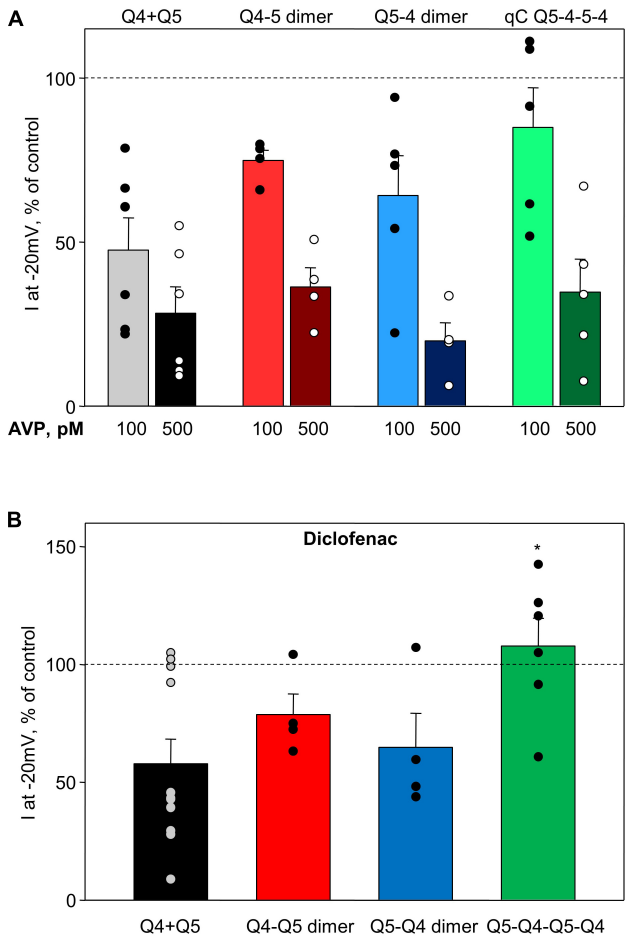

FIGURE 5 | Summary of AVP and diclofenac-induced decrease in M-current amplitude of Q4–Q5 dimers, Q5–Q4 dimers, and Q5–Q4–Q5–Q4 tetramers, in comparison with M-currents through channels formed from co-expressed individual Kv7.4 and Kv7.5 α-subunits (Q4 + Q5). **(A)** Summarized bar graph of AVP (100 pM light color and 500 μM dark color, respectively)-induced current suppression through co-expressed individual Kv7.4 and Kv7.5 α-subunits (Q4 + Q5, gray/black, $n = 6$), Q4–Q5 dimers (red, $n = 4$), Q5–Q4 dimers (blue, $n = 5$), and Q5–Q4–Q5–Q4 tetramers (green, $n = 5$), measured at −20 mV. **(B)** Summarized bar graph of diclofenac (100 μM)-induced current suppression through co-expressed individual Kv7.4 and Kv7.5 α-subunits (Q4 + Q5, black, $n = 11$), Q4–Q5 dimer (red, $n = 4$), Q5–Q4 dimers (blue, $n = 4$), and Q5–Q4–Q5–Q4 tetramers (green, $n = 6$), measured at −20 mV. *Significant difference from co-expressed individual Kv7.4 and Kv7.5 channels ($P = 0.031$, One Way ANOVA). Dashed lines indicate control current level.

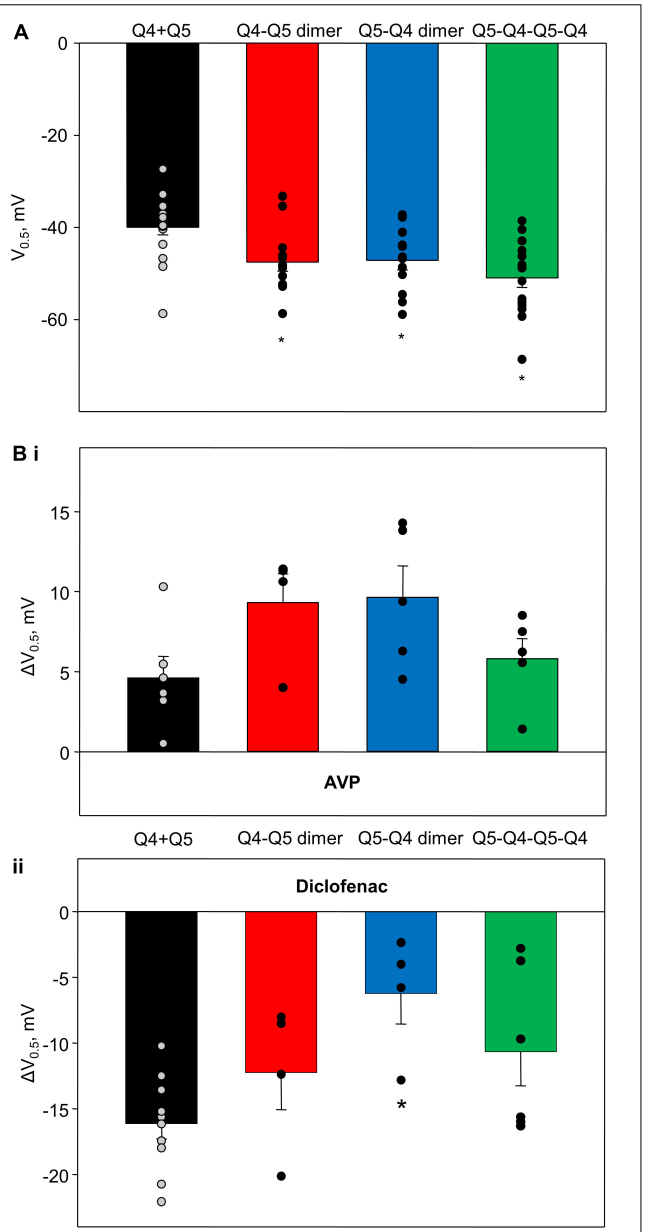

FIGURE 6 | Voltage of half-maximal activation of M-currents through channels formed from Q4–Q5 dimers, Q5–Q4 dimers, and Q5–Q4–Q5–Q4 tetramers, in comparison with co-expressed individual Kv7.4 and Kv7.5 α-subunits (Q4 + Q5), and effects of AVP and diclofenac on voltage of half-maximal activation of corresponding channels. **(A)** Voltage of half-maximal activation ($V_{0.5}$) of Kv7.4/Kv7.5 channels formed by co-expressed individual Kv7.4 and Kv7.5 V (Q4 + Q5, black, $n = 17$), Q4–Q5 dimers (red, $n = 12$), Q5–Q4 dimers (blue, $n = 13$), and Q5–Q4–Q5–Q4 tetramers (green, $n = 17$). *Significant difference from co-expressed individual Kv7.4 and Kv7.5 channel α-subunits ($P < 0.001$, One Way ANOVA). **(Bi)** AVP (100 pM)-induced positive shift of $V_{0.5}$ of Kv7.4/Kv7.5 channels formed by co-expressed individual Kv7.4 and Kv7.5 α-subunits (Q4 + Q5, black, $n = 6$), Q4–Q5 dimers (red, $n = 4$), Q5–Q4 dimers (blue, $n = 5$), and Q5–Q4–Q5–Q4 tetramers (green, $n = 5$). **(Bii)** Diclofenac (100 μM)-induced negative shift of $V_{0.5}$ of Kv7.4/Kv7.5 channels formed by co-expressed individual Kv7.4 and Kv7.5 α-subunits (Q4 + Q5, black, $n = 11$), Q4–Q5 dimers (red, $n = 4$), Q5–Q4 dimers (blue, $n = 4$), and Q5–Q4–Q5–Q4 tetramers (green, $n = 6$). *Significant difference from co-expressed individual Kv7.4 and Kv7.5 α-subunits ($P = 0.016$, One Way ANOVA).

to be greater in co-expressed Q4 + Q5 channels (**Figure 6Bii**, black bar), but was not significantly different from the effect measured in cells expressing the dimeric or tetrameric constructs (**Figure 6Bii**, red, blue, and green bars).

DISCUSSION

Heteromeric channels containing Kv7.4 and Kv7.5 α-subunits remain among the least characterized subtypes of Kv7 channels despite increasing evidence that they are likely the predominant

contributors to M-currents in many types of smooth muscle cells. A fundamental unanswered question is how do the α-subunits assemble to account for the properties of M-currents recorded in smooth muscle myocytes? Expressing concatenated dimers of Kv7.4 and Kv7.5, and concatenated tetramers with alternating Kv7.5 and Kv7.4 α-subunits in a smooth muscle cell line revealed that the previously reported unique characteristics of native smooth muscle M-currents can be largely reproduced under conditions that favor a 2 Kv7.4: 2 Kv7.5 stoichiometry, with alternating Kv7.4 and Kv7.5 α-subunits within a tetrameric structure. The results further revealed that responses to cAMP/PKA-activating stimuli appear to require unconstrained Kv7.5 N-termini for full effect.

Heteromeric Kv7.4/Kv7.5 Channels Behave Differently From Homomeric Kv7.4 and Homomeric Kv7.5 in a Smooth Muscle Expression System

Previous studies had revealed some notable differences in the effects of treatments on homomeric Kv7.4 and homomeric Kv7.5 currents using A7r5 smooth muscle cells as an expression system. Mani et al. reported that the combination of forskolin (10 μM) with IBMX (500 μM) increased current amplitude at −20 mV by ∼2.5-fold in cells overexpressing Kv7.5 channels, but had no detectable effect when Kv7.4 was overexpressed by itself (Mani et al., 2016). In another previous study, in A7r5 cells overexpressing Kv7.5 alone, AVP treatment significantly reduced Kv7.5 current amplitude at −20 mV by 66 ± 7% (n = 9) and 80 ± 6% (n = 6), with 100 and 500 pM AVP, respectively; in contrast, in A7r5 cells overexpressing Kv7.4 alone, AVP (100 or 500 pM) had no significant effect on the current amplitude (Brueggemann et al., 2014b). We also previously found that a pharmacological agent, diclofenac, had diametrically opposite effects on currents via Kv7.4 and Kv7.5 homomers overexpressed in A7r5 cells (Brueggemann et al., 2011). Stable Kv7.5 currents recorded at a −20 mV holding voltage were abruptly inhibited by 100 μM diclofenac treatment, whereas the same treatment in A7r5 cells overexpressing Kv7.4 alone resulted in ∼1.5-fold increase in current amplitude at the same holding voltage (Brueggemann et al., 2011).

In each of the previous studies (Brueggemann et al., 2011, 2014b; Mani et al., 2016), the effects of the treatments on cells co-expressing Kv7.4 and Kv7.5 were distinct from those elicited when either subunit was expressed alone. Notably the responses of the cells and the characteristics of the currents measured in A7r5 cells co-expressing Kv7.4 and Kv7.5 were similar to those measured in freshly isolated arterial myocytes from rat mesenteric arteries (Mackie et al., 2008; Brueggemann et al., 2011; Mani et al., 2016). Proximity ligation assays and results of co-immunoprecipitation studies supported a direct physical interaction between Kv7.4 and Kv7.5 α-subunits in both the A7r5 cell expression system and in the arterial myocytes (Brueggemann et al., 2014b), though it could not be determined whether channels with a particular subunit assembly pattern could account for the distinct responses to the treatments. To control the assembly of α-subunits within tetrameric channels, we constructed concatenated dimers of Kv7.4 and Kv7.5, and concatenated tetramers with alternating Kv7.5 and Kv7.4 α-subunits and measured their behavior in the same smooth muscle cell line.

Concatenated α-Subunits as a Model to Study Kv Channel Structure/Function

The pore-forming structures of many types of ion channels are thought to form as oligomeric assemblies of α-subunits, with Kv channels forming as tetramers of α-subunits (Catterall, 1988; Brueggemann et al., 2013). The Kv α-subunit proteins are encoded by individual genes in the cell, enabling multiple gene products to assemble in a variety of combinations. In native cell systems that express multiple Kv α-subunit genes, there is a distinct potential for a mix of Kv channel subtypes with different combinations of α-subunits, making the characteristics of tetrameric channels of a particular α-subunit composition difficult to resolve. One experimental approach that has been used to understand how α-subunit assembly affects channel function and pharmacological responsiveness is the overexpression of concatenated DNA constructs that constrain the assembly of α-subunits in certain orders or stoichiometries. For example, Hurst et al. (1992, 1995) created concatenated Kv1.1 constructs, linking four copies of the Kv1.1 cDNA 3′–5′, thereby producing a single DNA vector encoding four Kv1.1 α-subunits, with the C-terminus of one subunit connected to the N-terminus of the next. Expression of this construct in *Xenopus* oocytes yielded Kv currents that resembled the currents generated by overexpression of individual (non-concatenated) Kv1.1 α-subunits, which presumably assemble into tetramers (Hurst et al., 1992).

The characteristics of heteromeric Kv channels were also studied using concatenated constructs in the work of Wimmers et al. (2002). In that study, cDNAs encoding Kv11.1, Kv11.2, and Kv11.3 α-subunits (*erg1*, *erg2*, and *erg3*, respectively) were linked 5′–3′ in pairs, and expressed in Chinese Hamster Ovary (CHO) cells. The authors speculated that expression of alternating α-subunit dimeric constructs (e.g., *erg1–erg2*) would result in channels that formed as dimer pairs in a head-to-tail arrangement; for example, *erg1–erg2* dimer expression would produce channels with alternating Kv11.1 and Kv11.2 α-subunits in the tetrameric structure (Wimmers et al., 2002). They found that *erg1–erg1* dimer expression yielded Kv currents that were similar to currents generated when *erg1* monomer was expressed, with slight differences in kinetics of activation and inactivation; in contrast, *erg1–erg2*, *erg1–erg3*, and *erg3–erg2* dimer constructs generated channels with distinct electrophysiological characteristics, though their regulation by physiological or pharmacological modulators was not examined (Wimmers et al., 2002).

Recent work from the Kurata laboratory utilized concatenated *kcnq2* and *kcnq3* constructs to determine whether Kv7 channel activating drugs exert their effects by binding to individual α-subunits, or by binding to multiple α-subunits within the tetrameric channel structures (Wang et al., 2018; Yau et al., 2018).

They utilized mutations that prevent the drug effects to determine that retigabine, a Kv7 channel activator, need interact with only a single retigabine-sensitive α-subunit within a tetrameric Kv7.3 channel to exert its full effect (Wang et al., 2018), whereas another Kv7 channel activator, ICA-069673, required four responsive α-subunits within Kv7.2 channels for its full response (Yau et al., 2018). Although these studies demonstrated that concatenated Kv7 channels are functional in an expression system (*Xenopus* oocytes), the physiological regulation of the channels was not explored.

The findings presented in this article represent the first evidence that heteromeric Kv7.4/Kv7.5 channels can form from expressed concatenated dimers or tetramers of the Kv7.4 and Kv7.5 α-subunits. The features previously found to distinguish Kv7.4/Kv7.5 heteromers from Kv7.4 and Kv7.5 homomeric channels, including their responses to physiological signaling pathways that positively or negatively regulate channel activity, were generally reproduced in M-currents through channels formed from the concatenated Kv7.4 and Kv7.5 α-subunit dimers or tetramers.

In the present study, the concatenated dimer results reveal that the α-subunit order is important, particularly for sensitivity to cAMP/PKA-activating stimuli. M-currents derived from expression of Q4–Q5 dimers were insensitive to forskolin/IBMX, compared with at least modest responsiveness of M-currents derived from expression of Q5–Q4 dimers. This difference may relate to the position of a previously identified N-terminal target for PKA: a serine at position 53 of the Kv7.5 N-terminal segment. In channels formed from individually expressed α-subunits, the Kv7.5 N-terminus would have relatively unconstrained mobility on the cytosolic side of the channel. In contrast, in Q4–Q5 dimers, the Kv7.5 N-terminal S53 site would be found in the concatenated segment between subunits, which may constrain its position in a way that shields it from phosphorylation by PKA. Alternatively, its localization in the segment that tethers two adjacent α-subunits may prevent the phosphorylated serine residue from interacting with the channel structure in a way that would increase its open probability [e.g., by enhancing the channel's affinity for phosphatidylinositol 4,5-bisphosphate, as previously proposed (Brueggemann et al., 2020)]. According to these lines of reasoning, in the oppositely ordered Q5–Q4 dimer, the position of the Kv7.5 N-terminal S53 site is unconstrained, which would account for its greater sensitivity to cAMP/PKA-activating stimuli. Presumably, the second Q5 in the Q5–Q4–Q5–Q4 tetramer would be "shielded" from PKA regulation, though its enhancement by PKA-activating stimuli was about the same as for Q5–Q4 dimers, suggesting that availability of a single free Q5 N-terminus may be sufficient to confer PKA regulation.

The α-subunit order in concatenated dimers was apparently less important for other features, such as the $V_{0.5}$, suppression by AVP, and the effects of diclofenac on current amplitude and voltage sensitivity, all of which were similar in M-currents of cells expressing either Q4–Q5 or Q5–Q4 dimers. The Q5–Q4–Q5–Q4 concatenated tetramer differed only in its insensitivity to suppression of current amplitude by diclofenac (each of the dimer constructs generated M-currents whose amplitudes at −20 mV were modestly suppressed by diclofenac), though a diclofenac-induced negative shift in $V_{0.5}$ was apparent in both dimeric and tetrameric concatemers. It is notable that these responses to diclofenac are very different from the responses of homomeric Kv7.4 and homomeric Kv7.5. In A7r5 cells expressing Kv7.5 alone, 100 μM diclofenac induced a rapid voltage-dependent block, that was not observed in cells expressing Kv7.4 alone; the effect on Kv7.5 was accompanied by a robust (∼30 mV) negative shift in $V_{0.5}$ (Brueggemann et al., 2011). In the case of Kv7.4 homomers, 100 μM diclofenac enhanced the current amplitude (by ∼40% at −20 mV) and negatively shifted $V_{0.5}$ by ∼10 mV (Brueggemann et al., 2011). Co-expression of Kv7.4 and Kv7.5 in A7r5 cells produced M-currents that were neither enhanced nor inhibited by 100 μM diclofenac at −20 mV, but which demonstrated an intermediate negative shift in $V_{0.5}$ of ∼15 mV (Brueggemann et al., 2011). The native M-currents in freshly dissociated MASMCs behaved like the co-expressed Kv7.4 and Kv7.5 in terms of their insensitivity to diclofenac at −20 mV and a 15 mV negative shift in $V_{0.5}$, which was interpreted as evidence that the native channels are likely Kv7.4/Kv7.5 heteromers (Brueggemann et al., 2011). Like Q5–Q4–Q5–Q4, M-currents in MASMCs were also modestly enhanced by forskolin/IBMX (Mani et al., 2016), and modestly suppressed by AVP treatments (Mackie et al., 2008); these responses are markedly smaller than the responses of Kv7.5 homomers and markedly greater than the responses of Kv7.4 homomers to the same treatments (Brueggemann et al., 2014b; Mani et al., 2016). The similarity of MASMC M-currents to those derived from expression of Q5–Q4–Q5–Q4 concatenated tetramers, and their responses to diclofenac, as well as to forskolin/IBMX and AVP, further suggests that the native myocyte channels may be tetramers of alternating Kv7.4 and Kv7.5 α-subunits in a 2:2 stoichiometry.

While Q5–Q4–Q5–Q4 channels may be functionally present and contribute to M-currents in native myocytes, it cannot be ruled out that other functional channels (e.g., homomers or heteromers of Kv7.4 and Kv7.5) can also contribute to the native myocyte M-currents. In particular, a contribution of homomeric Kv7.4 might explain the findings that the voltage of half-maximal activation ($V_{0.5}$) of concatenated Q5–Q4–Q5–Q4 channels (around −50 mV) is much more negative than that of native MASMC M-currents (−35 mV; Brueggemann et al., 2011). On the other hand, the inhibitory response of the native current to diclofenac (Brueggemann et al., 2011) is lost in concatenated Q5–Q4–Q5–Q4 channels; and the native current in MASMC is markedly inhibited by AVP (100 pM; Mackie et al., 2008), but nearly unaffected in Q5–Q4–Q5–Q4 channels, which might support a contribution of the more responsive homomeric Kv7.5 channels in MASMCs.

Limitations

There are some limitations of our present study that should be considered. Perhaps the most obvious is the question how well can a concatenated construct mimic the properties of a channel formed from individually expressed α-subunits? We examined several characteristics of the channels ($V_{0.5}$, responses to physiological stimuli, drug responses) and found

many similarities to native channels, but there were also some dissimilarities. Concatenation necessarily introduces a link between the C-terminus of one α-subunit and the N-terminus of another, which would not normally be present. Research from our laboratory implicated both the N- and C-termini in the signaling responses of Kv7.5, specifically attributing the response to cAMP/PKA activation to the N-terminal segment and the response to PKC-activating stimuli (including AVP) to the C-terminus (Haick et al., 2017; Brueggemann et al., 2018, 2020). Some differences in signaling sensitivities might therefore arise if the targeted N- or C-terminal segments are tethered to an adjacent α-subunit and less free to interact with kinases or downstream effectors. We did not explore the possibility that longer or more flexible linkers between adjacent α-subunits might result in channels that more closely mimic the regulatory characteristics of channels formed by individual α -subunits.

Signal transduction via Kv7 channels may also involve scaffolding proteins, such as A-kinase anchoring protein (AKAPs; Hoshi et al., 2003; Bal et al., 2010; Zhang et al., 2011) or post-synaptic density protein 95 (PSD-95; Sedó-Cabezón et al., 2015)—it is unclear whether the roles of these scaffolding proteins are altered by concatenation of the α-subunits. Ancillary channel subunits, particularly KCNE proteins, can also modulate the expression and function of Kv channels (Brueggemann et al., 2013); KCNE4 was found to interact with both Kv7.4 and Kv7.5 in MASMCs (Jepps et al., 2015). These interactions, and any changes that result from concatenation of α-subunits, are not considered in the present study. We have detected both AKAP150 and PSD-95, but have not detected expression of any of the five mammalian KCNEs (KCNE1-5) in A7r5 cells (Brueggemann et al., unpublished results).

As summarized in **Figure 6A**, we consistently observed a difference in voltage dependence of activation of concatenated channel constructs compared with co-expression of the individual α-subunits, with the concatenated channels activating 5–10 mV more negatively. Our previous study implicated the C-termini of Kv7.4 and Kv7.5 as important determinants of the $V_{0.5}$ of the homomeric channels (Brueggemann et al., 2020). Those findings suggested that the cytosolic C-terminal tails of the α-subunits affect the movement of the membrane-resident voltage sensors. Hence, it is not entirely surprising that concatenation of α-subunits, involving links between C-termini and N-termini of adjacent α-subunits, might affect the interactions of C-termini with the voltage sensors, and thereby alter the voltage dependences of the fully formed channels, though we do not have enough structural information to explain why the voltage-dependence is shifted to a more negative range.

Another limitation of our study is that we did not explore an extended range of α-subunit stoichiometries to determine whether other Kv7.4/Kv7.5 subunit configurations are functional e.g., when constrained to assemble as heteromers with 3:1 stoichiometry (Q4–Q4–Q4–Q5, or Q5–Q5–Q5–Q4), or with like subunits adjacent within the tetramer (Q4–Q4–Q5–Q5). Future studies may determine whether these other configurations also reproduce features of the native smooth muscle Kv7.4/Kv7.5 channels. While it is important to emphasize that there may not be a single fixed stoichiometry or arrangement of α-subunits, our study illustrates that Kv7.4 and Kv7.5 heteromerization generates functional channels with distinct properties, and with the ability to serve as downstream targets in receptor-mediated smooth muscle signaling pathways.

Summary

Heteromeric Kv7.4/Kv7.5 channels formed from concatenated dimers or tetramers of Kv7.4 and Kv7.5 α-subunits conduct M-currents that exhibit many characteristics of native smooth muscle M-currents. Based on these findings, we speculate that in smooth muscle cells, such as MASMCs, where M-currents can be attributed primarily to heteromeric Kv7.4/Kv7.5 channels, the configuration of α-subunits within the tetrameric channel structure is likely alternating Kv7.4 and Kv7.5 in a 2:2 stoichiometry. Though the potential for contributions from channels with other arrangements of α-subunits is not ruled out, the alternating Kv7.4/Kv7.5 α-subunit configuration confers channel properties that are distinct from homomeric channels of either Kv7.4 or Kv7.5 α-subunits, in terms of their sensitivities to signaling pathways that target Kv7 channels to modulate smooth muscle contractility, and in terms of their responses to Kv7 channel modulating drugs. These findings have significance for our understanding of physiological smooth muscle signal transduction, as well as for development of smooth muscle therapeutics that target Kv7 channels.

DATA AVAILABILITY STATEMENT

The datasets generated for this study are available on request to the corresponding author.

AUTHOR CONTRIBUTIONS

LB conducted all the experiments and data analysis. LC designed and constructed the DNA vectors. All authors participated in the research design and writing of the manuscript.

FUNDING

The project described was supported by Award Number I01BX002344 from the Biomedical Laboratory Research & Development Service of the VA Office of Research and Development.

ACKNOWLEDGMENTS

The authors gratefully acknowledge the technical assistance of Minhua Wang in construction of DNA vectors.

SUPPLEMENTARY MATERIAL

The Supplementary Material for this article can be found online at: https://www.frontiersin.org/articles/10.3389/fphys.2020.00992/full#supplementary-material

REFERENCES

Bal, M., Zhang, J., Hernandez, C. C., Zaika, O., and Shapiro, M. S. (2010). Ca2+/calmodulin disrupts AKAP79/150 interactions with KCNQ (M-type) K+ channels. *J. Neurosci.* 30, 2311–2323. doi: 10.1523/jneurosci.5175-09.2010

Brueggemann, L. I., Cribbs, L. L., and Byron, K. L. (2020). Structural determinants of Kv7.5 potassium channels that confer changes in phosphatidylinositol 4,5-bisphosphate (PIP2) affinity and signaling sensitivities in smooth muscle cells. *Mol. Pharmacol.* 97, 145–158. doi: 10.1124/mol.119.117192

Brueggemann, L. I., Cribbs, L. L., Schwartz, J., Wang, M., Kouta, A., and Byron, K. L. (2018). Mechanisms of PKA-Dependent Potentiation of Kv7.5 Channel Activity in Human Airway Smooth Muscle Cells. *Int. J. Mol. Sci.* 19:E2223. doi: 10.3390/ijms19082223

Brueggemann, L. I., Gentile, S., and Byron, K. L. (2013). Social networking among voltage-activated potassium channels. *Prog. Mol. Biol. Transl. Sci.*117, 269–302. doi: 10.1016/b978-0-12-386931-9.00010-6

Brueggemann, L. I., Haick, J. M., Cribbs, L. L., and Byron, K. L. (2014a). Differential activation of vascular smooth muscle Kv7.4, Kv7.5, and Kv7.4/7.5 channels by ML213 and ICA-069673. *Mol Pharmacol.* 86, 330–341. doi: 10.1124/mol.114.093799

Brueggemann, L. I., Kakad, P. P., Love, R. B., Solway, J., Dowell, M. L., Cribbs, L. L., et al. (2012). Kv7 potassium channels in airway smooth muscle cells: signal transduction intermediates and pharmacological targets for bronchodilator therapy. *Am. J. Physiol. Lung. Cell Mol. Physiol.* 302, L120-L132.

Brueggemann, L. I., Mackie, A. R., Cribbs, L. L., Freda, J., Tripathi, A., Majetschak, M., et al. (2014b). Differential protein kinase C-dependent modulation of Kv7.4 *and Kv*7.5 subunits of vascular Kv7 channels. *J. Biol. Chem.* 289, 2099–2111. doi: 10.1074/jbc.m113.527820

Brueggemann, L. I., Mackie, A. R., Mani, B. K., Cribbs, L. L., and Byron, K. L. (2009). Differential effects of selective cyclooxygenase-2 inhibitors on vascular smooth muscle ion channels may account for differences in cardiovascular risk profiles. *Mol. Pharmacol.* 76, 1053–1061. doi: 10.1124/mol.109.057844

Brueggemann, L. I., Mackie, A. R., Martin, J. L., Cribbs, L. L., and Byron, K. L. (2011). Diclofenac distinguishes among homomeric and heteromeric potassium channels composed of KCNQ4 and KCNQ5 subunits. *Mol. Pharmacol.* 79, 10–23. doi: 10.1124/mol.110.067496

Brueggemann, L. I., Moran, C. J., Barakat, J. A., Yeh, J. Z., Cribbs, L. L., and Byron, K. L. (2007). Vasopressin stimulates action potential firing by protein kinase C-dependent inhibition of KCNQ5 in A7r5 rat aortic smooth muscle cells. *Am. J. Physiol. Heart Circ. Physiol.* 292, H1352–H1363.

Byron, K. L., and Brueggemann, L. I. (2018a). "Elucidation of vasopressin signal transduction pathways in vascular smooth muscle," in *Signal Transduction And Smooth Muscle*, eds M. Trebak, and S. Earley (Boca Raton, FL: CRC Press), 1-28.

Byron, K. L., and Brueggemann, L. I. (2018b). Kv7 potassium channels as signal transduction intermediates in the control of microvascular tone. *Microcirculation.* 25:e12419. doi: 10.1111/micc.12419

Byron, K. L., and Taylor, C. W. (1993). Spontaneous Ca2+ spiking in a vascular smooth muscle cell line is independent of the release of intracellular Ca2+ stores. *J. Biol. Chem.* 268, 6945–6952.

Catterall, W. A. (1988). Structure and function of voltage-sensitive ion channels. *Science* 242, 50–61. doi: 10.1126/science.2459775

Delmas, P., and Brown, D. A. (2005). Pathways modulating neural KCNQ/M (Kv7) potassium channels. *Nat. Rev. Neurosci.* 6, 850–862. doi: 10.1038/nrn1785

Haick, J. M., Brueggemann, L. I., Cribbs, L. L., Denning, M. F., Schwartz, J., and Byron, K. L. (2017). PKC-dependent regulation of Kv7.5 channels by the bronchoconstrictor histamine in human airway smooth muscle cells. *Am. J. Physiol. Lung. Cell Mol. Physiol.* 312, L822–l834. doi: 10.1152/ajplung.00567.2016

Hoshi, N., Zhang, J. S., Omaki, M., Takeuchi, T., Yokoyama, S., Wanaverbecq, N., et al. (2003). AKAP150 signaling complex promotes suppression of the M-current by muscarinic agonists. *Nat. Neurosci.* 6, 564–571. doi: 10.1038/nn1062

Hurst, R. S., Kavanaugh, M. P., Yakel, J., Adelman, J. P., and North, R. A. (1992). Cooperative interactions among subunits of a voltage-dependent potassium channel. Evidence from expression of concatenated cDNAs. *J. Biol. Chem.* 267, 23742–23745.

Hurst, R. S., North, R. A., and Adelman, J. P. (1995). Potassium channel assembly from concatenated subunits: effects of proline substitutions in S4 segments. *Recept. Channels* 3, 263–272.

Jepps, T. A., Carr, G., Lundegaard, P. R., Olesen, S. P., and Greenwood, I. A. (2015). Fundamental role for the KCNE4 ancillary subunit in Kv7.4 regulation of arterial tone. *J. Physiol.* 593, 5325–5340. doi: 10.1113/jp271286

Kimes, B. W., and Brandt, B. L. (1976). Characterization of two putative smooth muscle cell lines from rat thoracic aorta. *Exp. Cell Res.* 98, 349–366. doi: 10.1016/0014-4827(76)90446-8

Mackie, A. R., Brueggemann, L. I., Henderson, K. K., Shiels, A. J., Cribbs, L. L., Scrogin, K. E., et al. (2008). Vascular KCNQ potassium channels as novel targets for the control of mesenteric artery constriction by vasopressin, based on studies in single cells, pressurized arteries, and in vivo measurements of mesenteric vascular resistance. *J. Pharmacol. Exp. Ther.* 325, 475–483. doi: 10.1124/jpet.107.135764

Mani, B. K., Robakowski, C., Brueggemann, L. I., Cribbs, L. L., Tripathi, A., Majetschak, M., et al. (2016). Kv7.5 potassium channel subunits are the primary targets for PKA-dependent enhancement of vascular smooth muscle Kv7 currents. *Mol. Pharmacol.* 89, 323–334. doi: 10.1124/mol.115.101758

Sedó-Cabezón, L., Jedynak, P., Boadas-Vaello, P., and Llorens, J. (2015). Transient alteration of the vestibular calyceal junction and synapse in response to chronic ototoxic insult in rats. *Dis. Mod. Mech.* 8, 1323–1337. doi: 10.1242/dmm.021436

Sims, S. M., Singer, J. J., and Walsh, J. V. (1985). Cholinergic agonists suppress a potassium current in freshly dissociated smooth muscle cells of the toad. *J. Physiol.* 367, 503–529. doi: 10.1113/jphysiol.1985.sp015837

Wang, A. W., Yau, M. C., Wang, C. K., Sharmin, N., Yang, R. Y., Pless, S. A., et al. (2018). Four drug-sensitive subunits are required for maximal effect of a voltage sensor-targeted KCNQ opener. *J. Gen. Physiol.* 150, 1432–1443. doi: 10.1085/jgp.201812014

Wimmers, S., Bauer, C. K., and Schwarz, J. R. (2002). Biophysical properties of heteromultimeric erg K+ channels. *Pflugers. Arch.* 445, 423–430. doi: 10.1007/s00424-002-0936-4

Yau, M. C., Kim, R. Y., Wang, C. K., Li, J., Ammar, T., Yang, R. Y., et al. (2018). One drug-sensitive subunit is sufficient for a near-maximal retigabine effect in KCNQ channels. *J. Gen. Physiol.* 150, 1421–1431. doi: 10.1085/jgp.201812013

Zhang, J., Bal, M., Bierbower, S., Zaika, O., and Shapiro, M. S. (2011). AKAP79/150 signal complexes in G-protein modulation of neuronal ion channels. *J. Neurosci.* 31, 7199–7211. doi: 10.1523/jneurosci.4446-10.2011

Conflict of Interest: The authors declare that the research was conducted in the absence of any commercial or financial relationships that could be construed as a potential conflict of interest.

frontiers in Physiology

ORIGINAL RESEARCH
published: 04 September 2020
doi: 10.3389/fphys.2020.01040

A Novel Kv7.3 Variant in the Voltage-Sensing S_4 Segment in a Family With Benign Neonatal Epilepsy: Functional Characterization and *in vitro* Rescue by β-Hydroxybutyrate

Francesco Miceli[1], Lidia Carotenuto[1], Vincenzo Barrese[1], Maria Virginia Soldovieri[2], Erin L. Heinzen[3,4], Arthur M. Mandel[5], Natalie Lippa[4], Louise Bier[4], David B. Goldstein[4], Edward C. Cooper[6], Maria Roberta Cilio[7], Maurizio Taglialatela[1] and Tristan T. Sands[4,5]**

[1] Department of Neuroscience, University of Naples "Federico II", Naples, Italy, [2] Department of Medicine and Health Science, University of Molise, Campobasso, Italy, [3] Eshelman School of Pharmacy, Division of Pharmacotherapy and Experimental Therapeutics, University of North Carolina at Chapel Hill, Chapel Hill, NC, United States, [4] Institute for Genomic Medicine, Columbia University Irving Medical Center, New York, NY, United States, [5] Department of Neurology, Columbia University Irving Medical Center, New York, NY, United States, [6] Departments of Neurology, Neuroscience, and Molecular and Human Genetics, Baylor College of Medicine, Houston, TX, United States, [7] Department of Pediatrics and Institute of Experimental and Clinical Research, Cliniques universitaires Saint-Luc, Université catholique de Louvain, Brussels, Belgium

Pathogenic variants in *KCNQ2* and *KCNQ3*, paralogous genes encoding Kv7.2 and Kv7.3 voltage-gated K^+ channel subunits, are responsible for early–onset developmental/epileptic disorders characterized by heterogeneous clinical phenotypes ranging from benign familial neonatal epilepsy (BFNE) to early–onset developmental and epileptic encephalopathy (DEE). *KCNQ2* variants account for the majority of pedigrees with BFNE and *KCNQ3* variants are responsible for a much smaller subgroup, but the reasons for this imbalance remain unclear. Analysis of additional pedigrees is needed to further clarify the nature of this genetic heterogeneity and to improve prediction of pathogenicity for novel variants. We identified a BFNE family with two siblings and a parent affected. Exome sequencing on samples from both parents and siblings revealed a novel *KCNQ3* variant (c.719T>G; p.M240R), segregating in the three affected individuals. The M240 residue is conserved among human Kv7.2-5 and lies between the two arginines (R5 and R6) closest to the intracellular side of the voltage-sensing S_4 transmembrane segment. Whole cell patch-clamp recordings in Chinese hamster ovary (CHO) cells revealed that homomeric Kv7.3 M240R channels were not functional, whereas heteromeric channels incorporating Kv7.3 M240R mutant subunits with Kv7.2 and Kv7.3 displayed a depolarizing shift of about 10 mV in activation gating. Molecular modeling results suggested that the M240R substitution preferentially stabilized the resting state and possibly destabilized the activated state of the Kv7.3 subunits, a result consistent with functional data. Exposure to β-hydroxybutyrate (BHB), a ketone body generated during the ketogenic diet (KD), reversed channel dysfunction induced

OPEN ACCESS

Edited by:
Mark S. Shapiro, The University of Texas Health Science Center at San Antonio, United States

Reviewed by:
Rían Manville, University of Brighton, United Kingdom
Geoff Abbott, University of California, Irvine, United States
Carlos Alberto Villalba-Galea, University of the Pacific, United States

***Correspondence:**
Maurizio Taglialatela
mtaglial@unina.it
Tristan T. Sands
tts27@cumc.columbia.edu

Specialty section:
This article was submitted to Membrane Physiology and Membrane Biophysics, a section of the journal Frontiers in Physiology

Received: *05 June 2020*
Accepted: *29 July 2020*
Published: *04 September 2020*

Citation:
Miceli F, Carotenuto L, Barrese V, Soldovieri MV, Heinzen EL, Mandel AM, Lippa N, Bier L, Goldstein DB, Cooper EC, Cilio MR, Taglialatela M and Sands TT (2020) A Novel Kv7.3 Variant in the Voltage-Sensing S_4 Segment in a Family With Benign Neonatal Epilepsy: Functional Characterization and in vitro Rescue by β-Hydroxybutyrate. Front. Physiol. 11:1040. doi: 10.3389/fphys.2020.01040

by the M240R variant. In conclusion, we describe the first missense loss-of-function (LoF) pathogenic variant within the S_4 segment of Kv7.3 identified in patients with BFNE. Studied under conditions mimicking heterozygosity, the M240R variant mainly affects the voltage sensitivity, in contrast to previously analyzed BFNE Kv7.3 variants that reduce current density. Our pharmacological results provide a rationale for the use of KD in patients carrying LoF variants in Kv7.2 or Kv7.3 subunits.

Keywords: *KCNQ*, BFNE, encephalopathy, channelopathies, ketogenic diet

INTRODUCTION

Voltage-gated potassium (K^+) channels (Kv channels) regulate the resting membrane potential and set the threshold and duration of the action potential in excitable cells. Among these, Kv7.2 and Kv7.3 voltage-gated K^+ subunits, encoded by the *KCNQ2* and *KCNQ3* genes, are expressed in the central and peripheral nervous system (Brown and Adams, 1980; Wang et al., 1998). These subunits form homo- and heterotetrameric channels underlying the M-current (I_{KM}), a non-inactivating K^+ current with slow activation and deactivation kinetics that activates at the threshold potential of about −60/−50 mV, thus regulating the resting membrane potential and suppressing repetitive neuronal firing (Brown and Adams, 1980).

Pathogenic variants in *KCNQ2* cause early-onset epilepsies with wide phenotypic heterogeneity (Allen et al., 2014; Miceli et al., 2018). Indeed, some variants have been identified in patients with benign familial neonatal epilepsy (BFNE), an autosomal-dominant epilepsy with seizures affecting otherwise healthy infants in the first days of life and spontaneously disappearing over the next several months, with mostly normal neurocognitive development (Jentsch, 2000; Singh et al., 2003; Soldovieri et al., 2006). At the severe end of the *KCNQ2* spectrum is an early-onset developmental and epileptic encephalopathy (DEE) characterized by recurrent seizures starting in the neonatal period and neurodevelopmental disability (Weckhuysen et al., 2012). While more than 300 pathogenic variants have been described in *KCNQ2*, few variants in *KCNQ3* have been detected, mostly in families with BFNE. In addition, *de novo* variants in *KCNQ3* have been rarely described in children with DEE (Allen et al., 2013; Grozeva et al., 2015; Miceli et al., 2015; Ambrosino et al., 2018; Lauritano et al., 2019), intellectual disability (ID) apparently without epilepsy (Rauch et al., 2012; Deciphering Developmental Disorders, 2017), cortical visual impairment (Bosch et al., 2016), and in patients with ID and autism (Sands et al., 2019).

In most children affected with *KCNQ2*- or *KCNQ3*-related BFNE, seizures are controlled with conventional antiepileptic drugs, including sodium channel blockers (Sands et al., 2016). Instead, few options are available for patients with the most severe forms of *KCNQ2*- or *KCNQ3*-related disorders; in addition to sodium-channel blockers such as carbamazepine and phenytoin which appear to be highly effective (Pisano et al., 2015), ezogabine, a selective Kv7 channel activator, has been shown to improve seizure control and development in patients with Kv7.2 loss-of-function (LoF) variants (Millichap et al., 2016). Unfortunately, because of its unfavorable risk/benefit ratio, ezogabine has been withdrawn from the market. Among non-pharmacological therapies, ketogenic diet (KD) has been recently shown to be particularly effective in children with DEE caused by *KCNQ2* variants (Ko et al., 2018), but the mechanisms of action are not completely understood and there are no data on the effects on *KCNQ3* related disorders. KD is a low carbohydrate, high-fat, adequate-protein diet regimen that shifts the primary fuel source for neuronal activity from glucose to endogenous ketones: acetone, acetoacetate, and β-hydroxybutyrate (BHB). KD likely improves seizure control through a variety of mechanisms such as inhibition of the glycolysis, disruption of glutamatergic synaptic transmission, and activation of ATP-sensitive potassium channels (Lutas and Yellen, 2013). Recently, BHB has been shown to directly and specifically activate Kv7 channels containing Kv7.3 subunits by increasing current sensitivity to voltage (Manville et al., 2018, 2020).

In the present manuscript, we report the clinical, molecular and functional properties of a BFNE family carrying a novel *KCNQ3* variant (c.719T>G; p.M240R) segregating with epilepsy in the three affected individuals. Whole cell patch-clamp recordings in Chinese hamster ovary (CHO) cells revealed that homomeric Kv7.3 M240R channels were not functional, whereas heteromeric channels incorporating Kv7.3 M240R mutant subunits with Kv7.2 and Kv7.3 displayed a depolarizing shift of about 10 mV in activation gating, consistent with a LoF *in vitro* effect. Consistent with these functional data, molecular modeling suggested that the M240R substitution preferentially stabilized the resting state and possibly destabilize the activated state of the Kv7.3 subunits. Finally, we demonstrate that BHB was able to reverse the functional alterations observed in heteromeric channels carrying Kv7.3 M240R subunits.

MATERIALS AND METHODS

Patients

The BFNE family was referred for an epilepsy genetics research study by their treating clinician and written informed consent was obtained. Exome sequencing was performed in both parents and each sibling, and the presence of c.719T > G (p.M240R) in affected members was confirmed by Sanger sequencing in a clinical genetics laboratory. The study was approved by the human research ethics committee of Columbia University Irving Medical Center.

Mutagenesis and Heterologous Expression of *KCNQ2* and *KCNQ3* cDNAs

Mutations were engineered in *KCNQ3* human cDNA cloned into pcDNA3.1 by QuikChange site-directed mutagenesis (Agilent Technologies Italia SpA, Milan, Italy), as previously described (Miceli et al., 2013). Channel subunits were expressed in CHO cells by transient transfection. CHO cells were grown in 100 mm plastic Petri dishes in Dulbecco's modified Eagle's medium (DMEM) containing 10% foetal bovine serum (FBS), L-glutamine (0.1 mM), penicillin (50 U/ml), and streptomycin (50 μg/ml) in a humidified atmosphere at 37°C with 5% CO_2. For electrophysiological experiments, cells were seeded on glass coverslips (Carolina Biological Supply Company, Burlington, NC, United States) and transfected on the next day with the appropriate cDNAs using Lipofectamine 2000 (Invitrogen, Milan, Italy) according to the manufacturer's protocol. A plasmid encoding for enhanced green fluorescent protein (Clontech laboratories, Inc., Palo Alto, CA, United States) was used as transfection marker; total cDNA in the transfection mixture was kept constant at 4 μg.

Whole-Cell Electrophysiology

Currents from CHO cells were recorded at room temperature (20–22°C) 1–2 days after transfection, using a commercially available amplifier (Axopatch 200A, Molecular Devices, Union City, CA, United States) and the *whole-cell* configuration of the patch-clamp technique, with glass micropipettes of 3–5 MΩ resistance. The extracellular solution contained (in millimolar): 138 NaCl, 2 $CaCl_2$, 5.4 KCl, 1 $MgCl_2$, 10 glucose, and 10 HEPES, pH 7.4 with NaOH. The pipette (intracellular) solution contained (in millimolar): 140 KCl, 2 $MgCl_2$, 10 EGTA, 10 HEPES, 5 Mg-ATP, pH 7.3–7.4 with KOH. The pCLAMP software (version 10.0.2) was used for data acquisition and analysis. Current densities (expressed in picoamperes per picofarad) were calculated as peak K^+ currents divided by *C*. Data were acquired at 0.5–2 kHz and filtered at 1–5 kHz with the four-pole lowpass Bessel filter of the amplifier. No corrections were made for liquid junction potentials. To generate conductance-voltage curves, the cells were held at −80 mV, then depolarized for 1.5 s from −80 mV to +20/+80 mV in 10 mV increments, followed by an isopotential pulse at 0 mV of 300 ms duration; the current values recorded at the beginning of the 0 mV pulse were measured, normalized, and expressed as a function of the preceding voltages. Data were fit to a Boltzmann distribution of the following form $y = \max/[1 + \exp(V_{1/2} - V)/k]$, where V is the test potential, $V_{1/2}$ the half-activation potential, and k the slope factor.

For current-activation kinetics analysis, the current traces recorded in response to incremental voltage steps were fitted to a double-exponential function and then a single time constant, representing the weighted average of the slow and fast components, was obtained by using the following equation: $\tau = (\tau_f A_f + \tau_s A_s)/(A_f + A_s)$, where A_f and A_s indicate the amplitude of the fast and slow exponential components, τ_f and τ_s the time constants of each component (Miceli et al., 2013).

Structural Modeling

Three-dimensional models of $K_v7.3$ subunits in different gating states were generated by using as templates the coordinates of resting and activated states of the $K_v1.2/2.1$ chimera (Long et al., 2007; PDB accession number 2R9R; 26% of sequence identity with $K_v7.3$) subjected to long (>200 μs) molecular dynamic simulations (Jensen et al., 2012). Modeling of the S_1-S_4 VSD in each state was performed with SWISS-MODEL, as described (Sands et al., 2019). The models were optimized through all-atom energy minimization by using the GROMOS96 implementation of Swiss-PDBViewer, and analyzed using both the DeepView module of Swiss-PDBViewer (version 4.0.1[1]) and PyMOL[2].

Statistics

Data are expressed as the mean ± SEM. Statistically significant differences between the data were evaluated with the Student's *t*-test ($p < 0.05$).

RESULTS

Clinical and Genetic Features of the BFNE Pedigree With a Novel *KCNQ3* Variant

Case II-1

A term male neonate was hospitalized for seizures starting in the first week of life. The seizures lasted less than 1 min, recurring every 2 h. Electroencephalography (EEG) recorded variable lateralization of ictal onset. Clinically, there was bilateral arm stiffening, rightward head version, and right leg stiffening, lasting 45 s. Workup for acute etiologies, including an MRI of the brain, was unrevealing. The child was treated with phenobarbital, but continued to have seizures after hospital discharge. He was cross-titrated onto levetiracetam from 3 weeks of age and seizures stopped around that time. Levetiracetam was weaned at 12 months. At 18 months he was diagnosed with isolated language delay (one standard deviation below expected) and started speech therapy. There was no concern for autism.

Case II-2

Nineteen months later, a female sibling was born. She began having episodes on the 5th day of life, characterized by limb stiffening and eye rolling. EEG confirmed seizures. Workup included a normal MRI of the brain. She was treated with phenobarbital and levetiracetam, which were weaned off at 4 and 6 months, respectively. She had recurrence with two back-to-back seizures at 22 months, and she was started on oxcarbazepine with seizure freedom. Follow-up EEGs have been normal. Developmental milestones have all been met on time as of 26 months.

Family history was notable for an isolated seizure in the father (case I-1) during infancy. The father's interictal EEG was normal, the seizure did not recur, and he was not treated with anti-seizure

[1]http://spdbv.vital-it.ch/

[2]http://www.pymol.org/

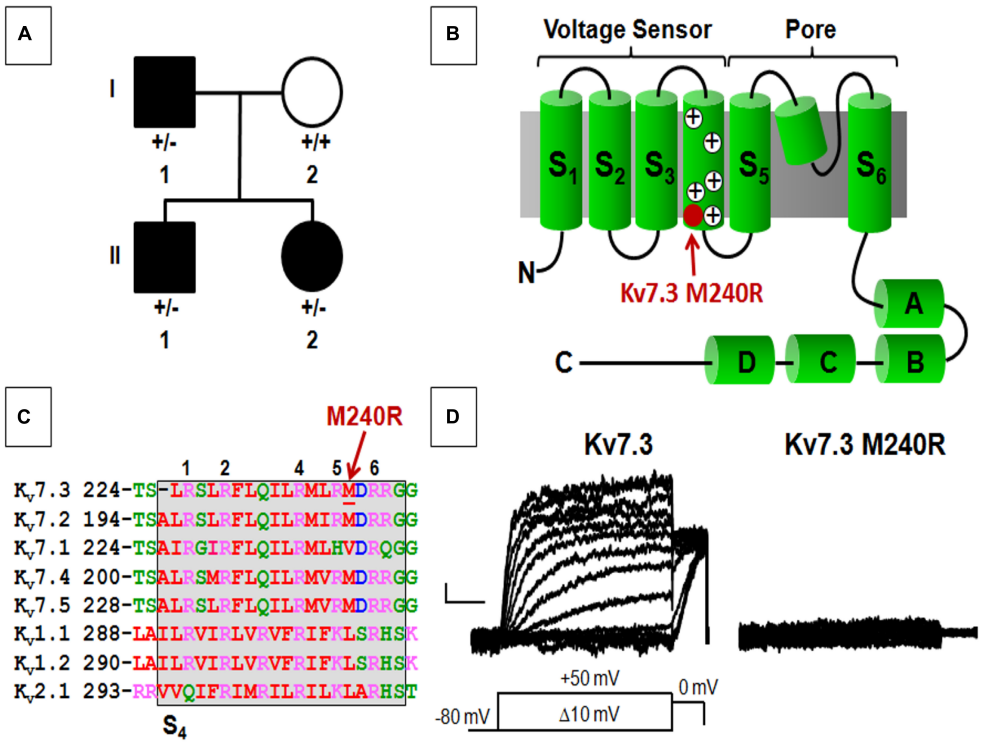

FIGURE 1 | Pedigree, schematic representation of a single Kv7.3 subunit, and functional analysis of mutation at position 240. **(A)** Pedigree of the family. **(B)** Topological representation of a single Kv7 subunit. Arrows indicate the location of the mutation investigated (shaded in red). **(A–D)** Indicate the four putative alpha-helical domains identified in the Kv7 C-terminal region. **(C)** Sequence alignment of the S_4 segments of the indicated Kv subunits (www.ebi.ac.uk/Tools/psa/). Residues are colored according to the following scheme: magenta represents basic; blue represents acid; red represents non-polar; green represents polar. 1, 2, 4, 5, and 6 refer to the positively charged arginines numbered according to their position along the S_4 primary sequence. **(D)** Macroscopic currents from the indicated homomeric channels. Current scale, 50 pA; time scale, 0.2 s.

medication. No seizure was ever described in the mother (case I-2; **Figure 1A**).

Exome sequencing, performed in all four family members, demonstrated a novel missense variant in *KCNQ3*, c.719T > G (p.M240R), in the two siblings and the affected father (**Figure 1A**), thus segregating with the phenotype. The variant is absent from gnomAD and predicted to be deleterious (polyphen-2, 0.989; SIFT, 0.9122; CADD score 27.3). The M240 residue lies between the R5 (R239) and R6 (R242) positions of the voltage-sensing S_4 transmembrane segment within the voltage-sensing domain (VSD; **Figure 1B**). This non-polar residue is conserved among human Kv7.2-5 subunits, but not in Kv7.1 and other Kv channels such as Kv1.1, Kv1.2, and Kv2.1, although residues with similar physicochemical properties are present at this position (**Figure 1C**).

Functional and Pharmacological Properties of Homomeric and Heteromeric Channels Carrying Kv7.3 M240R Subunits

Heterologous expression of wild-type Kv7.3 subunits led to the appearance of voltage-dependent K^+ −selective currents characterized by a rather slow time-course of activation and deactivation and a threshold for current activation of around −50 mV; the macroscopic K^+ currents density at + 20 mV was 12.6 ± 1.1 pA/pF, similarly to previously reported values (Wang et al., 1998; Sands et al., 2019). By contrast, no measurable currents were recorded in cells expressing Kv7.3 M240R subunits, consistent with the variant causing a complete LoF effect (**Figure 1D** and **Table 1**).

Kv7.3 subunits assemble with Kv7.2 subunits to form I_{KM} (Wang et al., 1998). Co-expression of Kv7.2 and Kv7.3 subunits generated currents which were considerably larger than those recorded upon expression as Kv7.2 or Kv7.3 subunits alone; in addition, currents from Kv7.2 + Kv7.3 heteromeric channels displayed an increased sensitivity to blockade by tetraethylammonium (TEA) when compared to homomeric Kv7.3 channels (**Table 1**). When compared to currents from wild-type Kv7.2 + Kv7.3 subunits, co-expression of Kv7.3 M240R with Kv7.2 subunits caused a marked rightward shift (by about + 40 mV) of the activation gating, a significant decrease of slope of the G/V curve (see section Materials and Methods for details), a reduced current density by about 50% at depolarized potential, with no change in sensitivity to TEA blockade (**Figures 2A–C** and **Table 1**). The marked rightward shift of the G/V curves of the heteromeric Kv7.2 + Kv7.3 M240R channels markedly reduced current density at the physiologically

TABLE 1 | Biophysical and pharmacological properties of mutant Kv7.3 channels.

	n	$V_{1/2}$ (mV)	*k* (mV/e-fold)	Current density at + 20 mV (pA/pF)	Blockade by 3 mM TEA (%)	100 μM BHB (Δ V, mV)
CHO	10	–	–	0.5 ± 0.05	–	–
Kv7.3	26	−37.2 ± 1.1*	7.2 ± 0.4*	12.6 ± 1.1*	8.0 ± 2.1*	–
Kv7.3 M240R	8	–	–	0.5 ± 0.2	–	–
Kv7.2	11	−26.8 ± 1.3	13.2 ± 0.9	42.1 ± 2.5	85.1 ± 3.1*	–
Kv7.2 + Kv7.3	18	−27.7 ± 1.4	11.2 ± 0.5	126.4 ± 17.9	50.1 ± 4.3	−8.1 ± 1.1
Kv7.2 + Kv7.3 M240R	7	18.1 ± 4.9*	22.6 ± 0.8*	70.2 ± 10.4*	45.2 ± 5.1	–
Kv7.2 + Kv7.3 + Kv7.3 M240R	18	−15.6 ± 1.7*	15.5 ± 0.7*	115.0 ± 15.2	48.5 ± 5.2	−8.7 ± 1.1

*TEA, tetraethylammonium; CHO, Chinese hamster ovary. *$p < 0.05$ vs. Kv7.2 + Kv7.3.*

relevant potentials of −50/−40 mV (**Figure 2C**). The activation kinetics of Kv7.2 + Kv7.3-M240R currents were slower than those of Kv7.2 + Kv7.3, particularly at more depolarized potentials. In fact, $\tau_{activation}$ at + 20 mV were 142 ± 19 ms and 274 ± 71 ms, for Kv7.2 + Kv7.3 and Kv7.2 + Kv7.3-M240R, respectively. In order to assess the influence of the depolarizing pulse length on the current steady-state properties from Kv7.2 + Kv7.3-M240R-expressing channels, additional experiments in which the pulse length was increased from 1.5 to 3 s were performed. The results obtained revealed no significant difference in the $V_{1/2}$ and *k* values on Kv7.2 + Kv7.3-M240R current using the two protocols; indeed, the $V_{1/2}$ and the *k* values were, respectively, + 12.2 ± 7.6 and + 10.2 ± 5.4 mV ($n = 4$; $p > 0.05$), and 23.0 ± 3.6 and 23.5 ± 1.4 mV/e-fold ($n = 4$; $p > 0.05$) for Kv7.2 + Kv7.3- and Kv7.2 + Kv7.3-M240R-expressing cells.

Altogether these data suggest that Kv7.3 M240R subunits are able to form heteromeric channels with Kv7.2 subunits, although their currents display gating properties very different from Kv7.2 + Kv7.3 heteromeric channels. To replicate *in vitro* the genetic combination occurring in the affected family members who are heterozygous for the pathogenic allele (Individuals I-1, II-1, and II-2), functional studies were also carried out upon transfection of cDNAs for Kv7.2 + Kv7.3 + Kv7.3 M240R at a cDNA ratio of 1:0.5:0.5. The current density measured in CHO cells expressing heteromeric channels formed by the described subunit combinations was very similar to that recorded in cells expressing Kv7.2 + Kv7.3 subunits at a transfection ratio 1:1 (mimicking a healthy individual) (**Figures 2A,B** and **Table 1**) and no difference in the activation kinetics was observed between the Kv7.2 + Kv7.3 and Kv7.2 + Kv7.3 + Kv7.3 M240R currents; indeed the $\tau_{activation}$ at + 20 mV were 142 ± 19 ms and 128 ± 28 ms, respectively. By contrast, the midpoint of activation of the currents recorded upon Kv7.2 + Kv7.3 + Kv7.3 M240R subunit co-expression was right-shifted by about 10 mV when compared to Kv7.2 + Kv7.3 (**Figures 2A–C** and **Table 1**), thus confirming LoF effects of the mutant subunits also when incorporated into channel tetramers with Kv7.2 + Kv7.3 subunits.

Structural Basis for the LoF Effect by the Kv7.3 M240R Substitution

The herein identified M240R variant introduces an extra positively charged residue into the S_4 segment of Kv7.3 subunits, between R5 and R6. To achieve a better understanding of the possible role of the M240 residue in the gating process and of the structural consequences of its replacement with an R, we built homology models of a Kv7.3 subunit in both resting and activated states, as previously described (Jensen et al., 2012; Sands et al., 2019). Our structural models suggested that, no electrostatic interaction between the M240 residue side chain and surrounding protein residues occurs in both the resting and the activated VSD configurations (**Figure 3A**); in particular, in the resting VSD state and in two of the four subunits, the M240 side chain points toward the N-terminal region of the same subunits, whereas in the other two subunits it points in the opposite direction, namely toward the S_5 segment (**Figure 3B**). Substitution of the non-polar M residue at position 240 with an R introduces a novel electrostatic interaction between R240 side chain and a highly conserved negatively charged N-terminal glutamate (E116) in one Kv7.3 subunit. This interaction only occurred in the resting state of the VSD (Long et al., 2007) (**Figure 3C**). Instead, VSD movement during the activation process translated the R240 side chain in a tight pocket surrounded by non-polar residues, possibly destabilizing the tight network of hydrophobic interactions within this pocket. As a result, our model suggests that the M240R substitution may preferentially stabilize the closed state and possibly destabilize the activated state of the Kv7.3 subunits.

Pharmacological Effects of BHB Exposure on Heteromeric Channels Incorporating the Kv7.3 Epilepsy-Causing Variant

The results described suggest that heteromeric channels incorporating Kv7.3 M240R subunits display a reduced sensitivity to voltage, strongly suggesting a LoF pathogenic mechanism. Given that BHB has been recently shown to potentiate Kv7.3 and Kv7.2 + Kv7.3 currents by a mechanism opposite to that introduced by the M240R variant (Manville et al., 2018, 2020), we further evaluated its ability to counteract *in vitro* the described functional alteration. We tested the effects of the BHB using a voltage protocol in which Kv7.2 + Kv7.3 and Kv7.2 + Kv7.3 + Kv7.3 M240R currents were activated by 3 s voltage ramps from −80 to +20 mV. Perfusion with 100 μM BHB enhanced ramp-evoked Kv7.2 + Kv7.3 and Kv7.2 + Kv7.3 + Kv7.3 M240R currents; this effect was reversible since the currents returned to basal values after about 10 s upon BHB removal from the bath (**Figure 4A**). In addition,

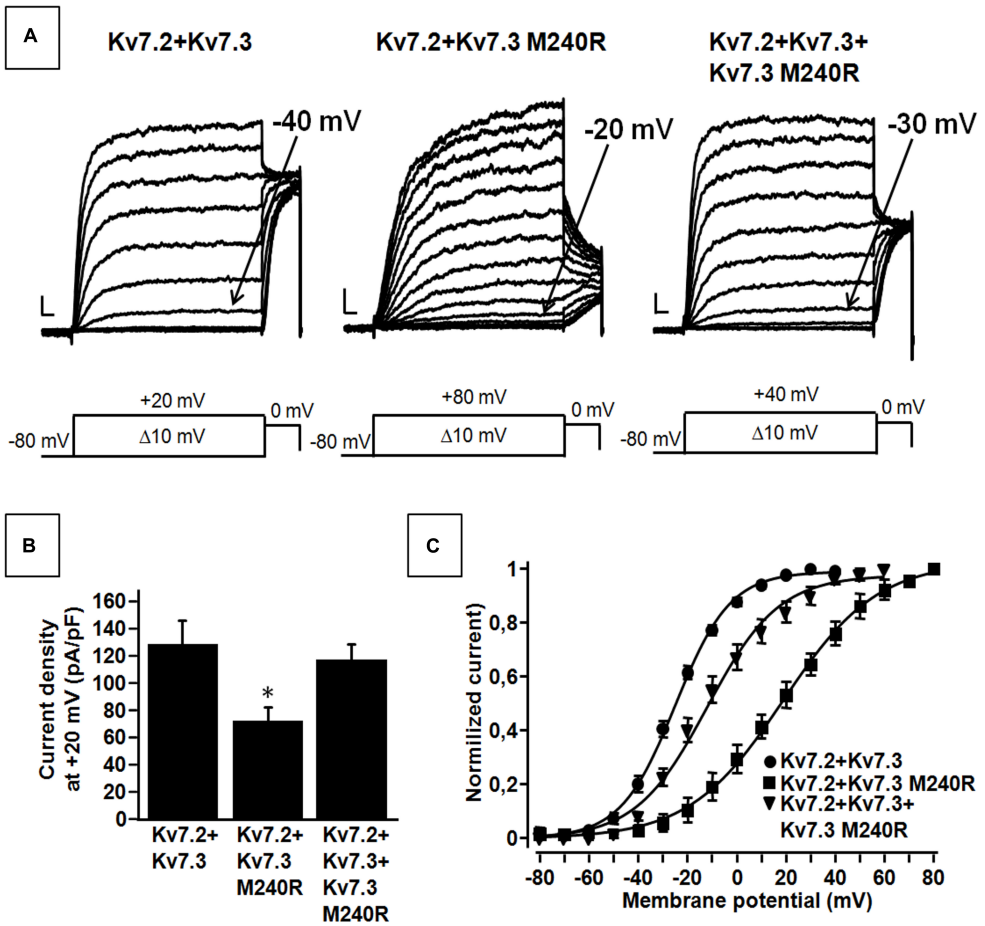

FIGURE 2 | Functional properties of heteromeric channels incorporating subunits carrying the benign familial neonatal epilepsy (BFNE) variant. **(A)** Macroscopic current traces from the indicated heteromeric channels in response to the indicated voltage protocol. Current scale, 200 pA; time scale, 0.1 s. **(B)** Current density from the indicated heteromeric channels calculated at +20 mV. The asterisk indicates a statistically-significant value versus Kv7.2 + Kv7.3. **(C)** Conductance/voltage curves for Kv7.2 + Kv7.3, Kv7.2 + Kv7.3 M240R, Kv7.2 + Kv7.3 + Kv7.3M240R. Continuous lines indicate Boltzmann fits of the experimental data. Current scale, 200 pA; time scale, 0.1 s. Each data point is the mean (SEM) of 7–18 cells recorded in at least three separate experimental sessions.

steady-state experiments revealed that at −40 mV, a membrane potential value close to the activation threshold, 100 μM BHB increased Kv7.2 + Kv7.3 and Kv7.2 + Kv7.3 + Kv7.3 M240R currents (**Figure 4B**) and also caused a 10 mV negative shift in the G/V curve (**Figure 4C**). Interestingly, the $V_{1/2}$ value of Kv7.2 + Kv7.3 + Kv7.3 M240R currents upon BHB exposure was similar to that of Kv7.2 + Kv7.3-expressing cells (**Figure 4C** and **Table 1**), suggesting the ability of the BHB to restore Kv7.2 + Kv7.3 + Kv7.3 M240R currents to that of wild-type.

DISCUSSION

Inherited variants in *KCNQ2* or *KCNQ3* cause BFNE, a neonatal-onset familial epilepsy, characterized by recurrent focal tonic seizures in otherwise well infants (Sands et al., 2016). While seizure onset is most often in the first days of life, seizures can present later in infancy (Zara et al., 2013), as demonstrated by the father in our pedigree, or not at all, as penetrance is incomplete. Seizures tend to remit over the first year, but ∼30% of individuals have seizures later in life (Grinton et al., 2015), as illustrated by case II-2.

Most BFNE families carry pathogenic variants in *KCNQ2*, whereas only a small percentage carry *KCNQ3* variants (Grinton et al., 2015; Sands et al., 2016; Miceli et al., 2017, 2018). *KCNQ2* variants responsible for BFNE are missense, stop-gain, frameshift, splice variants, and deletions randomly distributed along the entire primary sequence of the subunit. In contrast, BFNE-causing *KCNQ3* variants are all missense, affecting specific residues located in the pore region of the channel (S_5–S_6 and intervening loop; **Table 2**). Prior studies have reported 13 such variants, each affecting a different Kv7.3 residue located in and around the pore (**Table 2**); in addition, four Kv7.3 variants affecting residues in the long C-terminus have also been described, although the pathogenic role of these variants appears questionable due to their ample representation in the gnomAD population database without the benefit of supportive functional data (N821S, Bassi et al., 2005; R780C, Zara et al., 2013), or with

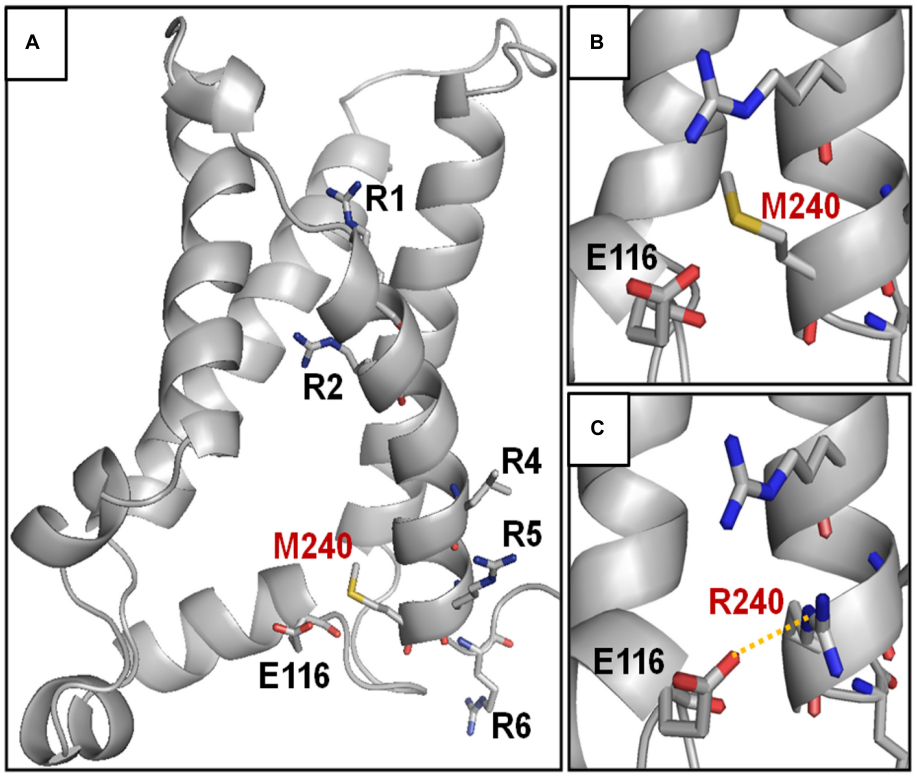

FIGURE 3 | Structural modeling of homomeric Kv7.3 channel subunits in resting gating states. **(A)** Homology model of a homotetrameric Kv7.3 channel subunits, obtained as described in the section "Materials and Methods." **(B,C)** Enlarged views showing the N-terminal domain encompassing the E116 residue in the wild-type **(B)** or M240R mutant **(C)** subunits, showing the occurrence the E116-R240 polar interaction (highlighted in yellow).

functional data that fail to support a disease association (N468S, Singh et al., 2003; P574S, Miceli et al., 2009). Out of the 13 *KCNQ3* variants causing BFNE, those nine with supportive functional data lie within a span of 51 residues (V279 to R330) in this region. Functional analyses of these variants to date, e.g., V279F, I317T, R330C, and R330L, have mostly demonstrated a reduction in maximal current with no effect on the voltage-dependence of activation (Soldovieri et al., 2014; Miceli et al., 2015; Maljevic et al., 2016), consistent with these variants being in the pore. Only W309R induced both a reduction in currents (by about 60%) and a rather small (3–4 mV) rightward shift in the $V_{1/2}$ value, when expressed together with Kv7.2 and Kv7.3 (Uehara et al., 2008).

In the present work, we report a BFNE family carrying the first variant in *KCNQ3* located in the S_4 helix of the VSD (M240R). Functional studies revealed that the M240R variant abolishes channel function in homomeric configuration, but that this is partially rescued in heteromeric channels with wild-type Kv7.2 and/or Kv7.2/3 subunits. Differently from all other Kv7.3 BFNE variants characterized to date, M240R subunits, when expressed with Kv7.2 and Kv7.3 subunits, show a significant decrease of channel sensitivity to voltage of about 10 mV, without major changes in pore properties and heteromerization. These functional results suggest that the introduction of an additional positively charged residue at the bottom of S_4 in Kv7.3 subunits destabilizes the activated conformation of the voltage sensor, thereby impeding pore opening. Structural modeling provides a potential explanation for such a conclusion; indeed, introduction of an R at position 240 stabilizes the VSD resting state by forming a novel strong ionic interaction with an highly conserved residue in the N-terminus; in addition, the larger R side chain may destabilize the tight network of hydrophobic interaction occurring in the activated state. Further studies using residue swapping or charge reversion are needed to confirm the potential interaction between the R240 and E116 residues. The available data do not allow us to determine whether the G/V shift introduced by the mutation originates from the participation of the 240 residue in voltage-sensing or in the subsequent steps along the activation pathway leading to pore opening. However, the fact that recent structural data from human Kv7.1 (Sun and MacKinnon, 2020), reveal that the V241 residue, corresponding to the M240 residue in Kv7.3, is located within a key region for VSD-pore electro-mechanical coupling (Hou et al., 2020), raises the possibility that this residue may play a similar functional role also in Kv7.3. Therefore, a LoF mechanism appears mainly responsible for BFNE pathogenesis in our family. Similar conclusions have been reached for BFNE-causing variants in Kv7.2, where haploinsufficiency, corresponding to an I_{KM} reduction of only ∼25%, appears responsible for disease pathogenesis (Jentsch, 2000).

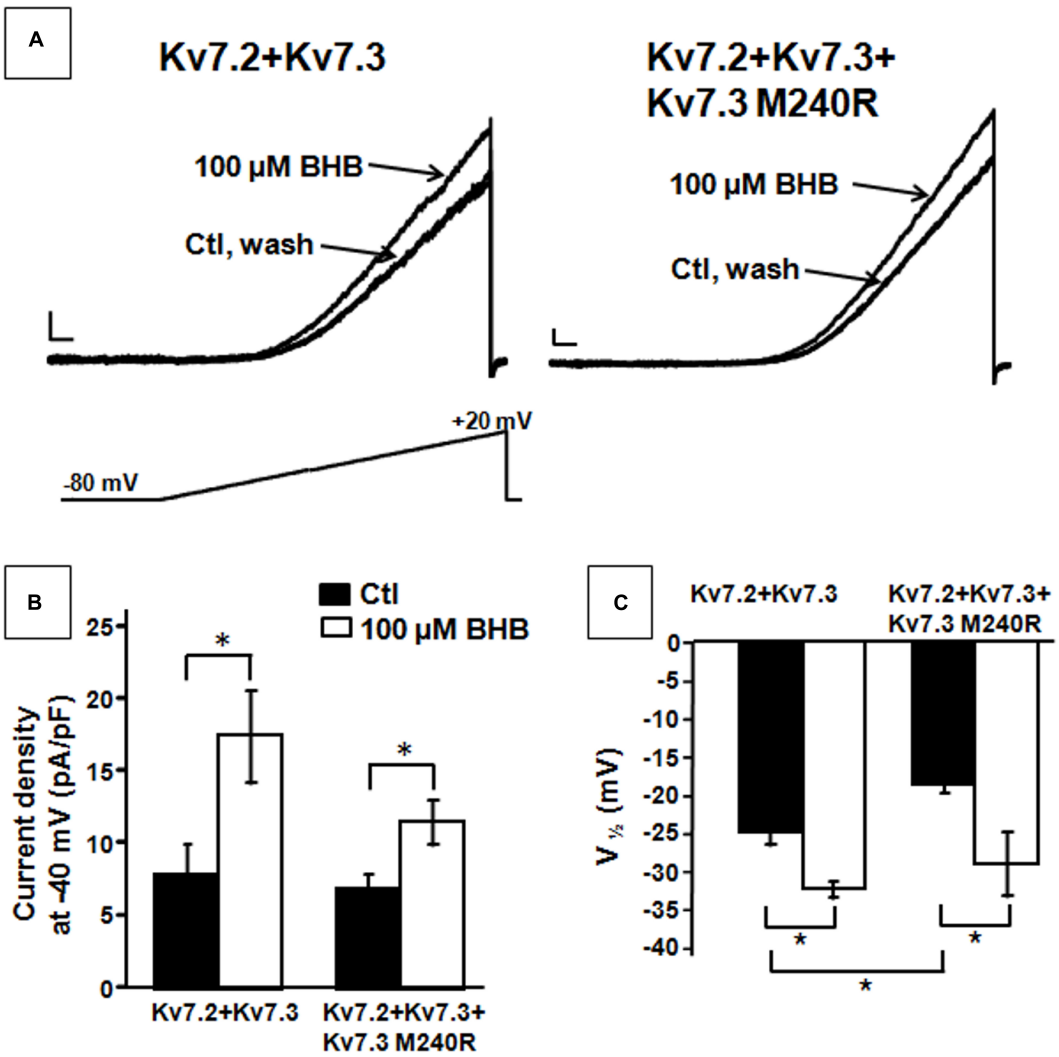

FIGURE 4 | Effect of β-hydroxybutyrate (BHB) on heteromeric Kv7.2 + Kv7.3, Kv7.2 + Kv7.3 + Kv7.3 M240R channels. **(A)** Current responses from the indicated heteromeric channels to voltage ramps from −80 to +20 mV. **(B,C)** Quantification of the effects of 100 μM BHB on the indicated heteromeric channels. Data are expressed as current density calculated at −40 mV **(B)** and in the $V_{1/2}$ values. Current scale, 200 pA; time scale, 200 ms. * indicates $p < 0.05$ vs. corresponding controls.

Benign familial neonatal epilepsy with normal neurocognitive development is not the only phenotype associated with variants in Kv7.3. In fact, individuals with mild/moderate ID have been described in BFNE pedigrees (I317T, R330L; Soldovieri et al., 2014; Miceli et al., 2015); moreover, *de novo* variants in *KCNQ3* have been described in children with DEE (Allen et al., 2013; Grozeva et al., 2015; Miceli et al., 2015; Ambrosino et al., 2018; Lauritano et al., 2019), ID apparently without epilepsy (Rauch et al., 2012; Deciphering Developmental Disorders, 2017), cortical visual impairment (Bosch et al., 2016), and in patients with ID and autism (Sands et al., 2019). Such phenotypic heterogeneity is at least in part correlated with variant-specific functional effects, by yet unknown mechanisms; in fact, opposite to BFNE variants causing LoF, gain-of-function (GoF) variants cause non-verbal ID, autism, and prominent sleep-activated multifocal epileptiform EEG discharges without neonatal seizures (Singh et al., 2003; Sands et al., 2019).

The observation that epilepsy-associated variants in *KCNQ2* are more than 10 times more frequent than those in *KCNQ3*, suggests that *KCNQ3* tolerates variation better than *KCNQ2*. Several pieces of evidence support this view; as an example, while heterozygous frameshift variants in *KCNQ2* are frequent causes of BFNE (Miceli et al., 2018), no heterozygous pathogenic frameshift *KCNQ3* variant has ever been associated with a human phenotype. In addition, no individual carrying *KCNQ2* frameshift variants in homozygosity has ever been described, as minimal *KCNQ2* residual activity is probably essential for survival (Lauritano et al., 2019); by contrast, two recent studies reported the occurrence of homozygous frameshift variants in *KCNQ3* (each inherited from an asymptomatic parent) in patients

TABLE 2 | Missense variants reported for *KCNQ3*.

Residue	Variant	Region	Phenotype	Effect	gnomAD	References
R227	R227Q	S_4 (R1)	ID/ASD	GoF	0	Sands et al., 2019
R230	R230C/H/S	S_4 (R2)	ID/ASD	GoF	1 (3.98E−06)^	Sands et al., 2019
M240	M240R	S_4	BFNE	LoF	0	Current work
Y266	Y266C	S_5	BFNE	LoF	0	Symonds et al., 2019
V279	V279F	S_5	BFNE	LoF	0	Maljevic et al., 2016
E299	E299K	Pore loop	BFNE	LoF	0	Neubauer et al., 2008
D305	D305G	Pore loop	BFNE	LoF	0	Singh et al., 2003
W308	W308S	Pore loop	BFNE		0	Sands et al., 2016
W309	W309R	Pore loop	BFNE	LoF	1 (3.98E−06)	Hirose et al., 2000; Uehara et al., 2008
G310	G310V	Pore loop	BFNE	LoF	0	Charlier et al., 1998; Schroeder et al., 1998
I317	I317T	Pore loop	BFNE*	LoF	0	Soldovieri et al., 2014
R330	R330L	Pore loop	BFNE*	LoF	0	Miceli et al., 2015
	R330C	Pore loop	BFNE	LoF	0	Li et al., 2008; Fister et al., 2013; Miceli et al., 2015
	R330H	Pore loop	BFNE		0	Allen et al., 2014
G340	G340V	S_6	BFNE		0	Grinton et al., 2015
R364	R364H	Prox C-term	BFIE		1 (3.18E−05)	Fusco et al., 2015
N468	N468S	C-terminus	BFIE	No effect	39 (1.38E−04)	Singh et al., 2003
P574	P574S	C-terminus	BFNE	No effect	586 (2.07E−03)	Miceli et al., 2009
R780	R780C	C-terminus	BFIE		26 (9.20E−05)	Zara et al., 2013
N821	N821S	C-terminus	BFNE		60 (2.12E−04)	Bassi et al., 2005

*Table gives number of observations of each variant (frequency) in gnomAD, associated phenotype, region within Kv7.3, and functional consequences in vitro if known; blue, intellectual disability (ID) with or without autism spectrum disorder (ASD); purple, benign familial neonatal epilepsy (BFNE) or benign infantile epilepsy (BFIE) phenotypes; gray, variants of questionable pathogenicity; LoF, loss-of-function; GoF, gain-of-function; * individuals with mild/moderate ID reported; ^ mosaic individual.*

with developmental delay and neonatal seizures (Kothur et al., 2018; Lauritano et al., 2019), demonstrating that, homozygous variants in *KCNQ3* are compatible with life. Moreover, a distinct functional role of these two genes emerging from developmental and genetic studies in humans, appears also to be recapitulated in mice. In fact, while *KCNQ2* homozygous KO mice died at birth, homozygous *KCNQ3* KO mice showed no seizures and survived until adulthood (Tzingounis and Nicoll, 2008; Kim et al., 2016); similarly, conditional deletion of *KCNQ2* in cortical pyramidal neurons increased neuronal excitability and decreased lifespan, whereas deletion of *KCNQ3* neither increased pyramidal neurons excitability nor affected mice survival (Soh et al., 2014).

Notably, in heteromeric channels, the functional effects of the M240R variant in Kv7.3 herein described in a BFNE family are quantitatively and qualitatively very similar to those triggered by the R213Q variant in Kv7.2, the latter identified in sporadic patients with DEE (Weckhuysen et al., 2012; Millichap et al., 2016). The fact that similar, dramatic *in vitro* functional consequences are associated to a severe phenotype in Kv7.2 and to self-limiting epilepsy in Kv7.3, further supports the hypothesis that Kv7.3 is more tolerant than Kv7.2 to genetic changes causing LoF effects. Among many others, such as inclusion/exclusion of both genes in panels for DEE, diagnostic NGS coverage, and epistatic compensation, an attractive explanation for such distinct functional role lies in the different developmental pattern of expression, with *KCNQ2* being expressed at earlier stages of development when compared to *KCNQ3*, in both mice and humans (Tinel et al., 1998; Kanaumi et al., 2008).

In patients with *KCNQ2*- and *KCNQ3*-related disorders, seizures are controlled with sodium channel blockers in most patients (Pisano et al., 2015; Sands et al., 2016). However, a percentage continues to have seizures, which may contribute to cognitive impairment. In addition, successful management of seizures does not address the neurodevelopmental disability that occurs in *KCNQ2* and *KCNQ3* DEEs. Efficacy of the KD, with greater than 90% seizure reduction, has been reported in patients with monogenic DEEs, including KCNQ2-DEE (Ko et al., 2018) and Dravet syndrome (Knupp and Wirrell, 2018). Our finding that the endogenous ketone BHB can activate heteromeric Kv7.2 + Kv7.3 channels containing Kv7.3 M240R subunits to the same extent as wild-type Kv7.2 + Kv7.3 channels (Manville et al., 2018, 2020), thereby counteracting the underlying pathophysiology, suggests that the KD could represent precision medicine for more severe phenotypes caused by *KCNQ2* and *KCNQ3* LoF variants. Further work is required to identify additional patients carrying *KCNQ3* or *KCNQ2* pathogenic LoF variants retaining responsiveness to BHB *in vitro* and who may benefit from KD treatment *in vivo*.

CONCLUSION

In conclusion, we describe the first missense LoF pathogenic variant located in the S_4 segment of *KCNQ3* as a cause of BFNE. In contrast to BFNE-*KCNQ3* variants previously described,

functional and modeling data suggest that the M240R variant primarily affects the voltage sensitivity of heteromeric channels. Our study provides a pharmacological rationale for investigating the use of KD in patients with DEE caused by *KCNQ3* and *KCNQ2* LoF variants.

DATA AVAILABILITY STATEMENT

The raw data supporting the conclusions of this article will be made available by the authors, without undue reservation.

ETHICS STATEMENT

The studies involving human participants were reviewed and approved by the Columbia University Irving Medical Center. Written informed consent to participate in this study was provided by the participants' legal guardian/next of kin. Written informed consent was obtained from the individual(s), and minor(s)' legal guardian/next of kin, for the publication of any potentially identifiable images or data included in this article.

AUTHOR CONTRIBUTIONS

FM, MT, and TS conceived the study, analyzed the data, and wrote the manuscript. EC, MC, and DG analyzed the data and wrote the manuscript. FM, LC, VB, MS, EH, AM, NL, and LB performed the research and analyzed the data. All authors contributed to the article and approved the submitted version.

FUNDING

The present work was supported by the Telethon Foundation (GGP15113) and by the Italian Ministry for University and Research (PRIN 2017ALCR7C) to MT, the Italian Ministry for University and Research (Project Scientific Independence of Researchers 2014 RBSI1444EM and PRIN 2017YH3SXK) to FM, the Italian Ministry of Health Ricerca Finalizzata Giovani Ricercatori 2016 (project GR-2016-02363337), the Italian Ministry for University and Research (PRIN 2017ALCR7C), and Research Funds from University of Molise to MS. This publication was supported by the National Center for Advancing Translational Sciences, National Institutes of Health, through Grant Number UL1TR001873. The content is solely the responsibility of the authors and does not necessarily represent the official views of the NIH.

ACKNOWLEDGMENTS

We thank Thomas J. Jentsch, Department of Physiology and Pathology of Ion Transport, Leibniz-Institut für Molekulare Pharmakologie, Berlin for sharing Kv7.2 and Kv7.3 cDNAs and David E. Shaw, D. E. Shaw Research, New York, for the coordinates of the Kv1.2/2.1 chimera.

REFERENCES

Allen, A. S., Berkovic, S. F., Cossette, P., Delanty, N., Dlugos, D., Eichler, E. E., et al. (2013). De novo mutations in epileptic encephalopathies. *Nature* 501, 217–221. doi: 10.1038/nature12439

Allen, N. M., Mannion, M., Conroy, J., Lynch, S. A., Shahwan, A., Lynch, B., et al. (2014). The variable phenotypes of KCNQ-related epilepsy. *Epilepsia* 55, e99–e105. doi: 10.1111/epi.12715

Ambrosino, P., Freri, E., Castellotti, B., Soldovieri, M. V., Mosca, I., Manocchio, L., et al. (2018). Kv7.3 Compound Heterozygous Variants in Early Onset Encephalopathy Reveal Additive Contribution of C-Terminal Residues to PIP2-Dependent K(+) Channel Gating. *Mol. Neurobiol.* 55, 7009–7024. doi: 10.1007/s12035-018-0883-5

Bassi, M. T., Balottin, U., Panzeri, C., Piccinelli, P., Castaldo, P., Barrese, V., et al. (2005). Functional analysis of novel KCNQ2 and KCNQ3 gene variants found in a large pedigree with benign familial neonatal convulsions (BFNC). *Neurogenetics* 6, 185–193. doi: 10.1007/s10048-005-0012-2

Bosch, D. G., Boonstra, F. N., de Leeuw, N., Pfundt, R., Nillesen, W. M., de Ligt, J., et al. (2016). Novel genetic causes for cerebral visual impairment. *Eur. J. Hum. Genet.* 24, 660–665. doi: 10.1038/ejhg.2015.186

Brown, D. A., and Adams, P. R. (1980). Muscarinic suppression of a novel voltage-sensitive K+ current in a vertebrate neurone. *Nature* 283, 673–676. doi: 10.1038/283673a0

Charlier, C., Singh, N. A., Ryan, S. G., Lewis, T. B., Reus, B. E., Leach, R. J., et al. (1998). A pore mutation in a novel KQT-like potassium channel gene in an idiopathic epilepsy family. *Nat. Genet.* 18, 53–55. doi: 10.1038/ng0198-53

Deciphering Developmental Disorders (2017). Prevalence and architecture of de novo mutations in developmental disorders. *Nature* 542, 433–438. doi: 10.1038/nature21062

Fister, P., Soltirovska-Salamon, A., Debeljak, M., and Paro-Panjan, D. (2013). Benign familial neonatal convulsions caused by mutation in KCNQ3, exon 6: a European case. *Eur. J. Paediatr. Neurol.* 17, 308–310. doi: 10.1016/j.ejpn.2012.10.007

Fusco, C., Frattini, D., and Bassi, M. T. (2015). A novel KCNQ3 gene mutation in a child with infantile convulsions and partial epilepsy with centrotemporal spikes. *Eur. J. Paediatr. Neurol.* 19, 102–103. doi: 10.1016/j.ejpn.2014.08.006

Grinton, B. E., Heron, S. E., Pelekanos, J. T., Zuberi, S. M., Kivity, S., Afawi, Z., et al. (2015). Familial neonatal seizures in 36 families: clinical and genetic features correlate with outcome. *Epilepsia* 56, 1071–1080. doi: 10.1111/epi.13020

Grozeva, D., Carss, K., Spasic-Boskovic, O., Tejada, M. I., Gecz, J., Shaw, M., et al. (2015). Targeted Next-Generation Sequencing Analysis of 1,000 Individuals with Intellectual Disability. *Hum. Mutat.* 36, 1197–1204. doi: 10.1002/humu.22901

Hirose, S., Zenri, F., Akiyoshi, H., Fukuma, G., Iwata, H., Inoue, T., et al. (2000). A novel mutation of KCNQ3 (c.925T–>C) in a Japanese family with benign familial neonatal convulsions. *Ann. Neurol.* 47, 822–826. doi: 10.1002/1531-8249(200006)47:6<822::aid-ana19>3.0.co;2-x

Hou, P., Kang, P. W., Kongmeneck, A. D., Yang, N. D., Liu, Y., Shi, J., et al. (2020). Two-stage electro-mechanical coupling of a KV channel in voltage-dependent activation. *Nat. Commun.* 11:676. doi: 10.1038/s41467-020-14406-w

Jensen, M. O., Jogini, V., Borhani, D. W., Leffler, A. E., Dror, R. O., and Shaw, D. E. (2012). Mechanism of voltage gating in potassium channels. *Science* 336, 229–233. doi: 10.1126/science.1216533

Jentsch, T. J. (2000). Neuronal KCNQ potassium channels: physiology and role in disease. *Nat. Rev. Neurosci.* 1, 21–30. doi: 10.1038/35036198

Kanaumi, T., Takashima, S., Iwasaki, H., Itoh, M., Mitsudome, A., and Hirose, S. (2008). Developmental changes in KCNQ2 and KCNQ3 expression in human brain: possible contribution to the age-dependent etiology of benign familial neonatal convulsions. *Brain Dev.* 30, 362–369. doi: 10.1016/j.braindev.2007.11.003

Kim, K. S., Duignan, K. M., Hawryluk, J. M., Soh, H., and Tzingounis, A. V. (2016). The voltage activation of cortical KCNQ channels depends on global PIP2 levels. *Biophys. J.* 110, 1089–1098. doi: 10.1016/j.bpj.2016.01.006

Knupp, K. G., and Wirrell, E. C. (2018). Treatment strategies for dravet syndrome. *CNS Drugs* 32, 335–350. doi: 10.1007/s40263-018-0511-y

Ko, A., Jung, D. E., Kim, S. H., Kang, H. C., Lee, J. S., Lee, S. T., et al. (2018). The Efficacy of Ketogenic Diet for Specific Genetic Mutation in Developmental and Epileptic Encephalopathy. *Front. Neurol.* 9:530. doi: 10.3389/fneur.2018.00530

Kothur, K., Holman, K., Farnsworth, E., Ho, G., Lorentzos, M., Troedson, C., et al. (2018). Diagnostic yield of targeted massively parallel sequencing in children with epileptic encephalopathy. *Seizure* 59, 132–140. doi: 10.1016/j.seizure.2018.05.005

Lauritano, A., Moutton, S., Longobardi, E., Tran Mau-Them, F., Laudati, G., Nappi, P., et al. (2019). A novel homozygous KCNQ3 loss-of-function variant causes non-syndromic intellectual disability and neonatal-onset pharmacodependent epilepsy. *Epilepsia Open* 4, 464–475. doi: 10.1002/epi4.12353

Li, H., Li, N., Shen, L., Jiang, H., Yang, Q., Song, Y., et al. (2008). A novel mutation of KCNQ3 gene in a Chinese family with benign familial neonatal convulsions. *Epilepsy Res.* 79, 1–5. doi: 10.1016/j.eplepsyres.2007.12.005

Long, S. B., Tao, X., Campbell, E. B., and MacKinnon, R. (2007). Atomic structure of a voltage-dependent K+ channel in a lipid membrane-like environment. *Nature* 450, 376–382. doi: 10.1038/nature06265

Lutas, A., and Yellen, G. (2013). The ketogenic diet: metabolic influences on brain excitability and epilepsy. *Trends Neurosci.* 36, 32–40. doi: 10.1016/j.tins.2012.11.005

Maljevic, S., Vejzovic, S., Bernhard, M. K., Bertsche, A., Weise, S., Docker, M., et al. (2016). Novel KCNQ3 mutation in a large family with benign familial neonatal epilepsy: a rare cause of neonatal seizures. *Mol. Syndromol.* 7, 189–196. doi: 10.1159/000447461

Manville, R. W., Papanikolaou, M., and Abbott, G. W. (2018). Direct neurotransmitter activation of voltage-gated potassium channels. *Nat. Commun.* 9:1847. doi: 10.1038/s41467-018-04266-w

Manville, R. W., Papanikolaou, M., and Abbott, G. W. (2020). M-Channel activation contributes to the anticonvulsant action of the ketone body beta-Hydroxybutyrate. *J. Pharmacol. Exp. Ther.* 372, 148–156. doi: 10.1124/jpet.119.263350

Miceli, F., Soldovieri, M. V., Ambrosino, P., Barrese, V., Migliore, M., Cilio, M. R., et al. (2013). Genotype-phenotype correlations in neonatal epilepsies caused by mutations in the voltage sensor of K(v)7.2 potassium channel subunits. *Proc. Natl. Acad. Sci. U.S.A.* 110, 4386–4391. doi: 10.1073/pnas.1216867110

Miceli, F., Soldovieri, M. V., Joshi, N., Weckhuysen, S., Cooper, E., and Taglialatela, M. (2018). "KCNQ2-Related Disorders," in *GeneReviews((R))*, eds M. P. Adam, H. H. Ardinger, R. A. Pagon, S. E. Wallace, L. J. H. Bean, K. Stephens, et al. (Seattle, WA: University of Washington).

Miceli, F., Soldovieri, M. V., Joshi, N., Weckhuysen, S., Cooper, E. C., and Taglialatela, M. (2017). "KCNQ3-Related Disorders," in *GeneReviews((R))*, eds M. P. Adam, H. H. Ardinger, R. A. Pagon, S. E. Wallace, L. J. H. Bean, K. Stephens, et al. (Seattle, WA: University of Washington).

Miceli, F., Soldovieri, M. V., Lugli, L., Bellini, G., Ambrosino, P., Migliore, M., et al. (2009). Neutralization of a unique, negatively-charged residue in the voltage sensor of K V 7.2 subunits in a sporadic case of benign familial neonatal seizures. *Neurobiol. Dis.* 34, 501–510. doi: 10.1016/j.nbd.2009.03.009

Miceli, F., Striano, P., Soldovieri, M. V., Fontana, A., Nardello, R., Robbiano, A., et al. (2015). A novel KCNQ3 mutation in familial epilepsy with focal seizures and intellectual disability. *Epilepsia* 56, e15–e20. doi: 10.1111/epi.12887

Millichap, J. J., Park, K. L., Tsuchida, T., Ben-Zeev, B., Carmant, L., Flamini, R., et al. (2016). KCNQ2 encephalopathy: features, mutational hot spots, and ezogabine treatment of 11 patients. *Neurol Genet.* 2:e96. doi: 10.1212/NXG.0000000000000096

Neubauer, B. A., Waldegger, S., Heinzinger, J., Hahn, A., Kurlemann, G., Fiedler, B., et al. (2008). KCNQ2 and KCNQ3 mutations contribute to different idiopathic epilepsy syndromes. *Neurology* 71, 177–183. doi: 10.1212/01.wnl.0000317090.92185.ec

Pisano, T., Numis, A. L., Heavin, S. B., Weckhuysen, S., Angriman, M., Suls, A., et al. (2015). Early and effective treatment of KCNQ2 encephalopathy. *Epilepsia* 56, 685–691. doi: 10.1111/epi.12984

Rauch, A., Wieczorek, D., Graf, E., Wieland, T., Endele, S., Schwarzmayr, T., et al. (2012). Range of genetic mutations associated with severe non-syndromic sporadic intellectual disability: an exome sequencing study. *Lancet* 380, 1674–1682. doi: 10.1016/S0140-6736(12)61480-9

Sands, T. T., Balestri, M., Bellini, G., Mulkey, S. B., Danhaive, O., Bakken, E. H., et al. (2016). Rapid and safe response to low-dose carbamazepine in neonatal epilepsy. *Epilepsia* 57, 2019–2030. doi: 10.1111/epi.13596

Sands, T. T., Miceli, F., Lesca, G., Beck, A. E., Sadleir, L. G., Arrington, D. K., et al. (2019). Autism and developmental disability caused by KCNQ3 gain-of-function variants. *Ann. Neurol.* 86, 181–192. doi: 10.1002/ana.25522

Schroeder, B. C., Kubisch, C., Stein, V., and Jentsch, T. J. (1998). Moderate loss of function of cyclic-AMP-modulated KCNQ2/KCNQ3 K+ channels causes epilepsy. *Nature* 396, 687–690. doi: 10.1038/25367

Singh, N. A., Westenskow, P., Charlier, C., Pappas, C., Leslie, J., Dillon, J., et al. (2003). KCNQ2 and KCNQ3 potassium channel genes in benign familial neonatal convulsions: expansion of the functional and mutation spectrum. *Brain* 126(Pt 12), 2726–2737. doi: 10.1093/brain/awg286

Soh, H., Pant, R., LoTurco, J. J., and Tzingounis, A. V. (2014). Conditional deletions of epilepsy-associated KCNQ2 and KCNQ3 channels from cerebral cortex cause differential effects on neuronal excitability. *J. Neurosci.* 34, 5311–5321. doi: 10.1523/JNEUROSCI.3919-13.2014

Soldovieri, M. V., Boutry-Kryza, N., Milh, M., Doummar, D., Heron, B., Bourel, E., et al. (2014). Novel KCNQ2 and KCNQ3 mutations in a large cohort of families with benign neonatal epilepsy: first evidence for an altered channel regulation by syntaxin-1A. *Hum. Mutat.* 35, 356–367. doi: 10.1002/humu.22500

Soldovieri, M. V., Castaldo, P., Iodice, L., Miceli, F., Barrese, V., Bellini, G., et al. (2006). Decreased subunit stability as a novel mechanism for potassium current impairment by a KCNQ2 C terminus mutation causing benign familial neonatal convulsions. *J. Biol. Chem.* 281, 418–428. doi: 10.1074/jbc.m510980200

Sun, J., and MacKinnon, R. (2020). Structural basis of human KCNQ1 modulation and gating. *Cell* 180, 340-347.e9. doi: 10.1016/j.cell.2019.12.003

Symonds, J. D., Zuberi, S. M., Stewart, K., McLellan, A., O'Regan, M., MacLeod, S., et al. (2019). Incidence and phenotypes of childhood-onset genetic epilepsies: a prospective population-based national cohort. *Brain* 142, 2303–2318. doi: 10.1093/brain/awz195

Tinel, N., Lauritzen, I., Chouabe, C., Lazdunski, M., and Borsotto, M. (1998). The KCNQ2 potassium channel: splice variants, functional and developmental expression. Brain localization and comparison with KCNQ3. *FEBS Lett.* 438, 171–176. doi: 10.1016/s0014-5793(98)01296-4

Tzingounis, A. V., and Nicoll, R. A. (2008). Contribution of KCNQ2 and KCNQ3 to the medium and slow afterhyperpolarization currents. *Proc. Natl. Acad. Sci. U.S.A.* 105, 19974–19979. doi: 10.1073/pnas.0810535105

Uehara, A., Nakamura, Y., Shioya, T., Hirose, S., Yasukochi, M., and Uehara, K. (2008). Altered KCNQ3 potassium channel function caused by the W309R pore-helix mutation found in human epilepsy. *J. Membr. Biol.* 222, 55–63. doi: 10.1007/s00232-008-9097-5

Wang, H. S., Pan, Z., Shi, W., Brown, B. S., Wymore, R. S., Cohen, I. S., et al. (1998). KCNQ2 and KCNQ3 potassium channel subunits: molecular correlates of the M-channel. *Science* 282, 1890–1893. doi: 10.1126/science.282.5395.1890

Weckhuysen, S., Mandelstam, S., Suls, A., Audenaert, D., Deconinck, T., Claes, L. R., et al. (2012). KCNQ2 encephalopathy: emerging phenotype of a neonatal epileptic encephalopathy. *Ann. Neurol.* 71, 15–25. doi: 10.1002/ana.22644

Zara, F., Specchio, N., Striano, P., Robbiano, A., Gennaro, E., Paravidino, R., et al. (2013). Genetic testing in benign familial epilepsies of the first year of life: clinical and diagnostic significance. *Epilepsia* 54, 425–436. doi: 10.1111/epi.12089

Conflict of Interest: The authors declare that the research was conducted in the absence of any commercial or financial relationships that could be construed as a potential conflict of interest.

frontiers in Physiology

ORIGINAL RESEARCH
published: 11 September 2020
doi: 10.3389/fphys.2020.571813

Two *KCNQ2* Encephalopathy Variants in the Calmodulin-Binding Helix A Exhibit Dominant-Negative Effects and Altered PIP_2 Interaction

*Baouyen Tran[1], Zhi-Gang Ji[2], Mingxuan Xu[2], Tammy N. Tsuchida[3] and Edward C. Cooper[1,2,4]**

[1]*Department of Neuroscience, Baylor College of Medicine, Houston, TX, United States,* [2]*Department of Neurology, Baylor College of Medicine, Houston, TX, United States,* [3]*Departments of Pediatrics and Neurology, Children's National Medical Center, Washington, DC, United States,* [4]*Department of Molecular and Human Genetics, Baylor College of Medicine, Houston, TX, United States*

OPEN ACCESS

Edited by:
Thomas Andrew Jepps, University of Copenhagen, Denmark

Reviewed by:
Jérôme J. Devaux, INSERM U1051 Institut des Neurosciences de Montpellier (INM), France
Enrique Soto, Meritorious Autonomous University of Puebla, Mexico

***Correspondence:**
Edward C. Cooper
ecc1@bcm.edu

Specialty section:
This article was submitted to Membrane Physiology and Membrane Biophysics, a section of the journal Frontiers in Physiology

Received: *11 June 2020*
Accepted: *18 August 2020*
Published: *11 September 2020*

Citation:
Tran B, Ji Z-G, Xu M, Tsuchida TN and Cooper EC (2020) Two KCNQ2 Encephalopathy Variants in the Calmodulin-Binding Helix A Exhibit Dominant-Negative Effects and Altered PIP_2 Interaction. Front. Physiol. 11:571813. doi: 10.3389/fphys.2020.571813

Heterozygous missense variants in *KCNQ2*, which encodes the potassium channel subunit Kv7.2, are among the most common genetic causes of severe neonatal-onset epileptic encephalopathy. Because about 20% of known severe Kv7.2 missense changes lie within the intracellular C-terminal region, improving understanding of the underlying pathogenic mechanisms is important. We analyzed the basis for the severe phenotypes of Kv7.2 A337T and A337G, variants in the C-terminal's calmodulin (CaM)-binding Helix A. When expressed heterologously in mammalian cells, alone or in combination with wild type Kv7.2 or with wild type Kv7.2 and Kv7.3, both variants strongly suppressed channel currents. A337T channels expressed alone exhibited significantly reduced protein half-life and surface trafficking and co-immunoprecipitated less CaM. For both variants, increasing cellular phosphatidylinositol 4,5-bisphosphate (PIP_2) by overexpression of PI(4)P5-kinase restored current densities. For both variants, the fraction of current suppressed by activation of M1 muscarinic receptors with 10 μM oxotremorine methiodide, which depletes PIP_2, was less than for controls. During voltage-sensitive phosphatase-induced transient PIP_2 depletion and resynthesize, potassium current inhibition and recovery kinetics were both markedly slowed. These results suggest that these variants may reduce currents by a mechanism not previously described: slowing of PIP_2 migration between the bulk membrane and binding sites mediating channel electromechanical coupling. A novel Kv7.2/3-selective opener, SF0034, rescued current amplitudes. Our findings show that these two Helix A variants suppress channel current density strongly, consistent with their severe heterozygous phenotypes, implicate impairment of CaM and PIP_2 regulation in *KCNQ2* encephalopathy pathogenesis, and highlight the potential usefulness of selective Kv7 openers for this distinctive pathogenic mechanism and patient subgroup.

Keywords: SF0034, Kv7.2, epileptic encephalopathy, phosphatidylinositol 4,5-bisphosphate, calmodulin

INTRODUCTION

Variants in *KCNQ2* can underlie a severe syndrome consisting of intractable neonatal onset seizures and profound global developmental delay called *KCNQ2* encephalopathy (Weckhuysen et al., 2012; Millichap et al., 2016). Indeed, recent cohort studies have shown that 10–30% of previously undiagnosed patients with early infantile epileptic encephalopathy (EIEE) have *de novo* heterozygous missense or single codon deletion variants in *KCNQ2* (Saitsu et al., 2012; Weckhuysen et al., 2012; Kato et al., 2013; Milh et al., 2013; Olson et al., 2017). *KCNQ2* was first discovered at the locus for a mild, self-limiting neonatal syndrome, benign familial neonatal epilepsy (BFNE) (Biervert et al., 1998; Charlier et al., 1998; Singh et al., 1998). *KCNQ2* variants causing BFNE are usually inherited as an autosomal dominant trait with high penetrance but sometimes appears *de novo*. It is important to understand *KCNQ2* genotype-phenotype relationships so that individuals with BFNE or with rare non-pathogenic variants can be rapidly distinguished from those with EIEE-causing variants. BFNE infants have a good prognosis, and ill infants with non-pathogenic *KCNQ2* variants need further diagnostic efforts. Individuals with pathogenic *KCNQ2* encephalopathy variants have ended their diagnostic odyssey, have a poor long-term prognosis, and are appropriate candidates for novel therapeutic trials.

KCNQ2 and its close homolog, *KCNQ3*, encode potassium channel subunits Kv7.2 and Kv7.3, respectively, which form tetrameric neuronal voltage-gated potassium channels. Both homomers (formed by Kv7.2 alone) and heteromers (combining Kv7.2 and Kv7.3) underlie the neuronal M-current (I_M), a voltage-dependent, slowly activating, non-inactivating current regulated by G_q-coupled receptors including M1 muscarinic acetylcholine receptors (M1Rs; Wang et al., 1998; Delmas and Brown, 2005). These channels are broadly expressed in the central nervous system, where they are highly concentrated at axon initial segments (AISs) and nodes of Ranvier, and can influence action potential generation and conduction (Cooper et al., 2000; Devaux et al., 2004; Pan et al., 2006; Shah et al., 2008; Battefeld et al., 2014). Kv7.2 and Kv7.3 have a classical 6-transmembrane voltage-gated potassium channel topology but possess a distinctive, large intracellular CT domain (**Figure 1A**). Known roles of the CT include integrating modulatory interactions, including with calmodulin (CaM; Wen and Levitan, 2002; Yus-Nájera et al., 2002) and phosphatidylinositol 4,5-bisphosphate (PIP_2; Zhang et al., 2003; Li et al., 2005; Brown et al., 2007; Gamper and Shapiro, 2007; Hernandez et al., 2008; Zaydman and Cui, 2014).

Considerable evidence indicates that CaM and PIP_2 interactions are allosterically coupled (Kosenko et al., 2012; Kosenko and Hoshi, 2013; Zaydman and Cui, 2014; Alberdi et al., 2015; Chen et al., 2015). Although Kv7.1 atomic structures have recently been obtained in the presence of CaM, with and without bound PIP_2 (Sun and MacKinnon, 2017, 2020), dynamic mechanisms of Ca^{2+}-CaM and PIP_2 regulation remain poorly understood. CaM binding at two α-helical segments of the Kv7.2 CT domain, Helix A and B, has been proposed to be required for ER exit and targeting to the axon (Etxeberria et al., 2008; Alaimo et al., 2009; Cavaretta et al., 2014; Liu and Devaux, 2014). PIP_2 binding is required for the voltage-dependent opening of Kv7 channels and appears to contribute directly to coupling voltage sensor movement and pore gate opening (Zaydman et al., 2013; Zaydman and Cui, 2014; Sun and MacKinnon, 2017, 2020). However, sites functionally implicated in Kv7 channel PIP_2 modulation extend beyond the binding pocket seen by cryoelectron microscopy and include conserved H, K, and R residues from the S2–3 linker, S4–5 linker, S6, the CT region upstream of the Helix A, and on linkers between the A, B, and C helices (Hernandez et al., 2008; Telezhkin et al., 2013; Zaydman and Cui, 2014; Hille et al., 2015).

Most BFNE missense variants cause mild loss-of-function when co-expressed with wild type (WT) subunits, whereas most EIEE variants cause severe dominant-negative suppression of activity. However, only a small proportion of known variants have been studied to date. Previous studies of human Kv7.2 variants from the CT domain have mostly focused on those causing BFNE (Richards et al., 2004; Alaimo et al., 2009; Orhan et al., 2014; Alberdi et al., 2015; Ambrosino et al., 2015). Recently, a heterozygous Kv7.2 EIEE variant in the proximal CT, R325G, was shown to suppress currents by directly impairing PIP_2 binding (Soldovieri et al., 2016). Here, we analyze the functional consequences of A337T and A337G, two *KCNQ2* encephalopathy variants (Saitsu et al., 2012; Millichap et al., 2016), at a conserved residue in the CaM-binding Helix A (**Figure 1A**). The pathogenicity of these variants has remained less certain due to rarity: To date, only one individual has been described with each. We found that both variants cause loss of current amplitude sufficient to be considered as dominant-negative, supporting the clinical diagnoses of *KCNQ2* encephalopathy. We obtained evidence that the suppression of Kv7.2 + Kv7.3 channel function involves a novel pattern of disruption of PIP_2 and (for A337T) CaM interaction. Ezogabine was previously used successfully to control seizures and improve EEG in the infant with A337T (Millichap et al., 2016). We show that SF0034, a close ezogabine analog with improved potency and KCNQ2/3 selectivity (Kalappa et al., 2015), rescued current loss. Our findings highlight the importance of PIP_2 interaction in causation and potential therapy for *KCNQ2* encephalopathy.

MATERIALS AND METHODS

Ethics

Animal procedures were approved by the Institutional Animal Care and Use Committee (IACUC) at Baylor College of Medicine, in accordance with guidelines of the Association for Assessment and Accreditation of Laboratory and Animal Care (AAALAC) and the U.S. National Institutes of Health (NIH). Clinical data were collected according to procedures reviewed and approved by the Institutional Review Board of Baylor College of Medicine. The study protocol allows inclusion of information on registered patients enrolled after informed written consent, as well as deidentified data regarding anonymous patients entered after verbal parental consent to the treating physician.

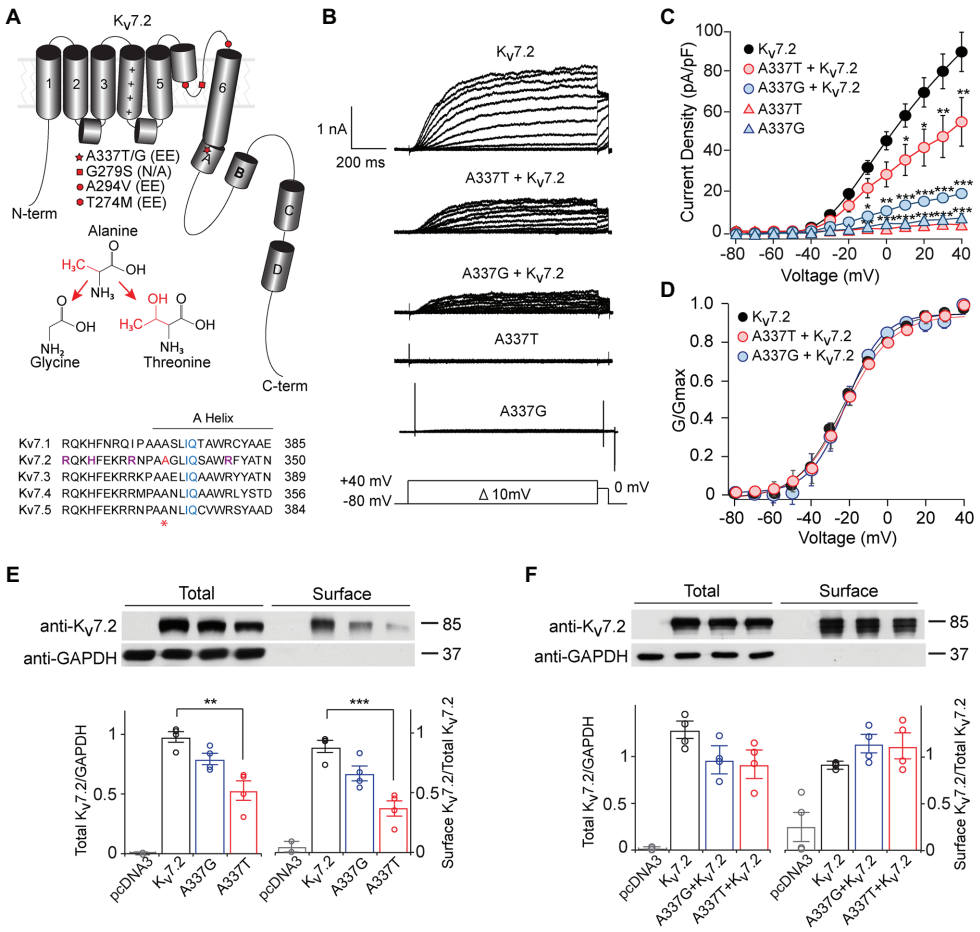

FIGURE 1 | A337T and A337G suppressed Kv7.2 currents. **(A)** Cartoon showing Kv7.2 membrane topology, highlighting positions of functionally important α-helical segments and domains, and the variants analyzed in this study. The side chain changes resulting from the two clinical variants at A337 are shown. Alignment of human *KCNQ* sequences around *KCNQ2* A337 (red and asterisk) shows high conservation across the gene family. Basic residues previously implicated in PIP_2 binding (Zhang et al., 2013; Kim et al., 2016a; Soldovieri et al., 2016; purple) and the canonical CaM binding IQ motif (blue), are highlighted. A337 (highlighted in red and asterisk) is near the proximal end of Helix A. **(B)** Representative currents from Chinese hamster ovary (CHO) cells transfected with WT Kv7.2, A337G, and A337T in response to depolarization steps from −80 mV to between −70 and +40 mV. **(C)** Current-voltage plots show significant current reductions in cells expressing either A337T or A337G (**$p < 0.01$, ***$p < 0.001$, Two-way ANOVA, Bonferroni test, $n = 14–31$, see **Table 1**). **(D)** Conductance-voltage plots show no significant differences of WT and mutant-containing channels (see **Table 1**). **(E)** Western blots of cell lysates (left lanes, **$p = 0.003$, One-way ANOVA, Tukey test) and surface biotinylated proteins (right lanes, ***$p < 0.001$, One-way ANOVA, Tukey test) from CHO cells electroporated with empty pcDNA3 vector (negative control), Kv7.2, A337G or A337T ($n = 4$). In plots, quantification of total channel protein normalized to GAPDH (left) and surface channel protein normalized to total channel protein are shown. Values are normalized to WT. **(F)** Western blot of cell lysates (left lanes) and surface membrane biotinylated proteins (right lanes) from CHO cells electroporated with WT Kv7.2 alone or with 1:1 ratio of Kv7.2 and A337G or A337T cDNAs ($n = 4$). The cropped blot images are from full-length gels shown as supplementary information **(Supplementary Figure S2)**.

cDNA Constructs, Drugs, and Nomenclature

Human KCNQ2 (Genbank: NM_004518) and KCNQ3 (NM_004519) cDNA (Biervert et al., 1998; Schroeder et al., 1998) clones were provided by Thomas Jentsch and subcloned into pcDNA3.1 (Thermo Fisher Scientific). Point mutations were introduced using QuikChange (Agilent Technologies). *C. intestinalis* voltage sensitive phosphatase (ciVSP) cDNA (Murata and Okamura, 2007) was provided by Yasushi Okamura (Osaka Univ.). Mouse phosphatidylinositol-4-phosphate 5-kinase type I gamma (PIP5K, NM_001293647) cDNA was provided by Robin Irvine (Cambridge Univ.). Human M1 muscarinic receptor (M1R, NM_000738.3) cDNA was provided by Bruce Conklin (University of California, San Francisco). SF0034 was provided by SciFluor Life Sciences (Cambridge, MA). Oxotremorine methiodide (Oxo-M) was purchased from (Sigma-Aldrich). Kv7.2 protein variants are listed with respect to the 872 codon reference sequence (NCBI Reference Sequence: NM 172107.3).

Cell Culture and cDNA Expression

Chinese hamster ovary (CHO) cells and human embryonic kidney (HEK) 293 T cells were maintained in Dulbecco's modified Eagle's medium (DMEM, Gibco) at 5% CO_2 and 37°C.

All patch clamp studies shown were conducted using CHO cells transfected using PolyJet (SignaGen). To achieve higher protein expression levels required for cycloheximide (CHX) protein stability experiments, HEK cells transfected using Lipofectamine 2000 (Thermo Fisher Scientific) were used. Electroporation using the Neon system (Thermo Fisher Scientific) was used with CHO cells for surface protein biotinylation experiments and CaM co-immunoprecipitation, and with acutely dissociated hippocampal neurons for AIS localization experiments.

Whole Cell Electrophysiology

Transfected CHO cells were recorded at room temperature (20–22°C), 1–3 days post-transfection, using an Axopatch 200B (Molecular Devices) amplifier, pCLAMP v.9, a cFlow perfusion controller and mPre8 manifold (Cell MicroControls), and glass micropipettes (VWR International) with 1–4 MΩ resistance. The extracellular solution consisted of (in mM): 138 NaCl, 5.4 KCl, 2 $CaCl_2$, 1 $MgCl_2$, 10 glucose, 10 HEPES, pH 7.4 with NaOH (Miceli et al., 2013). Pipette solution contained (in mM): 140 KCl, 2 $MgCl_2$, 10 EGTA, 10 HEPES, and 5 Mg-ATP, pH 7.4 with KOH. Series resistance was compensated by 70% after compensation using Axopatch 200B fast and slow capacitance controls. Currents were digitally sampled at 5–10 kHz, depending on the protocol, and filtered at 5 kHz using a low-pass Bessel filter. For voltage-activation experiments, cells were held at −80 mV and depolarized in 10 mV incremental steps from −80 to +40 mV for 1 s, then stepped to 0 mV for 60 ms. Tail currents at 0 mV were fitted using the Boltzmann function: $\frac{G}{Gmax} = \frac{1}{1+e^{\frac{V_{\frac{1}{2}}-Vm}{k}}}$ to obtain the half-maximum activation voltage ($V_{1/2}$) and the slope factor (k). Activation and deactivation rates were measured in SigmaPlot or Clampfit using a single exponential function: $I = Ae^{-t/\tau} + C$. TEA sensitivity experiments were performed as previously described (Soldovieri et al., 2016). Currents were elicited by 3 s ramp depolarizations from −80 to 40 mV. To monitor inhibition by Oxo-M, cells were pulsed every 2 s for 200 ms to +40 mV from a holding potential of −80 mV before, during and after perfusion with drug solution. In experiments using ciVSP to study recovery, cells were held at −80 mV, then pre-pulsed for 2 s at −20 mV before stepping to +100 mV for 10 s, and then held at −20 mV for 30 s to monitor recovery. Kinetic parameters for current depletion and recovery were determined by non-linear regression models in SigmaPlot. Rates of current decline after ciVSP activation were estimated by fitting to a sigmoidal equation: $y = \frac{1}{\left(1+e^{-t-t0/b}\right)}$. For WT Kv7.2 + Kv7.3 heteromers, current recovery kinetics after the end of a ciVSP-activating step were fit using the squared exponential function: $y^2 = \left(1-2e^{-\frac{t}{\tau}}+e^{-2t/\tau}\right)$ as described previously (Falkenburger et al., 2010; Alberdi et al., 2015). Current recovery for channels containing variants were fit poorly using this squared exponential but could be better fit using another sigmoidal equation, the 4-parameter logistic: $y = ymax + (y0 - \frac{ymax}{(1+\frac{t}{\left(ymax-\frac{ymin}{2}\right)^b})})$. A calculated liquid junction potential (−3.62 mV) was not corrected.

Biotinylation, Immunoprecipitation, and Western Blotting

CHO cell membrane protein biotinylation was performed 48 h after electroporation, using Sulfo-NHS-LC-Biotin (Pierce) as described previously (Kosenko et al., 2012). Excess biotin was quenched using 100 mM glycine and cells were lysed. After clearing by centrifugation, NeutrAvidin agarose beads (Pierce) were used to collect biotinylated proteins. For CaM co-IP, lysates were incubated with Dynabead protein A magnetic beads (Thermo Fisher) pre-coated with guinea pig anti-KCNQ2-C2 antibodies (Surti et al., 2005). Proteins were separated on 8% (Kv7) or 12% (CaM) SDS-PAGE gels, transferred onto nitrocellulose membranes, and analyzed by western blotting. For CaM blots, PVDF membranes were used, and protein gels were transferred in 0.1 M potassium phosphate buffer (pH 7.4) overnight and then fixed in 0.2% glutaraldehyde for 45 min. Membranes were blocked and then blotted with antibodies, imaged using enhance chemiluminescence (ThermoFisher Pierce Supersignal) and film, and bands were quantified as described previously (Cooper et al., 2001; Pan et al., 2006; Jin et al., 2009). Primary blotting antibodies were guinea pig-anti-KCNQ2-C2 and anti-KCNQ3-N1, mouse-anti-calmodulin (Pierce), and chicken-anti-GAPDH as loading control (Cell Signal) in 2% IgG-Free BSA (Jackson ImmunoResearch), blocking buffer was tris-buffered saline with 0.1% Tween-20 (TBS-T, Bio-Rad), and secondary antibodies were HRP-conjugated anti-guinea pig, anti-mouse or anti-chicken (Jackson ImmunoResearch). For quantification of channel or calmodulin expression in whole cell lysates, each channel band was normalized against the intensity of the anti-GAPDH band in the same lane. Bar graphs show results of normalized versus WT control samples. Band intensities were averaged across the indicated numbers of independent transfections and blots.

Cycloheximide Treatment

Forty-eight hours after transfection, HEK cells were treated with 100 μg/ml of CHX (Sigma-Aldrich) or dimethyl sulfoxide (DMSO) (Thermo Fisher) at the same start time and then processed for cell lysis at subsequent time points as shown.

Hippocampal Neuron Culture and Immunocytochemistry

Hippocampi from male and female Sprague-Dawley rats (Charles River) were dissected at E18–19 incubated with proteases at 37° C for 15 min, and cells were dissociated by trituration with fire-polished Pasteur pipettes. After electroporation (Thermo Fisher Neon, 1 μg total DNA per sample, 1,200 V, 40 ms, 1 pulse), neurons were plated on poly-D-lysine (Sigma-Aldrich) and rat tail collagen (Roche) coated 12 mm glass coverslips

(Warner Instruments) at 5 × 10^4 cells per well in a 24-well plate in a plating media [minimal essential medium (MEM), 10% FBS, 0.5% glucose, 1 mM sodium pyruvate, 25 μM glutamine, and 50 units penicillin/streptomycin]. After 4 h, medium was changed to Neurobasal medium supplemented with B-27 and 25 mM glutamine and 50 units pen/strep. At 3 days *in vitro* (DIV), neuronal cultures were treated with 2 μM cytosine arabinoside. Half of the neuronal culture medium was replaced with fresh medium every 5–6 days. At 7 DIV, the neurons were fixed with 1% PFA in Na-acetate, pH 6.0 for 20 min and washed with PBS. Coverslips were blocked in 3% BSA, 0.1% Triton X-100 for 1 h at RT and then incubated with lab-made primary rabbit-anti-KCNQ2-N1 and guinea pig-anti-KCNQ3-N1 antibodies as previously described (Cooper et al., 2001; Devaux et al., 2004; Pan et al., 2006). Labeling with mouse-anti-Ankyrin-G (clone N106/36; UC Davis/NINDS/NIMH NeuroMab Facility) was used to demark AISs. Secondary antibodies were anti-rabbit DyLight 488, anti-mouse Cy3, and anti-guinea-pig Cy5-conjugated secondary antibodies (Jackson ImmunoResearch). Cover slips were mounted in ProLong Gold with DAPI (Thermo Fisher). Images were acquired using a Nikon 80i microscope, a 60× NA 1.4 Plan Apo oil-immersion objective lens, NIS-Elements software (Nikon), and an ExiAqua (QImaging) CCD camera. In each experiment, acquisition settings for each color channel were identical for all samples. Quantification of the immunofluorescence signals along the AIS was performed as described previously (Battefeld et al., 2014). The NIS-Elements intensity profile tool was used to mark the AIS trajectory, using abrupt increases and decreases in labeling for ankyrin-G to mark the AIS origin and distal tip. For each color channel in each set of images acquired in parallel, the black (0 intensity) level was specified by measuring a minimal intensity value at a non-AIS location; this quantity was subtracted from all measurements for all images to be compared. Intensity values along each AIS trajectory were binned in 16 segments, and these values were averaged to determine mean segment intensities for each condition and fluorophore. These values were normalized to the mean maximal values measured in images of control neurons electroporated with WT Kv7.2 and Kv7.3 cDNAs to obtain relative intensity values at each distance along the AIS (Battefeld et al., 2014).

Statistics

Statistical analyses were performed in SigmaPlot (v.13). One- or two-way ANOVA was followed by Tukey's or Bonferroni's post-hoc test for multiple comparisons. For drug treatment studies, one- or two-way repeated measures (RM) ANOVA was performed. On figure panels: $*p < 0.05$, $**p < 0.01$ and $***p < 0.001$. All fluorescence intensities, band intensities, and electrophysiology analyses are reported as mean ± SEM.

RESULTS

Clinical Descriptions

Description of patients with EIEE and the *KCNQ2 de novo* variants c.1009G>A; p.Ala337Thr (Millichap et al., 2016) and c.1010C>G; p.Ala337Gly (Saitsu et al., 2012) appeared previously. The A337T individual is now age 8 years of age and has been followed clinically since birth. Electroencephalograms (EEGs) at ages 6 days, 5 months (prior to ezogabine use), and 6 months (with high dose ezogabine) were presented previously. Focal tonic seizures and clusters of flexor spasms, hypotonia, and encephalopathy were noted at age 2 days. The neonatal EEG background had primarily a burst-suppression appearance, except for brief intervals of continuity (high-amplitude delta activity with multifocal epileptiform discharges) during wakefulness. The EEG evolved by age 4 months to a modified hypsarrhythmia pattern with multifocal epileptiform activity and frequent electroclinical focal tonic seizures (several per day) continued despite serial anti-seizure medication trials including phenobarbital, topiramate, oxcarbazepine, and lamotrigine. Ezogabine treatment at age 5 months was followed closely with serum levels, EEG, and clinical observation. Ezogabine caused urinary retention at 23 mg/kg/day but this resolved easily and the treatment was resumed at 14 mg/kg/day and later increased to 21 mg/kg/day. Ezogabine exposure was associated with improvement in seizures, which was reflected in diminished epileptiform activity. The patient remained on ezogabine until it was removed from the market by the manufacturer almost 4.5 years later. Despite ezogabine, however, the patient remains globally developmentally delayed (nonverbal but can choose objects by pressing a button on an assistive device, non-ambulatory), although breakthrough seizures became rare. The A337G individual was described at 7 years old in 2012 (Saitsu et al., 2012). Very briefly, the patient was diagnosed with Ohtahara syndrome as a neonate, due to tonic seizure onset at age 7 days, burst-suppression EEG, and encephalopathy. The patient remained globally impaired at age 7 years, without the ability to speak meaningful words or walk.

Kv7.2 A337T and A337G Are Loss-of-Function Variants

Under whole cell voltage-clamp, CHO cells transfected with WT Kv7.2 produced large, slowly activating, non-inactivating currents, but cells expressing A337T alone or A337G alone gave little detectable voltage-activated current (**Figures 1B,C**). Compared to WT Kv7.2, CHO cells transfected with A337T + Kv7.2 plasmids in a 1:1 ratio to mimic the heterozygous genotype displayed about 40% less current at +40 mV and A337G + Kv7.2 about 80% less current (**Figure 1C**; Kv7.2: 89.6 ± 9.6 pA/pF; A337G + Kv7.2: 20.2 ± 3.6 pA/pF; A337T + Kv7.2: 55.3 ± 11.9 pA/pF). The conductance/voltage relationship of cells co-expressing WT and A337 variants 1:1 was not significantly changed compared to WT alone (**Figure 1D**). Experiments using co-expression with the tetraethylammonium (TEA)-resistant mutant, Kv7.2 Y284C (Hadley et al., 2003; Soldovieri et al., 2016), were used to assess for co-assembly. The principle of this assay is that channels formed by coassembly with Y284C exhibit an intermediate sensitivity to TEA. A337T and A337G, when co-expressed with Y284C (or with WT), indeed showed currents that were more sensitive to TEA than Y284C expressed alone (**Supplementary Figure S1**). Thus, the

A337 variants are capable of forming tetramers with Y284C, and the most parsimonious explanation of the results is that in homomers, A337T partly and A337G more fully exerts a current-suppressing effect on WT Kv7.2.

We used surface biotinylation and western blots to further assess whether the observed decreases in current could be explained by a reduction of protein levels. Total and surface-localized Kv7.2 protein levels from cells expressing A337G were not significantly different from WT controls. Cells expressing A337T alone showed significantly decreased total Kv7.2 protein (0.56 ± 0.08 of WT) and reduced surface abundance (0.43 ± 0.06 of WT). These reductions were insufficient to account for the nearly complete loss of current exhibited (**Figure 1E**). Moreover, when either A337T or A337G was co-expressed with WT Kv7.2 in a 1:1 ratio, total protein (Kv7.2: 1.00 ± 0.11; A337G + Kv7.2: 0.78 ± 0.17; A337T + Kv7.2: 0.73 ± 0.17) and surface abundance (Kv7.2: 1.00 ± 0.01; A337G + Kv7.2: 1.23 ± 0.12; A337T + Kv7.2: 1.20 ± 0.16) were restored to control levels (**Figure 1F**; see **Supplementary Figure S2** for full blots).

Although homomeric Kv7.2 channels are found within the nervous system, Kv7.2 + Kv7.3 heteromeric channels give much larger currents and appear to be the main contributors to neuronal somatic and axonal M-currents in many neuronal types (Wang et al., 1998; Cooper et al., 2000; Hadley et al., 2003; Devaux et al., 2004; Pan et al., 2006; Battefeld et al., 2014). Therefore, we co-transfected each A337 variant with WT Kv7.2 and Kv7.3 cDNAs in a 1:1:2 ratio, mimicking the heterozygous genotype and the heteromeric subunit composition. Remarkably, inclusion of either A337T or A337G as 25% of total cDNA suppressed maximal current density by about 60% (**Figures 2A,B**: at +40 mV, Kv7.2 + Kv7.3: 416.0 ± 30.9 pA/pF; A337T + Kv7.2 + Kv7.3: 164.7 ± 18.6 pA/pF; A337G + Kv7.2 + Kv7.3: 146.4 ± 30.3 pA/pF). Transfection with a 1:1 ratio of A337T or A337G and Kv7.3 cDNA produced current density levels that were decreased by nearly 80% compared to WT alone (at +40 mV, A337T + Kv7.3: 88.5 ± 14.3 pA/pF; A337G + Kv7.3: 87.8 ± 28.7 pA/pF). No differences were observed between the conductance-voltage curves of Kv7.2 + Kv7.3, A337T + Kv7.2 + Kv7.3, and A337G + Kv7.2 + Kv7.3, but a small rightward shift in $V_{1/2}$ was observed for A337T + Kv7.3, and the calculated steepness of voltage activation was slightly increased for both A337T + Kv7.3 and A337G + Kv7.3 (**Figure 2C**; **Table 1**). In addition, activation and deactivation rates were not changed in A337T + Kv7.2 + Kv7.3 channels compared to WT heteromers (**Figures 2D,E**). Neither variant reduced total or surface biotinylated Kv7.2 protein levels (**Figure 2F**; see **Supplementary Figure S3** for full blots).

To analyze the losses of total and membrane protein when A337T was expressed alone, we compared the protein stability of WT Kv7.2 and A337T channels in transfected HEK cells using the translation inhibitor, cycloheximide. After CHX treatment, A337T protein degradation was more rapid than WT (**Supplementary Figure S4**). Treatment with 0.1% DMSO (the CHX vehicle) gave no significant effects over 24 h, but A337T protein levels were lower than the WT, as shown above using CHO cells (see **Supplementary Figure S5** for full blots).

Next, we used co-immunoprecipitation to compare effects of A337T on the binding of CaM by homomers and heteromers. Expressed alone, A337T exhibited significantly decreased ability to co-precipitate CaM, whereas binding by G279S, a missense change at the GYG selectivity filter with strongly dominant-negative effects on conduction (Schroeder et al., 1998), was similar to WT (Kv7.2: 1.00 ± 0.16; G279S: 0.71 ± 0.22; A337T: 0.24 ± 0.12; **Figure 3A**). However, in heteromeric channels containing the A337T variant subunit, CaM-bound levels were comparable to WT and G279S controls (**Figure 3B**). Thus, for A337T, reduced protein levels were correlated with reduced half-life and CaM binding. However, the near-absence of current observed when A337T or A337G were expressed alone and the partial loss of current seen when the mutant subunits were co-expressed to mimic heterozygosity could not be explained by these mechanisms (see **Supplementary Figure S6** for full blots).

In Cultured Hippocampal Neurons, Three Pore Domain Variants (A274M, A294V, and G279S) Reduce AIS Trafficking, but A337T Localizes Normally to the AIS

Localization of Kv7.2/Kv7.3 heteromeric channels at the AIS is critical for their roles in regulating neuronal excitability (Battefeld et al., 2014). To assess for potential AIS trafficking effects of variants, we electroporated cDNAs into freshly dissociated hippocampal neurons at embryonic day 18–19 (E18–19) and analyzed their ability to become concentrated along the AIS as axons develop in culture. At 7 DIV, ankyrin-G is highly concentrated at the AIS but endogenous Kv7.2 and Kv7.3 remain weakly expressed and are undetectable at the AIS under our imaging conditions (Nakada et al., 2003; Rasmussen et al., 2007; Abidi et al., 2015). To maximize sensitivity for observing an effect of the pathogenic Kv7.2 variants, each was co-expressed with Kv7.3 in a 1:1 ratio, i.e., a subunit composition that produced 80% current loss in CHO cells. Neurons co-expressing WT Kv7.2 and Kv7.3 exhibited concentrated staining for both subunits in the AIS (**Figure 4A**). Quantification of the relative staining intensity along the AIS revealed a length profile similar to that seen *in vivo* (Battefeld et al., 2014), with light labeling proximally, and strong labeling in the middle and distal AIS (**Figure 4B**). By contrast, three previously studied pore domain variants, G279S, A294V, and T274M (Peters et al., 2005; Orhan et al., 2014; Abidi et al., 2015), did not concentrate at any portion of the AIS and were instead retained at the soma (**Figures 4C–H**). Unlike these pore variants, A337T proteins were concentrated in the AIS in a pattern that was similar to that seen in neurons co-expressing Kv7.2 and Kv7.3 only (**Figures 4I,J**). Thus, even as homozygous heteromers, A337T-containing channels traffic to the AIS similarly to WT Kv7.2 + Kv7.3 heteromers, while the three different pore domain variants appear to strongly suppress AIS trafficking.

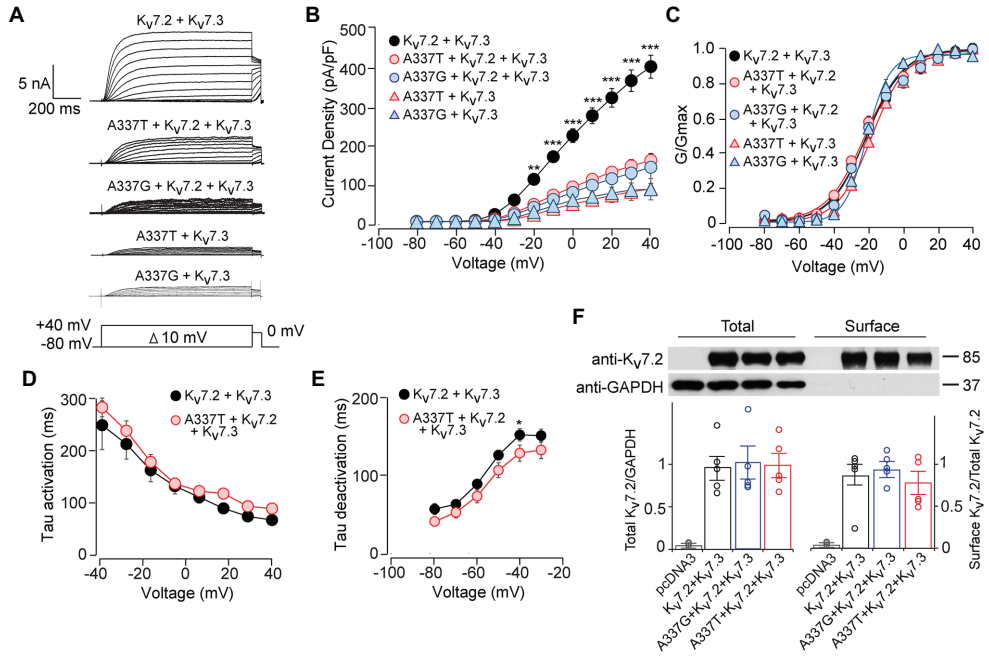

FIGURE 2 | A337T and A337G strongly suppressed heteromeric Kv7.2 + 7.3 currents. **(A)** Currents produced by the indicated combinations of subunits; voltage protocol is shown as an inset. **(B)** Current-voltage plots show significant reductions by A337T and A337G compared to control at voltages of −20 and above (**$p < 0.01$, ***$p < 0.001$, Two-way ANOVA, Bonferroni test, n = 10–20, see **Table 1**). **(C)** Conductance-voltage plots of WT only and mutant-containing channels (n = 5–20, *$p = 0.02$, ***$p < 0.001$, Two-way ANOVA, Bonferroni test; see **Table 1**). **(D,E)** Single exponential fits for heteromeric channels showing the **(D)** activation time constant and **(E)** deactivation time constant (at −40 mV, *$p < 0.05$, Two-way ANOVA, Bonferroni test, n = 6–10). **(F)** Western blot analysis of cell lysates (left lanes) and isolated biotinylated membrane surface proteins (right lanes) from CHO cells expressing Kv7.2 + Kv7.3 co-transfected with A337 variants (n = 5). Upper, representative results; lower, quantification performed as for **Figure 1**. Images are of the entire immunoblots are shown as supplementary information **(Supplementary Figure S3)**.

A337T and A337G Alter Channel Regulation by PIP_2

Activation of Gq-coupled receptors, including the M1 muscarinic acetylcholine receptor, rapidly inhibits neuronal Kv7 currents (Brown and Adams, 1980; Delmas and Brown, 2005). The primary signaling pathway for this inhibition is depletion of membrane PIP_2, leading to dissociation of PIP_2 from channel binding sites and uncoupling of voltage sensing from opening of the ion pore (**Figure 5A**; Suh and Hille, 2002; Zhang et al., 2003; Falkenburger et al., 2010; Zaydman et al., 2013). Given the obligatory role of PIP_2 in Kv7 activation, we investigated whether these variants affected PIP_2 interaction. Treatment of CHO cells co-expressing M1 receptors and WT Kv7.2 + Kv7.3 with the muscarinic agonist oxotremorine methiodide (Oxo-M) strongly inhibited currents (**Figure 5B**; pre-Oxo-M, 391.5 ± 48.5 pA/pF; after 20 s Oxo-M, 158.5 ± 28.0 pA/pF, 41 ± 7% of pre). As expected, channels formed from 1:1:2 co-expression of WT Kv7.2, an A337 variant, and Kv7.3, gave much smaller basal currents. However, these small currents were also, proportionally, less completely suppressed by Oxo-M (A337T: pre-Oxo-M, 140.9 ± 36.4 pA/pF; after 20 s Oxo-M, 107.8 ± 29.3 pA/pF, 77 ± 20% of pre; A337G: pre-Oxo-M, 104.4 ± 36.3 pA/pF; after 20 s Oxo-M, 71.7 ± 28.6 pA/pF, 69 ± 27% of pre).

The pattern of smaller basal currents and lessened suppression by Oxo-M resulting from co-expressing the variants could reflect reduced ability to be activated by depolarization, despite binding of PIP_2. To further assess this, we used co-expression of the PIP_2-synthesizing enzyme PIP5K to boost the bulk membrane PIP_2 concentration (Falkenburger et al., 2010; Kim et al., 2016b; Soldovieri et al., 2016). In cells expressing WT Kv7.2 subunits alone, PIP5K overexpression increased current density nearly 3-fold (**Figures 5C,D**) and shifted the conductance-voltage curve to the left (**Figure 5E**). Remarkably, co-expressing PIP5K with a 1:1 ratio of one variant and WT Kv7.2 subunits augmented currents strongly. Indeed, current densities were not significantly different from WT alone (At +40 mV, Kv7.2: 89.6 ± 9.6 pA/pF; Kv7.2 + PIP5K: 266.8 ± 35.8 pA/pF; A337T + Kv7.2 + PIP5K: 219.8 ± 43.7 pA/pF; A337G + Kv7.2 + PIP5K: 199.0 ± 37.3 pA/pF; **Figure 5D**; **Table 1**). Also, whereas expression of A337T or A337G alone gave current barely detectable above background, with PIP5K overexpression, A337T or A337G currents were readily detected (**Figure 5D**). Indeed, for A337T or A337G with PIP5K, current density at +40 mV was about half of WT without exogenous PIP5K (A337T: 4.9 ± 1.6 pA/pF; A337T + PIP5K: 47.5 ± 15.9 pA/pF; A337G: 6.5 ± 1.1 pA/pF; A337G + PIP5K: 48.4 ± 24.7 pA/pF; **Figure 5D**).

TABLE 1 | Current density and activation gating parameters of wild type or variant-containing Kv7.2 and Kv7.2/7.3 channels.

Transfection	*n*	Current density pA/pF, +40 mV	*p*	$V_{1/2}$ (mV)	*p*	*k*, fold (mV/e)	*p*
Kv7.2	13	89.6 ± 9.6		–21.7 ± 1.0		11.7 ± 0.5	
A337G	6	6.5 ± 1.1	<0.001[1]	n/a		n/a	
A337T	10	4.9 ± 1.6	<0.001[1]	n/a		n/a	
Kv7.2 + A337G	11	20.2 ± 3.6	<0.001[1]	–24.1 ± 1.2		12.1 ± 1.9	NS
Kv7.2 + A337T	15	55.3 ± 11.9	0.001[1]	–23.5 ± 0.8		12.7 ± 1.0	NS
Kv7.2 + Kv7.3	20	416.0 ± 30.9		–21.5 ± 0.8		10.6 ± 0.4	
Kv7.2 + Kv7.3 + A337G	9	146.4 ± 30.3	<0.001[2]	–21.7 ± 0.9		0.04 ± 1.0	NS
Kv7.2 + Kv7.3 + A337T	17	164.7 ± 18.6	<0.001[2]	–23.3 ± 1.2		11.7 ± 0.7	NS
Kv7.3 + A337G	6	87.8 ± 28.7	<0.001[2]	–23.7 ± 0.4		6.6 ± 0.5	<0.001[2]
Kv7.3 + A337T	12	88.5 ± 14.3	<0.001[2]	–18.0 ± 0.4		9.8 ± 0.5	<0.001[2]
Kv7.2 + PIP5K	10	238.8 ± 50.0	<0.001[3]	–39.6 ± 1.38	<0.001[3]	8.5 ± 0.6	<0.001[3]
A337G + PIP5K	10	48.4 ± 24.6	<0.001[3] <0.001[4]	n/a		n/a	
A337T + PIP5K	9	47.5 ± 15.9	<0.001[3] <0.001[4]	n/a		n/a	
Kv7.2 + A337G + PIP5K	9	199.0 ± 35.4	<0.001[3] NS[4]	–34.8 ± 0.8	<0.001[3] NS[4]	9.6 ± 0.9	NS
Kv7.2 + A337T + PIP5K	9	162.6 ± 47.9	<0.001[3] NS[4]	–39.0 ± 0.5	<0.001[3] NS[4]	10.0 ± 0.6	NS
Kv7.2 + Kv7.3 + PIP5K	8	643.0 ± 58.9	<0.001[3]	–33.5 ± 0.6	<0.001[3]	9.6 ± 0.7	NS
Kv7.2 + Kv7.3 + A337G + PIP5K	9	537.4 ± 46.9	<0.001[3] NS[5]	–33.5 ± 0.5	<0.001[3] NS[5]	9.2 ± 0.6	NS
Kv7.2 + Kv7.3 + A337T + PIP5K	9	725.4 ± 45.5	<0.001[3] NS[5]	–33.0 ± 0.5	<0.001[3] NS[5]	9.0 ± 0.6	NS

[1]*vs. WT Kv7.2 alone.*
[2]*vs. WT Kv7.2 + Kv7.3 alone.*
[3]*vs. same subunits, without PIP5K.*
[4]*vs. Kv7.2 + PIP5K.*
[5]*vs. Kv7.2 + Kv7.3 + PIP5K.*

Next, we repeated the PIP5K co-expression experiment for WT Kv7.2 + Kv7.3 heteromers with and without A337T or A337G. Whereas currents in this configuration were diminished strongly by the co-expression of the A337 variants (**Figures 2A,B**), PIP5K increased current in cells expressing either variant in 1:1:2 ratio with WT Kv7.2 and Kv7.3 to levels equal to WT (at +40 mV, Kv7.2 + Kv7.3: 416.0 ± 30.9 pA/pF; Kv7.2 + Kv7.3 + PIP5K: 643.0 ± 58.3 pA/pF; A337T + Kv7.2 + Kv7.3 + PIP5K: 725.4 ± 95.5 pA/pF; A337G + Kv7.2 + Kv7.3 + PIP5K: 537.4 ± 46.9 pA/pF, **Figures 5F,G**; see **Table 1**). The conductance-voltage curves of WT and A337T or A337G-containing heteromers were left-shifted equally (**Figure 5H**). In contrast, channels formed by 1:1 co-expression of Kv7.2 and G279S, a mutation within the selectivity filter that exhibits dominant-negative effects (Schroeder et al., 1998), were only partly restored in amplitude by overexpressed PIP5K (**Supplementary Figure S7**). In combination, the M1 receptor and PIP5K experiments indicated that including A337T or A337G subunits within channel tetramer confers reduced PIP_2 responsiveness upon channels formed by these subunits and WT Kv7.2 or Kv7.2 and Kv7.3. Furthermore, these effects can be reversed, all or in part, by raising the cellular PIP_2 concentration with PIP5K overexpression. In contrast to channels incorporating G279S variants, A337T and A337G containing channels appeared able to conduct well and to couple voltage-sensing and pore opening well, but to require higher levels of PIP_2.

To analyze these mechanisms further, we co-expressed the *Ciona intestinalis* voltage-sensitive phosphatase (ciVSP) with channel subunits. Previous studies have shown that strong membrane depolarization of cells expressing ciVSP rapidly depletes membrane PIP_2, and M-current is inhibited at rates reflecting net unbinding of PIP_2 from the channels (Murata and Okamura, 2007; Falkenburger et al., 2010). In CHO cells co-expressing ciVSP and WT channels, 10 s long step depolarizations induced currents that activated and then declined (**Figure 6A**; see **Supplementary Figure S8A**). The onset and rate of current decline increased progressively with membrane depolarizations above +30 mV (**Figure 6A**). Because the M1R and PIP5K experiments indicated that A337T and A337G may reduce basal PIP_2 binding, we expected ciVSP co-expression to reveal a hastening of unbinding for those variants, as seen in studies of R325G, a site 12 residues closer to the S6 membrane helix which may interact directly with PIP_2 (Soldovieri et al., 2016). Unexpectedly, in cells co-expressing ciVSP and A337T + Kv7.2 + Kv7.3, at steps to +30 mV and above, the rate of current decline was slower and the fraction of current depleted after 10 s was less than for WT (**Figure 6B**). At +100 mV, we found that inclusion of A337T or A337G significantly delayed ciVSP-induced current declines compared to controls (**Figure 6C**). The decay rate constants were 3.29 s (Kv7.2 + Kv7.3), 14.80 s (A337T + Kv7.2 + Kv7.3), and 9.38 s

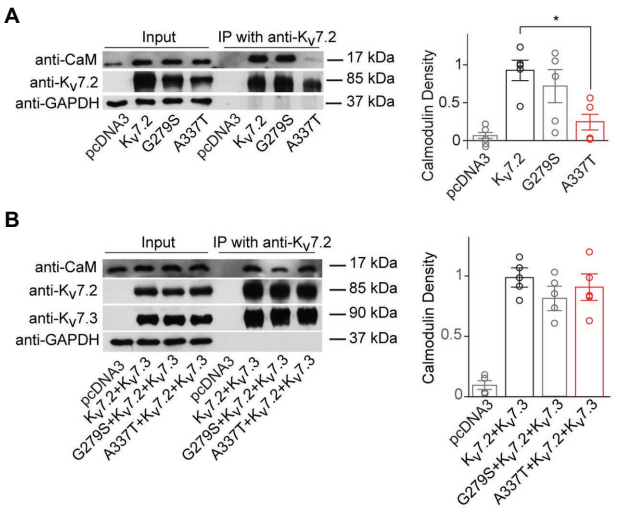

FIGURE 3 | A337T homomers are less able to co-immunoprecipitate calmodulin than WT Kv7.2 homomers. **(A)** Representative western blot analysis and quantification of calmodulin (CaM) co-immunoprecipitated using anti-Kv7.2 antibodies and transfected human embryonic kidney (HEK) cells expressing WT Kv7.2, G279S, or A337T. CaM co-immunoprecipitated is significantly reduced for A337T (*p = 0.04, One-way ANOVA, Tukey test, n = 5) but not G279S. In plots, CaM immunoprecipitated is normalized to wild type (WT). **(B)** Representative western blot analysis and quantification of CaM co-immunoprecipitated from cells expressing WT Kv7.2 + Kv7.3, alone or in a 1:1:2 ratio with G279S or A337T, show no differences between groups (n = 4). These cropped blot images are from full-length gels shown as supplementary information **(Supplementary Figure S6)**.

(A337G + Kv7.2 + Kv7.3). Current decline during ciVSP activation was also slowed by co-expression of either variant with WT Kv7.2 (i.e., in homomeric channels; see **Supplementary Figure S8B**). It is unlikely that co-expression of A337G or A337T was slowing the rate at which ciVSP activation was depleting unbound, bulk membrane PIP_2. Instead, inclusion of the variants seemed to slow the effective rate of dissociation from the channels (see Discussion).

Reduced equilibrium binding of a ligand to a single site can result from slowing of both "on" and "off" rates, if the change in "on" rate is greater. To investigate whether the variants very strongly slowed rates of PIP_2 binding, we used an established depletion-recovery protocol (Falkenburger et al., 2010). PIP_2 was extensively depleted by strong ciVSP activation (10 s at +100 mV), and then currents were monitored for 30 s at −20 mV, as PIP_2 was resynthesized (**Figure 6D**). As observed previously (Falkenburger et al., 2010), recovery followed an S-shaped time course, and the rate of recovery appeared independent of the extent of prior PIP_2 depletion (see **Supplementary Figure S8C**). Compared to WT channels, currents recovered more slowly in channels including the A337 variants than in WT-only channels, and this appeared due to an increase in the latency in initiation of recovery (**Figures 6D–F**; see **Supplementary Figure S9**), potentially contributing to reduced apparent affinity. However, the approximately 2-fold slowing in recovery was similar to the 3- to 5-fold change in the rate of current reduction seen in the depletion experiments. To further probe PIP_2 interactions with the gating machinery, we measured activation and deactivation kinetics, since mutations near some PIP_2 binding sites can affect the rate of deactivation (Chen et al., 2015). A337T did not influence voltage-dependent activation and deactivation rates (**Figures 2D,E**). Together, these data show that incorporation of A337T or A337G into heteromeric Kv7.2 + Kv7.3 channels impaired PIP_2 interaction in a novel pattern, appearing to decrease occupancy at sites required for electromechanical coupling at basal conditions of whole cell patch recording, without hastening the unidirectional rate of unbinding if membrane PIP_2 was strongly depleted.

SF0034 Rescued Subthreshold Current Density in Heterozygous A337T Channels

Ezogabine, an FDA-approved drug that increases Kv7.2/7.3 currents by shifting voltage activation to more hyperpolarized voltages and increasing maximal current density, has been proposed as a targeted therapeutic in *KCNQ2* encephalopathy and use with some apparent benefit has been described in small clinical case series, including in the A337T proband (Gunthorpe et al., 2012; Millichap and Cooper, 2012; Weckhuysen et al., 2013; Millichap et al., 2016). However, ezogabine exhibits modest selectivity and potency and has side effects, including acute urinary retention and blue skin discoloration, which limit its clinical usefulness (Brickel et al., 2012; Clark et al., 2015; Food and Drug Administration, U.S., 2015; Kalappa et al., 2015). The infant with neonatal onset epileptic encephalopathy and a heterozygous A337T variant was given ezogabine at 4.5 months of age, resulting in improved seizure control and interictal electroencephalographic pattern, but urinary retention limited dosing to 21 mg/kg/day (Millichap et al., 2016), which achieves a brain concentration estimated at approximately 1 μM (Gunthorpe et al., 2012). SF0034 is an ezogabine analogue with improved potency and selectivity in *in vitro* and *in vivo* (Kalappa et al., 2015). In HEK cells, SF0034 was ~5-fold more potent than ezogabine in shifting the voltage-dependence of activation of Kv7.2 + Kv7.3 heteromers but was less efficacious than ezogabine against Kv7.4 or Kv7.5 homomers. The effects of SF0034, like for ezogabine, were abolished by point mutation of Kv7.3 Trp265. SF0034 treatment was shown to slow spike frequency in mouse CA1 pyramidal neurons, but this effect was markedly reduced in littermate mice with Kv7.2 conditionally deleted from these neurons. To begin to assess whether such "second generation" openers merit exploration as candidate therapeutic agents for *KCNQ2* encephalopathy, we studied the effects of SF0034 on channels including the A337T pathogenic variant.

At 1 μM, SF0034 increased currents in cells expressing WT heteromeric channels and cells co-expressing A337T (**Figure 7A**). SF0034 shifted the conductance-voltage curve to hyperpolarized potentials equivalently (Kv7.2 + Kv7.3: pretreatment control $V_{1/2}$ = −23.8 ± 0.6 mV, SF0034 $V_{1/2}$ = −34.5 ± 0.6 mV; A337T + Kv7.2 + Kv7.3: pretreatment control $V_{1/2}$ = −23.0 ± 0.4 mV, SF0034 $V_{1/2}$ = −32.5 ± 0.4 mV; **Figures 7B,C**). Although absolute increases in current were greater with a strongly depolarizing voltage step to +40 mV compared to −40 mV (**Figure 7D**), relative increases

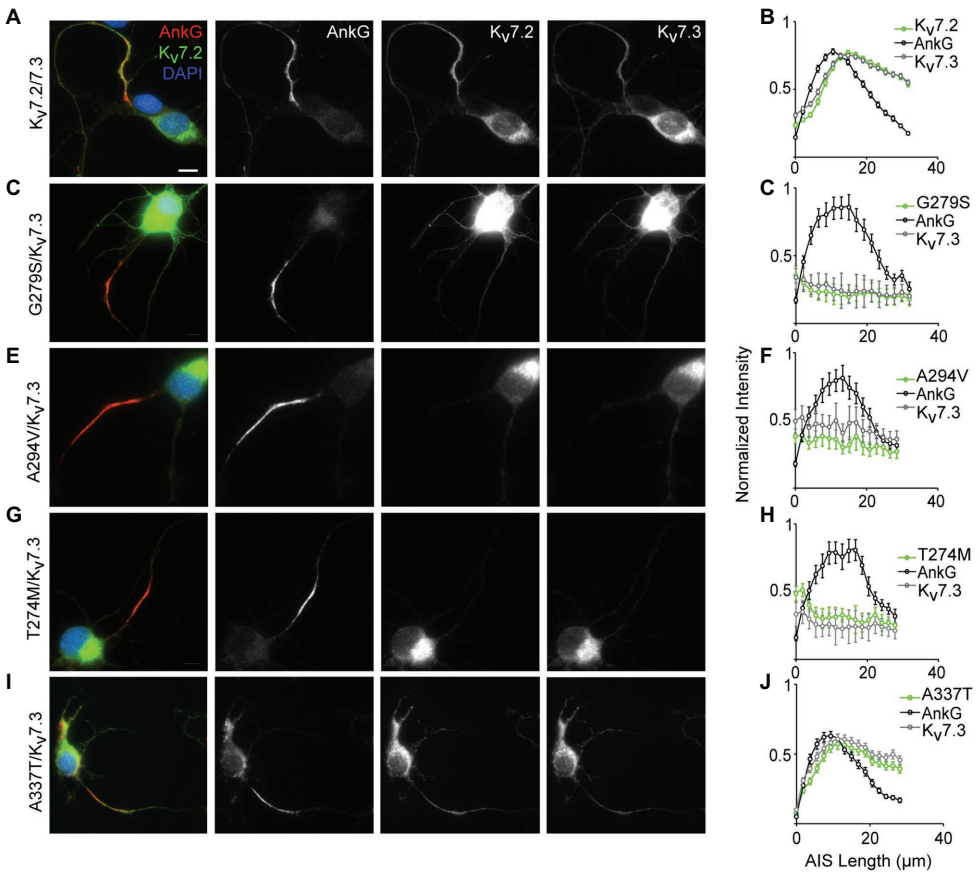

FIGURE 4 | A337T does not disrupt localization of Kv7.2 or Kv7.3 subunits at the AIS of hippocampal neurons. **(A)** Representative image of cultured rat hippocampal neurons electroporated with WT Kv7.2 + Kv7.3 cDNAs at E18 and imaged after 7 DIV. Neurons were labeled with DAPI, anti-AnkG, anti-Kv7.2, and anti-Kv7.3. Merged (color) and greyscale images show Kv7.2 + Kv7.3 localized at the AIS (scale, for all images: 10 μm). **(B)** Intensity profile quantifications of AnkG, Kv7.2, and Kv7.3 antibody labeling along the AIS. **(C–H)** Representative images of hippocampal neurons electroporated with pore mutations G279S, A294V, and T274M and their respective intensity profile quantifications. Expression of these variants prevents concentration of Kv7.2 and Kv7.3 at the AIS. **(I,J)** Representative image of A337T and its intensity profile quantification show a normal pattern of Kv7.2 and Kv7.3 localization at the AIS (histograms: n = 69–104 neurons).

were greatest at weak depolarizations (**Figures 7E,F**). Thus, 1 μM SF0034 increased current density of WT Kv7.2 + Kv7.3 channels about four-fold at −40 mV (**Figure 7E**; Ctrl: 21.3 ± 3.2 pA/pF, SF0034: 68.7 ± 9.89 pA/pF) and about 25% at +40 mV (**Figure 7F**; Ctrl: 422.0 ± 52.1 pA/pF, SF0034: 542.4 ± 62.1 pA/pF). SF0034 treatment of cells co-expressing A337T subunits were also significantly increased at both −40 mV (**Figure 7E**; Ctrl: 4.7 ± 0.9 pA/pF, SF0034: 24.3 ± 5.7 pA/pF) and + 40 mV (**Figure 7F**; A337T Ctrl 200.6 ± 46.7 pA/pF, SF0034 266.7 ± 66.5 pA/pF). Current density in SF0034-treated A337T co-expressing cells was equivalent to that of untreated WT only expressing cells (n.s. between Kv7.2 + Kv7.3 controls versus A337T + Kv7.2 + Kv7.3 SF0034 at both −40 and +40 mV; results summarized in **Supplementary Table S1**).

DISCUSSION

Our analysis of human *KCNQ2* variants from severely affected individuals, with particular attention to effects of co-expression with WT subunits to mimic heterozygosity as is observed in people, serves two important purposes. First, finding a markedly abnormal functional profile supports a variant's classification as pathogenic for a severe phenotype (Miceli et al., 2013; Orhan et al., 2014; Richards et al., 2015; Soldovieri et al., 2016). Second, characterization of novel variants giving severe phenotypes, even when heterozygous (i.e., expressed along with wild type subunits), builds an "intolerance map" of functionally critical sites within the protein structure and may highlight contributions to allosteric mechanisms that have been overlooked by hypothesis-driven experiments. Although heterozygous missense variants clustered near the CaM-binding Helix A and B of the intracellular CT domain account for approximately 21% of cases of *KCNQ2* encephalopathy (Millichap et al., 2016), studies to date have only begun to explain why very severe phenotypes result from some variants, while others cause benign familial neonatal epilepsy (Orhan et al., 2014; Soldovieri et al., 2016; Zhang et al., 2020). Understanding how these variants confer severe outcomes may aid development of targeted novel therapies.

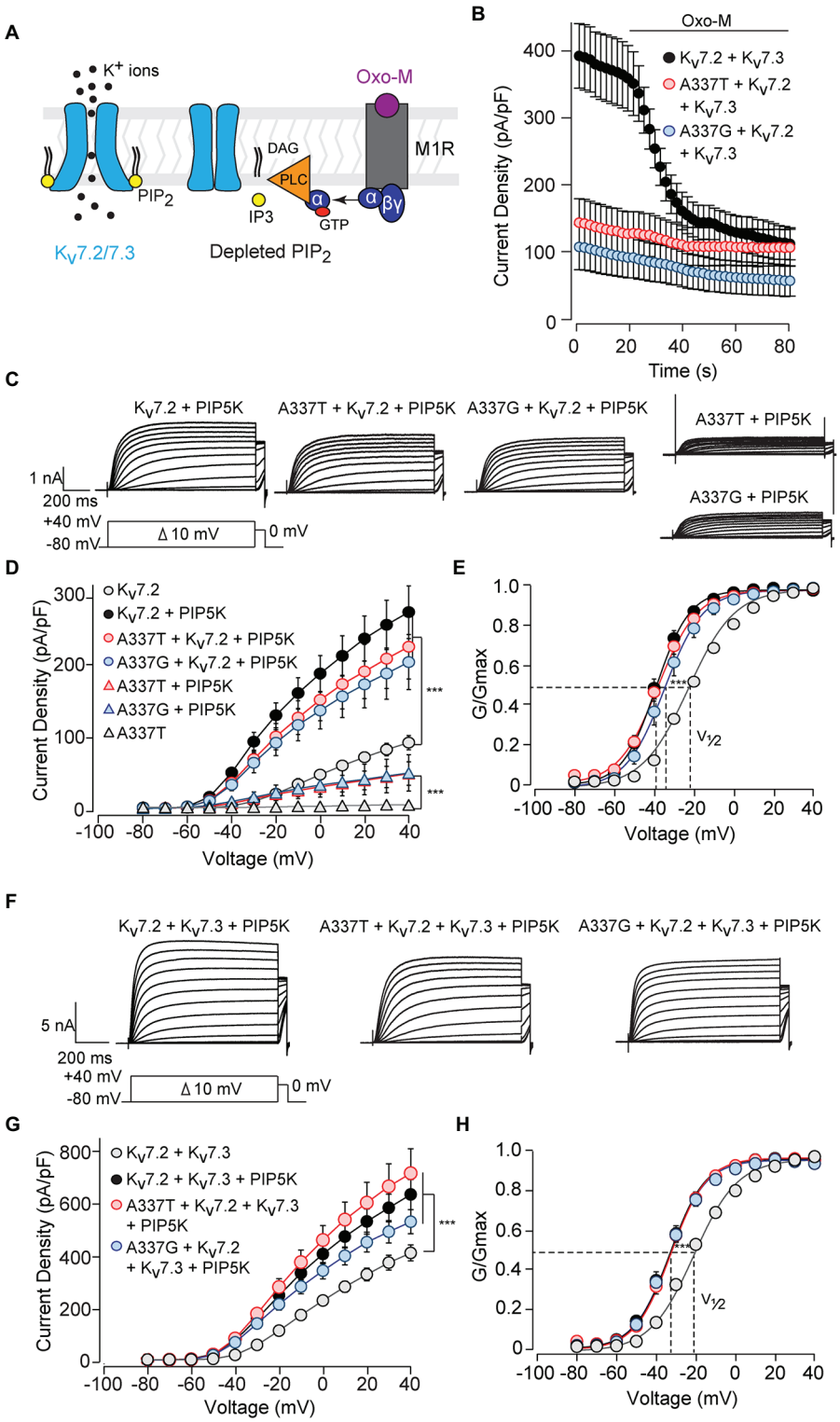

FIGURE 5 | Currents suppressed by A337 variants were restored by co-expression of PIP5K. **(A)** Diagram of the main transduction pathway underlying cholinergic inhibition of M-current. Agonist oxotremorine methiodide (Oxo-M) activates the M1 muscarinic receptor (M1R), activating a heterotrimeric G-protein (α, βγ) and phospholipase C (PLC). PLC cleaves phosphatidylinositol 4,5-bisphosphate (PIP_2) residing in the membrane, reducing PIP_2 available for binding to the channel. **(B)** Time course

(Continued)

FIGURE 5 | of current inhibition by Oxo-M (10 μM, bar) in CHO cells transfected with M1R, Kv7.2, and Kv7.3, with and without A337 variants. **(C)** Representative families of currents produced in response to step depolarizations by the indicated combinations of WT and mutant Kv7.2 subunits when co-transfected with PIP5K. **(D)** Current-voltage relationships for channels co-expressed with PIP5K compared to without PIP5K (***$p < 0.001$, two-way ANOVA, Bonferroni test, $n = 5–16$, see **Table 1**). **(E)** Conductance-voltage relationships from cells transfected with PIP5K compared to WT Kv7.2 without PIP5K. Activation of WT Kv7.2 expressed alone, WT + A337T, and WT + A337G are significantly shifted to hyperpolarized potentials (***$p < 0.001$, two-way ANOVA, Bonferroni test, $n = 5–16$, see **Table 1**). **(F)** Representative currents produced by the indicated combinations of heteromeric WT and mutant Kv7.2 subunits in cells co-transfected with PIP5K. **(G)** Current densities in cells co-expressing PIP5K compared to WT Kv7.2 + Kv7.3 (***$p < 0.001$, Two-way ANOVA, Bonferroni test, $n = 10–20$). **(H)** Conductance-voltage relationships from cells transfected with PIP5K compared to WT Kv7.2 + Kv7.3 expressed without PIP5K. PIP5K overexpression shifts activation significantly to hyperpolarized potentials (***$p < 0.001$, two-way ANOVA, Bonferroni test, $n = 10–20$, see **Table 1**).

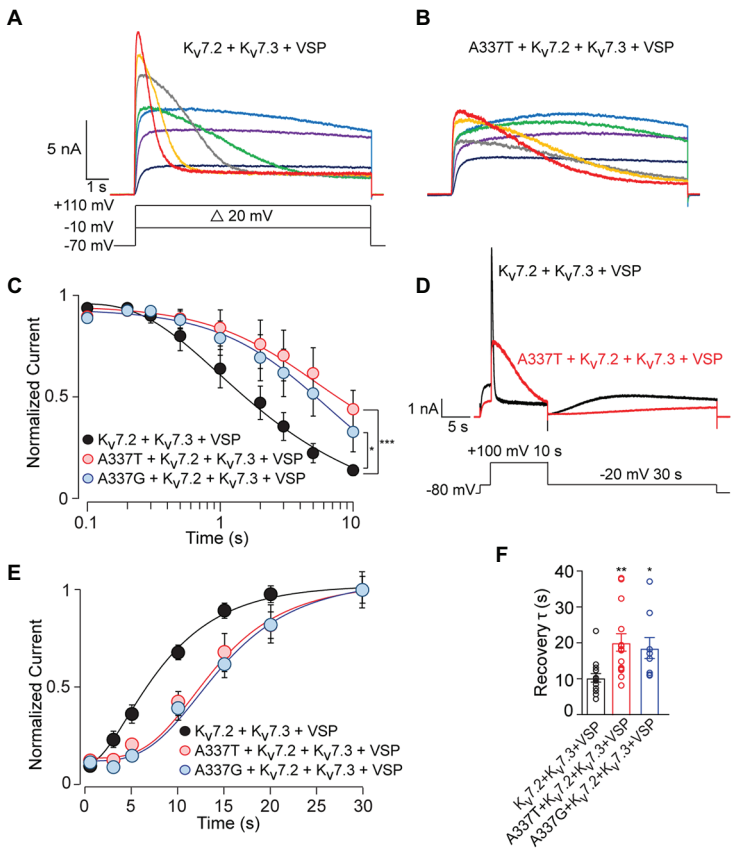

FIGURE 6 | *C. intestinalis* voltage sensitive phosphatase (ciVSP) induced current suppression and recovery is slower in cells expressing A337T or A337G. **(A,B)** Currents produced by Kv7.2 + Kv7.3 **(A)** or A337T + Kv7.2 + Kv7.3 **(B)**, in response to 10 s step depolarizations, in cells co-expressing ci-VSP. The voltage protocol in A applies. **(C)** Normalized current densities from cells co-transfected with the indicated subunits and ciVSP, at intervals during 10 s depolarizing steps to +100 mV (At 10 s, ***$p < 0.001$, *$p = 0.025$, two-way ANOVA, Bonferroni test, $n = 8–11$). **(D)** Voltage protocol and representative currents showing ciVSP induced current inhibition (at +100 mV) and recovery at −10 mV). Both appear faster for WT Kv7.2 + Kv7.3 heteromers, compared to A337T + Kv7.2 + Kv7.3. **(E)** Recovery is delayed in cells transfected with the mutant subunits, compared to WT heteromer only controls (***$p < 0.001$, **$p = 0.004$, two-way ANOVA, Bonferroni test, $n = 8–11$). **(F)** Recovery rates for A337T + Kv7.2 + Kv7.3, and A337G + Kv7.2 + Kv7.3 channels are significantly slowed compared to control (*$p = 0.02$, **$p < 0.004$, one-way ANOVA, Bonferroni test, $n = 9–15$).

Our analysis of Kv7.2 A337T and A337G, *de novo* missense variants within Helix A from patients with refractory seizures and developmental impairment (Saitsu et al., 2012; Millichap et al., 2016), yielded three main findings. First, these variants generated minimal or no detectable current when expressed alone and induced dominant-negative suppression when co-expressed with WT Kv7.2 (A337G) or with Kv7.2 and Kv7.3 (both A337T and A337G). The fractional reduction in conductance seen here was similar to that previously observed for T274M and G290D, two severe pore domain variants near the selectivity filter, and for R325G, a missense change at a proximal CT arginine residue that may contribute directly to PIP_2 binding (Orhan et al., 2014; Soldovieri et al., 2016). Thus, our findings support the conclusion that these rare variants are pathogenic and provide further support for the idea that dominant-negative current suppression is an informative *in vitro* signature of severe EIEE phenotypes. Second, although A337G was not studied, trafficking of A337T to the AIS was normal in hippocampal neurons, as also shown recently for R325G and I205V (Soldovieri et al., 2016; Niday et al., 2017).

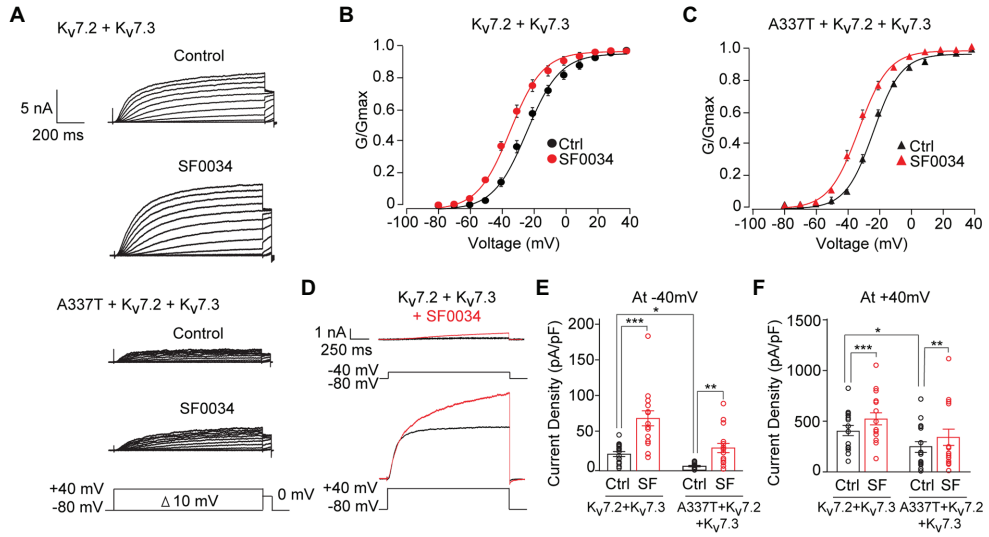

FIGURE 7 | SF0034 partially restored current loss due to A337T mutation. **(A)** Kv7.2 + Kv7.3 and A337T + Kv7.2 + Kv7.3 currents in CHO cells, before and after treatment with 1 μM SF0034. Protocol given in inset. **(B)** Conductance-voltage relationship of WT Kv7.2 + Kv7.3 before and after SF0034 treatment (Control (Ctrl): $V_{1/2}$ = −23.8 ± 0.6 mV, k = 10.7 ± 0.7 mV; SF0034: $V_{1/2}$ = −34.8 ± 0.6 mV, k = 10.5 ± 0.7 mV (n = 16). **(C)** Conductance-voltage relationship of A337T + Kv7.2 + Kv7.3 before and after SF0034 treatment. Ctrl: $V_{1/2}$ = 23.1 ± 0.4 mV, k = 8.9 ± 0.4 mV; SF0034: $V_{1/2}$ = −32.5 ± 0.4 mV, k = 9.6 ± 0.5 mV (n = 16). **(D)** Kv7.2 + Kv7.3 currents response to the indicated depolarizing steps, before and after SF0034. **(E,F)** Current densities before and after SF0034 treatment for the indicated subunit combinations at −40 mV (*p = 0.02; **p = 0.002; and ***p < 0.001) and +40 mV (*p = 0.03 and ***p < 0.001). SF0034 treated A337T-containing channel current density was not significantly different compared to untreated WT control at either −40 or +40 mV (two-way repeated measures ANOVA, Bonferroni test, one-way ANOVA, Kruskal-Wallis test, n = 16).

In contrast, we showed that three pore domain mutations, a well-studied experimental mutation of the selectivity filter, G279S, and two of the most highly recurrent human *KCNQ2* encephalopathy variants (Millichap et al., 2016), T274M and A294V, strongly prevent AIS trafficking. These findings indicate that severe variants fall into at least two classes with respect to trafficking, a major difference in disease mechanism that has implications for therapy. It is unknown why mutations buried within the transmembrane ion pore would prevent AIS surface expression. It is intriguing to imagine that neuronal quality control mechanisms could distinguish between available and pore-blocked channels, and this deserves more study. Third, we showed that PIP_2-dependent modulation was altered by both A337 variants, even though this residue, unlike the R325 studied by Soldovieri et al. 2016, lies within the CaM binding Helix A at a distance from any basic residue previously implicated in direct PIP_2 interaction. Our PIP5K experiments suggest that treatments increasing PIP_2 or making channels more responsive to PIP_2 represent potential therapeutic approaches for these variants. Although the above listed conclusions are robust, our studies also exposed questions that are highly intriguing, interrelated, and for the present time, incompletely resolved, in spite of new related information on the structure of Kv7 channels obtained by cryoelectron microscopy (Sun and MacKinnon, 2020). These questions concern the impact of the variants on CaM binding, the kinetics of PIP_2 association and dissociation from the channel, and on allosteric interaction between these two modulators.

A337T CaM Binding Changes and Relevance to Pathogenicity

We found that protein half-life, total and surface protein abundance, and CaM binding were all reduced by the A337T mutation, but only when A337T subunits were expressed alone, i.e., without WT subunits. Protein stability effects were not seen for A337G, even though A337G strongly reduced current amplitudes. These rare variants, like nearly all of those found in *KCNQ2* encephalopathy, cause clinical symptoms in heterozygous individuals, so the observed effects on CaM binding and protein expression may not contribute to clinical severity. Alternatively, important effects on CaM binding may be insensitively detected in the transient expression systems used here and may be informatively brought to light by expressing the mutated subunit alone. Another example suggesting the potential predictive utility of data from variants expressed alone experiments is provided by a recent analysis of R144Q, R198Q, R201C, and R201H, *KCNQ2* voltage-sensor domain variants associated with severe encephalopathy phenotypes. These variants gave strong hyperpolarizing shifts in gating voltage-dependence if expressed alone but much smaller effects when co-expressed with WT subunits (Miceli et al., 2015; Millichap et al., 2016; Mulkey et al., 2017). Nonetheless, the markedly altered voltage-dependence exhibited by the variants when expressed alone correlated with the delayed age of onset of seizures and impaired development, distinctive aspects of the otherwise severe clinical phenotypes. Analysis of a larger number of pathogenic variants *in vitro*, and, potentially, studies of mouse models where the mutant alleles are driven by native promoters (Ihara et al., 2016),

will clarify parameters for interpreting results obtained from variant-alone expression as part of efforts to assess pathogenicity and predict clinical severity.

PIP_2 Interaction Changes: Implications for Channel Allostery and Pathogenicity

PIP_2 binding is obligatory for Kv7 channel activation. The conserved site mediating electromechanical coupling has been determined *via* cryoelectron microscopy of Kv7.1 in the PIP2-bound, open state (Sun and MacKinnon, 2020). Nonetheless, the dynamic interactions between PIP_2 with the intact channel that result in macroscopic current properties remain very incompletely understood. These issues are potentially critical for learning how heterozygous variants can severely impair function within an assembled channel including both mutant and wild type subunits. Our experiments shed new light on PIP_2 interactions with WT channels. WT Kv7.2 homomers gave about 4-fold smaller currents than WT Kv7.2 + Kv7.3 heteromers, but PIP5K co-expression enhanced homomer currents about 3-fold and heteromer currents only about 50%. Also, recovery from ciVSP-induced current inhibition followed a sigmoid time course well-fitted by a squared exponential function, as seen previously—an indication that binding of more than one PIP_2 molecule is required for a channel to become active, as predicted by functional analysis (Falkenburger et al., 2010) and apparent in the new atomic structure. The ability of PIP5K co-expression to shift voltage-gating to the left, for both WT homomers and heteromers (**Figure 6**) suggests that elevated PIP_2 concentration increased binding stoichiometry above levels minimally sufficient for voltage-gating. In sum, these results indicate that, under our recording conditions without PIP5K co-expression, PIP_2 binding is not saturated and that Kv7.2 + Kv7.3 heteromers have higher affinity than Kv7.2 homomers, consistent with earlier single channel recordings (Hernandez et al., 2008).

Channels including A337T and A337G subunits gave reduced current amplitudes, whether the mutated subunits were expressed alone or co-expressed with WT subunits. The ability of M1 receptor or ciVSP activation to inhibit currents was reduced for heteromers containing mutant subunits, as if the mutations were occluding the PIP_2 depleting effects of these treatments. In addition, when either A337T or A337G was expressed alone or with WT subunits, PIP5K co-expression strongly enhanced currents to levels equal to WT-only channels, and shifted gating to hyperpolarized potentials, as also seen for WT channels. These findings suggest that the channels including the A337 variants carry out electromechanical coupling similarly to WT channels, but bind less PIP_2 under the basal conditions of our experiments. Further experiments, including recording of excised patches using application of PIP_2 analogues to assess effects on single channel open probability and kinetics, could be used to test this interpretation.

The striking observations that A337T and A337G slow the kinetics of both current inhibition and current recovery during and after a ciVSP activation step (**Figure 6**; **Supplementary Figures S8, S9**) were unexpected. Those results could be explained if A337T and A337G exert their main effects not by altering PIP_2 binding at the channel sites directly mediating electromechanical coupling, but instead, by delaying the migration of PIP_2 between those sites and the bulk membrane. The Kv7.1 atomic structure shows conspicuous water-filled portals between the bulk cytoplasm and the intracellular mouth of the ion pore which includes patches lined by a number of basic residues (Sun and MacKinnon, 2017, 2020). It is noteworthy that additional basic residue sites between Helix A and B have been shown to functionally contribute to PIP_2 interaction (Hernandez et al., 2008; Telezhkin et al., 2013; Kim et al., 2016a). These sites between Helix A and B are likely more peripherally located, but are not yet included in the known atomic structure. These basic sites may contribute to channel availability and modulation kinetics by maintaining an annular microdomain with an elevated local PIP_2 concentration around the channel and helping to orchestrate migration bidirectionally.

Structures of the Helix A from Kv7.1, Kv7.3, and Kv7.4, co-crystallized with Helix B and bound CaM, show the conserved Ala residue (homologous to KCNQ2 A337) buried under and interacting with sidechains from the CaM C-lobe (Sachyani et al., 2014; Strulovich et al., 2016; Chang et al., 2018). In the intact channel, the four subunits' Helix A-B/CaM modules form a ring below the transmembrane domain (Mruk et al., 2012; Sachyani et al., 2014; Alberdi et al., 2015; Sun and MacKinnon, 2017, 2020). CaM binding is highly dynamic (Mruk et al., 2012) and has been proposed to include multiple potential modes: binding to a Helix A alone, a Helix B alone, an A–B pair contributed by a single subunit, or crosslinked helices from two subunits (Alaimo et al., 2014; Sachyani et al., 2014; Alberdi et al., 2015; Chang et al., 2018; Sun and MacKinnon, 2020). Importantly, the Kv7.1 structure obtained with and without PIP_2 bound reveals a large, nearly 180° flipping of the entire Helix A–B/CaM complex between the two states. How the large segment between Helix A and B participates in this state change is unknown. A337T and A337G are centrally located near the pivot point for this remarkable conformational flip. They may impair PIP_2's migration between the bulk membrane and the S4-linker binding site by altering the preferred CaM binding configuration, or by slowing the rate of the c-terminal conformational flip that follows PIP_2 binding and unbinding. Evidence for dual impact on CaM and PIP_2 was developed for another pathogenic variant, L637R, located much more distally in Helix D (Alberdi et al., 2015). There is already functional evidence that several modulatory signals, including elevated $[Ca^{2+}]i$ and phosphorylation by PKC and protein kinase CK2, may coordinately regulate the CaM configuration and PIP_2 binding and thus, available current (Suh and Hille, 2008; Kosenko et al., 2012; Kosenko and Hoshi, 2013; Kang et al., 2014; Chang et al., 2018). It will be exciting to see a more integrated understanding of this refined and ancient mechanism emerge through future experiments.

Ezogabine, an activator of Kv7.2–5 subunit-containing channels that is approved for epilepsy in adults, has been shown to reverse effects of *KCNQ2* encephalopathy variants in patch clamp experiments (Miceli et al., 2013; Orhan et al., 2014; Soldovieri et al., 2016).

Although ezogabine has also shown some benefits in seizure control in several *KCNQ2* encephalopathy infants, including an individual heterozygous for A337T (Weckhuysen et al., 2013; Millichap et al., 2016), side effects have limited its use. SF0034 is an ezogabine analog showing greater potency and selectivity in both cell-based and *in vivo* models (Kalappa et al., 2015). We found that SF0034 can increase macroscopic currents of A337T-containing channels, by some measures restoring current density levels to that of WT channels in the absence of drug. Novel Kv7 openers merit further study as a candidate therapy for *KCNQ2* encephalopathy due to loss-of-function variants, including those in the CT region that impair PIP_2 modulation. Our A337T patient received ezogabine in the 6th month of life, with benefits for seizures but continued severe developmental impairment. Very early diagnosis and intervention may represent the best opportunity for favorable impact on development.

DATA AVAILABILITY STATEMENT

The raw data supporting the conclusions of this article will be made available by the authors, without undue reservation.

AUTHOR CONTRIBUTIONS

BT and Z-GJ performed all biochemistry, neuronal transfections, imaging, and electrophysiology experiments. BT and MX designed biochemical experiments. BT and Z-GJ designed electrophysiology experiments and analyzed data. TT provided clinical information. BT and EC designed the project and wrote the manuscript. All authors reviewed and revised the manuscript, and approved the submitted version. EC funded the project.

FUNDING

This study was supported by funding from the National Institutes of Health (R01 NS49119), a CURE Research Grant, the Jack Pribaz Foundation, the Miles Family Fund, an American Epilepsy Society Research Infrastructure Award and Predoctoral Research Fellowship (BT), and the Pediatric Epilepsy Research Foundation (TT).

ACKNOWLEDGMENTS

We thank Thomas Jentsch (human KCNQ2 and KCNQ3), Yasushi Okamura (ciVSP), Bruce Conklin (M1R) and Robin Irvine (PIP5K) for generous gifts of cDNA clones, SciFluor Life Sciences for gift of SF0034, and Joel Hirsch for generously sharing KCNQ1 structure model files. We thank Frank Horrigan for review of the manuscript and helpful discussion.

SUPPLEMENTARY MATERIAL

The Supplementary Material for this article can be found online at: https://www.frontiersin.org/articles/10.3389/fphys.2020.571813/full#supplementary-material

REFERENCES

Abidi, A., Devaux, J. J., Molinari, F., Alcaraz, G., Michon, F. X., Sutera-Sardo, J., et al. (2015). A recurrent KCNQ2 pore mutation causing early onset epileptic encephalopathy has a moderate effect on M current but alters subcellular localization of Kv7 channels. *Neurobiol. Dis.* 80, 80–92. doi: 10.1016/j.nbd.2015.04.017

Alaimo, A., Alberdi, A., Gomis-Perez, C., Fernández-Orth, J., Bernardo-Seisdedos, G., Malo, C., et al. (2014). Pivoting between calmodulin lobes triggered by calcium in the Kv7.2/calmodulin complex. *PLoS One* 9:e86711. doi: 10.1371/journal.pone.0086711

Alaimo, A., Gómez-Posada, J. C., Aivar, P., Etxeberría, A., Rodriguez-Alfaro, J. A., Areso, P., et al. (2009). Calmodulin activation limits the rate of KCNQ2 K^+ channel exit from the endoplasmic reticulum. *J. Biol. Chem.* 284, 20668–20675. doi: 10.1074/jbc.M109.019539

Alberdi, A., Gomis-Perez, C., Bernardo-Seisdedos, G., Alaimo, A., Malo, C., Aldaregia, J., et al. (2015). Uncoupling PIP2-calmodulin regulation of Kv7.2 channels by an assembly destabilizing epileptogenic mutation. *J. Cell Sci.* 128, 4014–4023. doi: 10.1242/jcs.176420

Ambrosino, P., Alaimo, A., Bartollino, S., Manocchio, L., De Maria, M., Mosca, I., et al. (2015). Epilepsy-causing mutations in Kv7.2 C-terminus affect binding and functional modulation by calmodulin. *Biochim. Biophys. Acta* 1852, 1856–1866. doi: 10.1016/j.bbadis.2015.06.012

Battefeld, A., Tran, B. T., Gavrilis, J., Cooper, E. C., and Kole, M. H. (2014). Heteromeric Kv7.2/7.3 channels differentially regulate action potential initiation and conduction in neocortical myelinated axons. *J. Neurosci.* 34, 3719–3732. doi: 10.1523/JNEUROSCI.4206-13.2014

Biervert, C., Schroeder, B. C., Kubisch, C., Berkovic, S. F., Propping, P., Jentsch, T. J., et al. (1998). A potassium channel mutation in neonatal human epilepsy. *Science* 279, 403–406. doi: 10.1126/science.279.5349.403

Brickel, N., Gandhi, P., Vanlandingham, K., Hammond, J., and Derossett, S. (2012). The urinary safety profile and secondary renal effects of retigabine (ezogabine): a first-in-class antiepileptic drug that targets KCNQ (K(v)7) potassium channels. *Epilepsia* 53, 606–612. doi: 10.1111/j.1528-1167.2012.03441.x

Brown, D. A., and Adams, P. R. (1980). Muscarinic suppression of a novel voltage-sensitive K^+ current in a vertebrate neurone. *Nature* 283, 673–676. doi: 10.1038/283673a0

Brown, D. A., Hughes, S. A., Marsh, S. J., and Tinker, A. (2007). Regulation of M(Kv7.2/7.3) channels in neurons by PIP2 and products of PIP2 hydrolysis: significance for receptor-mediated inhibition. *J. Physiol.* 582, 917–925. doi: 10.1113/jphysiol.2007.132498

Cavaretta, J. P., Sherer, K. R., Lee, K. Y., Kim, E. H., Issema, R. S., and Chung, H. J. (2014). Polarized axonal surface expression of neuronal KCNQ potassium channels is regulated by calmodulin interaction with KCNQ2 subunit. *PLoS One* 9:e103655. doi: 10.1371/journal.pone.0103655

Chang, A., Abderemane-Ali, F., Hura, G. L., Rossen, N. D., Gate, R. E., and Minor, D. L. Jr. (2018). A calmodulin C-lobe Ca(2+)-dependent switch governs Kv7 channel function. *Neuron* 97, 836.e6–852.e6. doi: 10.1016/j.neuron.2018.01.035

Charlier, C., Singh, N. A., Ryan, S. G., Lewis, T. B., Reus, B. E., Leach, R. J., et al. (1998). A pore mutation in a novel KQT-like potassium channel gene in an idiopathic epilepsy family. *Nat. Genet.* 18, 53–55. doi: 10.1038/ng0198-53

Chen, L., Zhang, Q., Qiu, Y., Li, Z., Chen, Z., Jiang, H., et al. (2015). Migration of PIP2 lipids on voltage-gated potassium channel surface influences channel deactivation. *Sci. Rep.* 5:15079. doi: 10.1038/srep15079

Clark, S., Antell, A., and Kaufman, K. (2015). New antiepileptic medication linked to blue discoloration of the skin and eyes. *Ther. Adv. Drug Saf.* 6, 15–19. doi: 10.1177/2042098614560736

Cooper, E. C., Aldape, K. D., Abosch, A., Barbaro, N. M., Berger, M. S., Peacock, W. S., et al. (2000). Colocalization and coassembly of two human

brain M-type potassium channel subunits that are mutated in epilepsy. *Proc. Natl. Acad. Sci. U. S. A.* 97, 4914–4919. doi: 10.1073/pnas.090092797

Cooper, E. C., Harrington, E., Jan, Y. N., and Jan, L. Y. (2001). M channel KCNQ2 subunits are localized to key sites for control of neuronal network oscillations and synchronization in mouse brain. *J. Neurosci.* 21, 9529–9540. doi: 10.1523/JNEUROSCI.21-24-09529.2001

Delmas, P., and Brown, D. A. (2005). Pathways modulating neural KCNQ/M (Kv7) potassium channels. *Nat. Rev. Neurosci.* 6, 850–862. doi: 10.1038/nrn1785

Devaux, J. J., Kleopa, K. A., Cooper, E. C., and Scherer, S. S. (2004). KCNQ2 is a nodal K^+ channel. *J. Neurosci.* 24, 1236–1244. doi: 10.1523/JNEUROSCI.4512-03.2004

Etxeberria, A., Aivar, P., Rodriguez-Alfaro, J. A., Alaimo, A., Villacé, P., Gómez-Posada, J. C., et al. (2008). Calmodulin regulates the trafficking of KCNQ2 potassium channels. *FASEB J.* 22, 1135–1143. doi: 10.1096/fj.07-9712com

Falkenburger, B. H., Jensen, J. B., and Hille, B. (2010). Kinetics of PIP2 metabolism and KCNQ2/3 channel regulation studied with a voltage-sensitive phosphatase in living cells. *J. Gen. Physiol.* 135, 99–114. doi: 10.1085/jgp.200910345

Food and Drug Administration, U.S. (2015). FDA Drug Safety Communication: FDA determines 2013 labeling adequate to manage risk of retinal abnormalities, potential vision loss, and skin discoloration with anti-seizure drug Potiga (ezogabine); requires additional study. Online. Available at: http://www.fda.gov/Drugs/DrugSafety/ucm451166.htm (Accessed August 8, 2016).

Gamper, N., and Shapiro, M. S. (2007). Regulation of ion transport proteins by membrane phosphoinositides. *Nat. Rev. Neurosci.* 8, 921–934. doi: 10.1038/nrn2257

Gunthorpe, M. J., Large, C. H., and Sankar, R. (2012). The mechanism of action of retigabine (ezogabine), a first-in-class K^+ channel opener for the treatment of epilepsy. *Epilepsia* 53, 412–424. doi: 10.1111/j.1528-1167.2011.03365.x

Hadley, J. K., Passmore, G. M., Tatulian, L., Al-Qatari, M., Ye, F., Wickenden, A. D., et al. (2003). Stoichiometry of expressed KCNQ2/KCNQ3 potassium channels and subunit composition of native ganglionic M channels deduced from block by tetraethylammonium. *J. Neurosci.* 23, 5012–5019. doi: 10.1523/JNEUROSCI.23-12-05012.2003

Hernandez, C. C., Zaika, O., and Shapiro, M. S. (2008). A carboxy-terminal inter-helix linker as the site of phosphatidylinositol 4,5-bisphosphate action on Kv7 (M-type) K^+ channels. *J. Gen. Physiol.* 132, 361–381. doi: 10.1085/jgp.200810007

Hille, B., Dickson, E. J., Kruse, M., Vivas, O., and Suh, B. -C. (2015). Phosphoinositides regulate ion channels. *BBA-Mol. Cell Biol. L.* 1851, 844–856. doi: 10.1016/j.bbalip.2014.09.010

Ihara, Y., Tomonoh, Y., Deshimaru, M., Zhang, B., Uchida, T., Ishii, A., et al. (2016). Retigabine, a Kv7.2/Kv7.3-channel opener, attenuates drug-induced seizures in Knock-in mice Harboring Kcnq2 mutations. *PLoS One* 11:e0150095. doi: 10.1371/journal.pone.0150095

Jin, Z., Liang, G. H., Cooper, E. C., and Jarlebark, L. (2009). Expression and localization of K channels KCNQ2 and KCNQ3 in the mammalian cochlea. *Audiol. Neurootol.* 14, 98–105. doi: 10.1159/000158538

Kalappa, B. I., Soh, H., Duignan, K. M., Furuya, T., Edwards, S., Tzingounis, A. V., et al. (2015). Potent KCNQ2/3-specific channel activator suppresses in vivo epileptic activity and prevents the development of tinnitus. *J. Neurosci.* 35, 8829–8842. doi: 10.1523/JNEUROSCI.5176-14.2015

Kang, S., Xu, M., Cooper, E. C., and Hoshi, N. (2014). Channel-anchored protein kinase CK2 and protein phosphatase 1 reciprocally regulate KCNQ2-containing M-channels via phosphorylation of calmodulin. *J. Biol. Chem.* 289, 11536–11544. doi: 10.1074/jbc.M113.528497

Kato, M., Yamagata, T., Kubota, M., Arai, H., Yamashita, S., Nakagawa, T., et al. (2013). Clinical spectrum of early onset epileptic encephalopathies caused by KCNQ2 mutation. *Epilepsia* 54, 1282–1287. doi: 10.1111/epi.12200

Kim, K. S., Duignan, K. M., Hawryluk, J. M., Soh, H., and Tzingounis, A. V. (2016b). The voltage activation of cortical KCNQ channels depends on global PIP2 levels. *Biophys. J.* 110, 1089–1098. doi: 10.1016/j.bpj.2016.01.006

Kim, H. J., Jeong, M. H., Kim, K. R., Jung, C. Y., Lee, S. Y., Kim, H., et al. (2016a). Protein arginine methylation facilitates KCNQ channel-PIP2 interaction leading to seizure suppression. *elife* 5:e17159. doi: 10.7554/eLife.17159

Kosenko, A., and Hoshi, N. (2013). A change in configuration of the calmodulin-KCNQ channel complex underlies Ca^{2+}-dependent modulation of KCNQ channel activity. *PLoS One* 8:e82290. doi: 10.1371/journal.pone.0082290

Kosenko, A., Kang, S., Smith, I. M., Greene, D. L., Langeberg, L. K., Scott, J. D., et al. (2012). Coordinated signal integration at the M-type potassium channel upon muscarinic stimulation. *EMBO J.* 31, 3147–3156. doi: 10.1038/emboj.2012.156

Li, Y., Gamper, N., Hilgemann, D. W., and Shapiro, M. S. (2005). Regulation of Kv7 (KCNQ) K^+ channel open probability by phosphatidylinositol 4,5-bisphosphate. *J. Neurosci.* 25, 9825–9835. doi: 10.1523/JNEUROSCI.2597-05.2005

Liu, W., and Devaux, J. J. (2014). Calmodulin orchestrates the heteromeric assembly and the trafficking of KCNQ2/3 (Kv7.2/3) channels in neurons. *Mol. Cell. Neurosci.* 58, 40–52. doi: 10.1016/j.mcn.2013.12.005

Miceli, F., Soldovieri, M. V., Ambrosino, P., Barrese, V., Migliore, M., Cilio, M. R., et al. (2013). Genotype-phenotype correlations in neonatal epilepsies caused by mutations in the voltage sensor of K(v)7.2 potassium channel subunits. *Proc. Natl. Acad. Sci. U. S. A.* 110, 4386–4391. doi: 10.1073/pnas.1216867110

Miceli, F., Soldovieri, M. V., Ambrosino, P., De Maria, M., Migliore, M., Migliore, R., et al. (2015). Early-onset epileptic encephalopathy caused by gain-of-function mutations in the voltage sensor of Kv7.2 and Kv7.3 potassium channel subunits. *J. Neurosci.* 35, 3782–3793. doi: 10.1523/JNEUROSCI.4423-14.2015

Milh, M., Boutry-Kryza, N., Sutera-Sardo, J., Mignot, C., Auvin, S., Lacoste, C., et al. (2013). Similar early characteristics but variable neurological outcome of patients with a de novo mutation of KCNQ2. *Orphanet J. Rare Dis.* 8:80. doi: 10.1186/1750-1172-8-80

Millichap, J. J., and Cooper, E. C. (2012). KCNQ2 potassium channel epileptic encephalopathy syndrome: divorce of an electro-mechanical couple? *Epilepsy Curr.* 12, 150–152. doi: 10.5698/1535-7511-12.4.150

Millichap, J. J., Park, K. L., Tsuchida, T., Ben-Zeev, B., Carmant, L., Flamini, R., et al. (2016). KCNQ2 encephalopathy: features, mutational hot spots, and ezogabine treatment of 11 patients. *Neurol. Genet.* 2:e96. doi: 10.1212/NXG.0000000000000096

Mruk, K., Shandilya, S. M. D., Blaustein, R. O., Schiffer, C. A., and Kobertz, W. R. (2012). Structural insights into neuronal K^+ channel–calmodulin complexes. *Proc. Natl. Acad. Sci. U. S. A.* 109, 13579–13583. doi: 10.1073/pnas.1207606109

Mulkey, S. B., Ben-Zeev, B., Nicolai, J., Carroll, J. L., Gronborg, S., Jiang, Y. H., et al. (2017). Neonatal nonepileptic myoclonus is a prominent clinical feature of KCNQ2 gain-of-function variants R201C and R201H. *Epilepsia* 58, 436–445. doi: 10.1111/epi.13676

Murata, Y., and Okamura, Y. (2007). Depolarization activates the phosphoinositide phosphatase ci-VSP, as detected in Xenopus oocytes coexpressing sensors of PIP(2). *J. Physiol.* 583, 875–889. doi: 10.1113/jphysiol.2007.134775

Nakada, C., Ritchie, K., Oba, Y., Nakamura, M., Hotta, Y., Iino, R., et al. (2003). Accumulation of anchored proteins forms membrane diffusion barriers during neuronal polarization. *Nat. Cell Biol.* 5, 626–632. doi: 10.1038/ncb1009

Niday, Z., Hawkins, V. E., Soh, H., Mulkey, D. K., and Tzingounis, A. V. (2017). Epilepsy-associated KCNQ2 channels regulate multiple intrinsic properties of layer 2/3 pyramidal neurons. *J. Neurosci.* 37, 576–586. doi: 10.1523/JNEUROSCI.1425-16.2016

Olson, H. E., Kelly, M., Lacoursiere, C. M., Pinsky, R., Tambunan, D., Shain, C., et al. (2017). Genetics and genotype–phenotype correlations in early onset epileptic encephalopathy with burst suppression. *Ann. Neurol.* 81, 419–429. doi: 10.1002/ana.24883

Orhan, G., Bock, M., Schepers, D., Ilina, E. I., Reichel, S. N., Löffler, H., et al. (2014). Dominant-negative effects of KCNQ2 mutations are associated with epileptic encephalopathy. *Ann. Neurol.* 75, 382–394. doi: 10.1002/ana.24080

Pan, Z., Kao, T., Horvath, Z., Lemos, J., Sul, J. Y., Cranstoun, S. D., et al. (2006). A common ankyrin-G-based mechanism retains KCNQ and NaV channels at electrically active domains of the axon. *J. Neurosci.* 26, 2599–2613. doi: 10.1523/JNEUROSCI.4314-05.2006

Peters, H. C., Hu, H., Pongs, O., Storm, J. F., and Isbrandt, D. (2005). Conditional transgenic suppression of M channels in mouse brain reveals functions in neuronal excitability, resonance and behavior. *Nat. Neurosci.* 8, 51–60. doi: 10.1038/nn1375

Rasmussen, H. B., Frøkjær-Jensen, C., Jensen, C. S., Jensen, H. S., Jørgensen, N. K., Misonou, H., et al. (2007). Requirement of subunit co-assembly and ankyrin-G for M-channel localization at the axon initial segment. *J. Cell Sci.* 120, 953–963. doi: 10.1242/jcs.03396

Richards, S., Aziz, N., Bale, S., Bick, D., Das, S., Gastier-Foster, J., et al. (2015). Standards and guidelines for the interpretation of sequence variants: a joint

consensus recommendation of the American College of Medical Genetics and Genomics and the Association for Molecular Pathology. *Genet. Med.* 17, 405–424. doi: 10.1038/gim.2015.30

Richards, M. C., Heron, S. E., Spendlove, H. E., Scheffer, I. E., Grinton, B., Berkovic, S. F., et al. (2004). Novel mutations in the KCNQ2 gene link epilepsy to a dysfunction of the KCNQ2-calmodulin interaction. *J. Med. Genet.* 41:e35. doi: 10.1136/jmg.2003.013938

Sachyani, D., Dvir, M., Strulovich, R., Tria, G., Tobelaim, W., Peretz, A., et al. (2014). Structural basis of a Kv7.1 potassium channel gating module: studies of the intracellular c-terminal domain in complex with calmodulin. *Structure* 22, 1582–1594. doi: 10.1016/j.str.2014.07.016

Saitsu, H., Kato, M., Koide, A., Goto, T., Fujita, T., Nishiyama, K., et al. (2012). Whole exome sequencing identifies KCNQ2 mutations in Ohtahara syndrome. *Ann. Neurol.* 72, 298–300. doi: 10.1002/ana.23620

Schroeder, B. C., Kubisch, C., Stein, V., and Jentsch, T. J. (1998). Moderate loss of function of cyclic-AMP-modulated KCNQ2/KCNQ3 K channels causes epilepsy. *Nature* 396, 687–690. doi: 10.1038/25367

Shah, M. M., Migliore, M., Valencia, I., Cooper, E. C., and Brown, D. A. (2008). Functional significance of axonal Kv7 channels in hippocampal pyramidal neurons. *Proc. Natl. Acad. Sci. U. S. A.* 105, 7869–7874. doi: 10.1073/pnas.0802805105

Singh, N. A., Charlier, C., Stauffer, D., Dupont, B. R., Leach, R. J., Melis, R., et al. (1998). A novel potassium channel gene, KCNQ2, is mutated in an inherited epilepsy of newborns. *Nat. Genet.* 18, 25–29. doi: 10.1038/ng0198-25

Soldovieri, M. V., Ambrosino, P., Mosca, I., De Maria, M., Moretto, E., Miceli, F., et al. (2016). Early-onset epileptic encephalopathy caused by a reduced sensitivity of Kv7.2 potassium channels to phosphatidylinositol 4,5-bisphosphate. *Sci. Rep.* 6:38167. doi: 10.1038/srep38167

Strulovich, R., Tobelaim, W. S., Attali, B., and Hirsch, J. A. (2016). Structural insights into the M-channel proximal C-terminus/Calmodulin complex. *Biochemistry* 55, 5353–5365. doi: 10.1021/acs.biochem.6b00477

Suh, B. -C., and Hille, B. (2002). Recovery from muscarinic modulation of M current channels requires phosphatidylinositol 4,5-bisphosphate synthesis. *Neuron* 35, 507–520. doi: 10.1016/S0896-6273(02)00790-0

Suh, B. -C., and Hille, B. (2008). PIP2 is a necessary cofactor for ion channel function: how and why? *Annu. Rev. Biophys.* 37, 175–195. doi: 10.1146/annurev.biophys.37.032807.125859

Sun, J., and Mackinnon, R. (2017). Cryo-EM structure of a KCNQ1/CaM complex reveals insights into congenital long QT syndrome. *Cell* 169, 1042.e9–1050.e9. doi: 10.1016/j.cell.2017.05.019

Sun, J., and Mackinnon, R. (2020). Structural basis of human KCNQ1 modulation and gating. *Cell* 180, 340.e9–347.e9. doi: 10.1016/j.cell.2019.12.003

Surti, T. S., Huang, L., Jan, Y. N., Jan, L. Y., and Cooper, E. C. (2005). Identification by mass spectrometry and functional characterization of two phosphorylation sites of KCNQ2/KCNQ3 channels. *Proc. Natl. Acad. Sci. U. S. A.* 102, 17828–17833. doi: 10.1073/pnas.0509122102

Telezhkin, V., Thomas, A. M., Harmer, S. C., Tinker, A., and Brown, D. A. (2013). A basic residue in the proximal C-terminus is necessary for efficient activation of the M-channel subunit Kv7.2 by PI(4,5)P(2). *Pflugers Arch.* 465, 945–953. doi: 10.1007/s00424-012-1199-3

Wang, H. -S., Pan, Z., Shi, W., Brown, B. S., Wymore, R. S., Cohen, I. S., et al. (1998). KCNQ2 and KCNQ3 potassium channel subunits: molecular correlates of the M-channel. *Science* 282, 1890–1893. doi: 10.1126/science.282.5395.1890

Weckhuysen, S., Ivanovic, V., Hendrickx, R., Van Coster, R., Hjalgrim, H., Moller, R. S., et al. (2013). Extending the KCNQ2 encephalopathy spectrum: clinical and neuroimaging findings in 17 patients. *Neurology* 81, 1697–1703. doi: 10.1212/01.wnl.0000435296.72400.a1

Weckhuysen, S., Mandelstam, S., Suls, A., Audenaert, D., Deconinck, T., Claes, L. R. F., et al. (2012). KCNQ2 encephalopathy: emerging phenotype of a neonatal epileptic encephalopathy. *Ann. Neurol.* 71, 15–25. doi: 10.1002/ana.22644

Wen, H., and Levitan, I. B. (2002). Calmodulin is an auxiliary subunit of KCNQ2/3 potassium channels. *J. Neurosci.* 22, 7991–8001. doi: 10.1523/JNEUROSCI.22-18-07991.2002

Yus-Nájera, E., Santana-Castro, I., and Villarroel, A. (2002). The identification and characterization of a noncontinuous calmodulin-binding site in noninactivating voltage-dependent KCNQ potassium channels. *J. Biol. Chem.* 277, 28545–28553. doi: 10.1074/jbc.M204130200

Zaydman, M. A., and Cui, J. (2014). PIP2 regulation of KCNQ channels: biophysical and molecular mechanisms for lipid modulation of voltage-dependent gating. *Front. Physiol.* 5:195. doi: 10.3389/fphys.2014.00195

Zaydman, M. A., Silva, J. R., Delaloye, K., Li, Y., Liang, H., Larsson, H. P., et al. (2013). Kv7.1 ion channels require a lipid to couple voltage sensing to pore opening. *Proc. Natl. Acad. Sci. U. S. A.* 110, 13180–13185. doi: 10.1073/pnas.1305167110

Zhang, H., Craciun, L. C., Mirshahi, T., Rohacs, T., Lopes, C. M., Jin, T., et al. (2003). PIP(2) activates KCNQ channels, and its hydrolysis underlies receptor-mediated inhibition of M currents. *Neuron* 37, 963–975. doi: 10.1016/S0896-6273(03)00125-9

Zhang, J., Kim, E. C., Chen, C., Procko, E., Pant, S., Lam, K., et al. (2020). Identifying mutation hotspots reveals pathogenetic mechanisms of KCNQ2 epileptic encephalopathy. *Sci. Rep.* 10:4756. doi: 10.1038/s41598-020-61697-6

Zhang, Q., Zhou, P., Chen, Z., Li, M., Jiang, H., Gao, Z., et al. (2013). Dynamic PIP2 interactions with voltage sensor elements contribute to KCNQ2 channel gating. *Proc. Natl. Acad. Sci. U. S. A.* 110, 20093–20098. doi: 10.1073/pnas.1312483110

Conflict of Interest: BT, MX, ZGJ, and TT declare no competing financial interests. EC has served as a consultant to and as PI of investigator-initiated research grants from SciFluor Life Sciences, Knopp Biosciences, and Xenon Pharmaceuticals. This consultancy work and sponsored research was reviewed and approved according to the conflict of interest policies of Baylor College of Medicine.

frontiers in Physiology

REVIEW
published: 16 September 2020
doi: 10.3389/fphys.2020.01004

Detrusor Smooth Muscle K_V7 Channels: Emerging New Regulators of Urinary Bladder Function

John Malysz[1] *and Georgi V. Petkov*[1,2,3]*

[1] Department of Pharmaceutical Sciences, College of Pharmacy, University of Tennessee Health Science Center, Memphis, TN, United States, [2] Department of Pharmacology, College of Medicine, University of Tennessee Health Science Center, Memphis, TN, United States, [3] Department of Urology, College of Medicine, University of Tennessee Health Science Center, Memphis, TN, United States

Relaxation and contraction of the urinary bladder smooth muscle, also known as the detrusor smooth muscle (DSM), facilitate the micturition cycle. DSM contractility depends on cell excitability, which is established by the synchronized activity of multiple diverse ion channels. K^+ channels, the largest family of channels, control DSM excitability by maintaining the resting membrane potential and shaping the action potentials that cause the phasic contractions. Among the members of the voltage-gated K^+ (K_V) channel superfamily, K_V type 7 (K_V7) channels — $K_V7.1$–$K_V7.5$ members encoded by *KCNQ1–KCNQ5* genes — have been recently identified as functional regulators in various cell types including vascular, cardiac, and neuronal cells. Their regulatory roles in DSM, however, are just now emerging and remain to be elucidated. To address this gap, our research group has initiated the systematic investigation of human DSM K_V7 channels in collaboration with clinical urologists. In this comprehensive review, we summarize the current understanding of DSM Kv7 channels and highlight recent discoveries in the field. We describe K_V7 channel expression profiles at the mRNA and protein levels, and further elaborate on functional effects of K_V7 channel selective modulators on DSM excitability, contractility, and intracellular Ca^{2+} dynamics in animal species along with *in vivo* studies and the limited data on human DSM. Within each topic, we highlight the main observations, current gaps in knowledge, and most pressing questions and concepts in need of resolution. We emphasize the lack of systematic studies on human DSM K_V7 channels that are now actively ongoing in our laboratory.

Keywords: KCNQ, smooth muscle, detrusor, excitability, contractility, overactive bladder, patch-clamp, electrophysiology

OPEN ACCESS

Edited by:
Vincenzo Barrese, University of Naples Federico II, Italy

Reviewed by:
Iain A. Greenwood, St George's, University of London, United Kingdom
Núria Comes, University of Barcelona, Spain

***Correspondence:**
Georgi V. Petkov
gpetkov@uthsc.edu

Specialty section:
This article was submitted to Membrane Physiology and Membrane Biophysics, a section of the journal Frontiers in Physiology

Received: *31 May 2020*
Accepted: *23 July 2020*
Published: *16 September 2020*

Citation:
Malysz J and Petkov GV (2020) Detrusor Smooth Muscle K_V7 Channels: Emerging New Regulators of Urinary Bladder Function. Front. Physiol. 11:1004. doi: 10.3389/fphys.2020.01004

Abbreviations: BPH, benign prostatic hyperplasia; Ca_V, L-type voltage-gated Ca^{2+} (channel); DO, detrusor overactivity; DSM, detrusor smooth muscle; EFS, electrical field stimulation; ICA-069673, *N*-(2-Chloro-5-pyrimidinyl)-3,4-difluorobenzamide; K_V7, voltage-gated potassium type 7 (channel); KCNE, K^+ voltage-gated channel subfamily E (member); ML213, *N*-(2,4,6-Trimethylphenyl)-bicyclo[2.2.1]heptane-2-carboxamide; ML277, (2R)-*N*-[4-(4-Methoxyphenyl)-2-thiazolyl]-1-[(4-methylphenyl)sulfonyl]-2-piperidinecarboxamide; MMSC, muscularis mucosae smooth muscle; qRT-PCR, quantitative reverse transcription polymerase chain reaction; RBC, rhythmic bladder contraction; SMC, smooth muscle cell; TC, transient contraction; XE991, 10,10-bis(4-Pyridinylmethyl)-9(10H)-anthracenone dihydrochloride.

INTRODUCTION

The urinary bladder smooth muscle, also referred to as the detrusor smooth muscle (DSM) forms the bladder wall and ultimately determines the two fundamental functions of the organ: urine storage and voiding (Andersson and Arner, 2004; Andersson and Wein, 2004). DSM relaxation along with the closure of the urinary bladder sphincter facilitates urine storage. On the other hand, coordinated DSM contractions and the opening of the urinary bladder sphincter promote urine voiding. The understanding of the complex factors regulating urinary bladder function is continuously evolving and involves myogenic, neuronal, and urothelial interacting mechanisms (see reviews by Andersson and Arner, 2004; de Groat et al., 2015; Fry and McCloskey, 2019; Dalghi et al., 2020). The myogenic concept stresses the intrinsic role of DSM cell excitability for regulating contractility. DSM cells express various types of ion channels including Ca^{2+}, K^+, non-selective cation, and Cl^- channels (for a general overview, please see the most recent review by Malysz and Petkov, 2020). In general, the opening of K^+ channels causes membrane hyperpolarization, reduction of L-type voltage-gated Ca^{2+} (Ca_V) channel open probability, decrease in net Ca^{2+} influx, and smooth muscle relaxation (Petkov, 2009; Brading and Brain, 2011; Petkov, 2012; Fry and McCloskey, 2019). Inhibition of K^+ channels has an opposite effect, promoting DSM excitability, and thus contractility (Petkov, 2009, 2012; Brading and Brain, 2011; Fry and McCloskey, 2019; Malysz and Petkov, 2020). Among the 40 genes encoding all of the known K_V channels, the functions the K_V7 subfamily are just beginning to be unraveled in the DSM of human and animal species. The K_V7 channel subfamily contains five members — named $K_V7.1$- $K_V7.5$ and encoded by *KCNQ1–KCNQ5* genes. They can form either a homotetrameric (e.g., $K_V7.1$) or a heterotetrameric (e.g., $K_V7.2/K_V7.3$) channel combination, with each exhibiting distinct electrophysiological and pharmacological properties (Barrese et al., 2018b). Further, K_V7 tetrameric channel complexes may preferentially associate with regulatory accessory subunits such as KCNE that fine-tune channel biophysical properties (e.g., $K_V7.1$-KCNE1) (Barrese et al., 2018b).

Recent and current medicinal chemistry efforts have discovered a number of excellent pharmacological tool compounds, either inhibitors or activators, which are K_V7 subtype-specific. They include (1) retigabine and flupirtine, both pan-specific activators of $K_V7.2$-$K_V7.5$ channels; (2) ICA-069673, a selective activator of $K_V7.2/K_V7.3$ channels; (3) ML213, a preferential activator of $K_V7.2$, $K_V7.2/K_V7.3$, and $K_V7.4$ channels; (4) XE991 and linopirdine, pan-selective inhibitors of $K_V7.1$-$K_V7.5$ channels (Miceli et al., 2008, 2018; Yu et al., 2010, 2011; Amato et al., 2011; Barrese et al., 2018b). More recently, the next generation of subtype-specific and selective modulators for $K_V7.2/K_V7.3$ and $K_V7.4/K_V7.5$ channels has been described (Liu et al., 2019; Osuma et al., 2019; Zhang et al., 2019; Ostacolo et al., 2020). These compounds provide an excellent opportunity to determine the functions of K_V7 channels subtypes in DSM and elsewhere.

Current knowledge of DSM K_V7 channels lags behind that of other cell types where K_V7 channels are already well recognized as critical regulators of cell function. A number of prior reviews describe in detail K_V7 channels in smooth muscle and other cell types including regulatory mechanisms under normal and pathophysiological conditions (Stott et al., 2014; Barrese et al., 2018b; Byron and Brueggemann, 2018; Nappi et al., 2020). For non-bladder smooth muscle, transcript and protein expressions of K_V7 channels as well as functional roles (patch-clamp electrophysiology and contractility) have been revealed in arteries (cerebral, basal, mesenteric, renal, gracilis, penile, and visceral adipose), portal vein, airway, gastrointestinal tract, uterus, and corpus cavernosum (Yeung and Greenwood, 2005; Yeung et al., 2008; Jepps et al., 2009; McCallum et al., 2009; Zhong et al., 2010; Ipavec et al., 2011; Mani et al., 2011, 2013; McCallum et al., 2011; Ng et al., 2011; Brueggemann et al., 2012a, 2014, 2018; Evseev et al., 2013; Chadha et al., 2014; Jepps et al., 2016; Barrese et al., 2018a; Stott et al., 2018; Zavaritskaya et al., 2020). The expression profiles of K_V7 channel subtypes differ substantially based on smooth muscle cell (SMC) type. In rodent and human blood vessels, evidence points to the predominant role of $K_V7.4$ and $K_V7.5$ channel subtypes – but not $K_V7.2$ or $K_V7.3$ – regulating vascular membrane potential and contractility (Mackie and Byron, 2008; Mackie et al., 2008; Zhong et al., 2010; Ng et al., 2011; Chadha et al., 2014). In airway smooth muscle, $K_V7.1$ – $K_V7.5$ channel subtypes demonstrate species-specific expression profiles (Brueggemann et al., 2012a; Evseev et al., 2013). In the heart, the expressed $K_V7.1$ channels co-assembled with KCNE1 proteins underlie the voltage-gated delayed rectifier K^+ channel currents that contribute to the late repolarization phase of the cardiac action potential (Barhanin et al., 1996). Neuronal heteromeric K_V7 channels incorporating $K_V7.2$, $K_V7.3$, $K_V7.4$, or $K_V7.5$ channel subtypes are expressed in various brain regions, and they control the membrane potential and action potential pattern generation (Brown and Passmore, 2009). Of note, the pharmacological activation of heteromeric $K_V7.2/K_V7.3$ channels is thought to underlie the primary mechanism of action for retigabine, a previously approved anti-epileptic drug (Wickenden et al., 2000). Mechanistically, retigabine shifts the voltage dependency of $K_V7.2$–$K_V7.5$ channels to hyperpolarized membrane potentials (due to an increase in open probability), accelerates the activation, and reduces deactivation of the currents (Tatulian et al., 2001; Tatulian and Brown, 2003). A single tryptophan within the S5 domain of $K_V7.2$-$K_V7.5$ channels has been shown to be essential for the effect of retigabine (Schenzer et al., 2005).

This review summarizes our current understanding of the K_V7 channels' physiological roles in DSM. First, we highlight the initial findings for retigabine, a $K_V7.2$–$K_V7.5$ channel activator causing urinary retention in clinical trials for epilepsy, which suggested for the first time a role for K_V7 channels in the control of urinary bladder function. Next, we provide an overview of subsequent *in vivo* animal model studies of urinary bladder function with retigabine and other K_V7 channel

modulators. Then, we describe the current understanding of the roles of K_V7 channels in DSM based on systematic studies that our group — initially at the University of South Carolina and now at the recently established Urology Research Center, University of Tennessee, Memphis — has pioneered in this field and those of other investigators. We summarize the expression profiles for K_V7 channel subtypes in DSM whole-tissue and single-cell preparations, electrophysiological findings for K_V7 channel modulators in DSM cell patch-clamp and tissue conventional microelectrode electrophysiological experiments, and how K_V7 channel pharmacological modulators affect intracellular Ca^{2+} concentrations and DSM contractility. Within each topic, we highlight the main findings and current knowledge gaps and emphasize the most pressing questions and concepts regarding DSM K_V7 channels that await scientific resolution.

K_V7 CHANNEL PHARMACOLOGICAL ACTIVATION IS ASSOCIATED WITH URINARY RETENTION IN PATIENTS

The initial realization that K_V7 channels may be involved in regulating urinary bladder function dates to the very first clinical testing of retigabine as an adjunct therapy for controlling epilepsy (Brickel et al., 2012). Safety analyses of clinical data for retigabine (phases 2/3) revealed urinary retention as a notable side-effect. Indeed, subjects taking retigabine in comparison to placebo reported a ∼2-fold higher incidence of urinary retention (0.9% versus 0.5%) and a relative risk of 1.32 (95% confidence interval, 0.986 – 1.761) of reporting a urinary/renal side effect (Brickel et al., 2012). Intriguingly, these findings suggested that retigabine, by activating K_V7 channels, might prove beneficial in ameliorating overactive bladder/detrusor overactivity. Retigabine, however, has not been clinically examined specifically for any urinary bladder condition. In contrast, its very close structural analog flupirtine has progressed into a phase 2 study for overactive bladder (Michel et al., 2012). Flupirtine has a long history (since 1981) of clinical use in Europe (but was not approved in the US) as a centrally acting, non-opioid analgesic (Devulder, 2010). Unfortunately, discoveries of other unexpected side-effects hampered clinical uses of retigabine and flupirtine (Brickel et al., 2012; Michel et al., 2012). For retigabine, this includes a prolongation of the QT interval and potential development of cardiac arrhythmias in certain patients (Barrese et al., 2010; Splinter, 2013). The mechanism involved remains to be elucidated; however, a direct effect on the heart is unlikely. When tested in guinea pig and human cardiomyocytes, retigabine induced a reduction rather than a prolongation of the action potential (Rubi et al., 2017). Other limitations for retigabine and flupirtine are their non-selectivity among K_V7 channel subtypes (both are active at $K_V7.2$-$K_V7.5$ channels), and their relatively weak potency (Miceli et al., 2008, 2011, 2018). Thus, novel subtype-specific K_V7 channel activators are needed. Both retigabine and flupirtine remain as excellent tools for preclinical investigations of K_V7 channels, including their roles in DSM, as described below.

K_V7 CHANNEL MODULATORS AFFECT URINARY BLADDER FUNCTION *IN VIVO* IN EXPERIMENTAL ANIMAL MODELS

A seminal report, published back in 2004, described that retigabine altered urinary bladder function *in vivo* (Streng et al., 2004). In conscious female adult rats, with continuously monitored bladder function by cystometry, retigabine applied intravenously (i.v., 0.5–5 mg/kg), intracerebroventricularly (10 or 50 μg bolus), and intravesically (100–1000 ng/ml) increased micturition volume and voiding intervals, and when given intravesically, decreased capsaicin-induced DO. Since XE991, a pan-selective K_V7 channel blocker, completely inhibited the effects of retigabine, the study authors concluded that *"KCNQ channels can be interesting targets aiming at micturition control"* (Streng et al., 2004).

A later report on unanesthetized adult female rats confirmed the inhibitory effects of retigabine (applied orally at 0.5 mg/kg) on capsaicin-induced DO where the K_V7 channel activator compound retigabine decreased micturition volume output (Svalo et al., 2012). This study also demonstrated retigabine efficacy in an animal model of acetic-acid-induced DO examined under anesthesia. Specifically, retigabine (i.v.) increased micturition interval (doses 0.001–1 mg/kg) and micturition volume (0.1 mg/kg). While cardiovascular effects on blood pressure were observed, they occurred only at the highest dose tested (1 mg/kg). The lower doses (0.01–0.3 mg/kg) still displayed positive effects on urinary bladder function, and these data, thus, showed separation of desirable urinary bladder effects and unwanted cardiovascular effects *in vivo*. Similarly, in rats, retigabine at a dose of 0.1 mg/kg (i.p.) reduced the frequency of spontaneous contractions during bladder filling, and it also completely abolished (10 mg/kg i.p.) acetic acid-enhanced (0.25%) micturition activity (Argentieri and Sheldon, 2006).

More recently, the effects of retigabine (0.01–3 mg/kg, i.v.) were examined on rhythmic bladder contractions (RBCs) in adult female rats under anesthesia (Aizawa et al., 2017). Retigabine dose-dependently decreased both the frequency and amplitude of RBCs with the former parameter showing higher sensitivity. This study also revealed a reduction in afferent nerve fiber firing activities of myelinated Aδ and unmyelinated C-fibers by retigabine at 1 mg/kg, but not at lower doses (Aizawa et al., 2017). Interestingly, retigabine at 0.3 mg/kg reduced the frequency of RBCs by ∼50% without affecting the afferent neuronal firing, suggesting that the primary cellular site of action for retigabine at this particular dose involved DSM (Aizawa et al., 2017).

Similarly, in adult mice, retigabine almost completely attenuated the afferent nerve firing associated with RBCs (referred to as transient contractions/TCs in this publication) during *ex vivo* bladder filling (Tykocki et al., 2019). Of note, retigabine reduced the magnitude of RBCs (i.e., TC integral in the report). Since XE991 prevented the effects of retigabine on afferent firing and RBCs, the findings supported the involvement

of K_V7 channels. Interestingly, XE991 examined alone did not change the RBC magnitude (integral), but rather its frequency, in contrast to observations with retigabine (Tykocki et al., 2019).

Collectively, K_V7 channel modulators exhibit *in vivo* efficacy in experimental animal models, supporting that K_V7 channels play a regulatory role in the urinary bladder. Below, we summarize the experimental evidence based on systematic studies initiated and continued today by our group and others on K_V7 channel subtypes in DSM by describing their expression and function in DSM.

EXPRESSION OF K_V7 CHANNEL SUBTYPES IN DSM WHOLE-TISSUE AND SINGLE CELLS

K_V7 channel subtypes have been detected at mRNA or protein levels in guinea pig, rat, and human DSM whole tissues or isolated cells (Svalo et al., 2012; Afeli et al., 2013; Anderson et al., 2013; Svalo et al., 2013, 2015; Provence et al., 2015, 2018). An important consideration for interpretation of the results from whole-DSM tissue preparations is that — since RT-PCR is a very sensitive technique —a detected mRNA signal can potentially originate from any cell type present in the whole tissue preparation, including DSM cells, interstitial cells, nerve fibers, and fibroblasts. Thus, to conclude that a given mRNA product is expressed directly in DSM cells, positive detections in isolated single DSM cells are required. In adult male guinea pig DSM whole-tissues and single cells, all $K_V7.1$–$K_V7.5$ were detected at mRNA and protein levels (Afeli et al., 2013; Anderson et al., 2013; Provence et al., 2015). Our qRT-PCR experiments revealed the following rank order of expressions in DSM whole-tissue: ($K_V7.1 \sim K_V7.2 > K_V7.3 \sim K_V7.5 > K_V7.4$) and single cells ($K_V7.1 \sim K_V7.2 > K_V7.5 > K_V7.3 \sim K_V7.4$) (Afeli et al., 2013). Further confirmations were made with RT-PCR, immunohistochemistry (with co-labeled DSM cells), and DSM cell immunocytochemistry determinations (Afeli et al., 2013; Anderson et al., 2013; Provence et al., 2015). Since K_V7 channels can assemble as preferential heteromers, the expression data suggested that guinea pig DSM K_V7 channels could potentially comprise $K_V7.2/K_V7.3$, $K_V7.3/K_V7.5$, and $K_V7.4/K_V7.5$ heteromeric complexes as well as homomeric channels. Experimental evidence from DSM cells based on *in situ* proximity ligation assay supported the presence of $K_V7.4/K_V7.5$ channel complexes (Provence et al., 2018). The positive detection of $K_V7.2$ and $K_V7.3$ subtypes in DSM cells along with functional findings of efficacy on excitability and contractility by the selective $K_V7.2/K_V7.3$ channel activator ICA-069673 were consistent with the existence of $K_V7.2/K_V7.3$ heteromeric channels (Provence et al., 2015). A remaining question is to determine which of the possible homomeric or heteromeric combinations comprise the most physiologically relevant native DSM K_V7 channel.

In contrast, the published K_V7 channel expression data in rats, pigs, and humans are only available for whole-DSM tissues (Argentieri and Sheldon, 2006; Svalo et al., 2012, 2013, 2015; Bientinesi et al., 2017; Seefeld et al., 2018). Although initially in rat DSM mRNAs for $K_V7.1$, $K_V7.3$, and $K_V7.5$ channels were detected, subsequent studies also confirmed the presence of $K_V7.4$ channels (Argentieri and Sheldon, 2006). In adult female rats, qRT-PCR analysis showed the highest level of expression for the $K_V7.4$ subtype followed by lower but still detectible $K_V7.1$ and $K_V7.5$ subtypes and marginal/not present $K_V7.2$ and $K_V7.3$ subtypes (Svalo et al., 2012). Western blot studies of whole DSM tissue preparations found protein expression for $K_V7.4$ but not $K_V7.2$ (Svalo et al., 2012). Comparative parallel qRT-PCR expression analyses on the heart ($K_V7.1 > K_V7.4 > K_V7.2 \sim K_V7.3 > K_V7.5$), aorta ($K_V7.1 > K_V7.4 > K_V7.5 > K_V7.3 > K_V7.2$), and brain ($K_V7.3 > K_V7.2 \sim K_V7.5 > K_V7.4 > K_V7.1$) revealed differential mRNA expression profiles for K_V7 channel subtypes (Svalo et al., 2012). The relative level of $K_V7.4$ channel mRNA expression in the bladder approximated or reached a level slightly lower than that identified for the other three organs (Svalo et al., 2012). qRT-PCR analyses of $K_V7.3$–$K_V7.5$ channel mRNAs in pig DSM tissue provided similar findings with the following rank order of expression: $K_V7.4 > K_V7.5 > K_V7.3$ subtypes (Svalo et al., 2013). For the $K_V7.4$ subtype, the relative levels of mRNA expression were 0.6-fold and 2.8-fold lower in the bladder than in the cortex and the heart (Svalo et al., 2013). When compared to $K_V7.3$ and $K_V7.5$ channel subtypes, the relative DSM mRNA expression levels of the $K_V7.4$ channel subtype were, respectively, 10- and 2.5-fold lower in the heart and 200- and 2500-fold lower in the cortex (Svalo et al., 2013). These observations reinforced a high level of expression for $K_V7.4$ channels in DSM and organ-specific expression profiles of K_V7 channel subtypes.

Initial qRT-PCR investigations on human whole DSM tissue preparations detected K_V7 channel subunits with relative mRNA expression: $K_V7.3 \sim K_V7.4 \sim K_V7.5 \sim K_V7.1 > K_V7.2$ (Svalo et al., 2015). Two other groups found a similar rank order in human DSM tissues: $K_V7.4 \geq K_V7.5 \sim K_V7.1 > K_V7.3 > K_V7.2$ (Bientinesi et al., 2017) and $K_V7.4 \sim K_V7.5 > K_V7.3 > K_V7.2$ (Seefeld et al., 2018). Thus, these studies identified the $K_V7.4$ channel subtype as the most highly expressed while the $K_V7.2$ channel subtype was the lowest. There is, however, an earlier publication where mRNAs for only $K_V7.3$ and $K_V7.5$ channels were detected but not for $K_V7.1$, $K_V7.2$, and $K_V7.4$ channels in human bladder specimens, which raised the possibility of some experimental variability (Argentieri and Sheldon, 2006). Interestingly, in DSM tissues obtained from urinary bladders with partial outlet obstruction (POO) due to benign prostatic hyperplasia (BPH), the transcript expression of $K_V7.1$ channels increased 3.4-fold (Svalo et al., 2015). For other K_V7 subtypes, mRNA expression remained unchanged except for $K_V7.2$ channels, which were undetectable in POO-bladders (Svalo et al., 2015). The observed $K_V7.1$ channel expression increase may reflect a compensatory upregulation that developed to counteract DO under POO. Since accessory KCNE subunits can assemble with K_V7 channels altering the K_V7 channel complex properties, it is of interest to elucidate their expression and function in DSM. Currently, only a single report has provided such expression data using qRT-PCR. That analysis showed transcript expressions of all KCNE1-5 subunits with comparative relative mRNA expressions, which did not change under POO due to

BPH (Svalo et al., 2015). A key limitation of human and animal model expression studies is the lack of data on single DSM cells at both mRNA and protein levels. Thus, future studies of DSM specimens from patient-donors and animal models with both normal and aberrant bladder function are needed.

K_V7 CHANNEL FUNCTIONAL STUDIES ON DSM CELL EXCITABILITY

Electrophysiological Characterizations of K_V7 Channels in Regulating DSM Cell Excitability

Studies on Single DSM Cell Excitability

The initial evidence for a role of K_V7 channels in determining DSM cell excitability dates back to 2013. At that time, two independent research laboratories, Karen McCloskey's and our group, found that retigabine and flupirtine, both $K_V7.2$–$K_V7.5$ channel activators, affected electrophysiological properties of guinea pig DSM cells (Afeli et al., 2013; Anderson et al., 2013). As shown in **Figure 1**, retigabine hyperpolarized the DSM cell membrane potential by ∼7 mV when examined with the perforated whole-cell patch-clamp technique (Afeli et al., 2013). Of note, in DSM cells that exhibited spontaneous action potentials, retigabine caused their inhibition via membrane potential hyperpolarization (Afeli et al., 2013). This key finding, thus, mechanistically linked activation of K_V7 channels with inhibition of L-type Ca_V channels in DSM cells. In a separate study using the conventional whole-cell approach, voltage step-induced K^+ currents were increased by flupirtine and also meclofenamic acid, another K_V7 channel activator displaying preference for $K_V7.2/K_V7.3$ channels (Anderson et al., 2013). Flupirtine also caused a reversible hyperpolarization of ∼5 mV in DSM cells measured with the conventional whole-cell current-clamp method (Anderson et al., 2013). XE991 and linopirdine, both $K_V7.1$–$K_V7.5$ channel blockers, displayed effects opposite of those of either retigabine or flupirtine (Anderson et al., 2013; Provence et al., 2015, 2018). XE991 induced DSM cell depolarization (examined with either the perforated or conventional whole-cell current-clamp approach) and inhibited the voltage-step-induced K^+ currents (conventional whole-cell) (Anderson et al., 2013; Provence et al., 2015, 2018). Linopirdine mimicked the effects of XE991 on the membrane potential (conventional current-clamp) and whole-cell K^+ currents (conventional voltage-clamp). Additionally, chromanol 293B, a $K_V7.1$ and $K_V7.1$/KCNE1 channel inhibitor (Lerche et al., 2000), attenuated the voltage-step induced K^+ currents (conventional whole-cell) in DSM cells suggesting a regulatory role of this channel subtype (Anderson et al., 2013). Collectively, these electrophysiological studies solidified the notion that multiple K_V7 channel subtypes determine guinea pig DSM cell excitability.

Recent medicinal chemistry efforts have led to the discovery of new channel-selective tool compounds for the study of K_V7 channel subtypes. These novel compounds exhibit K_V7 channel subtype preferential targeted profiles. Two such novel K_V7 channel activators are ICA-069673 and ML213 (Yu et al., 2010, 2011; Amato et al., 2011). ICA-069673 has 20-fold or higher selectivity for $K_V7.2/K_V7.3$ channels (EC_{50} = 0.69 μM) over $K_V7.3/K_V7.5$ and $K_V7.1$ channels, and this novel K_V7 activator exhibited no measurable activity against a panel of cardiac ion channels including hERG, $Na_V1.5$, L-type Ca_V and $K_V7.1$ channels (Amato et al., 2011). ML213 shows a preference for $K_V7.2$ (EC_{50} = 0.33 μM), $K_V7.2/K_V7.3$ (EC_{50} = 0.37 μM), and $K_V7.4$ (EC_{50} = 0.51 μM) channels with a high degree of selectivity (at least 80-fold, EC_{50} > 30 μM) over $K_V7.1$, $K_V7.1$/KCNE1, $K_V7.3$, and $K_V7.5$ channels (Yu et al., 2010, 2011). Both ICA-069673 and ML213, when studied on guinea pig DSM isolated cells with the perforated whole-cell patch-clamp approach, hyperpolarized the cell membrane potential in an XE991-dependent manner (Provence et al., 2015, 2018). Specifically, pretreatment of DSM cells with XE991 prevented the hyperpolarizing effects of ICA-069673 and ML213 (Provence et al., 2015, 2018). Further, XE991 applied in the presence of either one of these K_V7 channel activators caused reversal of the compound-induced membrane hyperpolarization (Provence et al., 2015, 2018).

The pharmacological efficacy of ML213 extends to DSM whole-cell K^+ currents (Provence et al., 2018). ML213 increased voltage-step induced K^+ currents under experimental conditions that maximized the detection of K_V7 channel currents, specifically recording the electrical activity in the presence of paxilline, a BK channel inhibitor, and $GdCl_3$, an inhibitor of both L-type Ca_V and nonselective cation channels, using a depolarized holding potential of -10 mV, which ensures inactivation of non-K_V7 channels (Provence et al., 2018). The ML213-induced channel activation was fully reversible upon washout of the compound (Provence et al., 2018). Indeed, this seminal finding made by our group was the very first-ever successful recording of native K_V7 channel currents in DSM cells with the perforated patch-clamp approach, complementing previous findings with the conventional whole-cell approach (Anderson et al., 2013; Provence et al., 2018). The studies with ICA-069673 and ML213, therefore, demonstrated that K_V7 channel subtype-specific targeting by selective pharmacological activation decreases DSM cell excitability by promoting hyperpolarization.

In contrast to results for these animal models, the precise physiological role of K_V7 channels in human DSM cells has yet to be evaluated by systematic approaches. Initial data from our group revealed the effects of K_V7 channel modulators on single DSM cell excitability (Provence et al., 2015, 2018). In these studies, single human DSM cells were obtained using a highly optimized methodology (Malysz et al., 2020). Retigabine and XE991, respectively, hyperpolarized and depolarized DSM cell membrane potentials recorded with the amphotericin perforated current-clamp (Provence et al., 2015, 2018). Retigabine also increased ramp-protocol evoked K_V currents under experimental conditions optimized for recording of native K_V7 currents with the perforated voltage-clamp approach (Provence et al., 2018). In addition, a preliminary report on cultured human DSM cells using patch-clamp electrophysiology revealed retigabine induced membrane potential hyperpolarization and an increase in voltage-step-induced currents. Future comprehensive studies —

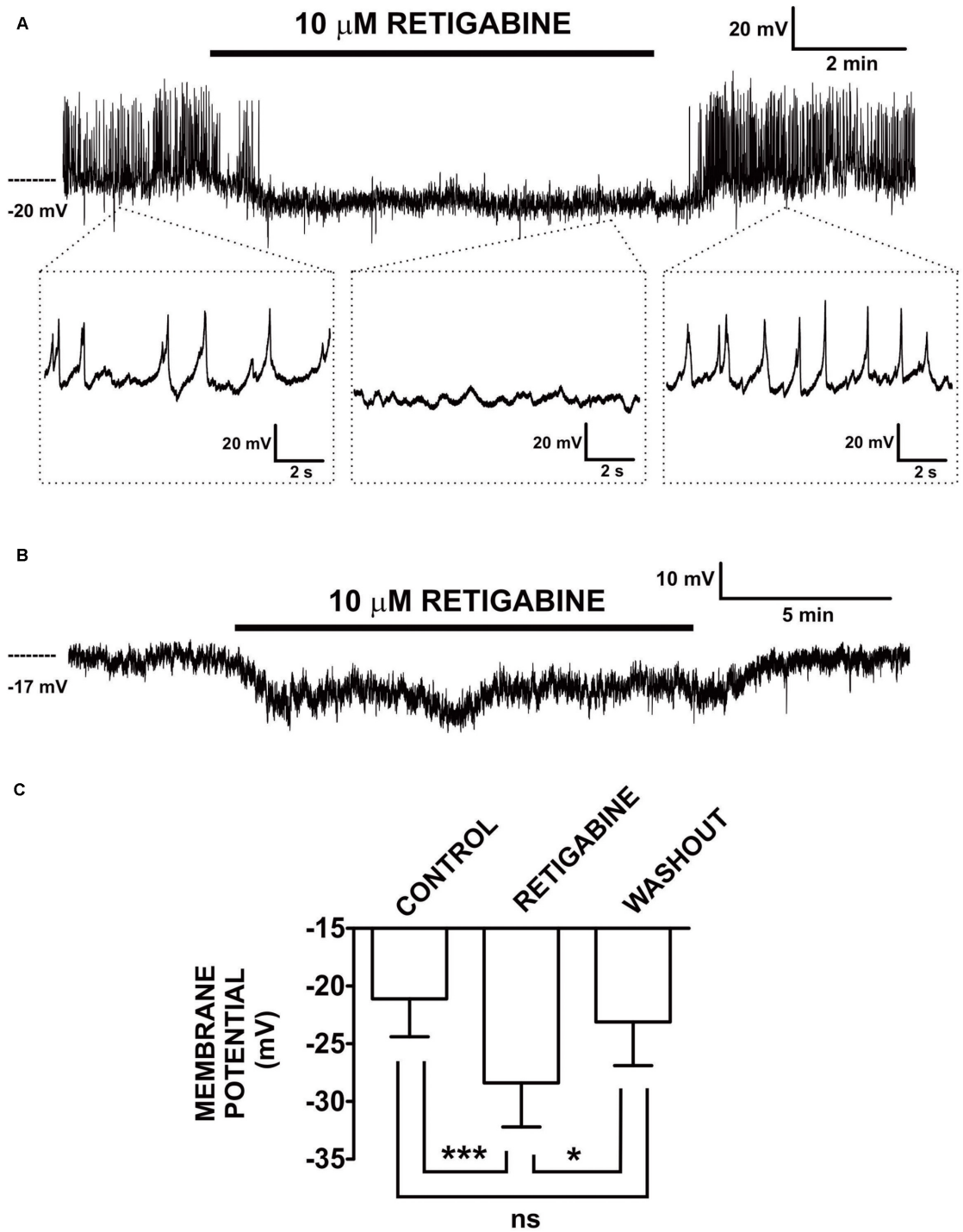

FIGURE 1 | Retigabine, a $K_V7.2$–$K_V7.5$ channel activator, induced hyperpolarization and inhibited generation of spontaneous action potentials in freshly isolated guinea pig DSM single cells. **(A)** An original current-clamp membrane potential recording in a DSM cell — obtained with the amphotericin-B perforated patch-clamp method — shows spontaneous action potentials. Retigabine (10 μM) inhibited these spontaneous action potentials and caused membrane hyperpolarization. Upon washout, membrane potential and action potentials fully recovered. The insets in **(A)** depict electrical activity on an expanded time scale for the time points indicated. **(B)** An original membrane potential recording from a DSM cell in which spontaneous action potentials were absent. Retigabine (10 μM) induced membrane hyperpolarization that recovered following washout of the compound. **(C)** Summary data show statistically significant hyperpolarization of DSM cells by retigabine (10 μM) (n = 12 DSM cells, N = 11 guinea pigs) and the recovery from hyperpolarization upon its washout (n = 8 DSM cells, N = 7 guinea pigs). The bars depict the actual mean membrane potential and SEM values for each experimental condition. The comparisons showed statistical significance of $^{***}P < 0.001$ and $^{*}P < 0.05$ for the specified conditions, ns, non-significant ($P > 0.05$). This figure is a reproduction from our previous *PLoS One* publication (Afeli et al., 2013) and used according to the publisher's copyright policy.

already underway in our laboratory — will reveal the specific details as to how K_V7 channel modulators, both pan- and subtype-selective, alter human DSM cell excitability.

Two other common animal models, rat and mouse, have not been comprehensively evaluated for the electrophysiological properties of DSM K_V7 channels. A patent application from Wyeth/Pfizer (Argentieri and Sheldon, 2006), revealed that in rat DSM cells, retigabine (1) enhanced voltage step- or ramp-induced K^+ currents by 2–3-fold as measured, and (2) hyperpolarized the membrane potential by ∼10 mV (Argentieri and Sheldon, 2006). Subsequent applications of XE991 in the presence of retigabine at least partially reversed the effects of retigabine on whole-cell currents and the cell membrane potential in rat DSM cells (Argentieri and Sheldon, 2006).

The role of K_V7 channels in mouse DSM cells has not been well studied. Currently, there are no publications using direct molecular biology approaches to detect K_V7 channel expression in mouse DSM, and the single available report using patch-clamp electrophysiology did not record K_V7 currents in mouse DSM cells, most likely due to the use of non-optimal conventional whole-cell patch-clamp recording protocols (Tykocki et al., 2019). The utilized protocol consisted of 500 ms duration depolarizing steps from −60 to +20 mV (10 mV increments with a 10 s pause between steps), but the holding potential was not specified although it appeared to be ≤−60 mV (Tykocki et al., 2019). The voltage-step induced K^+ currents that they recorded were reduced by XE991 (10 μM, at +20 mV from ∼ 6 to 3 pA/pF) but not affected by retigabine, although kinetic response time courses and washout effects were not reported (Tykocki et al., 2019). A possible confounding issue related to the interpretation of the pharmacological effects of XE991 in that study was that this compound also inhibits $K_V2.1$ and $K_V2.1/K_V9.3$ channel currents at 10–100 μM rather modestly (20–25%); in comparison, IC_{50} values of XE991 (0.6–5.5 μM) for K_V7 channel subtypes are much lower (Wang et al., 1998; Wladyka and Kunze, 2006; Zhong et al., 2010). $K_V2.1$ channels and currents have been reported in mouse DSM cells (Thorneloe and Nelson, 2003) and also in guinea pig and likely in human DSM cells (Hristov et al., 2012a,b). Of note, retigabine (0.3–3 μM) is known to effectively inhibit recombinant $K_V2.1$ channel currents (Stas et al., 2016) and, therefore, is expected to attenuate $K_V2.1$ channel currents in DSM cells. Furthermore, native SMC K_V7 channel currents are best studied using an optimized voltage protocol and the perforated patch-clamp method (Mani et al., 2011, 2013, 2016; Brueggemann et al., 2012b, 2014, 2018), which was not used in the Tykocki et al. (2019) study. The optimized K_V7 current recording protocol involves holding SMCs at a very depolarized membrane potential such as –4 mV and conducting voltage steps within a range of voltages from −70 mV up to ∼+20 mV for at least 1 s (1–5 s) and, importantly, in the presence of Gd^{3+}. Gd^{3+} blocks non-selective cation currents as well as L- and T-type Ca_V channels, while the highly depolarized membrane potential promotes inactivation of non-K_V7 channel currents (Mani et al., 2011). These specific conditions facilitate experimental isolation of native K_V7 channel currents. Indeed, native K_V7 channel currents in guinea pig DSM cells were previously recorded using this optimized protocol and in the presence of the BK channel blocker paxilline. These K_V7 currents were increased by the novel K_V7 channel activator ML213 (Provence et al., 2018). Tykocki et al. (2019) also reported that DSM cell membrane potentials (∼−45 mV on average and the majority of DSM cells ≤ −40 mV, up to ∼ −60 mV), recorded with the perforated patch-clamp approach, were not hyperpolarized by retigabine (Tykocki et al., 2019). Not surprisingly, whole-cell currents (conventional patch-clamp method) measured at −40 mV in a gap-free recording mode under elevated extracellular K^+ (E_K = −10 mM) were not affected by 10 μM retigabine (Tykocki et al., 2019). In contrast, in guinea pig DSM cells where the DSM cell membrane potential is more depolarized at ∼ −20 mV (perforated patch-clamp method), retigabine induced hyperpolarization (Afeli et al., 2013). Hence, the dissimilar effects of retigabine reported by Tykocki et al. (2019) may be related to specific experimental conditions, including the membrane potential level and voltage-protocol steps utilized, or to species differences. Tykocki et al. (2019) provided a caveat regarding mouse urinary bladder smooth muscle (UBSM) *"it is conceivable that K_V7 currents could be present and necessary for maintaining UBSM, but were undetectable using our patch-clamp parameters"* (Tykocki et al., 2019). Hence, future studies should address what may have been methodological issues and confirm the functional presence of K_V7 channels in mouse DSM cells using more precise patch-clamp protocols for recording native K_V7 channel currents.

Tykocki et al. (2019) also suggested that retigabine may cause partial inhibition of the L-type Ca_V channels in mouse DSM cells, consistent with prior findings (Mani et al., 2013; Rubi et al., 2017). At 10 μM, retigabine weakly attenuated the mouse DSM inward voltage-gated Ca_V current by ∼25% (from 8 to 6 pA/pF, evoked by the voltage step from −60 to +20 mV), while 60 mM KCl induced tonic contraction (primarily mediated via L-type Ca_V channel activation) by ∼20% (Tykocki et al., 2019). Similarly, recombinant peak L-type Ca_V channel currents (human $Ca_V1.2$ channels expressed in ts201 cells) were reduced ∼10 and ∼50% by 10 and 100 μM retigabine, respectively, while native L-type Ca_V currents in basal artery SMCs displayed a slightly higher sensitivity to 10 μM retigabine and showed ∼60% inhibition in the peak Ca_V channel current amplitude at +10 mV (Mani et al., 2013). In contrast to retigabine, the dihydropyridine L-type Ca_V channel blocker isradipine almost completely inhibited both the mouse DSM inward voltage step-induced Ca_V channel currents (from ∼−3.5 to −0.5 pA/pF, evoked by the step from −80 to +0 mV) and the 85 mM K^+ induced tonic contraction by >85% (Wegener et al., 2004). Similarly, in guinea pig DSM cells and DSM strips, nifedipine induced comparable near-complete inhibition of inward L-type Ca_V channel currents and 60 mM K^+ induced tonic contractions (Malysz et al., 2014; Provence et al., 2015). However, since comparative concentration-responses to retigabine attenuating DSM strip contractility under low (physiological; e.g., 5 or 20 mM) and elevated (e.g., 60 mM) extracellular K^+ were not yet studied in mouse DSM including by Tykocki et al. (2019) it remains unknown how the relatively minor inhibition on L-type Ca_V channels contributes to the overall effect of retigabine in mouse DSM. Hence, the conclusion that L-type Ca_V channel

blockade accounts solely for the effect of retigabine on mouse DSM requires validation and additional experimental evidence. In contrast, elevation of extracellular K^+ from 5 or 20 to 60 mM reduced retigabine-, ICA-069673-, and ML213-induced relaxation in rat or guinea pig DSM strips, consistent with a K^+ conductance underlying the effect of these K_V7 channel activators on DSM contractility (Argentieri and Sheldon, 2006; Rode et al., 2010; Provence et al., 2015). Given the potential confounding issues with retigabine and XE991 — especially their selectivity — systematic examinations of the effects of newer K_V7 channel modulators on DSM cells should reveal what role K_V7 channels play in the regulation of mouse DSM excitability. Such additional studies should also involve determinations of expression profiles of K_V7 channel subtypes in freshly isolated DSM cells (mRNA and protein), whole tissues, and afferent urinary bladder neurons, as these datasets are currently not well understood. Indeed, published findings by multiple groups have confirmed expressions and functional roles of K_V7 channels in guinea pig, rat, pig, and human DSM tissues and/or isolated DSM cells (Argentieri and Sheldon, 2006; Rode et al., 2010; Svalo et al., 2012, 2013, 2015; Afeli et al., 2013; Anderson et al., 2013; Provence et al., 2015, 2018; Bientinesi et al., 2017).

Electrophysiological Investigations of DSM Muscle Bundle/Tissue Strip Preparations

Pharmacological effects of K_V7 channel modulators have been examined with the conventional ("sharp") microelectrode electrophysiology in DSM muscle bundles/strips and muscularis mucosae smooth muscle (MMSM) preparations in the guinea pig urinary bladder. These two types of urinary bladder smooth muscle display similar types of electrical activity encompassing electrical quiescence as well as regular and irregular action potentials (Takagi and Hashitani, 2016; Lee et al., 2018). Flupirtine either completely abolished DSM action potentials or slowed their generation by decreasing frequency without any changes in the resting membrane potential attenuated or in action potential parameters (Takagi and Hashitani, 2016). On the other hand, XE991 induced membrane potential depolarization (∼4 mV) and this effect was associated with an increased action potential discharge (Takagi and Hashitani, 2016). In MMSM intact preparations, XE991 alone did not alter any of the action potential parameters or the resting membrane potential, although an increase of ∼30% in the number of spontaneous action potentials occurring during a burst of action potentials was observed (Lee et al., 2018). Flupirtine decreased the MMSM peak action potential amplitude by ∼25%, and the action potential after-hyperpolarization amplitude by ∼15%, without a significant change in resting membrane potential (Lee et al., 2018). These observations suggest a relatively higher contribution of K_V7 channels to the regulation of DSM excitability rather than of MMSM in guinea pigs, although in both types of urinary bladder smooth muscle, pharmacological modulators of K_V7 channels clearly affected the function.

In summary, evidence supports a role for K_V7 channels in regulating DSM excitability, but very few studies are currently available, thus additional systematic research efforts are warranted, especially on human DSM, and such systematic studies are currently underway in our laboratory.

K_V7 Channel Pharmacological Modulators Affect DSM Contractility and Intracellular Ca^{2+}

Studies of DSM Contractility in Experimental Animal Models

As of now, the guinea pig is the most thoroughly characterized species for determining the functional effects of K_V7 channel modulators, both activators and blockers, on DSM contractility. Our group and others have evaluated how diverse compounds acting on K_V7 channels affect spontaneous phasic, 20 mM KCl-induced, and electrical field stimulated (EFS)-induced contractions (**Tables 1**, **2**). K_V7 channel activators — including retigabine (pan-selective for $K_V7.2$–$K_V7.5$ channels), flupirtine (pan-selective for $K_V7.2$–$K_V7.5$ channels), L-364373 (active on $K_V7.1$ channels), ICA-069673 (selective for $K_V7.2/K_V7.3$ channels), ML213 (preferential selectivity for $K_V7.2$, $K_V7.2/K_V7.3$, and $K_V7.4$ channels), and meclofenamic acid (preferential activity on $K_V7.2/K_V7.3$ channels)—have shown inhibitory effects on guinea pig DSM contractions as summarized in **Table 1**. Conversely, K_V7 channel blockers — XE991 and linopirdine (both inhibitors of $K_V7.1$–$K_V7.5$ channels) and chromanol 293B (a $K_V7.1$ channel inhibitor) — enhanced DSM contractility as summarized in **Table 2**. Of critical importance are the findings of pretreatment of DSM tissue strips with an inhibitor such as XE991 on subsequent relaxation-inducing responses of K_V7 channel activators. Since K_V7 channel inhibition attenuated or prevented the subsequent effects of K_V7 channel activators, these findings substantiated that the underling pharmacological mechanism-of-action for the compounds involves K_V7 channels. Specifically, XE991 effectively attenuated both ICA-069673-induced and ML213-mediated inhibitions of DSM spontaneous phasic contractions (Provence et al., 2015, 2018). Collectively, to date all published pharmacological studies using diverse K_V7 channel modulators support a role of multiple K_V7 channel subtypes in the regulation of guinea pig DSM contractility.

The rat is the next most common animal species in which DSM K_V7 channels have been studied, but only three publications are currently available (Argentieri and Sheldon, 2006; Rode et al., 2010; Wang et al., 2014) and a single report on pig DSM (Svalo et al., 2013). In rat DSM, retigabine and ML213 effectively inhibited DSM spontaneous phasic, 20 mM KCl-induced phasic, or carbachol-potentiated phasic contractions (Argentieri and Sheldon, 2006; Rode et al., 2010; Wang et al., 2014). The elevation of extracellular K^+, which results in a reduction of the driving force for K^+, caused attenuation in retigabine-induced relaxation (Argentieri and Sheldon, 2006). This finding indicates that retigabine effects on DSM involve activation of K^+ channels. In contrast, the inhibitor XE991 displayed either no effect or a strong potentiation of DSM contractility (Rode et al., 2010; Wang et al., 2014). The reason for the differential experimental outcomes for XE991 remains to be resolved. In pig DSM, retigabine inhibited both EFS- and carbachol-induced

TABLE 1 | Effects of K_V7 channel activators on DSM contractility in various animal species and humans.

Activator	Species	Experimental DSM contraction protocol	Observation on DSM contractility	References
L-364373 ($K_V7.1$ channel activator)	Guinea pig	Spontaneous phasic	Inhibition of phasic contractions, effects on amplitude and muscle force, but weak changes in frequency and duration	Afeli et al., 2013
	Guinea pig	EFS-induced	Inhibition of EFS contractions, effects on amplitude and muscle force, but a weak change in the duration	Afeli et al., 2013
Retigabine ($K_V7.2$–$K_V7.5$ channel activator)	Guinea pig	Spontaneous phasic	Inhibition of phasic contractions, effects on amplitude, muscle force, frequency, and duration	Afeli et al., 2013
	Rat	Spontaneous phasic	Inhibition of phasic contractions, effects on amplitude and tension	Rode et al., 2010; Wang et al., 2014
	Rat	Carbachol-induced phasic	Inhibition of phasic contractions, effects on amplitude and tension	Rode et al., 2010
	Pig	Carbachol-induced phasic	Inhibition of phasic contractions, effects on amplitude and tension	Svalo et al., 2013
	Human	Carbachol-induced tonic	Inhibition of tonic contraction	Svalo et al., 2015
	Human	Bethanechol-induced tonic	Inhibition of tonic contraction	Bientinesi et al., 2017
	Rat	20 mM KCl-induced phasic	Inhibition of phasic contractions, effects on amplitude, tension, and frequency	Argentieri and Sheldon, 2006; Rode et al., 2010
	Human	20 mM KCl-induced phasic	Inhibition of tonic contraction	Svalo et al., 2015
	Guinea pig	EFS-induced	Inhibition of phasic contractions, effects on amplitude, muscle force, and duration	Afeli et al., 2013
	Rat	EFS-induced	Inhibition of EFS contractions, effects on amplitude and tension	Rode et al., 2010
	Pig	EFS-induced	Inhibition of EFS contractions (amplitude)	Svalo et al., 2013
Flupirtine ($K_V7.2$–$K_V7.5$ channel activator)	Guinea pig	Spontaneous phasic	Inhibition of phasic contractions, effects on amplitude and muscle force but not on frequency; also reduced muscle tone	Anderson et al., 2013
	Human	Bethanechol-induced tonic	Inhibition of tonic contraction	Bientinesi et al., 2017
Meclofenamic acid ($K_V7.2$/$K_V7.3$ channel activator)	Guinea pig	Spontaneous phasic	Inhibition of phasic contractions, effects on amplitude and muscle force but not on frequency; also reduced muscle tone	Anderson et al., 2013
ICA-069673 ($K_V7.2$/$K_V7.3$ channel activator)	Guinea pig	Spontaneous phasic	Inhibition of phasic contractions effects on amplitude, muscle force, frequency, and duration	Provence et al., 2015
	Guinea pig	Carbachol-induced phasic	Inhibition of phasic contractions, effects on amplitude, muscle force, duration, and frequency	Provence et al., 2015
	Guinea pig	20 mM KCl-induced phasic	Inhibition of phasic contractions, effects on amplitude, muscle force, duration, and frequency	Provence et al., 2015
	Guinea pig	EFS-induced	Inhibition of EFS contractions, effects on amplitude and muscle force	Provence et al., 2015
ML213 ($K_V7.2$, $K_V7.2$/$K_V7.3$, and $K_V7.4$ channel activator)	Guinea pig	Spontaneous phasic	Inhibition of contractions, effects on amplitude, muscle force, frequency, and duration	Provence et al., 2018
	Guinea pig	Carbachol-induced phasic	Inhibition of contractions, effects on amplitude, muscle force, duration, and frequency	Provence et al., 2018
	Pig	Carbachol-induced phasic	Inhibition of tonic contractions	Svalo et al., 2013
	Human	Carbachol-induced phasic	Inhibition of tonic contractions	Svalo et al., 2015
	Guinea pig	20 mM KCl-induced phasic	Inhibition of phasic contractions, effects on amplitude, muscle force, duration, and frequency	Provence et al., 2018
	Human	20 mM KCl-induced phasic	No effect on tonic contraction	Svalo et al., 2015
	Guinea pig	EFS-induced	Inhibition of EFS contraction, effects on amplitude and muscle force	Provence et al., 2018
ML277	Human	Carbachol-induced	Inhibition of tonic contractions	Svalo et al., 2015
($K_V7.1$ channel activator)	Human	20 mM KCl-induced	No effect on tonic contraction	Svalo et al., 2015
	Human	40 mM KCl-induced	Inhibition of tonic contraction	Svalo et al., 2015

TABLE 2 | Effects of K_V7 channel inhibitors on DSM contractions in various animal species and humans.

Inhibitor	Species	Experimental DSM Contraction Protocol	Observation on DSM contractility	References
XE991 ($K_V7.1$–$K_V7.5$ channel blocker)	Guinea pig	Spontaneous phasic	Enhancement of phasic contractions, effects on amplitude and muscle force but weak/unchanged on frequency and duration; also increase or no change in muscle tone	Afeli et al., 2013; Anderson et al., 2013
	Rat	Spontaneous phasic	No effect on contractions	Wang et al., 2014
	Rat	Spontaneous phasic	Enhancement of phasic contractions; effects on amplitude and tension	Rode et al., 2010
	Guinea pig	EFS-induced	Enhancement of EFS contractions, effects on amplitude and muscle force but weak/unchanged on duration; also increase in muscle tone	Afeli et al., 2013
	Rat	20 mM KCl-induced	Enhancement of phasic contractions, effects on amplitude, tension, and frequency	Rode et al., 2010
	Pig	20 mM KCl-induced	Enhancement of phasic contractions, effects on amplitude and tension	Svalo et al., 2013
	Rat	Carbachol-induced	No/weak effects on phasic contractions	Rode et al., 2010
	Pig	Carbachol-induced	No effect on phasic contractions	Svalo et al., 2013
	Pig	EFS-induced	No effect on EFS contractions	Svalo et al., 2013
	Human	Spontaneous tonic activity (lacking phasic contractions)	Enhancement of tonic contraction	Bientinesi et al., 2017
	Human	20 mM K^+-induced	Enhancement of tonic contraction	Svalo et al., 2015
	Human	40 mM K^+-induced	No effect on tonic contraction	Svalo et al., 2015
	Human	Carbachol-induced	No effect on tonic contraction	Svalo et al., 2015
Linopirdine ($K_V7.1$–$K_V7.5$ channel blocker)	Guinea pig	Spontaneous phasic	Enhancement of phasic contractions, effects on amplitude and muscle force but weak/unchanged on frequency and duration; also increase or no change in muscle tone	Afeli et al., 2013; Anderson et al., 2013
	Guinea pig	EFS-induced	Enhancement of EFS contractions, effects on amplitude and muscle force but weak/unchanged on duration; also increase in muscle tone	Afeli et al., 2013
Chromanol 293B ($K_V7.1$ channel blocker)	Guinea pig	Spontaneous phasic	Enhancement of phasic contractions, effects on amplitude and muscle force but weak/unchanged on frequency also no effect on muscle tone	Anderson et al., 2013
	Pig	20 mM KCl-induced	No effect on phasic contractions	Svalo et al., 2013
	Pig	EFS-induced	No effect on EFS contractions	Svalo et al., 2013
	Pig	Carbachol-induced	No effect on phasic contractions	Svalo et al., 2013

contractions only in the absence but not in the presence of XE991. XE991 alone enhanced 20 mM KCl-induced but not EFS-induced contractions; chromanol 293B was ineffective in altering either of these two types of stimulated contractions, indicating a negligible role of $K_V7.1$ channels in pig DSM (Svalo et al., 2013). In mouse DSM, the effects of retigabine and XE991 on isolated strip contractility have only been described, so far, under the condition of highly elevated extracellular K^+ (60 mM) and the resultant non-physiological tonic contraction (Tykocki et al., 2019). Since responses to K_V7 channel modulators have not yet been examined under conditions of physiological extracellular K^+ concentration (i.e., ∼5 mM K^+), the role of K_V7 channels in mouse DSM strip contractility remains to be determined. The limited number of publications on rat, pig, and mouse DSM seeking to determine pharmacological modulation of K_V7 channels provide inconsistent findings and this scientific controversy needs clarification. Given that these initial studies found substantial pharmacological modulatory effects on contractility with K_V7 channels in these animal models, additional studies of the effects of new and improved subtype-specific K_V7 channel modulators are highly warranted.

Initial Studies on Human DSM Contractility

The gap in the understanding of DSM K_V7 channels lies in the lack of systematic studies on human DSM contractility; such studies are already ongoing in our laboratory in collaboration with clinical urologists. Currently, there are only two publications with very limited data available on this topic (Svalo et al., 2015; Bientinesi et al., 2017). In an earlier study, retigabine inhibited DSM contractility that was enhanced by carbachol and K^+ (20 or 40 mM) (Svalo et al., 2015). ML213 also inhibited carbachol-potentiated but not KCl-enhanced DSM contractions (Svalo et al., 2015). The $K_V7.1$ channel activator ML277 displayed inhibitory effects on carbachol- and 20 mM KCl-induced contractions, but not on 40 mM KCl (Svalo et al., 2015). XE991 could only increase contractions potentiated by 20 mM K^+, but not by carbachol or 40 mM K^+ (Svalo et al., 2015). The specific experimental conditions

employed, hence, influenced the outcome of pharmacological experiments. The second study on human DSM showed that DSM strips exhibiting quiescence and lacking phasic contractions responded to increasing concentrations of XE991 with the development of step-wise enhanced tonic contractions (Bientinesi et al., 2017). While application of XE991 caused an appearance of DSM phasic contractions, they were very low in amplitude and therefore could not be reliably analyzed (Bientinesi et al., 2017). Further, retigabine and flupirtine attenuated muscarinic agonist (bethanechol)-potentiated DSM tonic contractions (phasic contractions were minimal under the stimulated condition) in a concentration-dependent manner (Bientinesi et al., 2017). The effects of flupirtine and retigabine were reduced in the presence of XE991 but not affected by either the Na_V channel inhibitor tetrodotoxin or the N-type Ca_V blocker ω-conotoxin GVIA. The lack of efficacy of tetrodotoxin as well as ω-conotoxin GVIA on retigabine- and flupirtine-induced DSM relaxations suggested that K_V7 channels expressed on DSM cells mediated the inhibitory effects of these two activators (Bientinesi et al., 2017). These two reports — while valuable, interesting, and providing some initial evidence for a role of K_V7 channels in regulating human DSM contractility — have multiple experimental limitations (Svalo et al., 2015; Bientinesi et al., 2017). The stimulated (e.g., carbachol and high KCl) and non-stimulated DSM contraction patterns recorded had all very low amplitudes, and the only experimental variable reliably quantified was average muscle tone. Other DSM phasic contraction parameters, especially amplitude, muscle force, duration, and frequency, were not quantified. Since these characteristics can be measured only for robust contractions (as previously reported by our group and others) on human DSM (Sibley, 1984; Darblade et al., 2006; Hristov et al., 2011, 2012a,c, 2013, 2016, 2017; Oger et al., 2011; Afeli et al., 2012; Soder et al., 2013; Xin et al., 2016), additional studies conducted under physiologically relevant experimental conditions are needed. The second limitation involves the absence of spontaneous phasic contractions under non-stimulated conditions (e.g., without elevated K^+ or cholinergic agonists). These DSM spontaneous contractions are attributed to the inherent intrinsic contractility of DSM cells; also, when excessive, they drive the development of DO (Brading et al., 1986; Turner and Brading, 1997; Andersson and Arner, 2004). The third limitation lies in the current lack of knowledge of how K_V7 channel modulators alter bladder contractility under pathophysiological conditions. Future and ongoing systematic studies on human DSM contractility — including those underway in our laboratory — that will overcome these limitations are needed to comprehensively validate K_V7 channel subtypes as critical regulators of human DSM contractility, and to identify them as potential therapeutic targets for urinary bladder dysfunction.

Pharmacological Effects of K_V7 Channel Modulators on DSM Intracellular Ca^{2+} Concentration

In DSM as in other types of smooth muscle preparations, intracellular Ca^{2+} regulates contractility (Andersson and Arner, 2004; Andersson and Wein, 2004). Thus, it is important to elucidate how K_V7 channel modulators affect intracellular Ca^{2+} concentrations in DSM cells. Currently, only studies on guinea pig DSM are available in the literature (Anderson et al., 2013; Provence et al., 2015, 2018). DSM muscle bundles displayed either coordinated whole bundle Ca^{2+} flashes or spontaneous Ca^{2+} transients and smaller localized Ca^{2+} events in individual DSM cells, detected using the Ca^{2+} fluorescence indicator Fluo-4AM (Anderson et al., 2013). The K_V7 channel blocker XE991 increased all three types of Ca^{2+} events in DSM cells (bundle Ca^{2+} flashes, individual whole-cell Ca^{2+} oscillations, and localized Ca^{2+} events) (Anderson et al., 2013). Although that particular study (Anderson et al., 2013) did not examine the effects of a K_V7 channel activator, two more recent studies by our group did (Provence et al., 2015, 2018). We found that intracellular Ca^{2+} concentration in DSM tissue and cells, imaged by Fura-2AM, was decreased following the application of two subtype-preferential K_V7 channel activators, ICA-069673 (Provence et al., 2015) and ML213 (Provence et al., 2018). Further, the study with the channel blocker ML213 showed that pretreatment of DSM with nifedipine, an L-type Ca_V channel blocker, prevented the decrease in intracellular Ca^{2+} concentration induced by the K_V7 channel activator (Provence et al., 2018). This finding provided experimental support that the K_V7 channel activator-induced decrease in intracellular Ca^{2+} concentrations mechanistically involves L-type Ca_V channels. Since the studies examining the effects of K_V7 channel modulators on intracellular Ca^{2+} concentration are limited only to the guinea pig and to a very few compounds tested, additional investigations are needed. These critical follow-up studies on DSM that are crucial in humans should also be examined in animals models including rat, mouse, and pig testing novel subtype-specific K_V7 channel modulators under highly optimized experimental imaging conditions (such as newer generation Ca^{2+} dyes, genetically encoded Ca^{2+} indicators selectively expressed in DSM cells, and high resolution, fast speed, whole-tissue microscopy). Our laboratory has already initiated systematic studies in this context.

DISCUSSION AND CLOSING REMARKS

In this comprehensive review, we have summarized the current knowledge of DSM K_V7 channels, highlighting expression profiles (mRNA and protein) in DSM whole-tissue and single cells and pharmacological effects of K_V7 channel modulators on DSM excitability (whole-cell patch-clamp and sharp microelectrode electrophysiology), intracellular Ca^{2+} concentrations (muscle bundle/tissue and DSM cells), and DSM contractility examined in various species (guinea pig, rat, mouse, pig, and human). Since humans are the target for therapeutic intervention, determining how K_V7 channels regulate human urinary bladder function at the cellular, tissue, organ, and whole-body levels is essential. However, our present understanding is rudimentary and limited to only a few studies. Although the initial clinical finding from epilepsy clinical trials identified urinary bladder retention as a retigabine use-associated side effect that has been further supported by animal *in vivo* and *in vitro* studies, the concept that K_V7 channels provide a potential

novel therapeutic target for overactive bladder remains to be adequately validated. Additional systematic studies on human DSM are needed to fill current critical gaps in knowledge to determine how K_V7 channels regulate urinary bladder function under normal and pathophysiological conditions. Our laboratory has already initiated systematic investigations in this area in collaboration with clinical urologists from multiple clinical settings in the US. These studies will validate the K_V7 channel as a viable therapeutic target for urinary bladder dysfunction.

Among the animal models examined, most studies of DSM K_V7 channels, until now, have been conducted primarily on guinea pigs, which have revealed expression of all K_V7 channel subtypes ($K_V7.1$–$K_V7.5$) and functional roles for K_V7 channel subtypes in determining DSM cell excitability, intracellular Ca^{2+} concentration, and tissue contractility. Guinea pig DSM, however, displays a differential K_V7 channel subtype expression profile compared to that of humans and rats. Further, *in vivo* urinary bladder functional assessments with K_V7 channel modulators in guinea pigs are lacking. The translational usefulness of the mouse model for DSM K_V7 channel studies has been questioned (Tykocki et al., 2019).

Therefore, the rat appears to be the best animal model for future studies of DSM K_V7 channels given the subtype expression similarity to human (whole-tissue level), the already demonstrated *in vivo* efficacy of K_V7 channel modulators on urinary bladder function, and initial DSM excitability and contractility outcomes. To fully validate the rat model, additional studies are needed on single DSM cells and tissues illustrating expression and functional roles of K_V7 channels, including supportive findings based on dysfunction in smooth muscle-specific K_V7 channel animal knock-out models.

While in this review we have focused on DSM, with an emphasis on K_V7 channel expression and its functional roles, K_V7 channels expressed on urinary bladder innervating neurons and fibers, in the spinal cord, and the brain, as well as non-DSM cells (e.g., interstitial cells) in the bladder can affect overall urinary bladder function. Indeed, some limited experimental evidence has been provided for K_V7 channels expressed in interstitial cells and dorsal root ganglia/sensory afferents (Anderson et al., 2009; Tykocki et al., 2019). These additional cell types provide other opportunities for future research endeavors on K_V7 channels in the urinary bladder.

In conclusion, the currently available experimental evidence strongly supports the functional expression and regulatory roles of K_V7 channels in DSM. The reported findings, however, are based on limited studies in humans and animal models, as summarized here. To advance our understanding of K_V7 channel subtypes in DSM and urinary bladder, additional dedicated research efforts on human DSM tissues and cells (obtained from patient donors exhibiting healthy/control and pathological urinary bladder phenotypes) as well as a translationally relevant animal model, such as the rat, are urgently needed. The already initiated systematic research investigations in collaboration with clinical urologists at our Urology Research Center, University of Tennessee, Memphis will reveal how DSM K_V7 channels impact urinary bladder function and whether they can be targeted for management of urinary bladder diseases.

AUTHOR CONTRIBUTIONS

JM prepared the initial draft, edited the content, and approved the final version. GP edited the initial draft and content, and approved the final version. Both the authors contributed to the article and approved the submitted version.

FUNDING

This study was supported by grants from the National Institutes of Health R01-DK106964 and P20-DK123971 and Van Fleet Endowment to GP.

ACKNOWLEDGMENTS

The authors thank Drs. Amanda Clarke, Viktor Yarotskyy, Daniel Collier, and Ms. Sarah E. Maxwell for their help and constructive criticism that significantly contributed to improving the scientific quality of this comprehensive review.

REFERENCES

Afeli, S. A., Malysz, J., and Petkov, G. V. (2013). Molecular expression and pharmacological evidence for a functional role of K_V7 channel subtypes in Guinea pig urinary bladder smooth muscle. *PLoS One* 8:e75875. doi: 10.1371/journal.pone.0075875

Afeli, S. A., Rovner, E. S., and Petkov, G. V. (2012). SK but not IK channels regulate human detrusor smooth muscle spontaneous and nerve-evoked contractions. *Am. J. Physiol. Renal Physiol.* 303, F559–F568.

Aizawa, N., Wakamatsu, D., Kida, J., Otsuki, T., Saito, Y., Matsuya, H., et al. (2017). Inhibitory effects of retigabine, a K_V7 channel activator, on mechanosensitive primary bladder afferent activities and nociceptive behaviors in rats. *Neurourol. Urodyn.* 36, 280–285. doi: 10.1002/nau.22920

Amato, G., Roeloffs, R., Rigdon, G. C., Antonio, B., Mersch, T., Mcnaughton-Smith, G., et al. (2011). N-Pyridyl and Pyrimidine Benzamides as KCNQ2/Q3 Potassium Channel Openers for the Treatment of Epilepsy. *ACS Med. Chem. Lett.* 2, 481–484. doi: 10.1021/ml200053x

Anderson, U. A., Carson, C., Johnston, L., Joshi, S., Gurney, A. M., and Mccloskey, K. D. (2013). Functional expression of KCNQ (K_V7) channels in guinea pig bladder smooth muscle and their contribution to spontaneous activity. *Br. J. Pharmacol.* 169, 1290–1304. doi: 10.1111/bph.12210

Anderson, U. A., Carson, C., and Mccloskey, K. D. (2009). KCNQ currents and their contribution to resting membrane potential and the excitability of interstitial cells of Cajal from the guinea pig bladder. *J. Urol.* 182, 330–336. doi: 10.1016/j.juro.2009.02.108

Andersson, K. E., and Arner, A. (2004). Urinary bladder contraction and relaxation: physiology and pathophysiology. *Physiol. Rev.* 84, 935–986. doi: 10.1152/physrev.00038.2003

Andersson, K. E., and Wein, A. J. (2004). Pharmacology of the lower urinary tract: basis for current and future treatments of urinary incontinence. *Pharmacol. Rev.* 56, 581–631. doi: 10.1124/pr.56.4.4

Argentieri, T. M., and Sheldon, J. H. (2006). *Methods of Selecting Compounds for Modulation of Bladder Function*. US2006/0252201A1. Madison, NJ: Wyeth.

Barhanin, J., Lesage, F., Guillemare, E., Fink, M., Lazdunski, M., and Romey, G. (1996). K_VLQT1 and lsK (minK) proteins associate to form the I_{Ks} cardiac potassium current. *Nature* 384, 78–80. doi: 10.1038/384078a0

Barrese, V., Miceli, F., Soldovieri, M. V., Ambrosino, P., Iannotti, F. A., Cilio, M. R., et al. (2010). Neuronal potassium channel openers in the management of epilepsy: role and potential of retigabine. *Clin. Pharmacol.* 2, 225–236.

Barrese, V., Stott, J. B., Figueiredo, H. B., Aubdool, A. A., Hobbs, A. J., Jepps, T. A., et al. (2018a). Angiotensin II Promotes K_V7.4 channels degradation through reduced interaction with HSP90 (heat shock protein 90). *Hypertension* 71, 1091–1100. doi: 10.1161/hypertensionaha.118.11116

Barrese, V., Stott, J. B., and Greenwood, I. A. (2018b). KCNQ-encoded potassium channels as therapeutic targets. *Annu. Rev. Pharmacol. Toxicol.* 58, 625–648. doi: 10.1146/annurev-pharmtox-010617-052912

Bientinesi, R., Mancuso, C., Martire, M., Bassi, P. F., Sacco, E., and Curro, D. (2017). K_V7 channels in the human detrusor: channel modulator effects and gene and protein expression. *Naunyn Schmiedebergs Arch. Pharmacol.* 390, 127–137. doi: 10.1007/s00210-016-1312-9

Brading, A. F., and Brain, K. L. (2011). "Ion channel modulators and urinary tract function," in *Part of Handbook of Experimental Pharmacology book series*, eds K. E. Andersson and M. C. Michel (Berlin: Springer-Verlag), 375–393. doi: 10.1007/978-3-642-16499-6_18

Brading, A. F., Mostwin, J. L., Sibley, G. N., and Speakman, M. J. (1986). The role of smooth muscle and its possible involvement in diseases of the lower urinary tract. *Clin. Sci.* 70(Suppl. 14), 7s–13s. doi: 10.1042/cs070s007

Brickel, N., Gandhi, P., Vanlandingham, K., Hammond, J., and Derossett, S. (2012). The urinary safety profile and secondary renal effects of retigabine (ezogabine): a first-in-class antiepileptic drug that targets KCNQ (K_V7) potassium channels. *Epilepsia* 53, 606–612. doi: 10.1111/j.1528-1167.2012.03441.x

Brown, D. A., and Passmore, G. M. (2009). Neural KCNQ (K_V7) channels. *Br. J. Pharmacol.* 156, 1185–1195. doi: 10.1111/j.1476-5381.2009.00111.x

Brueggemann, L. I., Cribbs, L. L., Schwartz, J., Wang, M., Kouta, A., and Byron, K. L. (2018). Mechanisms of PKA-dependent potentiation of K_V7.5 channel activity in human airway smooth muscle cells. *Int. J. Mol. Sci.* 19:2223. doi: 10.3390/ijms19082223

Brueggemann, L. I., Haick, J. M., Cribbs, L. L., and Byron, K. L. (2014). Differential activation of vascular smooth muscle K_V7.4, K_V7.5, and K_V7.4/7.5 channels by ML213 and ICA-069673. *Mol. Pharmacol.* 86, 330–341. doi: 10.1124/mol.114.093799

Brueggemann, L. I., Kakad, P. P., Love, R. B., Solway, J., Dowell, M. L., Cribbs, L. L., et al. (2012a). K_V7 potassium channels in airway smooth muscle cells: signal transduction intermediates and pharmacological targets for bronchodilator therapy. *Am. J. Physiol. Lung. Cell Mol. Physiol.* 302, L120–L132.

Brueggemann, L. I., Mani, B. K., Haick, J., and Byron, K. L. (2012b). Exploring arterial smooth muscle K_V7 potassium channel function using patch clamp electrophysiology and pressure myography. *J. Vis. Exp.* 67:e4263.

Byron, K. L., and Brueggemann, L. I. (2018). K_V7 potassium channels as signal transduction intermediates in the control of microvascular tone. *Microcirculation* 25:e12419. doi: 10.1111/micc.12419

Chadha, P. S., Jepps, T. A., Carr, G., Stott, J. B., Zhu, H. L., Cole, W. C., et al. (2014). Contribution of K_V7.4/K_V7.5 heteromers to intrinsic and calcitonin gene-related peptide-induced cerebral reactivity. *Arterioscler. Thromb. Vasc. Biol.* 34, 887–893. doi: 10.1161/atvbaha.114.303405

Dalghi, M. G., Montalbetti, N., Carattino, M. D., and Apodaca, G. (2020). The urothelium: life in a liquid environment. *Physiol. Rev.* 100, 1621–1705. doi: 10.1152/physrev.00041.2019 [Epub ahead of print].

Darblade, B., Behr-Roussel, D., Oger, S., Hieble, J. P., Lebret, T., Gorny, D., et al. (2006). Effects of potassium channel modulators on human detrusor smooth muscle myogenic phasic contractile activity: potential therapeutic targets for overactive bladder. *Urology* 68, 442–448. doi: 10.1016/j.urology.2006.03.039

de Groat, W. C., Griffiths, D., and Yoshimura, N. (2015). Neural control of the lower urinary tract. *Compr. Physiol.* 5, 327–396.

Devulder, J. (2010). Flupirtine in pain management: pharmacological properties and clinical use. *CNS Drugs* 24, 867–881. doi: 10.2165/11536230-000000000-00000

Evseev, A. I., Semenov, I., Archer, C. R., Medina, J. L., Dube, P. H., Shapiro, M. S., et al. (2013). Functional effects of KCNQ K^+ channels in airway smooth muscle. *Front. Physiol.* 4:277. doi: 10.3389/fphys.2013.00277

Fry, C. H., and McCloskey, K. D. (2019). Spontaneous activity and the urinary bladder. *Adv. Exp. Med. Biol.* 1124, 121–147. doi: 10.1007/978-981-13-5895-1_5

Hristov, K. L., Afeli, S. A., Parajuli, S. P., Cheng, Q., Rovner, E. S., and Petkov, G. V. (2013). Neurogenic detrusor overactivity is associated with decreased expression and function of the large conductance voltage- and Ca^{2+}-activated K^+ channels. *PLoS One* 8:e68052. doi: 10.1371/journal.pone.0068052

Hristov, K. L., Chen, M., Afeli, S. A., Cheng, Q., Rovner, E. S., and Petkov, G. V. (2012a). Expression and function of K_V2-containing channels in human urinary bladder smooth muscle. *Am. J. Physiol. Cell Physiol.* 302, C1599–C1608.

Hristov, K. L., Chen, M., Kellett, W. F., Rovner, E. S., and Petkov, G. V. (2011). Large conductance voltage- and Ca^{2+}-activated K^+ channels regulate human detrusor smooth muscle function. *Am. J. Physiol. Cell Physiol.* 301, C903–C912.

Hristov, K. L., Chen, M., Soder, R. P., Parajuli, S. P., Cheng, Q., Kellett, W. F., et al. (2012b). K_V2.1 and electrically silent K_V channel subunits control excitability and contractility of guinea pig detrusor smooth muscle. *Am. J. Physiol. Cell. Physiol.* 302, C360–C372.

Hristov, K. L., Parajuli, S. P., Provence, A., Rovner, E. S., and Petkov, G. V. (2017). Nongenomic modulation of the large conductance voltage- and Ca^{2+}-activated K^+ channels by estrogen: a novel regulatory mechanism in human detrusor smooth muscle. *Physiol. Rep.* 5:e13351. doi: 10.14814/phy2.13351

Hristov, K. L., Parajuli, S. P., Soder, R. P., Cheng, Q., Rovner, E. S., and Petkov, G. V. (2012c). Suppression of human detrusor smooth muscle excitability and contractility via pharmacological activation of large conductance Ca^{2+}-activated K^+ channels. *Am. J. Physiol. Cell Physiol.* 302, C1632–C1641.

Hristov, K. L., Smith, A. C., Parajuli, S. P., Malysz, J., Rovner, E. S., and Petkov, G. V. (2016). Novel regulatory mechanism in human urinary bladder: central role of transient receptor potential melastatin 4 channels in detrusor smooth muscle function. *Am. J. Physiol. Cell Physiol.* 310, C600–C611.

Ipavec, V., Martire, M., Barrese, V., Taglialatela, M., and Curro, D. (2011). K_V7 channels regulate muscle tone and nonadrenergic noncholinergic relaxation of the rat gastric fundus. *Pharmacol. Res.* 64, 397–409. doi: 10.1016/j.phrs.2011.06.016

Jepps, T. A., Greenwood, I. A., Moffatt, J. D., Sanders, K. M., and Ohya, S. (2009). Molecular and functional characterization of K_V7 K^+ channel in murine gastrointestinal smooth muscles. *Am. J. Physiol. Gastrointest. Liver Physiol.* 297, G107–G115.

Jepps, T. A., Olesen, S. P., Greenwood, I. A., and Dalsgaard, T. (2016). Molecular and functional characterization of K_V7 channels in penile arteries and corpus cavernosum of healthy and metabolic syndrome rats. *Br. J. Pharmacol.* 173, 1478–1490. doi: 10.1111/bph.13444

Lee, K., Isogai, A., Antoh, M., Kajioka, S., Eto, M., and Hashitani, H. (2018). Role of K^+ channels in regulating spontaneous activity in the muscularis mucosae of guinea pig bladder. *Eur. J. Pharmacol.* 818, 30–37. doi: 10.1016/j.ejphar.2017.10.024

Lerche, C., Seebohm, G., Wagner, C. I., Scherer, C. R., Dehmelt, L., Abitbol, I., et al. (2000). Molecular impact of MinK on the enantiospecific block of I_{Ks} by chromanols. *Br. J. Pharmacol.* 131, 1503–1506. doi: 10.1038/sj.bjp.0703734

Liu, R., Tzounopoulos, T., and Wipf, P. (2019). Synthesis and optimization of K_V7 (KCNQ) potassium channel agonists: the role of fluorines in potency and selectivity. *ACS Med. Chem. Lett.* 10, 929–935. doi: 10.1021/acsmedchemlett.9b00097

Mackie, A. R., Brueggemann, L. I., Henderson, K. K., Shiels, A. J., Cribbs, L. L., Scrogin, K. E., et al. (2008). Vascular KCNQ potassium channels as novel targets for the control of mesenteric artery constriction by vasopressin, based on studies in single cells, pressurized arteries, and in vivo measurements of mesenteric vascular resistance. *J. Pharmacol. Exp. Ther.* 325, 475–483. doi: 10.1124/jpet.107.135764

Mackie, A. R., and Byron, K. L. (2008). Cardiovascular KCNQ (K_V7) potassium channels: physiological regulators and new targets for therapeutic intervention. *Mol. Pharmacol* 74, 1171–1179. doi: 10.1124/mol.108.049825

Malysz, J., Afeli, S. A., Provence, A., and Petkov, G. V. (2014). Ethanol-mediated relaxation of guinea pig urinary bladder smooth muscle: involvement of BK and L-type Ca^{2+} channels. *Am. J. Physiol. Cell Physiol.* 306, C45–C58.

Malysz, J., and Petkov, G. V. (2020). Urinary bladder smooth muscle ion channels: expression, function, and regulation in health and disease. *Am. J. Physiol. Renal Physiol.* 319, F257–F283. doi: 10.1152/ajprenal.00048.02020

Malysz, J., Rovner, E. S., Wake, R., and Petkov, G. V. (2020). Preparation and utilization of freshly isolated human detrusor smooth muscle cells for characterization of 9-phenanthrol-sensitive cation currents. *J. Vis. Exp.* 155:59884.

Mani, B. K., Brueggemann, L. I., Cribbs, L. L., and Byron, K. L. (2011). Activation of vascular KCNQ (K_V7) potassium channels reverses spasmogen-induced constrictor responses in rat basilar artery. *Br. J. Pharmacol.* 164, 237–249. doi: 10.1111/j.1476-5381.2011.01273.x

Mani, B. K., O'dowd, J., Kumar, L., Brueggemann, L. I., Ross, M., and Byron, K. L. (2013). Vascular KCNQ (K_V7) potassium channels as common signaling intermediates and therapeutic targets in cerebral vasospasm. *J. Cardiovasc. Pharmacol.* 61, 51–62. doi: 10.1097/fjc.0b013e3182771708

Mani, B. K., Robakowski, C., Brueggemann, L. I., Cribbs, L. L., Tripathi, A., Majetschak, M., et al. (2016). $K_V7.5$ potassium channel subunits are the primary targets for PKA-dependent enhancement of vascular smooth muscle K_V7 currents. *Mol. Pharmacol.* 89, 323–334. doi: 10.1124/mol.115.101758

McCallum, L. A., Greenwood, I. A., and Tribe, R. M. (2009). Expression and function of K_V7 channels in murine myometrium throughout oestrous cycle. *Pflugers Arch.* 457, 1111–1120. doi: 10.1007/s00424-008-0567-5

McCallum, L. A., Pierce, S. L., England, S. K., Greenwood, I. A., and Tribe, R. M. (2011). The contribution of K_V7 channels to pregnant mouse and human myometrial contractility. *J. Cell Mol. Med.* 15, 577–586. doi: 10.1111/j.1582-4934.2010.01021.x

Miceli, F., Soldovieri, M. V., Ambrosino, P., Manocchio, L., Mosca, I., and Taglialatela, M. (2018). Pharmacological targeting of neuronal $K_V7.2/3$ channels: a focus on chemotypes and receptor sites. *Curr. Med. Chem.* 25, 2637–2660. doi: 10.2174/0929867324666171012122852

Miceli, F., Soldovieri, M. V., Iannotti, F. A., Barrese, V., Ambrosino, P., Martire, M., et al. (2011). The voltage-sensing domain of $K_V7.2$ channels as a molecular target for epilepsy-causing mutations and anticonvulsants. *Front. Pharmacol.* 2:2. doi: 10.3389/fphar.2011.00002

Miceli, F., Soldovieri, M. V., Martire, M., and Taglialatela, M. (2008). Molecular pharmacology and therapeutic potential of neuronal K_V7-modulating drugs. *Curr. Opin. Pharmacol.* 8, 65–74. doi: 10.1016/j.coph.2007.10.003

Michel, M. C., Radziszewski, P., Falconer, C., Marschall-Kehrel, D., and Blot, K. (2012). Unexpected frequent hepatotoxicity of a prescription drug, flupirtine, marketed for about 30 years. *Br. J. Clin. Pharmacol.* 73, 821–825. doi: 10.1111/j.1365-2125.2011.04138.x

Nappi, P., Miceli, F., Soldovieri, M. V., Ambrosino, P., Barrese, V., and Taglialatela, M. (2020). Epileptic channelopathies caused by neuronal K_V7 (KCNQ) channel dysfunction. *Pflugers Arch.* 47, 881–898. doi: 10.1007/s00424-020-02404-2

Ng, F. L., Davis, A. J., Jepps, T. A., Harhun, M. I., Yeung, S. Y., Wan, A., et al. (2011). Expression and function of the K^+ channel KCNQ genes in human arteries. *Br. J. Pharmacol.* 162, 42–53. doi: 10.1111/j.1476-5381.2010.01027.x

Oger, S., Behr-Roussel, D., Gorny, D., Bernabe, J., Comperat, E., Chartier-Kastler, E., et al. (2011). Effects of potassium channel modulators on myogenic spontaneous phasic contractile activity in human detrusor from neurogenic patients. *BJU Int.* 108, 604–611. doi: 10.1111/j.1464-410x.2010.09935.x

Ostacolo, C., Miceli, F., Di Sarno, V., Nappi, P., Iraci, N., Soldovieri, M. V., et al. (2020). Synthesis and pharmacological characterization of conformationally restricted retigabine analogues as novel neuronal K_V7 channel activators. *J. Med. Chem.* 63, 163–185. doi: 10.1021/acs.jmedchem.9b00796

Osuma, A. T., Xu, X., Wang, Z., Van Camp, J. A., and Freiberg, G. M. (2019). Design and evaluation of pyrazolopyrimidines as KCNQ channel modulators. *Bioorg. Med. Chem. Lett.* 29:126603. doi: 10.1016/j.bmcl.2019.08.007

Petkov, G. V. (2009). "Ion channels," in *Pharmacology: Principles and Practice*, eds M. Hader, W. S. Messer, and K. A. Bachmann (Cambridge, MA: Academic Press), 387–427.

Petkov, G. V. (2012). Role of potassium ion channels in detrusor smooth muscle function and dysfunction. *Nat. Rev. Urol.* 9, 30–40. doi: 10.1038/nrurol.2011.194

Provence, A., Angoli, D., and Petkov, G. V. (2018). K_V7 channel pharmacological activation by the novel activator ML213: role for heteromeric $K_V7.4/K_V7.5$ channels in guinea pig detrusor smooth muscle function. *J. Pharmacol. Exp. Ther.* 364, 131–144. doi: 10.1124/jpet.117.243162

Provence, A., Malysz, J., and Petkov, G. V. (2015). The novel $K_V7.2/K_V7.3$ channel opener ICA-069673 reveals subtype-specific functional roles in guinea pig detrusor smooth muscle excitability and contractility. *J. Pharmacol. Exp. Ther.* 354, 290–301. doi: 10.1124/jpet.115.225268

Rode, F., Svalo, J., Sheykhzade, M., and Ronn, L. C. (2010). Functional effects of the KCNQ modulators retigabine and XE991 in the rat urinary bladder. *Eur. J. Pharmacol.* 638, 121–127. doi: 10.1016/j.ejphar.2010.03.050

Rubi, L., Kovar, M., Zebedin-Brandl, E., Koenig, X., Dominguez-Rodriguez, M., Todt, H., et al. (2017). Modulation of the heart's electrical properties by the anticonvulsant drug retigabine. *Toxicol. Appl. Pharmacol.* 329, 309–317. doi: 10.1016/j.taap.2017.06.018

Schenzer, A., Friedrich, T., Pusch, M., Saftig, P., Jentsch, T. J., Grotzinger, J., et al. (2005). Molecular determinants of KCNQ (K_V7) K^+ channel sensitivity to the anticonvulsant retigabine. *J. Neurosci.* 25, 5051–5060. doi: 10.1523/jneurosci.0128-05.2005

Seefeld, M. A., Lin, H., Holenz, J., Downie, D., Donovan, B., Fu, T., et al. (2018). Novel K_V7 ion channel openers for the treatment of epilepsy and implications for detrusor tissue contraction. *Bioorg. Med. Chem. Lett.* 28, 3793–3797. doi: 10.1016/j.bmcl.2018.09.036

Sibley, G. N. (1984). A comparison of spontaneous and nerve-mediated activity in bladder muscle from man, pig and rabbit. *J. Physiol.* 354, 431–443. doi: 10.1113/jphysiol.1984.sp015386

Soder, R. P., Parajuli, S. P., Hristov, K. L., Rovner, E. S., and Petkov, G. V. (2013). SK channel-selective opening by SKA-31 induces hyperpolarization and decreases contractility in human urinary bladder smooth muscle. *Am. J. Physiol. Regul. Integr. Comp. Physiol.* 304, R155–R163.

Splinter, M. Y. (2013). Efficacy of retigabine in adjunctive treatment of partial onset seizures in adults. *J. Cent. Nerv. Syst. Dis.* 5, 31–41.

Stas, J. I., Bocksteins, E., Jensen, C. S., Schmitt, N., and Snyders, D. J. (2016). The anticonvulsant retigabine suppresses neuronal K_V2-mediated currents. *Sci. Rep.* 6:35080.

Stott, J. B., Barrese, V., Suresh, M., Masoodi, S., and Greenwood, I. A. (2018). Investigating the role of G protein betagamma in K_V7-dependent relaxations of the rat vasculature. *Arterioscler. Thromb. Vasc. Biol.* 38, 2091–2102. doi: 10.1161/atvbaha.118.311360

Stott, J. B., Jepps, T. A., and Greenwood, I. A. (2014). K_V7 potassium channels: a new therapeutic target in smooth muscle disorders. *Drug Discov. Today* 19, 413–424. doi: 10.1016/j.drudis.2013.12.003

Streng, T., Christoph, T., and Andersson, K. E. (2004). Urodynamic effects of the K^+ channel (KCNQ) opener retigabine in freely moving, conscious rats. *J. Urol.* 172, 2054–2058. doi: 10.1097/01.ju.0000138155.33749.f4

Svalo, J., Bille, M., Parameswaran Theepakaran, N., Sheykhzade, M., Nordling, J., and Bouchelouche, P. (2013). Bladder contractility is modulated by K_V7 channels in pig detrusor. *Eur. J. Pharmacol.* 715, 312–320. doi: 10.1016/j.ejphar.2013.05.005

Svalo, J., Hansen, H. H., Ronn, L. C., Sheykhzade, M., Munro, G., and Rode, F. (2012). K_V7 positive modulators reduce detrusor overactivity and increase bladder capacity in rats. *Basic Clin. Pharmacol. Toxicol.* 110, 145–153. doi: 10.1111/j.1742-7843.2011.00765.x

Svalo, J., Sheykhzade, M., Nordling, J., Matras, C., and Bouchelouche, P. (2015). Functional and molecular evidence for K_V7 channel subtypes in human detrusor from patients with and without bladder outflow obstruction. *PLoS One* 10:e0117350. doi: 10.1371/journal.pone.0117350

Takagi, H., and Hashitani, H. (2016). Effects of K^+ channel openers on spontaneous action potentials in detrusor smooth muscle of the guinea-pig urinary bladder. *Eur. J. Pharmacol.* 789, 179–186. doi: 10.1016/j.ejphar.2016.07.041

Tatulian, L., and Brown, D. A. (2003). Effect of the KCNQ potassium channel opener retigabine on single KCNQ2/3 channels expressed in CHO cells. *J. Physiol.* 549, 57–63. doi: 10.1113/jphysiol.2003.039842

Tatulian, L., Delmas, P., Abogadie, F. C., and Brown, D. A. (2001). Activation of expressed KCNQ potassium currents and native neuronal M-type potassium currents by the anti-convulsant drug retigabine. *J. Neurosci.* 21, 5535–5545. doi: 10.1523/jneurosci.21-15-05535.2001

Thorneloe, K. S., and Nelson, M. T. (2003). Properties and molecular basis of the mouse urinary bladder voltage-gated K^+ current. *J. Physiol.* 549, 65–74. doi: 10.1113/jphysiol.2003.039859

Turner, W. H., and Brading, A. F. (1997). Smooth muscle of the bladder in the normal and the diseased state: pathophysiology, diagnosis and treatment. *Pharmacol. Ther.* 75, 77–110. doi: 10.1016/s0163-7258(97)00038-7

Tykocki, N. R., Heppner, T. J., Dalsgaard, T., Bonev, A. D., and Nelson, M. T. (2019). The K_V7 channel activator retigabine suppresses mouse urinary bladder afferent nerve activity without affecting detrusor smooth muscle K^+ channel currents. *J. Physiol.* 597, 935–950. doi: 10.1113/jp277021

Wang, H. S., Pan, Z., Shi, W., Brown, B. S., Wymore, R. S., Cohen, I. S., et al. (1998). KCNQ2 and KCNQ3 potassium channel subunits: molecular correlates of the M-channel. *Science* 282, 1890–1893. doi: 10.1126/science.282.5395.1890

Wang, Y., Tar, M. T., Fu, S., Melman, A., and Davies, K. P. (2014). Diabetes attenuates urothelial modulation of detrusor contractility and spontaneous activity. *Int. J. Urol.* 21, 1059–1064. doi: 10.1111/iju.12491

Wegener, J. W., Schulla, V., Lee, T. S., Koller, A., Feil, S., Feil, R., et al. (2004). An essential role of $Ca_V1.2$ L-type calcium channel for urinary bladder function. *FASEB J.* 18, 1159–1161. doi: 10.1096/fj.04-1516fje

Wickenden, A. D., Yu, W., Zou, A., Jegla, T., and Wagoner, P. K. (2000). Retigabine, a novel anti-convulsant, enhances activation of KCNQ2/Q3 potassium channels. *Mol. Pharmacol.* 58, 591–600. doi: 10.1124/mol.58.3.591

Wladyka, C. L., and Kunze, D. L. (2006). KCNQ/M-currents contribute to the resting membrane potential in rat visceral sensory neurons. *J. Physiol.* 575, 175–189. doi: 10.1113/jphysiol.2006.113308

Xin, W., Li, N., Fernandes, V. S., Chen, B., Rovner, E. S., and Petkov, G. V. (2016). BK channel regulation by phosphodiesterase type 1: a novel signaling pathway controlling human detrusor smooth muscle function. *Am. J. Physiol. Renal Physiol.* 310, F994–F999.

Yeung, S., Schwake, M., Pucovsky, V., and Greenwood, I. (2008). Bimodal effects of the K_V7 channel activator retigabine on vascular K^+ currents. *Br. J. Pharmacol.* 155, 62–72. doi: 10.1038/bjp.2008.231

Yeung, S. Y., and Greenwood, I. A. (2005). Electrophysiological and functional effects of the KCNQ channel blocker XE991 on murine portal vein smooth muscle cells. *Br. J. Pharmacol.* 146, 585–595. doi: 10.1038/sj.bjp.0706342

Yu, H., Wu, M., Hopkins, C., Engers, J., Townsend, S., Lindsley, C., et al. (2010). *A Small Molecule Activator of KCNQ2 and KCNQ4 Channels*. Bethesda, MD: NIH Molecular Libraries Program.

Yu, H., Wu, M., Townsend, S. D., Zou, B., Long, S., Daniels, J. S., et al. (2011). Discovery, synthesis, and structure activity relationship of a series of N-aryl-bicyclo[2.2.1]heptane-2-carboxamides: Characterization of ML213 as a novel KCNQ2 and KCNQ4 potassium channel opener. *ACS Chem. Neurosci.* 2, 572–577. doi: 10.1021/cn200065b

Zavaritskaya, O., Dudem, S., Ma, D., Rabab, K. E., Albrecht, S., Tsvetkov, D., et al. (2020). Vasodilation of rat skeletal muscle arteries by the novel BK channel opener GoSlo is mediated by the simultaneous activation of BK and K_V7 channels. *Br. J. Pharmacol.* 177, 1164–1186. doi: 10.1111/bph.14910

Zhang, F., Liu, Y., Tang, F., Liang, B., Chen, H., Zhang, H., et al. (2019). Electrophysiological and pharmacological characterization of a novel and potent neuronal K_V7 channel opener SCR2682 for antiepilepsy. *FASEB J.* 33, 9154–9166. doi: 10.1096/fj.201802848rr

Zhong, X. Z., Harhun, M. I., Olesen, S. P., Ohya, S., Moffatt, J. D., Cole, W. C., et al. (2010). Participation of KCNQ (K_V7) potassium channels in myogenic control of cerebral arterial diameter. *J. Physiol.* 588, 3277–3293. doi: 10.1113/jphysiol.2010.192823

Conflict of Interest: The authors declare that the research was conducted in the absence of any commercial or financial relationships that could be construed as a potential conflict of interest.

frontiers in Physiology

MINI REVIEW
published: 18 September 2020
doi: 10.3389/fphys.2020.568667

The Role of K_v7 Channels in Neural Plasticity and Behavior

*Brian C. Baculis[1], Jiaren Zhang[2] and Hee Jung Chung[1,2]**

[1]Neuroscience Program, University of Illinois at Urbana-Champaign, Urbana, IL, United States, [2]Department of Molecular Integrative Physiology, University of Illinois at Urbana-Champaign, Urbana, IL, United States

Activity-dependent persistent changes in neuronal intrinsic excitability and synaptic strength are widely thought to underlie learning and memory. Voltage-gated KCNQ/K_v7 potassium channels have been of great interest as the potential targets for memory disorders due to the beneficial effects of their antagonists in cognition. Importantly, *de novo* dominant mutations in their neuronal subunits *KCNQ2*/$K_v7.2$ and *KCNQ3*/$K_v7.3$ are associated with epilepsy and neurodevelopmental disorder characterized by developmental delay and intellectual disability. The role of K_v7 channels in neuronal excitability and epilepsy has been extensively studied. However, their functional significance in neural plasticity, learning, and memory remains largely unknown. Here, we review recent studies that support the emerging roles of K_v7 channels in intrinsic and synaptic plasticity, and their contributions to cognition and behavior.

Keywords: KCNQ channel, K_v7, intrinsic excitability, synaptic transmission, neural plasticity, learning, memory, behavior

OPEN ACCESS

Edited by:
Francesco Miceli,
University of Naples Federico II, Italy

Reviewed by:
Hailin Zhang,
Hebei Medical University, China
Yang Li,
Shanghai Institute of Materia Medica (CAS), China

****Correspondence:***
Hee Jung Chung
chunghj@illinois.edu

Specialty section:
This article was submitted to Membrane Physiology and Membrane Biophysics, a section of the journal Frontiers in Physiology

Received: *01 June 2020*
Accepted: *28 August 2020*
Published: *18 September 2020*

Citation:
Baculis BC, Zhang J and Chung HJ (2020) The Role of K_v7 Channels in Neural Plasticity and Behavior. Front. Physiol. 11:568667. doi: 10.3389/fphys.2020.568667

INTRODUCTION

Voltage-gate channel potassium (K^+) subfamily Q member 1–5 (*KCNQ* 1–5) encodes $K_v7.1$–$K_v7.5$ channels (Gutman et al., 2005) that are critical regulators of excitability in neurons, muscles, and sensory cells (Soldovieri et al., 2011). All K_v7 subunits have six transmembrane segments (S1–S6; Robbins, 2001). The S1–S4 comprise a voltage-sensing domain with the S4 being the main voltage-sensor (Robbins, 2001). The pore domain consists of the S5-S6 flanking the pore loop important for K^+ ion selectivity (Sun and MacKinnon, 2017). The gate is formed by the intersection of four S6 segments (Cui, 2016; Sun and MacKinnon, 2017). Upon depolarization, the electric field on the basic residues of S4 promotes its translational rotation and outward displacement, which leads to the opening of the gate (Cui, 2016; Sun and MacKinnon, 2017). All K_v7 channels require phosphatidylinositol-4,5-bisphosphate (PIP_2) in the plasma membrane for channel opening (Zhang et al., 2003; Suh and Hille, 2008; Zaydman and Cui, 2014), and PIP_2 is proposed to couple the voltage-sensing domain to the pore domain in $K_v7.1$ (Zaydman et al., 2013; Sun and MacKinnon, 2020). Each K_v7 subunit also has a short intracellular N-terminal domain and a long intracellular C-terminal tail that harbors four helices (helices A–D; Haitin and Attali, 2008). Helices A and B bind to calmodulin (CaM; Strulovich et al., 2016; Sun and MacKinnon, 2017), whereas helices C–D mediate subunit assembly (Haitin and Attali, 2008).

In neurons, K_v7 channels open at subthreshold potentials around −60 mV and produce slowly-activating and non-inactivating outward K^+ currents that potently suppress repetitive and

burst firing of action potentials (APs; Brown and Passmore, 2009). Their functional significance in inhibiting neuronal excitability is underscored by the fact that mutations in their subunits cause epilepsy (Nappi et al., 2020), whereas K_v7 agonist retigabine inhibits seizures in rodents and humans (Miceli et al., 2008). Importantly, emerging new evidence suggests that K_v7 channels may contribute to activity-dependent persistent changes in neuronal intrinsic excitability and synaptic strength that are widely thought to underlie learning and memory. This review will summarize the function of K_v7 channels in the hippocampus and discuss recent studies that investigate their contributions to hippocampal plasticity, cognition, and behavior.

BRAIN DISTRIBUTION OF K_V7 SUBUNITS AND THEIR CHANNELOPATHIES

$K_v7.2$, $K_v7.3$, and $K_v7.5$ are the major neuronal K_v7 subunits (**Table 1**). $K_v7.2$ and $K_v7.3$ show strong overlapping expression in the cerebral cortex, hippocampal formation, amygdala, basal ganglia, and hypothalamus (Wang et al., 1998; Cooper et al., 2001; Klinger et al., 2011). $K_v7.5$ is highly expressed in the brain stem and to less extent in the cerebral cortex, hippocampus, occipital, frontal, and temporal lobes (Lerche et al., 2000; Schroeder et al., 2000; Tzingounis et al., 2010; Fidzinski et al., 2015). While $K_v7.1$ and $K_v7.4$ are mainly found in the heart and cochlear hair cells, respectively (Wang et al., 1996; Kubisch et al., 1999), they are also detected at low level in multiple regions of the brain (Casimiro et al., 2001; Hansen et al., 2006; Goldman et al., 2009; Su et al., 2019; **Table 1**).

Importantly, >300 dominant mutations in *KCNQ2* and *KCNQ3* cause epilepsy including benign familial neonatal epilepsy (BFNE) and epileptic encephalopathy (EE; Rikee and ClinVar database). *KCNQ2* is the second most frequently mutated gene in neurodevelopmental disorder (Traynelis et al., 2017; Coe et al., 2019) characterized by cognitive and behavioral deficits (Mullin et al., 2013). A few mutations in *KCNQ1*, *KCNQ4*, and *KCNQ5* have been associated with epilepsy, autism, schizophrenia, and developmental disorder (**Table 1**). Haploinsufficiency in K_v7 function seems to underlie BFNE variants that cause the transient appearance of neonatal seizures (Soldovieri et al., 2011). EE patients display severe and often drug-resistant neonatal seizures and psychomotor retardation (Weckhuysen et al., 2012), and *de novo* EE mutations in *KCNQ2* and *KCNQ3* induce multiple defects in current and surface expression of K_v7 channels (Weckhuysen et al., 2012, 2013; Milh et al., 2013; Miceli et al., 2015; Kim et al., 2018; Zhang et al., 2020).

GENERAL PROPERTIES AND REGULATION OF K_V7 CURRENTS

$K_v7.1$ assembles with auxiliary β subunit KCNE1 to produce the slow delayed rectifier K^+ current (I_{Ks}) important for the repolarization of cardiac APs (Barhanin et al., 1996). Importantly, coassembly with KCNE1 slows the activation

TABLE 1 | Distribution of K_v7 subunit in the brain and the diseases associated with its pathogenic variants.

Gene	Protein	Primary location	Distribution in the brain		Pathogenic variants	
			Regions	Reference	Associated diseases	Reference
KCNQ1	$K_v7.1$	Heart	CTX, HPF, MB, CB, BS	Casimiro et al., 2001; Goldman et al., 2009. AIBS, THPA	Long QT syndrome 1, JLNS, familial atrial fibrillation epilepsy, SUDEP, ASD, developmental disorder	ClinVar, LOVD, *denovo*-db
KCNQ2	$K_v7.2$	Nervous system	CTX, HPF, A, HY, TH, OA, MD, SN, P, MY, CB	Wang et al., 1998; Cooper et al., 2001; Devaux et al., 2004; Klinger et al., 2011; D'Este et al., 2016; Galvin et al., 2020. AIBS, THPA	BFNE, EE, ASD, intellectual disability, developmental disorder, sporadic infantile spasm syndrome	ClinVar, RIKEE, *denovo*-db
KCNQ3	$K_v7.3$	Nervous system	CTX, HPF, A, HY, TH, OA, MD, SN, P, MY, CB	Wang et al., 1998; Devaux et al., 2004; Klinger et al., 2011; Galvin et al., 2020. AIBS, THPA	BFNE, EE, ASD, intellectual disability, developmental disorder	ClinVar, RIKEE, *denovo*-db
KCNQ4	$K_v7.4$	Inner ear	BS, OA, MD, RN, NA, MY, VTA, P	Hansen et al., 2006; Su et al., 2019. AIBS, THPA	DFNA2, ASD	ClinVar, *denovo*-db
KCNQ5	$K_v7.5$	Nervous system	CTX, HPF, BS, CB	Lerche et al., 2000; Schroeder et al., 2000; Tzingounis et al., 2010; Fidzinski et al., 2015; Galvin et al., 2020. AIBS, THPA	EE, ASD, intellectual disability, schizophrenia	ClinVar, RIKEE, *denovo*-db

Brain regions: CTX, cortex; OA, olfactory areas; HPF, hippocampal formation; A, amygdala; NA, nucleus accumbens; BS, brain stem; TH, thalamus; HY, hypothalamus; MB, midbrain; RN, raphe nuclei; SN, substantia nigra; VTA, ventral tegmental area; PAL, pallidum; HB, hindbrain; CB, cerebellum; P, pons; MY, medulla. K_v7 channelopathies: JLNS, Jervell and Lange-Nielsen syndrome; SUDEP, sudden unexpected death in epilepsy; BFNE, benign familial neonatal epilepsy; EE, epileptic encephalopathy; ASD, autism spectrum disorder; DFNA2, nonsyndromic sensorineural deafness type 2. Database website: Allen Institute for Brain Science (AIBS, https://alleninstitute.org/what-we-do/brain-science/), The Human Protein Atlas (THPA, https://www.proteinatlas.org/), ClinVar (https://www.ncbi.nlm.nih.gov/clinvar/), Leiden Open Variation Database (LOVD, https://research.cchmc.org/LOVD2/home.php), denovo-db (http://denovo-db.gs.washington.edu/denovo-db/index.jsp), and Rational Intervention for KCNQ2/3 Epileptic Encephalopathy (RIKEE, https://www.rikee.org/).

kinetics of $K_v7.1$ channel, potentiates its current amplitude, and eliminates its voltage-dependent inactivation (Barhanin et al., 1996; Sanguinetti et al., 1996; Tristani-Firouzi and Sanguinetti, 1998). Homomeric $K_v7.2$ channels activate at −60 mV and produce slow-activating and non-inactivating currents (Biervert et al., 1998). In comparison, currents through $K_v7.3$ channels are negligible due to an Ala residue in the pore domain (Wang et al., 1998; Gomez-Posada et al., 2010). $K_v7.5$ activates at −60 mV with slower kinetics than $K_v7.2$ and $K_v7.3$ (Schroeder et al., 2000; Gamper et al., 2003). $K_v7.4$ activates at −40 mV with slower activation kinetics than other K_v7 channels (Kubisch et al., 1999).

Neuronal K_v7 channels are mostly heterotetrameric channels composed of $K_v7.2$ and $K_v7.3$, and to a lesser extent $K_v7.3$ and $K_v7.5$ (Wang et al., 1998; Shah et al., 2002; **Table 1**). Compared to homomeric channels, significantly larger currents are generated by $K_v7.2/K_v7.3$ channels (Schroeder et al., 1998; Wang et al., 1998; Schwake et al., 2000) and $K_v7.3/K_v7.5$ channels (Schroeder et al., 2000; Gilling et al., 2013). $K_v7.2/K_v7.3$ channels produce M-current (I_M; Wang et al., 1998), which potently suppresses neuronal hyperexcitability (Wang et al., 1998; Yue and Yaari, 2004). I_M is inhibited by muscarinic acetylcholine receptor activation (Selyanko et al., 2000) and the depletion of PIP_2 (Suh and Hille, 2002; Zhang et al., 2003). K_v7 channels are also inhibited by other G-protein coupled receptors, including substance P, bradykinin, serotonin, angiotensin, luteinizing hormone-releasing hormone, opioid, and metabotropic glutamate receptors (Marrion, 1997). General properties and diverse regulation of K_v7 channels are described in detail in a previous review (Soldovieri et al., 2011).

ROLE OF K_V7 CHANNELS IN INTRINSIC EXCITABILITY AND PLASTICITY IN THE HIPPOCAMPUS

Brown and Adams have first reported in 1980 that inhibition of I_M upon stimulation of muscarinic acetylcholine receptor results in repetitive firing of APs in bullfrog sympathetic ganglion neurons (Brown and Adams, 1980). In the hippocampus, strong expression of $K_v7.2$, $K_v7.3$, and $K_v7.5$ is detected in pyramidal neurons (Schroeder et al., 2000; Cooper et al., 2001; Devaux et al., 2004). K_v7 antagonists XE991 and linopirdine depolarize resting membrane potential (RMP) and reduce AP threshold of hippocampal CA1 pyramidal neurons, resulting in spontaneous AP firing (Aiken et al., 1995; Shah et al., 2008; **Figure 1A**). K_v7 antagonists also increase intrinsic excitability (Yue and Yaari, 2004, 2006; Shah et al., 2008), contribute to medium and slow afterhyperpolarization (AHP) currents (Gu et al., 2005), reduce spike frequency adaptation (Aiken et al., 1995), and ultimately lead to an increased AP firing rate (Lezmy et al., 2020; **Figure 1A**). Consistent with pharmacologic inhibition, suppression of K_v7 current by overexpressing $K_v7.2$ containing dominant-negative pore mutation G279S enhances intrinsic excitability and reduces spike frequency adaptation and mAHP in CA1 neurons (Peters et al., 2005). Similarly, conditional homozygous deletion of *KCNQ2* increases CA1 excitability due to longer-lasting spike afterdepolarization (ADP) and reduced medium AHP (Soh et al., 2014; **Figure 1A**). Thus, K_v7 channels serve as critical "brakes" on neuronal excitability (Soldovieri et al., 2011).

The inhibitory effects of K_v7 currents on neuronal excitability are largely attributed to axonal K_v7 channels. $K_v7.2/K_v7.3$ channels are preferentially enriched at the axonal plasma membrane compared to the somatodendritic plasma membrane in hippocampal neurons (Chung et al., 2006) with the highest concentration at the axonal initial segments (AIS; Chung et al., 2006; Pan et al., 2006) where AP initiates (Clark et al., 2009). CaM binding to $K_v7.2$ is critical for targeting $K_v7.2/K_v7.3$ channels to the axonal surface (Cavaretta et al., 2014), whereas disruption of this binding decreases I_M and increases hippocampal neuronal excitability (Shahidullah et al., 2005). Furthermore, disrupting the enrichment of K_v7 channels at the AIS by blocking their interaction with ankyrin-G results in spontaneous firing of CA1 neurons by depolarizing RMP and reducing AP threshold (Shah et al., 2008).

In contrast to the well-documented function of axonal K_v7 channels discussed above, the existence and role of dendritic K_v7 channels are still in debate. Non-inactivating K_v7 current sensitive to muscarinic agonist is detected in the distal apical dendrites of CA1 neurons (Chen and Johnston, 2004). Dendritic K_v7 current can increase the threshold for initiating calcium (Ca^{2+}) spikes and induce spike bursts only in hyperexcitable conditions that promote Ca^{2+} electrogenesis in these dendrites (Yue and Yaari, 2006). However, XE991 and linopirdine do not affect input resistance of CA1 dendrites (Shah et al., 2008), and focal inhibition of dendritic I_M has no effect on the excitatory postsynaptic potential (EPSP) summation and excitability of CA1 neuron (Hu et al., 2007), indicating very low level of dendritic K_v7 current.

There is accumulating evidence for activity-dependent modulation of K_v7 channels and their contribution to persistent changes in intrinsic excitability termed "intrinsic plasticity." In the pilocarpine model of temporal lobe epilepsy, reduced K_v7 function and expression may contribute to muscarinic-dependent ictogenesis (Maslarova et al., 2013). However, acute induction of seizures increases *KCNQ2* and *KCNQ3* transcripts in the hippocampi as a homeostatic response to suppress neuronal hyperexcitability, and this regulation requires activation of L-type voltage-gated Ca^{2+} channels (Zhang and Shapiro, 2012). Enhancing neuronal activity by K_v7 inhibition with XE991 also results in homeostatic suppression of firing rate over 48 h (Lezmy et al., 2020). In contrast, prolonged blockade of neuronal activity or N-methyl-D-aspartate (NMDA) receptors increases firing rate and reduces in *KCNQ3* transcript and K_v7 current in hippocampal neurons (Lee and Chung, 2014; Lee et al., 2015). In the avian cochlear neurons, depriving afferent inputs induces a switch from fast activating K_v1 to slow activating $K_v7.2$ channels at the AIS, resulting in enhanced excitability (Kuba et al., 2015). This activity-dependent regulation of K_v7 transcript and distribution offers a powerful means to control intrinsic excitability.

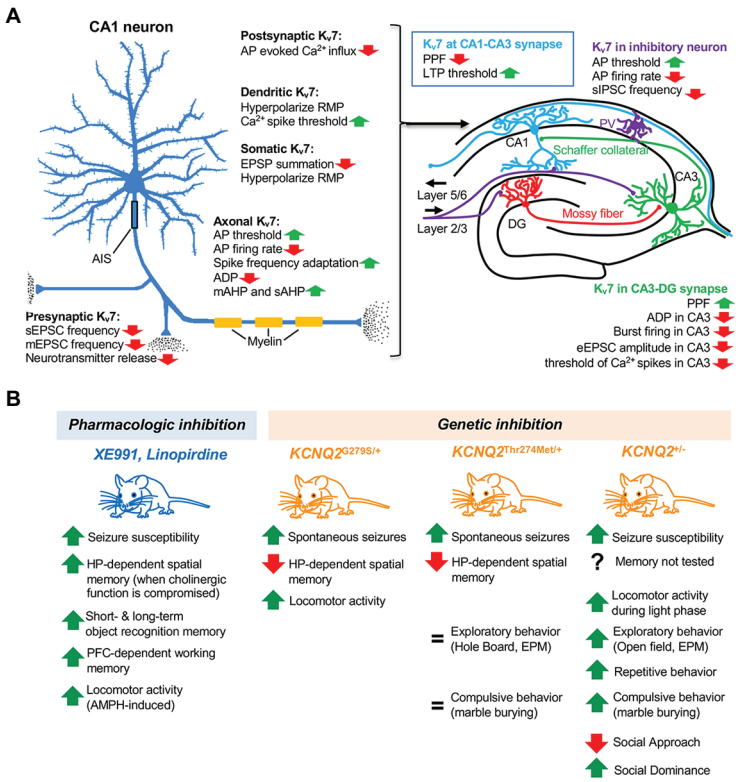

FIGURE 1 | The role of K_v7 channels in hippocampal neurons, memory, and behavior. **(A)** Function of K_v7 channels in excitatory pyramidal neuron and GABAergic inhibitory neuron in the hippocampus. AP, action potential; RMP, resting membrane potential; EPSP, excitatory postsynaptic potential; ADP, afterdepolarization; mAHP, medium afterhyperpolarization; sAHP, slow afterhyperpolarization; sEPSC, spontaneous excitatory postsynaptic current; mEPSC, miniature excitatory postsynaptic current; PPF, paired-pulse facilitation; LTP, long-term potential; sIPSC, spontaneous inhibitory postsynaptic current; PV, parvalbumin; and eEPSC, evoked excitatory postsynaptic current. **(B)** Effects of pharmacological or genetic inhibition of K_v7 channels on memory and behavior. HP, hippocampus; PFC, pre-frontal cortex; AMPH, amphetamine; and EPM, elevated plus maze.

ROLE OF K_V7 CHANNELS IN SYNAPTIC TRANSMISSION AND PLASTICITY IN THE HIPPOCAMPUS

Since the discovery of long-term potentiation (LTP) in the dentate gyrus of the hippocampus (Bliss and Lomo, 1973), persistent modification in synaptic strength termed "synaptic plasticity" has attracted significant attention as the cellular correlate of learning and memory (Nicoll, 2017). LTP at excitatory synapses can exert destabilizing influence on neural circuits by generating unconstrained synaptic strengthening (Turrigiano, 2012). Homeostatic plasticity counteracts such destabilizing condition by allowing neurons to adjust their synaptic strength (Turrigiano, 2012). While activity-dependent modulation of glutamate release and glutamate receptors serves as key mechanisms for LTP expression (Turrigiano, 2012; Humeau and Choquet, 2019), K_v7 channels and upstream muscarinic acetylcholine receptors have emerged as important regulators of excitatory synaptic transmission and plasticity.

Synaptic functions of K_v7 channels have been extensively studied at the excitatory synapses formed by hippocampal CA1 and CA3 pyramidal neurons (**Figure 1A**). These neurons show strong expression of $K_v7.2$ and $K_v7.3$ (Cooper et al., 2001; Pan et al., 2006). Conditional deletion of *KCNQ2* and *KCNQ3* increases the frequency of spontaneous excitatory postsynaptic currents (EPSC) in CA1 neurons (Soh et al., 2018), suggesting enhanced presynaptic release at CA1–CA3 synapses. Consistent with this notion, application of K_v7 antagonist XE991 increases whereas K_v7 agonist Flupirtine decreases miniature EPSC frequency in CA1 neurons (Sun and Kapur, 2012). Furthermore, K_v7 inhibition with linopirdine and XE991 treatment also increases neurotransmitter release (Nickolson et al., 1990; Martire et al., 2004; Peretz et al., 2007). While K_v7 current restrains AP-evoked Ca^{2+} influx into the presynaptic terminal and decreases the paired pulse ratio of evoked EPSCs at the mossy fiber–CA3 synapses (Martinello et al., 2019), paired pulse facilitation of EPSP is higher at CA1–CA3 synapses in XE991-treated mice (Fontan-Lozano et al., 2011), suggesting differential roles of K_v7 channels in short-term plasticity at two different synapses.

$K_v7.2$ and $K_v7.3$ are expressed in GABAergic neurons including parvalbumin (PV)- and somatostatin (SST)-positive interneurons in the hippocampus (Cooper et al., 2001; Lawrence et al., 2006). Application of XE991 abolishes I_M, depolarizes RMP, and increases AP firing in SST+ interneurons (Lawrence et al., 2006) and enhances intrinsic excitability of PV+ interneurons

(Soh et al., 2018; **Figure 1A**). Furthermore, conditional deletion of *KCNQ2* and *KCNQ3* from PV+ interneurons increases their firing and spontaneous inhibitory postsynaptic current (sIPSC) frequency of CA1 neurons in the hippocampus (Soh et al., 2018).

These studies highlight the presynaptic influence of K_v7 channels at glutamatergic and GABAergic synapses. Given that increased firing rate and burst firing can enhance neurotransmitter release probabilities (Hansen et al., 2008), K_v7 inhibition may increase neurotransmitter release as a consequence of increased axonal excitability (Devaux et al., 2004; Shah et al., 2008; Klinger et al., 2011). Indeed, when CA3 neurons are depolarized upon elevating extracellular K^+ concentration, XE991 enhances EPSP amplitude in CA1 neurons as a consequence of increasing spike ADP and burst firing of CA3 neurons (Vervaeke et al., 2006). Alternatively, K_v7 channels at the presynaptic terminals (Cooper et al., 2001; Martire et al., 2004; Regev et al., 2009) may directly counteract the depolarization of the presynaptic membrane necessary for synaptic vesicle fusion and neurotransmitter release.

The postsynaptic role of K_v7 channels is unclear. A recent electron microscopy study shows that $K_v7.2$, $K_v7.3$, and $K_v7.5$ colocalize with muscarinic acetylcholine receptors at dendritic spines in layer III pyramidal neurons of the primate prefrontal cortex (Galvin et al., 2020), although the specificity of the immunolabeling needs to be further validated. In the CA1–CA3 synapses, the mEPSC amplitude is unaltered by agonist nor antagonists of K_v7 channels (Sun and Kapur, 2012), suggesting their negligible role in regulating postsynaptic glutamate receptor function at this synapse (**Figure 1A**).

Nonetheless, accumulating evidence suggests that K_v7 channels regulate hippocampal synaptic plasticity. At CA1–CA3 synapses, XE991 induces LTP by subthreshold theta-burst stimulation (Petrovic et al., 2012). Systemic administration of XE991 also decreases the threshold for LTP induction in the hippocampal CA1 area *in vivo* without affecting the field EPSP amplitude (Song et al., 2009; Fontan-Lozano et al., 2011). Lastly, homeostatic increase in excitatory synaptic transmission in CA1 neurons has been observed upon conditional deletion of *KCNQ2* and *KCNQ3* from GABAergic interneurons (Soh et al., 2018), suggesting the contribution of K_v7 channels in synaptic scaling.

ROLE OF K_V7 CHANNELS IN HIPPOCAMPUS-DEPENDENT LEARNING AND MEMORY

Hippocampal LTP occurs during hippocampus-dependent learning and memory (Bliss et al., 2018) and its reduction is linked to memory loss in mouse models of Alzheimer's disease (Mango et al., 2019). Facilitation of LTP induction by XE991 (Song et al., 2009; Fontan-Lozano et al., 2011; Petrovic et al., 2012) suggests that pharmacologic K_v7 inhibition may enhance learning and memory. Indeed, linopirdine enhances the performance of rats in a hippocampus-dependent active avoidance test (Cook et al., 1990). XE991 improves memory in object recognition task in wild-type mice and mouse models of dementia induced by cholinergic depletion and neurodegeneration (Fontan-Lozano et al., 2011; Ballinger et al., 2016; Dennis et al., 2016) despite its ability to induce seizures at a higher dose (Fontan-Lozano et al., 2011; **Figure 1B**). In contrast, K_v7 agonists have yielded mixed results on affecting memory in rodents (Li et al., 2014; Frankel et al., 2016).

The cognition-enhancing effect of linopirdine is correlated with the increased release of acetylcholine in the hippocampus (Nickolson et al., 1990; Fontana et al., 1994), and stimulation of muscarinic acetylcholine receptor inhibits I_M in hippocampal neurons (Shah et al., 2002). Consistently, muscarinic agonist improves whereas anticholinergic agent scopolamine impairs performance in hippocampus-dependent memory tasks (Fontana et al., 1994; Fontan-Lozano et al., 2011). Muscarinic acetylcholine receptors in the prefrontal cortex also modulate working memory in primates *via* K_v7 channels (Galvin et al., 2020). Since cholinergic depletion and dysfunction in the hippocampus and prefrontal cortex are implicated in age-related cognitive decline and Alzheimer's disease (Ballinger et al., 2016; Haam and Yakel, 2017), these studies support the therapeutic potential for K_v7 antagonists as cognitive enhancers.

Surprisingly, genetic inhibition or reduction of K_v7 currents induces an opposite effect on memory (**Figure 1B**). Deficits in hippocampal-dependent spatial memory and spontaneous seizures are observed in mice with conditional transgenic expression of dominant-negative mutant $K_v7.2$-G279S (Peters et al., 2005) and heterozygous knock-in mice for $K_v7.2$ containing epileptic encephalopathy loss-of-function variant T274M (Milh et al., 2020). Considering that K_v7 channels are critical for development and inhibition of neonatal brain (Peters et al., 2005; Soh et al., 2014), the memory impairment in these genetic models could be attributed to abnormal hippocampal morphology and/or hyperexcitability (Peters et al., 2005; Milh et al., 2020).

K_v7 channels also regulate multiple behaviors (**Figure 1B**). Behavioral phenotyping of the global or conditional homozygous *KCNQ2* knock-out mice has not been possible due to their early postnatal lethality or premature death, respectively (Watanabe et al., 2000; Soh et al., 2014). However, heterozygous *KCNQ2* knock-out mice are viable and display increased locomotor activity and exploratory behavior (Kim et al., 2020), consistent with behavioral hyperactivity induced by transgenic suppression of K_v7 currents (Peters et al., 2005) and amphetamine and XE991 (Sotty et al., 2009). These mice also show decreased sociability and increased repetitive and compulsive behavior (Kim et al., 2020), reminiscent of autism seen in some EE patients with dominant *KCNQ2* mutations (Weckhuysen et al., 2012, 2013; Milh et al., 2013). However, the precise circuitries responsible for these abnormal behaviors remain unknown.

FUTURE PERSPECTIVES

The studies discussed in this review support the emerging concept that K_v7 channels contribute to neural plasticity, memory, and behavior. However, there is a significant knowledge gap in our understanding of the underlying molecular and cellular mechanisms. Future studies should continue to investigate structure-function and subcellular targeting of K_v7 channels, which will provide mechanistic insights for developing specific

modulators of their function and trafficking. Generation of mouse models in which deletion of a K_v7 subunit from specific neurons and subcellular localization with temporal control will be critical to delineate cell- and circuit-specific function of K_v7 channels in neural plasticity, cognition, and behavior.

AUTHOR CONTRIBUTIONS

BCB and HC contributed to the conception and design of the manuscript. BCB, JZ, and HC also drafted and revised the manuscript. All authors contributed to the article and approved the submitted version.

FUNDING

This work was supported by the National Institute of Neurological Disorders and Stroke (NINDS) Research Project Grant NS083402 (HC). Understanding the Brain: Training the Next Generation of Researchers in Engineering and Deciphering of Miniature Brain Machinery. NSF training grant 1735252 (BCB).

REFERENCES

Aiken, S. P., Lampe, B. J., Murphy, P. A., and Brown, B. S. (1995). Reduction of spike frequency adaptation and blockade of M-current in rat CA1 pyramidal neurones by linopirdine (DuP 996), a neurotransmitter release enhancer. *Br. J. Pharmacol.* 115, 1163–1168. doi: 10.1111/j.1476-5381.1995.tb15019.x

Ballinger, E. C., Ananth, M., Talmage, D. A., and Role, L. W. (2016). Basal forebrain cholinergic circuits and signaling in cognition and cognitive decline. *Neuron* 91, 1199–1218. doi: 10.1016/j.neuron.2016.09.006

Barhanin, J., Lesage, F., Guillemare, E., Fink, M., Lazdunski, M., and Romey, G. (1996). K(V)LQT1 and lsK (minK) proteins associate to form the I(Ks) cardiac potassium current. *Nature* 384, 78–80. doi: 10.1038/384078a0

Biervert, C., Schroeder, B. C., Kubisch, C., Berkovic, S. F., Propping, P., Jentsch, T. J., et al. (1998). A potassium channel mutation in neonatal human epilepsy. *Science* 279, 403–406. doi: 10.1126/science.279.5349.403

Bliss, T., Collingridge, G., Morris, R., and Reymann, K. (2018). Long-term potentiation in the hippocampus: discovery, mechanisms and function. *Neuroforum* 24, 103–120. doi: 10.1515/nf-2017-A059

Bliss, T. V., and Lomo, T. (1973). Long-lasting potentiation of synaptic transmission in the dentate area of the anaesthetized rabbit following stimulation of the perforant path. *J. Physiol.* 232, 331–356. doi: 10.1113/jphysiol.1973.sp010273

Brown, D. A., and Adams, P. R. (1980). Muscarinic suppression of a novel voltage-sensitive K^+ current in a vertebrate neurone. *Nature* 283, 673–676. doi: 10.1038/283673a0

Brown, D. A., and Passmore, G. M. (2009). Neural KCNQ (Kv7) channels. *Br. J. Pharmacol.* 156, 1185–1195. doi: 10.1111/j.1476-5381.2009.00111.x

Casimiro, M. C., Knollmann, B. C., Ebert, S. N., Vary, J. C. Jr., Greene, A. E., Franz, M. R., et al. (2001). Targeted disruption of the Kcnq1 gene produces a mouse model of Jervell and Lange-Nielsen syndrome. *Proc. Natl. Acad. Sci. U. S. A.* 98, 2526–2531. doi: 10.1073/pnas.041398998

Cavaretta, J. P., Sherer, K. R., Lee, K. Y., Kim, E. H., Issema, R. S., and Chung, H. J. (2014). Polarized axonal surface expression of neuronal KCNQ potassium channels is regulated by calmodulin interaction with KCNQ2 subunit. *PLoS One* 9:e103655. doi: 10.1371/journal.pone.0103655

Chen, X., and Johnston, D. (2004). Properties of single voltage-dependent K^+ channels in dendrites of CA1 pyramidal neurones of rat hippocampus. *J. Physiol.* 559, 187–203. doi: 10.1113/jphysiol.2004.068114

Chung, H. J., Jan, Y. N., and Jan, L. Y. (2006). Polarized axonal surface expression of neuronal KCNQ channels is mediated by multiple signals in the KCNQ2 and KCNQ3 C-terminal domains. *Proc. Natl. Acad. Sci. U. S. A.* 103, 8870–8875. doi: 10.1073/pnas.0603376103

Clark, B. D., Goldberg, E. M., and Rudy, B. (2009). Electrogenic tuning of the axon initial segment. *Neuroscientist* 15, 651–668. doi: 10.1177/1073858409341973

Coe, B. P., Stessman, H. A. F., Sulovari, A., Geisheker, M. R., Bakken, T. E., Lake, A. M., et al. (2019). Neurodevelopmental disease genes implicated by de novo mutation and copy number variation morbidity. *Nat. Genet.* 51, 106–116. doi: 10.1038/s41588-018-0288-4

Cook, L., Nickolson, V., Steinfels, G., Rohrbach, K., and Denoble, V. (1990). Cognition enhancement by the acetylcholine releaser DuP 996. *Drug Dev. Res.* 19, 301–314. doi: 10.1002/ddr.430190308

Cooper, E. C., Harrington, E., Jan, Y. N., and Jan, L. Y. (2001). M channel KCNQ2 subunits are localized to key sites for control of neuronal network oscillations and synchronization in mouse brain. *J. Neurosci.* 21, 9529–9540. doi: 10.1523/JNEUROSCI.21-24-09529.2001

Cui, J. (2016). Voltage-dependent gating: novel insights from KCNQ1 channels. *Biophys. J.* 110, 14–25. doi: 10.1016/j.bpj.2015.11.023

Dennis, S. H., Pasqui, F., Colvin, E. M., Sanger, H., Mogg, A. J., Felder, C. C., et al. (2016). Activation of muscarinic M1 acetylcholine receptors induces long-term potentiation in the hippocampus. *Cereb. Cortex* 26, 414–426. doi: 10.1093/cercor/bhv227

D'Este, E., Kamin, D., Balzarotti, F., and Hell, S. (2016). Ultrastructural anatomy of nodes of Ranvier in the peripheral nervous system as revealed by STED microscopy. *Proc. Natl. Acad. Sci. U. S. A.* 114, E191–E199. doi: 10.1073/pnas.1619553114

Devaux, J. J., Kleopa, K. A., Cooper, E. C., and Scherer, S. S. (2004). KCNQ2 is a nodal K^+ channel. *J. Neurosci.* 24, 1236–1244. doi: 10.1523/JNEUROSCI.4512-03.2004

Fidzinski, P., Korotkova, T., Heidenreich, M., Maier, N., Schuetze, S., Kobler, O., et al. (2015). KCNQ5 K(+) channels control hippocampal synaptic inhibition and fast network oscillations. *Nat. Commun.* 6:6254. doi: 10.1038/ncomms7254

Fontana, D. J., Inouye, G. T., and Johnson, R. M. (1994). Linopirdine (DuP 996) improves performance in several tests of learning and memory by modulation of cholinergic neurotransmission. *Pharmacol. Biochem. Behav.* 49, 1075–1082. doi: 10.1016/0091-3057(94)90267-4

Fontan-Lozano, A., Suarez-Pereira, I., Delgado-Garcia, J. M., and Carrion, A. M. (2011). The M-current inhibitor XE991 decreases the stimulation threshold for long-term synaptic plasticity in healthy mice and in models of cognitive disease. *Hippocampus* 21, 22–32. doi: 10.1002/hipo.20717

Frankel, S., Medvedeva, N., Gutherz, S., Kulick, C., Kondratyev, A., and Forcelli, P. A. (2016). Comparison of the long-term behavioral effects of neonatal exposure to retigabine or phenobarbital in rats. *Epilepsy Behav.* 57, 34–40. doi: 10.1016/j.yebeh.2016.01.018

Galvin, V. C., Yang, S. T., Paspalas, C. D., Yang, Y., Jin, L. E., Datta, D., et al. (2020). Muscarinic M1 receptors modulate working memory performance and activity via KCNQ potassium channels in the primate prefrontal cortex. *Neuron* 106, 649.e4–661.e4. doi: 10.1016/j.neuron.2020.02.030

Gamper, N., Stockand, J. D., and Shapiro, M. S. (2003). Subunit-specific modulation of KCNQ potassium channels by Src tyrosine kinase. *J. Neurosci.* 23, 84–95. doi: 10.1523/JNEUROSCI.23-01-00084.2003

Gilling, M., Rasmussen, H. B., Calloe, K., Sequeira, A. F., Baretto, M., Oliveira, G., et al. (2013). Dysfunction of the heteromeric KV7.3/KV7.5 potassium channel is associated with autism spectrum disorders. *Front. Genet.* 4:54. doi: 10.3389/fgene.2013.00054

Goldman, A. M., Glasscock, E., Yoo, J., Chen, T. T., Klassen, T. L., and Noebels, J. L. (2009). Arrhythmia in heart and brain: KCNQ1 mutations link epilepsy and sudden unexplained death. *Sci. Transl. Med.* 1:2ra6. doi: 10.1126/scitranslmed.3000289

Gomez-Posada, J. C., Etxeberria, A., Roura-Ferrer, M., Areso, P., Masin, M., Murrell-Lagnado, R. D., et al. (2010). A pore residue of the KCNQ3 potassium M-channel subunit controls surface expression. *J. Neurosci.* 30, 9316–9323. doi: 10.1523/JNEUROSCI.0851-10.2010

Gu, N., Vervaeke, K., Hu, H., and Storm, J. F. (2005). Kv7/KCNQ/M and HCN/h, but not $K_{Ca}2$/SK channels, contribute to the somatic medium after-hyperpolarization and excitability control in CA1 hippocampal pyramidal cells. *J. Physiol.* 566, 689–715. doi: 10.1113/jphysiol.2005.086835

Gutman, G. A., Chandy, K. G., Grissmer, S., Lazdunski, M., Mckinnon, D., Pardo, L. A., et al. (2005). International Union of Pharmacology. LIII.

Nomenclature and molecular relationships of voltage-gated potassium channels. *Pharmacol. Rev.* 57, 473–508. doi: 10.1124/pr.57.4.10

Haam, J., and Yakel, J. L. (2017). Cholinergic modulation of the hippocampal region and memory function. *J. Neurochem.* 142, 111–121. doi: 10.1111/jnc.14052

Haitin, Y., and Attali, B. (2008). The C-terminus of Kv7 channels: a multifunctional module. *J. Physiol.* 586, 1803–1810. doi: 10.1113/jphysiol.2007.149187

Hansen, H. H., Ebbesen, C., Mathiesen, C., Weikop, P., Ronn, L. C., Waroux, O., et al. (2006). The KCNQ channel opener retigabine inhibits the activity of mesencephalic dopaminergic systems of the rat. *J. Pharmacol. Exp. Ther.* 318, 1006–1019. doi: 10.1124/jpet.106.106757

Hansen, H. H., Waroux, O., Seutin, V., Jentsch, T. J., Aznar, S., and Mikkelsen, J. D. (2008). Kv7 channels: interaction with dopaminergic and serotonergic neurotransmission in the CNS. *J. Physiol.* 586, 1823–1832. doi: 10.1113/jphysiol.2007.149450

Hu, H., Vervaeke, K., and Storm, J. F. (2007). M-channels (Kv7/KCNQ channels) that regulate synaptic integration, excitability, and spike pattern of CA1 pyramidal cells are located in the perisomatic region. *J. Neurosci.* 27, 1853–1867. doi: 10.1523/JNEUROSCI.4463-06.2007

Humeau, Y., and Choquet, D. (2019). The next generation of approaches to investigate the link between synaptic plasticity and learning. *Nat. Neurosci.* 22, 1536–1543. doi: 10.1038/s41593-019-0480-6

Kim, E. C., Patel, J., Zhang, J., Soh, H., Rhodes, J. S., Tzingounis, A. V., et al. (2020). Heterozygous loss of epilepsy gene KCNQ2 alters social, repetitive and exploratory behaviors. *Genes Brain Behav.* 19:e12599. doi: 10.1111/gbb.12599

Kim, E. C., Zhang, J., Pang, W., Wang, S., Lee, K. Y., Cavaretta, J. P., et al. (2018). Reduced axonal surface expression and phosphoinositide sensitivity in Kv7 channels disrupts their function to inhibit neuronal excitability in Kcnq2 epileptic encephalopathy. *Neurobiol. Dis.* 118, 76–93. doi: 10.1016/j.nbd.2018.07.004

Klinger, F., Gould, G., Boehm, S., and Shapiro, M. S. (2011). Distribution of M-channel subunits KCNQ2 and KCNQ3 in rat hippocampus. *Neuroimage* 58, 761–769. doi: 10.1016/j.neuroimage.2011.07.003

Kuba, H., Yamada, R., Ishiguro, G., and Adachi, R. (2015). Redistribution of Kv1 and Kv7 enhances neuronal excitability during structural axon initial segment plasticity. *Nat. Commun.* 6:8815. doi: 10.1038/ncomms9815

Kubisch, C., Schroeder, B. C., Friedrich, T., Lutjohann, B., El-Amraoui, A., Marlin, S., et al. (1999). KCNQ4, a novel potassium channel expressed in sensory outer hair cells, is mutated in dominant deafness. *Cell* 96, 437–446. doi: 10.1016/S0092-8674(00)80556-5

Lawrence, J. J., Saraga, F., Churchill, J. F., Statland, J. M., Travis, K. E., Skinner, F. K., et al. (2006). Somatodendritic Kv7/KCNQ/M channels control interspike interval in hippocampal interneurons. *J. Neurosci.* 26, 12325–12338. doi: 10.1523/JNEUROSCI.3521-06.2006

Lee, K. Y., and Chung, H. J. (2014). NMDA receptors and L-type voltage-gated Ca^{2+} channels mediate the expression of bidirectional homeostatic intrinsic plasticity in cultured hippocampal neurons. *Neuroscience* 277, 610–623. doi: 10.1016/j.neuroscience.2014.07.038

Lee, K. Y., Royston, S. E., Vest, M. O., Ley, D. J., Lee, S., Bolton, E. C., et al. (2015). N-methyl-D-aspartate receptors mediate activity-dependent down-regulation of potassium channel genes during the expression of homeostatic intrinsic plasticity. *Mol. Brain* 8:4. doi: 10.1186/s13041-015-0094-1

Lerche, C., Scherer, C. R., Seebohm, G., Derst, C., Wei, A. D., Busch, A. E., et al. (2000). Molecular cloning and functional expression of KCNQ5, a potassium channel subunit that may contribute to neuronal M-current diversity. *J. Biol. Chem.* 275, 22395–22400. doi: 10.1074/jbc.M002378200

Lezmy, J., Gelman, H., Katsenelson, M., Styr, B., Tikochinsky, E., Lipinsky, M., et al. (2020). M-current inhibition in hippocampal excitatory neurons triggers intrinsic and synaptic homeostatic responses at different temporal scales. *J. Neurosci.* 40, 3694–3706. doi: 10.1523/JNEUROSCI.1914-19.2020

Li, C., Huang, P., Lu, Q., Zhou, M., Guo, L., and Xu, X. (2014). KCNQ/Kv7 channel activator flupirtine protects against acute stress-induced impairments of spatial memory retrieval and hippocampal LTP in rats. *Neuroscience* 280, 19–30. doi: 10.1016/j.neuroscience.2014.09.009

Mango, D., Saidi, A., Cisale, G. Y., Feligioni, M., Corbo, M., and Nistico, R. (2019). Targeting synaptic plasticity in experimental models of Alzheimer's disease. *Front. Pharmacol.* 10:778. doi: 10.3389/fphar.2019.00778

Marrion, N. V. (1997). Control of M-current. *Annu. Rev. Physiol.* 59, 483–504. doi: 10.1146/annurev.physiol.59.1.483

Martinello, K., Giacalone, E., Migliore, M., Brown, D. A., and Shah, M. M. (2019). The subthreshold-active KV7 current regulates neurotransmission by limiting spike-induced Ca^{2+} influx in hippocampal mossy fiber synaptic terminals. *Commun. Biol.* 2:145. doi: 10.1038/s42003-019-0408-4

Martire, M., Castaldo, P., D'amico, M., Preziosi, P., Annunziato, L., and Taglialatela, M. (2004). M channels containing KCNQ2 subunits modulate norepinephrine, aspartate, and GABA release from hippocampal nerve terminals. *J. Neurosci.* 24, 592–597. doi: 10.1523/JNEUROSCI.3143-03.2004

Maslarova, A., Salar, S., Lapilover, E., Friedman, A., Veh, R. W., and Heinemann, U. (2013). Increased susceptibility to acetylcholine in the entorhinal cortex of pilocarpine-treated rats involves alterations in KCNQ channels. *Neurobiol. Dis.* 56, 14–24. doi: 10.1016/j.nbd.2013.02.016

Miceli, F., Soldovieri, M. V., Martire, M., and Taglialatela, M. (2008). Molecular pharmacology and therapeutic potential of neuronal Kv7-modulating drugs. *Curr. Opin. Pharmacol.* 8, 65–74. doi: 10.1016/j.coph.2007.10.003

Miceli, F., Striano, P., Soldovieri, M. V., Fontana, A., Nardello, R., Robbiano, A., et al. (2015). A novel KCNQ3 mutation in familial epilepsy with focal seizures and intellectual disability. *Epilepsia* 56, e15–e20. doi: 10.1111/epi.12887

Milh, M., Boutry-Kryza, N., Sutera-Sardo, J., Mignot, C., Auvin, S., Lacoste, C., et al. (2013). Similar early characteristics but variable neurological outcome of patients with a de novo mutation of KCNQ2. *Orphanet J. Rare Dis.* 8:80. doi: 10.1186/1750-1172-8-80

Milh, M., Roubertoux, P., Biba, N., Chavany, J., Spiga Ghata, A., Fulachier, C., et al. (2020). A knock-in mouse model for KCNQ2-related epileptic encephalopathy displays spontaneous generalized seizures and cognitive impairment. *Epilepsia* 61, 868–878. doi: 10.1111/epi.16494

Mullin, A. P., Gokhale, A., Moreno-De-Luca, A., Sanyal, S., Waddington, J. L., and Faundez, V. (2013). Neurodevelopmental disorders: mechanisms and boundary definitions from genomes, interactomes and proteomes. *Transl. Psychiatry* 3:e329. doi: 10.1038/tp.2013.108

Nappi, P., Miceli, F., Soldovieri, M. V., Ambrosino, P., Barrese, V., and Taglialatela, M. (2020). Epileptic channelopathies caused by neuronal Kv7 (KCNQ) channel dysfunction. *Pflugers Arch.* 472, 881–898. doi: 10.1007/s00424-020-02404-2

Nickolson, V., William Tam, S., Myers, M., and Cook, L. (1990). DuP 996 (3,3-bis(4-pyrindinylmethyl)-1-phenylindolin-2-one) enhances the stimulus-induced release of acetylcholine from rat brain in vitro and in vivo. *Drug Dev. Res.* 19, 285–300. doi: 10.1002/ddr.430190307

Nicoll, R. A. (2017). A brief history of long-term potentiation. *Neuron* 93, 281–290. doi: 10.1016/j.neuron.2016.12.015

Pan, Z., Kao, T., Horvath, Z., Lemos, J., Sul, J. Y., Cranstoun, S. D., et al. (2006). A common ankyrin-G-based mechanism retains KCNQ and NaV channels at electrically active domains of the axon. *J. Neurosci.* 26, 2599–2613. doi: 10.1523/JNEUROSCI.4314-05.2006

Peretz, A., Sheinin, A., Yue, C., Degani-Katzav, N., Gibor, G., Nachman, R., et al. (2007). Pre- and postsynaptic activation of M-channels by a novel opener dampens neuronal firing and transmitter release. *J. Neurophysiol.* 97, 283–295. doi: 10.1152/jn.00634.2006

Peters, H. C., Hu, H., Pongs, O., Storm, J. F., and Isbrandt, D. (2005). Conditional transgenic suppression of M channels in mouse brain reveals functions in neuronal excitability, resonance and behavior. *Nat. Neurosci.* 8, 51–60. doi: 10.1038/nn1375

Petrovic, M. M., Nowacki, J., Olivo, V., Tsaneva-Atanasova, K., Randall, A. D., and Mellor, J. R. (2012). Inhibition of post-synaptic Kv7/KCNQ/M channels facilitates long-term potentiation in the hippocampus. *PLoS One* 7:e30402. doi: 10.1371/journal.pone.0030402

Regev, N., Degani-Katzav, N., Korngreen, A., Etzioni, A., Siloni, S., Alaimo, A., et al. (2009). Selective interaction of syntaxin 1A with KCNQ2: possible implications for specific modulation of presynaptic activity. *PLoS One* 4:e6586. doi: 10.1371/journal.pone.0006586

Robbins, J. (2001). KCNQ potassium channels: physiology, pathophysiology, and pharmacology. *Pharmacol. Ther.* 90, 1–19. doi: 10.1016/S0163-7258(01)00116-4

Sanguinetti, M. C., Curran, M. E., Zou, A., Shen, J., Spector, P. S., Atkinson, D. L., et al. (1996). Coassembly of K(V)LQT1 and minK (IsK) proteins to form cardiac I(Ks) potassium channel. *Nature* 384, 80–83. doi: 10.1038/384080a0

Schroeder, B. C., Hechenberger, M., Weinreich, F., Kubisch, C., and Jentsch, T. J. (2000). KCNQ5, a novel potassium channel broadly expressed in brain, mediates M-type currents. *J. Biol. Chem.* 275, 24089–24095. doi: 10.1074/jbc.M003245200

Schroeder, B. C., Kubisch, C., Stein, V., and Jentsch, T. J. (1998). Moderate loss of function of cyclic-AMP-modulated KCNQ2/KCNQ3 K^+ channels causes epilepsy. *Nature* 396, 687–690. doi: 10.1038/25367

Schwake, M., Pusch, M., Kharkovets, T., and Jentsch, T. J. (2000). Surface expression and single channel properties of KCNQ2/KCNQ3, M-type K^+ channels involved in epilepsy. *J. Biol. Chem.* 275, 13343–13348. doi: 10.1074/jbc.275.18.13343

Selyanko, A. A., Hadley, J. K., Wood, I. C., Abogadie, F. C., Jentsch, T. J., and Brown, D. A. (2000). Inhibition of KCNQ1-4 potassium channels expressed in mammalian cells via M1 muscarinic acetylcholine receptors. *J. Physiol.* 522, 349–355. doi: 10.1111/j.1469-7793.2000.t01-2-00349.x

Shah, M. M., Migliore, M., Valencia, I., Cooper, E. C., and Brown, D. A. (2008). Functional significance of axonal Kv7 channels in hippocampal pyramidal neurons. *Proc. Natl. Acad. Sci. U. S. A.* 105, 7869–7874. doi: 10.1073/pnas.0802805105

Shah, M., Mistry, M., Marsh, S. J., Brown, D. A., and Delmas, P. (2002). Molecular correlates of the M-current in cultured rat hippocampal neurons. *J. Physiol.* 544, 29–37. doi: 10.1113/jphysiol.2002.028571

Shahidullah, M., Santarelli, L. C., Wen, H., and Levitan, I. B. (2005). Expression of a calmodulin-binding KCNQ2 potassium channel fragment modulates neuronal M-current and membrane excitability. *Proc. Natl. Acad. Sci. U. S. A.* 102, 16454–16459. doi: 10.1073/pnas.0503966102

Soh, H., Pant, R., Loturco, J. J., and Tzingounis, A. V. (2014). Conditional deletions of epilepsy-associated KCNQ2 and KCNQ3 channels from cerebral cortex cause differential effects on neuronal excitability. *J. Neurosci.* 34, 5311–5321. doi: 10.1523/JNEUROSCI.3919-13.2014

Soh, H., Park, S., Ryan, K., Springer, K., Maheshwari, A., and Tzingounis, A. V. (2018). Deletion of KCNQ2/3 potassium channels from PV+ interneurons leads to homeostatic potentiation of excitatory transmission. *Elife* 7:e38617. doi: 10.7554/eLife.38617

Soldovieri, M. V., Miceli, F., and Taglialatela, M. (2011). Driving with no brakes: molecular pathophysiology of Kv7 potassium channels. *Physiology* 26, 365–376. doi: 10.1152/physiol.00009.2011

Song, M. K., Cui, Y. Y., Zhang, W. W., Zhu, L., Lu, Y., and Chen, H. Z. (2009). The facilitating effect of systemic administration of Kv7/M channel blocker XE991 on LTP induction in the hippocampal CA1 area independent of muscarinic activation. *Neurosci. Lett.* 461, 25–29. doi: 10.1016/j.neulet.2009.05.042

Sotty, F., Damgaard, T., Montezinho, L. P., Mork, A., Olsen, C. K., Bundgaard, C., et al. (2009). Antipsychotic-like effect of retigabine [N-(2-amino-4-(fluorobenzylamino)-phenyl)carbamic acid ester], a KCNQ potassium channel opener, via modulation of mesolimbic dopaminergic neurotransmission. *J. Pharmacol. Exp. Ther.* 328, 951–962. doi: 10.1124/jpet.108.146944

Strulovich, R., Tobelaim, W. S., Attali, B., and Hirsch, J. A. (2016). Structural insights into the M-channel proximal C-terminus/calmodulin complex. *Biochemistry* 55, 5353–5365. doi: 10.1021/acs.biochem.6b00477

Su, M., Li, L., Wang, J., Sun, H., Zhang, L., Zhao, C., et al. (2019). Kv7.4 channel contribute to projection-specific auto-inhibition of dopamine neurons in the ventral tegmental area. *Front. Cell. Neurosci.* 13:557. doi: 10.3389/fncel.2019.00557

Suh, B. C., and Hille, B. (2002). Recovery from muscarinic modulation of M current channels requires phosphatidylinositol 4,5-bisphosphate synthesis. *Neuron* 35, 507–520. doi: 10.1016/S0896-6273(02)00790-0

Suh, B. C., and Hille, B. (2008). PIP2 is a necessary cofactor for ion channel function: how and why? *Annu. Rev. Biophys.* 37, 175–195. doi: 10.1146/annurev.biophys.37.032807.125859

Sun, J., and Kapur, J. (2012). M-type potassium channels modulate Schaffer collateral-CA1 glutamatergic synaptic transmission. *J. Physiol.* 590, 3953–3964. doi: 10.1113/jphysiol.2012.235820

Sun, J., and Mackinnon, R. (2017). Cryo-EM structure of a KCNQ1/CaM complex reveals insights into congenital long QT syndrome. *Cell* 169, 1042.e1049–1050.e1049. doi: 10.1016/j.cell.2017.05.019

Sun, J., and Mackinnon, R. (2020). Structural basis of human KCNQ1 modulation and gating. *Cell* 180, 340.e349–347.e349. doi: 10.1016/j.cell.2019.12.003

Traynelis, J., Silk, M., Wang, Q., Berkovic, S. F., Liu, L., Ascher, D. B., et al. (2017). Optimizing genomic medicine in epilepsy through a gene-customized approach to missense variant interpretation. *Genome Res.* 27, 1715–1729. doi: 10.1101/gr.226589.117

Tristani-Firouzi, M., and Sanguinetti, M. C. (1998). Voltage-dependent inactivation of the human K^+ channel KvLQT1 is eliminated by association with minimal K^+ channel (minK) subunits. *J. Physiol.* 510, 37–45. doi: 10.1111/j.1469-7793.1998.037bz.x

Turrigiano, G. (2012). Homeostatic synaptic plasticity: local and global mechanisms for stabilizing neuronal function. *Cold Spring Harb. Perspect. Biol.* 4:a005736. doi: 10.1101/cshperspect.a005736

Tzingounis, A. V., Heidenreich, M., Kharkovets, T., Spitzmaul, G., Jensen, H. S., Nicoll, R. A., et al. (2010). The KCNQ5 potassium channel mediates a component of the afterhyperpolarization current in mouse hippocampus. *Proc. Natl. Acad. Sci. U. S. A.* 107, 10232–10237. doi: 10.1073/pnas.1004644107

Vervaeke, K., Gu, N., Agdestein, C., Hu, H., and Storm, J. F. (2006). Kv7/KCNQ/M-channels in rat glutamatergic hippocampal axons and their role in regulation of excitability and transmitter release. *J. Physiol.* 576, 235–256. doi: 10.1113/jphysiol.2006.111336

Wang, Q., Curran, M. E., Splawski, I., Burn, T. C., Millholland, J. M., Vanraay, T. J., et al. (1996). Positional cloning of a novel potassium channel gene: KVLQT1 mutations cause cardiac arrhythmias. *Nat. Genet.* 12, 17–23. doi: 10.1038/ng0196-17

Wang, H. S., Pan, Z., Shi, W., Brown, B. S., Wymore, R. S., Cohen, I. S., et al. (1998). KCNQ2 and KCNQ3 potassium channel subunits: molecular correlates of the M-channel. *Science* 282, 1890–1893. doi: 10.1126/science.282.5395.1890

Watanabe, H., Nagata, E., Kosakai, A., Nakamura, M., Yokoyama, M., Tanaka, K., et al. (2000). Disruption of the epilepsy KCNQ2 gene results in neural hyperexcitability. *J. Neurochem.* 75, 28–33. doi: 10.1046/j.1471-4159.2000.0750028.x

Weckhuysen, S., Ivanovic, V., Hendrickx, R., Van Coster, R., Hjalgrim, H., Moller, R. S., et al. (2013). Extending the KCNQ2 encephalopathy spectrum: clinical and neuroimaging findings in 17 patients. *Neurology* 81, 1697–1703. doi: 10.1212/01.wnl.0000435296.72400.a1

Weckhuysen, S., Mandelstam, S., Suls, A., Audenaert, D., Deconinck, T., Claes, L. R., et al. (2012). KCNQ2 encephalopathy: emerging phenotype of a neonatal epileptic encephalopathy. *Ann. Neurol.* 71, 15–25. doi: 10.1002/ana.22644

Yue, C., and Yaari, Y. (2004). KCNQ/M channels control spike afterdepolarization and burst generation in hippocampal neurons. *J. Neurosci.* 24, 4614–4624. doi: 10.1523/JNEUROSCI.0765-04.2004

Yue, C., and Yaari, Y. (2006). Axo-somatic and apical dendritic Kv7/M channels differentially regulate the intrinsic excitability of adult rat CA1 pyramidal cells. *J. Neurophysiol.* 95, 3480–3495. doi: 10.1152/jn.01333.2005

Zaydman, M. A., and Cui, J. (2014). PIP2 regulation of KCNQ channels: biophysical and molecular mechanisms for lipid modulation of voltage-dependent gating. *Front. Physiol.* 5:195. doi: 10.3389/fphys.2014.00195

Zaydman, M. A., Silva, J. R., Delaloye, K., Li, Y., Liang, H., Larsson, H. P., et al. (2013). Kv7.1 ion channels require a lipid to couple voltage sensing to pore opening. *Proc. Natl. Acad. Sci. U. S. A.* 110, 13180–13185. doi: 10.1073/pnas.1305167110

Zhang, H., Craciun, L. C., Mirshahi, T., Rohacs, T., Lopes, C. M., Jin, T., et al. (2003). PIP(2) activates KCNQ channels, and its hydrolysis underlies receptor-mediated inhibition of M currents. *Neuron* 37, 963–975. doi: 10.1016/S0896-6273(03)00125-9

Zhang, J., Kim, E. C., Chen, C., Procko, E., Pant, S., Lam, K., et al. (2020). Identifying mutation hotspots reveals pathogenetic mechanisms of KCNQ2 epileptic encephalopathy. *Sci. Rep.* 10:4756. doi: 10.1038/s41598-020-61697-6

Zhang, J., and Shapiro, M. S. (2012). Activity-dependent transcriptional regulation of M-Type (Kv7) K(+) channels by AKAP79/150-mediated NFAT actions. *Neuron* 76, 1133–1146. doi: 10.1016/j.neuron.2012.10.019

Conflict of Interest: The authors declare that the research was conducted in the absence of any commercial or financial relationships that could be construed as a potential conflict of interest.

frontiers in Physiology

REVIEW
published: 28 October 2020
doi: 10.3389/fphys.2020.570588

The Role of Kv7.2 in Neurodevelopment: Insights and Gaps in Our Understanding

*Nina Dirkx[1], Francesco Miceli[2], Maurizio Taglialatela[2] and Sarah Weckhuysen[1,3,4]**

[1]*Applied and Translational Neurogenomics Group, VIB Center for Molecular Neurology, Vlaams Instituut voor Biotechnologie, Antwerp, Belgium,* [2]*Section of Pharmacology, Department of Neuroscience, University of Naples Federico II, Naples, Italy,* [3]*Department of Translational Neurosciences, Faculty of Medicine and Health Sciences, University of Antwerp, Antwerp, Belgium,* [4]*Department of Neurology, Antwerp University Hospital, Antwerp, Belgium*

Kv7.2 subunits encoded by the *KCNQ2* gene constitute a critical molecular component of the M-current, a subthreshold voltage-gated potassium current controlling neuronal excitability by dampening repetitive action potential firing. Pathogenic loss-of-function variants in *KCNQ2* have been linked to epilepsy since 1998, and there is ample functional evidence showing that dysfunction of the channel indeed results in neuronal hyperexcitability. The recent description of individuals with severe developmental delay with or without seizures due to pathogenic variants in *KCNQ2* (*KCNQ2*-encephalopathy) reveals that Kv7.2 channels also have an important role in neurodevelopment. Kv7.2 channels are expressed already very early in the developing brain when key developmental processes such as proliferation, differentiation, and synaptogenesis play a crucial role in brain morphogenesis and maturation. In this review, we will discuss the available evidence for a role of Kv7.2 channels in these neurodevelopmental processes, focusing in particular on insights derived from *KCNQ2*-related human phenotypes, from the spatio-temporal expression of Kv7.2 and other Kv7 family member, and from cellular and rodent models, highlighting critical gaps and research strategies to be implemented in the future. Lastly, we propose a model which divides the M-current activity in three different developmental stages, correlating with the cell characteristics during these particular periods in neuronal development, and how this can be linked with *KCNQ2*-related disorders. Understanding these mechanisms can create opportunities for new targeted therapies for *KCNQ2*-encephalopathy.

Keywords: KCNQ2, M-current, neurodevelopment, KCNQ2-encephalopathy, Kv7.2

OPEN ACCESS

Edited by:
Walter Sandtner,
Medical University of Vienna, Austria

Reviewed by:
Jerome J. Lacroix,
Western University of Health Sciences, United States
Isabella Salzer,
Medical University of Vienna, Austria

****Correspondence:***
Sarah Weckhuysen
sarah.weckhuysen@uantwerpen.vib.be

Specialty section:
This article was submitted to Membrane Physiology and Membrane Biophysics, a section of the journal Frontiers in Physiology

Received: *08 June 2020*
Accepted: *07 September 2020*
Published: *28 October 2020*

Citation:
Dirkx N, Miceli F, Taglialatela M and Weckhuysen S (2020) The Role of Kv7.2 in Neurodevelopment: Insights and Gaps in Our Understanding. Front. Physiol. 11:570588. doi: 10.3389/fphys.2020.570588

INTRODUCTION

The *KCNQ* gene subfamily consist of five members (*KCNQ1*–5), all encoding voltage-gated potassium (K^+) channel subunits (Kv7.1–5). The Kv7.1 subunit is predominantly expressed in the heart tissue, while Kv7.2-5 subunits are expressed most abundantly in the nervous system; Kv7.2 and Kv7.3 subunits expression is mostly restricted to the nervous system, whereas that of Kv7.4 and Kv7.5 subunits are more widespread, also including smooth and skeletal muscles (Sanguinetti et al., 1996; Schroeder et al., 2000; Cooper et al., 2001; Yeung et al., 2007). In adult neurons, Kv7 channels consist most frequently of tetramers containing Kv7.2 and Kv7.3, and more rarely Kv7.5 subunits (Wang et al., 1998; Schroeder et al., 2000). Independently of subunit composition,

all Kv7 channels generate voltage-dependent K^+ currents and represent the molecular basis of the M-current, a voltage-gated and K^+-selective current which derives its name from its suppression upon activation of M_1 muscarinic receptors (Brown and Adams, 1980). Muscarinic-dependent M-current suppression is caused by M_1 receptor-dependent activation of phospholipase C, which hydrolyses phosphatidylinositol-4,5-bisphosphate (PIP_2), a molecule which is necessary for Kv7 channel opening (Suh and Hille, 2002). The M-current is a slowly activating, non-inactivating, time- and voltage-dependent potassium current, which regulates the resting membrane potential (RMP) and dampens repetitive neuronal firing, thereby controlling neuronal excitability (Wang et al., 1998; Brown and Passmore, 2009).

During the last decade, an emerging number of studies pointed out that severe disruption of the function of Kv7.2, Kv7.3, and Kv7.5 subunits due to de pathogenic variants in the encoding gene leads to developmental and epileptic encephalopathy (DEE; Weckhuysen et al., 2012; Lehman et al., 2017; Lauritano et al., 2019). DEEs are a heterogeneous group of mostly neonatal-, infantile- or childhood-onset disorders characterized by severe, drug-resistant seizures, characteristic electroencephalographic (EEG) signatures, and different levels of developmental delay or regression, often with a poor prognosis. Although anti-seizure drugs can have some effect on seizure control in *KCNQ*-related DEEs, and several patients become seizure free after a few weeks to months, these patients invariably suffer from severe developmental delay (Pisano et al., 2015). A complex relationship is known to exist between epilepsy and neurodevelopment; before the most recent International League Against Epilepsy classification introducing the DEE term (Fisher et al., 2017), the most-commonly used term of "epileptic encephalopathy" was meant to highlight the classical belief that epileptic activity by itself is the primary cause of cognitive and developmental deterioration. However, some patients can have developmental impairment before seizure onset, or cognitive deterioration may progress despite complete seizure control; given the variable relationship between seizures and cognition, these conditions have been more recently referred to as DEEs. Thus, the possibility that the control exerted over neuronal excitability by Kv7.2, Kv7.3, and Kv7.5 subunits may play a role in neurodevelopment deserves to be investigated. In this review, we will focus on what is currently known about the role of Kv7.2 channels in neurodevelopment.

HUMAN PATHOGENIC *KCNQ2* VARIANTS AND NEURODEVELOPMENT

The best proof for a role of the M-current in neurodevelopment is the observation that pathogenic variants in *KCNQ2* are responsible for a spectrum of neurodevelopmental disorders in humans. Already in 1998, inherited pathogenic variants in *KCNQ2* were identified as a cause of benign familial neonatal epilepsy (BFNE; *KCNQ2*-B; Singh et al., 1998). This disorder is characterized by neonatal seizures, but development in these patients is generally normal (Maljevic and Lerche, 2014). However, the risk of seizure recurrence in BFNE individuals is 10–20 times higher than the general population (Plouin, 1994), and a few BFNE families with individuals affected with various degrees of developmental disability have been described (Dedek et al., 2003; Borgatti et al., 2004). In 2012, some heterozygous pathogenic variants in *KCNQ2* were surprisingly shown to result in DEE, with a developmental delay ranging from mild to profound, nowadays referred to as "*KCNQ2*-encephalopathy" (*KCNQ2*-E; Weckhuysen et al., 2012). Pathogenic variants in *KCNQ2* are shown to be the most common genetic cause of neonatal-onset DEE. A recent prospective cohort study showed that 83% of newborns with a DEE had an identifiable genetic etiology, of whom 40% had a pathogenic variant in *KCNQ2* (Shellhaas et al., 2017). The incidence of *KCNQ2*-E is reported to be 1–3/100.000 births (Lopez-Rivera et al., 2020). By contrast, only a handful of DEE patients with pathogenic variants in *KCNQ3* or *KCNQ5* have been described (Rauch et al., 2012; Epi4k Consortium et al., 2013; Lehman et al., 2017; Ambrosino et al., 2018; Kothur et al., 2018; Lauritano et al., 2019; Rosti et al., 2019; Sands et al., 2019).

Interestingly, the degree of developmental delay does not completely correlate with the frequency or severity of the epileptic seizures (Weckhuysen et al., 2013). Furthermore, there seems to be a clear distinction between pathogenic variants leading to either *KCNQ2*-B or *KCNQ2*-E (**Figure 1**). Pathogenic variants associated with *KCNQ2*-B are truncating (splice, nonsense, and frameshift), whole gene deletions, or heterozygous missense variants resulting in haploinsufficiency with a 20–30% reduction of the M-current density when mutant subunits are expressed together with wild-type subunits in heterologous cell systems (Maljevic and Lerche, 2014). *KCNQ2*-E, on the other hand, is caused by heterozygous missense or in-frame indel mutations shown to have a dominant negative (DN; >50% reduction of the M-current density), or more rarely gain of function effect (GOF; >100% of the M-current density) when co-expressed with wild-type subunits (Miceli et al., 2013, 2015). Interestingly, *KCNQ2* GOF variants can lead to distinct neurodevelopmental phenotypes. For example, patients with the mild GOF variant R198Q present infantile spasms without prior neonatal seizure (Millichap et al., 2017), whereas patients with the strong GOF variants R201C/H showed severe neonatal-onset encephalopathy without neonatal seizures but prominent startle-like myoclonus and a burst-suppression EEG pattern

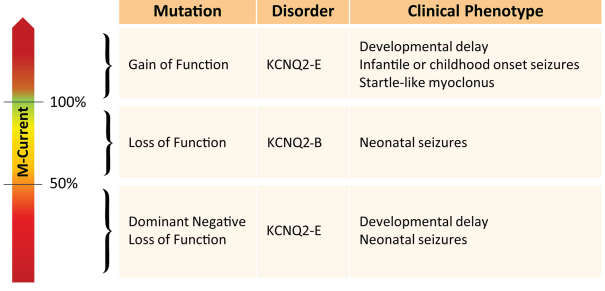

FIGURE 1 | Overview of the effect of different KCNQ2 pathogenic variants on the M-current and their associated clinical phenotype.

(Mulkey et al., 2017). *KCNQ2* has also gained interest in the field of autism spectrum disorder (ASD). First of all, many of the reported *KCNQ2*-E patients show autistic features or have ASD as a behavioral comorbidity (Milh et al., 2013; Millichap et al., 2016). Second, *KCNQ2* variants are also commonly identified in genetic studies on ASD cohorts (Jiang et al., 2013; Long et al., 2019). The mechanism by which two opposite effects on the M-channel, either a reduction of more than 50% of the M-current (DN effect) or an increase of the M-current density (GOF effect), both lead to developmental delay, is not known yet. However, this shows that the level of the M-current has to be regulated in a very precise manner to maintain homeostasis of the neuronal network.

Heterologous cellular systems have been used abundantly to study the functional consequences of human pathogenic *KCNQ2* variants, and electrophysiological assays have been used as a read-out to assess genotype-phenotype correlations (Orhan et al., 2014; Abidi et al., 2015; Miceli et al., 2015; Millichap et al., 2017; Kim et al., 2018; Soldovieri et al., 2019). These systems have the advantage of being relatively straightforward, cost-efficient, and relatively high-throughput (Maljevic et al., 2017). The disadvantage of this approach is that the lack of native-neuronal environment may influence channel behavior in such a way that those variant-induced functional changes that affect channel subcellular localization or interaction with neuronally-expressed proteins may not become apparent. This was demonstrated by two recent studies on two different recurrent *KCNQ2*-E variants, A294V and R560W. Both generated similar currents as seen for *KCNQ2*-B variants when overexpressed in heterologous systems (Orhan et al., 2014; Abidi et al., 2015). The DN effect could only be observed in transfected neurons; the A294V variant altered distribution of Kv7.2 containing channels to the somato-dendritic compartment, while the R560W variant reduced Kv7.2 axonal surface expression and impaired gating regulation by phosphoinositides (Kim et al., 2018). This data underline the importance of a neuronal environment to fully understand the disease pathomechanism(s) triggered by each pathogenic *KCNQ2* variant.

An interesting side note is that the Kv7.2 channel has several accessory proteins, many of which are also associated with neurodevelopmental disorders. *SCN1B* encodes for $Na_V\beta1$, a multifunctional molecule that is involved in modulation of sodium and potassium channels (including Kv7.2 channels), neurite outgrowth, axon pathfinding, and cell migration (Brackenbury and Isom, 2011; Nguyen et al., 2012). Bi-allelic pathogenic variants in the *SCN1B* gene are linked with DEE with phenotypic properties similar to Dravet syndrome, whereas heterozygous pathogenic variants lead to generalized epilepsy with febrile seizures plus (Scheffer et al., 2007; Aeby et al., 2019). Another important accessory protein of the Kv7.2 channel is Ankyrin-G, which is encoded by the *ANK3* gene. Ankyrin-G has the essential role to anchor the Kv7.2 subunit at the axon initial segment (AIS) and nodes of Ranvier (Devaux et al., 2004; Pan et al., 2006). Heterozygous pathogenic missense variants have been linked to intellectual disability, ASD, bipolar disorder, and schizophrenia (Ferreira et al., 2008; Bi et al., 2012; Iqbal et al., 2013). Lastly, syntaxin-1A is a member of the soluble N-ethylmaleimide-sensitive fusion protein attachment protein receptors (SNARE) superfamily. The SNARE protein complex facilitates the docking and fusion of synaptic vesicles at presynaptic membrane to enable neurotransmission (Rizo, 2018). Syntaxin-1A can bind to the C-terminus of Kv7.2 subunit, thereby decreasing open probability *via* facilitation of the interaction between the C-terminus and the N-terminus (Regev et al., 2009). To date, malfunction of syntaxin-1A itself is not known to be directly associated with neurodevelopmental disorders, however, pathogenic variants in the gene that encodes for the binding partner syntaxin binding protein 1 (STXBP1) are known to cause several DEE forms including a similar phenotype to *KCNQ2*-encephalopathy (Stamberger et al., 2016). STXBP1-Loss-of-function (LOF) mutations results in an increased binding of syntaxin-1A to the Kv7.2 channel, and thus, a decrease in M-current density (Devaux et al., 2017). Therefore, alterations in M-current density could be a convergence point between STXBP1-E and *KCNQ2*-E.

SPATIOTEMPORAL EXPRESSION OF Kv7.2 SUBUNIT AND ITS RELATION TO NEURODEVELOPMENT

In this section, we will focus on Kv7.2 channel expression in the central nervous system. However, it should be noted that Kv7 channels are also expressed in the peripheral nervous system (PNS) (Passmore et al., 2003). To date, only few studies are available regarding the Kv7 subunit distribution in the PNS; nonetheless, most of those document a high Kv7.2 and Kv7.3 subunits expression in rat small-diameter dorsal root ganglionic neurons and non-myelinated C fibers (Passmore et al., 2003; King and Scherer, 2012; Huang et al., 2016). In rat peripheral sciatic nerves, most small- and medium-sized axons were shown to express Kv7.2/Kv7.3 heteromers, while in the largest sciatic nerve axons, mostly Kv7.2 homomers are observed (Cooper, 2011).

Kv7.2 Subunit Expression in Mature Neurons in the CNS

Kv7.2 channels are expressed widely throughout the brain in both excitatory and inhibitory neurons. In the adult human brain, immunohistochemistry shows a high level of Kv7.2 channels in the cortex, and lower levels in the hippocampus (Cooper et al., 2000). Within the neuron, Kv7.2 channels are located at the AIS, nodes of Ranvier, the soma, and presynaptic terminals (Cooper et al., 2001; Cooper, 2011). Depending on the Kv7.2 channel subcellular localization in the neuron, Kv7.2 subunits may play different roles. In fact, at the AIS and nodes of Ranvier, Kv7.2 has an important role in stabilizing the RMP and increasing the steady state availability of the sodium channels (Nav) (Battefeld et al., 2014). At the soma, it is a key player for the inhibition of repetitive action potential firing by attenuating after depolarization, and at presynaptic terminals of neurons, the Kv7.2 channel has been shown to regulate presynaptic neurotransmitter release (Martire et al., 2004; Luisi et al., 2009; Regev et al., 2009; Battefeld et al., 2014).

Temporal Regulation of *KCNQ2* Transcripts and Kv7.2 Subunit Expression During Neurodevelopment

KCNQ2 Transcripts Expression During Neurodevelopment

KCNQ2 transcripts are already significantly expressed at the stem cell stage and during the whole course of neurodevelopment, with different transcripts showing differences in temporal expression. *KCNQ2* has six curated transcripts based on the Reference Sequence (RefSeq) database. Transcript a (NM_172107) is the canonical transcript and counts 17 exons. The two most studied transcripts are transcript c (NM_004518; contains a distinct three prime untranslated region and is missing exon 9 and 12) and d (NM_172108; missing exon 12 and has a shorter exon 13), both generating functional channels (Orhan et al., 2014; Abidi et al., 2015; Ambrosino et al., 2015; Devaux et al., 2017). This suggests that exon 9 and 12 are not essential to form a functional channel. In support, no known *KCNQ2*-E pathogenic variant is located in these exons. Transcript b (NM_172106) and f (NM_001382235), both missing exon 12, are not well studied. Lastly, transcript e (NM_172109) is a shorter *KCNQ2* transcript. It consists of exon 1 until exon 8 and has an alternative extension of exon 8 due to alternative splicing, which results in a frameshift. This shorter *KCNQ2* transcript is expressed most abundantly in the fetal brain and its expression levels decrease during neuronal development. Therefore, we will refer to this transcript as the "short fetal transcript." The opposite is seen for the longer *KCNQ2* transcripts; they are upregulated during neuronal differentiation and increase with ongoing maturation (Smith et al., 2001); however, the probe used in this study recognizes all transcripts, thus, the specific role of each individual transcript cannot be assessed. Nonetheless, in support of this human brain tissue study, the transcriptome data from the LIBD stem cell browser[1] show a similar temporal expression pattern for the different *KCNQ2* transcripts in induced pluripotent stem cells (iPSCs) and iPSC-derived neuronal cells. This database shows the expression of all exons over the course of neuronal development, from self-renewal toward neuronal progenitor cells (NPCs) and neurons. Interestingly, the data show that exon 1 until 8 (present in the short fetal transcript) are already significantly expressed during the self-renewal stage, and expression stays relatively stable throughout neuronal development. Exon 10–11 and 13–17, but not exon 9 and 12, show a low expression in the self-renewal and NPC stage, with an increased expression when NPCs differentiate into neurons. Lastly, exon 9 and 12 only show a significant expression in neurons. Because transcript c is the only curated long transcript that is missing exon 9 and 12, this suggests that transcript c is the longer transcript seen in self-renewal and NPC stage. Indeed, the expression of the short fetal transcript and transcript c in iPSCs and embryonic stem cells (ESCs) was confirmed in other studies, where they even demonstrated that *KCNQ2* shows the highest expression of all ion channels (Wang et al., 2005; Jiang et al., 2010; Linta et al., 2013). It should, however, be noted that we cannot rule out that additional alternative transcripts without exon 9 and 12 exist that are not included in the curated RefSeq transcripts.

[1]http://stemcell.libd.org/scb/

So far, on a protein level, the expression of these different transcript has not been studied during early neurodevelopmental stages. The presence of a shorter transcript of ~40 kDa on western blot has only been observed in adult mouse brain using an antibody targeting the N-terminal of the Kv7.2 subunit (which is conserved among all the Kv7.2 transcripts; Cooper et al., 2001). The size of this transcript is similar to the predicted size of protein encoded by the short fetal transcript. Unfortunately, no subsequent effort has been made in investigating this shorter transcript further.

M-Current Density During Neurodevelopment

Functional Kv7.2-containing channels are expressed early in neurodevelopment, and their expression increases during development, thereby influencing neuronal differentiation by altering the neuronal membrane potential. Not with standing the ample evidence at the transcript level for expression of Kv7.2 transcripts c and e from the stem cell stage, evidence at the protein level is so far lacking. In this context, it is however interesting to note that HEK293T cells transfected with the short fetal transcript do not generate a detectable M-current. Co-transfection with the short fetal transcript and the canonical transcript a suppresses the M-current density compared to transfection with transcript a alone (Smith et al., 2001). At the time of this publication, the necessity of PIP2 binding for the opening of the channel was not known yet (Suh and Hille, 2002). Based on the knowledge we have today, the short fetal transcript misses two important PIP2 binding sites, located at the A-B linker and B-C linker (Hernandez et al., 2008; Kim et al., 2018; Zhang et al., 2020). Therefore, if the short fetal Kv7.2 subunit would reach the plasma membrane and would form tetramers, this would result in a strongly reduced open probability of the channel due to reduced PIP2 binding. However, it is very unlikely that the short fetal Kv7.2 subunit will reach the plasma membrane, as it also lacks the subunit-interaction domain (SID), important for tertramerization, and the calmodulin domain, important for the transport to the plasma membrane (Schwake et al., 2003; Cavaretta et al., 2014).

Kv7.2 subunits are nevertheless definitely present at the plasma membrane of immature neurons, and levels are shown to increase during differentiation (Safiulina et al., 2008; Figueiro-Silva et al., 2015; Telezhkin et al., 2018). A low M-current density and a weak Kv7.2 channel expression was shown in neonatal mouse P0 CA3 neurons using a C-terminal antibody recognizing the long transcripts. After the first postnatal weeks, both the M-current density and Kv7.2 channels markedly increase. The low expression of Kv7.2 channels in neonatal neurons allows intrinsic bursting and neuronal synchronization, leading to generation of giant depolarizing potential, which are important for hippocampal network stabilization (Safiulina et al., 2008). Moreover, during neuronal differentiation of iPSC-derived neurons, hyperpolarization of the RMP was shown to be correlated with the expression levels of Kv7.2/3 (Telezhkin et al., 2018). The RMP is a known regulator of cell fate, as highlighted in several studies (Sontheimer et al., 1989; Ng et al., 2010; Rao et al., 2015). To initiate differentiation, mouse embryonic stem cells (mESC) become more depolarized to enter the G1/G0 phase, after which the cell gradually hyperpolarizes during differentiation (Ng et al., 2010). Therefore, more mature differentiated neurons

have a more hyperpolarized RMP compared to immature neurons. It is thus not surprising that forced membrane potential changes can alter the fate of cells. (MacFarlane and Sontheimer, 2000; Sundelacruz et al., 2008). This is in line with the observation that overexpression of Kv7.2/3 channels speeded up the maturation of the iPSC-derived neurons and facilitated spontaneous firing, by forcing the RMP to reach the optimal range for Nav channel activation (Telezhkin et al., 2018).

Based on the currently available studies outlined above, we hypothesize that there are three crucial, temporally-distinct phases in M-current density regulated by *KCNQ2* transcript expression that coordinate proper neuronal development. A schematic overview is provided in **Figure 2**.

Phase 1, occurring at very early developmental stages in which a very low M-current density correlates with a strongly depolarized RMP of the cells, a necessary prerequisite to maintain a high proliferation to differentiation ratio. The *KCNQ2* expression profile during this period, i.e., a high expression of short fetal *KCNQ2* and low expression of long *KCNQ2*, makes us believe that the short fetal Kv7.2 isoform serves as guard to prevent a large M-current to be generated and prevent hyperpolarization of the cell. Therefore, it may be hypothesized that pathogenic variants in *KCNQ2* that reduce the M-current will not lead to large clinical consequence during Phase 1.

Phase 2, in which an enhanced M-current density occurs as a consequence of a gradual increase in Kv7.2 expression, in order to support neuronal differentiation. A tight regulation of fetal and long Kv7.2 isoforms expression is necessary for a gradual increase in M-current density to hyperpolarize the RMP during differentiation. During the second phase, the first clinical consequence of Kv7.2-mediated developmental channelopathy can be expected.

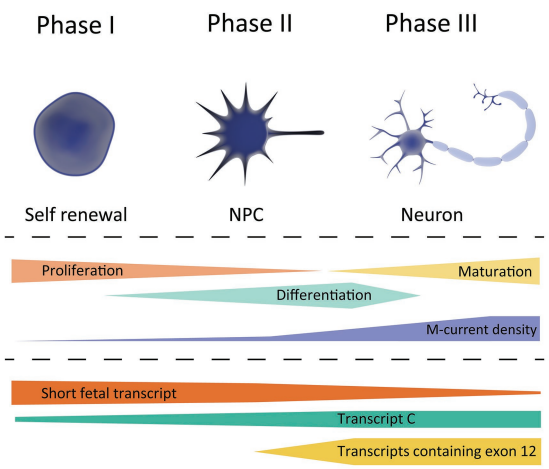

FIGURE 2 | Schematic overview of *KCNQ2* transcript expression during the different phases of neuronal development. Top, showing the different cell types during differentiation; stem cell (left), neuronal progenitor cell (NPC, middle), and neuron (right). Middle, showing the cell characteristics during neuronal development, and its correlation with the M-current density. Bottom, expression profile of the different *KCNQ2* transcripts based on the data exported from the LIBD stem cell browser.

Finally, **Phase 3**, when a stable M-current density and Kv7.2 expression supports neuronal maturation, corresponding mainly to the postnatal period. During this phase, Kv7.2 channels fulfill their better-known role in neurons; regulating the RMP, dampening repetitive firing, and controlling neurotransmitter release. In this phase, pathogenic variants in *KCNQ2* would lead to the different (mostly-neonatal) phenotypes of *KCNQ2*-B or *KCNQ2*-E, depending on the extent of M-current functional derangement.

Temporal Regulation of Kv7.2 and Kv7.3 Subunit Expression

In addition to the temporal changes in Kv7.2 subunit expression during development, available data also suggest a time-dependent regulation of the expression of other members of the Kv7 subfamily, the Kv7.3 subunit in particular. In mice, Kv7.2 subunits are already significantly expressed at birth, and its levels are relatively stable or even increase postnatally (Tinel et al., 1998; Safiulina et al., 2008). Expression of Kv7.3 subunit, on the other hand, is very low at birth and gradually increases to eventually become even higher than that of Kv7.3 subunit (Tinel et al., 1998; Zhang et al., 2016). Therefore, the ratio of M-channels consisting of Kv7.2 homomers and Kv7.2/Kv7.3 heteromers will shift during development. A similar pattern of age-dependent expression, with Kv7.2 subunits being already detected in fetal life and Kv7.3 subunits increasing from late fetal life to infancy, has also been shown in human brain tissue (**Figure 3**; Kanaumi et al., 2008). Interestingly, the M-current density of the Kv7.2/Kv7.3 heteromers is 3.8 times bigger than Kv7.2 homomers (Selyanko et al., 2001). Furthermore, when studying DN *KCNQ2*-E variants in heterologous cell systems, the incorporation of the Kv7.3 subunit is able to (partially) rescue the mutational effect on the M-current observed in homomeric Kv7.2 channels (Gomis-Perez et al., 2019). Therefore, the differences in the

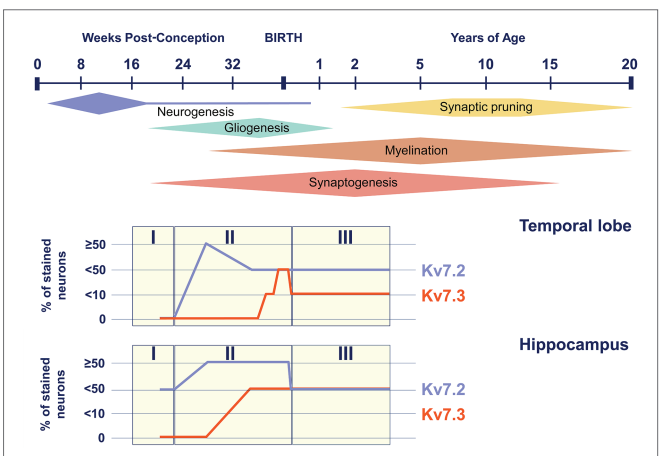

FIGURE 3 | Kv7.2 and Kv7.3 expression during human brain development. Top, timeline of key neural developmental cellular processes in the human brain (adapted from Semple et al., 2013). Bottom, representation of Kv7.2 and Kv7.3 positive neurons in the temporal lobe and the hippocampus during the three neurodevelopmental phases (adapted from Kanaumi et al., 2008).

temporal expression of Kv7.2 and Kv7.3 subunits probably contribute to the typical age-dependent characteristics of *KCNQ2*-related disorders: (i) the neonatal or even prenatal onset, at a time where Kv7.2 homomers are the predominant M-channels and (ii) the transient epileptic phenotype in which the increased expression of Kv7.3 subunits could play a role (Singh et al., 1998; Weckhuysen et al., 2012).

Kv7.2 Subunit Expression in Fetal Astrocytes

RNA sequencing data show preliminary evidence for early expression of kv7.2 subunits in human astrocytes. In a study on bulk RNA extracted from isolated cell types from mouse and both fetal and adult human cortex, a high expression of *KCNQ2* was found in neurons and oligodendrocyte precursor cells of mice, whereas in humans, the highest expression of *KCNQ2* was found in fetal astrocytes or astrocyte precursor cells, with rather low expression in neurons (Zhang et al., 2016). Open source, adult human brain, single-nuclei RNAseq databases such as the Allen Brain Map[2] and the UCSC cell browser,[3] on the other hand, show expression of *KCNQ2* in neurons, but no clear evidence of *KCNQ2* in astrocytes, suggesting expression in astrocytes is restricted to the early neurodevelopmental period. To date, no proof exists for a functional role of Kv7.2 channels in astrocytes. However, if this proves to be the case, this could open a whole new level of complexity to *KCNQ2*-related disorders, as astrocytes are known to contribute to the maintenance and formation of neuronal circuits and are known to play a role in the pathogenesis of several neurodevelopmental disorders, including ASD, Rett syndrome, and Fragile X (Molofsky et al., 2012; Sloan and Barres, 2014; Petrelli et al., 2016)

NEURONAL CELL MODELS AS A TOOL TO STUDY THE ROLE OF Kv7.2 SUBUNITS IN NEURODEVELOPMENT

A common method to study the function of M-channels is the use of pharmacological blockers or openers in *in vitro* or *ex vivo* cell models. Retigabine and flupirtine are the most commonly used openers and have a specificity for Kv7.2-5 subunits (Gribkoff, 2003; Yeung et al., 2008). In 2011, retigabine was approved as a treatment for epilepsy by the Food and Drug Administration and the European Medicines Agency; however, it was withdrawn from the market in June 2017 due to side effects including blue discoloration of skin and retina (Tompson et al., 2016). 10,10-bis(pyridin-4-ylmethyl)anthracen-9-one (XE991) and linopirdine are the most commonly used Kv7 channel blockers, both inhibiting all members of the Kv7 family. When interpreting these pharmacological studies, it is, thus, important to realize that none of these drugs are truly Kv7.2 subunit specific.

A clear distinction should also be made between studies using acute and chronic interventions. Acutely blocking the M-current in neurons is known to increase the intrinsic excitability, whereas chronic blocking gradually reduces the intrinsic excitability again. The chronic block induces a compensatory distal shift of the AIS and a relocation away from the soma of Nav and Kv7-channels, thus, again stabilizing network excitability (Lezmy et al., 2017). Chronical blocking of the M-current does not only influence excitability properties but has also been shown to alter neurodevelopmental processes, such as neurite outgrowth and synaptogenesis in different neuronal cell models (an overview of the studies is given in **Table 1**).

Chronic blocking of the M-current with XE991 in PC12 and P0 rat cortical neurons was shown to result in an increased neurite outgrowth, while retigabine had the opposite effect (Zhou et al., 2016). Additionally, Kv7.2 channels have been described to play a key role in the regulation of synaptic plasticity through its interaction with neuronal pentraxin 1 (NP1) at presynaptic terminals of excitatory synapses and the axonal growth cones of fetal cortical neurons. Chronic blocking of Kv7.2 channels in these neurons increases excitatory synaptogenesis (Figueiro-Silva et al., 2015). Remarkably, another study using chronic XE991 treatment in differentiating mESC and embryonic hippocampal neurons was shown to decrease synaptic and vesicular proteins in inhibitory neurons but not in excitatory neurons (Zhou et al., 2011). A possible explanation for these opposite results could be the difference in studied cell type and cell maturity between the two studies, as Kv7 subunits and transcripts show distinct expression levels, spatial expression, and interactors depending on cell type and maturity stage.

MOUSE MODELS AS TOOLS TO STUDY THE ROLE OF Kv7.2 SUBUNITS IN NEURODEVELOPMENT

To date, animal models have led to many fundamental discoveries of brain function and have given us a better understanding

TABLE 1 | Overview of *in vitro* studies that use pharmacological blockers or openers to chronically block the M-current.

Cell type	Intervention	Observed effect	References
P0–2 mouse hippocampal CA1 pyramidal neurons	Acute XE991	Increased the intrinsic excitability	(Lezmy et al., 2017)
	Chronic XE991	Gradual decrease in intrinsic excitability and a distal shift of AIS	
PC12 and P0 rat cortical neurons	Chronic XE991	Increased neurite outgrowth	(Zhou et al., 2016)
	Chronic retigabine	Decreased neurite outgrowth	
Rat fetal cortical neurons	Chronic linopiridine	Increased excitatory synaptogenesis	(Figueiro-Silva et al., 2015)
mESC and mouse embryonic hippocampal neurons	Chronic XE991 or chronic linopirdine	Decreased synaptic and vesicular proteins in inhibitory, but not excitatory neurons	(Zhou et al., 2011)

P0–2, 0–2 days postnatally; CA1, cornu ammonis 1; XE991, 10,10-bis(pyridin-4-ylmethyl)anthracen-9-one; AIS, axon initial segment; PC12, pheochromocytoma 12; mESC, mouse embryonic stem cells.

[2]https://celltypes.brain-map.org/rnaseq/human/cortex
[3]https://autism.cells.ucsc.edu/

of the regulation of neurodevelopmental processes. Both knockout (KO) or knock-in (KI) mice models have been generated to study the role of Kv7.2 channels *in vivo*.

KCNQ2 KO Mouse Models

The first mouse models to study the function of Kv7.2 channels were KO models, some generated already 2 decades ago. They have taught us that specific neuronal subtypes are more vulnerable to changes in Kv7.2 expression levels and/or function, and especially that loss of Kv7.2 channels leads to complex homeostatic network changes that generally favor hyperexcitability. Heterozygous deletion of *KCNQ2*, engineered in attempt to mimic the human BFNE genotype, fails to prompt spontaneous seizures but lowers the seizure threshold to proconvulsants in adult mice (Watanabe et al., 2000; Yang et al., 2003). The focus of these earlier studies was mainly on seizure susceptibility, as Kv7.2 was not linked yet to behavioral abnormalities. With the current evidence that the Kv7.2 channel plays a role in neurodevelopment and that variants in *KCNQ2* are enriched in ASD cohorts, the *KCNQ2* KO model was also subjected to extensive behavioral analysis; an in-depth behavioral study, indeed, recently showed autism-associated behaviors such as a decrease in social behavior and enhanced repetitive behaviors in *KCNQ2* heterozygous KO mice (Kim et al., 2020).

Homozygous *KCNQ2* KO mice die within hours after birth, which highlights the importance of Kv7.2 channels for survival. To circumvent lethality, brain region-specific *KCNQ2*-null mice have been developed to enable studying complete Kv7.2 channel loss in specific cell types (Soh et al., 2014, 2018; Niday et al., 2017). Transgenic mice with conditional deletion of *KCNQ2* in cortical pyramidal neurons are characterized by abnormal electrocorticogram activity and early death and showed increased excitability of CA1 pyramidal neurons. Interestingly, *KCNQ2*-null neurons did not show alterations in the RMP although they presented a decrease by ~85% of the M-current, suggesting that the contribution of K7.2 subunits to the RMP in p15-p20 mice cerebral cortical pyramidal neurons is small and/or that homeostatic adaptations occur to correct for the absence of Kv7.2 channels (Soh et al., 2014). A follow-up study furthermore showed neuronal hyperexcitability in layer 2/3 pyramidal neurons and alterations in action potential properties (AP), including increase in AP amplitude, decrease in medium after hyperpolarization (mAHP) and a (subsequent) increase in AP frequency (Niday et al., 2017). Specific ablation of Kv7.2 in interneurons, on the other hand, led to elevated excitability of parvalbumin positive (PV+), but not somatostatin positive, neurons. This, in turn, resulted in homeostatic potentiation of excitatory transmission in pyramidal neurons and increased seizure susceptibility in PV-*KCNQ2* null mice (Soh et al., 2018). Importantly, this study shows that Kv7.2 loss induced an increase in interneuron excitability, which influences the course of excitatory network development. In this respect, it is important to point out that γ-aminobutyric acid (GABA) drives excitatory synapse maturation and formation in pyramidal neurons and that early in neurodevelopment, GABA is known to act as an excitatory, instead of an inhibitory neurotransmitter, due to high $Na^+ - K^+ - Cl^-$ cotransporters 1 (NKCC1) expression (Li and Xu, 2008; Le Magueresse and Monyer, 2013).

KI Mouse Models of Human Pathogenic *KCNQ2* Variants

Most KI mouse models published so far express human *KCNQ2*-B variants and show a decreased seizure threshold similar to the heterozygous KO mice (Singh et al., 2008; Tomonoh et al., 2014). Interestingly, the BFNE *KCNQ2*-Y284C KI mouse also showed an increase in presynaptic GABA release at brain examination in the first postnatal week (Uchida et al., 2017). Because of the excitatory behavior of GABA early in neurodevelopment, the M-current is one of the most important regulators of neuronal inhibition during this period (Peters et al., 2005). Therefore, the combination of a reduction of the M-current and an increase in GABA release is believed to strongly contribute to the observed neonatal brain hyperexcitability in *KCNQ2*-B.

Until recently, the only genetic *KCNQ2*-E mouse model that had been published was a conditional overexpression model of the DN *KCNQ2*-G279S variant, inserted on the mouse X chromosome (Peters et al., 2005). This variant was modeled based on a DN variant in *KCNQ1*, and has, in the meantime, been described in a patient with *KCNQ2*-E (Sharawat et al., 2019). The mice displayed spontaneous seizures, as well as cognitive and behavioral impairments when scored with the Morris water maze and open-field tests. Morphological characterization of the hippocampus showed loss of mossy fiber terminals in the infrapyramidal layer. Remarkably, the observed phenotype was reversed when mutated *KCNQ2* expression was turned off, using a Tet-off system, in the first postnatal weeks (Peters et al., 2005). In a follow-up study, the authors showed that bumetanide treatment during this same critical period also resulted in a rescue of the phenotype (Marguet et al., 2015). Bumetanide is a NKCC1 antagonist reducing the GABA-mediated depolarization that is seen in early neurodevelopment (Wang and Kriegstein, 2011). In conclusion, both the model with conditional *KCNQ2* KO in PV+ neurons discussed above, the *KCNQ2*-Y284C KI and the *KCNQ2*-E overexpression mouse models, point toward an important role for GABA during early neurodevelopment in *KCNQ2*-related disorders.

Very recently, the first KI mouse model of a recurrent *KCNQ2*-E variant, *KCNQ2*-T274M, has been published, reproducing several phenotypic traits of human *KCNQ2*-E (Weckhuysen et al., 2012; Milh et al., 2020). These mice show learning and memory deficits when tested in the Morris water maze or the Barnes maze, as well as reduced exploratory behavior, suggesting that hippocampal dysfunction is involved in the disease pathology, although no abnormalities were observed upon morphological examination of the hippocampus. Furthermore, these mice present spontaneous clinical seizures starting from P20, which are rarely observed after P100 (Milh et al., 2020). This nicely mimics what is seen in patients, as most of them become seizure free a few months after seizure onset (Weckhuysen et al., 2012). This mouse model will contribute significantly to the understanding of *KCNQ2*-E phenotypic traits, which are often impossible to fully recapitulate in simplistic cell models and will be a very valuable tool for future drug discovery (Maljevic et al., 2017).

THE ROLE OF Kv7.2 CHANNELS IN NEURODEGENERATION

The role of the Kv7.2 channel in neurodegeneration is not the focus of this review; however, it is interesting to note that common genetic variation in *KCNQ2* has recently been associated with risk of cognitive decline in healthy elderly (Bonham et al., 2018). Furthermore, some evidence exists for an (indirect) role of Kv7.2 in neurodegeneration disorders. Amyloid beta (Aβ) oligomers, involved in the pathogenesis of Alzheimer's disease (AD), were reported to reduce Kv7.2 expression, resulting in a decrease of the M-current (Colom et al., 2011; Leao et al., 2012; Duran-Gonzalez et al., 2013; Mayordomo-Cava et al., 2015). In the medial septal neurons in mice, Aβ seems to reduce the M-current only in the glutamatergic neurons, resulting in increased firing and altered medial septal rhythmicity (Leao et al., 2012). As the medial septal nucleus is a key to generate the theta waves in the hippocampus, which is important for memory formation, alterations in the rhythmicity might underlie the cognitive deficits in AD patients (Winson, 1978; Seager et al., 2002). If the hypothesis is correct that hyperexcitability contributes to cognitive decline, specific Kv7.2 channels openers could be of benefit in AD patients. This could also be part of the explanation why no significant improvements in cognition were observed during a clinical trial of linopirdine, a Kv7.2 blocker, in AD patients (Rockwood et al., 1997). Furthermore, Kv7.2 channels openers could also be beneficial for Huntington's disease (HD), as retigabine has been reported to rescue the electrophysiological and behavioral phenotype of transgenic HD model (Cao et al., 2015). Moreover, retigabine was described to block the hyperexcitability and to improve motor neuron survival of iPSC-derived motor neurons from amyotrophic lateral sclerosis patients (Wainger et al., 2014). Lastly, for Parkinson's disease, several studies have shown that blocking of Kv7 channels with XE991 increased excitability of the dopaminergic neurons and has a neuroprotective effect toward dopaminergic degeneration in a mouse model of Parkinson's disease (Shi et al., 2013; Liu et al., 2018). Altogether, those results support the idea that Kv7 subunits, possibly including Kv7.2 subunits, are interesting therapeutic target for different neurodegenerative diseases and cognitive impairment.

FURTHER PERSPECTIVES

Since the discovery of the *KCNQ2* gene in 1998, *KCNQ2*-encoded Kv7.2 subunits have been studied extensively (Singh et al., 1998). Although multiple lines of evidence show that Kv7.2 channels are involved in neurodevelopment, most studies have focused on the function of the Kv7.2 channels in a mature neuronal environment. Therefore, in this review, we highlight the importance of Kv7.2 in (early) neurodevelopment. Thanks to the increasing use of RNA-sequencing and the availability of transcriptome databases, a large amount of information on *KCNQ2* expression has become available, leading to the consensus that an increasing expression of this gene is consistently observed during neuronal development (Safiulina et al., 2008; Telezhkin et al., 2018). Interestingly, multiple transcriptome datasets show evidence for the expression of a shorter fetal *KCNQ2* transcript (transcript e) in iPSCs and neuronal derivatives, in addition to the longer transcript transcript c (Wang et al., 2005; Jiang et al., 2010; Linta et al., 2013). The presence of the short transcript was already reported in 2001 in brain, both at the transcript and protein levels; however, no follow up studies investigating this transcript were performed (Cooper et al., 2001; Smith et al., 2001). Unfortunately, functional evidence for the presence of Kv7.2 protein at stem cell and neuronal progenitor stages is currently lacking. Future studies confirming or negating the presence of Kv7.2 isoforms in stem cells will be needed to clarify this issue. In the meantime, and based on the available data, we introduce a model dividing the M-current density in three phases: (1) very low density important to maintain cell proliferation, (2) increasing M-current density to hyperpolarize the membrane and support neuronal differentiation, and (3) a stable high M-current density present in maturing or mature neurons to dampen repetitive firing and control neurotransmitter release.

Regarding human disease related to Kv7.2 channel dysfunction, more specifically *KCNQ2*-E, it is clear that pathology goes beyond a simple increased open or closed state of the channel, but includes impact on temporo-spatial expression levels, binding partners, and widespread homeostatic network changes that are difficult to study in simplified models. The recent publication of a *KCNQ2*-E KI mouse model is certainly promising and will be an important tool for further in-depth studies (Milh et al., 2020). Another promising model that would contribute to our understanding of the role of Kv7.2 channels in neurodevelopment is neuronal cultures derived from human iPSCs, as they provide the neuronal environment which is lacking in heterologous cell systems. Their ability to differentiate in several different brain cell types allows us to look not only at network changes but also to the contribution of different cell types to pathology. They are especially useful in the study of neurodevelopmental disorders, since they largely recapitulate fetal development (Tidball and Parent, 2016; Logan et al., 2019). Compared to monolayer neuronal cultures, brain organoids have the ability to foster even more complex cell interactions that stimulate cellular maturation, better recapitulating potential pathological cascades (Logan et al., 2019). Both 2D iPSC-derived neuronal cultures and 3D brain organoids have already successfully been used for the study of several neurodevelopmental disorders to identify disease mechanisms and potential new therapeutic targets (Fink and Levine, 2018; Russo et al., 2019). To date, no iPSC-derived neuronal model for *KCNQ2*-E has been reported in the literature yet. Furthermore, the current research performed to understand the role of the Kv7.2 channel in neurodevelopment has focused mainly on LOF of Kv7.2 channels, whereas *KCNQ2* GOF variants give rise to an at least equally severe neurodevelopmental phenotype in human patients (Miceli et al., 2015). How both DN and GOF variants lead to neurodevelopmental delay is not understood yet. Future efforts comparing the effects of both DN and GOF variants on the neuronal network *in vitro* and *in vivo* are necessary to understand how Kv7.2 regulates neurodevelopment and can potentially open new doors for innovative therapeutic tools. Lastly, the development of Kv7 channel blockers and openers overcoming some of the

pharmacokinetic and pharmacodynamic limitations shown by the available drugs (all of which have been synthesized and started to be developed well before the discovery of the *KCNQ* gene subfamily and the description of their multiple pathophysiological roles) could not only be beneficial for patients suffering from *KCNQ2*-B and *KCNQ2*-E but could also positively impact patients affected with multiple neurodegenerative disorders (Wainger et al., 2014; Kumar et al., 2016; Ostacolo et al., 2020).

AUTHOR CONTRIBUTIONS

All authors listed have made a substantial, direct and intellectual contribution to the work, and approved it for publication. ND and SW designed the scope and structure of the review. ND, SW, FM, and MT wrote and edited the final manuscript.

FUNDING

ND receives support from FWO-SB (1S59219N) and SW receives support from FWO-FKM (1861419N) and GSKE. MT receives support from the Italian Ministry for University and Research (PRIN 2017ALCR7C). FM receives support from the Italian Ministry for University and Research (Project Scientific Independence of Researchers 2014 RBSI1444EM; PRIN 2017YH3SXK) and the University of Naples "Federico II" and Compagnia di San Paolo (STAR Program; project number 6-CSP-UNINA-120).

REFERENCES

Abidi, A., Devaux, J. J., Molinari, F., Alcaraz, G., Michon, F. X., Sutera-Sardo, J., et al. (2015). A recurrent KCNQ2 pore mutation causing early onset epileptic encephalopathy has a moderate effect on M current but alters subcellular localization of Kv7 channels. *Neurobiol. Dis.* 80, 80–92. doi: 10.1016/j.nbd.2015.04.017

Aeby, A., Sculier, C., Bouza, A. A., Askar, B., Lederer, D., Schoonjans, A. S., et al. (2019). SCN1B-linked early infantile developmental and epileptic encephalopathy. *Ann. Clin. Transl. Neurol.* 6, 2354–2367. doi: 10.1002/acn3.50921

Ambrosino, P., Alaimo, A., Bartollino, S., Manocchio, L., De Maria, M., Mosca, I., et al. (2015). Epilepsy-causing mutations in Kv7.2 C-terminus affect binding and functional modulation by calmodulin. *Biochim. Biophys. Acta* 1852, 1856–1866. doi: 10.1016/j.bbadis.2015.06.012

Ambrosino, P., Freri, E., Castellotti, B., Soldovieri, M. V., Mosca, I., Manocchio, L., et al. (2018). Kv7.3 compound heterozygous variants in early onset encephalopathy reveal additive contribution of C-terminal residues to PIP2-dependent K(+) channel gating. *Mol. Neurobiol.* 55, 7009–7024. doi: 10.1007/s12035-018-0883-5

Battefeld, A., Tran, B. T., Gavrilis, J., Cooper, E. C., and Kole, M. H. (2014). Heteromeric Kv7.2/7.3 channels differentially regulate action potential initiation and conduction in neocortical myelinated axons. *J. Neurosci.* 34, 3719–3732. doi: 10.1523/JNEUROSCI.4206-13.2014

Bi, C., Wu, J., Jiang, T., Liu, Q., Cai, W., Yu, P., et al. (2012). Mutations of ANK3 identified by exome sequencing are associated with autism susceptibility. *Hum. Mutat.* 33, 1635–1638. doi: 10.1002/humu.22174

Bonham, L. W., Evans, D. S., Liu, Y., Cummings, S. R., Yaffe, K., and Yokoyama, J. S. (2018). Neurotransmitter pathway genes in cognitive decline during aging: evidence for GNG4 and KCNQ2 genes. *Am. J. Alzheimers Dis. Other Dement.* 33, 153–165. doi: 10.1177/1533317517739384

Borgatti, R., Zucca, C., Cavallini, A., Ferrario, M., Panzeri, C., Castaldo, P., et al. (2004). A novel mutation in KCNQ2 associated with BFNC, drug resistant epilepsy, and mental retardation. *Neurology* 63, 57–65. doi: 10.1212/01.wnl.0000132979.08394.6d

Brackenbury, W. J., and Isom, L. L. (2011). Na channel beta subunits: overachievers of the ion channel family. *Front. Pharmacol.* 2:53. doi: 10.3389/fphar.2011.00053

Brown, D. A., and Adams, P. R. (1980). Muscarinic suppression of a novel voltage-sensitive K^+ current in a vertebrate neurone. *Nature* 283, 673–676. doi: 10.1038/283673a0

Brown, D. A., and Passmore, G. M. (2009). Neural KCNQ (Kv7) channels. *Br. J. Pharmacol.* 156, 1185–1195. doi: 10.1111/j.1476-5381.2009.00111.x

Cao, Y., Bartolome-Martin, D., Rotem, N., Rozas, C., Dellal, S. S., Chacon, M. A., et al. (2015). Rescue of homeostatic regulation of striatal excitability and locomotor activity in a mouse model of Huntington's disease. *Proc. Natl. Acad. Sci. U. S. A.* 112, 2239–2244. doi: 10.1073/pnas.1405748112

Cavaretta, J. P., Sherer, K. R., Lee, K. Y., Kim, E. H., Issema, R. S., and Chung, H. J. (2014). Polarized axonal surface expression of neuronal KCNQ potassium channels is regulated by calmodulin interaction with KCNQ2 subunit. *PLoS One* 9:e103655. doi: 10.1371/journal.pone.0103655

Colom, L. V., Castaneda, M. T., Hernandez, S., Perry, G., Jaime, S., and Touhami, A. (2011). Intrahippocampal amyloid-beta (1-40) injections injure medial septal neurons in rats. *Curr. Alzheimer Res.* 8, 832–840. doi: 10.2174/156720511798192763

Cooper, E. C. (2011). Made for "anchorin": Kv7.2/7.3 (KCNQ2/KCNQ3) channels and the modulation of neuronal excitability in vertebrate axons. *Semin. Cell Dev. Biol.* 22, 185–192. doi: 10.1016/j.semcdb.2010.10.001

Cooper, E. C., Aldape, K. D., Abosch, A., Barbaro, N. M., Berger, M. S., Peacock, W. S., et al. (2000). Colocalization and coassembly of two human brain M-type potassium channel subunits that are mutated in epilepsy. *Proc. Natl. Acad. Sci. U. S. A.* 97, 4914–4919. doi: 10.1073/pnas.090092797

Cooper, E. C., Harrington, E., Jan, Y. N., and Jan, L. Y. (2001). M channel KCNQ2 subunits are localized to key sites for control of neuronal network oscillations and synchronization in mouse brain. *J. Neurosci.* 21, 9529–9540. doi: 10.1523/JNEUROSCI.21-24-09529.2001

Dedek, K., Fusco, L., Teloy, N., and Steinlein, O. K. (2003). Neonatal convulsions and epileptic encephalopathy in an Italian family with a missense mutation in the fifth transmembrane region of KCNQ2. *Epilepsy Res.* 54, 21–27. doi: 10.1016/s0920-1211(03)00037-8

Devaux, J., Dhifallah, S., De Maria, M., Stuart-Lopez, G., Becq, H., Milh, M., et al. (2017). A possible link between KCNQ2- and STXBP1-related encephalopathies: STXBP1 reduces the inhibitory impact of syntaxin-1A on M current. *Epilepsia* 58, 2073–2084. doi: 10.1111/epi.13927

Devaux, J. J., Kleopa, K. A., Cooper, E. C., and Scherer, S. S. (2004). KCNQ2 is a nodal K^+ channel. *J. Neurosci.* 24, 1236–1244. doi: 10.1523/JNEUROSCI.4512-03.2004

Duran-Gonzalez, J., Michi, E. D., Elorza, B., Perez-Cordova, M. G., Pacheco-Otalora, L. F., Touhami, A., et al. (2013). Amyloid beta peptides modify the expression of antioxidant repair enzymes and a potassium channel in the septohippocampal system. *Neurobiol. Aging* 34, 2071–2076. doi: 10.1016/j.neurobiolaging.2013.02.005

Epi4k ConsortiumEpilepsy Phenome/Genome ProjectAllen, A. S., Berkovic, S. F., Cossette, P., Delanty, N., et al. (2013). De novo mutations in epileptic encephalopathies. *Nature* 501, 217–221. doi: 10.1038/nature12439

Ferreira, M. A., O'Donovan, M. C., Meng, Y. A., Jones, I. R., Ruderfer, D. M., Jones, L., et al. (2008). Collaborative genome-wide association analysis supports a role for ANK3 and CACNA1C in bipolar disorder. *Nat. Genet.* 40, 1056–1058. doi: 10.1038/ng.209

Figueiro-Silva, J., Gruart, A., Clayton, K. B., Podlesniy, P., Abad, M. A., Gasull, X., et al. (2015). Neuronal pentraxin 1 negatively regulates excitatory synapse density and synaptic plasticity. *J. Neurosci.* 35, 5504–5521. doi: 10.1523/JNEUROSCI.2548-14.2015

Fink, J. J., and Levine, E. S. (2018). Uncovering true cellular phenotypes: using induced pluripotent stem cell-derived neurons to study early insults in neurodevelopmental disorders. *Front. Neurol.* 9:237. doi: 10.3389/fneur.2018.00237

Fisher, R. S., Cross, J. H., French, J. A., Higurashi, N., Hirsch, E., Jansen, F. E., et al. (2017). Operational classification of seizure types by the international league against epilepsy: position paper of the ILAE Commission for Classification and Terminology. *Epilepsia* 58, 522–530. doi: 10.1111/epi.13670

Gomis-Perez, C., Urrutia, J., Marce-Grau, A., Malo, C., Lopez-Laso, E., Felipe-Rucian, A., et al. (2019). Homomeric Kv7.2 current suppression is a common feature in KCNQ2 epileptic encephalopathy. *Epilepsia* 60, 139–148. doi: 10.1111/epi.14609

Gribkoff, V. K. (2003). The therapeutic potential of neuronal KCNQ channel modulators. *Expert Opin. Ther. Targets* 7, 737–748. doi: 10.1517/14728222.7.6.737

Hernandez, C. C., Zaika, O., and Shapiro, M. S. (2008). A carboxy-terminal inter-helix linker as the site of phosphatidylinositol 4,5-bisphosphate action on Kv7 (M-type) K^+ channels. *J. Gen. Physiol.* 132, 361–381. doi: 10.1085/jgp.200810007

Huang, D., Huang, S., Gao, H., Liu, Y., Qi, J., Chen, P., et al. (2016). Redox-dependent modulation of T-type Ca(2+) channels in sensory neurons contributes to acute anti-nociceptive effect of substance P. *Antioxid. Redox Signal.* 25, 233–251. doi: 10.1089/ars.2015.6560

Iqbal, Z., Vandeweyer, G., van der Voet, M., Waryah, A. M., Zahoor, M. Y., Besseling, J. A., et al. (2013). Homozygous and heterozygous disruptions of ANK3: at the crossroads of neurodevelopmental and psychiatric disorders. *Hum. Mol. Genet.* 22, 1960–1970. doi: 10.1093/hmg/ddt043

Jiang, P., Rushing, S. N., Kong, C. W., Fu, J., Lieu, D. K., Chan, C. W., et al. (2010). Electrophysiological properties of human induced pluripotent stem cells. *Am. J. Phys. Cell Phys.* 298, C486–C495. doi: 10.1152/ajpcell.00251.2009

Jiang, Y. H., Yuen, R. K., Jin, X., Wang, M., Chen, N., Wu, X., et al. (2013). Detection of clinically relevant genetic variants in autism spectrum disorder by whole-genome sequencing. *Am. J. Hum. Genet.* 93, 249–263. doi: 10.1016/j.ajhg.2013.06.012

Kanaumi, T., Takashima, S., Iwasaki, H., Itoh, M., Mitsudome, A., and Hirose, S. (2008). Developmental changes in KCNQ2 and KCNQ3 expression in human brain: possible contribution to the age-dependent etiology of benign familial neonatal convulsions. *Brain Dev.* 30, 362–369. doi: 10.1016/j.braindev.2007.11.003

Kim, E. C., Patel, J., Zhang, J., Soh, H., Rhodes, J. S., Tzingounis, A. V., et al. (2020). Heterozygous loss of epilepsy gene KCNQ2 alters social, repetitive and exploratory behaviors. *Genes Brain Behav.* 19:e12599. doi: 10.1111/gbb.12599

Kim, E. C., Zhang, J., Pang, W., Wang, S., Lee, K. Y., Cavaretta, J. P., et al. (2018). Reduced axonal surface expression and phosphoinositide sensitivity in Kv7 channels disrupts their function to inhibit neuronal excitability in Kcnq2 epileptic encephalopathy. *Neurobiol. Dis.* 118, 76–93. doi: 10.1016/j.nbd.2018.07.004

King, C. H., and Scherer, S. S. (2012). Kv7.5 is the primary Kv7 subunit expressed in C-fibers. *J. Comp. Neurol.* 520, 1940–1950. doi: 10.1002/cne.23019

Kothur, K., Holman, K., Farnsworth, E., Ho, G., Lorentzos, M., Troedson, C., et al. (2018). Diagnostic yield of targeted massively parallel sequencing in children with epileptic encephalopathy. *Seizure* 59, 132–140. doi: 10.1016/j.seizure.2018.05.005

Kumar, M., Reed, N., Liu, R., Aizenman, E., Wipf, P., and Tzounopoulos, T. (2016). Synthesis and evaluation of potent KCNQ2/3-specific channel activators. *Mol. Pharmacol.* 89, 667–677. doi: 10.1124/mol.115.103200

Lauritano, A., Moutton, S., Longobardi, E., Tran Mau-Them, F., Laudati, G., Nappi, P., et al. (2019). A novel homozygous KCNQ3 loss-of-function variant causes non-syndromic intellectual disability and neonatal-onset pharmacodependent epilepsy. *Epilepsia Open* 4, 464–475. doi: 10.1002/epi4.12353

Le Magueresse, C., and Monyer, H. (2013). GABAergic interneurons shape the functional maturation of the cortex. *Neuron* 77, 388–405. doi: 10.1016/j.neuron.2013.01.011

Leao, R. N., Colom, L. V., Borgius, L., Kiehn, O., and Fisahn, A. (2012). Medial septal dysfunction by Abeta-induced KCNQ channel-block in glutamatergic neurons. *Neurobiol. Aging* 33, 2046–2061. doi: 10.1016/j.neurobiolaging.2011.07.013

Lehman, A., Thouta, S., Mancini, G. M. S., Naidu, S., van Slegtenhorst, M., McWalter, K., et al. (2017). Loss-of-function and gain-of-function mutations in KCNQ5 cause intellectual disability or epileptic encephalopathy. *Am. J. Hum. Genet.* 101, 65–74. doi: 10.1016/j.ajhg.2017.05.016

Lezmy, J., Lipinsky, M., Khrapunsky, Y., Patrich, E., Shalom, L., Peretz, A., et al. (2017). M-current inhibition rapidly induces a unique CK2-dependent plasticity of the axon initial segment. *Proc. Natl. Acad. Sci. U. S. A.* 114, E10234–E10243. doi: 10.1073/pnas.1708700114

Li, K., and Xu, E. (2008). The role and the mechanism of gamma-aminobutyric acid during central nervous system development. *Neurosci. Bull.* 24, 195–200. doi: 10.1007/s12264-008-0109-3

Linta, L., Stockmann, M., Lin, Q., Lechel, A., Proepper, C., Boeckers, T. M., et al. (2013). Microarray-based comparisons of ion channel expression patterns: human keratinocytes to reprogrammed hiPSCs to differentiated neuronal and cardiac progeny. *Stem Cells Int.* 2013:784629. doi: 10.1155/2013/784629

Liu, H., Jia, L., Chen, X., Shi, L., and Xie, J. (2018). The Kv7/KCNQ channel blocker XE991 protects nigral dopaminergic neurons in the 6-hydroxydopamine rat model of Parkinson's disease. *Brain Res. Bull.* 137, 132–139. doi: 10.1016/j.brainresbull.2017.11.011

Logan, S., Arzua, T., Canfield, S. G., Seminary, E. R., Sison, S. L., Ebert, A. D., et al. (2019). Studying human neurological disorders using induced pluripotent stem cells: from 2D monolayer to 3d organoid and blood brain barrier models. *Compr. Physiol.* 9, 565–611. doi: 10.1002/cphy.c180025

Long, S., Zhou, H., Li, S., Wang, T., Ma, Y., Li, C., et al. (2019). The clinical and genetic features of co-occurring epilepsy and autism spectrum disorder in chinese children. *Front. Neurol.* 10:505. doi: 10.3389/fneur.2019.00505

Lopez-Rivera, J. A., Perez-Palma, E., Symonds, J., Lindy, A. S., McKnight, D. A., Leu, C., et al. (2020). A catalogue of new incidence estimates of monogenic neurodevelopmental disorders caused by de novo variants. *Brain* 143, 1099–1105. doi: 10.1093/brain/awaa051

Luisi, R., Panza, E., Barrese, V., Iannotti, F. A., Viggiano, D., Secondo, A., et al. (2009). Activation of pre-synaptic M-type K^+ channels inhibits [3H]D-aspartate release by reducing Ca^{2+} entry through P/Q-type voltage-gated Ca^{2+} channels. *J. Neurochem.* 109, 168–181. doi: 10.1111/j.1471-4159.2009.05945.x

MacFarlane, S. N., and Sontheimer, H. (2000). Changes in ion channel expression accompany cell cycle progression of spinal cord astrocytes. *Glia* 30, 39–48. doi: 10.1002/(sici)1098-1136(200003)30:1<39::aid-glia5>3.0.co;2-s

Maljevic, S., and Lerche, H. (2014). Potassium channel genes and benign familial neonatal epilepsy. *Prog. Brain Res.* 213, 17–53. doi: 10.1016/B978-0-444-63326-2.00002-8

Maljevic, S., Reid, C. A., and Petrou, S. (2017). Models for discovery of targeted therapy in genetic epileptic encephalopathies. *J. Neurochem.* 143, 30–48. doi: 10.1111/jnc.14134

Marguet, S. L., Le-Schulte, V. T., Merseburg, A., Neu, A., Eichler, R., Jakovcevski, I., et al. (2015). Treatment during a vulnerable developmental period rescues a genetic epilepsy. *Nat. Med.* 21, 1436–1444. doi: 10.1038/nm.3987

Martire, M., Castaldo, P., D'Amico, M., Preziosi, P., Annunziato, L., and Taglialatela, M. (2004). M channels containing KCNQ2 subunits modulate norepinephrine, aspartate, and GABA release from hippocampal nerve terminals. *J. Neurosci.* 24, 592–597. doi: 10.1523/JNEUROSCI.3143-03.2004

Mayordomo-Cava, J., Yajeya, J., Navarro-Lopez, J. D., and Jimenez-Diaz, L. (2015). Amyloid-beta(25-35) modulates the expression of GirK and KCNQ channel genes in the hippocampus. *PLoS One* 10:e0134385. doi: 10.1371/journal.pone.0134385

Miceli, F., Soldovieri, M. V., Ambrosino, P., Barrese, V., Migliore, M., Cilio, M. R., et al. (2013). Genotype-phenotype correlations in neonatal epilepsies caused by mutations in the voltage sensor of K(v)7.2 potassium channel subunits. *Proc. Natl. Acad. Sci. U. S. A.* 110, 4386–4391. doi: 10.1073/pnas.1216867110

Miceli, F., Soldovieri, M. V., Ambrosino, P., De Maria, M., Migliore, M., Migliore, R., et al. (2015). Early-onset epileptic encephalopathy caused by gain-of-function mutations in the voltage sensor of Kv7.2 and Kv7.3 potassium channel subunits. *J. Neurosci.* 35, 3782–3793. doi: 10.1523/JNEUROSCI.4423-14.2015

Milh, M., Boutry-Kryza, N., Sutera-Sardo, J., Mignot, C., Auvin, S., Lacoste, C., et al. (2013). Similar early characteristics but variable neurological outcome of patients with a de novo mutation of KCNQ2. *Orphanet J. Rare Dis.* 8:80. doi: 10.1186/1750-1172-8-80

Milh, M., Roubertoux, P., Biba, N., Chavany, J., Spiga Ghata, A., Fulachier, C., et al. (2020). A knock-in mouse model for KCNQ2-related epileptic encephalopathy displays spontaneous generalized seizures and cognitive impairment. *Epilepsia* 61, 868–878. doi: 10.1111/epi.16494

Millichap, J. J., Miceli, F., De Maria, M., Keator, C., Joshi, N., Tran, B., et al. (2017). Infantile spasms and encephalopathy without preceding neonatal seizures caused by KCNQ2 R198Q, a gain-of-function variant. *Epilepsia* 58, e10–e15. doi: 10.1111/epi.13601

Millichap, J. J., Park, K. L., Tsuchida, T., Ben-Zeev, B., Carmant, L., Flamini, R., et al. (2016). KCNQ2 encephalopathy: features, mutational hot spots, and ezogabine treatment of 11 patients. *Neurol. Genet.* 2:e96. doi: 10.1212/NXG.0000000000000096

Molofsky, A. V., Krencik, R., Ullian, E. M., Tsai, H. H., Deneen, B., Richardson, W. D., et al. (2012). Astrocytes and disease: a neurodevelopmental perspective. *Genes Dev.* 26, 891–907. doi: 10.1101/gad.188326.112

Mulkey, S. B., Ben-Zeev, B., Nicolai, J., Carroll, J. L., Grønborg, S., Jiang, Y. H., et al. (2017). Neonatal nonepileptic myoclonus is a prominent clinical feature of KCNQ2 gain-of-function variants R201C and R201H. *Epilepsia* 58, 436–445. doi: 10.1111/epi.13676

Ng, S. Y., Chin, C. H., Lau, Y. T., Luo, J., Wong, C. K., Bian, Z. X., et al. (2010). Role of voltage-gated potassium channels in the fate determination of embryonic stem cells. *J. Cell. Physiol.* 224, 165–177. doi: 10.1002/jcp.22113

Nguyen, H. M., Miyazaki, H., Hoshi, N., Smith, B. J., Nukina, N., Goldin, A. L., et al. (2012). Modulation of voltage-gated K^+ channels by the sodium channel beta1 subunit. *Proc. Natl. Acad. Sci. U. S. A.* 109, 18577–18582. doi: 10.1073/pnas.1209142109

Niday, Z., Hawkins, V. E., Soh, H., Mulkey, D. K., and Tzingounis, A. V. (2017). Epilepsy-associated KCNQ2 channels regulate multiple intrinsic properties of layer 2/3 pyramidal neurons. *J. Neurosci.* 37, 576–586. doi: 10.1523/JNEUROSCI.1425-16.2016

Orhan, G., Bock, M., Schepers, D., Ilina, E. I., Reichel, S. N., Loffler, H., et al. (2014). Dominant-negative effects of KCNQ2 mutations are associated with epileptic encephalopathy. *Ann. Neurol.* 75, 382–394. doi: 10.1002/ana.24080

Ostacolo, C., Miceli, F., Di Sarno, V., Nappi, P., Iraci, N., Soldovieri, M. V., et al. (2020). Synthesis and pharmacological characterization of conformationally restricted retigabine analogues as novel neuronal Kv7 channel activators. *J. Med. Chem.* 63, 163–185. doi: 10.1021/acs.jmedchem.9b00796

Pan, Z., Kao, T., Horvath, Z., Lemos, J., Sul, J. Y., Cranstoun, S. D., et al. (2006). A common ankyrin-G-based mechanism retains KCNQ and NaV channels at electrically active domains of the axon. *J. Neurosci.* 26, 2599–2613. doi: 10.1523/JNEUROSCI.4314-05.2006

Passmore, G. M., Selyanko, A. A., Mistry, M., Al-Qatari, M., Marsh, S. J., Matthews, E. A., et al. (2003). KCNQ/M currents in sensory neurons: significance for pain therapy. *J. Neurosci.* 23, 7227–7236. doi: 10.1523/JNEUROSCI.23-18-07227.2003

Peters, H. C., Hu, H., Pongs, O., Storm, J. F., and Isbrandt, D. (2005). Conditional transgenic suppression of M channels in mouse brain reveals functions in neuronal excitability, resonance and behavior. *Nat. Neurosci.* 8, 51–60. doi: 10.1038/nn1375

Petrelli, F., Pucci, L., and Bezzi, P. (2016). Astrocytes and microglia and their potential link with autism spectrum disorders. *Front. Cell. Neurosci.* 10:21. doi: 10.3389/fncel.2016.00021

Pisano, T., Numis, A. L., Heavin, S. B., Weckhuysen, S., Angriman, M., Suls, A., et al. (2015). Early and effective treatment of KCNQ2 encephalopathy. *Epilepsia* 56, 685–691. doi: 10.1111/epi.12984

Plouin, P. (1994). "Benign familial neonatal convulsions" in *Idiopathic generalized epilepsies: Clinical, experimental and genetic aspects*. eds. A. Malafosse, E. Hirsch, C. Marescaux, D. Broglin and R. Bernasconi (London: John Libbey and Co., Ltd.), 39–44.

Rao, V. R., Perez-Neut, M., Kaja, S., and Gentile, S. (2015). Voltage-gated ion channels in cancer cell proliferation. *Cancer* 7, 849–875. doi: 10.3390/cancers7020813

Rauch, A., Wieczorek, D., Graf, E., Wieland, T., Endele, S., Schwarzmayr, T., et al. (2012). Range of genetic mutations associated with severe non-syndromic sporadic intellectual disability: an exome sequencing study. *Lancet* 380, 1674–1682. doi: 10.1016/S0140-6736(12)61480-9

Regev, N., Degani-Katzav, N., Korngreen, A., Etzioni, A., Siloni, S., Alaimo, A., et al. (2009). Selective interaction of syntaxin 1A with KCNQ2: possible implications for specific modulation of presynaptic activity. *PLoS One* 4:e6586. doi: 10.1371/journal.pone.0006586

Rizo, J. (2018). Mechanism of neurotransmitter release coming into focus. *Protein Sci.* 27, 1364–1391. doi: 10.1002/pro.3445

Rockwood, K., Beattie, B. L., Eastwood, M. R., Feldman, H., Mohr, E., Pryse-Phillips, W., et al. (1997). A randomized, controlled trial of linopirdine in the treatment of Alzheimer's disease. *Can. J. Neurol. Sci.* 24, 140–145. doi: 10.1017/s031716710002148x

Rosti, G., Tassano, E., Bossi, S., Divizia, M. T., Ronchetto, P., Servetti, M., et al. (2019). Intragenic duplication of KCNQ5 gene results in aberrant splicing leading to a premature termination codon in a patient with intellectual disability. *Eur. J. Med. Genet.* 62:103555. doi: 10.1016/j.ejmg.2018.10.007

Russo, F. B., Brito, A., de Freitas, A. M., Castanha, A., de Freitas, B. C., and Beltrao-Braga, P. C. B. (2019). The use of iPSC technology for modeling autism spectrum disorders. *Neurobiol. Dis.* 130:104483. doi: 10.1016/j.nbd.2019.104483

Safiulina, V. F., Zacchi, P., Taglialatela, M., Yaari, Y., and Cherubini, E. (2008). Low expression of Kv7/M channels facilitates intrinsic and network bursting in the developing rat hippocampus. *J. Physiol.* 586, 5437–5453. doi: 10.1113/jphysiol.2008.156257

Sands, T. T., Miceli, F., Lesca, G., Beck, A. E., Sadleir, L. G., Arrington, D. K., et al. (2019). Autism and developmental disability caused by KCNQ3 gain-of-function variants. *Ann. Neurol.* 86, 181–192. doi: 10.1002/ana.25522

Sanguinetti, M. C., Curran, M. E., Zou, A., Shen, J., Spector, P. S., Atkinson, D. L., et al. (1996). Coassembly of K(V)LQT1 and minK (IsK) proteins to form cardiac I(Ks) potassium channel. *Nature* 384, 80–83. doi: 10.1038/384080a0

Scheffer, I. E., Harkin, L. A., Grinton, B. E., Dibbens, L. M., Turner, S. J., Zielinski, M. A., et al. (2007). Temporal lobe epilepsy and $GEFS^+$ phenotypes associated with SCN1B mutations. *Brain* 130, 100–109. doi: 10.1093/brain/awl272

Schroeder, B. C., Hechenberger, M., Weinreich, F., Kubisch, C., and Jentsch, T. J. (2000). KCNQ5, a novel potassium channel broadly expressed in brain, mediates M-type currents. *J. Biol. Chem.* 275, 24089–24095. doi: 10.1074/jbc.M003245200

Schwake, M., Jentsch, T. J., and Friedrich, T. (2003). A carboxy-terminal domain determines the subunit specificity of KCNQ K^+ channel assembly. *EMBO Rep.* 4, 76–81. doi: 10.1038/sj.embor.embor715

Seager, M. A., Johnson, L. D., Chabot, E. S., Asaka, Y., and Berry, S. D. (2002). Oscillatory brain states and learning: impact of hippocampal theta-contingent training. *Proc. Natl. Acad. Sci. U. S. A.* 99, 1616–1620. doi: 10.1073/pnas.032662099

Selyanko, A. A., Hadley, J. K., and Brown, D. A. (2001). Properties of single M-type KCNQ2/KCNQ3 potassium channels expressed in mammalian cells. *J. Physiol.* 534, 15–24. doi: 10.1111/j.1469-7793.2001.00015.x

Semple, B. D., Blomgren, K., Gimlin, K., Ferriero, D. M., and Noble-Haeusslein, L. J. (2013). Brain development in rodents and humans: identifying benchmarks of maturation and vulnerability to injury across species. *Prog. Neurobiol.* 106-107, 1–16. doi: 10.1016/j.pneurobio.2013.04.001

Sharawat, I. K., Kasinathan, A., Sahu, J. K., and Sankhyan, N. (2019). Response to carbamazepine in KCNQ2 related early infantile epileptic encephalopathy. *Indian J. Pediatr.* 86, 301–302. doi: 10.1007/s12098-018-2796-8

Shellhaas, R. A., Wusthoff, C. J., Tsuchida, T. N., Glass, H. C., Chu, C. J., Massey, S. L., et al. (2017). Profile of neonatal epilepsies: characteristics of a prospective US cohort. *Neurology* 89, 893–899. doi: 10.1212/WNL.0000000000004284

Shi, L., Bian, X., Qu, Z., Ma, Z., Zhou, Y., Wang, K., et al. (2013). Peptide hormone ghrelin enhances neuronal excitability by inhibition of Kv7/KCNQ channels. *Nat. Commun.* 4:1435. doi: 10.1038/ncomms2439

Singh, N. A., Charlier, C., Stauffer, D., DuPont, B. R., Leach, R. J., Melis, R., et al. (1998). A novel potassium channel gene, KCNQ2, is mutated in an inherited epilepsy of newborns. *Nat. Genet.* 18, 25–29. doi: 10.1038/ng0198-25

Singh, N. A., Otto, J. F., Dahle, E. J., Pappas, C., Leslie, J. D., Vilaythong, A., et al. (2008). Mouse models of human KCNQ2 and KCNQ3 mutations for benign familial neonatal convulsions show seizures and neuronal plasticity without synaptic reorganization. *J. Physiol.* 586, 3405–3423. doi: 10.1113/jphysiol.2008.154971

Sloan, S. A., and Barres, B. A. (2014). Mechanisms of astrocyte development and their contributions to neurodevelopmental disorders. *Curr. Opin. Neurobiol.* 27, 75–81. doi: 10.1016/j.conb.2014.03.005

Smith, J. S., Iannotti, C. A., Dargis, P., Christian, E. P., and Aiyar, J. (2001). Differential expression of kcnq2 splice variants: implications to m current function during neuronal development. *J. Neurosci.* 21, 1096–1103. doi: 10.1523/JNEUROSCI.21-04-01096.2001

Soh, H., Pant, R., LoTurco, J. J., and Tzingounis, A. V. (2014). Conditional deletions of epilepsy-associated KCNQ2 and KCNQ3 channels from cerebral cortex cause differential effects on neuronal excitability. *J. Neurosci.* 34, 5311–5321. doi: 10.1523/JNEUROSCI.3919-13.2014

Soh, H., Park, S., Ryan, K., Springer, K., Maheshwari, A., and Tzingounis, A. V. (2018). Deletion of KCNQ2/3 potassium channels from PV+ interneurons leads to homeostatic potentiation of excitatory transmission. *elife* 7:e38617. doi: 10.7554/eLife.38617

Soldovieri, M. V., Ambrosino, P., Mosca, I., Miceli, F., Franco, C., Canzoniero, L. M. T., et al. (2019). Epileptic encephalopathy in a patient with a novel variant in the Kv7.2 S2 transmembrane segment: clinical, genetic, and functional features. *Int. J. Mol. Sci.* 20:3382. doi: 10.3390/ijms20143382

Sontheimer, H., Trotter, J., Schachner, M., and Kettenmann, H. (1989). Channel expression correlates with differentiation stage during the development of oligodendrocytes from their precursor cells in culture. *Neuron* 2, 1135–1145. doi: 10.1016/0896-6273(89)90180-3

Stamberger, H., Nikanorova, M., Willemsen, M. H., Accorsi, P., Angriman, M., Baier, H., et al. (2016). STXBP1 encephalopathy: a neurodevelopmental disorder including epilepsy. *Neurology* 86, 954–962. doi: 10.1212/WNL.0000000000002457

Suh, B. C., and Hille, B. (2002). Recovery from muscarinic modulation of M current channels requires phosphatidylinositol 4,5-bisphosphate synthesis. *Neuron* 35, 507–520. doi: 10.1016/s0896-6273(02)00790-0

Sundelacruz, S., Levin, M., and Kaplan, D. L. (2008). Membrane potential controls adipogenic and osteogenic differentiation of mesenchymal stem cells. *PLoS One* 3:e3737. doi: 10.1371/journal.pone.0003737

Telezhkin, V., Straccia, M., Yarova, P., Pardo, M., Yung, S., Vinh, N. N., et al. (2018). Kv7 channels are upregulated during striatal neuron development and promote maturation of human iPSC-derived neurons. *Pflugers Arch.* 470, 1359–1376. doi: 10.1007/s00424-018-2155-7

Tidball, A. M., and Parent, J. M. (2016). Concise review: exciting cells: modeling genetic epilepsies with patient-derived induced pluripotent stem cells. *Stem Cells* 34, 27–33. doi: 10.1002/stem.2203

Tinel, N., Lauritzen, I., Chouabe, C., Lazdunski, M., and Borsotto, M. (1998). The KCNQ2 potassium channel: splice variants, functional and developmental expression. Brain localization and comparison with KCNQ3. *FEBS Lett.* 438, 171–176. doi: 10.1016/s0014-5793(98)01296-4

Tomonoh, Y., Deshimaru, M., Araki, K., Miyazaki, Y., Arasaki, T., Tanaka, Y., et al. (2014). The kick-in system: a novel rapid knock-in strategy. *PLoS One* 9:e88549. doi: 10.1371/journal.pone.0088549

Tompson, D. J., Buraglio, M., Andrews, S. M., and Wheless, J. W. (2016). Adolescent clinical development of ezogabine/retigabine as adjunctive therapy for partial-onset seizures: pharmacokinetics and tolerability. *J. Pediatr. Pharmacol. Ther.* 21, 404–412. doi: 10.5863/1551-6776-21.5.404

Uchida, T., Lossin, C., Ihara, Y., Deshimaru, M., Yanagawa, Y., Koyama, S., et al. (2017). Abnormal gamma-aminobutyric acid neurotransmission in a Kcnq2 model of early onset epilepsy. *Epilepsia* 58, 1430–1439. doi: 10.1111/epi.13807

Wainger, B. J., Kiskinis, E., Mellin, C., Wiskow, O., Han, S. S., Sandoe, J., et al. (2014). Intrinsic membrane hyperexcitability of amyotrophic lateral sclerosis patient-derived motor neurons. *Cell Rep.* 7, 1–11. doi: 10.1016/j.celrep.2014.03.019

Wang, D. D., and Kriegstein, A. R. (2011). Blocking early GABA depolarization with bumetanide results in permanent alterations in cortical circuits and sensorimotor gating deficits. *Cereb. Cortex* 21, 574–587. doi: 10.1093/cercor/bhq124

Wang, H. S., Pan, Z., Shi, W., Brown, B. S., Wymore, R. S., Cohen, I. S., et al. (1998). KCNQ2 and KCNQ3 potassium channel subunits: molecular correlates of the M-channel. *Science* 282, 1890–1893. doi: 10.1126/science.282.5395.1890

Wang, K., Xue, T., Tsang, S. Y., Van Huizen, R., Wong, C. W., Lai, K. W., et al. (2005). Electrophysiological properties of pluripotent human and mouse embryonic stem cells. *Stem Cells* 23, 1526–1534. doi: 10.1634/stemcells.2004-0299

Watanabe, H., Nagata, E., Kosakai, A., Nakamura, M., Yokoyama, M., Tanaka, K., et al. (2000). Disruption of the epilepsy KCNQ2 gene results in neural hyperexcitability. *J. Neurochem.* 75, 28–33. doi: 10.1046/j.1471-4159.2000.0750028.x

Weckhuysen, S., Ivanovic, V., Hendrickx, R., Van Coster, R., Hjalgrim, H., Moller, R. S., et al. (2013). Extending the KCNQ2 encephalopathy spectrum: clinical and neuroimaging findings in 17 patients. *Neurology* 81, 1697–1703. doi: 10.1212/01.wnl.0000435296.72400.a1

Weckhuysen, S., Mandelstam, S., Suls, A., Audenaert, D., Deconinck, T., Claes, L. R., et al. (2012). KCNQ2 encephalopathy: emerging phenotype of a neonatal epileptic encephalopathy. *Ann. Neurol.* 71, 15–25. doi: 10.1002/ana.22644

Winson, J. (1978). Loss of hippocampal theta rhythm results in spatial memory deficit in the rat. *Science* 201, 160–163. doi: 10.1126/science.663646

Yang, Y., Beyer, B. J., Otto, J. F., O'Brien, T. P., Letts, V. A., White, H. S., et al. (2003). Spontaneous deletion of epilepsy gene orthologs in a mutant mouse with a low electroconvulsive threshold. *Hum. Mol. Genet.* 12, 975–984. doi: 10.1093/hmg/ddg118

Yeung, S. Y., Pucovsky, V., Moffatt, J. D., Saldanha, L., Schwake, M., Ohya, S., et al. (2007). Molecular expression and pharmacological identification of a role for K(v)7 channels in murine vascular reactivity. *Br. J. Pharmacol.* 151, 758–770. doi: 10.1038/sj.bjp.0707284

Yeung, S., Schwake, M., Pucovsky, V., and Greenwood, I. (2008). Bimodal effects of the Kv7 channel activator retigabine on vascular K^+ currents. *Br. J. Pharmacol.* 155, 62–72. doi: 10.1038/bjp.2008.231

Zhang, J., Kim, E. C., Chen, C., Procko, E., Pant, S., Lam, K., et al. (2020). Identifying mutation hotspots reveals pathogenetic mechanisms of KCNQ2 epileptic encephalopathy. *Sci. Rep.* 10:4756. doi: 10.1038/s41598-020-61697-6

Zhang, Y., Sloan, S. A., Clarke, L. E., Caneda, C., Plaza, C. A., Blumenthal, P. D., et al. (2016). Purification and characterization of progenitor and mature human astrocytes reveals transcriptional and functional differences with mouse. *Neuron* 89, 37–53. doi: 10.1016/j.neuron.2015.11.013

Zhou, N., Huang, S., Li, L., Huang, D., Yan, Y., Du, X., et al. (2016). Suppression of KV7/KCNQ potassium channel enhances neuronal differentiation of PC12 cells. *Neuroscience* 333, 356–367. doi: 10.1016/j.neuroscience.2016.07.024

Zhou, X., Song, M., Chen, D., Wei, L., and Yu, S. P. (2011). Potential role of KCNQ/M-channels in regulating neuronal differentiation in mouse hippocampal and embryonic stem cell-derived neuronal cultures. *Exp. Neurol.* 229, 471–483. doi: 10.1016/j.expneurol.2011.03.018

Conflict of Interest: The authors declare that the research was conducted in the absence of any commercial or financial relationships that could be construed as a potential conflict of interest.

frontiers in Physiology

ORIGINAL RESEARCH
published: 07 December 2020
doi: 10.3389/fphys.2020.598779

K_V7 Channel Expression and Function Within Rat Mesenteric Endothelial Cells

Samuel N. Baldwin[1], Shaun L. Sandow[2], Gema Mondéjar-Parreño[3], Jennifer B. Stott[1] and Iain A. Greenwood[1]**

[1] Vascular Biology Research Centre, Institute of Molecular and Clinical Sciences, St George's University of London, London, United Kingdom, [2] Biomedical Science, School of Health and Sports Science, University of the Sunshine Coast, Maroochydore, QLD, Australia, [3] Department of Pharmacology and Toxicology, School of Medicine, Complutense University of Madrid, Madrid, Spain

OPEN ACCESS

Edited by:
Francesco Miceli,
University of Naples Federico II, Italy

Reviewed by:
Vincenzo Calderone,
University of Pisa, Italy
Nikita Gamper,
University of Leeds, United Kingdom

***Correspondence:**
Iain A. Greenwood
grenwood@sgul.ac.uk
Samuel N. Baldwin
m1405629@sgul.ac.uk

Specialty section:
This article was submitted to Membrane Physiology and Membrane Biophysics, a section of the journal Frontiers in Physiology

Received: 25 August 2020
Accepted: 13 November 2020
Published: 07 December 2020

Citation:
Baldwin SN, Sandow SL, Mondéjar-Parreño G, Stott JB and Greenwood IA (2020) K_V7 Channel Expression and Function Within Rat Mesenteric Endothelial Cells. Front. Physiol. 11:598779. doi: 10.3389/fphys.2020.598779

Background and Purpose: Arterial diameter is dictated by the contractile state of the vascular smooth muscle cells (VSMCs), which is modulated by direct and indirect inputs from endothelial cells (ECs). Modulators of KCNQ-encoded k_V7 channels have considerable impact on arterial diameter and these channels are known to be expressed in VSMCs but not yet defined in ECs. However, expression of k_V7 channels in ECs would add an extra level of vascular control. This study aims to characterize the expression and function of K_V7 channels within rat mesenteric artery ECs.

Experimental Approach: In rat mesenteric artery, KCNQ transcript and K_V7 channel protein expression were determined via RT-qPCR, immunocytochemistry, immunohistochemistry and immunoelectron microscopy. Wire myography was used to determine vascular reactivity.

Key Results: KCNQ transcript was identified in isolated ECs and VSMCs. $K_V7.1$, $K_V7.4$ and $K_V7.5$ protein expression was determined in both isolated EC and VSMC and in whole vessels. Removal of ECs attenuated vasorelaxation to two structurally different $K_V7.2$-5 activators S-1 and ML213. $K_{IR}2$ blockers ML133, and $BaCl_2$ also attenuated S-1 or ML213-mediated vasorelaxation in an endothelium-dependent process. K_V7 inhibition attenuated receptor-dependent nitric oxide (NO)-mediated vasorelaxation to carbachol, but had no impact on relaxation to the NO donor, SNP.

Conclusion and Implications: In rat mesenteric artery ECs, $K_V7.4$ and $K_V7.5$ channels are expressed, functionally interact with endothelial $K_{IR}2.x$ channels and contribute to endogenous eNOS-mediated relaxation. This study identifies K_V7 channels as novel functional channels within rat mesenteric ECs and suggests that these channels are involved in NO release from the endothelium of these vessels.

Keywords: pharmacology, vascular biology, endothelial cell, K_V7 channel, K_{IR} channel, carbachol

INTRODUCTION

KCNQ-encoded K_V7 channels are key regulators of arterial reactivity. Within the vasculature, of the five KCNQ subtypes, KCNQ4 is predominantly expressed, followed by KCNQ5 > KCNQ1; with little to no contribution from KCNQ2/3 (Ohya et al., 2003; Yeung et al., 2007; Ng et al., 2011). In human and rodent blood vessels K_V7 channels contribute to resting tone (Ohya et al., 2003; Yeung et al., 2007; Mackie et al., 2008; Ng et al., 2011), whereby their blockers such as linopirdine or XE991 produce contractions or enhance vasoconstrictor responses. In addition, a range of K_V7 channel activators including retigabine, S-1 and ML213 are effective relaxants of pre-contracted arterial tone. Furthermore, K_V7 channels also represent functional end targets for a myriad of endogenous vasoactive responses, wherein channel activity is impaired during PKC-mediated vasoconstriction (Brueggemann et al., 2006) and enhanced as a result of cGMP and cAMP dependent receptor-mediated vasodilation (e.g., Chadha et al., 2012; Khanamiri et al., 2013; Stott et al., 2014, 2015; Mani et al., 2016; Brueggemann et al., 2018; Mondéjar-Parreño et al., 2019). To date, vascular K_V7 channel studies have focused predominantly on vascular smooth muscle cells (VSMCs) or whole arteries, and as a result it is currently unclear whether endothelial cells (ECs) express K_V7 channels and if so, what their functional role may be.

Endothelial cells form the inner layer of blood vessels and constitute a paracrine signaling platform which regulates VSMC contractility, vascular resistance and ultimately blood flow through the release of nitric oxide (NO), prostacyclin, epoxyeicosatrienoic acid and others; including the generation and spread of endothelium-derived hyperpolarization (EDH) (McGuire et al., 2001). Myoendothelial (ME) projections within fenestrations (holes) of the internal elastic lamina (IEL) facilitate the presence gap junctions (MEGJs) at a proportion of such sites (∼50% in adult rat 1st–3rd order 'large' mesenteric arteries; MA; Sandow et al., 2009) which permits heterocellular electrochemical coupling via connexin proteins (Sandow et al., 2012). These sites enable the transfer of EC-derived signals via the flow of both small molecules < ∼1 kDa and current between the cells. In endothelium-dependent relaxation of rat MA, a fundamental role for small/intermediate conductance calcium-activated potassium (SK_{Ca} and IK_{Ca}, respectively; Sandow et al., 2006; Dora et al., 2008), transient receptor potential canonical type 3 (Senadheera et al., 2012), inwardly rectifying potassium channels ($K_{IR}2$) (Goto et al., 2004), as well as inositol-1,3,4 trisphosphate receptor/s (Fukao et al., 1997) has been demonstrated.

Identification of K_V7 expression in ECs would open up a new layer of vascular control by these channels and is a necessary requisite for understanding the role of these channels in vascular health and disease. This study aims to ascertain whether rat mesenteric ECs express K_V7 channels, and if so, what their functional implications may be. This study shows that K_V7 channels are expressed in rat mesenteric artery ECs and contribute to both K_V7 activator-mediated relaxation via a potential functional interaction with $K_{IR}2$ channels and endothelial NO synthase (eNOS)-dependent axis of carbachol (CCh)-mediated vasorelaxation.

Abbreviations: 4-AP, 4-aminopyridine; Acta2, α-smooth muscle actin-2; CCh, carbachol; cGMP, cyclic guanosine monophosphate; Cq, quantification cycle; CYC1, cytochrome C1; EC, endothelial cell; EDH, endothelium derived hyperpolarization; GAPD, glyceraldehyde-3-phosphate dehydrogenase; eNOS, endothelial nitric oxide synthase; IK_{Ca}, intermediate conductance calcium-activated potassium channel; IEL, internal elastic lamina; K_{IR}, inwardly rectifying potassium channel; K_V, voltage-gated potassium channel; L-NAME, L-nitroarginine methyl ester; MA, mesenteric artery; MO, methoxamine; Myh11, myosin heavy chain 11; NO, nitric oxide; PECAM-1, platelet endothelial cell adhesion molecule-1; RT-qPCR, reverse-transcription quantitative polymerase chain reaction; SEM, standard error of the mean; SK_{Ca}, small conductance calcium-activated potassium channel; SNP, *S*-nitroprusside; TEA, tetraethylammonium; VSMC, vascular smooth muscle cell; vWBF, von-Willebrand factor.

MATERIALS AND METHODS

Animal Models

Experiments were performed on MA from Male Wistar rats (Charles River, Margate, United Kingdom) ages 11–14 weeks (200–350 g) from the Biological Research Facility, St George's, London, United Kingdom; and from the Animal Resources Center, Perth, Australia. Animals were housed in cages with free access to water and food (RM1; Dietex Inter-national, United Kingdom) *ad libitum*, with a 12-h light/dark cycle and constant temperature and humidity (21 ± 1°C; 50% ± 10% humidity) in accordance with the Animal (Scientific Procedures) Act 1986, the guidelines of the National Health and Medical Research Council of Australia and the UNSW Animal Ethics and Experimentation Committee (AEEC #18/86B). Animals were kept in LSB Aspen woodchip bedding. Animals were culled by either cervical dislocation with secondary confirmation via cessation of the circulation by femoral artery severance or were anesthetized with sodium pentathol (intraperitoneal, 100 mg/kg) in accordance with Schedule 1 of the ASPA 1986.

Either whole mesenteric plexus or 2nd/3rd/4th order MA were used with vessel order identified from the second bifurcation of the superior MA. Arteries were dissected, cleaned of fat and adherent tissue and stored on ice within physiological salt solution (PSS) of the following composition (mmol-L^{-1}); 119 NaCl, 4.5 KCl, 1.17 $MgSO_4.7H_20$, 1.18 NaH_2PO_4, 25 $NaHCO_3$, 5 glucose, 1.25 $CaCl_2$.

Reverse Transcription Quantitative Polymerase Chain Reaction

Second and third order MA segments were enzymatically digested to obtain either freshly isolated ECs (as previous, Greenberg et al., 2016) or VSMCs. Briefly, vessels were washed in Hanks' Balanced Salt Solution (HBSS; ThermoFisher Scientific, GIBCO, 14170-088) containing 50 μmol-L^{-1} $CaCl_2$ for 5 min at 37°C, the media was then replaced in HBSS containing 50 μmol-L^{-1} $CaCl_2$ with 1 mg/mL collagenase IA (Sigma Aldrich, C9891, United Kingdom) for 15 min at 37°C. Vessels were washed

in HBSS containing 50 μmol-L^{-1} $CaCl_2$ for 10 min at 37°C. The supernatant was removed and the vessels suspended in fresh HBSS containing 75 μmol-L^{-1} $CaCl_2$. For RT-qPCR, ECs were dissociated using a wide-bore smooth-tipped pipette and identified under the microscope (x10) as sheets of cells independent from the vessel which were harvested and stored separately from the residual VSMCs.

mRNA from both isolated ECs and VSMCs was extracted using Monarch Total RNA Miniprep Kit (New England BioLabs, Ipswich, MA, United States) and reverse transcribed via LunaScript RT SuperMix Kit (New England BioLabs, Ipswich, MA, United States). Quantitative analysis of relative gene expression was assessed via CFX-96 Real-Time PCR Detection System (BioRad, Hertfordshire, United Kingdom). Samples were run in duplicate to account for variation. Samples were run in BrightWhite qPCR plate (Primer Design, Camberley, United Kingdom), with each well containing 20 μL of reaction solution containing: 10 μL of PrecisionPLUS qPCR Master Mix (Primer Design, Camberley, United Kingdom), 300 nmol-L^{-1} of gene specific target primer (Thermofisher scientific, Waltham, MA, United States) and 10 ng of cDNA sample made up to 20 μL total volume with nuclease free water. Run protocol: (1) activation step (15 min:95°C), (2) denaturation step (15 s: 94°C), (3) annealing step (30 s: 55°C), and (4) extension step (30 s: 70°C). Steps 2- 4 were repeated x 40. Quantification cycle (Cq) was determined via Bio-Rad CFX96 Manager 3.0. Cq values were normalised to housekeeper genes expressed as a $2^{-\Delta Cq}$ when compared to appropriate reference genes including 14-3-3 Zeta (YWHAZ) and glyceraldehyde-3-phosphate dehydrogenase (GAPD). Cell isolation for VSMCs and ECs was validated by either positive expression of VSMC specific marker α-actin 2 (*Acta2)* or EC specific marker-platelet endothelial cell adhesion molecule-1 *(Pecam-1)* respectively. See **Table 1** for a list of the primers used in the following (Jepps et al., 2011; Askew Page et al., 2019; ThermoFisher Scientific).

TABLE 1 | RT-qPCR primer sequences.

Gene	(+) Forward primer sequence (–) Reverse primer sequence	Gene accession number	Amplicon (bp)
Acta2	ATCCGATAGAACACGGCATC AGGCATAGAGGGACAGCACA	NM_031004.2	228
Pecam1	CTCCTAAGAGCAAAGAGCAACTTC TACACTGGTATTCCATGTCTCTGG	NM_031591.1	100
Kcnq1	TGGGTCTCATCTTCTCCTCC GTAGCCAATGGTGGTGACTG	NM_032073	124
Kcnq2	AAGAGCAGCATCGGCAAAAA GGTGCGTGAGAGGTTAGTAGCA-	NM_133322	101
Kcnq3	CAGCAAAGAACTCATCACCG ATGGTGGCCAGTGTGATCAG	AF091247	161
Kcnq4	GAATGAGCAGCTCCCAGAAG AAGCTCCAGCTTTTCTGCAC	XM_233477.8	133
Kcnq5	AACTGATGAGGAGGTCGGTG GATGACCGTGACCTTCCAGT	XM_001071249.3	120

Immunocytochemistry

Freshly dispersed ECs (as above), together with residual VSMCs were left for 1hr before use. Cells were then fixed in 4% paraformaldehyde (Sigma-Aldrich, United Kingdom) in PBS for 20 min at RT as previously described (Barrese et al., 2018a). Cells were treated with 0.1 mol-L^{-1} glycine for 5 min and incubated for 1 h with blocking solution (PBS-0.1% Triton X-100-10% bovine serum albumin) at RT. Following incubation overnight at 4°C with primary antibodies (**Table 2**) diluted in blocking solution (anti-PECAM-1 for ECs, anti-α-actin for VSMCs and anti-$K_V7.1$, $K_V7.4$, and $K_V7.5$ channel for ECs/VSMCs), cells were then washed for 20 min with PBS, incubated for 1 h at RT with the secondary conjugated antibodies diluted in blocking solution. Excess secondary antibody was removed by washing with PBS and cells mounted using media containing 4′,6-diamidino-2-phenylindole (DAPI) for nuclear counterstaining. Using triple staining, ECs and VSMC were differentiated via the following: ECs were positive for anti PECAM-1 and negative for anti-α-actin; while VSMC was positive for anti-α-actin and negative for anti-PECAM-1 (data not shown). Cells were analyzed using a Zeiss LSM 510 Meta argon/krypton laser scanning confocal microscope (Image Resource Facility, St George's University, London).

Cell Culture

Chinese Hamster Ovary (CHO) cells were maintained in DMEM supplemented with 10% fetal bovine serum, 2 mmol-L^{-1} L-glutamine, and 1% penicillin/streptomycin (Sigma Aldrich, Dorset, United Kingdom) and maintained at 37°C with 5% CO_2 in an incubator. Cells were plated in a 24-well plate, incubated for 24hr then transfected with either $K_V7.1$, $K_V7.4$ or $K_V7.5$ plasmids using Lipofecamine 2000 (Thermofisher, Paisley, United Kingdom) as described previously (Barrese et al., 2018a). After 24 h, cells were fixed and stained as described above.

Immunohistochemistry

Animals were anesthetized with sodium pentathol (intraperitoneal, 100 mg/kg) and perfusion fixed (Sandow et al., 2004) in 2% paraformaldehyde in 0.1 mol-L^{-1} PBS. Third to 4th order MA segments were dissected, opened laterally and pinned as a sheet to a Sylgard dish. Segments were washed in PBS (3 × 5 min), incubated in blocking buffer (PBS with 1% BSA and 0.2% Triton) at room temperature (RT) for 2 h and then overnight with primary antibody (**Table 2**) in blocking buffer at 4°C, washed again (3 × 5 min with gentle agitation), and incubated in secondary antibody (**Table 2**; matched to the respective primary) in PBS with 0.1% Triton in PBS for 2 h at RT. Tissue was mounted on slides in anti-fade media containing propidium iodide (PI) or DAPI (**Table 2**) and imaged with uniform confocal settings. Incubation of tissue with secondary only was used as a 'zero' setting for confocal imaging. Controls involved substitution of primary with isotype control, with concentration (where provided by manufacturer) matched, or 10-fold higher than the respective antibody of interest (**Table 2**). Working Ab dilutions were prepared in accordance with previous work (Jepps et al., 2009; Chadha et al., 2012). Confocal image

TABLE 2 | Immunocyto/histochemistry reagents and use (Jepps et al., 2009; Chadha et al., 2012).

Reagent purpose	Detail	Source	Predicted MW, kDa	Epitope	[used]	Peptide availability	Raised in
Primary antibodies	Kv7.1/KCNQ1	Pineda Antikörper-Service, Germany	75	N-terminus	1:100	No	Rabbit
	Kv7.4/KCNQ4	NeuroMab, cat no 75-082, 1 mg/ml	77	Hu aa 2-77, clone N4/36 IgG	1:200 (5 μg/ml)	No	Mouse
	Kv7.4/KCNQ4*	Abcam, ab65797, lot GR94754, whole serum	77	N' domain	1:100 not available	No	Rabbit
	Kv7.5/KCNQ5*	Millipore ABN1372-q2476155; 1 ml/ml	∼103	Human IgG	1:100 (10 μg/ml)	No	Rabbit
	PECAM-1/CD31	Santa Cruz Biotechnology, Sc-1506, 200 μg/ml	130	699–727 aa at the C-terminus	1:100 (2 μg/ml)	–	Goat
	SM-α-actin	Sigma Aldrich A2547	∼42	N-terminal	(1:100) not available	–	Mouse
Nuclear labels/cell patency markers	DAPI, Vectasheild	Vectorlabs	–	Nucleic acid		–	–
	propidium iodide (PI)	Sigma, P4170	–	Nucleic acid	10 nM	–	–
Immuno-histochemistry secondary antibodies	Mouse 568	Abcam, ab175700, lot GR320062-4, 2 mg/ml	–	IgG	1:100 (20 μg/ml)	–	Donkey
	Rabbit 546	Thermofisher, A-11035	–	IgG	1:100 (20 μg/ml)	–	Goat
	Rabbit 633	Merck, SAB4600132, lot 15C0423, 2 mg/ml	–	IgG	1:100 (20 μg/ml)	–	Donkey
Immuno-cytochemistry secondary antibodies	Mouse 488	Thermofisher, A21202, 2 mg/mL	–	IgG	1:100 (0.02 mg/ml)	–	Donkey
	Rabbit 568	Thermofisher, A10042, 2 mg/mL	–	IgG	1:100 (0.02 mg/ml)	–	Donkey
	Goat 633	Thermofisher, A21082, 2 mg/mL	–	IgG	1:100 (0.02 mg/ml)	–	Donkey
Isotype controls	Mouse IgG	ThermoFisher, 10400C	–	IgG	5 mg/ml	–	Mouse
	Rabbit IgG	ThermoFisher, S31235	–	IgG	10 mg/ml	–	Rabbit
Immunoelectron microscopy secondary antibodies	5 nm Au anti- rabbit	Merck, G7277, lot SLB3882V	–	IgG	1:100	–	Goat
	10 nm Au anti- rabbit	Merck, G7402	–	IgG	1:100	–	Goat

CD31, cluster of differentiation 31; DAPI, 4',6-diamidino-2-phenylindole; PECAM, platelet endothelial cell adhesion molecule.

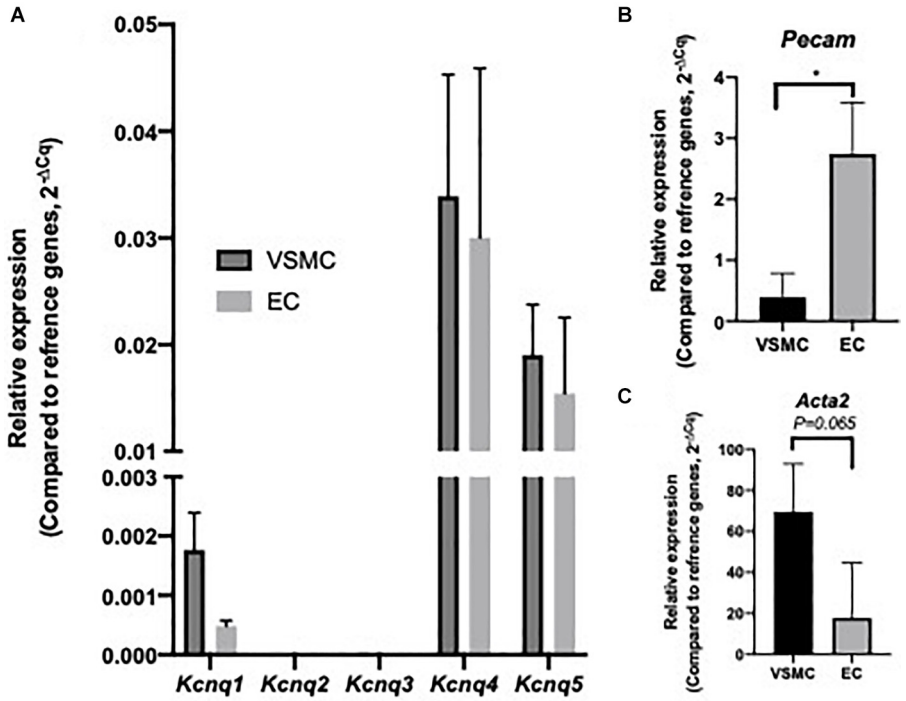

FIGURE 1 | Expression profile of *Kcnq* genes within isolated rat mesenteric vascular smooth muscle cells (VSMCs) and endothelial cells (ECs). RT-qPCR analysis of relative expression of *Kcnq1-5* in isolated VSMCs and ECs **(A)**. Cell specific markers *Acta2* and *Pecam,* for VSMCs and ECs respectively, were measured to determine sample purity **(B,C)**. Values expressed as mean ± SEM of ($2^{-\Delta Cq}$) of ΔCq values generated from appropriate housekeeper genes ($n = 3$). Statistical significance is defined as $^*P < 0.05$ **(B,C)**.

stacks were collected at 0.2 μm intervals. The optimal rinsing protocol was determined by incubating in secondary only; and rinsing after successive 5 min incubations until fluorescence was reduced to background. Note that if this was not done secondary alone was specifically and highly localized to IEL hole sites; as potential false positives at such sites; suggesting that such sites have an affinity for IgG-secondary label alone.

Electron Microscopy

Animals were anesthetized as above and perfusion fixed in 0.2% glutaraldehyde and 2% paraformaldehyde in 0.1 mol-L^{-1} PBS (pH 7.4). MA segments (∼2 mm in length) were washed (3 × 5 min) and processed in a Leica EMPACT 2 high-pressure freezer using 0.7% low melting agarose as a cryoprotectant. Samples were then freeze-substituted in a Leica AFS2 into 0.2% uranyl acetate in 95% acetone (from −85 to −50°C) and infiltrated with Lowicryl (at −50°C), before UV polymerization (2 days each at −50 and 20°C; Zechariah et al., 2020). Conventional transmission electron microscopy (TEM) was conducted using standard procedures (Sandow et al., 2002, 2004).

Individual serial transverse sections (∼100 nm) were mounted on Formvar-coated slot grids and processed for antigen localization as for confocal immunohistochemistry (per above and **Table 2**). The secondary used was 5 or 10 nmol-L^{-1} colloidal gold-conjugated antibody (1:40; 2 h) in 0.01% Tween-20. Sections were imaged at x10-40,000 on a JEOL transmission electron microscope at 16 MP (Emsis, Morada G3). Background gold label density was determined from randomly selected (4x) 1 × 1 μm regions per sample of lumen and IEL, compared to the same sized regions of interest in EC profiles.

Wire Myography

Second order MA segments (∼2 mm in length) were mounted on 40 μm diameter tungsten wire in a tension myograph chamber (Danish Myo Technology, Arhus, Denmark) containing 5 mL of PSS (composition, as above) oxygenated with 95% O_2 and 5% CO_2 at 37°C. Vessels then underwent a passive force normalization process to achieve an internal luminal circumference at a transmural pressure of 100 mmHg (13.3 kPa) to standardize pre-experimental conditions (Mulvany and Halpern, 1976). Force generated was first amplified by a PowerLab (ADInstruments, Oxford, United Kingdom), and recorded by LabChart software (ADInstruments, Oxford, United Kingdom). Vessels were then challenged with 60 mmol-L^{-1} [K^+] to determine viability, and then constricted with 10 μmol-L^{-1} methoxamine (MO), an α-1 adrenoreceptor agonist, EC integrity was then determined via addition of 10 μmol-L^{-1} carbachol (CCh), a synthetic acetylcholine analog. Vessels displaying ≥ 90% vasorelaxation in response to CCh were considered EC positive (EC+). Vessels were denuded of ECs by gently passing a human hair through the lumen. Vessels expressing ≤ 10% vasorelaxation in response to CCh were considered EC negative (EC−). During functional investigations,

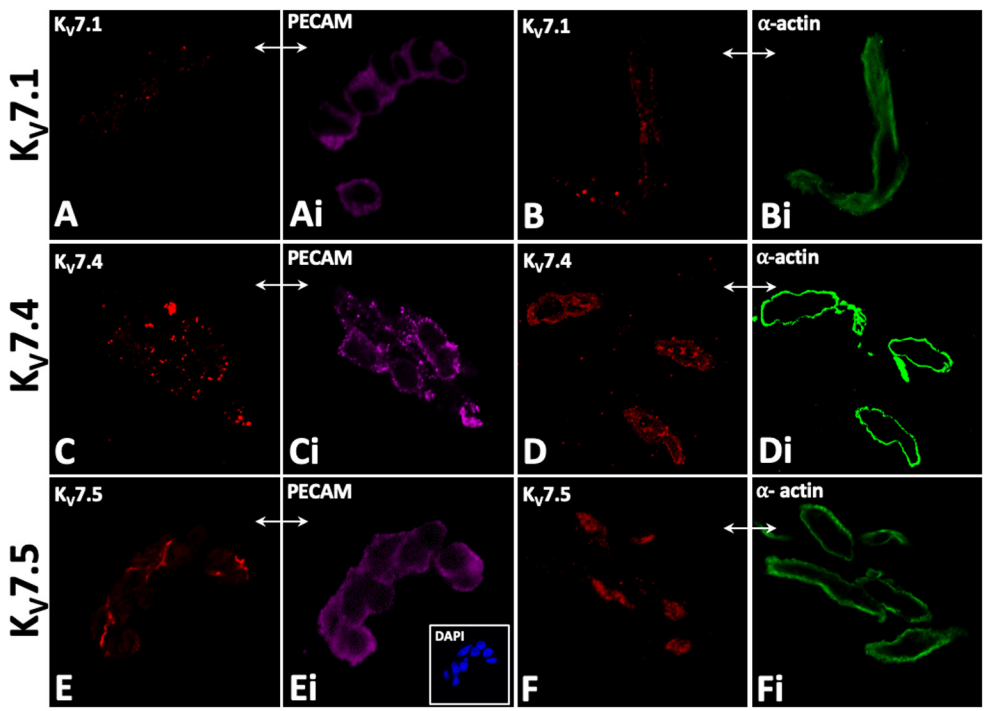

FIGURE 2 | Immunocytochemistry demonstrates K_V7.1, K_V7.4, and 7_V.5 localization in rat mesenteric artery isolated endothelial (EC; **A,C,E**) and smooth muscle cells (SMC; **B,D,F**). Punctate labelling for Kv7.1, Kv7.4, and 7.5 was present in isolated EC and SMCs (**A,C,E** and **B,D,F**). PECAM and smooth muscle a-actin were used as markers for isolated endothelial and smooth muscle cells, respectively (**Ai,Ci,Ei** and **Bi,Di,Fi** respectively); e.g. comparative-same cells, double arrows, **A–Fi**). 4′,6-diamidino-2-phenylindole (DAPI; e.g. inset, **C**) were used as nuclear markers to verify cell patency. *n* = 4–6, representative of different source tissue **(A–Fi)**. Double arrows from insets indicate same panel as main, but to different marker.

all vessels were pre-constricted with the thromboxane A2 receptor agonist U46619 (300 nmol-L^{-1}) to elicit an EC_{80} contraction. Concentration-dependent relaxant responses to S-1 (0.1–10 μmol-L^{-1}), ML213 (0.1–10 μmol-L^{-1}), ML277 (0.03–10 μmol-L^{-1}), CCh (0.3–10 μmol-L^{-1}) and *S*-nitroprusside (SNP; 0.01–3 μmol-L^{-1}) were determined in the presence and absence of ECs, linopirdine (10 μmol-L^{-1}), HMR-1556 (10 μmol-L^{-1}), carbenoxolone (100 μmol-L^{-1}), ML133 (20 μmol-L^{-1}), barium chloride ($BaCl_2$; 100 μmol-L^{-1}), L-nitroarginine methyl ester (L-NAME; 100 μmol-L^{-1}), TRAM34 (1 μmol-L^{-1}), Apamin (10 nmol-L^{-1}), 4-aminopyridine (4-AP; 1 mmol-L^{-1}), and tetraethylamonium (TEA; 1 mmol-L^{-1}).

Data and Statistical Analysis

All functional figures express mean data from at least 5 animals ± standard error of the mean (SEM). Experiments comparing groups of unequal numbers are present due to technical failure or expiry of tissue during isometric tension recording. For functional experiments involving cumulative concentrations, a transformed data set was generated using; X = Log(X), to reduce representative skew. A four parametric linear regression analysis was then performed using the following equation; [Log(Agonist) vs. response – variable slope (four parameters bottom/hillslope/top/EC_{50})] using GraphPad Prism (Version 8.2.0) to fit a concentration effect curve (CEC) to the figure. For data comparing multiple groups, a two way-ANOVA followed by a *post hoc* Bonferonni test in order to account for type 1 errors in multiple comparisons was performed for comparison of mean values. For data comparing two groups, an unpaired parametric T-test was was performed. Significance values are represented as follows; $P < 0.05$ (*). *n* = (x), number of animals used. *N* = (x), number of segments used. The data and statistical analysis comply with the recommendations on experimental design and analysis in pharmacology (Curtis et al., 2018).

RESULTS

Identification of K_V7 Channels Within MA ECs

Initial investigation sought to identify *Kcnq*/K_V7 transcript and protein within MA ECs. Transcript levels for *Kcnq1-5* and EC and VSMC markers were determined in cell lysates from isolated MA VSMC and EC (per Methods). Both ECs and VSMCs expressed *Kcnq4* > *Kcnq5* > *Kcnq1* with no expression of *Kcnq2/3* (**Figure 1A**) similar to previous studies (Ohya et al., 2003; Yeung et al., 2007; Ng et al., 2011). However, a comparative reduction in the relative abundance of *Kcnq1* was observed in MA ECs when compared to VSMCs (**Figure 1A**). Cell isolation efficiency is demonstrated by a reduction in EC marker *Pecam*

within VSMCs cell lysates when compared to ECs ($P \leq 0.05$) and a reduction in VSMCs marker *Acta2* in EC cell lysates when compared to VSMCs ($P = 0.065$, **Figures 1B,C**).

K_V7.1, K_V7.4, and K_V7.5 were detected in isolated ECs by immunodetection (**Figures 2A,C,E**). K_V7.4 had a punctate distribution in isolated ECs (**Figure 2C**) whereas K_V7.5 label appeared to be predominantly cytoplasmic with some diffuse label around the nucleus (**Figure 2E**). Similar to previous reports (Zhong et al., 2010; Oliveras et al., 2014; Mills et al., 2015; Morales-Cano et al., 2015; Barrese et al., 2018a). K_V7.1, K_V7.4, and 7.5 were also identified in isolated MA VSMCs (**Figures 2B,D,F**). K_V7.1 staining in ECs was negligible compared to VMSCs (**Figures 2A,B**). ECs and VSMCs were identified by positive expression of either PECAM (**Figures 2Ai,Ci,Ei**) or α-actin (**Figures 2Bi,Di,Fi**) respectively. Antibody specificity was determined via positive staining in CHO cells transfected with purported target and negative staining in non-transfected control cells (**Supplementary Figure 1**). Importantly, as ion channel expression can alter in isolated cells K_V7.4 and K_V7.5 were also detected in both ECs and VSMCs in *en face* whole-mount arteries (**Figures 3A,B,E,F**). Notably, both K_V7.4 and 7.5 were expressed at a proportion of IEL hole sites at an apparently higher level than the associated EC membrane label (**Figures 3C,D,G,H**). We also detected K_V7.4 and K_V7.5 in EC by immuno-gold electron microscopy (**Supplementary Figure 2**). These studies identify K_V7.4 and K_V7.5 in ECs as well as smooth muscle cells.

Removal of ECs Modulates K_V7.2-5 Activator Efficacy

A comprehensive pharmacological analysis was undertaken to determine if K_V7 channels have a functional role in MA ECs via a reductive approach. Initially, the effects of K_V7 channel modulators were examined in endothelium intact or denuded MAs. The structurally dissimilar K_V7.2–7.5 activators S-1 and ML213 interact with the same pharmacophore centered around a tryptophan in the S5 domain (Schenzer, 2005; Bentzen et al., 2006; Brueggemann et al., 2014; Jepps et al., 2014). ML277 is a potent activator of K_V7.1 (Yu et al., 2013) with a 100-fold increase in selectivity for K_V7.1 compared to K_V7.2-5 (Yu et al., 2013). Consistent with previous findings (Chadha et al., 2012; Jepps et al., 2014), S-1- and ML213-mediated vasorelaxation was ablated by pre-incubation with 10 μmol-L^{-1} of the pan-K_V7 channel inhibitor linopirdine (Schnee and Brown, 1998; **Figures 4A,B,D**). Relaxation produced by 10–300 nmol-L^{-1} ML277 were also prevented by pre-incubation with linopirdine (**Figure 4C**). However, relaxation produced by concentrations > 1 μmol-L^{-1} ML277 was not attenuated by linopirdine and are therefore not mediated by K_V7.1 activation.

Endothelial removal for the following experiments was confirmed by ablation of vasorelaxation in response to 10 μmol-L^{-1} CCh (**Figure 5A**). Endothelium denudation by mechanical abrasion has no impact on the peak contraction produced by 300 nmol-L^{-1} U46619 (**Figure 5B**), but significantly attenuated the potency of S-1 mediated vasorelaxation increasing EC_{50} from

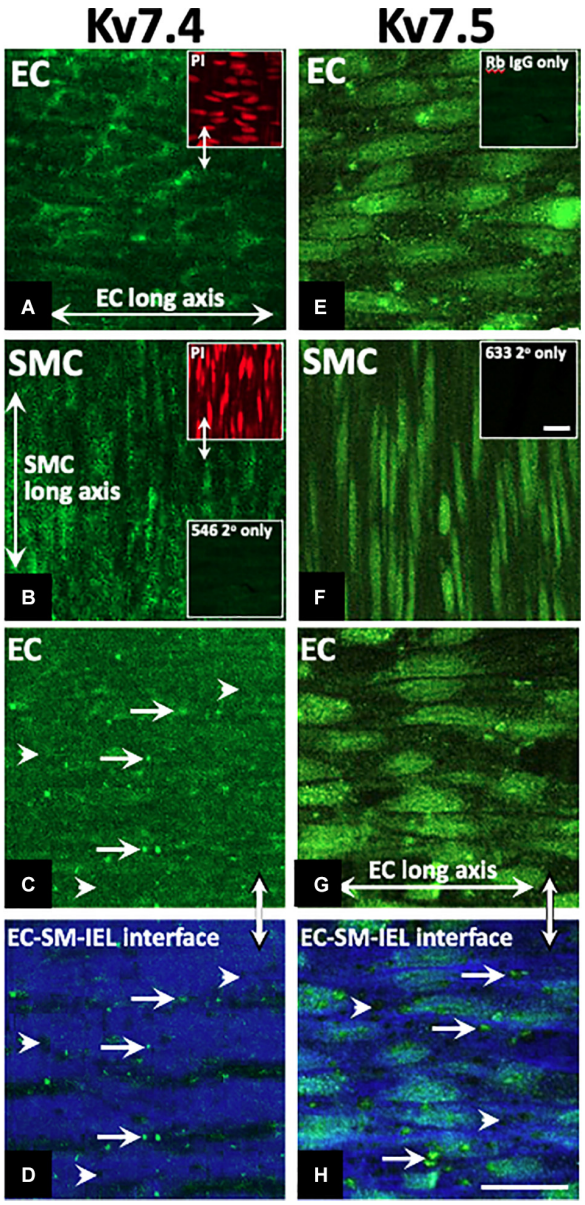

FIGURE 3 | Immunohistochemistry demonstrates Kv7.4 and 7.5 localization in rat mesenteric artery endothelium (EC) and smooth muscle cells (SMCs) with a focus on internal elastic lamina (IEL) hole sites in whole mount tissue. Whole mounts of confocal stacks through the EC and SMC of K_V7.4 (**A,B**, respectively) and Kv7.5 (**E,F**, respectively). Confocal image stacks through the luminal EC to SM border **(C,G)** show diffuse/punctate K_V7.4/K_V7.5 across the cell membrane with some punctate higher-level fluorescence at localized sites (e.g. full arrows; **C**). When single images were taken at the EC-IEL-SM interface **(D,H)**, punctate higher-level fluorescence densities were present (e.g. **D,H** arrows; **H**, higher magnification inset) at *a proportion* of IEL hole sites (e.g., **D,H** arrowheads). Propidium iodide (PI; e.g., upper left inset, **A,B**) were used as nuclear markers to verify cell and layer patency. Incubation in secondary only separately for each of the 3 fluorophores (**Table 2**; e.g. lower left inset, **B**; inset, **F**) were used to set 'zero' confocal settings. Incubation in isotype IgG control only (e.g., **E**, inset) showed fluorescence equivalent to secondary alone (e.g., **B**, lower inset; **F**, inset). $n = 4$, representative of different source. Longitudinal vessel axis, left to right. Double arrows indicate same site, but at different focal planes **(C,D,G,H)**, and location of inset **(D)**. Bar, 25 μm.

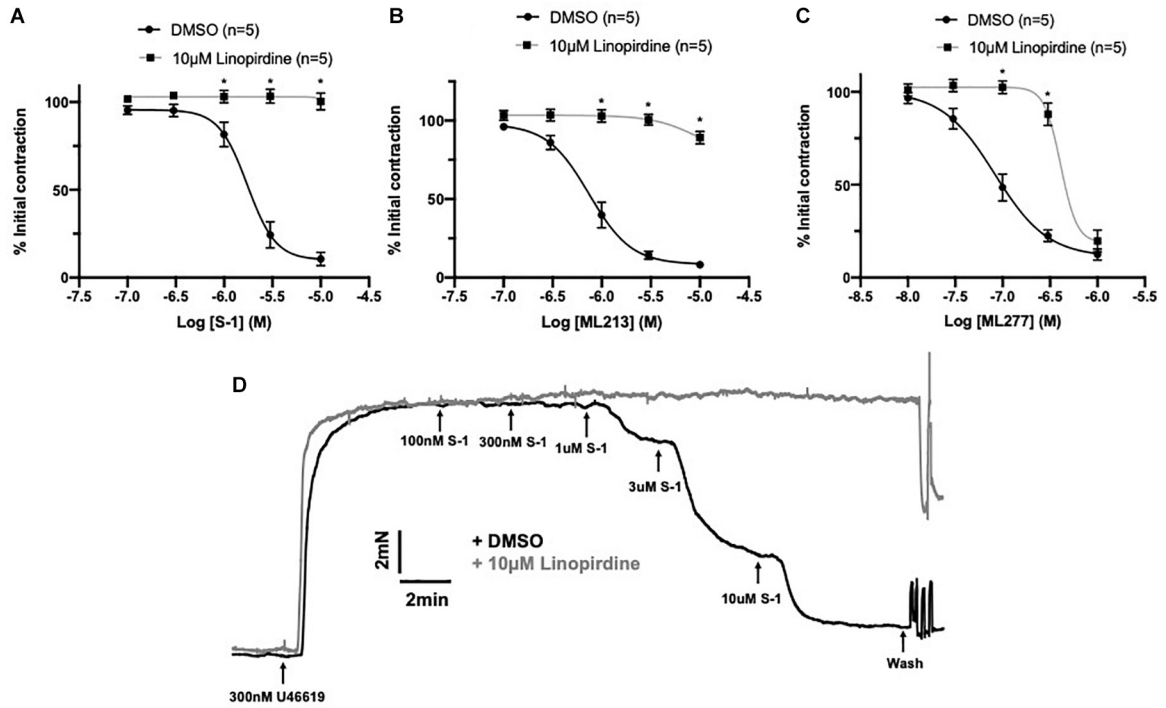

FIGURE 4 | Sensitivity of Kv7 activator relaxations to 10 μmol-L^{-1} linopirdine. In vessels pre-incubated in DMSO solvent control, K_V7.2-5 channel activators S-1 and ML213 relax pre-constricted arterial tone (300 nmol-L^{-1} U46619; black) and are ablated by pre-incubation with pan K_V7 channel inhibitor linopirdine (10 μmol-L^{-1}; gray; n = 5; **A,B**). In vessels pre-incubated in DMSO solvent control, K_V7.1 channel activator ML277 relaxes pre-constricted arterial tone (300 mol-L^{-1} U46619; black) and is ablated by linopirdine (10 μmol-L^{-1}; gray) to a threshold of 300 nmol-L^{-1} ML277 (n = 5; **C**). A representative trace of S-1-mediated vasorelaxation ± 10 μmol-L^{-1} linopirdine **(D)**. All values are expressed as mean + SEM. A two-way statistical ANOVA with a *post hoc* Bonferroni test was used to generate significance values. Statistical significance is defined as $^*P < 0.05$ **(A–C)**.

2 ± 0.2 μmol-L^{-1} to 3 ± 0.7 μmol-L^{-1} (**Figures 5C,D**). S-1 mediated relaxation was also impaired via the non-selective gap junction inhibitor carbenoxolone (Tare et al., 2002) (water E_{max} = 6.11 ± 1.82% vs. carbenoxolone E_{max} = 18.7 ± 3.25%; **Figure 5E**). In addition, the potency of ML213 was also impaired by endothelial removal (EC(+) EC_{50} = 1 ± 0.2 μmol-L^{-1} vs. EC(−) EC_{50} = 3 ± 0.2 μmol-L^{-1}; **Figure 5F**) in a fashion analogous to S-1. However, the linopirdine-sensitive relaxation produced by ML277 was not affected by endothelial removal (**Figure 5G**).

EC K_{IR} Channels Modulate K_V7.2-5 Activator Sensitivity

Having identified that the presence of the endothelium modulates responses to K_V7 activators, experiments were performed to identify the underlying mechanism/s involved. *Murine* endothelial KCNJ2-encoded K_{IR}2.1 channels have been identified as 'signal boosters' that enhance EC-derived relaxation (Sonkusare et al., 2016). Comparatively, the current literature regarding *rat* mesenteric K_{IR}2 channels is limited. In brief, rat MA endothelium expresses K_{IR}2.1 (Dora et al., 2008), inwardly rectifying Ba^{2+} sensitive channels are restricted to the endothelial layer (Crane et al., 2003a) and K_{IR} channels contribute to acetylcholine-mediated responses (Goto et al., 2004). We propose that like mice, rat mesenteric ECs express functional K_{IR}2 channels that propagate EC signals in a similar process. Therefore, we performed a series of studies investigating the effect of two characterized K_{IR}2 blockers, $BaCl_2$ (Hagiwara et al., 1978) and ML133 (Wang et al., 2011) on K_V7 activator-mediated vasorelaxation.

In arteries with a functional endothelium, K_{IR}2 blockers, $BaCl_2$ (100 μmol-L^{-1}) and ML133 (20 μmol-L^{-1}), significantly impaired relaxations produced by S-1 (**Figure 6A**, EC_{50} = DMSO, 1.89 ± 0.2 μmol-L^{-1}/$BaCl_2$, 2.3 ± 0.31 μmol-L^{-1}; **Figure 6B**, EC_{50} = DMSO, 0.52 ± 0.12 μmol-L^{-1}/ML133, 3.1 ± 1.5 μmol-L^{-1}) and ML213 (**Figures 6C,D**, EC_{50} = DMSO, 0.9 ± 0.3 μmol/L^{-1}/$BaCl_2$, 2.2 ± 0.5 μmol/L^{-1}/ML133, 2.5 ± 0.25 μmol-L^{-1}) when compared to DMSO solvent control (**Figures 6A–D**). No attenuation of the response to ML277 was observed when pre-incubated with either blocker (**Figures 6E,F**), consistent with EC removal. Furthermore, in arteries where the endothelium had been removed neither ML133 nor $BaCl_2$ had any effect on ML213 mediated relaxations (**Figures 6G,H**).

IK_{Ca}/SK_{Ca} Inhibitors Had No Impact on K_V7 Activator Mediated Relaxation

Endothelial IK_{Ca} and SK_{Ca} channels contribute to relaxation responses in rat MA (Crane et al., 2003b). Thus, it is feasible that K_V7 channels interact with other key endothelial

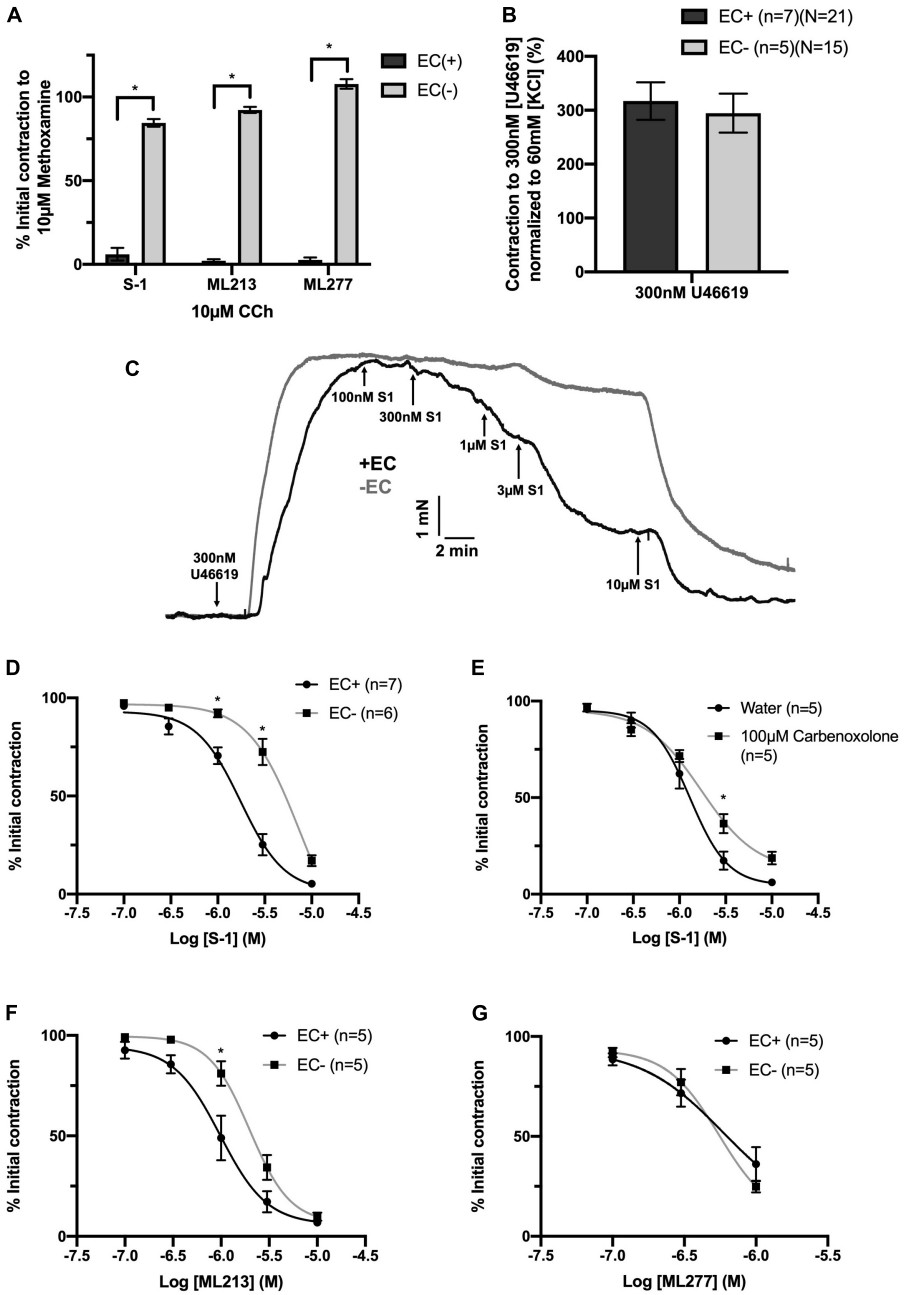

FIGURE 5 | $K_V7.2$-5 channel activator mediated vasorelaxation was significantly attenuated by EC removal. Removal of ECs ablated vasorelaxation in response to 10 μmol-L^{-1} CCh following pre-constriction with 10 μmol-L^{-1} MO **(A)**. Removal of ECs (gray) has no effect on vasoconstriction to U46619 (300 nmol-L^{-1}) when normalized to vasoconstriction to KCl (60 mmol-L^{-1}; n = 5–7; n = 15-21; **B**). Representative trace of EC S-1-mediated vasorelaxation in EC(–) denuded vessels (gray) vs. EC(+) vessels (black; **C**). S-1-mediated vasorelaxation was significantly attenuated by EC removal and 100 μmolL^{-1} carbenoxolone (gray; n = 5–7; **D,E**). ML213 but not ML277-mediated vasorelaxation was significantly attenuated by EC removal (gray; n = 5–7; **D,E**). Removal of ECs (gray) has no effect on ML277 within its range of linopirdine sensitivity (n = 5; **F**). All values are expressed as mean + SEM **(A–G)**. A two-way statistical ANOVA with a *post hoc* Bonferroni test was used to generate significance values. Statistical significance is defined as $^*P < 0.05$ **(A–G)**.

potassium channels; particularly those expressed within microdomains (Sandow et al., 2009). However, consistent with previous reports (Jepps et al., 2016), pre-incubation with a combination of IK_{Ca} inhibitor TRAM-34 (1 μmol-L^{-1}; Wulff et al., 2000) and SK_{Ca} inhibitor apamin (100 nmol-L^{-1}; Spoerri et al., 1975) had no effect on K_V7 activator mediated vasorelaxation (**Figures 7A–C**). These data suggest that the endothelium-dependent increase in potency to the K_V7 activators involves endothelial K_{IR}, but not IK_{Ca} or SK_{Ca} channels.

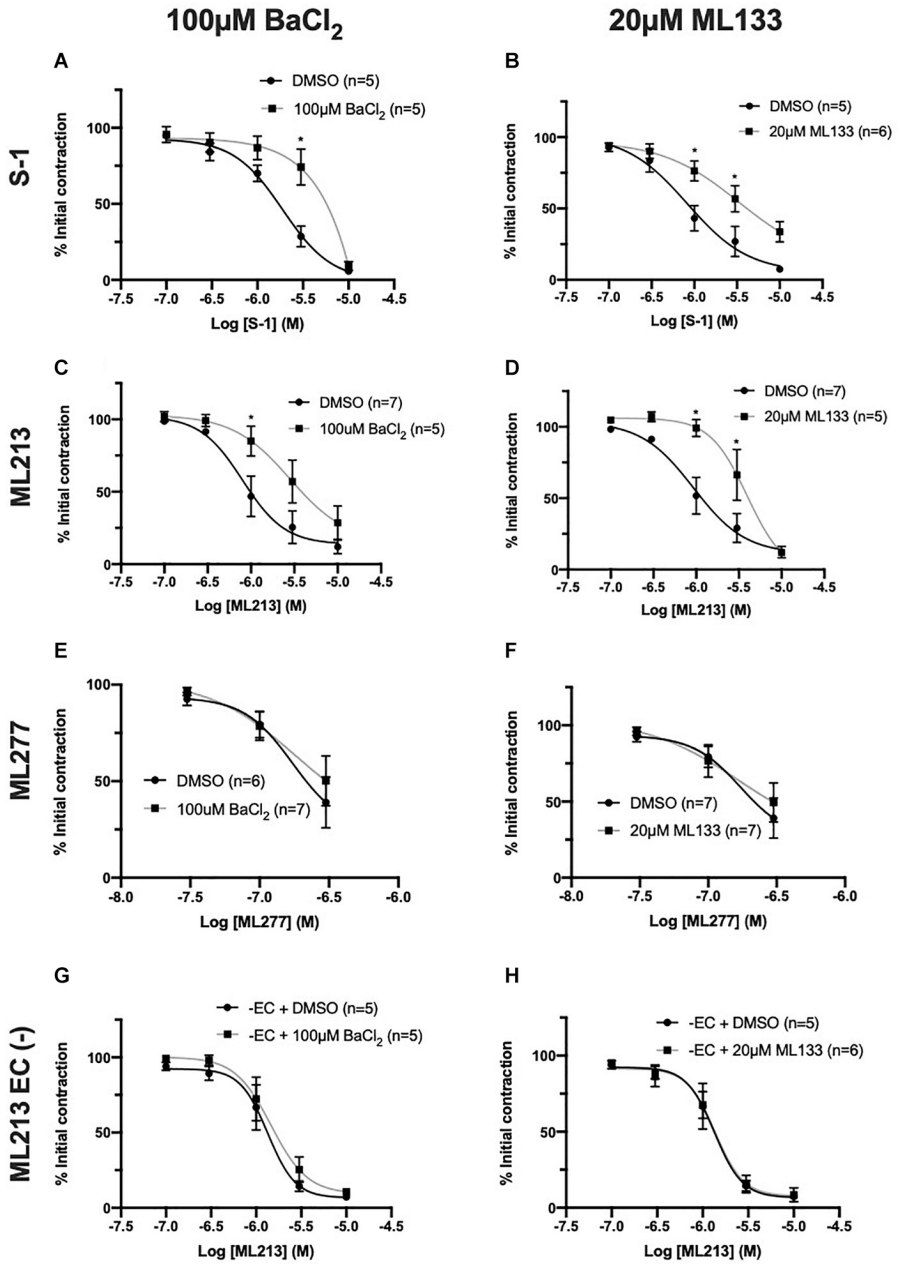

FIGURE 6 | $K_V7.2$-5 channel activator-mediated vasorelaxation was attenuated by two structurally different K_{IR} channel blockers, $BaCl_2$ and ML133, but not In EC denuded vessels. $K_V7.2$-5 channel activator S-1 and ML213 effects were significantly attenuated by pre-incubation with the $K_{IR}2$ channel inhibitor $BaCl_2$ (100 μmol-L^{-1}; black; n = 5–7; **A,C**). $K_V7.2$-5 channel activator S-1 and ML213 effects were significantly attenuated by pre-incubation with a selective K_{Ir} 2.1 channel inhibitor, ML133 (20 μmol-L^{-1}; gray; n = 5–7; **B,D**). $K_V7.1$ channel activator ML277-mediated vasorelaxation was not affected by pre-incubation with either $BaCl_2$ (100 μmol-L^{-1}) or ML133 (20 μmol-L^{-1}; gray; n = 6–7; **E,F**). In EC denuded vessels, $K_V7.2$-5 channel activator ML213 responses were not affected by pre-incubation with either $K_{IR}2$ channel inhibitor $BaCl_2$ (100 μmol-L^{-1}; gray; n = 5; **G**) or ML133 (20 μmol-L^{-1}; gray; n = 5–6; **H**). All values are expressed as mean + SEM **(A–H)**. A two-way statistical ANOVA with a *post hoc* Bonferroni test was used to generate significance values. Statistical significance is defined as $^*P < 0.05$ **(A–H)**.

K_V7 Channels Contribute to CCh Evoked Vasorelaxation

The expression of functional K_V7 channels within ECs begs the question - do they contribute to EC-derived responses? Acetylcholine produces endothelium-dependent relaxation through NO-, EDH- and prostanoid-dependent mechanisms in rat MA (Parsons et al., 1994; Shimokawa et al., 1996; Peredo et al., 1997).

A distinct rightward shift in the sensitivity to vasorelaxation in response to CCh, a synthetic acetylcholine analog, was

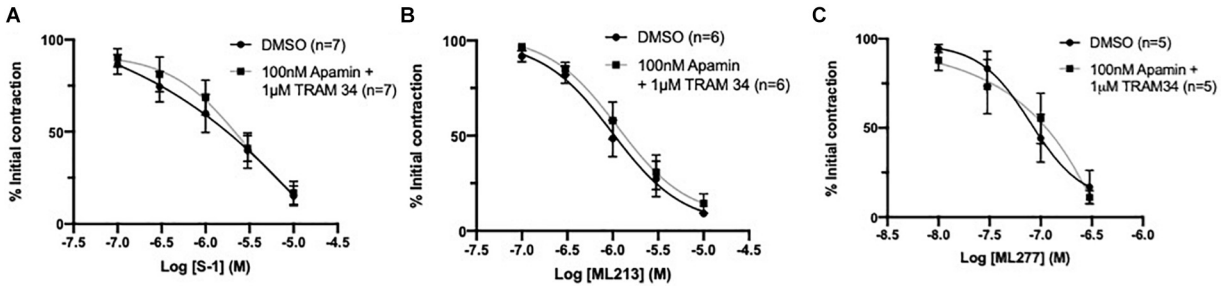

FIGURE 7 | K_V7 channel activator mediated vasorelaxation was not affected by preincubation with IK_{Ca}/SK_{Ca} channel antagonists. Pre-incubation with both IK_{Ca} channel inhibitor TRAM34 (1 μmol-L^{-1}) and SK_{Ca} channel inhibitor Apamin (100 nmol-L^{-1}) had no effect on S-1, ML213 nor ML277 mediated vasorelaxation (n = 5–7; gray, **A–C**). All values are expressed are expressed as mean values ± SEM. A two-way statistical ANOVA with a *post hoc* Bonferroni test was used to generate significance values; no significant values were observed **(A–C)**.

produced by the eNOS inhibitor L-NAME (100 μmol-L^{-1}) when compared to DMSO control (EC_{50} DMSO = 0.59 ± 0.1 μmol-L^{-1}; L-NAME = 0.94 ± 0.1 μmol-L^{-1}; **Figure 8A**). A combination IK_{Ca} and SK_{Ca} inhibitors, TRAM-34 (1 μmol-L^{-1}) and apamin (100 nmol-L^{-1}) respectively, suppress EDH in rat MA, and produced greater attenuation (EC_{50} TRAM34/apamin = 1.5 ± 0.7 μmol-L^{-1}; **Figure 8A**) when compared to L-NAME. Pre-incubating vessels with the pan K_V7 channel inhibitor linopirdine (10 μmol-L^{-1}) significantly attenuated CCh-mediated relaxation when compared to DMSO control (EC_{50} DMSO = 0.2 ± 0.08 μmol-L^{-1}; linopirdine = 0.7 ± 0.3 μmol-L^{-1}; **Figure 8B**). In contrast, pre-incubating vessels with either the $K_V7.1$ specific inhibitor HMR-1556 (10 μmol-L^{-1}) or a combination of non-specific K_V channel inhibitors TEA (1 mmol-L^{-1}; Choi et al., 1991) and 4-AP (1 mmol-L^{-1}; Kurata and Fedida, 2006) had no significant effect on CCh-evoked vasorelaxation (**Figures 8C,D**).

Additionally, CCh-evoked relaxations were significantly attenuated in vessels pre-incubated in TRAM34/apamin (1 μmol-L^{-1}/100 nmol-L^{-1}) and linopirdine (10 μmol-L^{-1}) compared to vessels only pre-incubated in TRAM34/apamin alone (EC_{50} DMSO = 0.24 ± 0.05 μmol-L^{-1}; TRAM34/Apamin = 0.27 ± 0.03 μmol-L^{-1}; TRAM34/Apamin + linopirdine = 0.61 ± 0.2 μmol-L^{-1}; **Figure 8E**). In contrast, linopirdine failed to attenuate CCh relaxation in arteries pre-incubated with L-NAME (100 μmol-L^{-1}; **Figure 8F**), thus suggesting K_V7 contribution to eNOS sensitive proportion of CCh-mediated relaxation.

Furthermore, the present data demonstrates that pre-incubation with linopirdine (10 μmol-L^{-1}) has no effect on vasorelaxation produced by the NO-donor SNP (**Figure 8G**). However, in contrast with previous reports (Jepps et al., 2016), pre-incubation with L-NAME (100 μmol-L^{-1}) significantly attenuated $K_V7.2$-5 activator mediated vasorelaxation (**Figure 8H**).

DISCUSSION

The present study identified *Kcnq1, Kcnq4,* and *Kcnq5* transcripts in EC marker expressing cells and the consequent $K_V7.1$, $K_V7.4$, and $K_V7.5$ protein in isolated and whole mount rat MA ECs/VSMCs. Functionally, the present study demonstrates that the relaxation produced by two structurally different $K_V7.2$-5 activators, but not a $K_V7.1$ activator, were modulated by the presence of the endothelium and gap junction inhibition. Said relaxation was also sensitive to $K_{IR}2$ inhibition, which was dependent on the presence of ECs, suggestive of a novel functional interaction between K_V7 and endothelial $K_{IR}2.x$ channels. Furthermore, the present data suggest that $K_V7.4/K_V7.5$ channels contribute to the NO-mediated axis of CCh-evoked endothelium-dependent relaxation downstream of eNOS. Thus, K_V7 channels are expressed in ECs, when pharmacologically upregulated, are functionally coupled to other EC potassium channels in rat MA and contribute to endothelium-derived responses.

K_V7 Channel Expression and Function Within ECs

Kv7 channel modulators have considerable impact on arterial tone. In VSMCs, active K_V7 channels hyperpolarize the membrane potential, decreasing voltage-dependent calcium channel (VDCC) open probability and extracellular calcium influx resulting in relaxation. Within rodent models, the pharmacopeia of K_V7 channel modulators has revealed $K_V7.4$ and 7.5 channels are; (1) key determinants of resting vascular tone via regulation of resting membrane potential; (2) upregulated during cGMP and cAMP/EPAC/PKA-mediated vasodilation; (3) suppressed via PKC-mediated vasoconstriction. Comparatively, no functional role for $K_V7.1$ has been identified in arteries (see Barrese et al., 2018b; Byron and Brueggemann, 2018 for review). A caveat of these observations is a lack of differentiation between VSMCs and ECs. However, recently K_V7 channels were identified in pig coronary artery ECs (Chen et al., 2016), the novel findings presented here expand on these findings and demonstrate K_V7 transcript and channel expression, functional activity and contribution to EC-derived vasodilatory signaling cascades in rat MA endothelium.

In most arteries, the endothelium and smooth muscle are electrochemically linked via MEGJs formed from connexin proteins within heterocellular communicating microdomains

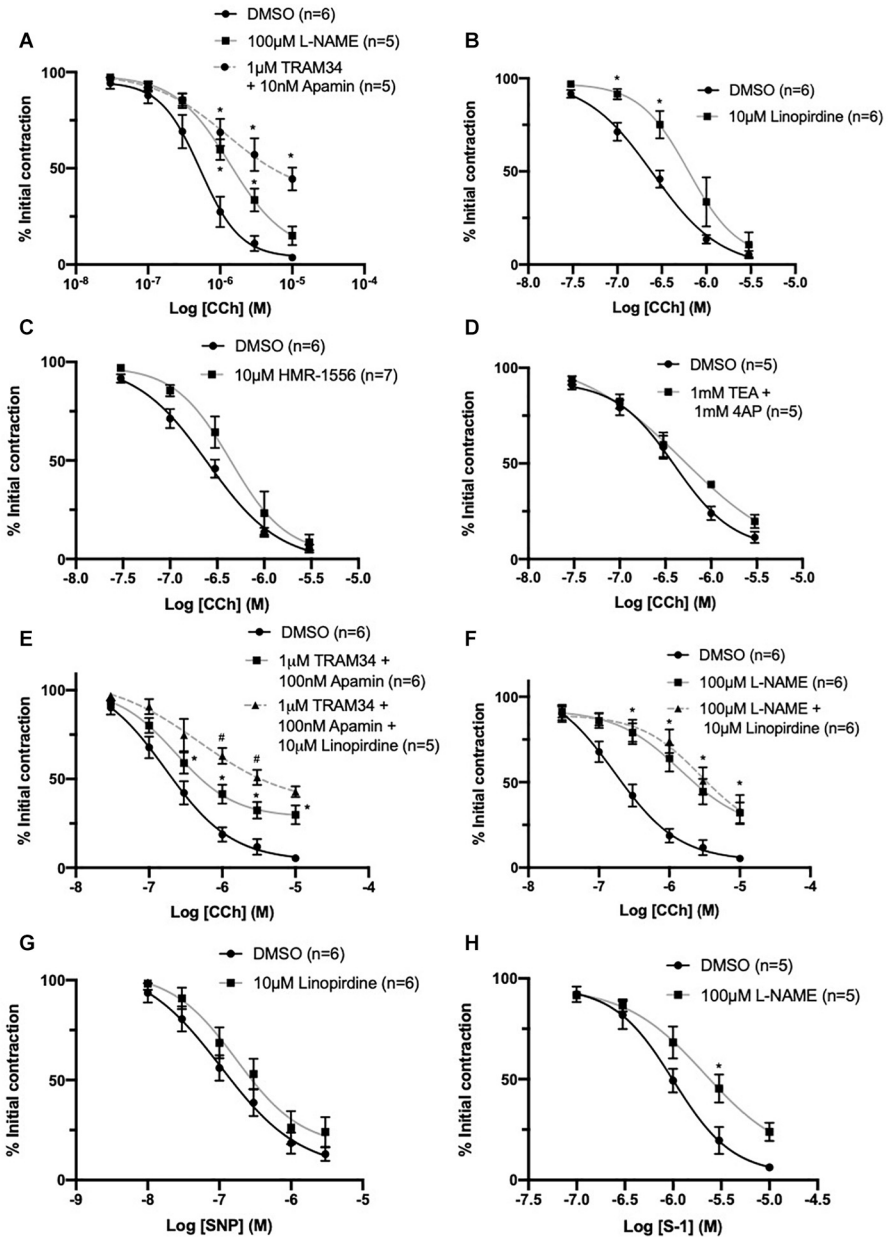

FIGURE 8 | CCh evoked vasorelaxation is mediated through both eNOS and IK_{Ca}/SK_{Ca} channels and is partially attenuated by inhibition of K_V7 channels upstream of NO. Both eNOS inhibitor L-nitroarginine methyl ester (L-NAME; 100 μmol-L^{-1}; gray) and IK_{Ca}/SK_{Ca} channel inhibitors TRAM-34 (1 μmol-L^{-1})/apamin (100 nmol-L^{-1}; red, dashed line) significantly attenuated CCh mediated vasorelaxation (n = 5–6; **A**). The pan K_V7 channel inhibitor linopirdine (10 μmol-L^{-1}; gray) significantly attenuated CCh mediated vasorelaxation (n = 6; **B**). The $K_V7.1$ channel inhibitor HMR-1556 (10 μmol-L^{-1}; gray) did not modulate CCh-mediated vasorelaxation (n = 6; **C**). A combination of non-specific K^+ channel inhibitors 4-aminopyridine (4-AP; 1 mmol-L^{-1}) and tetraethylammonium (TEA; 1 mmol-L^{-1}; gray) did not modulate CCh-mediated vasorelaxation (n = 5; **D**). Additive attenuation to CCh-evoked relaxation in the presence of TRAM-34 (1 μmol-L^{-1})/apamin (100 nmol-L^{-1}) + linopirdine (10 μmol-L^{-1}; gray, dashed line) was observed when compared to vessels pre-incubated in only TRAM34/apamin (gray; n = 5–6; **E**). No additive attenuation to CCh evoked vasorelaxation was observed between vessels pre-incubated in L-NAME (100 μmol-L^{-1}) + linopirdine (10 μmol-L^{-1}; gray, dashed line) when compared with L-NAME (100 μmol-L^{-1}; gray; n = 5; **F**). SNP-mediated vasorelaxation was no effected by the pan-K_V7 channel inhibitor linopirdine (10 μmol-L^{-1}; gray) when compared to DMSO solvent control (black; **G**). $K_V7.2$-5 channel activator S-1 was significantly attenuated by pre-incubation with eNOS inhibitor L-NAME (100 μmol-L^{-1}; gray; n = 5; **H**). All values are expressed as mean + SEM. A two-way statistical ANOVA with a *post hoc* Bonferroni test was used to generate significance values (*, drug v DMSO solvent control; #=Group B vs. Group C) Statistical significance is defined as $^{\#/*}P < 0.05$ **(A–H)**.

present within holes in the IEL (see Sandow et al., 2012 for review). Via these connections, current injection in to ECs passes into VSMCs (Sandow et al., 2002) supporting the presence of such coupling. The present data suggests a potential role for electrochemical heterocellular communication during $K_V7.2$-5 activator-mediated vasorelaxation (**Figure 9**). This conjecture is

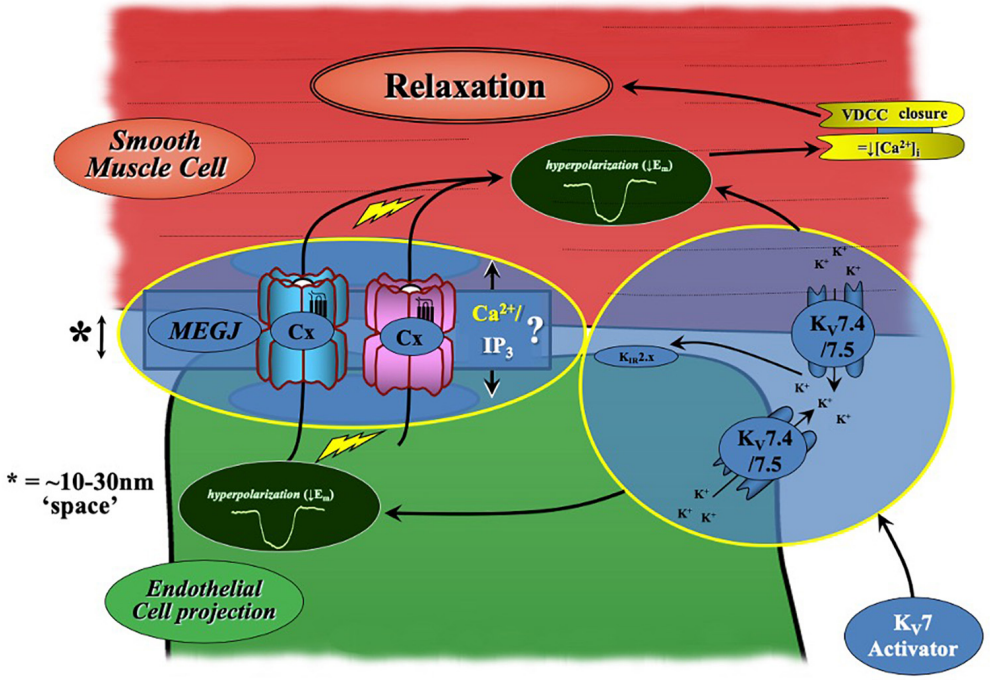

FIGURE 9 | Schematic of K_V7.2-5 activator-mediated vasorelaxation. K_V7.2-5 activator-mediated vasorelaxation occurs predominantly via K_V7.4/7.5 activation within VSMCs. However, our findings suggest a novel contribution of endothelial-K_V7.4/7.5 channels to K_V7.2-5 activator mediated responses which augments relaxation. A process which is sensitive to both gap-junction and endothelial-K_{IR}2.x inhibition (modified from Senadheera et al., 2012).

supported by apparently higher level expression of K_V7.4/K_V7.5 in a proportion of IEL holes than that at the EC membrane as well as a significant attenuation of relaxation of pre-constricted arterial tone by two structurally different K_V7.2-5 activators in the absence of ECs and presence of a (putative) gap junction inhibitor. In contrast, EC removal had no impact on K_V7.1 activator-mediated vasorelaxation, which was observed in conjunction with reduced expression of *Kcnq1* transcript and K_V7.1 labeling within ECs compared to VSMCs. Collectively suggesting that only K_V7.4/K_V7.5 channels of the K_V7 sub-family are functionally expressed within MA ECs. An extrapolation of these results indicates a novel role for K_V7.4/K_V7.5 channels in the regulation of EC membrane potential within myoendothelial projections. It is plausible, that localized EC K_V7 channels negate the influx of depolarization from VSMCs into the endothelium, providing tight regulation of EC V_m during VSMC contraction. However, further studies would be required to validate this hypothesis.

A Novel Functional Interaction With Endothelial K_{IR} Channels

K_{IR}2.x channels have been characterized in a variety of rat vascular beds including cerebral and coronary arteries (Smith et al., 2008), where their selective inhibition by Ba^{2+} revealed K_{IR} channel amplification of a K^+ channel activator conductance (Smith et al., 2008). However, there is a degree of conflict regarding the role of K_{IR}2.x channels within rat MAs. As above, Ba^{2+} sensitive currents and K_{IR}2.x expression has been demonstrated in rat MA ECs (Crane et al., 2003a) which are purported to contribute to K_{Ca} mediated-hyperpolarization during ACh-derived EC-dependent responses (Goto et al., 2004). In contrast, Smith et al. (2008) demonstrated that within 3rd order MAs, ACh-mediated K^+ conductance-dependent relaxation was insensitive to Ba^{2+}, indicating that K_{IR}2.x channels do not augment K^+ conductance in these vessels during receptor-mediated vasodilation.

In the present study, significant attenuation of both S-1 and ML213 K_V7.2-5 activator-mediated vasorelaxation was found following pre-incubation with two structurally different K_{IR}2.x blockers ML133 (Wu et al., 2010) and Ba^{2+} (Hagiwara et al., 1978) when compared to a solvent control. ML133 has been identified via high-throughput and mutagenesis investigation as a novel inhibitor of K_{IR}2.1 channels via D172 and I176 residues within the M2 region of K_{IR}2.1 (Wang et al., 2011) with an IC_{50} of 1.8 μmol-L^{-1} at pH 7.4, with little to no effect against other K_{IR}2.x family members (Wu et al., 2010; Wang et al., 2011). Presently, ML133 is the most selective inhibitor of the K_{IR}2 family. In analogous fashion to our endothelium denudation experiments, no effect was seen on the K_V7.1 activator ML277-mediated vasorelaxation; implying a specific interplay with K_V7.4 and 7.5 channels. Furthermore, K_{IR}2 blockers had no effect on K_V7.2–7.5 activator-mediated relaxation in EC-denuded arteries, supporting the notion that functional K_{IR}2 channels (in the rat MA bed) are restricted to the endothelium (Crane et al., 2003b). The present study suggests that pharmacological activation of

endothelial $K_V7.4/7.5$ channels also activates an endothelial $K_{IR}2$ channels, increasing K^+ conductance, which in turn accounts for a proportion of EC augmentation of $K_V7.2$-5 activator-mediated vasorelaxation (**Figure 9**). This may be due to a localized increase in potassium ion concentration in the proximity of the $K_{IR}2$ channels or an alternative modulation. However, based on the findings described by Goto et al. (2004) and Smith et al. (2008), the collective data suggest that this phenomenon is dependent on the branch order of MA. Furthermore, it remains unclear if this occurs during receptor mediated signaling, or if it is only present during pharmacological activation of endothelial K_V7 channels.

A primary concern for identification of novel functional interactions between ion channels using pharmacological tools is potential off-target effects. However, K_V7 activator-mediated relaxation in vessels pre-incubated in 10 μmol-L^{-1} linopirdine was abolished. If S-1 or ML213 were activating non-K_V channels such as K_{IR}, a degree of relaxation would still be observed in the presence of linopirdine. The present findings therefore suggest that both S-1 and ML213 work exclusively via K_V7 channels and that attenuation of their response within rat MA occurs via a novel functional coupling of $K_V7.4/7.5$ and $K_{IR}2$ within ECs.

The Contribution of K_V7 Channels to CCh Evoked Relaxations Within Rat MA

Our findings demonstrate that both NO- and EDH-dependent signaling contributes to CCh-mediated vasodilation, though the main contributor to endothelial-dependent vasodilation in 2nd order MA appears to be EDH, consistent with previous studies (Shimokawa et al., 1996). In light of the significant impact of K_V7 inhibition on CCh-mediated vasorelaxation during the suppression of EDH, the present study suggests that K_V7 channels contribute to the eNOS sensitive axis of CCh-evoked relaxation within rat MA.

However, in a similar manner to rat renal artery (Stott et al., 2015), rat MA K_V7 channels do not represent downstream targets of NO signaling as K_V7 inhibition does not impair NO-donor SNP-mediated relaxation. However, eNOS inhibition does impair relaxation to a K_V7 activator, potentially implying K_V7 channel involvement in the production or release of NO in response to CCh. Interestingly, this appears to be a vascular bed specific phenomenon, as L-NAME has no effect on K_V7 activator-mediated relaxation within rat penile artery (Jepps et al., 2016).

Limitations

Ideally, direct functional evidence for a functional role of K_v7 channels in ECs would be provided by either single cell electrophysiology of sharp microelectrode impalement in whole arteries. However, this was not possible within the constraints of this study. Instead, we inferred a functional role for EC K_v7 channels using a reductive approach, i.e., comparison of functional responses without or with EC ablation. These studies implicate K_v7 channels as functional component of the EC physiology that merit consideration in future studies.

CONCLUSION

In conclusion, the present data reveal that mesenteric ECs express $K_V7.4/K_V7.5$ channels and their presence boosts K_V7 activator-mediated relaxation. Furthermore, the data indicated a novel functional interaction with endothelial $K_{IR}2$ channels and support the proposition that endothelial K_V7 channels contribute to endogenous endothelium-derived responses. These findings highlight the complex nature of the vascular response to K_V7 channel upregulation and emphasize the importance of these channels to vascular signaling. The present data are consistent with K_V7 channels representing a novel therapeutic target in endothelial dysfunction.

DATA AVAILABILITY STATEMENT

The original contributions presented in the study are included in the article/**Supplementary Material**, further inquiries can be directed to the corresponding author/s.

ETHICS STATEMENT

The animal study was reviewed and approved by UNSW Animal Ethics and Experimentation Committee (AEEC #18/86B). For investigations performed at St George's University, London, investigators strictly adhered to the Animal (Scientific Procedures) Act 1986.

AUTHOR CONTRIBUTIONS

SB, SS, GM-P, and JS performed the research. IG and JS designed the research study. SS contributed essential reagents or tools. SB, SS, and GM-P analyzed the data. SB and IG wrote the manuscript. All the authors contributed to the article and approved the submitted version.

FUNDING

SB was funded by the British Heart Foundation (Grant #FS/18/41/33762) awarded to IG.

ACKNOWLEDGMENTS

The authors would like to thank Miss Aditi Gunjal for her excellent assistance in wire myography.

SUPPLEMENTARY MATERIAL

The Supplementary Material for this article can be found online at: https://www.frontiersin.org/articles/10.3389/fphys.2020.598779/full#supplementary-material

REFERENCES

Askew Page, H. R., Dalsgaard, T., Baldwin, S. N., Jepps, T. A., Povstyan, O., Olesen, S. P., et al. (2019). TMEM16A is implicated in the regulation of coronary flow and is altered in hypertension. *Br. J. Pharmacol.* 176, 1635–1648. doi: 10.1111/bph.14598

Barrese, V., Stott, J. B., Figueiredo, H. B., Aubdool, A. A., Hobbs, A. J., Jepps, T. A., et al. (2018b). Angiotensin II Promotes $K_V7.4$ channels degradation through reduced interaction with HSP90. *Hypertension* 71, 1091–1100. doi: 10.1161/HYPERTENSIONAHA.118.11116

Barrese, V., Stott, J. B., and Greenwood, I. A. (2018a). KCNQ-encoded potassium channels as therapeutic targets. *Ann. Rev. Pharmacol. Toxicol.* 58, 625–648. doi: 10.1146/annurev-pharmtox-010617-052912

Bentzen, B. H., Schmitt, N., Calloe, K., Dalby Brown, W., Grunnet, M., and Olesen, S. P. (2006). The acrylamide (S)-1 differentially affects Kv7 (KCNQ) potassium channels. *Neuropharmacology* 51, 1068–1077. doi: 10.1016/j.neuropharm.2006.07.001

Brueggemann, L. I., Cribbs, L. L., Schwartz, J., Wang, M., Kouta, A., and Byron, K. L. (2018). Mechanisms of PKA-dependent potentiation of Kv7.5 channel activity in human airway smooth muscle cells. *Int. J. Mol. Sci.* 12:2223. doi: 10.3390/ijms19082223

Brueggemann, L. I., Haick, J. M., Cribbs, L. L., and Byron, K. L. (2014). Differential activation of vascular smooth muscle Kv7.4, Kv7.5, and Kv7.4/7.5 channels by ML213 and ICA-069673. *Mol. Pharmacol.* 86, 330–341. doi: 10.1124/mol.114.093799

Brueggemann, L. I., Moran, C. J., Barakat, J. A., Yeh, J. Z., Cribbs, L. L., and Byron, K. L. (2006). Vasopressin stimulates action potential firing by protein kinase C-dependent inhibition of KCNQ5 in A7r5 rat aortic smooth muscle cells. *AJP Heart Circ. Physiol.* 292, H1352–H1363. doi: 10.1152/ajpheart.00065.2006

Byron, K. L., and Brueggemann, L. I. (2018). Kv7 potassium channels as signal transduction intermediates in the control of microvascular tone. *Microcirculation* 25:e12419. doi: 10.1111/micc.12419

Chadha, P. S., Zunke, F., Zhu, H. L., Davis, A. J., Jepps, T. A., Olesen, S. P., et al. (2012). Reduced KCNQ4-encoded voltage-dependent potassium channel activity underlies impaired β-adrenoceptor-mediated relaxation of renal arteries in hypertension. *Hypertension* 59, 877–884. doi: 10.1161/HYPERTENSIONAHA.111.187427

Chen, X., Li, W., Hiett, S. C., and Obukhov, A. G. (2016). Novel Roles for Kv7 channels in shaping histamine-induced contractions and bradykinin-dependent relaxations in Pig Coronary Arteries. *PLoS One* 11:e1048569. doi: 10.1371/journal.pone.0148569

Choi, K. L., Aldricht, R. W., Yellen, G., and Hughes, H. (1991). Tetraethylammonium blockade distinguishes two inactivation mechanisms in voltage-activated Ki channels. *Proc. Natl. Acad. Sci. U. S. A.* 88, 5092–5095. doi: 10.1073/pnas.88.12.5092

Crane, G. J., Gallagher, N., Dora, K. A., and Garland, C. J. (2003a). Small- and intermediate-conductance calcium-activated K+ channels provide different facets of endothelium-dependent hyperpolarization in rat mesenteric artery. *J. Physiol.* 553(Pt 1), 183–189. doi: 10.1113/jphysiol.2003.051896

Crane, G. J., Walker, S. D., Dora, K. A., and Garland, C. J. (2003b). Evidence for a differential cellular distribution of inward rectifier K channels in the rat isolated mesenteric artery. *J. Vasc. Res.* 40, 159–168. doi: 10.1159/000070713

Curtis, M. J., Alexander, S., Cirino, G., Docherty, J. R., George, C. H., Giembycz, M. A., et al. (2018). Experimental design and analysis and their reporting II: updated and simplified guidance for authors and peer reviewers. *Br. J. Pharmacol.* 175, 987–993. doi: 10.1111/bph.14153

Dora, K. A., Gallagher, N. T., McNeish, A., and Garland, C. J. (2008). Modulation of endothelial cell KCa3.1 channels during endothelium-derived hyperpolarizing factor signaling in mesenteric resistance arteries. *Circ. Res.* 102, 1247–1255. doi: 10.1161/CIRCRESAHA.108.172379

Fukao, M., Hattori, Y., Kanno, M., Sakuma, I., and Kitabatake, A. (1997). Sources of Ca2+ in relation to generation of acetylcholine-induced endothelium-dependent hyperpolarization in rat mesenteric artery. *Br. J. Pharmacol.* 120, 1328–1334. doi: 10.1038/sj.bjp.0701027

Goto, K., Rummery, N. M., Grayson, T. H., and Hill, C. E. (2004). Attenuation of conducted vasodilatation in rat mesenteric arteries during hypertension: role of inwardly rectifying potassium channels. *J. Physiol.* 561(Pt 1), 215–231. doi: 10.1113/jphysiol.2004.070458

Grayson, T. H., Chadha, P. S., Bertrand, P. P., Chen, H., Morris, M. J., Senadheera, S., et al. (2013). Increased caveolae density and caveolin-1 expression accompany impaired NO-mediated vasorelaxation in diet-induced obesity. *Histochem. Cell Biol.* 139, 309–321. doi: 10.1007/s00418-012-1032-2

Greenberg, H. Z. E., Shi, J., Jahan, K. S., Martinucci, M. C., Gilbert, S. J., Ho, W. S., et al. (2016). Stimulation of calcium-sensing receptors induces endothelium-dependent vasorelaxations via nitric oxide production and activation of IKCa channels. *Vasc. Pharmacol.* 80, 75–84. doi: 10.1016/j.vph.2016.01.001

Hagiwara, S., Miyazaki, S., Moody, W., and Patlak, J. (1978). Blocking effects of barium and hydrogen ions on the potassium current during anomalous rectification in the starfish egg. *J. Physiol.* 279, 167–185. doi: 10.1113/jphysiol.1978.sp012338

Howitt, L., Hilton Grayson, T., Morris, M. J., Sandow, S. L., and Murphy, T. V. (2012). Dietary obesity increases NO and inhibits BKCa-mediated, endothelium-dependent dilation in rat cremaster muscle artery: association with caveolins and caveolae. *Am. J. Physiol. Heart Circ. Physiol.* 302, H2464–H2476. doi: 10.1152/ajpheart.00965.2011

Jepps, T. A., Bentzen, B. H., Stott, J. B., Povstyan, O. V., Sivaloganathan, K., Dalby-Brown, W., et al. (2014). Vasorelaxant effects of novel Kv7.4 channel enhancers ML213 and NS15370. *Br. J. Pharmacol.* 171, 4413–4424. doi: 10.1111/bph.12805

Jepps, T. A., Chadha, P. S., Davis, A. J., Harhun, M. I., Cockerill, G. W., Olesen, S. P., et al. (2011). Downregulation of Kv7.4 channel activity in primary and secondary hypertension. *Circulation* 124, 602–611. doi: 10.1161/CIRCULATIONAHA.111.032136

Jepps, T. A., Greenwood, I. A., Moffatt, J. D., Sanders, K. M., and Ohya, S. (2009). Molecular and functional characterization of K_v7 K^+ channel in murine gastrointestinal smooth muscles. *Am. J. Physiol. Gastrointest. Liver Physiol.* 297, G107–G115. doi: 10.1152/ajpgi.00057.2009

Jepps, T. A., Olesen, S. P., Greenwood, I. A., and Dalsgaard, T. (2016). Molecular and functional characterization of Kv7 channels in penile arteries and corpus cavernosum of healthy and metabolic syndrome rats. *Br. J. Pharmacol.* 173, 1478–1490. doi: 10.1111/bph.13444

Khanamiri, S., Soltysinska, E., Jepps, T. A., Bentzen, B. H., Chadha, P. S., Schmitt, N., et al. (2013). Contribution of K_v7 channels to basal coronary flow and active response to ischemia. *Hypertension* 62, 1090–1097. doi: 10.1161/HYPERTENSIONAHA.113.01244

Kurata, H. T., and Fedida, D. (2006). A structural interpretation of voltage-gated potassium channel inactivation. *Prog. Biophys. Mol. Biol.* 92, 185–208. doi: 10.1016/j.pbiomolbio.2005.10.001

Mackie, A. R., Brueggemann, L. I., Henderson, K. K., Shiels, A. J., Cribbs, L. L., Scrogin, K. E., et al. (2008). Vascular KCNQ potassium channels as novel targets for the control of mesenteric artery constriction by vasopressin, based on studies in single cells, pressurized arteries, and in vivo measurements of mesenteric vascular resistance. *J. Pharmacol. Exp. Ther.* 325, 475–483. doi: 10.1124/jpet.107.135764

Mani, B. K., Robakowski, C., Brueggemann, L. I., Cribbs, L. L., Tripathi, A., Majetschak, M., et al. (2016). Kv7.5 potassium channel subunits are the primary targets for PKA-dependent enhancement of vascular smooth muscle Kv7 Currents. *Mol. Pharmacol.* 89, 323–334. doi: 10.1124/mol.115.101758

McGuire, J. J., Ding, H., and Triggle, C. R. (2001). Endothelium-derived relaxing factors: a focus on endothelium-derived hyperpolarizing factor(s). *Can. J. Physiol. Pharmacol.* 79, 443–470. doi: 10.1139/y01-025

Mills, T. A., Greenwood, S. L., Devlin, G., Shweikh, Y., Robinson, M., Cowley, E., et al. (2015). Activation of K_V7 channels stimulates vasodilatation of human placental chorionic plate arteries. *Placenta* 36, 638–644. doi: 10.1016/j.placenta.2015.03.007

Mondéjar-Parreño, G., Moral-Sanz, J., Barreira, B., De la Cruz, A., Gonzalez, T., Callejo, M., et al. (2019). Activation of Kv7 channels as a novel mechanism for NO/cGMP-induced pulmonary vasodilation. *Br. J. Pharmacol.* 176, 2131–2145. doi: 10.1111/bph.14662

Morales-Cano, D., Moreno, L., Barreira, B., Pandolfi, R., Chamorro, V., Jimenez, R., et al. (2015). Kv7 channels critically determine coronary artery reactivity: left-right differences and down-regulation by hyperglycaemia. *Cardiovasc. Res.* 106, 98–108. doi: 10.1093/cvr/cvv020

Mulvany, M. J., and Halpern, W. (1976). Mechanical properties of vascular smooth muscle cells *in situ*. *Nature* 260, 617–619. doi: 10.1038/260617a0

Ng, F. L., Davis, A. J., Jepps, T. A., Harhun, M. I., Yeung, S. Y., Wan, A., et al. (2011). Expression and function of the K + channel KCNQ genes in human arteries. *Br. J. Pharmacol.* 162, 42–53. doi: 10.1111/j.1476-5381.2010.01027.x

Ohya, S., Sergeant, G. P., Greenwood, I. A., and Horowitz, B. (2003). Molecular variants of KCNQ channels expressed in murine portal vein myocytes: a role in delayed rectifier current. *Circ. Res.* 92, 1016–1023. doi: 10.1161/01.RES.0000070880.20955.F4

Oliveras, A., Roura-Ferrer, M., Solé, L., De La Cruz, A., Prieto, A., Etxebarria, A., et al. (2014). Functional assembly of Kv7.1/Kv7.5 channels with emerging properties on vascular muscle physiology. *Arterioscler. Thromb. Vasc. Biol.* 23, 1522–1530. doi: 10.1161/ATVBAHA.114.303801

Parsons, S. J. W., Hill, A., Waldron, G. J., Plane, T., and Garland, C. J. (1994). The relative importance of nitric oxide and nitric oxide—independent mechanisms in acetylcholine—evoked dilatation of the rat mesenteric bed. *Br. J. Pharmacol.* 113, 1275–1280. doi: 10.1111/j.1476-5381.1994.tb17136.x

Peredo, H. A., Feleder, E. C., and Adler-Graschinsky, E. (1997). Differential effects of acetylcholine and bradykinin on prostanoid release from the rat mesenteric bed: role of endothelium and of nitric oxide. *Prostaglandins Leukot. Essent. Fatty Acids* 56, 253–258. doi: 10.1016/S0952-3278(97)90567-6

Sandow, S. L., Goto, K., Rummery, N. M., and Hill, C. E. (2004). Developmental changes in myoendothelial gap junction mediated vasodilator activity in the rat saphenous artery. *J. Physiol.* 556(Pt 3), 875–886. doi: 10.1113/jphysiol.2003.058669

Sandow, S. L., Haddock, R. E., Hill, C. E., Chadha, P. S., Kerr, P. M., Welsh, D. G., et al. (2009). What's where and why at a vascular myoendothelial microdomain signalling complex. *Clin. Exp. Pharmacol. Physiol.* 36, 67–76. doi: 10.1111/j.1440-1681.2008.05076.x

Sandow, S. L., Neylon, C. B., Chen, M. X., and Garland, C. J. (2006). Spatial separation of endothelial small- and intermediate-conductance calcium-activated potassium channels (KCa) and connexins: possible relationship to vasodilator function? *J. Anat.* 209, 689–698. doi: 10.1111/j.1469-7580.2006.00647.x

Sandow, S. L., Senadheera, S., Bertrand, P. P., Murphy, T. V., and Tare, M. (2012). Myoendothelial contacts, gap junctions, and microdomains: anatomical links to function? *Microcirculation* 19, 403–415. doi: 10.1111/j.1549-8719.2011.00146.x

Sandow, S. L., Tare, M., Coleman, H. A., Hill, C. E., and Parkington, H. C. (2002). Involvement of myoendothelial gap junctions in the actions of endothelium-derived hyperpolarizing factor. *Circ. Res.* 90, 1108–1113. doi: 10.1161/01.RES.0000019756.88731.83

Schenzer, A. (2005). Molecular Determinants of KCNQ (Kv7) K+ channel sensitivity to the anticonvulsant retigabine. *J. Neurosci.* 25, 5051–5060. doi: 10.1523/JNEUROSCI.0128-05.2005

Schnee, M. E., and Brown, B. S. (1998). Selectivity of linopirdine (DuP 996), a neurotransmitter release enhancer, in blocking voltage-dependent and calcium-activated potassium currents in hippocampal neurons. *J. Pharmacol. Exp. Ther.* 286, 709–717.

Senadheera, S., Kim, Y., Grayson, T. H., Toemoe, S., Kochukov, M. Y., Abramowitz, J., et al. (2012). Transient receptor potential canonical type 3 channels facilitate endothelium-derived hyperpolarization-mediated resistance artery vasodilator activity. *Cardiovasc. Res.* 95, 439–447. doi: 10.1093/cvr/cvs208

Shimokawa, H., Yasutake, H., Fujii, K., Owada, M. K., Nakaike, R., Fukumoto, Y., et al. (1996). The importance of the hyperpolarizing mechanism increases as the vessel size decreases in endothelium-dependent relaxations in rat mesenteric circulation. *J. Cardiovasc. Pharmacol.* 28, 703–711. doi: 10.1097/00005344-199611000-00014

Smith, P. D., Brett, S. E., Luykenaar, K. D., Sandow, S. L., Marrelli, S. P., Vigmond, E. J., et al. (2008). KIR channels function as electrical amplifiers in rat vascular smooth muscle. *J. Physiol.* 586, 1147–1160. doi: 10.1113/jphysiol.2007.145474

Sonkusare, S. K., Dalsgaard, T., Bonev, A. D., and Nelson, M. T. (2016). Inward rectifier potassium (Kir2.1) channels as end-stage boosters of endothelium-dependent vasodilators. *J. Physiol.* 594, 3271–3285. doi: 10.1113/JP271652

Spoerri, E., Jentsch, J., and Glees, P. (1975). Apamin from bee venom. Effects of the neurotoxin on subcellular particles of neural cultures. *FEBS Lett.* 52, 143–147. doi: 10.1016/0014-5793(75)80006-8

Stott, J. B., Barrese, V., Jepps, T. A., Leighton, E. V., and Greenwood, I. A. (2015). Contribution of Kv7 channels to natriuretic peptide mediated vasodilation in normal and hypertensive rats. *Hypertension* 65, 676–682. doi: 10.1161/HYPERTENSIONAHA.114.04373

Stott, J. B., Jepps, T. A., and Greenwood, I. A. (2014). K_V7 potassium channels: a new therapeutic target in smooth muscle disorders. *Drug Discov. Today* 19, 413–424. doi: 10.1016/j.drudis.2013.12.003

Tare, M., Coleman, H. A., and Parkington, H. C. (2002). Glycyrrhetinic derivatives inhibit hyperpolarization in endothelial cells of guinea pig and rat arteries. *Am. J. Physiol. Heart Circ. Physiol.* 282, H335–H341. doi: 10.1152/ajpheart.2002.282.1.H335

Wang, H. R., Wu, M., Yu, H., Long, S., Stevens, A., Engers, D. W., et al. (2011). Selective inhibition of the Kir2 family of inward rectifier potassium channels by a small molecule probe: The discovery, SAR, and pharmacological characterization of ML133. *ACS Chem. Biol.* 6, 845–856. doi: 10.1021/cb200146a

Wu, M., Wang, H., Yu, H., Makhina, E., Xu, J., Dawson, E. S., et al. (2010). "A potent and selective small molecule Kir2.1 inhibitor," in *Probe Reports from the NIH Molecular Libraries Program*, (Bethesda, MD: National Center for Biotechnology Information).

Wulff, H., Miller, M. J., Hänsel, W., Grissmer, S., Cahalan, M. D., and Chandy, K. G. (2000). Design of a potent and selective inhibitor of the intermediate- conductance Ca2+-activated K+ channel, IKCa1: a potential immunosuppressant. *Proc. Natl. Acad. Sci. U. S. A.* 97, 8151–8156. doi: 10.1073/pnas.97.14.8151

Yeung, S. Y. M., Pucovský, V., Moffatt, J. D., Saldanha, L., Schwake, M., Ohya, S., et al. (2007). Molecular expression and pharmacological identification of a role for Kv7 channels in murine vascular reactivity. *Br. J. Pharmacol.* 151, 758–770. doi: 10.1038/sj.bjp.0707284

Yu, H., Lin, Z., Xu, K., Huang, X., Long, S., Wu, M., et al. (2013). "Identification of a novel, small molecule activator of KCNQ1 channels," in *Probe Reports from the NIH Molecular Libraries Program*, (Bethesda, MD: National Center for Biotechnology Information).

Zechariah, A., Tran, C. H. T., Hald, B. O., Sandow, S. L., Sancho, M., Kim, M. S. M., et al. (2020). Intercellular conduction optimizes arterial network function and conserves blood flow homeostasis during cerebrovascular challenges. *Arterioscler. Thromb. Vasc. Biol.* 40, 733–750. doi: 10.1161/ATVBAHA.119.313391

Zhong, X. Z., Harhun, M. I., Olesen, S. P., Ohya, S., Moffatt, J. D., Cole, W. C., et al. (2010). Participation of KCNQ (Kv7) potassium channels in myogenic control of cerebral arterial diameter. *J. Physiol.* 588(Pt 17), 3277–3293. doi: 10.1113/jphysiol.2010.192823

Conflict of Interest: The authors declare that the research was conducted in the absence of any commercial or financial relationships that could be construed as a potential conflict of interest.

frontiers in Physiology

ORIGINAL RESEARCH
published: 15 December 2020
doi: 10.3389/fphys.2020.597395

The Functional Availability of Arterial Kv7 Channels Is Suppressed Considerably by Large-Conductance Calcium-Activated Potassium Channels in 2- to 3-Month Old but Not in 10- to 15-Day Old Rats

*Dongyu Ma[1,2], Dina Gaynullina[1,3], Nadine Schmidt[1], Mitko Mladenov[4,5] and Rudolf Schubert[1,6]**

[1] European Center for Angioscience (ECAS), Research Division Cardiovascular Physiology, Medical Faculty Mannheim, Heidelberg University, Mannheim, Germany, [2] Department of Cardiology, The First Affiliated Hospital of Anhui Medical University, Anhui, China, [3] Faculty of Biology, M.V. Lomonosov Moscow State University, Moscow, Russia, [4] Department of Fundamental and Applied Physiology, Russian National Research Medical University, Moscow, Russia, [5] Institute of Biology, Faculty of Natural Sciences and Mathematics, Ss Cyril and Methodius University, Skopje, Macedonia, [6] Department of Physiology, Institute of Theoretical Medicine, Medical Faculty, University of Augsburg, Augsburg, Germany

Background: Voltage-gated potassium (Kv) channels, especially Kv7 channels, are major potassium channels identified in vascular smooth muscle cells with a great, albeit differential functional impact in various vessels. Vascular smooth muscle Kv7 channels always coexist with other K channels, in particular with BK channels. BK channels differ in the extent to which they influence vascular contractility. Whether this difference also causes the variability in the functional impact of Kv7 channels is unknown. Therefore, this study addressed the hypothesis that the functional impact of Kv7 channels depends on BK channels.

Experimental Approach: Experiments were performed on young and adult rat *gracilis* and *saphenous* arteries using real-time PCR as well as pressure and wire myography.

Key Results: Several subfamily members of Kv7 (KCNQ) and BK channels were expressed in saphenous and gracilis arteries: the highest expression was observed for BKα, BKβ1 and KCNQ4. Arterial contractility was assessed with methoxamine-induced contractions and pressure-induced myogenic responses. In vessels of adult rats, inhibition of Kv7 channels or BK channels by XE991 or IBTX, respectively enhanced arterial contractility to a similar degree, whereas activation of Kv7 channels or BK channels by retigabine or NS19504, respectively reduced arterial contractility to a similar degree. Further, IBTX increased both the contractile effect of XE991 and the anticontractile effect of retigabine, whereas NS19504 reduced the effect of retigabine and impaired the effect of XE991. In vessels of young rats, inhibition of Kv7 channels by XE991 enhanced arterial contractility much stronger than inhibition of BK channels by IBTX, whereas activation of Kv7 by retigabine reduced arterial contractility to a

OPEN ACCESS

Edited by:
Thomas Andrew Jepps, University of Copenhagen, Denmark

Reviewed by:
William F. Jackson, Michigan State University, United States
Geoff Abbott, University of California, Irvine, United States
Iain A. Greenwood, St George's, University of London, United Kingdom

***Correspondence:**
Rudolf Schubert
rudolf.schubert@med.uni-augsburg.de;
rudolf.schubert@medma.uni-heidelberg.de

Specialty section:
This article was submitted to Membrane Physiology and Membrane Biophysics, a section of the journal Frontiers in Physiology

Received: *21 August 2020*
Accepted: *24 November 2020*
Published: *15 December 2020*

Citation:
Ma D, Gaynullina D, Schmidt N, Mladenov M and Schubert R (2020) The Functional Availability of Arterial Kv7 Channels Is Suppressed Considerably by Large-Conductance Calcium-Activated Potassium Channels in 2- to 3-Month Old but Not in 10- to 15-Day Old Rats. Front. Physiol. 11:597395. doi: 10.3389/fphys.2020.597395

greater extent than activation of BK channels by NS19504. Further, IBTX increased the anticontractile effect of retigabine but not the contractile effect of XE991, whereas NS19504 reduced the effect of retigabine and impaired the effect of XE991.

Conclusion: Kv7 and BK channels are expressed in young and adult rat arteries and function as negative feedback modulators in the regulation of contractility of these arteries. Importantly, BK channels govern the extent of functional impact of Kv7 channels. This effect depends on the relationship between the functional activities of BK and Kv7 channels.

Keywords: arteries, ion channels, BK channel, Kv7 channel, ontogenesis, vascular smooth muscle

INTRODUCTION

In vascular smooth muscle cells (VSMCs), potassium channels evoke membrane hyperpolarization, reduce the entry of extracellular Ca^{2+} through voltage-dependent Ca^{2+} channels (VDCCs) and hence decrease their contractility (Nelson and Quayle, 1995; Coetzee et al., 1999; Jackson, 2000; Thorneloe and Nelson, 2005; Tykocki et al., 2017). VSMC contractility plays an essential role in the determination of vascular tone. The latter contributes considerably to the setting of blood pressure and the regulation of blood flow distribution to different organs and tissues.

Kv7 channels (Kv7.1–7.5), a subfamily of Kv channels (Kv1–12) (Wulff et al., 2009) are encoded by KCNQ (KCNQ1–5) genes. These channels play an important role in vasodilation and contribute to the negative feedback control of vasoconstriction. This role of Kv7 channels is based on their regulation by a number of factors including the membrane potential and signaling pathways involving PKC, PKA, PKG as well as G-protein βγ subunits (Mackie et al., 2008; Chadha et al., 2012; Stott et al., 2015a,b).

Another factor with potential regulatory impact on Kv7 channels are other K channels expressed in VSMCs (for an overview of VSMC K channels see Tykocki et al., 2017). Interestingly, a recent publication suggested a largely unexplored explanation for this phenomenon (Coleman et al., 2017). When VSMC membrane potential is close to the potassium equilibrium potential, driving force for potassium ions is small. Due to the small driving force, blockade of a particular potassium channel under these conditions will result in only a small change or in no change in membrane potential and vessel tone, hence a small functional role of this channel. A membrane potential close to the potassium equilibrium potential may be produced by another potassium channel underlying a dominant potassium conductance. Blockade of the latter potassium conductance will move the membrane potential away from the potassium equilibrium potential. This will result in a larger driving force for potassium and a larger functional role of the non-blocked K channels. Thus, the functional impact of a particular potassium channel will depend on the relative activities of the other potassium channels expressed, i.e., potassium channels will interact functionally.

Of note, a recent study showed an increased functional role of Kv7 channels in rat pulmonary arteries after inhibition of Kv1 and TASK-1 channels suggesting a functional interaction of Kv7 and Kv1/TASK-1 channels (Mondéjar-Parreño et al., 2020). A detailed investigation of this interaction was not the focus of the latter study.

BK channel expression has been shown in smooth muscle cells of all systemic arteries. These channels are involved in the negative feedback regulation of myogenic tone, they contribute to vasoconstriction and mediate vasodilation in almost all vessels studied (Nelson and Quayle, 1995; Jackson and Blair, 1998; Tykocki et al., 2017). Thus, BK channels seem to be a good candidate for the above mentioned dominant potassium conductance able to affect the functional role of other K channels including Kv7 channels. Indeed, BK channels have been shown to be the dominant negative feedback regulator of vasocontraction in adult rat saphenous arteries, whereas K_{ATP}-, Kv1-, Kv2- and TASK-1 channels, each one tested for itself, are not involved in this response and Kir2- and Kv7-channels play only a small role (Shvetsova et al., 2019, 2020). However, none of the latter studies explores the interaction of K channels. Thus, the hypothesis was tested that the functional impact of Kv7 channels depends on BK channels. This interaction was studied initially for agonist-induced vasocontraction in rat saphenous arteries, where the role of different VSMC K channels has been described recently in detail (Shvetsova et al., 2019, 2020) and extended to the gracilis artery myogenic response, another important contractile stimulus. The gracilis artery was used because it possesses prominent myogenic reactivity (see data of the present manuscript), in contrast to the larger saphenous artery and belongs to the same vascular region as the saphenous artery.

MATERIALS AND METHODS

Animals

The investigation conforms with the US Guide for the Care and Use of Laboratory Animals (Eighth edition, National Academy of Sciences, 2011) and approval for the use of laboratory animals in this study was granted by a governmental committee on animal welfare (I-17/17). Adult, 2- to 3-month old, and young, 10- to 15-days old, male Wistar rats (Janvier, France) were used. Food and water *ad libitum* was provided for the animals which were housed in a room with a controlled temperature and a 12-h light-dark cycle.

Vessel Preparation

Rats were sacrificed under CO_2 narcosis by decapitation. The lower extremity (limb) was quickly removed. It was placed in an ice-cold physiological saline solution composed of (in mM): 145 NaCl, 4.5 KCl, 1.2 NaH_2PO_4, 0.1 $CaCl_2$, 1.0 $MgSO_4$, 0.025 EDTA, 5 HEPES (pH 7.4). The gracilis artery and the saphenous artery were isolated by removing all surrounding skeletal muscle and connective tissue. Further experiments were performed on small rings 2 mm in length.

Isobaric Mounting of Gracilis Arteries

The gracilis artery was mounted on two glass pipettes which were fixed in the experimental chamber of a pressure myograph (DMT 201CM, Danish Myotechnology, Denmark). This chamber contained experimental solution (physiological saline solution, PSS) consisting of (in mM) 146 NaCl, 4.5 KCl, 1.2 NaH_2PO_4, 1.0 $MgSO_4$, 1.6 $CaCl_2$, 0.025 EDTA, 5.5 glucose and 5 HEPES at pH 7.4. The microscope image of the vessel was viewed with a CCD camera and digitized by a frame-grabber card (Hasotec, Germany). Diameter changes were measured continuously at a sampling rate of 0.5 Hz with use of a custom-made program (Fischer et al., 1996). Of note, the internal diameter is the most appropriate parameter to characterize the functional state of the vessels. However, when we tested the combined effect of IBTX and XE991 a strong constriction occurred. Under these conditions the connective tissue remaining even after careful dissection (more rigorous removal of the connective tissue led to a loss of myogenic reactivity) masked the inner diameter; in fact the inner diameter could not be determined any more. Thus, the external diameter had to be used to assess myogenic reactivity. Vessels were kept at a pressure of 80 mmHg without any luminal flow at a temperature of 37°C. Leaking vessels were discarded at any stage of the experiment to ensure complete non-flow conditions. After development of a spontaneous myogenic tone vessel viability was tested by application of 10^{-5} M methoxamine to test smooth muscle cell function and 10^{-6} M acetylcholine to test endothelial cell function. All vessels were exposed to calcium-free solution to determine the fully relaxed diameter at 80 mmHg at the end of the experiment. The fully relaxed diameter of the vessels in this study was in the range from 210 to 235 μm. All diameter values were normalized to the diameter of the same fully relaxed vessel at 80 mmHg in calcium-free solution. Normalization was done in order to eliminate variability due to differences in the size of different vessels.

Isometric Mounting of Saphenous Arteries

The isolated saphenous artery was mounted in a wire myograph (model 620M, Danish Myotechnology, Denmark) on two 40 μm wires. Isometric tension was recorded where data acquisition and analysis was performed using Labchart (ADInstruments, United States). The vessels were stretched to their optimal lumen diameter (90% of the diameter they would have at a transmural pressure of 100 mmHg (Mulvany and Halpern, 1977). They were placed in PSS consisting of (in mM) 120 NaCl, 4.5 KCl, 1.2 NaH_2PO_4, 1.0 $MgSO_4$, 1.6 $CaCl_2$, 0.025 EDTA, 5.5 glucose, 26 $NaHCO_3$, and 5 HEPES at pH 7.4 oxygenated with carbogen (95% O_2 and 5% CO_2) at 37°C. Viability of the vessels was tested by application of 10^{-5} M methoxamine to test smooth muscle cell function and of 10^{-5} M acetylcholine after preconstriction with 10^{-7} M methoxamine to test endothelial cell function. Vessel tension was normalized to the tension developed in response to 10^{-5} M methoxamine applied directly after the viability test. This was done in order to eliminate variability due to differences in the contractility of different vessels. Special care was taken to carefully match vessel tension before the intervention to be able to compare vessel responses to different interventions. Thus, when 4 groups of vessels with different interventions (e.g., application of IBTX, NS19504, IBTX + NS19504, control = application of vehicle) were compared, it was ensured that the averaged methoxamine-induced concentration-response relationships (or the pressure-diameter relationships in isobaric preparations) of these 4 vessel groups obtained directly after the 10^{-5} M methoxamine-test and before the addition of the above mentioned substances did not differ (see for example Schmid et al., 2018, **Supplementary Figure 1A**).

Functional Removal of the Endothelium

The endothelium was removed from all vessels studied in pressure or wire myographs. In isobaric experiments this was done by passing an air bubble through the lumen of the vessel. In isometric experiments the endothelium was disrupted mechanically using a rat whisker. Functional removal of the endothelium was considered successful when acetylcholine-induced vasodilation was absent during the viability test.

Real-Time PCR

Vessels (saphenous and gracilis arteries) were isolated in two groups, with endothelium(E+) and without endothelium(E−) as described above. They were cut into small pieces and homogenized for 3 min at 30 Hz in the TissueLyser II (Qiagen). Total RNA was isolated using the "RNeasy Mini-Kit" (Qiagen) according to the manufacturer instructions. Optional On-Column DNase Digestion using the RNase-Free DNase Set (Qiagen) was performed as described in the manufacturer instructions. In the final step, RNA was collected from the affinity column using 30 μl RNase-free H2O, which was passed twice over the column. RNA concentration was determined on the Tecan infinite 200 PRO.

Reverse transcription to cDNA was performed by Mastercyler (Gradient 5333, Eppendorf) using 5 × Reaction Buffer (Thermo scientific), dNTP Mix (10 nM each, Thermo scientific), RevertAid H Minus ReverseTranscriptase (Thermo scientific), and Random Primers (Invitrogen) according to the manufacturer's standard protocol. All samples were diluted to a starting concentration of 5 ng RNA per μL of reaction.

Samples were quantified with real-time PCR using SensiFAST^{TM} SYBR No-ROX Kit, 2× (Bioline, Cat# BIO-98020) on Light Cycler 480 (Roche) according to the manufacturer's standard protocol. Primers were purchased or self-designed and ordered from Eurofins. Amplicon context sequence and amplicon length can be found on the Bio-Rad

Homepage[1] in accordance with the Guidelines for Minimum Information for Publication of Quantitative Digital PCR Experiments (MIQE) guidelines (Huggett et al., 2013). The following genes (with their Sequence) have been tested: Kcnq1 (ffw: GGCTCTGGGTTTGCACTG, rev: CATAGCA CCTCCATGCAGTC), Kcnq2 (ffw: ACACAGACTCAGACCTC TGCAC, rev: AGCCCAACCCAGAATCACTTCC), Kcnq3 (ffw: GCTAGGGACCGGAGCCGACA, rev: CCCCTCGGTCTCTCC AGGGC), Kcnq4 (ffw: CCCCGCTGCTCTACTGAG, rev: ATG ACATCATCCACCGTGAG), Kcnq5 (ffw: GATGCCAGTGTGA CGTGTCCGTGG, rev: CCTTTCCGAGGACCTGCTGGTAG), rBKalpha (ffw: AAACAAGTAATTCCATCAAGCTGGTG, rev: CGTAAGTGCCTGGTTGTTTTGG), rBKbeta1 (ffw: ACCAAT CTCTTCTGCACAGCAGC, rev: AGAGCTGTGACTGGCAGT TCCTT), eNOS (ffw: GGATTCTGGCAAGACCGATTAC, rev: GGTGAGGACTTGTCCAAACACT), Hmbs (ffw: GCGGAAG AAAACGGCTCAATG, rev: AGCATCGCTACCACAGTGTC), Gapdh (ffw: CACCAGCATCACCCCATTT; rev: CCATCAAGG ACCCCTTCATT). Hmbs was used as reference gene for the expression analysis of endothelium-denuded and endothelium-intact vessels; Gapdh was used as reference gene for the expression analysis of vessels from young and adult rats. For each reaction of 20 μL, a volume of 2 μL cDNA was used (as an equivalent of 10 ng starting RNA). At the end of reaction, melting curves were checked by use of the Light Cycler 480 software to ensure the specificity of qPCR products. The LinRegPCR program (Academic Medical Center, Netherlands) was used to analyze the real-time PCR data. mRNA expression levels were calculated as E^{-Ct}, where E is the primer efficiency and Ct is the cycle number on which product fluorescence rose above the threshold level. Primer efficiency was determined for every primer pair using LinReg. These expression values were related to the expression values of the housekeeping gene detected in the same sample. Expression data from vessels from young and adult rats were normalized to the mean of the expression of vessels from adult rats.

Selection Criteria for BK and Kv7 Channel Blocker and Opener Concentrations

Iberiotoxin (IBTX) has widely been employed as a BK channel inhibitor starting from 1990 (Galvez et al., 1990). It has been used since then in an uncountable number of reports and proven to be a specific BK channel blocker. IBTX was reported to have an IC_{50} of 1.7 nM (Tykocki et al., 2017). Since a complete block of BK channels was desired, 100 nM IBTX was employed.

NS19504 is a relatively new opener of BK channels with an EC_{50} of 11 μM for bladder smooth muscle BK channels (determined with a Tl^+ assay under conditions differing quite a lot compared to the conditions employed in experiments on intact organs) and 640 nM for the inhibition of bladder spontaneous contractile activity (Nausch et al., 2014). Of note, the inhibition of spontaneous bladder activity by NS19504 was not blocked completely by IBTX pointing to a non-specific effect of this new compound at higher concentrations. Data on the effect of NS19504 on vascular smooth muscle BK channels are not available. Therefore, we studied the effect of NS19504 on rat arteries in detail (see "Results" section). NS19504 at $6*10^{-6}$ M was selected as the most appropriate concentration, i.e., the concentration that produces the largest but still selective effect on vascular contractility.

XE991 is a well-known blocker of Kv7 channels with an IC_{50} of 5.5 μM determined for Kv7.4 channels expressed in HEK cells (Søgaard et al., 2001; Gollasch et al., 2018). Kv7.4 channels are the most prominent isoform expressed in the vessels studied in the present investigation (see **Figure 1** of the present manuscript for saphenous and gracilis arteries and Figure 3 in Zavaritskaya et al., 2013 for gracilis arteries). Taking into account the considerable differences in experimental conditions between patch-clamp studies on channels or currents and myography experiments on intact vessels, this IC_{50} value was used as a first orientation. Additionally, recent data were considered where we found that in an intact vessel preparation the effect of a Kv7 channel opener was inhibited by $3*10^{-6}$ M XE991 and 10^{-5}M XE991 to the same degree (Zavaritskaya et al., 2020). In addition, unpublished data on gracilis arteries showed that the effect of $3*10^{-5}$ M XE991 on spontaneous myogenic tone was smaller compared to $3*10^{-6}$ M XE991 and 10^{-5}M XE991 pointing to an unspecific effect at this high concentration. Thus, in order to ensure the largest but still selective inhibitory effect of XE991, $3*10^{-6}$ M was employed.

Retigabine is a well described opener of Kv7 channels with EC_{50} values between 1 and 5 μM for expressed Kv7.4 channels (Gollasch et al., 2018). We used previous data from intact vessel preparations to select the most appropriate concentration of retigabine. Retigabine at concentrations $> 3*10^{-5}$ M was able to dilate KCl-preconstricted vessels (Zavaritskaya et al., 2013) suggesting an effect independent of K channels at this concentration. The present study shows that the effect of retigabine at $3*10^{-5}$ M could be abolished by XE991. Therefore, this concentration of retigabine was selected.

Drugs and Chemicals

Methoxamine, acetylcholine as well as the salts for the solutions were obtained from Sigma (Germany). Iberiotoxin was purchased from Alomone Labs (Israel). NS19504, Retigabine and XE991 were obtained from Tocris (United Kingdom).

Data Analysis and Statistics

The anti-contractile or contractile effect of a certain substance was calculated as the area between the methoxamine-induced concentration-response relationships or the pressure-diameter relationships obtained in the absence and in the presence of this substance (see also Schmid et al., 2018).

All values are given as mean ± SEM; n is the number of animals tested. Statistical analysis was performed using GraphPadPrism 6.0 (GraphPad Software, Inc.) employing ANOVA or paired *t*-tests as appropriate and a value of $p < 0.05$ was considered statistically significant.

[1] www.bio-rad.com

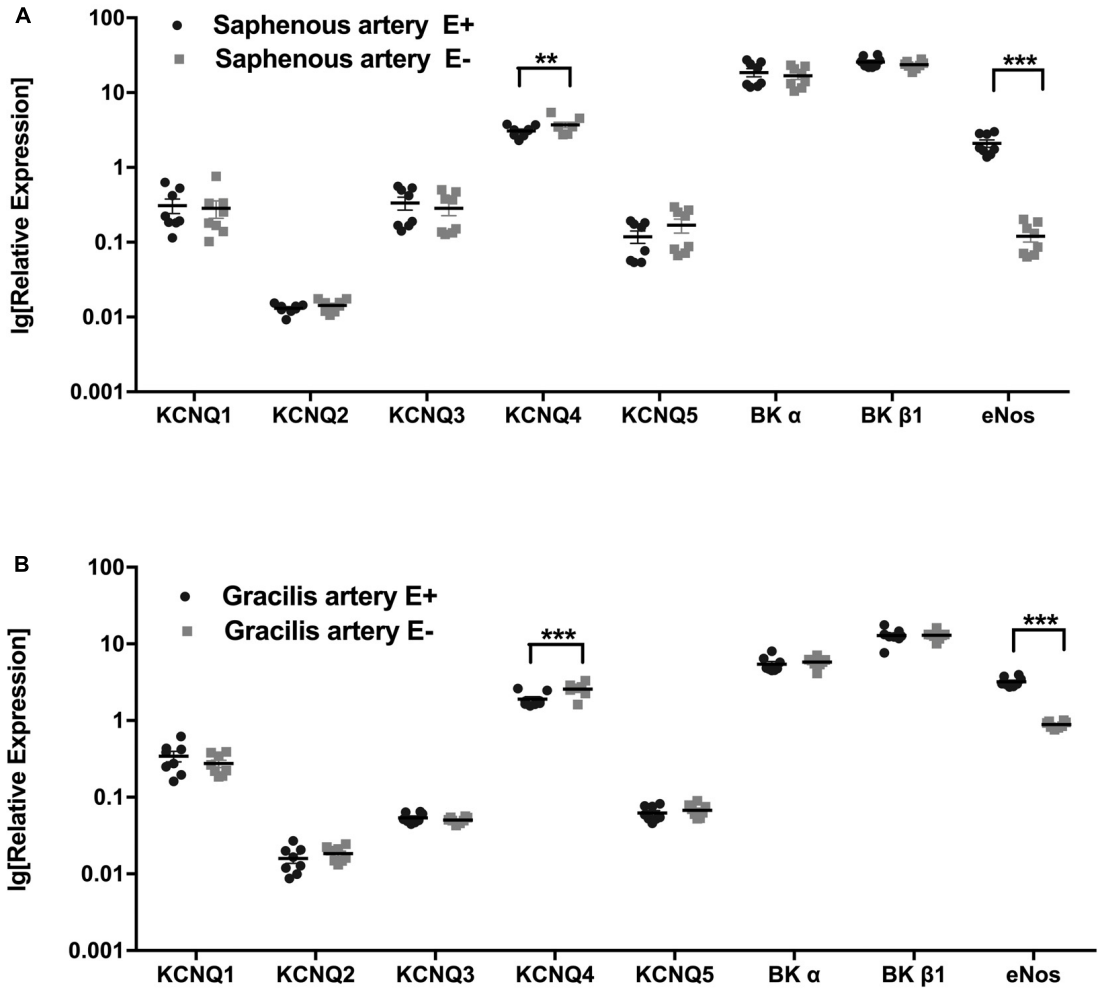

FIGURE 1 | Expression of KCNQ and BK channel genes. **(A)** Relative expression profile (related to Hmbs) of KCNQ and BK channel genes in Saphenous artery with endothelium (E+) and without endothelium (E–). **(B)** Relative expression profile of KCNQ and BK channel genes in gracilis artery with endothelium (E+) and without endothelium (E–). $n = 8$; $^{**}p < 0.01$; $^{***}p < 0.001$.

RESULTS

Expression of Kv7 and BK Channel Genes in Arteries of Adult Rats

The expression profiles of the subunits of KCNQ and BK channel genes in saphenous arteries were similar to those in gracilis arteries: the highest expression was observed for BKα, BKβ1 and KCNQ4, followed by KCNQ1, KCNQ3 and KCNQ5 at considerably lower expression levels. The lowest expressed gene was KCNQ2 (**Figures 1A,B**).

Expression profiles were compared for vessels without (E−) and with (E+) endothelium. Successful removal of the endothelium was verified by a substantially lower expression of the endothelial marker eNOS in vessels without endothelium (**Figures 1A,B**). In both vessels, no differences in KCNQ and BK channel genes were detected between vessel without and with endothelium, except for KCNQ4, which was expressed at a slightly lower level in vessels with endothelium (**Figures 1A,B**).

Functional Interaction of Kv7 and BK Channels in Arteries of Adult Rats

The functional interaction of Kv7 and BK channels was studied by addition of their respective blockers and activators. Specifically, XE991 was used as a selective blocker of Kv7 channels, retigabine as a selective activator of Kv7 channels; iberiotoxin (IBTX) was used as a selective blocker of BK channels, and NS19504 as a novel activator of BK channels (for more details on the selection criteria for the BK and Kv7 channel blocker and opener concentrations see methods section).

Kv7 and BK channel functional interaction was studied using two approaches addressing different mechanisms regulating vessel contractility. Firstly, isometric preparations of saphenous arteries, a larger artery showing stable vasoconstrictor-induced contractions without spontaneous basal tone, were employed. Contractility was tested over a wide range of vessel tension achieved by application of methoxamine at concentrations between 10^{-8} M and 10^{-5} or 10^{-4}M. Secondly, isobaric

preparations of gracilis arteries, a smaller, myogenically active artery, were used. Contractility was tested over a wide pressure range between 10 and 120 mmHg.

Effect of Retigabine and XE991 on Arterial Contraction

Retigabine at $3*10^{-5}$M strongly attenuated methoxamine-induced contractions, i.e., demonstrated an anti-contractile effect, whereas for XE991 at $3*10^{-6}$M an effect was not detected in this experiment (**Supplementary Figures 1A,B**). In the presence of retigabine, however, XE991 enhanced methoxamine-induced contractions compared to these contractions in the presence of retigabine alone, i.e., demonstrated a contractile effect (**Supplementary Figure 1B**). Of note, in the presence of XE991 retigabine was without effect on methoxamine-induced contractions compared to these contractions in the presence of XE991 alone (**Supplementary Figure 1B**). Thus, the anti-contractile effect of retigabine was abolished by XE991 (**Supplementary Figure 1C**). Such an effect of XE991 was also observed when contractility was assessed based on the myogenic response of gracilis arteries (**Supplementary Figures 2A–C**).

Effect of NS19504 and IBTX on Arterial Contraction

Because there is no agent commonly recognized and confirmed as a selective activator of vascular smooth muscle BK channels, NS19504 as a novel candidate was tested in more detail, i.e., at three concentrations ($3*10^{-6}$M, $6*10^{-6}$M, 10^{-5}M).

NS19504 at $3*10^{-6}$M attenuated methoxamine-induced contractions, while IBTX at 10^{-7}M enhanced it (**Supplementary Figures 3A,B,E1**). In the presence of NS19504 IBTX also enhanced methoxamine-induced contractions compared to these contractions in the presence of NS19504 alone (**Supplementary Figure 3E1**). Of note, in the presence of IBTX NS19504 was without effect on methoxamine-induced contractions compared to these contractions in the presence of IBTX alone (**Supplementary Figure 3E1**). Thus, the anti-contractile effect of $3*10^{-6}$M NS19504 was abolished by IBTX (**Supplementary Figure 3F1**). Such an effect of IBTX was also observed when contractility was assessed based on the myogenic response of gracilis arteries (**Supplementary Figures 4A–C**).

NS19504 at $6*10^{-6}$M attenuated methoxamine-induced contractions, while IBTX at 10^{-7}M enhanced it (**Supplementary Figures 3A,C,E2**). In the presence of NS19504 IBTX also enhanced methoxamine-induced contractions compared to these contractions in the presence of NS19504 alone (**Supplementary Figure 3E2**). Of note, in the presence of IBTX NS19504 was without effect on methoxamine-induced contractions compared to these contractions in the presence of IBTX alone (**Supplementary Figure 3E2**). Thus, the anti-contractile effect of $6*10^{-6}$M NS19504 was abolished by IBTX (**Supplementary Figure 3F2**).

NS19504 at 10^{-5}M attenuated methoxamine-induced contractions, while IBTX at 10^{-7}M enhanced it (**Supplementary Figures 3A,D,E3**). In the presence of NS19504 IBTX also enhanced methoxamine-induced contractions compared to these contractions in the presence of NS19504 alone (**Supplementary Figure 3E3**). In the presence of IBTX NS19504 attenuated methoxamine-induced contractions compared to these contractions in the presence of IBTX alone (**Supplementary Figure 3E3**). Thus, the anti-contractile effect of 10^{-5}M NS19504 was reduced but not abolished by IBTX (**Supplementary Figure 3F3**).

The Functional Impact of Kv7 Channels Increases After Blocking BK Channels

XE991 at $3*10^{-6}$M as well as IBTX at 10^{-7}M enhanced methoxamine-induced contractions (**Figure 2A**). In the presence of IBTX, XE991 also enhanced methoxamine-induced contractions compared to these contractions in the presence of IBTX alone (**Figure 2A**). Further, in the presence of XE991,

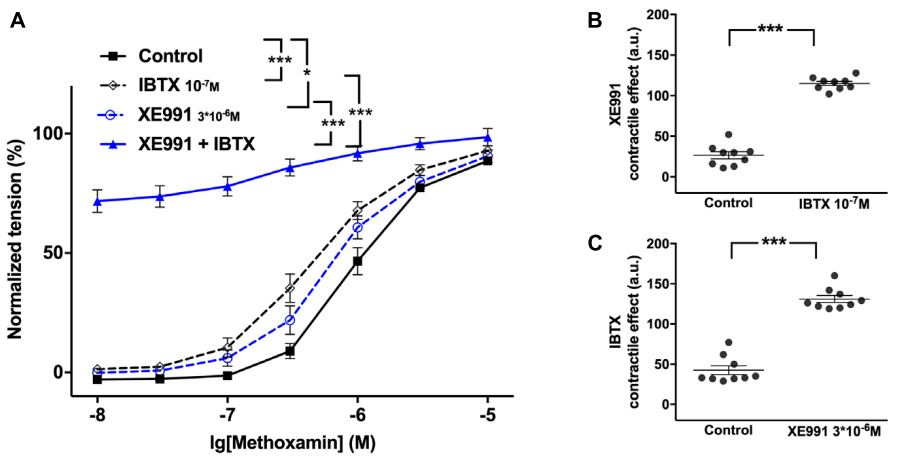

FIGURE 2 | Effect of XE991 and IBTX on methoxamine-induced contractions of the saphenous artery. **(A)** Normalized tension of saphenous arteries with different methoxamine concentrations in the absence of potassium channel active agents (Control), in the presence of IBTX (IBTX 10^{-7}M), in the presence of XE991 (XE991 $3*10^{-6}$M) and in the combined presence of XE991 and IBTX (XE991 + IBTX). **(B)** XE991 contractile effect in the absence (Control) and presence of IBTX (IBTX 10^{-7}M). **(C)** IBTX contractile effect in the absence (Control) and presence of XE991 (XE991 $3*10^{-6}$M). $n = 12$; $^{*}p < 0.05$, $^{***}p < 0.001$.

IBTX enhanced methoxamine-induced contractions compared to these contractions in the presence of XE991 alone (**Figure 2A**). Thus, the contractile effect of XE991 was enhanced by IBTX (**Figure 2B**), and the contractile effect of IBTX was enhanced by XE991 (**Figure 2C**). Such effects of IBTX and XE991 were also observed when contractility was assessed based on the myogenic response of gracilis arteries (**Supplementary Figures 5A–C**).

Further, retigabine at $3*10^{-6}$M attenuated methoxamine-induced contractions, whereas IBTX at 10^{-7}M enhanced methoxamine-induced contractions (**Figure 3A1**). In the presence of retigabine IBTX also enhanced methoxamine-induced contractions compared to these contractions in the presence of retigabine alone (**Figure 3A1**). In the presence of IBTX retigabine also attenuated methoxamine-induced contractions compared to these contractions in the presence of IBTX alone (**Figure 3A1**). Thus, the anti-contractile effect of retigabine was enhanced by IBTX (**Figure 3B1**), whereas the contractile effect of IBTX was reduced by retigabine (**Figure 3C1**). Such effects of IBTX and retigabine were also observed when contractility was assessed based on the myogenic response of gracilis arteries (**Supplementary Figures 6A–C**).

Retigabine at 10^{-5}M attenuated methoxamine-induced contractions, whereas IBTX at 10^{-7}M enhanced methoxamine-induced contractions (**Figure 3A2**). Of note, in the presence of retigabine IBTX did not affect methoxamine-induced contractions compared to these contractions in the presence of retigabine alone (**Figure 3A2**). In the presence of IBTX retigabine also attenuated methoxamine-induced contractions compared to

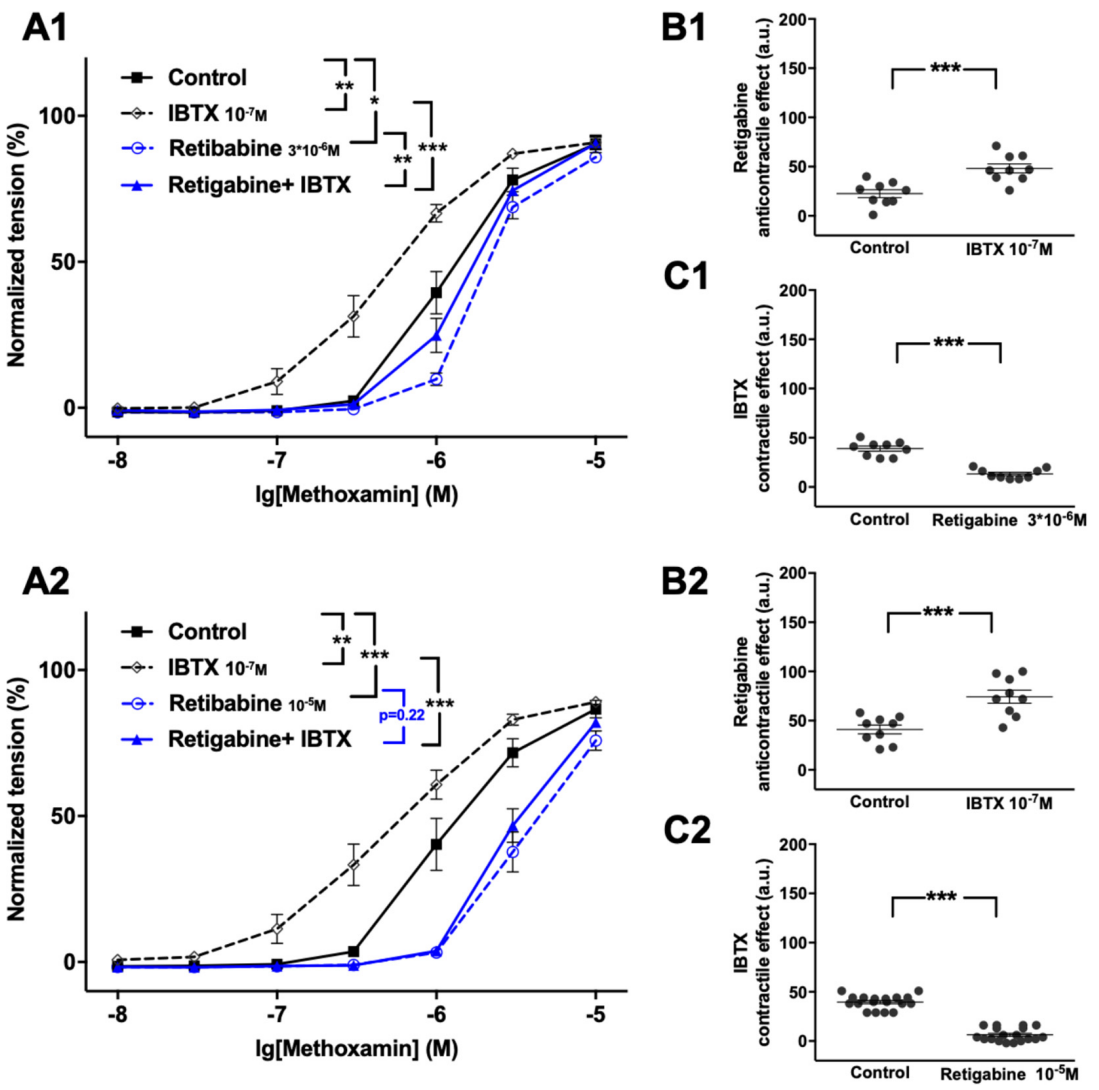

FIGURE 3 | Effect of retigabine and IBTX on methoxamine-induced contractions of the saphenous artery. **(A1,A2)** Normalized tension of saphenous arteries with different methoxamine concentrations in the absence of potassium channel active agents (Control), in the presence of IBTX (IBTX 10^{-7}M), in the presence of retigabine (**A1**: Retigabine $3*10^{-6}$M; **A2**: Retigabine 10^{-5}M) and in the combined presence of retigabine and IBTX (Retigabine + IBTX). **(B1,B2)** Retigabine anti-contractile effect in the absence of (Control) and presence of IBTX (IBTX 10^{-7}M). **(C1,C2)** IBTX contractile effect in the absence of (Control) and presence of retigabine (**C1**: Retigabine $3*10^{-6}$M, **C2**: Retigabine 10^{-5}M). n1 = 9, n2 = 9; $*p < 0.05$, $**p < 0.01$; $***p < 0.001$.

these contractions in the presence of IBTX alone (**Figure 3A2**). Thus, the anti-contractile effect of retigabine was considerably enhanced by IBTX (**Figure 3B2**), whereas the contractile effect of IBTX was abolished by retigabine (**Figure 3C2**).

The Functional Impact of Kv7 Channels Decreases After Activating BK Channels

Retigabine at 10^{-5}M as well as NS19504 at $3*10^{-6}$M attenuated methoxamine-induced contractions (**Figure 4A1**). In the presence of NS19504 retigabine also attenuated methoxamine-induced contractions compared to these contractions in the presence of NS19504 alone (**Figure 4A1**). Further, in the presence of retigabine NS19504 attenuated methoxamine-induced contractions compared to these contractions in the presence of retigabine alone (**Figure 4A1**). Thus, the anti-contractile effect of retigabine was reduced by NS19504 (**Figure 4B1**), and the anti-contractile effect of NS19504 was reduced by retigabine (**Figure 4C1**). The same effects where observed for NS19504 at $6*10^{-6}$M (**Figures 4A2,B2,C2**). Such effects of NS19504 and retigabine were also observed when contractility was assessed based on the myogenic response of gracilis arteries (**Supplementary Figures 7A–C**).

Further, NS19504 at $6*10^{-6}$M attenuated methoxamine-induced contractions, whereas XE991 at $3*10^{-6}$M enhanced

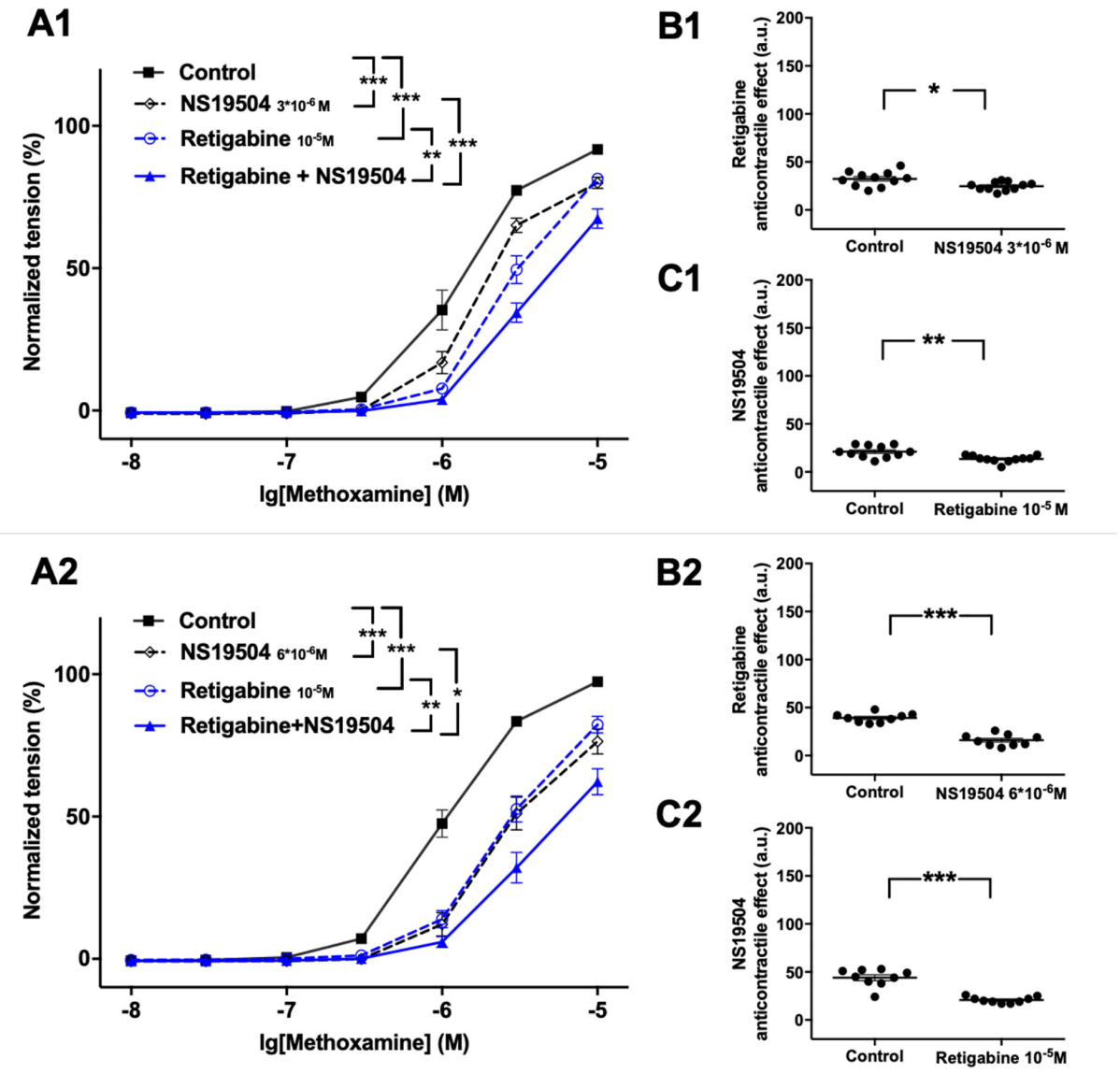

FIGURE 4 | Effect of retigabine and NS19504 on methoxamine-induced contractions of the saphenous artery. **(A1,A2)** Normalized tension of saphenous arteries at different methoxamine concentration in the absence of potassium channel active agents (Control), in the presence of retigabine (Retigabine 10^{-5}M), in the presence of NS19504 (**A1**: NS19504 $3*10^{-6}$M, A2: NS19504 $6*10^{-6}$M) and in the combined presence of retigabine and NS19504 (Retigabine + NS19504). **(B1,B2)** Retigabine anti-contractile effect in the absence (Control) and presence of NS19504 (**B1**: NS19504 $3*10^{-6}$M, B2: NS19504 $6*10^{-6}$M). **(C1,C2)** NS19504 anti-contractile effect in the absence (Control) and presence of retigabine (Retigabine 10^{-5}M). n1 = 11, n2 = 9; $^{*}p < 0.05$, $^{**}p < 0.01$; $^{***}p < 0.001$.

methoxamine-induced contractions (**Figure 5A**). In the presence of NS19504 XE991 did not affect methoxamine-induced contractions compared to these contractions in the presence of NS19504 alone (**Figure 5A**). In the presence of XE991 NS19504 also attenuated methoxamine-induced contractions compared to these contractions in the presence of XE991 alone (**Figure 5A**). Thus, the anti-contractile effect of NS19504 was enhanced by XE991 (**Figure 5B**), whereas the contractile effect of XE991 was abolished by NS19504 (**Figure 5C**). Such effects of XE991 and NS19504 were also observed when contractility was assessed based on the myogenic response of gracilis arteries (**Supplementary Figures 8A–C**).

The Functional Impact of BK and Kv7 Channels in Arteries of Young Rats

The functional impact of BK and Kv7 channels on methoxamine-induced contractions was determined also in saphenous arteries of young rats.

Expression of Kv7 and BK Channel Genes in Saphenous Arteries of Adult and Young Rats

Comparison of the most highly expressed potassium channel genes of interest in the saphenous artery showed that the expression of BKα and BKβ1 was smaller in vessels from young compared to adult rats, whereas for KCNQ4 no difference was detected (**Figure 6**). Thus, vessels of young rats may serve as a model of a functional situation resembling a considerable block of BK channels.

Effect of Retigabine and XE991 on Arterial Contraction

Retigabine at $3^{*}10^{-5}$M attenuated methoxamine-induced contractions, whereas XE991 at $3^{*}10^{-6}$M strongly enhanced this effect (**Supplementary Figure 9A**). In the presence of retigabine XE991 enhanced methoxamine-induced contractions compared to these contractions in the presence of retigabine alone (**Supplementary Figure 9A**). Of note, in the presence

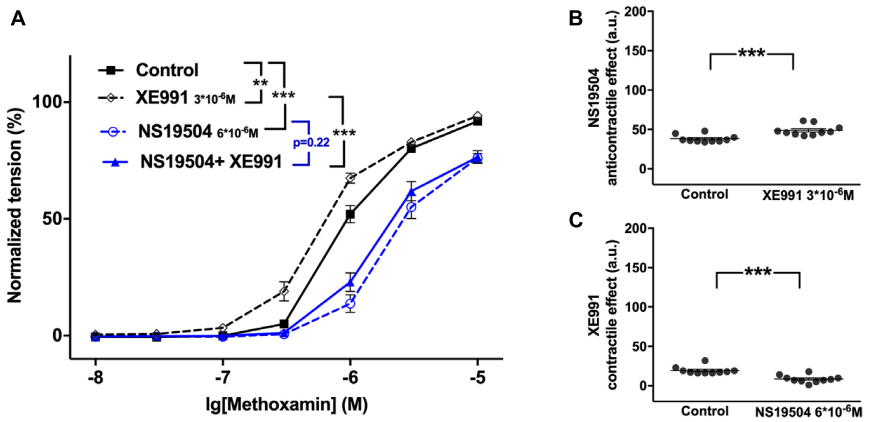

FIGURE 5 | Effect of NS19504 and XE991 on methoxamine-induced contractions of the saphenous artery. **(A)** Normalized tension of saphenous arteries with different methoxamine concentrations in the absence of potassium channel active agents (Control), in the presence of XE991 (XE991 $3^{*}10^{-6}$M), in the presence of NS19504 (NS19504 $6^{*}10^{-6}$M) and in the combined presence of NS19504 and XE991 (NS19504 + XE991). **(B)** NS19504 anti-contractile effect in the absence (Control) and presence of XE991 (XE991 $3^{*}10^{-6}$M). **(C)** XE991 contractile effect in the absence (Control) and presence of NS19504 (NS19504 $6^{*}10^{-6}$M). n = 10; $^{**}p < 0.01$; $^{***}p < 0.001$.

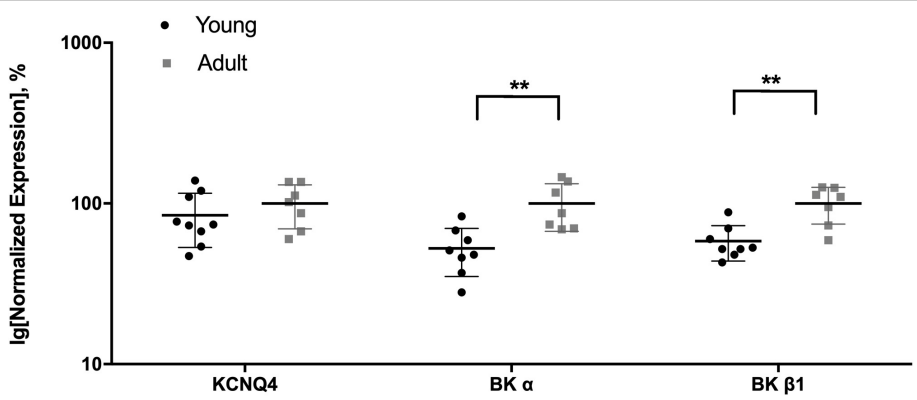

FIGURE 6 | Expression of KCNQ4 and BK channel genes in the saphenous artery of young and adult rats. Normalized expression (related to Gapdh and normalized to the mean of the expression of vessels from adult rats) of KCNQ4 and BK channel genes in saphenous arteries from young (n = 8) and adult (n = 7) rats. $^{**}p < 0.01$.

of XE991 retigabine was without effect on methoxamine-induced contractions compared to these contractions in the presence of XE991 alone (**Supplementary Figure 9A**). Thus, the anti-contractile effect of retigabine was abolished by XE991 (**Supplementary Figure 9B**).

Effect of NS19504 and IBTX on Arterial Contraction

NS19504 at $6*10^{-6}$M attenuated methoxamine-induced contractions, while IBTX at 10^{-7}M enhanced it (**Supplementary Figure 10A**). In the presence of NS19504, IBTX also enhanced methoxamine-induced contractions compared to these contractions in the presence of NS19504 alone (**Supplementary Figure 10A**). Of note, in the presence of IBTX NS19504 was without effect on methoxamine-induced contractions compared to these contractions in the presence of IBTX alone (**Supplementary Figure 10A**). Thus, the anti-contractile effect of NS19504 was abolished by IBTX (**Supplementary Figure 10B**).

Together these data show that (i) in adults IBTX and NS19504 shifted the concentration-response relationship of methoxamine to the left and to the right, respectively, to a similar degree (**Figure 7A**) demonstrating that BK channels exert an anticontractile effect during methoxamine-induced contractions; (ii) in young rats, a similar effect of IBTX and NS19504 was observed, albeit with smaller magnitude (**Figure 7C**) also demonstrating an anticontractile effect of BK channels; (iii) in adults XE991 had no considerable effect on the methoxamine-induced concentration-response relationship, whereas retigabine shifted the concentration-response relationship of methoxamine to the right (**Figure 7B**), demonstrating that Kv7 channels showed no considerable anticontractile effect; (iv) in contrast in young rats, XE991 and retigabine shifted the concentration-response relationship of methoxamine to the left and to the right, respectively, where the effect of XE991 is more pronounced (**Figure 7D**) demonstrating a strong anticontractile effect of Kv7 channels.

The Functional Impact of Kv7 Channels Changed Little After Blocking BK Channels in Young Rats

XE991 at $3*10^{-6}$M as well as IBTX at 10^{-7}M enhanced methoxamine-induced contractions (**Figure 8A**). In the

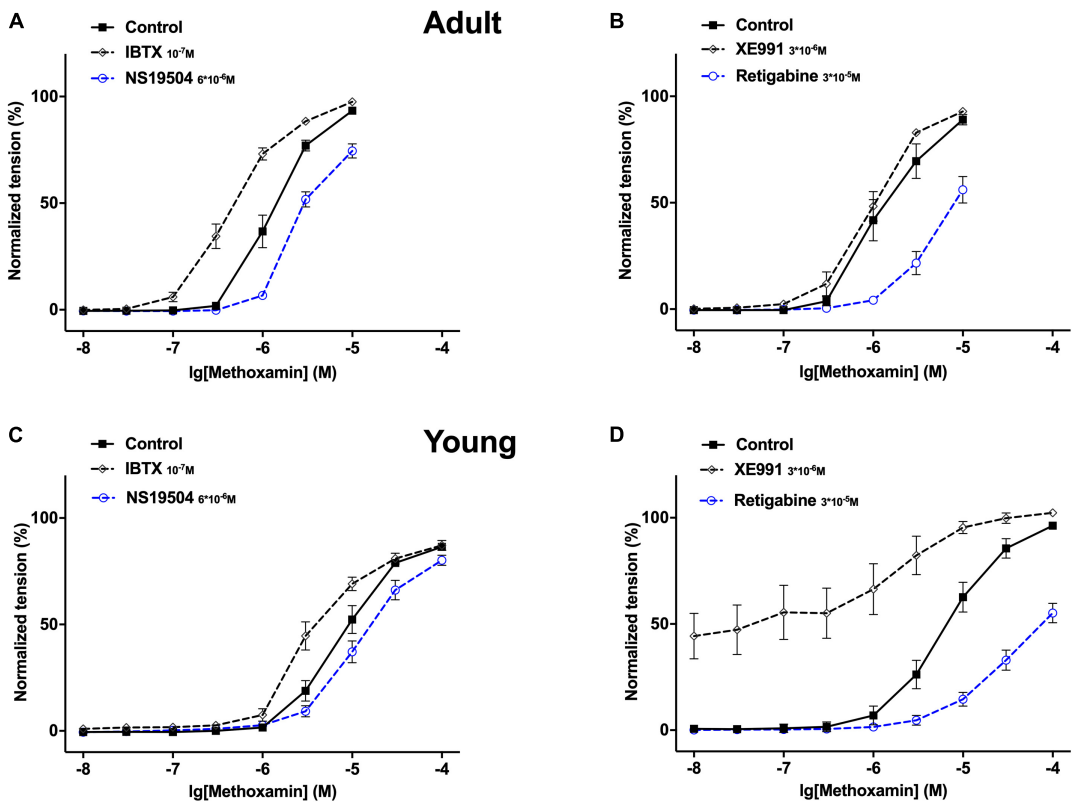

FIGURE 7 | Effect of NS19504, IBTX, Retigabine and XE991 on methoxamine-induced contractions of the saphenous artery in adult and young rats. **(A)** Normalized tension of adult saphenous arteries with different methoxamine concentrations in the absence of BK channel active agents (Control), in the presence of IBTX (IBTX 10^{-7}M) and in the presence of NS19504 (NS19504 $6*10^{-6}$M). **(B)** Normalized tension of adult saphenous arteries at different methoxamine concentrations in the absence of Kv7 channel active agents (Control), in the presence of XE991 (XE991 $3*10^{-6}$M), in the presence of retigabine (Retigabine $3*10^{-5}$M). **(C)** Normalized tension of young saphenous arteries with different methoxamine concentrations in the absence of BK channel active agents (Control), in the presence of IBTX (IBTX 10^{-7}M) and in the presence of NS19504 (NS19504 $6*10^{-6}$M). **(D)** Normalized tension of young saphenous arteries at different methoxamine concentrations in the absence of Kv7 channel active agents (Control), in the presence of XE991 (XE991 $3*10^{-6}$M), in the presence of retigabine (Retigabine $3*10^{-5}$M).

presence of IBTX, XE991 also enhanced methoxamine-induced contractions compared to these contractions in the presence of IBTX alone (**Figure 8A**). Further, in the presence of XE991, IBTX did not affect methoxamine-induced contractions compared to these contractions in the presence of XE991 alone (**Figure 8A**). Thus, the contractile effect of XE991 was not affected by IBTX (**Figure 8B**), but the contractile effect of IBTX was abolished by XE991 (**Figure 8C**).

Retigabine at 10^{-5}M attenuated methoxamine-induced contractions, whereas IBTX at 10^{-7}M enhanced methoxamine-induced contractions (**Figure 9A**). Of note, in the presence of retigabine IBTX did not affect methoxamine-induced contractions compared to these contractions in the presence of retigabine alone (**Figure 9A**). In the presence of IBTX retigabine also attenuated methoxamine-induced contractions compared to these contractions in the presence of IBTX alone (**Figure 9A**). Thus, the anti-contractile effect of retigabine was enhanced by IBTX (**Figure 9B**), whereas the contractile effect of IBTX was abolished by retigabine (**Figure 9C**).

Retigabine at 10^{-5}M as well as NS19504 at $6*10^{-6}$M attenuated methoxamine-induced contractions (**Figure 10A**). In the presence of NS19504 retigabine also attenuated methoxamine-induced contractions compared to these contractions in the presence of NS19504 alone (**Figure 10A**). Further, in the presence of retigabine NS19504 did not affect methoxamine-induced contractions compared to these contractions in the presence of retigabine alone (**Figure 10A**). Thus, the anti-contractile effect of retigabine was reduced by

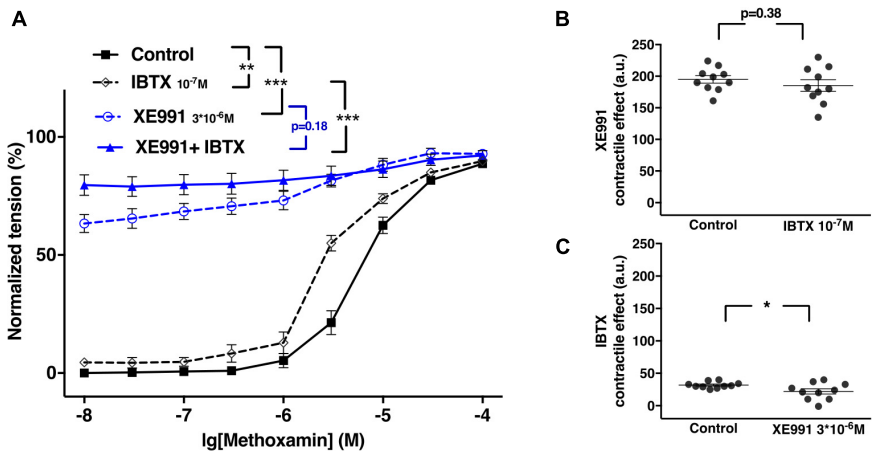

FIGURE 8 | Effect of XE991 and IBTX on methoxamine-induced contractions of the saphenous artery of young rats. **(A)** Normalized tension of saphenous arteries with different methoxamine concentrations in the absence of potassium channel active agents (Control), in the presence of IBTX (IBTX 10^{-7}M), in the presence of XE991 (XE991 $3*10^{-6}$M) and in the combined presence of XE991 and IBTX (XE991 + IBTX). **(B)** XE991 contractile effect in the absence (Control) and presence of IBTX (IBTX 10^{-7}M). **(C)** IBTX contractile effect in the absence (Control) and presence of XE991 (XE991 $3*10^{-6}$M). $n = 11$; $^{*}p < 0.05$, $^{**}p < 0.01$; $^{***}p < 0.001$.

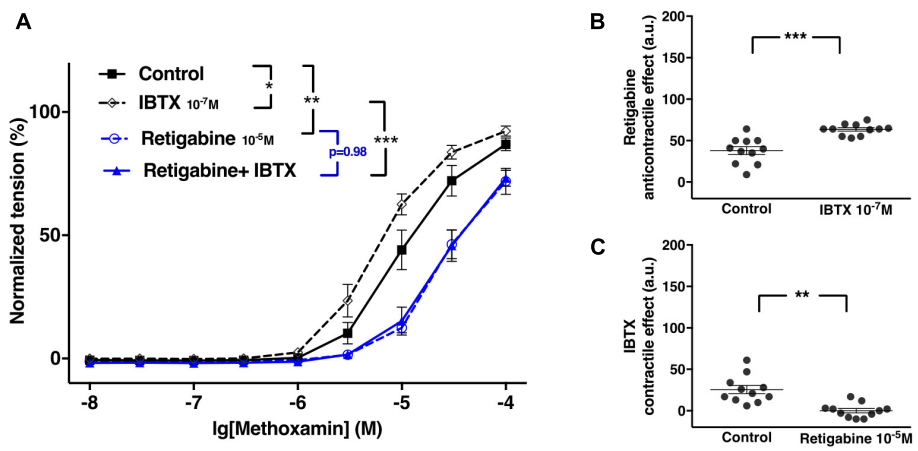

FIGURE 9 | Effect of retigabine and IBTX on methoxamine-induced contractions of the saphenous artery of young rats. **(A)** Normalized tension of saphenous arteries with different methoxamine concentrations in the absence of potassium channel active agents (Control), in the presence of IBTX (IBTX 10^{-7}M), in the presence of retigabine (Retigabine 10^{-5}M) and in the combined presence of retigabine and IBTX (Retigabine + IBTX). **(B)** Retigabine anti-contractile effect in the absence of (Control) and presence of IBTX (IBTX 10^{-7}M). **C)** IBTX contractile effect in the absence of (Control) and presence of retigabine (Retigabine 10^{-5}M). $n = 11$; $^{*}p < 0.05$, $^{**}p < 0.01$; $^{***}p < 0.001$.

NS19504 (**Figure 10B**), and the anti-contractile effect of NS19504 was abolished by retigabine (**Figure 10C**).

NS19504 at $6*10^{-6}$M attenuated methoxamine-induced contractions, whereas XE991 at $3*10^{-6}$M enhanced methoxamine-induced contractions (**Figure 11A**). In the presence of NS19504, XE991 also enhanced methoxamine-induced contractions compared to these contractions in the presence of NS19504 alone (**Figure 11A**). In the presence of XE991, NS19504 also attenuated methoxamine-induced contractions compared to these contractions in the presence of XE991 alone (**Figure 11A**). Thus, the anti-contractile effect of NS19504 was enhanced by XE991 (**Figure 11B**), whereas the contractile effect of XE991 was reduced by NS19504 (**Figure 11C**).

DISCUSSION

Expression of Kv7 and BK Channels in Arteries of Adult Rats

The expression of mRNA for Kv7 (KCNQ) and BK channels was determined in two types of skeletal muscle arteries, the larger saphenous artery and the smaller gracilis artery. The potassium channel genes studied were expressed at different levels. In

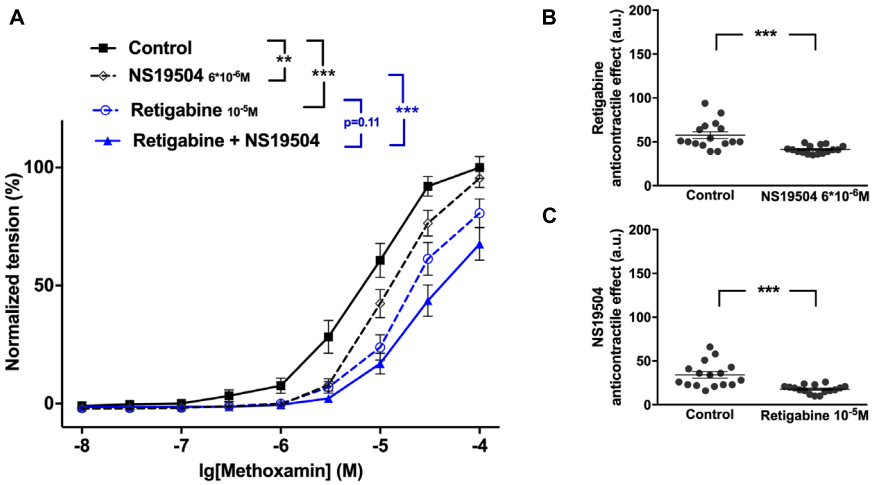

FIGURE 10 | Effect of retigabine and NS19504 on methoxamine-induced contractions of the saphenous artery of young rats. **(A)** Normalized tension of saphenous arteries at different methoxamine concentration in the absence of potassium channel active agents (Control), in the presence of retigabine (Retigabine 10^{-5}M), in the presence of NS19504 (NS19504 $6*10^{-6}$M) and in the combined presence of retigabine and NS19504 (Retigabine + NS19504). **(B)** Retigabine anti-contractile effect in the absence (Control) and presence of NS19504 (NS19504 $6*10^{-6}$M). **(C)** NS19504 anti-contractile effect in the absence (Control) and presence of retigabine (Retigabine 10^{-5}M). $n = 16$; $^{**}p < 0.01$; $^{***}p < 0.001$.

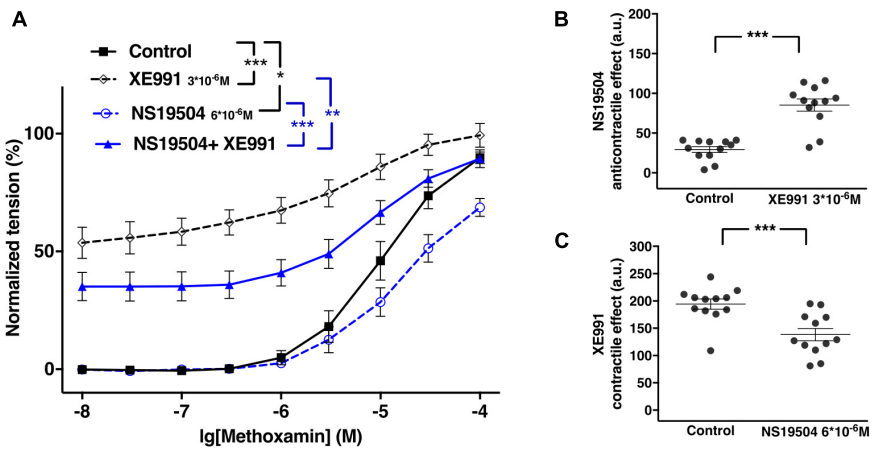

FIGURE 11 | Effect of NS19504 and XE991 on methoxamine-induced contractions of the saphenous artery of young rats. **(A)** Normalized tension of saphenous arteries with different methoxamine concentrations in the absence of potassium channel active agents (Control), in the presence of XE991 (XE991 $3*10^{-6}$M), in the presence of NS19504 (NS19504 $6*10^{-6}$M) and in the combined presence of NS19504 and XE991 (NS19504 + XE991). **(B)** NS19504 anti-contractile effect in the absence (Control) and presence of XE991 (XE991 $3*10^{-6}$M). **(C)** XE991 contractile effect in the absence (Control) and presence of NS19504 (NS19504 $6*10^{-6}$M). $n = 12$; $^{*}p < 0.05$, $^{**}p < 0.01$; $^{***}p < 0.001$.

particular, BK channels (BK α and BK β1 subunits) prevail as in other systemic blood vessels (Nelson and Quayle, 1995; Tykocki et al., 2017). Further, KCNQ4 is the most highly expressed KCNQ gene, followed by KCNQ1 and KCNQ5. This expression profile is similar to other rat (e.g., gracilis arteries, cerebral arteries, coronary arteries, pulmonary arteries and mesenteric arteries) and human arteries (e.g., visceral arteries and mesenteric arteries) (Søgaard et al., 2001; Joshi et al., 2009; Zhong et al., 2010; Ng et al., 2011; Zavaritskaya et al., 2013; Haick and Byron, 2016). The observed expression pattern was similar in both vessels studied. In addition, a comparable expression profile was detected for most channels in endothelium-intact and endothelium-denuded vessels. In contrast, eNOS, expressed preferentially in endothelial cells, showed a much smaller expression in endothelium-denuded vessels. Thus, our findings indicate that the potassium channel genes studied are not predominantly expressed in the endothelium but are expressed in both the endothelium and smooth muscle. An exception is KNCQ4, which was expressed at a lower level in endothelium-intact vessels, pointing to a preferential expression of this channel in smooth muscle cells. To enable the investigation of the functional role of Kv7 and BK channels located in smooth muscle cells, vessels without endothelium have been used in the functional experiments in this study.

Function of Kv7 and BK Channels in Arteries of Adult Rats

The myogenic response as well as vasoactive substance-induced contractions are two main mechanisms governing vascular contractility (Brozovich et al., 2016). Therefore, in this study, the interaction of Kv7 and BK channels in the regulation of the contractility of isolated arteries was examined based on pressure-induced myogenic responses and methoxamine-induced contractions. The characteristics of the myogenic response of the gracilis artery observed in this study are in accordance with the characteristics of typical myogenic responses (Bayliss, 1902; Davis and Hill, 1999; Schubert et al., 2008). Methoxamine-induced contractions of the saphenous artery have been described previously (Shvetsova et al., 2019).

Of note, in several experiments K channel blocker or their combination produced an increase in basal tone of isometric vessel preparations. Also under these conditions the lowest concentration of methoxamine used (10 nM) did not produce an increase of vessel tension on its own. Thus, the increased values of vessel tension at 10nM methoxamine (most obvious to see in **Figures 2**, **8**, **11** and **Supplementary Figure 9**) do not represent an increased sensitivity to low concentrations of methoxamine. In fact, they show the increased basal tone induced by K channel blockers or their combinations.

Negative Feedback Regulation of Vascular Contractility by Kv7 and BK Channels

The BK channel blocker IBTX enhanced methoxamine-induced contractions and strengthened the myogenic response; the Kv7 channel blocker XE991 also strengthened the myogenic response but did not affect considerably methoxamine-induced contractions in adult animals. NS19504, the BK channel opener, and retigabine, the Kv7 channel opener both attenuated methoxamine-induced contractions and the myogenic response. These data are supported by previous observations in different arteries (Brayden and Nelson, 1992; Rosenfeld et al., 2000; Greenwood and Ohya, 2009; Hill et al., 2010; Zhong et al., 2010; Haick and Byron, 2016; Tykocki et al., 2017; Schmid et al., 2018; Shvetsova et al., 2019). In summary, the data of the present study suggest that Kv7 and BK channels play a negative feedback role in methoxamine-induced contractions as well as in the myogenic response to prevent excessive vasoconstriction by limiting agonist- and pressure-induced depolarization.

The data suggest that Kv7 and BK channels can replace each other, at least regarding the studied negative feedback regulation of methoxamine-induced contraction and the myogenic response. However, this was observed only for the saphenous artery from adult animals. In this vessel from young animals BK channels cannot substitute Kv7 channels. Since BK and Kv7 channels have been shown to differ in their expression and/or functional impact in various vessels, we suggest that in some vessels (like adult saphenous arteries) they can substitute for one another but in other vessels (like young saphenous arteries) either BK or Kv7 channels will secure the negative feedback regulation of vasocontraction. Thus, both channels are needed to ensure negative feedback regulation of vasocontraction in all vessels. The reason for differences in expression and/or functional impact of BK and Kv7 channels in different vessels has to be established yet.

The presented data also show that, at the concentrations used in this study, the Kv7 channel blocker XE991 and the BK channel blocker IBTX are able to abolish the effects of the Kv7 channel opener retigabine and the BK channel opener NS19504, respectively. Thus, when used at appropriate concentrations these agents are selective openers/blockers of their respective channels (see also selection criteria for the BK and Kv7 channel blocker and opener concentrations in the methods section).

Of note, whereas XE991, IBTX and retigabine have been used at the reported concentrations in intact vessels as selective tools to study the function of Kv7 and BK channels previously (Galvez et al., 1990; Wickenden et al., 2000; Yeung and Greenwood, 2005; Ng et al., 2011; Hannigan et al., 2016; Gollasch et al., 2018; Shvetsova et al., 2019; Zavaritskaya et al., 2020), the BK channel opener NS19504 has not been explored on intact vessels before. The data of the present study show, that effects not related to BK channels, i.e., not blocked by IBTX, are observed at higher concentrations of NS19504 (10^{-5} M). However, at lower concentrations ($3*10^{-6}$ M, $6*10^{-6}$ M) the effects of NS19504 can be blocked completely by IBTX. A similar effect has been observed in guinea pig bladder strips (Nausch et al., 2014). These novel findings demonstrate that at appropriate concentrations NS19504 can be used as a selective opener of vascular smooth muscle BK channels.

Regulation of the Functional Impact of Kv7 Channels by BK Channels

Experiments on both pressure-induced myogenic responses and methoxamine-induced contractions in adult rats showed that

blockade of BK channels induced or increased a contractile effect of the Kv7 channel blocker XE991 and increased the anti-contractile effect of the Kv7 channel opener retigabine. This suggests that the functional impact of Kv7 channels increases after blocking BK channels. Accordingly, the opposite action on BK channels, their activation, decreased the anti-contractile effect of the Kv7 channel opener retigabine and abolished the contractile effect of the Kv7 channel blocker XE991. These data show that inhibition of BK channels increased the functional impact of Kv7 channels, while activation of BK channels decreased the functional impact of Kv7 channels.

Our findings can be explained based on a recently published idea (Coleman et al., 2017). When functional BK channels have been inhibited by IBTX the accompanying depolarization will move the membrane potential away from the potassium equilibrium potential resulting in a larger driving force (electrochemical gradient) for potassium ions. Further, Kv7 and BK channels are part of a plasma membrane equivalent electrical circuit where each type of potassium channel is in parallel contributing to the total membrane resistance. Blocking BK channels will increase membrane resistance so that for a given change in potassium current a larger change in membrane potential is achieved. In summary, due to the larger driving force and the increased membrane resistance after blocking BK channels changes in Kv7 channel activity, induced by either blockers or openers, will result in

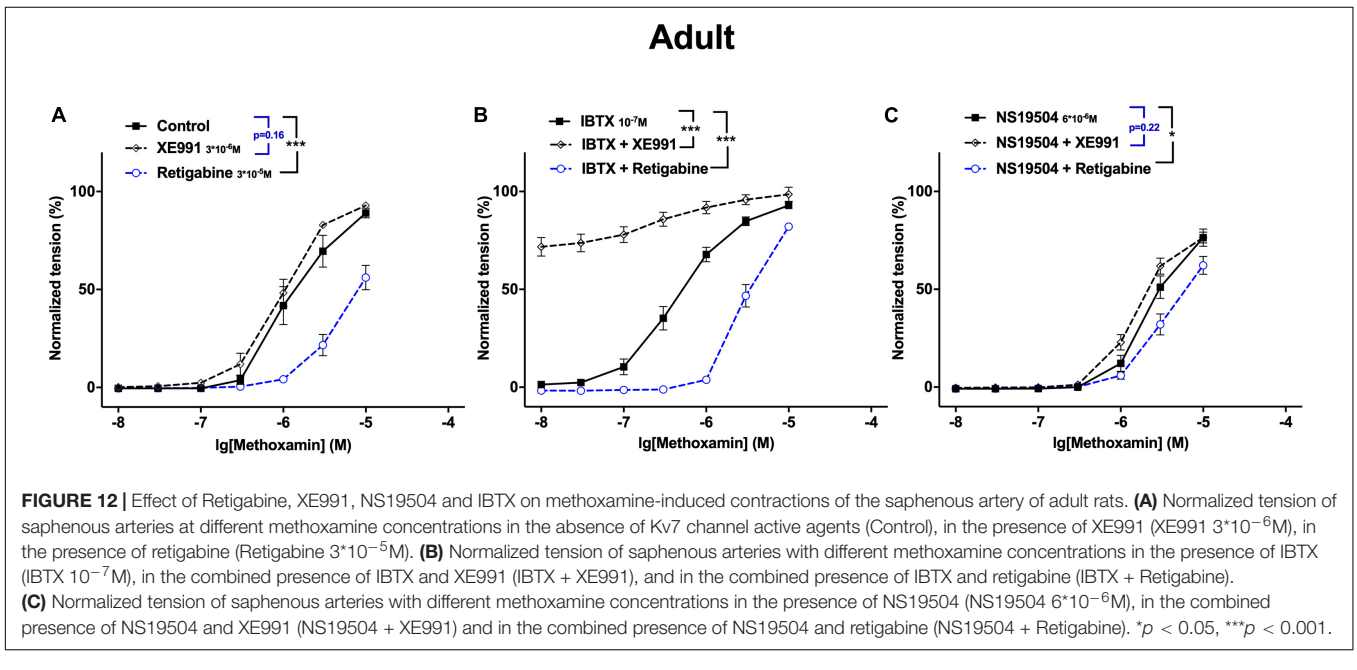

FIGURE 12 | Effect of Retigabine, XE991, NS19504 and IBTX on methoxamine-induced contractions of the saphenous artery of adult rats. **(A)** Normalized tension of saphenous arteries at different methoxamine concentrations in the absence of Kv7 channel active agents (Control), in the presence of XE991 (XE991 $3*10^{-6}$M), in the presence of retigabine (Retigabine $3*10^{-5}$M). **(B)** Normalized tension of saphenous arteries with different methoxamine concentrations in the presence of IBTX (IBTX 10^{-7}M), in the combined presence of IBTX and XE991 (IBTX + XE991), and in the combined presence of IBTX and retigabine (IBTX + Retigabine). **(C)** Normalized tension of saphenous arteries with different methoxamine concentrations in the presence of NS19504 (NS19504 $6*10^{-6}$M), in the combined presence of NS19504 and XE991 (NS19504 + XE991) and in the combined presence of NS19504 and retigabine (NS19504 + Retigabine). $*p < 0.05$, $***p < 0.001$.

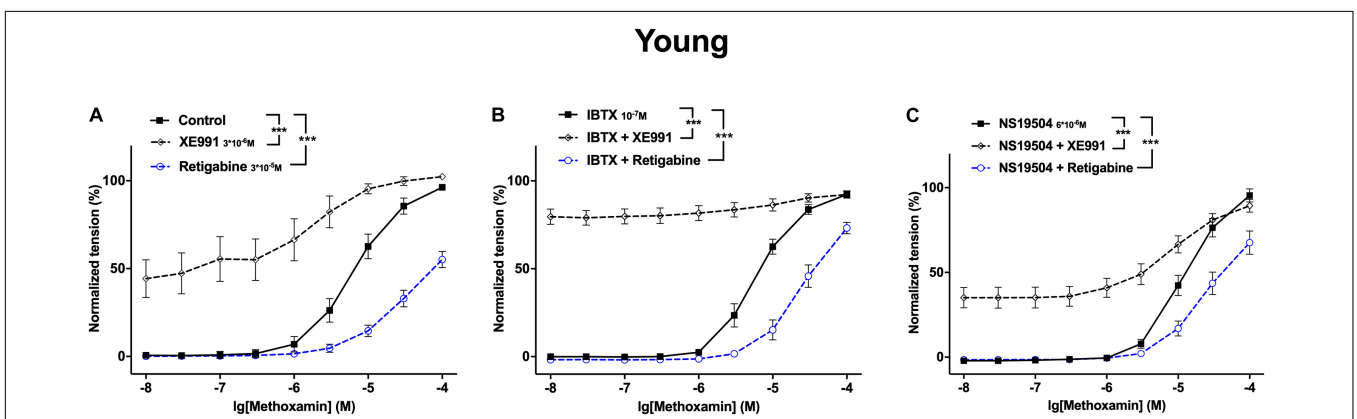

FIGURE 13 | Effect of Retigabine, XE991, NS19504 and IBTX on methoxamine-induced contractions of the saphenous artery of young rats. **(A)** Normalized tension of saphenous arteries at different methoxamine concentrations in the absence of Kv7 channel active agents (Control), in the presence of XE991 (XE991 $3*10^{-6}$M), in the presence of retigabine (Retigabine $3*10^{-5}$M). **(B)** Normalized tension of saphenous arteries with different methoxamine concentrations in the presence of IBTX (IBTX 10^{-7}M), in the combined presence of IBTX and XE991 (IBTX + XE991), and in the combined presence of IBTX and retigabine (IBTX + Retigabine). **(C)** Normalized tension of saphenous arteries with different methoxamine concentrations in the presence of NS19504 (NS19504 $6*10^{-6}$M), in the combined presence of NS19504 and XE991 (NS19504 + XE991) and in the combined presence of NS19504 and retigabine (NS19504 + Retigabine). $***p < 0.001$.

a larger change in membrane potential and vessel tension. Furthermore, when functional BK channels have been stimulated by NS19504 the accompanying hyperpolarization will move the membrane potential closer to the potassium equilibrium potential resulting in a smaller driving force for potassium ions. Further, activating BK channels will decrease membrane resistance so that for a given change in potassium current a smaller change in membrane potential is achieved. In summary, due to the smaller driving force and the decreased membrane resistance after activating BK channels, changes in Kv7 channel activity, induced by either blockers or openers, will result in a smaller change in membrane potential and vessel tension. Of note, this reasoning has been successfully applied to explain the differential effects of dual Kv7 and BK channel opener substances, GoSlo compounds (Zavaritskaya et al., 2020).

Of note, a detailed electrophysiological examination (either membrane potential or ion currents) of this model would help to clarify this idea further. The lack of such data is a weakness of the present study. However, this complex and extensive exploration is beyond the scope of the present study.

Notwithstanding the focus of the present study, the Kv7 channels, these data also show that inhibition of Kv7 channels increased the functional impact of BK channels, while activation of Kv7 channels decreased the functional impact of BK channels. Thus, changes in the activity of Kv7 channels affect the activity of BK channels, and vice versa.

The Functional Impact of Kv7 Channels Is Suppressed Considerably by BK Channels in Adult but Not in Young Rats

As IBTX, XE991, NS19504 and retigabine, when used at appropriate concentrations, are selective blockers/openers of their respective channels, it can be concluded that BK channels exert an anticontractile effect during methoxamine-induced contractions in adult as well as in young rats (see **Figures 7A,C**). In young rats, however, the degree of modulation of methoxamine-induced contractions was somewhat smaller compared to adult rats. In contrast, Kv7 channels showed a very small anticontractile effect in adult rats, but a strong anticontractile effect in young rats (see **Figures 7B,D**). These data are consistent with and nicely reproduce recently published findings showing a strongly increased negative feedback regulation of vasocontraction by Kv7 channels in arteries of young rats (compared to adult animals) which was accompanied by a lower BK channel gene expression and an increased abundance of Kv7 channels (**Figure 6** and Shvetsova et al., 2019).

Comparative evaluation of the functional impact of Kv7 and BK channels on arterial contractility in adult and young rats was performed on the basis of methoxamine-induced contractions. Pressure-induced myogenic responses could not be employed because of the very small size of the gracilis artery in young rats. As described above in detail, in adult rats, inhibition of BK channels increased the functional impact of Kv7 channels, while activation of BK channels decreased the functional impact of Kv7 channels. Interestingly, in young rats, blockade of BK channels did not affect the contractile effect of the Kv7 channel blocker XE991 (in contrast to adult rats) but increased the anti-contractile effect of the Kv7 channel opener retigabine (as in adult rats). The opposite action on BK channels, their activation, decreased the anti-contractile effect of the Kv7 channel opener retigabine (as in adult rats) and reduced the contractile effect of the Kv7 channel blocker XE991 (as in adult rats).

A different look at the data revealed that in adult rats Kv7 channels showed no considerable anticontractile effect on methoxamine-induced contraction, although they are available as the effect of retigabine shows (**Figure 12A**). However, a considerable anticontractile effect of Kv7 channels was observed after blockade of BK channels (**Figure 12B**); this effect was eliminated after activation of BK channels (**Figure 12C**). Thus, the functional impact of Kv7 channels is limited by BK channels in adult rats. In young rats, Kv7 channels showed a strong anticontractile effect on methoxamine-induced contraction (**Figure 13A**). This effect was still observed after blockade (**Figure 13B**) as well as after activation (**Figure 13C**) of BK channels. Only the range of vessel tension that Kv7 channels could affect was increased after blockade and decreased after activation of BK channels (**Figures 13B,C**). Thus, the functional impact of Kv7 channels is not limited by BK channels in young rats.

This observation is in accordance with the idea mentioned above (Coleman et al., 2017). In young rats BK channels exerted an anticontractile effect during methoxamine-induced contractions, as in adult rats. However, in young rats, the range of vessel tension that BK channels could affect was smaller. Thus, vessels of young rats were in a functional situation resembling a considerable block of BK channels. When the remaining functional BK channels have been blocked by IBTX the accompanying depolarization will be small, and will almost not move the membrane potential in relation to the potassium equilibrium potential resulting in only a slightly larger driving force for potassium ions. Further, blocking BK channels will almost not increase membrane resistance so that for a given change in potassium current only a slightly increased change in membrane potential is achieved. In summary, due to the very small increase in driving force and membrane resistance after blocking BK channels, blockade of Kv7 channels will result in almost the same change in membrane potential and vessel tension as with unblocked BK channels. Furthermore, when functional BK channels have been stimulated by NS19504 the accompanying hyperpolarization will move the membrane potential closer to the potassium equilibrium potential resulting in a smaller driving force for potassium ions. Further, BK channels activation will decrease membrane resistance so that for a given change in potassium current a smaller change in membrane potential is achieved. In summary, due to the smaller driving force and the decreased membrane resistance after activation of BK channels changes in Kv7 channel activity, induced by either blockers or openers, will result in a smaller change in membrane potential and vessel tension.

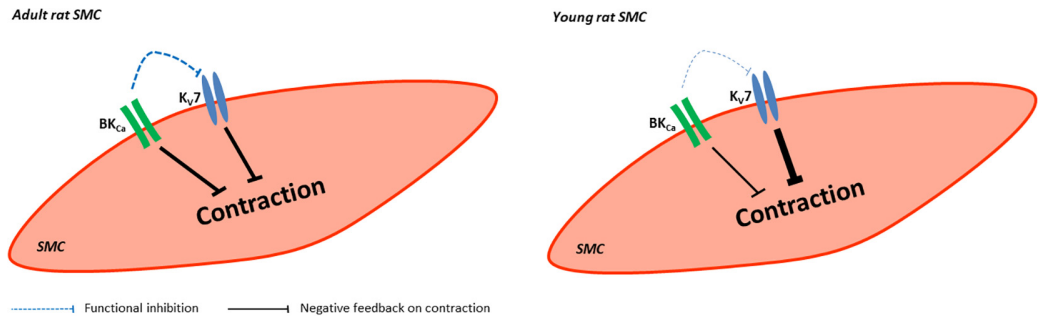

FIGURE 14 | Summary of the role of BK and KV7 channels in saphenous arteries of young and adult rats. In vessels from adult rats BK and Kv7 channels evoke a similar negative feedback regulation on vessel contraction whereby BK channels produce a considerable functional inhibition on Kv7 channels. In vessels from young rats BK and Kv7 channels evoke different negative feedback regulation on vessel contraction with Kv7 channels dominating. BK channels produce almost no functional inhibition on Kv7 channels.

CONCLUSION

Kv7 channels and BK channels are expressed in rat arteries, the saphenous and gracilis arteries. They mainly function as a negative feedback mechanism in the regulation of the contractility of these arteries. In adult rats, the functional impact of Kv7 channels is suppressed by BK channels, this effect was not observed in young rats (**Figure 14**).

As an additional finding, it was observed that the selectivity of NS19504 for BK channels is concentration dependent. Under the conditions of this study, NS19504 at $6*10^{-6}$ M selectively activates vascular smooth muscle BK channels.

DATA AVAILABILITY STATEMENT

The raw data supporting the conclusions of this article will be made available by the authors, without undue reservation.

ETHICS STATEMENT

The study was reviewed and approved by Regierungspräsidium Karlsruhe, Germany (I-17/17).

AUTHOR CONTRIBUTIONS

DM and RS designed the study and wrote the manuscript. DM, DG, MM, and NS performed the experiments. DM, DG, MM, NS, and RS analyzed the data and read and approved the manuscript. All the authors contributed to the article and approved the submitted version.

FUNDING

DM was supported by a scholarship from the China Scholarship Council (CSC) (201408080102) and by the Deutsche Forschungsgemeinschaft (IRTG 1874 DIAMICOM-SP 4 to RS).

SUPPLEMENTARY MATERIAL

The Supplementary Material for this article can be found online at: https://www.frontiersin.org/articles/10.3389/fphys.2020.597395/full#supplementary-material

Supplementary Figure 1 | Effect of retigabine and XE991 on methoxamine-induced contractions of the saphenous artery. **(A)** Original recordings of methoxamine-induced contractions in the presence of XE991 and retigabine in a wire myograph experiment on saphenous arteries. **(B)** Normalized tension of saphenous arteries at different methoxamine concentrations in the absence of Kv7 channel active agents (Control), in the presence of XE991 (XE991 $3*10^{-6}$M), in the presence of retigabine (Retigabine $3*10^{-5}$M) and in the combined presence of retigabine and XE991 (Retigabine + XE991). **(C)** Anti-contractile effect of retigabine in the absence (Control) and presence of XE991 (XE991 $3*10^{-6}$M). $n = 8$; $^{***}p < 0.001$.

Supplementary Figure 2 | Effect of retigabine and XE991 on the myogenic response of the gracilis artery. **(A)** Original recordings of myogenic responses in the presence of XE991 and retigabine in a pressure myograph experiment on gracilis arteries**. (B)** Normalized diameter of gracilis arteries at different intra-luminal pressures in the absence of Kv7 channel active agents (Control), in the presence of XE991 (XE991 $3*10^{-6}$M), in the presence of retigabine (Retigabine $3*10^{-6}$M) and in the combined presence of retigabine and XE991 (Retigabine and XE991). **(C)** Anti-contractile effect of retigabine in the absence (Control) and presence of XE991 (XE991 $3*10^{-6}$M). $n = 10$; $^{*}p < 0.05$, $^{**}p < 0.01$; $^{***}p < 0.001$.

Supplementary Figure 3 | Effect of NS19504 and IBTX on methoxamine-induced contractions of the saphenous artery. **(A–D)** Original recordings of methoxamine-induced contractions in the presence of IBTX and NS19504 in a wire myograph experiment on saphenous arteries**. (E1–E3)** Normalized tension of saphenous arteries with different methoxamine concentrations in the absence of BK channel active agents (Control), in the presence of IBTX (IBTX 10^{-7}M), in the presence of NS19504 (**E1**: NS19504 $3*10^{-6}$M; **E2**: NS19504 $6*10^{-6}$M; **E3**: NS19504 10^{-5}M) and in the combined presence of NS19504 and IBTX (NS19504 and IBTX). **(F1–F3)** NS19504 anti-contractile effect in the absence (Control) and presence of IBTX (IBTX 10^{-7}M). n1 = 7; n2 = 7; n3 = 8; $^{*}p < 0.05$, $^{**}p < 0.01$; $^{***}p < 0.001$.

Supplementary Figure 4 | Effect of NS19504 and IBTX on the myogenic response of the gracilis artery. **(A)** Original recordings of myogenic responses in the presence of IBTX and NS19504 in a pressure myograph experiment on gracilis arteries. **(B)** Normalized diameter of gracilis arteries at different intra-luminal pressures in the absence of BK channel active agents (Control), in the presence of IBTX (IBTX 10^{-7}M), in the presence of NS19504 (NS19504 $3*10^{-6}$M) and in the combined presence of NS19504 and IBTX (NS19504 and IBTX). **(C)** NS19504 anti-contractile effect in the absence (Control) and presence of IBTX (IBTX 10^{-7}M). $n = 10$; $^{*}p < 0.05$, $^{**}p < 0.01$; $^{***}p < 0.001$.

Supplementary Figure 5 | Effect of XE991 and IBTX on the myogenic response of the gracilis artery. **(A1,A2)** Normalized diameter of gracilis arteries with different intra-luminal pressures in the absence of potassium channel blockers (Control), in the presence of IBTX (IBTX 10^{-7}M), in the presence of XE991 (XE991 $3*10^{-6}$M) and in the combined presence of IBTX and XE991 (**A1** in sequence XE991 + IBTX, **A2** in sequence IBTX + XE991). **(B1,B2)** XE991 contractile effect in the absence (Control) and presence of IBTX (IBTX 10^{-7}M). **(C1,C2)** IBTX contractile effect in the absence (Control) and presence of XE991 (XE991 $3*10^{-6}$M). n1 = 10, n2 = 10; $*p < 0.05$, $***p < 0.001$.

Supplementary Figure 6 | Effect of retigabine and IBTX on the myogenic response of the gracilis artery. **(A)** Normalized diameter of gracilis arteries at different intra-luminal pressures in the absence of potassium channel active agents (Control), in the presence of IBTX (IBTX 10^{-7}M), in the presence of retigabine (Retigabine $3*10^{-6}$M) and in the combined presence of retigabine and IBTX (Retigabine and IBTX). **(B)** Retigabine anti-contractile effect in the absence (Control) and presence of IBTX (IBTX 10^{-7}M). **(C)** IBTX contractile effect in the absence (Control) and presence of retigabine (Retigabine $3*10^{-6}$M). $n = 10$; $*p < 0.05$, $**p < 0.01$.

Supplementary Figure 7 | Effect of retigabine and NS19504 on the myogenic response of the gracilis artery. **(A)** Normalized diameter of gracilis arteries at different intra-luminal pressures in the absence of potassium channel active agents (Control), in the presence of retigabine (Retigabine $3*10^{-6}$M), in the presence of NS19504 (NS19504 $3*10^{-6}$M) and in the combined presence of retigabine and NS19504 (Retigabine + NS19504). **(B)** Retigabine anti-contractile effect in the absence of (Control) and presence of NS19504 (NS19504 $3*10^{-6}$M). **(C)** NS19504 anti-contractile effect in the absence of (Control) and presence of retigabine (Retigabine $3*10^{-6}$M). $n = 9$; $*p < 0.05$, $**p < 0.01$.

Supplementary Figure 8 | Effect of NS19504 and XE991 on the myogenic response of the gracilis artery. **(A)** Normalized diameter of gracilis arteries at different intra-luminal pressures in the absence of potassium channel active agents (Control), in the presence of XE991 (XE991 $3*10^{-6}$M), in the presence of NS19504 (NS19504 $3*10^{-6}$M) and in the combined presence of NS19504 and XE991 (NS19504 + XE991). **(B)** NS19504 anti-contractile effect in the absence (Control) and presence of XE991 (XE991 $3*10^{-6}$M). **(C)** XE991 contractile effect in the absence (Control) and presence of NS19504 (NS19504 $3*10^{-6}$M). $n = 9$; $*p < 0.05$, $**p < 0.01$; $***p < 0.001$.

Supplementary Figure 9 | Effect of retigabine and XE991 on methoxamine-induced contractions of the saphenous artery of young rats. **(A)** Normalized tension of saphenous arteries at different methoxamine concentrations in the absence of Kv7 channel active agents (Control), in the presence of XE991 (XE991 $3*10^{-6}$M), in the presence of retigabine (Retigabine $3*10^{-5}$M) and in the combined presence of retigabine and XE991 (Retigabine + XE991). **(B)** Anti-contractile effect of retigabine in the absence (Control) and presence of XE991 (XE991 $3*10^{-6}$M). $n = 10$; $***p < 0.001$.

Supplementary Figure 10 | Effect of NS19504 and IBTX on methoxamine-induced contractions of the saphenous artery of young rats. **(A)** Normalized tension of saphenous arteries with different methoxamine concentrations in the absence of BK channel active agents (Control), in the presence of IBTX (IBTX 10^{-7}M), in the presence of NS19504 (NS19504 $6*10^{-6}$M) and in the combined presence of NS19504 and IBTX (NS19504 and IBTX). **(B)** NS19504 anti-contractile effect in the absence (Control) and presence of IBTX (IBTX 10^{-7}M). $n = 13$; $*p < 0.05$, $**p < 0.01$; $***p < 0.001$.

REFERENCES

Bayliss, W. M. (1902). On the local reactions of the arterial wall to changes of internal pressure. *J. Physiol.* 28, 220–231. doi: 10.1113/jphysiol.1902.sp000911

Brayden, J., and Nelson, M. (1992). Regulation of arterial tone by activation of calcium-dependent potassium channels. *Science* 256, 532–535. doi: 10.1126/science.1373909

Brozovich, F. V., Nicholson, C. J., Degen, C. V., Gao, Y. Z., Aggarwal, M., and Morgan, K. G. (2016). Mechanisms of Vascular Smooth Muscle Contraction and the Basis for Pharmacologic Treatment of Smooth Muscle Disorders. *Pharmacol. Rev.* 68, 476–532. doi: 10.1124/pr.115.010652

Chadha, P. S., Zunke, F., Zhu, H.-L., Davis, A. J., Jepps, T. A., Olesen, S. P., et al. (2012). Reduced KCNQ4-Encoded Voltage-Dependent Potassium Channel Activity Underlies Impaired β-Adrenoceptor–Mediated Relaxation of Renal Arteries in Hypertension. *Hypertension* 59, 877–884. doi: 10.1161/HYPERTENSIONAHA.111.187427

Coetzee, W. A., Amarillo, Y., Chiu, J., Chow, A., Lau, D., McCormack, T., et al. (1999). Molecular diversity of K+ channels. *Ann. N Y. Acad. Sci.* 868, 233–285. doi: 10.1111/j.1749-6632.1999.tb11293.x

Coleman, H. A., Tare, M., and Parkington, H. C. (2017). Nonlinear effects of potassium channel blockers on endothelium-dependent hyperpolarization. *Acta Physiol.* 219, 324–334. doi: 10.1111/apha.12805

Davis, M. J., and Hill, M. A. (1999). Signaling Mechanisms Underlying the Vascular Myogenic Response. *Physiol. Rev.* 79, 387–423. doi: 10.1152/physrev.1999.79.2.387

Fischer, J. G., Mewes, H., Hopp, H. H., and Schubert, R. (1996). Analysis of pressurized resistance vessel diameter changes with a low cost digital image processing device. *Comput. Methods Programs Biomed.* 50, 23–30. doi: 10.1016/0169-2607(96)01726-9

Galvez, A., Gimenez-Gallego, G., Reuben, J. P., Roy-Contancin, L., Feigenbaum, P., Kaczorowski, G. J., et al. (1990). Purification and characterization of a unique, potent, peptidyl probe for the high conductance calcium-activated potassium channel from venom of the scorpion Buthus tamulus. *J. Biol. Chem.* 265, 11083–11090.

Gollasch, M., Welsh, D. G., and Schubert, R. (2018). Perivascular adipose tissue and the dynamic regulation of K v 7 and K ir channels: Implications for resistant hypertension. *Microcirculation* 25:e12434. doi: 10.1111/micc.12434

Greenwood, I. A., and Ohya, S. (2009). New tricks for old dogs: KCNQ expression and role in smooth muscle. *Br. J. Pharmacol.* 156, 1196–1203. doi: 10.1111/j.1476-5381.2009.00131.x

Haick, J. M., and Byron, K. L. (2016). Novel treatment strategies for smooth muscle disorders: Targeting Kv7 potassium channels. *Pharmacol. Ther.* 165, 14–25. doi: 10.1016/j.pharmthera.2016.05.002

Hannigan, K. I., Large, R. J., Bradley, E., Hollywood, M. A., Sergeant, G. P., McHale, N. G., et al. (2016). Effect of a novel BK Ca opener on BK Ca currents and contractility of the rabbit corpus cavernosum. *Am. J. Physiol. Cell Physiol.* 310, C284–C292. doi: 10.1152/ajpcell.00273.2015

Hill, M. A., Yang, Y., Ella, S. R., Davis, M. J., and Braun, A. P. (2010). Large conductance. Ca2+-activated K+ channels (BKCa) and arteriolar myogenic signaling. *FEBS Lett.* 584, 2033–2042. doi: 10.1016/j.febslet.2010.02.045

Huggett, J. F., Foy, C. A., Benes, V., Emslie, K., Garson, J. A., Haynes, R., et al. (2013). The digital MIQE guidelines: Minimum Information for Publication of Quantitative Digital PCR Experiments. *Clin. Chem.* 59, 892–902. doi: 10.1373/clinchem.2013.206375

Jackson, W. F. (2000). Ion channels and vascular tone. *Hypertension* 35, 173–178. doi: 10.1161/01.hyp.35.1.173

Jackson, W. F., and Blair, K. L. (1998). Characterization and function of Ca(2+)-activated K+ channels in arteriolar muscle cells. *Am. J. Physiol.* 274, H27–H34. doi: 10.1152/ajpheart.1998.274.1.H27

Joshi, S., Sedivy, V., Hodyc, D., Herget, J., and Gurney, A. M. (2009). KCNQ Modulators Reveal a Key Role for KCNQ Potassium Channels in Regulating the Tone of Rat Pulmonary Artery Smooth Muscle. *J. Pharmacol. Exp. Ther.* 329, 368–376. doi: 10.1124/jpet.108.147785

Mackie, A. R., Brueggemann, L. I., Henderson, K. K., Shiels, A. J., Cribbs, L. L., Scrogin, K. E., et al. (2008). Vascular KCNQ Potassium Channels as Novel Targets for the Control of Mesenteric Artery Constriction by Vasopressin. Based on Studies in Single Cells, Pressurized Arteries, and in Vivo Measurements of Mesenteric Vascular Resistance. *J. Pharmacol. Exp. Ther.* 325, 475–483. doi: 10.1124/jpet.107.135764

Mondéjar-Parreño, G., Barreira, B., Callejo, M., Morales-Cano, D., Barrese, V., Esquivel-Ruiz, S., et al. (2020). Uncovered Contribution of Kv7 Channels to Pulmonary Vascular Tone in Pulmonary Arterial Hypertension. *Hypertension* 76, 1134–1146. doi: 10.1161/HYPERTENSIONAHA.120.15221

Mulvany, M. J., and Halpern, W. (1977). Contractile properties of small arterial resistance vessels in spontaneously hypertensive and normotensive rats. *Circ. Res.* 41, 19–26. doi: 10.1161/01.RES.41.1.19

Nausch, B., Rode, F., Jørgensen, S., Nardi, A., Korsgaard, M. P. G., Hougaard, C., et al. (2014). NS19504: A Novel BK Channel Activator with Relaxing Effect on Bladder Smooth Muscle Spontaneous Phasic Contractions. *J. Pharmacol. Exp. Ther.* 350, 520–530. doi: 10.1124/jpet.113.212662

Nelson, M. T., and Quayle, J. M. (1995). Physiological roles and properties of potassium channels in arterial smooth muscle. *Am. J. Physiol. Physiol.* 268, C799–C822. doi: 10.1152/ajpcell.1995.268.4.C799

Ng, F. L., Davis, A. J., Jepps, T. A., Harhun, M. I., Yeung, S. Y., Wan, A., et al. (2011). Expression and function of the K+ channel KCNQ genes in human arteries. *Br. J. Pharmacol.* 162, 42–53. doi: 10.1111/j.1476-5381.2010.01027.x

Rosenfeld, C. R., White, R. E., Roy, T., and Cox, B. E. (2000). Calcium-activated potassium channels and nitric oxide coregulate estrogen-induced vasodilation. *Am. J. Physiol. Circ. Physiol.* 279, H319–H328. doi: 10.1152/ajpheart.2000.279.1.H319

Schmid, J., Müller, B., Heppeler, D., Gaynullina, D., Kassmann, M., Gagov, H., et al. (2018). The Unexpected Role of Calcium-Activated Potassium Channels: Limitation of NO-Induced Arterial Relaxation. *J. Am. Heart Assoc.* 7:7808. doi: 10.1161/JAHA.117.007808

Schubert, R., Lidington, D., and Bolz, S. S. (2008). The emerging role of Ca2+ sensitivity regulation in promoting myogenic vasoconstriction. *Cardiovasc. Res.* 77, 8–18. doi: 10.1016/j.cardiores.2007.07.018

Shvetsova, A. A., Gaynullina, D. K., Schmidt, N., Bugert, P., Lukoshkova, E. V., Tarasova, O. S., et al. (2020). TASK-1 channel blockade by AVE1231 increases vasocontractile responses and BP in 1- to 2-week-old but not adult rats. *Br. J. Pharmacol.* 177, 5148–5162. doi: 10.1111/bph.15249

Shvetsova, A. A., Gaynullina, D. K., Tarasova, O. S., and Schubert, R. (2019). Negative feedback regulation of vasocontraction by potassium channels in 10- to 15-day-old rats: Dominating role of Kv7 channels. *Acta Physiol.* 225:e13176. doi: 10.1111/apha.13176

Søgaard, R., Ljungstrøm, T., Pedersen, K. A., Olesen, S.-P., and Jensen, B. S. (2001). KCNQ4 channels expressed in mammalian cells: functional characteristics and pharmacology. *Am. J. Physiol. Cell Physiol.* 280, C859–C866. doi: 10.1152/ajpcell.2001.280.4.C859

Stott, J. B., Barrese, V., Jepps, T. A., Leighton, E. V., and Greenwood, I. A. (2015a). Contribution of Kv7 Channels to Natriuretic Peptide Mediated Vasodilation in Normal and Hypertensive Rats. *Hypertension* 65, 676–682. doi: 10.1161/HYPERTENSIONAHA.114.04373

Stott, J. B., Povstyan, O. V., Carr, G., Barrese, V., and Greenwood, I. A. (2015b). G-protein βγ subunits are positive regulators of Kv7.4 and native vascular Kv7 channel activity. *Proc. Natl. Acad. Sci. U S A.* 112, 6497–6502. doi: 10.1073/pnas.1418605112

Thorneloe, K. S., and Nelson, M. T. (2005). Ion channels in smooth muscle: regulators of intracellular calcium and contractility. *Can. J. Physiol. Pharmacol.* 83, 215–242. doi: 10.1139/y05-016

Tykocki, N. R., Boerman, E. M., and Jackson, W. F. (2017). Smooth Muscle Ion Channels and Regulation of Vascular Tone in Resistance Arteries and Arterioles. *Compr. Physiol.* 7, 485–581. doi: 10.1002/cphy.c160011

Wickenden, A. D., Yu, W., Zou, A., Jegla, T., and Wagoner, P. K. (2000). Retigabine. A Novel Anti-Convulsant, Enhances Activation of KCNQ2/Q3 Potassium Channels. *Mol. Pharmacol.* 58, 591–600. doi: 10.1124/mol.58.3.591

Wulff, H., Castle, N. A., and Pardo, L. A. (2009). Voltage-gated potassium channels as therapeutic targets. *Nat. Rev. Drug Discov.* 8, 982–1001. doi: 10.1038/nrd2983

Yeung, S. Y. M., and Greenwood, I. A. (2005). Electrophysiological and functional effects of the KCNQ channel blocker XE991 on murine portal vein smooth muscle cells. *Br. J. Pharmacol.* 146, 585–595. doi: 10.1038/sj.bjp.0706342

Zavaritskaya, O., Dudem, S., Ma, D., Rabab, K. E., Albrecht, S., Tsvetkov, D., et al. (2020). Vasodilation of rat skeletal muscle arteries by the novel BK channel opener GoSlo is mediated by the simultaneous activation of BK and Kv7 channels. *Br. J. Pharmacol.* 177, 1164–1186. doi: 10.1111/bph.14910

Zavaritskaya, O., Zhuravleva, N., Schleifenbaum, J., Gloe, T., Devermann, L., Kluge, R., et al. (2013). Role of KCNQ Channels in Skeletal Muscle Arteries and Periadventitial Vascular Dysfunction. *Hypertension* 61, 151–159. doi: 10.1161/HYPERTENSIONAHA.112.197566

Zhong, X. Z., Harhun, M. I., Olesen, S. P., Ohya, S., Moffatt, J. D., Cole, W. C., et al. (2010). Participation of KCNQ (Kv7) potassium channels in myogenic control of cerebral arterial diameter. *J. Physiol.* 588, 3277–3293. doi: 10.1113/jphysiol.2010.192823

Conflict of Interest: The authors declare that the research was conducted in the absence of any commercial or financial relationships that could be construed as a potential conflict of interest.

frontiers in Physiology

ORIGINAL RESEARCH
published: 20 January 2021
doi: 10.3389/fphys.2020.604134

The S2–S3 Loop of Kv7.4 Channels Is Essential for Calmodulin Regulation of Channel Activation

Wenhui Zhuang[1] *and Zhiqiang Yan*[1,2]*

[1]State Key Laboratory of Medical Neurobiology and MOE Frontiers Center for Brain Science, Department of Physiology and Biophysics, School of Life Sciences, Human Phenome Institute, Fudan University, Shanghai, China, [2]Shenzhen Bay Laboratory, Institute of Molecular Physiology, Shenzhen, China

Kv7.4 (KCNQ4) voltage-gated potassium channels control excitability in the inner ear and the central auditory pathway. Mutations in Kv7.4 channels result in inherited progressive deafness in humans. Calmodulin (CaM) is crucial for regulating Kv7 channels, but how CaM affects Kv7 activity has remained unclear. Here, based on electrophysiological recordings, we report that the third EF hand (EF3) of CaM controls the calcium-dependent regulation of Kv7.4 activation and that the S2–S3 loop of Kv7.4 is essential for the regulation mediated by CaM. Overexpression of the mutant CaM_{1234}, which loses the calcium binding ability of all four EF hands, facilitates Kv7.4 activation by accelerating activation kinetics and shifting the voltage dependence of activation leftwards. The single mutant CaM_3, which loses the calcium binding ability of the EF3, phenocopies facilitating effects of CaM_{1234} on Kv7.4 activation. Kv7.4 channels co-expressed with wild-type (WT) CaM show inhibited activation when intracellular calcium levels increase, while Kv7.4 channels co-expressed with CaM_{1234} or CaM_3 are insensitive to calcium. Mutations C156A, C157A, C158V, R159, and R161A, which are located within the Kv7.4 S2–S3 loop, dramatically facilitate activation of Kv7.4 channels co-expressed with WT CaM but have no effect on activation of Kv7.4 channels co-expressed with CaM_3, indicating that these five mutations decrease the inhibitory effect of Ca^{2+}/CaM. The double mutation C156A/R159A decreases Ca^{2+}/CaM binding and completely abolishes CaM-mediated calcium-dependent regulation of Kv7.4 activation. Taken together, our results provide mechanistic insights into CaM regulation of Kv7.4 activation and highlight the crucial role of the Kv7.4 S2–S3 loop in CaM regulation.

Keywords: Kv7.4 channels, calmodulin regulation, calcium-dependent regulation, channel activation, voltage-dependent activation

OPEN ACCESS

Edited by:
Francesco Miceli, University of Naples Federico II, Italy

Reviewed by:
Álvaro Villarroel, University of the Basque Country, Spain
Jérôme J. Devaux, INSERM U1051 Institut des Neurosciences de Montpellier (INM), France

***Correspondence:**
Zhiqiang Yan
zqyan@fudan.edu.cn

Specialty section:
This article was submitted to Membrane Physiology and Membrane Biophysics, a section of the journal Frontiers in Physiology

Received: *08 September 2020*
Accepted: *23 December 2020*
Published: *20 January 2021*

Citation:
Zhuang W and Yan Z (2021) The S2–S3 Loop of Kv7.4 Channels Is Essential for Calmodulin Regulation of Channel Activation. Front. Physiol. 11:604134. doi: 10.3389/fphys.2020.604134

INTRODUCTION

Kv7 (KCNQ) voltage-gated potassium channels (Kv7.1–7.5; Gutman et al., 2003) produce Iks current (Kv7.1; Barhanin et al., 1996; Sanguinetti et al., 1996; Wang et al., 1996; Jentsch, 2000) and M current (Kv7.2–7.5; Wang et al., 1998; Delmas and Brown, 2005; Hernandez et al., 2008), playing critical roles in controlling cellular excitability in the brain, heart, and ear. Kv7 channels

open at subthreshold membrane potentials and function as a brake on membrane excitation (Delmas and Brown, 2005; Brown and Passmore, 2009). Kv7.4 channels are expressed in the inner ear and the central auditory pathway in the brainstem (Kubisch et al., 1999; Beisel et al., 2000, 2005; Kharkovets et al., 2000). Mutations in Kv7.4 result in an autosomal-dominant, non-syndromic, progressive, high-frequency hearing loss, denoted as DFNA2 (Kubisch et al., 1999).

Calmodulin (CaM) appears to be an essential auxiliary subunit of Kv7 channels and strongly modulates Kv7 function. The Kv7 A and B helices, which are located in the cytoplasmic C-terminal domain and close to the pore, are identified as CaM binding sites (Wen and Levitan, 2002; Yus-Najera et al., 2002; Sachyani et al., 2014; Strulovich et al., 2016; Sun and MacKinnon, 2017; Chang et al., 2018). Disrupted CaM interactions with Kv7.1 (Ghosh et al., 2006; Shamgar et al., 2006), Kv7.2 (Etxeberria et al., 2008; Alaimo et al., 2009, 2018), heteromeric Kv7.2/Kv7.3 (Liu and Devaux, 2014), or Kv7.4 (Chang et al., 2018) have been shown to be tightly associated with severely impaired Kv7 surface expression, which illustrates the vital role of CaM in Kv7 assembly and trafficking. Numerous studies about the effects of calcium on the interaction between CaM and Kv7 revealed that both Ca^{2+}/CaM and Apo/CaM forms bind to the channels (Wen and Levitan, 2002; Yus-Najera et al., 2002; Ghosh et al., 2006; Shamgar et al., 2006; Bal et al., 2008), whereas details of the structure of the Kv7:CaM complex are calcium dependent. Apo/CaM embraces an antiparallel pair of the Kv7 A and B helices, with the Apo/C-lobe interacting with the A helix and the Apo/N-lobe interacting with the B helix (Bernardo-Seisdedos et al., 2018; Chang et al., 2018). Calcium binding allows the Ca^{2+}/N-lobe to stay anchored on the Kv7 B helix in a similar configuration to the apo/N-lobe (Sachyani et al., 2014; Strulovich et al., 2016; Sun and MacKinnon, 2017; Bernardo-Seisdedos et al., 2018; Chang et al., 2018), while there are striking differences between the Ca^{2+}/C-lobe and Apo/C-lobe conformations. Structural studies of the interaction between CaM and the Kv7.4 A and B helices showed that calcium binding makes the C-lobe lose interaction with the A helix and bind to the B helix weakly through a much smaller interaction surface (Xu et al., 2013; Chang et al., 2018). CaM acts as a calcium sensor and regulates Kv7 currents in a calcium-dependent manner. Ca^{2+}/CaM facilitates Kv7.1 function (Sachyani et al., 2014; Tobelaim et al., 2017; Chang et al., 2018) but inhabits Kv7.2–7.5 (Gamper and Shapiro, 2003; Gamper et al., 2005; Sihn et al., 2016; Gomis-Perez et al., 2017; Chang et al., 2018). Nevertheless, the exact mechanism by which CaM regulates Kv7 channels remains unclear.

The cryo-EM structure of the Kv7.1/CaM complex reports a newly discovered interaction between the third EF hand (EF3) of CaM and the Kv7.1 S2–S3 loop (Sun and MacKinnon, 2017), which is unique to Kv7 channels but absent in the other voltage-gated potassium channels (**Supplementary Figure S1**), raising a possibility that CaM contacts the voltage sensor of Kv7 channels through the S2–S3 loop. In our study, using electrophysiological recordings and co-immunoprecipitation assays, we demonstrate that CaM regulates Kv7.4 activation through the S2–S3 loop and propose a new model accounting for CaM-mediated regulation of Kv7 channels.

MATERIALS AND METHODS

Plasmid Constructs

The plasmids (EX-U0210-M98-5) expressing human Kv7.4 (NP_004691.2) were purchased from GeneCopoeia. Each amino acid of the Kv7.4 S2–S3 loop was substituted by an alanine or a valine to generate Kv7.4 mutants. DNA encoding CaM (NP_008819.1) was a gift from Jiahuai Han (Xiamen University, China). CaM mutants with impaired calcium affinities had an alanine substitution of the first residue, an aspartate, and in the calcium-binding loop of each EF hand (CaM_3, D94A; CaM_4, D130A; CaM_{12}, D21A/D57A; CaM_{34}, D94A/D130A; and CaM_{1234}, D21A/D57A/D94A/D130A; Geiser et al., 1991; Xia et al., 1998). Mutations G97A, N98A, G99A, and Y100A were introduced into wild-type (WT) CaM (referred to as CaM G97A, CaM N98A, CaM G99A, and CaM Y100A) or CaM_3 (referred to as CaM_3 G97A, CaM_3 N98A, CaM_3 G99A, and CaM_3 Y100A). All mutants were generated by homologous recombination and verified by automated sequencing. DNA segments encoding WT or mutant Kv7.4 were subcloned into pIRES2-EGFP plasmids, and segments encoding WT or mutant CaM were subcloned into pIRES2-mCherry plasmids.

There are two alternatively spliced isoforms of human Kv7.4, called Kv7.4 isoform a and Kv7.4 isoform b (NP_751895.1). Most studies including ours used Kv7.4 isoform a, which we and others called Kv7.4. Our study also performed experiments on Kv7.4 isoform b, which we called Kv7.4b to distinguish from isoform a. DNA segments encoding Kv7.4b were generated by deleting residues 377–430 of Kv7.4 isoform a by homologous recombination and subcloned into pIRES2-EGFP plasmids. The sequence was verified by automated sequencing.

For surface labeling, the Kv7.4 subunit was tagged with a modified Myc epitope that was flanked with the extracellular D1–D2 loop of ClC-5 chloride channels to increase accessibility in the extracellular loop that connects the transmembrane domains S1 and S2 as previously described (Kim et al., 2011; referred to as Myc-Kv7.4). The amino acid sequence of the Kv7.4 S1–S2 loop was changed to STIQEHQELANENSE HEQKLISEEDLVTFEERDKCPEWNC. The Myc-Kv7.4 segments were subcloned into pcDNA3.1 plasmids without fluorescent tags. DNA encoding CD8α was kindly provided by Lan Bao (the Chinese Academy of Sciences, China), and an HA epitope was inserted between the signal peptide and the mature protein of CD8α (referred to as HA-CD8α). The HA-CD8α segments were subcloned into pcDNA3.1 plasmids as well.

For measurements of Kv7.4 and CaM total expressions and co-immunoprecipitation experiments, the Kv7.4 subunit was tagged with a Flag epitope (DYKDDDDK) at the N-terminus (referred to as Flag-Kv7.4), and CaM was tagged with an HA epitope (YPYDVPDYA) at the C-terminus (referred to as CaM-HA).

Electrophysiology

Chinese hamster ovary (CHO) cells were obtained from the Cell Bank of the Chinese Academy of Sciences, and cultured in DMEM/F-12 (Gibco) with 10% fetal bovine serum (FBS) at 37°C with 5% CO_2. Cells in 35 mm diameter wells were transfected using Lipofectamine 3000 (Invitrogen) with 1 μg of DNA encoding Kv7.4 channels and 1 μg of either DNA encoding CaM or empty vectors per dish.

Twenty-four hours following transfection, the media were replaced with bath solution. The bath solution contained 145 mM NaCl, 4 mM KCl, 1.8 mM $CaCl_2$, 0.5 mM $MgCl_2$, 10 mM HEPES, and 5 mM D-glucose (pH 7.4 adjusted with NaOH). Electrophysiology experiments were performed at room temperature by whole-cell voltage clamp recordings using polished pipettes filled with pipette solution. The pipettes were pulled from borosilicate glass capillaries (BF150-86-10, Sutter Instrument, Novato) using a Flaming/Brown micropipette puller (P-97, Sutter Instrument, Novato) and polished to obtain 3–5 MΩ resistance. The normal pipette solution contained 140 mM KCl, 1 mM $MgCl_2$, 10 mM HEPES, 10 mM EGTA, 3 mM $CaCl_2$, and 4 mM K_2ATP (pH 7.2 adjusted with KOH).

Pipette solutions containing various free calcium concentrations were used to change intracellular calcium levels. Whole-cell recordings were performed on transfected cells using pipette solutions containing 140 mM KCl, 1 mM $MgCl_2$, 10 mM HEPES, 4 mM K_2ATP, and 10 mM EGTA plus 0, 3, or 6 mM $CaCl_2$. The free calcium concentrations of the pipette solutions were 0, 77.6, and 275.9 nM, respectively, as calculated by the Webmax software online.[1]

BAPTA-AM (Abcam) was used to decrease intracellular calcium levels. BAPTA-AM was prepared as a stock solution in 20 mM in DMSO. One microliter of the BAPTA-AM stock solution was added to 1 ml of DMEM/F-12 media without FBS to obtain a final concentration of 20 μM BAPTA-AM. Twenty-four hours following transfection, cells were pretreated with the media containing 20 μM BAPTA-AM for 6 h at 37°C with 5% CO_2. Whole-cell recordings were performed on transfected cells pretreated with BAPTA-AM using the pipette solution containing 140 mM KCl, 1 mM $MgCl_2$, 10 mM HEPES, 4 mM K_2ATP, and 10 mM EGTA (pH 7.2 adjusted with KOH).

All recordings were carried out using pClamp10.5 software [(Axon Instruments, United States), an Axopatch 200B amplifier (Axon Instruments, United States), and an Axon Digidata 1550 digitizer (Axon Instruments, United States)]. Data were filtered at 1 kHz and digitized at 10 kHz. Kv7.4 channel current traces were recorded from a holding potential of −80 mV to depolarizing step potentials ranging from −100 to 40 mV with 20 mV increments for 1,000 ms, followed by −50 mV pulses for 500 ms to generate tail currents. Currents were measured after at least 80% series resistance compensation. Leakage currents were digitally subtracted after P/N leak subtraction. Kv7.4 current amplitudes at varying test potentials were measured at steady-state levels, and the currents were then divided by the cell capacitance (pF) to generate a current density-voltage relationship. Tail currents were measured immediately after pulsing to −50 mV. To obtain voltage-dependent activation curves, the normalized tail current vs. voltage was plotted and fitted with the following Boltzmann equation: $I/Imax = 1/\{1 + \exp[(V_{1/2} - Vm)/k]\}$, where $V_{1/2}$ is the half-activation potential, Vm is the membrane potential, and k is the slope factor. Parameters of Kv7.4 activation kinetics were determined by fitting the activation phase of the traces with a two-component exponential function: $I(t) = A_1 \exp(-t/\tau_1) + A_2 \exp(-t/\tau_2) + C$, where I is the recorded current, A is the current amplitude, τ is the time constant, and C is the amplitude at which the activation starts. A_1, τ_1 and A_2, τ_2 represent the parameters for the fast and slow activation components, respectively. The deactivation time constants were measured by fitting the deactivating phase to a single exponential at −50 mV, as described above.

Immunofluorescence and Quantification of Surface Expression

Chinese hamster ovary cells in 35 mm diameter wells were transfected with 1 μg of DNA encoding Myc-tagged Kv7.4 channels, 0.3 μg of DNA encoding HA-tagged CD8α, and 1 μg of either DNA encoding CaM or empty vectors per dish. Forty-eight hours after co-transfection with Myc-Kv7.4, HA-CD8α, and CaM, live CHO cells were placed in phosphate-buffered saline (PBS) with 3% bovine serum albumin (BSA) for 1 h to block unspecific binding. The cells were then incubated for 30 min with primary antibodies, mouse monoclonal anti-Myc (30601ES20, Yeasen), and rabbit monoclonal anti-HA (ab236632, Abcam). After three washes with PBS, the cells were incubated for 30 min with the secondary antibodies, Alexa-594-conjugated donkey anti-mouse IgG (H + L; 34112ES60, Yeasen), and Alexa-488-conjugated donkey anti-rabbit IgG (H + L; 34206ES60, Yeasen). All procedures were performed at room temperature.

Confocal images were acquired on a laser scanning confocal microscope (FV1200, Olympus, Japan) using a 60× oil immersion objective, in multitracking mode to minimize channel crosstalk. The surface expression of Kv7.4 channels was quantified by the ratio of Myc fluorescence intensity to HA fluorescence intensity of all the cells captured in random subsets, and fluorescence intensities were measured using ImageJ (National Institutes of Health, United States). HA-CD8α was used here as a control for its stable and exclusive expression on the cell surface (Zhang et al., 2008).

Co-immunoprecipitation and Western Blot

Chinese hamster ovary cells in 100 mm diameter wells were transfected with 9 μg of DNA encoding Flag-tagged Kv7.4 channels and 9 μg of DNA encoding HA-tagged CaM per dish. Forty-eight hours after transfection, cells were lysed in lysis buffer containing 50 mM Tris-HCl (pH 8), 150 mM NaCl, 0.5% Nonidet P-40, 200 μM Na_3VO_4, and protease inhibitor cocktail (B14001, Bimake), rotating at 4°C for 30 min. Cell lysates were centrifuged at 14,000 *g* for 10 min at 4°C. Collected supernatants were incubated with rabbit monoclonal anti-Flag antibodies (ab205606, Abcam) in the presence of either 2 mM

[1]https://somapp.ucdmc.ucdavis.edu/pharmacology/bers/maxchelator/webmaxc/webmaxcS.htm

$CaCl_2$ or 2 mM EGTA overnight at 4°C. Protein A + G agarose beads (P2012, Beyotime) were added, and the mixture was incubated for additional 3 h at 4°C. The beads that pulled down the immune complexes were collected by centrifugation at 1,000 *g* for 2 min, and then washed three times with lysis buffer. SDS-PAGE loading buffer was added and boiled for 5 min to elute proteins. Immunoprecipitated proteins were separated by SDS-PAGE and blotted onto nitrocellulose membranes (10600001, GE Healthcare). The blots were blocked in TBST (10 mM Tris-HCl, 150 mM NaCl, and 0.1% Tween 20, pH 7.5) with 5% nonfat milk at room temperature for 1 h, and then incubated with mouse anti-Flag antibodies (30502ES20, Yeasen) and mouse anti-HA antibodies (30701ES20, Yeasen) overnight. After three washes with TBST, the blots were incubated with horseradish peroxidase (HRP)-labeled goat anti-mouse IgG (H + L; 33201ES60, Yeasen) for 1 h at room temperature. Proteins were visualized using Immun-Star HRP Substrate (1705041, Bio-Rad) and ChemiDoc Imaging System (Bio-Rad, United States). Chemiluminescent signals were collected by Image Lab software (Bio-Rad, United States) and analyzed by ImageJ (National Institutes of Health, United States).

Statistics

The statistical significances were determined by unpaired Student's *t*-test for comparisons between two groups and by one-way ANOVA for comparisons of more groups. All statistical data in the figures were presented as mean ± SEM.

RESULTS

CaM Regulates Kv7.4 Activation in a Calcium-Dependent Manner

Previous studies reported CaM conferred calcium sensitivity to Kv7.4 channels and affected Kv7.4 activity (Sihn et al., 2016; Chang et al., 2018). To test the calcium-dependent regulation mediated by CaM, we first measured currents of CHO cells transfected with Kv7.4 alone or together with WT CaM or the mutant CaM_{1234} that lost the calcium binding ability of all four EF hands. CHO cells have endogenous CaM (Xu et al., 2007), and overexpression of endogenous WT CaM or CaM_{1234} could knock down the effects of endogenous CaM. Shown in **Figure 1A** are whole-cell current traces of Kv7.4 channels with only endogenous CaM but no overexpressed exogenous CaM and Kv7.4 channels with overexpression of exogenous WT CaM or CaM_{1234}. Compared with Kv7.4 channels with only endogenous CaM of CHO cells, overexpression of exogenous WT CaM and CaM_{1234} significantly increased current amplitudes, and Kv7.4 co-expressed with CaM_{1234} generated the largest current amplitudes (**Figures 1B,C**; current densities at 40 mV: Kv7.4 = 76.7 ± 6.6 pA/pF; Kv7.4:CaM = 178.2 ± 17.9 pA/pF; and Kv7.4:CaM_{1234} = 377.6 ± 35.9 pA/pF). Kv7.4 with overexpression of exogenous WT CaM showed activation properties similar to Kv7.4 channels with only endogenous CaM in terms of activation kinetics (**Figure 1D**; τ values at 40 mV: Kv7.4 = 72.4 ± 3.7 ms; Kv7.4:CaM = 72.0 ± 8.6 ms) and the voltage dependence of activation (**Figures 1E,F**; $V_{1/2}$ values: Kv7.4 = −19.9 ± 0.8 mV; Kv7.4:CaM = −18.8 ± 1.6 mV), while overexpression of exogenous CaM_{1234} sharply accelerated the activation rate (**Figure 1D**; τ value at 40 mV: Kv7.4:CaM_{1234} = 20.8 ± 3.1 ms) and shifted the half-activation voltage leftward markedly (**Figures 1E,F**; $V_{1/2}$ value: Kv7.4:CaM_{1234} = −47.9 ± 1.0 mV). Overexpression of exogenous WT CaM or CaM_{1234} did not change deactivation kinetics (**Figure 1G**).

We also measured the surface expression of Kv7.4 without overexpression of exogenous CaM and Kv7.4 with overexpression of exogenous WT CaM or CaM_{1234} to further interpret the different current amplitudes. To quantify surface expression, we developed a new method based on immunofluorescence assays. CHO cells were co-transfected with Myc-Kv7.4, HA-CD8α and empty vectors, WT CaM or CaM_{1234}. The Kv7.4 subunit was tagged with a Myc epitope in the extracellular loop that connects the transmembrane domains S1 and S2, which has been used to detect Kv7.4 surface expression in previous studies (Kim et al., 2011). Our electrophysiological data showed that the extracellular Myc tag had no effects on Kv7.4 currents or CaM regulation of Kv7.4 (**Supplementary Figure S2**). An extracellular HA tag was inserted between the signal peptide and the mature protein of CD8α. Previous studies have shown that CD8α could be stably and exclusively present on the cell surface (Zhang et al., 2008). Hence, HA-CD8α was used as an indicator to observe the expression of exogenous protein and as a ruler to quantify the membrane area of the transfected cells. The fluorescence intensity of Myc-Kv7.4 was divided by the fluorescence intensity of the co-expressed HA-CD8α, and this ratio could represent an average surface expression of Kv7.4 channels. Statistically, overexpression of exogenous WT CaM or CaM_{1234} significantly increased Kv7.4 surface expression about 3.5-fold (**Figures 1H,I**). Therefore, overexpression of exogenous WT CaM increased Kv7.4 current amplitudes by enhancing Kv7.4 surface expression without changing activation properties, while overexpression of exogenous CaM_{1234} increased Kv7.4 current amplitudes by enhancing Kv7.4 surface expression as well as facilitating channel activation. There was no significant difference in surface expression between Kv7.4 co-expressed with WT CaM and Kv7.4 co-expressed with CaM_{1234} (**Figures 1H,I**), which emphasized that only facilitated activation of Kv7.4 co-expressed with CaM_{1234} accounted for its greater current amplitudes than Kv7.4 co-expressed with WT CaM. Thus, we focused on the effects of WT or mutant CaM on Kv7.4 activation in the subsequent study.

We next sought to verify the role of calcium in CaM regulation of Kv7.4 activation to explain the differences in activation properties between Kv7.4 co-expressed with WT CaM and Kv7.4 co-expressed with CaM_{1234}. We prepared different pipette solutions containing 10 mM EGTA plus 0, 3, or 6 mM $CaCl_2$, and the free calcium concentrations are calculated by the MaxChelator software to be about 0, 80, and 270 nM, respectively. We performed whole-cell recordings using the different pipette solutions to change intracellular calcium levels of the recorded cells. Increasing free calcium concentrations in the pipette solutions exerted inhibitory effects on Kv7.4:CaM

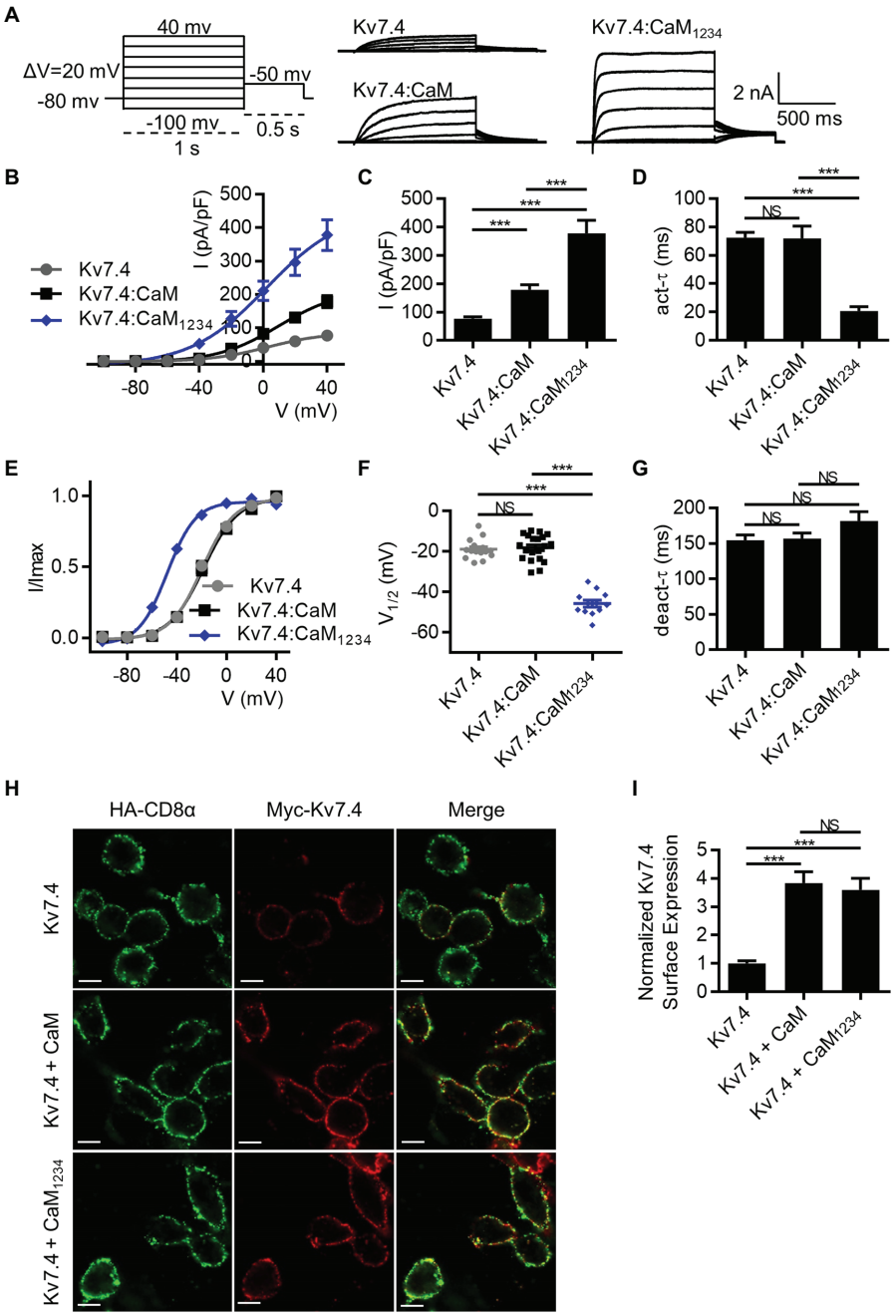

FIGURE 1 | Calmodulin (CaM) regulates Kv7.4 activation and trafficking. **(A)** Representative current traces of Kv7.4 channels without overexpression of exogenous CaM and Kv7.4 channels with overexpression of exogenous CaM or CaM_{1234} using the indicated protocol. **(B)** Corresponding current density-voltage relations of Kv7.4 (*N* = 20), Kv7.4:CaM (*N* = 20), and Kv7.4:CaM_{1234} (*N* = 12). **(C)** Average current densities at 40 mV for Kv7.4 (*N* = 20), Kv7.4:CaM (*N* = 20), and Kv7.4:CaM_{1234} (*N* = 12). **(D)** Average time constants at 40 mV for the fast activation component of Kv7.4 (*N* = 20), Kv7.4:CaM (*N* = 20), and Kv7.4:CaM_{1234} (*N* = 12). **(E)** Voltage-dependent activation curves for Kv7.4 (*N* = 20), Kv7.4:CaM (*N* = 20), and Kv7.4:CaM_{1234} (*N* = 12). **(F)** Individual $V_{1/2}$ values for Kv7.4 (*N* = 20), Kv7.4:CaM (*N* = 20), and Kv7.4:CaM_{1234} (*N* = 12). **(G)** Average time constants at 40 mV for the deactivation of Kv7.4 (*N* = 20), Kv7.4:CaM (*N* = 20), and Kv7.4:CaM_{1234} (*N* = 12). **(H)** Immunofluorescence analysis of surface expression of Kv7.4 channels without overexpression of exogenous CaM and Kv7.4 channels with overexpression of exogenous CaM or CaM_{1234}. Live transfected cells were double labeled with anti-HA (green) and anti-Myc (red) antibodies to detect surface expression of HA-CD8α and Myc-Kv7.4, respectively. The scale bars indicate 10 μm. **(I)** Quantification of surface expression of K7.4 channels without overexpression of exogenous CaM (*n* = 30) and Kv7.4 channels with overexpression of exogenous CaM (*n* = 30) or CaM_{1234} (*n* = 30), in which the ratio (Myc intensity/HA intensity) of each subset was normalized to the average ratio of Kv7.4 without overexpression of exogenous CaM. *n* indicates the number of captured subsets obtained from five replications of experiments. Error bars show SEM. *N* indicates the number of cells. Asterisks indicate significance: $^{**}p < 0.01$; $^{***}p < 0.001$. *NS* indicates not significant.

activation, decreasing the activation rate (**Figure 2A**; τ values at 40 mV: Kv7.4:CaM with 10 mM EGTA = 52.3 ± 1.2 ms; Kv7.4:CaM with 10 mM EGTA plus 3 mM $CaCl_2$ = 76.0 ± 2.0 ms; Kv7.4:CaM with 10 mM EGTA plus 6 mM $CaCl_2$ = 102.4 ± 9.2 ms), and shifting the voltage-dependent activation rightwards (**Figure 2B**; $V_{1/2}$ values at 40 mV: Kv7.4:CaM with 10 mM EGTA = −27.8 ± 1.4 mV; Kv7.4:CaM with 10 mM EGTA plus 3 mM $CaCl_2$ = −17.3 ± 1.6 mV; Kv7.4:CaM with 10 mM EGTA plus 6 mM $CaCl_2$ = −10.1 ± 1.1 mV). However, both activation kinetics (**Figure 2C**; τ values at 40 mV: Kv7.4:CaM_{1234} with 10 mM EGTA = 20.5 ± 2.5 ms; Kv7.4:CaM_{1234} with 10 mM EGTA plus 3 mM $CaCl_2$ = 17.7 ± 2.6 ms; Kv7.4:CaM_{1234} with 10 mM EGTA plus 6 mM $CaCl_2$ = 18.4 ± 2.2 ms) and voltage-dependent activation (**Figure 2B**; $V_{1/2}$ values at 40 mV: Kv7.4:CaM_{1234} with 10 mM EGTA = −48.0 ± 1.4 mV; Kv7.4:CaM_{1234} with 10 mM EGTA plus 3 mM $CaCl_2$ = −47.2 ± 1.8 mV; Kv7.4:CaM_{1234} with 10 mM EGTA plus 6 mM $CaCl_2$ = −45.7 ± 1.1 mV) of Kv7.4:CaM_{1234} remained unchanged when we used different pipette solutions. Therefore, we further confirmed that functional CaM mediated calcium-dependent inhibition to Kv7.4 channel activation and that the calcium-insensitive CaM_{1234} facilitated Kv7.4 activation essentially by abolishing the calcium-dependent inhibition.

Compared with the pipette solutions with $CaCl_2$ added, the pipette solution containing only 10 mM EGTA facilitated Kv7.4:CaM activation. Nevertheless, there are still differences between Kv7.4:CaM with the pipette solution containing only 10 mM EGTA and Kv7.4:CaM_{1234} in both the activation rate and the voltage dependence of activation, possibly because binding to Kv7.4 made CaM obtain high affinities for calcium *in vivo* and the calcium chelating ability of 10 mM EGTA was not enough to make all CaM in Apo/CaM forms, which CaM_{1234} mimicked, in such a limited time of the whole-cell recording. We pretreated transfected cells with 20 μM BAPTA-AM, a cell permeable calcium chelator, for 6 h and performed whole-cell recordings using the pipette solution containing only 10 mM EGTA. Pretreating with BAPTA-AM further facilitated Kv7.4:CaM activation but had no effect on Kv7.4:CaM_{1234} activation in terms of the activation rate (**Figures 2A,C**; τ values at 40 mV: Kv7.4:CaM pretreated with 20 μM BAPTA-AM = 28.4 ± 2.8 ms; Kv7.4:CaM_{1234} pretreated with

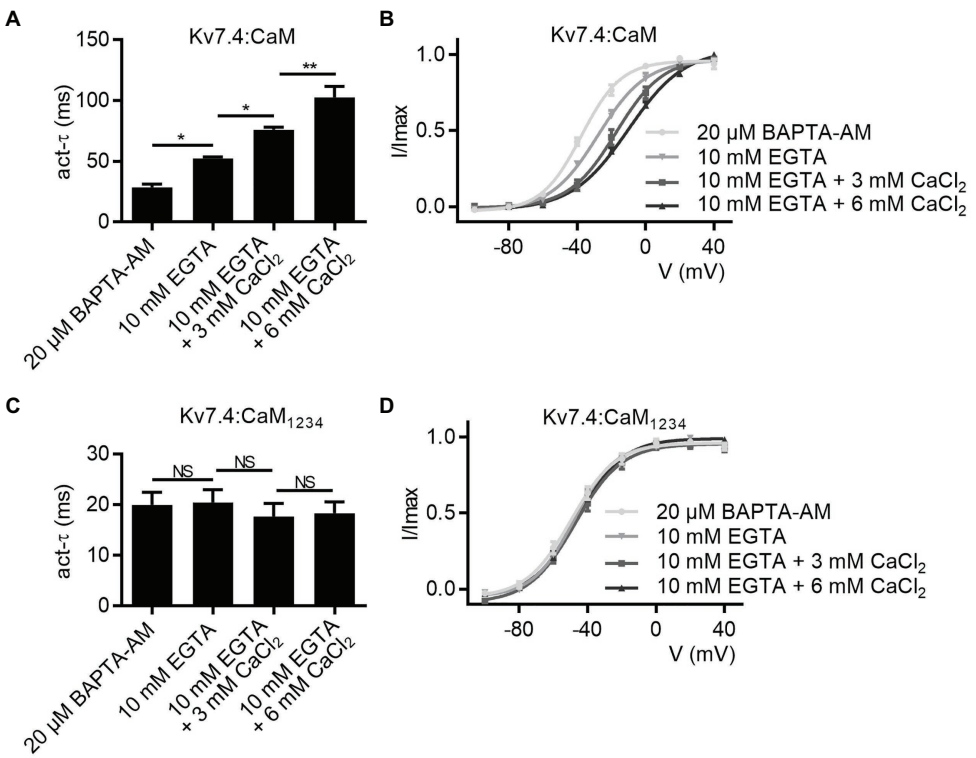

FIGURE 2 | CaM mediates calcium-dependent inhibition to Kv7.4 activation. **(A)** Average time constants at 40 mV for the fast activation component of Kv7.4:CaM with pipette solutions containing only 10 mM EGTA (*N* = 7), 10 mM EGTA plus 3 mM $CaCl_2$ (*N* = 7), or 10 mM EGTA plus 6 mM $CaCl_2$ (*N* = 7) and Kv7.4:CaM pretreated with BAPTA-AM (*N* = 8; **B**) Voltage-dependent activation curves for Kv7.4:CaM with pipette solutions containing only 10 mM EGTA (*N* = 7), 10 mM EGTA plus 3 mM $CaCl_2$ (*N* = 7), or 10 mM EGTA plus 6 mM $CaCl_2$ (*N* = 7) and Kv7.4:CaM pretreated with BAPTA-AM (*N* = 8). **(C)** Average time constants at 40 mV for the fast activation component of Kv7.4:CaM_{1234} with pipette solutions containing only 10 mM EGTA (*N* = 7), 10 mM EGTA plus 3 mM $CaCl_2$ (*N* = 7), or 10 mM EGTA plus 6 mM $CaCl_2$ (*N* = 7) and Kv7.4:CaM pretreated with BAPTA-AM (*N* = 9) **(D)** Voltage-dependent activation curves for Kv7.4:CaM_{1234} with pipette solutions containing only 10 mM EGTA (*N* = 7), 10 mM EGTA plus 3 mM $CaCl_2$ (*N* = 7), or 10 mM EGTA plus 6 mM $CaCl_2$ (*N* = 7) and Kv7.4:CaM pretreated with BAPTA-AM (*N* = 9). Error bars show SEM. *N* indicates the number of cells. Asterisks indicate significance: $^*p < 0.05$; $^{**}p < 0.01$. *NS* indicates not significant.

20 μM BAPTA-AM = 19.9 ± 2.5 ms) and the voltage dependence of activation (**Figures 2B,D**; $V_{1/2}$ values: Kv7.4:CaM pretreated with 20 μM BAPTA-AM = −37.6 ± 1.0 mV; Kv7.4:$CaM2_{234}$ pretreated with 20 μM BAPTA-AM = −49.8 ± 1.7 mV).

Taken together, our results proved that CaM regulates Kv7.4 channels in a calcium-dependent manner, in which Apo/CaM facilitated Kv7.4 activation and Ca^{2+}/CaM inhibited Kv7.4 activation.

The CaM EF3 Is Vital to the Regulation of Kv7.4 Activation

Earlier studies have reported calcium-dependent structural properties of the Kv7.4:CaM complex, in which calcium binding to the CaM N-lobe or C-lobe led to different interactions between CaM and Kv7.4 (Xu et al., 2013; Chang et al., 2018). To test if the calcium-dependent structural properties had effects on the calcium-dependent regulation of Kv7.4 activation mediated by CaM, we sought to explore the role of each lobe or EF hand of CaM in regulating Kv7.4 channels. Hence, we co-expressed Kv7.4 with the CaM mutants that lost the calcium binding affinity of the N-lobe (CaM_{12}) or the C-lobe (CaM_{34}), and the effects of CaM_{12} and CaM_{34} were compared with the effects of WT CaM and CaM_{1234}. There was no significant difference among the expression levels of WT CaM and the CaM mutants (**Supplementary Figure S4**). Shown in **Figure 3A** are whole-cell current traces of Kv7.4 channels co-expressed with WT CaM and the CaM mutants. CaM_{34} mirrored the effects of CaM_{1234} on the current amplitudes (**Figures 3B,C**; current densities at 40 mV: Kv7.4:CaM_{1234} = 375.7 ± 40.8 pA/pF; Kv7.4:CaM_{34} = 408.9 ± 28.0 pA/pF), the activation rate (**Figure 3D**; τ values at 40 mV: Kv7.4:CaM_{1234} = 20.6 ± 2.0 ms; Kv7.4:CaM_{34} = 20.4 ± 2.0 ms), and the voltage dependence (**Figures 3E,F**; $V_{1/2}$ values: Kv7.4:CaM_{34} = −46.3 ± 1.0 mV; CaM_{34} = −47.1 ± 1.2 mV). Compared with CaM_{1234} and CaM_{34}, CaM_{12} caused much smaller changes to the indicated Kv7.4 channel properties, only generating a small increase in the current amplitudes (**Figures 3B,C**; current densities at 40 mV: Kv7.4:CaM_{12} = 293.5 ± 22.2 pA/pF), a mildly faster activation rate (**Figure 3D**; τ values at 40 mV: Kv7.4:CaM_{12} = 42.9 ± 4.7 ms), and a slightly leftward shift in the voltage-dependent activation curve (**Figures 3E,F**; $V_{1/2}$ values: Kv7.4:CaM_{12} = −36.9 ± 1.4 mV). These results suggested that the CaM C-lobe played a key role in the calcium-dependent regulation of Kv7.4 activation, although calcium binding to the N-lobe also conferred a slight inhibition to Kv7.4.

Next, we used the CaM mutants with disabled calcium binding ability of the EF3 (CaM_3) or the EF4 (CaM_4) in the C-lobe. CaM_3 phenocopied the effects of CaM_{1234} and CaM_{34} on current amplitudes (**Figures 3B,C**; current densities at 40 mV: Kv7.4:CaM_3 = 385.8 ± 30.3 pA/pF), activation kinetics (**Figure 3D**; τ values at 40 mV: Kv7.4:CaM_3 = 18.5 ± 1.0 ms), and voltage-dependent activation (**Figures 3E,F**; $V_{1/2}$ values: Kv7.4:CaM_3 = −48.0 ± 0.9 mV). However, CaM_4, which caused effects almost equivalent to WT CaM, made no difference to the current amplitudes (**Figures 3B,C**; current densities at 40 mV: Kv7.4:CaM_4 = 216.0 ± 24.2 pA/pF), the activation rate (**Figure 3D**; τ values at 40 mV: Kv7.4:CaM_4 = 75.2 ± 5.4 ms), or the voltage dependence of activation (**Figures 3E,F**; $V_{1/2}$ values: Kv7.4:CaM_4 = −22.2 ± 1.2 mV). Like Kv7.4:CaM_{1234}, Kv7.4:CaM_3 showed insensitivity to the changing intracellular calcium levels, and both varying free calcium concentrations of the pipette solutions and application of BAPTA-AM have no effect on the activation rate (**Figure 3G**; τ values at 40 mV: Kv7.4:CaM_3 pretreated with 20 μM BAPTA-AM = 19.6 ± 2.1 ms; Kv7.4:CaM_3 with 10 mM EGTA = 19.2 ± 1.6 ms; Kv7.4:CaM_3 with 10 mM EGTA plus 3 mM $CaCl_2$ = 17.9 ± 1.4 ms; Kv7.4:CaM_3 with 10 mM EGTA plus 6 mM $CaCl_2$ = 18.1 ± 2.2 ms) or the voltage-dependent activation (**Figure 3H**; $V_{1/2}$ values: Kv7.4:CaM_3 pretreated with 20 μM BAPTA-AM = −45.3 ± 1.5 mV; Kv7.4:CaM_3 with 10 mM EGTA = −47.3 ± 1.7 mV; Kv7.4:CaM_3 with 10 mM EGTA plus 3 mM $CaCl_2$ = −48.5 ± 1.2 mV; Kv7.4:CaM_3 with 10 mM EGTA plus 6 mM $CaCl_2$ = −47.1 ± 1.3 mV) of Kv7.4:CaM_3. These results emphasized a critical role of the CaM EF3 in modulating Kv7.4 activation, which supported the possibility that the CaM EF3 interacted with the Kv7.4 S2–S3 loop to contact the voltage sensor (Sun and MacKinnon, 2017).

The Kv7.4 S2–S3 Loop Is Required for CaM Regulation of Kv7.4 Activation

We sought to interpret the importance of the CaM EF3 in regulating Kv7.4 activation based on the potential interaction between the CaM EF3 and the Kv7 S2–S3 loop (Sun and MacKinnon, 2017). Each residue of the nine-amino-acid S2–S3 loop was changed to an alanine or a valine. Because the current traces from CHO cells expressing C158A or G162A were quite noisy (**Supplementary Figure S6A**), we generated the mutants C158V and G162V for further investigation. When co-expressed with WT CaM, five of the nine Kv7.4 mutants displayed facilitated channel activation (**Figure 4A**) with a faster activation rate (**Figure 4D**; τ values at 40 mV: Kv7.4:CaM = 72.7 ± 4.8 ms, Kv7.4 C156A:CaM = 31.3 ± 2.9 ms, Kv7.4 C157A:CaM = 38.2 ± 4.6 ms, Kv7.4 C158V:CaM = 33.3 ± 1.7 ms, Kv7.4 R159A:CaM = 28.3 ± 3.0 ms, and Kv7.4 R161A:CaM = 37.4 ± 2.1 ms) and a leftward shift in the voltage-dependent activation (**Figure 4F**; $V_{1/2}$ values: Kv7.4:CaM = −18.2 ± 1.1 mV, Kv7.4 C156A:CaM = −33.9 ± 1.2 mV, Kv7.4 C157A:CaM = −29.6 ± 1.1 mV, Kv7.4 C158V:CaM = −30.6 ± 1.2 mV, Kv7.4 R159A:CaM = −35.7 ± 1.2 mV, and Kv7.4 R161A:CaM = −33.0 ± 1.1 mV). However, these five mutants co-expressed CaM_3 showed activation properties similar to WT Kv7.4 co-expressed with CaM_3 in terms of both the activation kinetics (**Figure 4E**; τ values at 40 mV: Kv7.4:CaM_3 = 18.8 ± 1.0 ms, Kv7.4 C156A: Kv7.4:CaM_3 = 20.2 ± 1.4 ms, Kv7.4 C157A:CaM_3 = 19.2 ± 1.4 ms, Kv7.4 C158V:CaM_3 = 19.3 ± 1.8 ms, Kv7.4 R159A:CaM_3 = 21.0 ± 1.7 ms, and Kv7.4 R161A:CaM_3 = 19.3 ± 2.0 ms) and the voltage dependence of activation (**Figure 4G**; $V_{1/2}$ values: Kv7.4:CaM_3 = −47.9 ± 0.8 mV, Kv7.4 C156A:CaM_3 = −49.1 ± 1.5 mV, Kv7.4 C157A:CaM_3 = −48.1 ± 1.4 mV, Kv7.4 C158V:CaM_3 = −50.1 ± 1.3 mV, Kv7.4 R159A:CaM_3 = −51.2 ± 1.5 mV, and Kv7.4 R161A:CaM_3 = −49.6 ± 0.9 mV), indicating that these five mutations had no effect on activation of Kv7.4 co-expressed with CaM_3. These results suggested that mutations within the S2–S3 loop of Kv7.4 channels decreased the calcium-dependent inhibition mediated by functional CaM

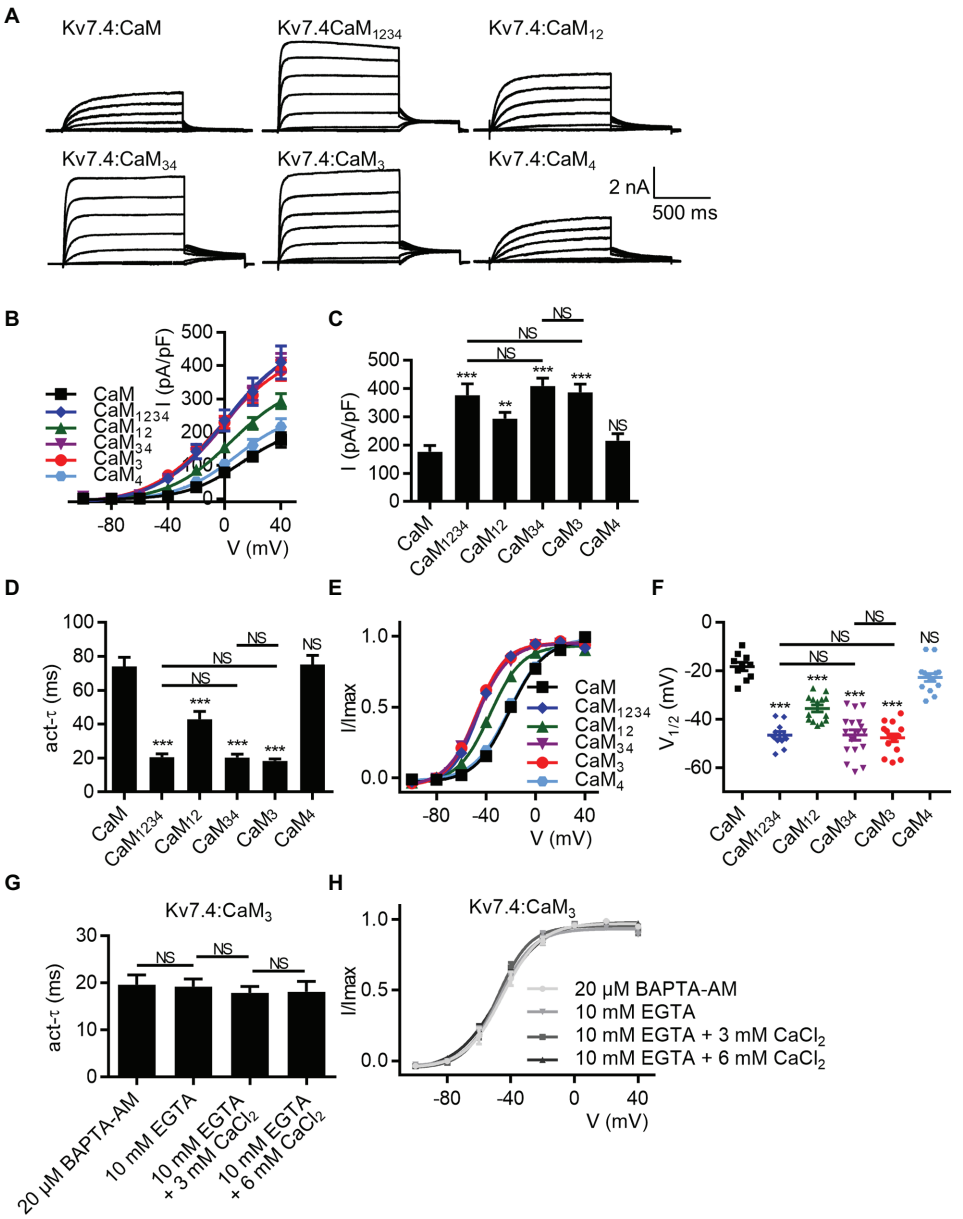

FIGURE 3 | The CaM EF3 controls the regulation of Kv7.4 activation. **(A)** Representative current traces of cells co-expressing Kv7.4 channels with CaM or CaM mutants. **(B)** Corresponding current density-voltage relations of Kv7.4 channels with CaM (N = 10) or CaM mutants: CaM_{1234} (N = 11), CaM_{12} (N = 14), CaM_{34} (N = 17), CaM_3 (N = 15), and CaM_4 (N = 14). **(C)** Average current densities at 40 mV for Kv7.4 channels with CaM (N = 10) or CaM mutants: CaM_{1234} (N = 11), CaM_{12} (N = 14), CaM_{34} (N = 17), CaM_3 (N = 15), and CaM_4 (N = 14). **(D)** Average time constants at 40 mV for the fast activation component of Kv7.4 with CaM (N = 10) or CaM mutants: CaM_{1234} (N = 11), CaM_{12} (N = 14), CaM_{34} (N = 17), CaM_3 (N = 15), and CaM_4 (N = 14). **(E)** Voltage-dependent activation curves for Kv7.4 with CaM (N = 10) or CaM mutants: CaM_{1234} (N = 11), CaM_{12} (N = 14), CaM_{34} (N = 17), CaM_3 (N = 15), and CaM_4 (N = 14). **(F)** Individual $V_{1/2}$ values for Kv7.4 with CaM (N = 10) or CaM mutants: CaM_{1234} (N = 11), CaM_{12} (N = 14), CaM_{34} (N = 17), CaM_3 (N = 15), and CaM_4 (N = 14). **(G)** Average time constants at 40 mV for the fast activation component of Kv7.4:CaM_3 with pipette solutions containing only 10 mM EGTA (N = 8), 10 mM EGTA plus 3 mM $CaCl_2$ (N = 7), or 10 mM EGTA plus 6 mM $CaCl_2$ (N = 8) and Kv7.4:CaM_3 pretreated with BAPTA-AM (N = 9). **(H)** Voltage-dependent activation curves for Kv7.4:CaM_3 with pipette solutions containing only 10 mM EGTA (N = 8), 10 mM EGTA plus 3 mM $CaCl_2$ (N = 7), or 10 mM EGTA plus 6 mM $CaCl_2$ (N = 8) and Kv7.4:CaM_3 pretreated with BAPTA-AM (N = 9). Error bars show SEM. N indicates the number of cells. Asterisks indicate significance: $^{**}p < 0.01$; $^{***}p < 0.001$. *NS* indicates not significant.

(**Supplementary Figure S7**) and proved that the S2–S3 loop of Kv7.4 is required for CaM regulation of Kv7.4 activation. We could not probe the role of the residues Tyr160 and Gly162 in CaM regulation, because the mutants Y160A and G162V did not yield functional currents (**Supplementary Figures S6B**, **S8A,B**). Moreover, the mutations

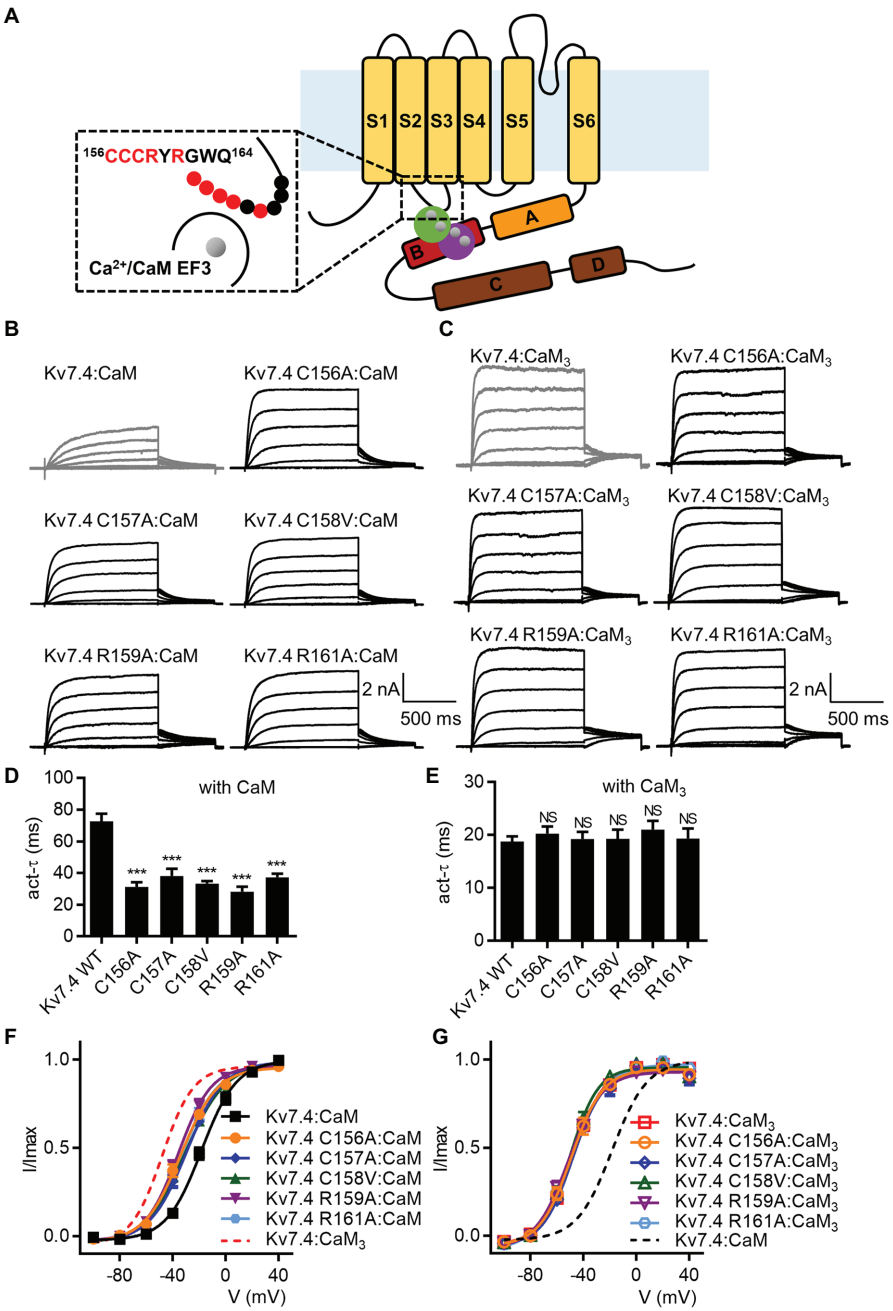

FIGURE 4 | Mutations in the Kv7.4 S2-S3 loop affect CaM regulation of channel activation. **(A)** A schematic depicting a possible structural model of Ca^{2+}/CaM interacting with the Kv7.4 subunit, in which both the Ca^{2+}/N-lobe and Ca^{2+}/C-lobe interact with the B helix of Kv7.4 channels, based on structural studies of Ca^{2+}/CaM with the Kv7.4 A and B helices (Xu et al., 2013; Chang et al., 2018). A magnified view of the potential interface between the Kv7.4 S2–S3 loop and the Ca^{2+}/CaM EF3 is shown in the dashed box. The nine residues of the Kv7.4 S2–S3 loop studied in this work are labeled with circles. Red circles indicate residues required for CaM regulation of Kv7.4 activation (according to our electrophysiological). **(B)** Representative current traces of cells co-expressing Kv7.4 WT or Kv7.4 mutants with CaM. **(C)** Representative current traces of cells co-expressing Kv7.4 WT or Kv7.4 mutants with CaM_3. **(D)** Average time constants at 40 mV for the fast activation component of Kv7.4:CaM (N = 12), Kv7.4 C156A:CaM (N = 13), Kv7.4 C157A:CaM (N = 8), Kv7.4 C158V:CaM (N = 10), Kv7.4 R159A:CaM (N = 9), and Kv7.4 R161A:CaM (N = 13). **(E)** Average time constants at 40 mV for the fast activation component of Kv7.4:CaM_3 (N = 11), Kv7.4 C156A:CaM_3 (N = 11), Kv7.4 C157A:CaM_3 (N = 10), Kv7.4 C158V:CaM_3 (N = 9), Kv7.4 R159A:CaM_3 (N = 8), and Kv7.4 R161A:CaM_3 (N = 9). **(F)** Voltage-dependent activation curves for Kv7.4:CaM (N = 12), Kv7.4 C156A:CaM (N = 13), Kv7.4 C157A:CaM (N = 8), Kv7.4 C158V:CaM (N = 10), Kv7.4 R159A:CaM (N = 9), and Kv7.4 R161A:CaM (N = 13). **(G)** Voltage-dependent activation curves for Kv7.4:CaM_3 (N = 11), Kv7.4 C156A:CaM_3 (N = 11), Kv7.4 C157A:CaM_3 (N = 10), Kv7.4 C158V:CaM_3 (N = 9), Kv7.4 R159A:CaM_3 (N = 8), and Kv7.4 R161A:CaM_3 (N = 9). Error bars show SEM. N indicates the number of cells. Asterisks indicate significance: ***$p < 0.001$. *NS* indicates not significant.

W163A and Q164A did not affect the currents of Kv7.4 co-expressed with WT CaM (**Supplementary Figures S8C,E**) or CaM_3 (**Supplementary Figures S8D,F**), implying that the two residues were not involved in CaM regulation.

The Kv7.4 Double Mutation C156A/R159A Completely Abolishes CaM Regulation of Kv7.4 Activation

Although the five Kv7.4 mutations (C156A, C157A, C158V, R159A, and R161A) facilitated activation of Kv7.4 channels co-expressed with WT CaM, the activation time constants and the half-activation voltages of the five single mutants were still different from the parameters of Kv7.4 channels co-expressed with CaM_3, suggesting that the inhibitory effects of Ca^{2+}/CaM was decreased but not abolished completely. For further investigation on the necessity of the S2–S3 loop, we sought to enhance the facilitating effects by generating double mutants (C156A/R159A, C156A/R161A, C158V/R159A, and R159A/R158A). Shown in **Figure 5A** are whole-cell current traces of the double mutants co-expressed with WT CaM or CaM_3. When co-expressed with WT CaM, all the double mutants displayed further facilitated channel activation in terms of activation kinetics (**Figure 5B**; τ values at 40 mV: Kv7.4:CaM = 71.9 ± 5.0 ms, Kv7.4 C156A/R159A:CaM = 19.1 ± 1.7 ms, Kv7.4 C156A/R161A:CaM = 31.7 ± 3.1 ms, Kv7.4 C158V/R159A:CaM = 23.9 ± 2.0 ms, and Kv7.4 R159A/R161A:CaM = 25.5 ± 1.9 ms) and voltage-dependent activation (**Figures 5C,D**; $V_{1/2}$ values: Kv7.4:CaM = −21.1 ± 1.2 mV, Kv7.4 C156A/R159A = −47.3 ± 1.2 mV, Kv7.4 C156A/R161A:CaM = −43.3 ± 0.7 mV, Kv7.4 C158V/R159A:CaM = −41.3 ± 0.8 mV, and Kv7.4 C158V/R159A:CaM = −41.7 ± 1.1 mV). As expected, all the double mutants co-expressed with CaM_3 generated activation rates (**Figure 4B**; τ values at 40 mV: Kv7.4:CaM_3 = 19.2 ± 1.4 ms, Kv7.4 C156A/R159A:CaM_3 = 20.5 ± 1.6 ms, Kv7.4 C156A/R161A:CaM_3 = 20.8 ± 1.7 ms, Kv7.4 C158V/R159A:CaM_3 = 18.6 ± 1.1 ms, and Kv7.4 R159A/R161A:CaM_3 = 19.9 ± 1.6 ms) and half-activation voltages (**Figures 4C,D**; $V_{1/2}$ values: Kv7.4:CaM_3 = −48.6 ± 0.9 mV, Kv7.4 C156A/R159A: CaM_3 = −49.9 ± 0.8 mV, Kv7.4 C156A/R161A:CaM_3 = −50.0 ± 1.8 mV, Kv7.4 C158V/R159A:CaM_3 = −49.0 ± 0.9 mV, and Kv7.4 R159A/R161A:CaM_3 = −48.8 ± 1.8 mV; **Figures 4C,D**) similar to WT Kv7.4 channels with CaM_3. Importantly, according to our statistical results, there was no significant difference among Kv7.4 C156A/R159A:CaM, Kv7.4 C156A/R159A:CaM_3, and Kv7.4:CaM_3 in both activation kinetics (**Figure 5B**) and voltage-dependent activation (**Figure 5C**). This indicated that the double mutation C156A/R159A generated facilitating effects equivalent to CaM_3 and suggested that CaM regulation of Kv7.4 activation was abolished completely by this mutation. Additionally, both varying free calcium concentrations of the pipette solutions and application of BAPTA-AM have no effect on activation kinetics (**Figure 5E**; τ values at 40 mV: Kv7.4 C156A/R159A:CaM pretreated with 20 μM BAPTA-AM = 21.6 ± 2.1 ms; Kv7.4 C156A/R159A:CaM with 10 mM EGTA = 20.2 ± 1.9 ms; Kv7.4 C156A/R159A:CaM with 10 mM EGTA plus 3 mM CaCl2 = 18.5 ± 3.0 ms; Kv7.4 C156A/R159A:CaM with 10 mM EGTA plus 6 mM CaCl2 = 19.0 ± 2.3 ms) or voltage-dependent activation (**Figure 5F**; V1/2 values: Kv7.4 C156A/R159A:CaM pretreated with 20 μM BAPTA-AM = −48.6 ± 1.7 mV; Kv7.4 C156A/R159A:CaM with 10 mM EGTA = −47.2 ± 1.3 mV; Kv7.4 C156A/R159A:CaM with 10 mM EGTA plus 3 mM CaCl2 = −50.9 ± 1.4 mV; Kv7.4 C156A/R159A:CaM with 10 mM EGTA plus 6 mM CaCl2 = −48.6 ± 1.1 mV) of Kv7.4 C156A/R159A:CaM. Taken together, these results of Kv7.4 C156A/R159A further emphasized the essential role of the Kv7.4 S2–S3 loop in CaM-mediated calcium-dependent regulation.

We used co-immunoprecipitation experiments to probe the effects of the double mutation C156/R159A, which completely abolished CaM regulation of Kv7.4 activation, on Kv7.4 forming complex with CaM, a requirement for their interaction. A Flag tag and an HA tag were introduced to the N-terminus of Kv7.4 and the C-terminus of CaM, respectively. Electrophysiological recordings revealed no noticeable distinction between tagged and untagged combinations of Kv7.4 with CaM in channel currents (**Supplementary Figure S3A**) or in the effects of CaM regulation (**Supplementary Figures S3B,C**). Immunoprecipitation accomplished using anti-Flag antibodies to precipitate Flag-Kv7.4 or Flag-Kv7.4 C156A/R159A in the presence of either 2 mM CaCl2 or 2 mM EGTA. The immunoprecipitates were probed with anti-Flag antibodies to confirm precipitation of Flag-Kv7.4 or Flag-Kv7.4 C156A/R159A and were probed with anti-HA antibodies to detect CaM-HA or CaM_3-HA pulled down with the channels. In the presence of 2 mM $CaCl_2$, WT CaM showed a detectable but much weaker association with the Kv7.4 C156A/R159A mutant than with WT Kv7.4, while the signals of CaM_3 pulled down with WT Kv7.4 and Kv7.4 C156A/R159A are similar (**Figure 6**). These results implied that the Kv7.4 S2-S3 loop interacted with Ca^{2+}/CaM but had no association with Ca^{2+}/CaM_3 that had an empty EF3 and calcium-bound EF hands 1, 2, and 4. Of note, the signal of CaM_3 pulled down with Kv7.4 channels was stronger than WT CaM in the presence of 2 mM $CaCl_2$, matching the observation by Kosenko and Hoshi (2013), who reported that longer exposure to calcium decreased CaM binding to Kv7.2 channels. This difference might result from the different interactions of the Kv7.4 C-terminal domain with Ca^{2+}/CaM and with CaM_3, in which calcium binding disturbed the interaction between the CaM C-lobe and the Kv7.4 A helix and the Ca^{2+}/C-lobe bound to the B helix weakly through a much smaller interaction surface (Xu et al., 2013; Chang et al., 2018). Therefore, the stronger binding of CaM_3 than Ca^{2+}/CaM is not contradictory to our hypothesis that Ca^{2+}/CaM interacted with the Kv7.4 S2–S3 loop, whereas Ca^{2+}/CaM_3 lost this interaction. In the presence of 2 mM EGTA through the whole immunoprecipitation overnight, both WT CaM and CaM_3 would exist in Apo/CaM forms, and there were no significant differences among the signals of WT CaM pulled down with WT Kv7.4, WT CaM pulled down with Kv7.4 C156A/R159A, CaM_3 pulled down with WT Kv7.4, and CaM_3 pulled down with Kv7.4 C156A/R159A (**Figure 6**). Additionally, the binding of Apo/CaM is stronger than Ca^{2+}/CaM and similar to Ca^{2+}/CaM_3, suggesting an important role of the EF3 in CaM

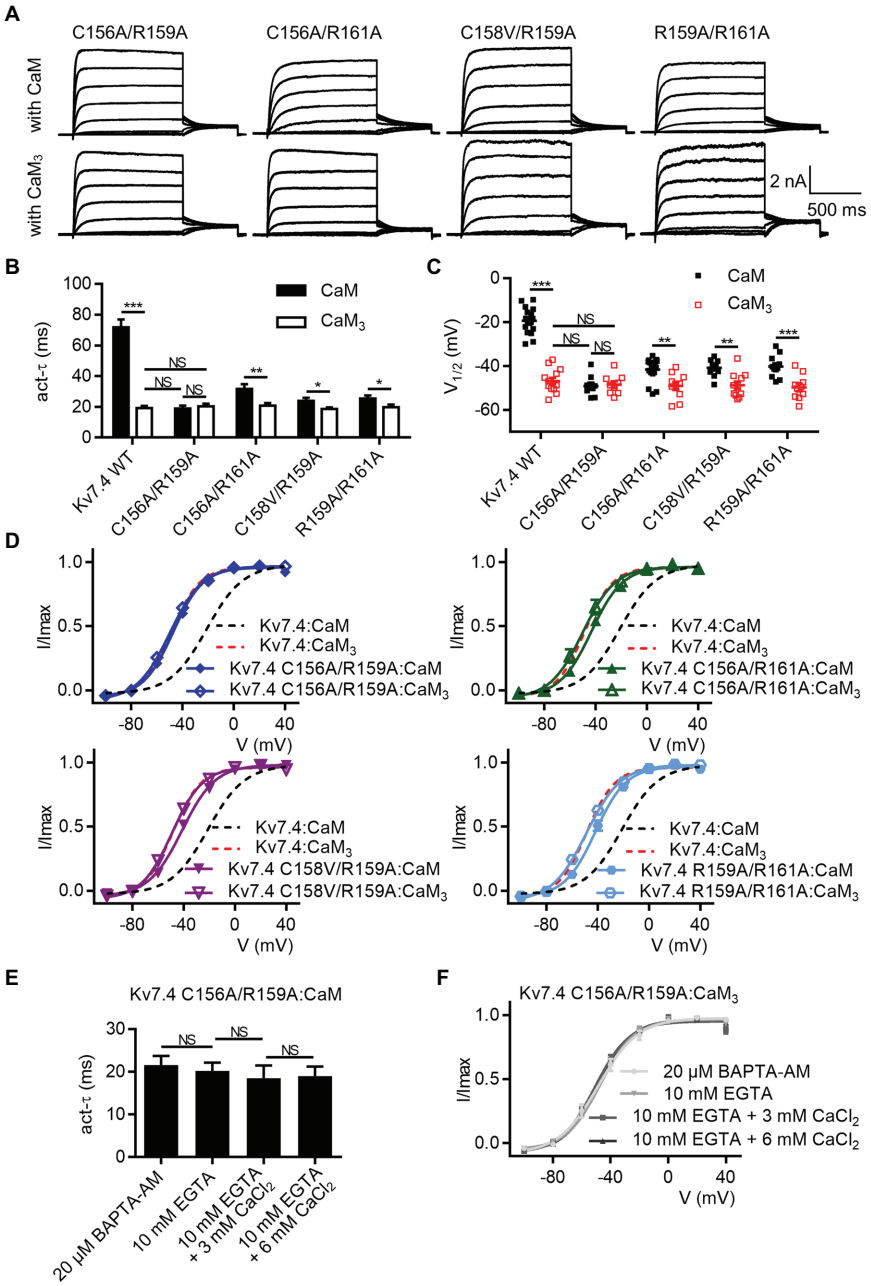

FIGURE 5 | The Kv7.4 double mutation C156A/R159A completely abolishes CaM regulation of channel activation. **(A)** Representative current traces of cells co-expressing Kv7.4 double mutants with CaM (top) or CaM_3 (bottom). **(B)** Average time constants at 40 mV for the fast activation component of Kv7.4:CaM (N = 17), Kv7.4:CaM_3 (N = 13), Kv7.4 C156A/R159A:CaM (N = 9), Kv7.4 C156A/R159A:CaM_3 (N = 9), Kv7.4 C156A/R161A:CaM (N = 17), Kv7.4 C156A/R161A:CaM_3 (N = 10), Kv7.4 C158V/R159A:CaM (N = 10), Kv7.4 C158V/R159A:CaM_3 (N = 11), Kv7.4 R159A/R161A:CaM (N = 11), and Kv7.4 R159A/R161A:CaM_3 (N = 10). **(C)** Individual $V_{1/2}$ values for Kv7.4:CaM (N = 17), Kv7.4:CaM_3 (N = 13), Kv7.4 C156A/R159A:CaM (N = 9), Kv7.4 C156A/R159A:CaM_3 (N = 9), Kv7.4 C156A/R161A:CaM (N = 17), Kv7.4 C156A/R161A:CaM_3 (N = 10), Kv7.4 C158V/R159A:CaM (N = 10), Kv7.4 C158V/R159A:CaM_3 (N = 11), Kv7.4 R159A/R161A:CaM (N = 11), and Kv7.4 R159A/R161A:CaM_3 (N = 10). **(D)** Voltage-dependent activation curves for Kv7.4:CaM (N = 17), Kv7.4:CaM_3 (N = 13), Kv7.4 C156A/R159A:CaM (N = 9), Kv7.4 C156A/R159A:CaM_3 (N = 9), Kv7.4 C156A/R161A:CaM (N = 17), Kv7.4 C156A/R161A:CaM_3 (N = 10), Kv7.4 C158V/R159A:CaM (N = 10), Kv7.4 C158V/R159A:CaM_3 (N = 11), Kv7.4 R159A/R161A:CaM (N = 11), and Kv7.4 R159A/R161A:CaM_3 (N = 10). **(E)** Average time constants at 40 mV for the fast activation component of Kv7.4 C156A/R159A:CaM with pipette solutions containing only 10 mM EGTA (N = 7), 10 mM EGTA plus 3 mM $CaCl_2$ (N = 7), or 10 mM EGTA plus 6 mM $CaCl_2$ (N = 7) and Kv7.4 C156A/R159A:CaM pretreated with BAPTA-AM (N = 8). **(F)** Voltage-dependent activation curves for Kv7.4 C156A/R159A:CaM with pipette solutions containing only 10 mM EGTA (N = 7), 10 mM EGTA plus 3 mM $CaCl_2$ (N = 7), or 10 mM EGTA plus 6 mM $CaCl_2$ (N = 7) and Kv7.4 C156A/R159A:CaM pretreated with BAPTA-AM (N = 8). N indicates the number of cells. Asterisks indicate significance: $^*p < 0.05$; $^{**}p < 0.01$; $^{***}p < 0.001$. *NS* indicates not significant.

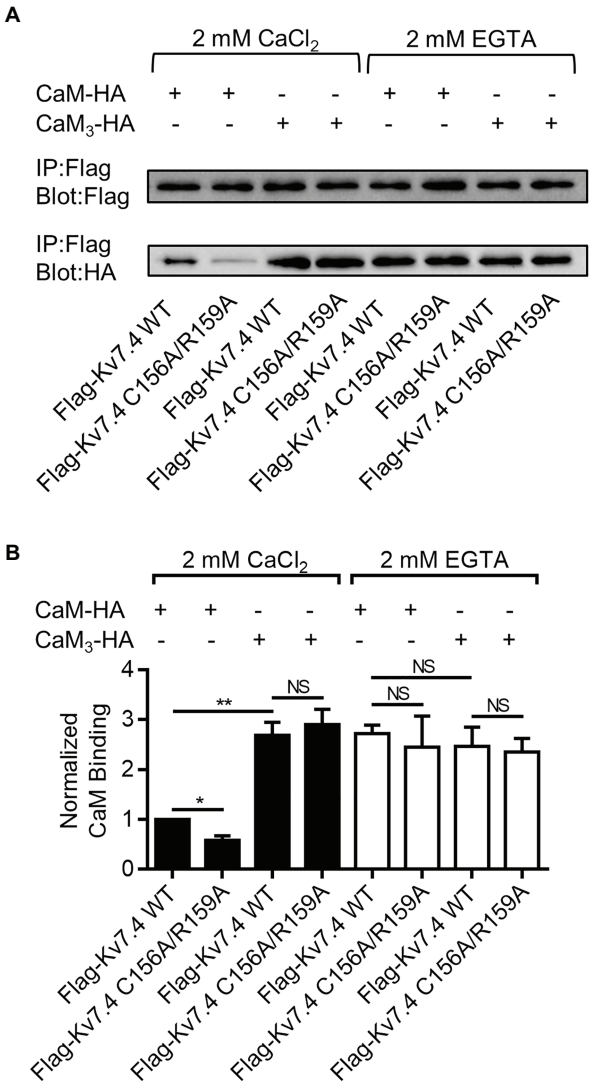

FIGURE 6 | The Kv7.4 double mutation C156A/R159A decreased Ca^{2+}/CaM binding. **(A)** Co-immunoprecipitation analysis of CaM or CaM_3 binding to Kv7.4 or Kv7.4 C156A/R159A. Chinese hamster ovary (CHO) cells were co-transfected with Flag-Kv7.4 and CaM-HA, Flag Kv7.4 C156A/R159A and CaM-HA, Flag-Kv7.4 and CaM_3-HA, or Flag-Kv7.4 C156A/R159A:CaM_3-HA. Immunoprecipitation was accomplished using anti-Flag antibodies in the presence of either 2 mM $CaCl_2$ or 2 mM EGTA. The immunoprecipitates were probed with anti-Flag antibodies to confirm precipitation of Flag-Kv7.4 or Flag-Kv7.4 C156A/R159A and were probed with anti-HA antibodies to detect CaM-HA or CaM_3-HA pulled down with the channels. The experiments were replicated four times and showed similar results. **(B)** Quantification of CaM or CaM_3 binding to Kv7.4 or Kv7.4 C156A/R159A. The binding efficiency is represented as the ratio of HA intensity to Flag intensity, and all ratios are normalized to the ratio representing CaM binding to Kv7.4 in the presence of $CaCl_2$. Asterisks indicate significance: $^*p < 0.05$; $^{**}p < 0.01$. *NS* indicates not significant.

binding. Taken together, these results of the co-immunoprecipitation experiments coincided with our electrophysiological data, supporting an potential correlation between the structure and function of the Kv7.4:CaM complex.

The Residues N98 and N99 in the CaM EF3 Are Required for the Regulation of Kv7.4 Activation

Sun and MacKinnon (2017) have previously shown that four residues in the CaM EF3 (Gly97, Asn98, Gly99, and Tyr100) are involved in the newly discovered interface between CaM and the S2–S3 loop of Kv7.1 channels (**Supplementary Figure S9**). We generated CaM mutants in which Gly97, Asn98, Gly99, or Tyr100 were mutated to an alanine based on WT CaM (CaM G97A, CaM N98A, CaM G99A, and CaM Y100A) or CaM_3 (CaM_3 G97A, CaM_3 N98A, CaM_3 G99A, and CaM_3 Y100A). Kv7.4 channels co-expressed with all these CaM mutants yielded functional currents (**Figures 7A,B**). Compared with WT CaM, CaM N98A and CaM G99A accelerated the activation rate (**Figure 7C**; τ values at 40 mV: Kv7.4:CaM = 73.1 ± 4.8 ms, Kv7.4:CaM N98A = 29.1 ± 2.5 ms, and Kv7.4:CaM G99A = 35.2 ± 2.3 ms) and shifted the voltage-dependent activation curve leftwards (**Figure 7E**; $V_{1/2}$ values: Kv7.4:CaM = −18.7 ± 1.0 mV, Kv7.4:CaM N98A = −32.8 ± 0.9 ms, and Kv7.4:CaM G99A = −31.9 ± 1.8 ms). Kv7.4 co-expressed with CaM G97A or CaM Y100A generated activation properties identical to Kv7.4 co-expressed with WT CaM in terms of both the activation rate (**Figure 7C**; τ values at 40 mV: Kv7.4:CaM G97A = 68.6 ± 3.1 ms and Kv7.4:CaM Y100A = 70.0 ± 7.0 ms) and the voltage dependence of activation (**Figure 7E**; $V_{1/2}$ values: Kv7.4:CaM N98A = −20.4 ± 1.0 ms and Kv7.4:CaM G99A = −21.6 ± 0.8 ms), suggesting that the two residues of CaM were not involved in the regulation of Kv7.4 activation. All mutants based on CaM_3 (CaM_3 G97A, CaM_3 N98A, CaM_3 G99A, and CaM_3 Y100A) phenocopied the effects of CaM_3 on the activation rate (**Figure 7D**; τ values at 40 mV: Kv7.4:CaM_3 = 19.2 ± 1.1 ms, Kv7.4:CaM_3 G97A = 19.5 ± 1.4 ms, Kv7.4:CaM_3 N98A = 21.3 ± 2.0 ms, Kv7.4:CaM_3 G99A = 20.7 ± 1.3 ms, and Kv7.4:CaM_3 Y100A = 22.1 ± 1.1 ms) and the voltage dependence of activation (**Figure 7F**; $V_{1/2}$ values: Kv7.4:CaM_3 = −48.4 ± 1.0 mV, Kv7.4:CaM_3 G97A = −46.3 ± 1.2 mV, Kv7.4:CaM_3 N98A = −45.4 ± 1.3 mV, Kv7.4:CaM_3 G99A = −48.1 ± 1.1 mV, and Kv7.4:CaM_3 Y100A = −48.0 ± 0.9 mV). Taken together, the effects of the two mutations N98A and G99A in the CaM EF3 were similar to the effects of the five mutations (C156A, C157A, C158V, R159A, and R161A) in the Kv7.4 S2–S3 loop, which potentially interacted with the CaM EF3, providing further supporting evidence for the model in which CaM modulated Kv7.4 activation through the S2-S3 loop.

CaM Regulates Activation of Kv7.4 Isoform b

There are two alternatively spliced isoforms of human Kv7.4, called Kv7.4 isoform a and Kv7.4 isoform b. Most studies including ours, used Kv7.4 isoform a, which we and others called Kv7.4. To further the understanding of CaM regulation of both the two isoforms, we also performed experiments on Kv7.4 isoform b, which we called Kv7.4b to distinguish from isoform a. Whole-cell recordings were performed on CHO cells transfected with Kv7.4b alone or together with WT CaM, CaM_{1234}, or CaM_3. Kv7.4b with only endogenous CaM and

Kv7.4b with overexpression of exogenous WT CaM showed the same activation rate (τ values at 40 mV: Kv7.4b = 52.5 ± 5.0 ms; Kv7.4b:CaM = 48.0 ± 4.2 ms) and voltage dependence of activation ($V_{1/2}$ values: Kv7.4b = −22.2 ± 2.0 mV; Kv7.4b:CaM = −24.9 ± 1.0 mV). Overexpression of CaM_{1234} significantly accelerated the activation rate (τ value at 40 mV: Kv7.4b:CaM_{1234} = 23.4 ± 2.7 ms) and shifted the voltage dependent activation leftwards markedly ($V_{1/2}$ value: Kv7.4b:CaM_{1234} = −48.8 ± 1.1 mV). CaM_3 mirrored the facilitating effects of CaM_{1234} on both activation kinetics (τ value at 40 mV: Kv7.4b:CaM_3 = 21.8 ± 2.2 ms) and voltage-dependence activation ($V_{1/2}$ value: Kv7.4b:CaM_3 = −51.6 ± 1.1 mV). To probe effects of the Kv7.4b S2–S3 loop on CaM regulation, we also performed whole-cell recordings on CHO cells transfected with Kv7.4b C156A/R159A alone or together with WT CaM, CaM_{1234}, or CaM_3. According to the statistical results, there was no significant difference among the four groups in both the activation rate (τ values at 40 mV: Kv7.4b C156A/R156A = 23.5 ± 3.4 ms; Kv7.4b C156A/R159A:CaM = 22.5 ± 2.0 ms; Kv7.4b C156A/R159A:CaM_{1234} = 23.6 ± 1.8 ms; Kv7.4b C156A/R159A:CaM_3 = 21.6 ± 1.9 ms) and the voltage dependence of activation ($V_{1/2}$ values: Kv7.4b C156A/R156A = −53.2 ± 2.0 mV; Kv7.4b C156A/R159A:CaM = −53.5 ± 0.9 mV; Kv7.4b C156A/R159A:CaM_{1234} = −52.4 ± 1.3 mV; Kv7.4b C156A/

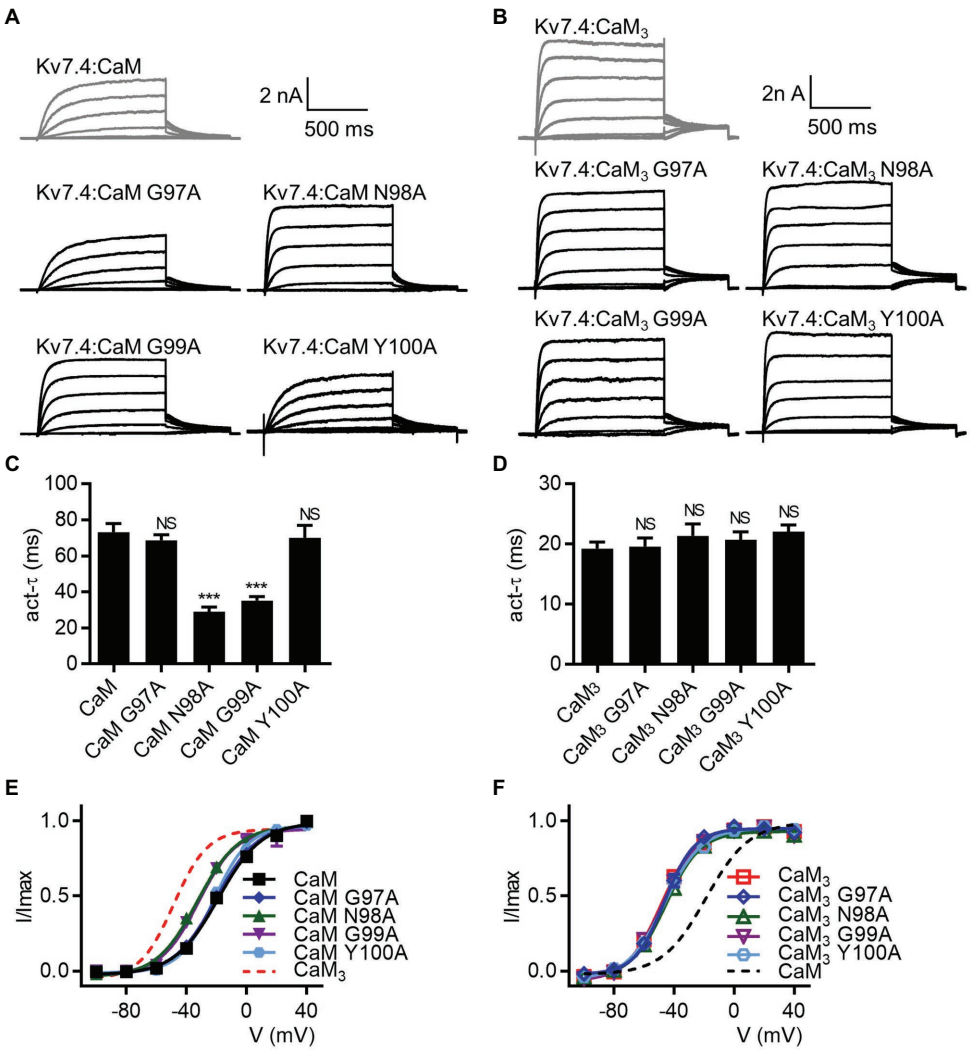

FIGURE 7 | CaM mutations N98A and G99A affect the regulation of Kv7.4 activation. **(A)** Representative current traces of cells co-expressing Kv7.4 with CaM-based mutants. **(B)** Representative current traces of cells co-expressing Kv7.4 with CaM_3-based mutants. **(C)** Average time constants at 40 mV for the fast activation component of Kv7.4:CaM (*N* = 13), Kv7.4:CaM G97A (*N* = 15), Kv7.4:CaM N98A (*N* = 12), Kv7.4:CaM G99A (*N* = 10), and Kv7.4:CaM Y100A (*N* = 17). **(D)** Average time constants at 40 mV for the fast activation component of Kv7.4:CaM_3 (*N* = 11), Kv7.4:CaM_3 G97A (*N* = 11), Kv7.4:CaM_3 N98A (*N* = 11), Kv7.4:CaM_3 G99A (*N* = 14), and Kv7.4:CaM_3 Y100A (*N* = 9). **(E)** Voltage-dependent activation curves for Kv7.4:CaM (*N* = 13), Kv7.4:CaM G97A (*N* = 15), Kv7.4:CaM N98A (*N* = 12), Kv7.4:CaM G99A (*N* = 10), and Kv7.4:CaM Y100A (*N* = 17). **(F)** Voltage-dependent activation curves for Kv7.4:CaM_3 (*N* = 11), Kv7.4:CaM_3 G97A (*N* = 11), Kv7.4:CaM_3 N98A (*N* = 11), Kv7.4:CaM_3 G99A (*N* = 14), and Kv7.4:CaM_3 Y100A (*N* = 9). Error bars show SEM. *N* indicates the number of cells. Asterisks indicate significance: ***$p < 0.001$. *NS* indicates not significant.

R159A:CaM_3 = −53.3 ± 0.9 mV), suggesting that the double mutation C156A/R159A in the S2–S3 loop also abolished CaM regulation of Kv7.4b activation. Taken together, our work revealed a unified mechanism for CaM regulation of both isoforms of Kv7.4 channels (**Figure 8**).

DISCUSSION

With the properties of opening at subthreshold membrane potentials and lacking inactivation, Kv7 channels hold a pivotal position in controlling excitability in the heart and the nervous system (Barhanin et al., 1996; Sanguinetti et al., 1996; Wang et al., 1996, 1998; Jentsch, 2000; Delmas and Brown, 2005; Hernandez et al., 2008; Brown and Passmore, 2009). CaM conferred effective regulation to Kv7 channels. Though the importance of CaM regulation of Kv7 channels has been recognized, the regulation mechanism remains elusive. Earlier studies mostly focused on the role of the C-terminal domain of Kv7 channels in CaM binding and CaM regulation. Mutations in the C-terminal domain impairing CaM binding affect channel assembly, trafficking, and gating (Ghosh et al., 2006; Shamgar et al., 2006; Etxeberria et al., 2008; Alaimo et al., 2009, 2018; Liu and Devaux, 2014; Tobelaim et al., 2017; Chang et al., 2018). Here, our data provided new insight into CaM regulation of Kv7 channels by proving that the S2–S3 loop of Kv7.4 channels is essential for CaM-mediated calcium-dependent regulation of Kv7.4 activation.

Previous studies have shown that CaM conferred intracellular calcium signals to Kv7 channels (Gamper and Shapiro, 2003; Gamper et al., 2005; Sihn et al., 2016; Gomis-Perez et al., 2017; Tobelaim et al., 2017; Chang et al., 2018). To probe the calcium-dependent regulation of Kv7.4 channels mediated by CaM, we performed electrophysiology experiments on CHO cells transfected with Kv7.4 anole or together with WT CaM or CaM mutants with impaired calcium binding abilities. CHO cells have endogenous CaM, which is important for many cellular physiological activities, and thus cannot be knocked out. Overexpression of exogenous CaM or CaM mutants could knockdown the effects of endogenous CaM, which is a common method used by most of the previous studies to probe calcium-dependent CaM regulation. Compared with Kv7.4 channels with only endogenous CaM of CHO cells, overexpression of exogenous WT CaM increased current amplitudes over 2-fold but did not change activation properties, and overexpression of exogenous CaM_{1234} increased current amplitudes about 5-fold and facilitated channel activation as well. CaM_{1234} sharply accelerated the activation rate and produced a large leftward shift in the voltage-dependent activation, similar to the effects of CaM_{1234} on Kv7.2 (Gomis-Perez et al., 2017), Kv7.3 (Gomis-Perez et al., 2017), and Kv7.5 (Chang et al., 2018) and implying a unified mechanism in which Apo/CaM facilitates Kv7.2–7.5 activation, or in other words, in which Ca^{2+}/CaM inhibits Kv7.2–7.5 activation.

We also measured surface expression of Kv7.4 with only endogenous CaM and Kv7.4 with overexpression of exogenous WT CaM and CaM_{1234} to further explain the different current amplitudes. Kv7.4 co-expressed with WT CaM and Kv7.4 co-expressed with CaM_3 showed similar surface expression and about 3.5-fold the surface expression of Kv7.4 with only endogenous CaM, suggesting that CaM enhances Kv7.4 surface expression in a calcium-independent manner. We also measured Kv7.4 total expression of the three groups, and the total expression of Kv7.4 with overexpression of exogenous WT CaM or CaM_{1234} was about twice the total expression of Kv7.4 channels with only endogenous CaM (**Supplementary Figures S4A,B**). Taken together, increased surface expression accounted for the greater current amplitudes of Kv7.4 with overexpression of exogenous WT CaM than Kv7.4 with only endogenous CaM, and Kv7.4 with overexpression of exogenous CaM_{1234} generated further greater current amplitudes due to both facilitated activation and increased surface expression. As the facilitating effect of the overexpression of exogenous WT CaM or CaM_{1234} on Kv7.4 surface expression is more significant than the facilitating effect on Kv7.4 total expression, we deem that the increase of Kv7.4 surface expression is likely due to not only the increase of Kv7.4 total expression but also enhanced channel trafficking.

Of note, Kv7.4 with overexpression of exogenous WT CaM showed activation properties equivalent to Kv7.4 with only endogenous CaM, possibly because exogenous WT CaM is essentially the same as endogenous CaM except the much higher expression level. CaM was reported to be an auxiliary subunit of Kv7 channels (Wen and Levitan, 2002). Disrupted CaM interactions with Kv7 channels have been shown to be tightly associated with severely impaired Kv7 surface expression (Ghosh et al., 2006; Shamgar et al., 2006; Etxeberria et al., 2008; Alaimo et al., 2009, 2018; Liu and Devaux, 2014; Chang et al., 2018), illustrating the vital role of CaM in Kv7 assembly and trafficking, which is also supported by our study. Additionally, the stoichiometry for CaM binding to the Kv7 subunit was 1:1 (Sun and MacKinnon, 2017), and Bernardo-Seisdedos et al. (2018) reported that the Kv7.2 A and B helices could not be purified in the absence of CaM and that the complex could not be dissociated at any calcium concentration *in vitro*. Therefore, we deem that there would be CaM strongly and stably binding to the functional plasma membrane Kv7.4 channels, which has been properly assembled and transported, at a stoichiometry of 1:1, although more Kv7.4 channels was expressed on the cell surface due to the overexpression of exogenous WT CaM. However, the already bound CaM controls the regulating activation of the plasma membrane Kv7.4 channels, so the different expression levels of endogenous CaM and overexpressed exogenous WT CaM did not change Kv7.4 activation.

We also studied the effects CaM_{12}, CaM_{34}, CaM_3, and CaM_4 on Kv7.4 activation to probe the role of each lobe or EF hand in regulating Kv7.4 channels. CaM_{34} and CaM_3 caused facilitating effects equivalent to CaM_{1234} on Kv7.4 activation kinetics and the voltage dependence of activation, supporting a key role of the EF3 in CaM regulation of Kv7.4 activation. CaM_{12} did not mirror the effects of WT CaM of Kv7.4 activation, possibly because calcium binding could enhance the binding of the N-lobe to the B helix of Kv7.4 (Chang et al., 2018), and such configuration changes might have slight effects on channel function. However, the changes of Kv7.4 activation caused by CaM_{12} were much slighter than the changes caused

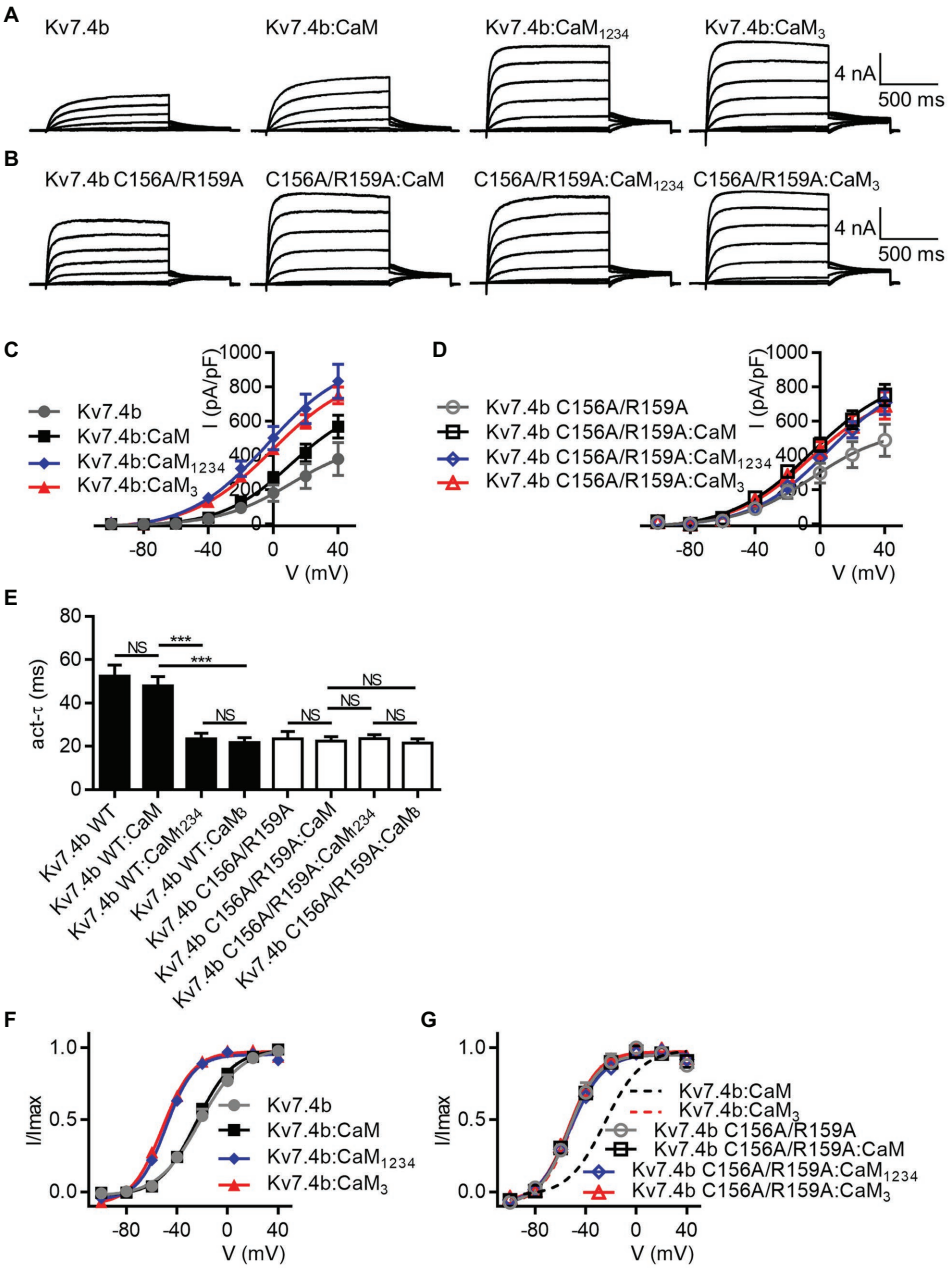

FIGURE 8 | CaM regulates activation of Kv7.4 isoform b. **(A)** Representative current traces of Kv7.4b without overexpression of exogenous CaM and Kv7.4b with overexpression of exogenous CaM, CaM_{1234}, or CaM_3. **(B)** Representative current traces of Kv7.4b C156A/R159A without overexpression of exogenous CaM and Kv7.4b C156A/R159A with overexpression of exogenous CaM, CaM_{1234}, or CaM_3. **(C)** Corresponding current density-voltage relations of Kv7.4b (*N* = 7), Kv7.4b:CaM (*N* = 10), Kv7.4b:CaM_{1234} (*N* = 9), and Kv7.4b:CaM_3 (*N* = 10). **(D)** Corresponding current density-voltage relations of Kv7.4b C156A/R159A (*N* = 7), Kv7.4b C156A/R159A:CaM (*N* = 9), Kv7.4b C156A/R159A:CaM_{1234} (*N* = 8), and Kv7.4b C156A/R159A:CaM_3 (*N* = 8). **(E)** Average time constants at 40 mV for the fast activation component of Kv7.4b (*N* = 7), Kv7.4b:CaM (*N* = 10), Kv7.4b:CaM_{1234} (*N* = 9), Kv7.4b:CaM_3 (*N* = 10), Kv7.4b C156A/R159A (*N* = 7), Kv7.4b C156A/R159A:CaM (*N* = 9), Kv7.4b C156A/R159A:CaM_{1234} (*N* = 8), and Kv7.4b C156A/R159A:CaM_3 (*N* = 8). **(F)** Voltage-dependent activation curves for Kv7.4b (*N* = 7), Kv7.4b:CaM (*N* = 10), Kv7.4b:CaM_{1234} (*N* = 9), and Kv7.4b:CaM_3 (*N* = 10). **(G)** Voltage-dependent activation curves for Kv7.4b C156A/R159A (*N* = 7), Kv7.4b C156A/R159A:CaM (*N* = 9), Kv7.4b C156A/R159A:CaM_{1234} (*N* = 8), and Kv7.4b C156A/R159A:CaM_3 (*N* = 8). Error bars show SEM. *N* indicates the number of cells. Asterisks indicate significance: ***$p < 0.001$. *NS* indicates not significant.

by CaM_{1234}, CaM_{34}, and CaM_3. Our data largely match the results by Chang et al. (2018), but there is a difference in the effects of CaM_4 on Kv7.4 activation. We found that CaM_4 did not change Kv7.4 activation kinetics or the voltage dependence of activation, whereas Chang et al. (2018) showed that CaM_4 facilitated Kv7.4 activation though the facilitating

effects is much weaker than CaM_3, CaM_{34}, and CaM_{1234}. This difference might result from the different experimental approaches, in which Chang et al. (2018) used perforated-patch configuration to test cells under natural resting calcium levels but we used whole-cell configuration to substitute the cell cytosolic composition by the pipette solution. Moreover, activation of Kv7.4 co-expressed with WT CaM was inhibited by increasing intracellular calcium levels, while CaM_{1234} and CaM_3 rendered Kv7.4 insensitive to the changing calcium concentrations, further emphasizing the role of calcium in CaM regulation of Kv7.4 channels and implying that CaM_{1234} and CaM_3 facilitate Kv7.4 activation essentially by abolishing the calcium-dependent inhibition.

The free calcium concentration in the regular pipette solution is 80 nM, which is within the basal cytosolic calcium concentrations (10–100 nM). Free CaM exists in its Apo-forms in the basal cytosolic calcium concentrations [K_d(C-lobe) = 3.4 μM, K_d(N-lobe) = 14 μM; Linse et al., 1991]. However, CaM binding to some target peptides or proteins can dramatically increase calcium affinities (Olwin et al., 1984; Olwin and Storm, 1985; Peersen et al., 1997; Black et al., 2005; Evans and Shea, 2009; Findeisen et al., 2013). For instance, the calcium affinities of CaM binding to the IQ motif of Cav channels, kinase skMLCK or kinase MKII are quite high with Kd values much lower than 100 nM (Peersen et al., 1997; Black et al., 2005). In this study, the calcium chelators, EGTA and BAPTA-AM exerted effects on Kv7.4 activation in the same facilitating direction as CaM_{1234}, CaM_{12}, CaM_{34}, and CaM_3, suggesting that there are some tonic occupations by calcium in the EF hands under the basal intracellular calcium level. Previous studies have also reported changed Kv7 currents by decreasing intracellular calcium concentrations from the basal level (Ghosh et al., 2006; Shamgar et al., 2006; Chang et al., 2018). These observations are possibly due to increased calcium affinities of CaM when binding to Kv7 channels.

Structural studies have reported that the CaM EF3 interacted with the Kv7.1 S2–S3 loop, which is conserved among Kv7 isoforms (Sun and MacKinnon, 2017). To explore if the important functional role of the CaM EF3 is associated with the potential interaction between the CaM EF3 and the Kv7.4 S2–S3, we mutated amino acids either in the Kv7.4 S2–S3 loop or in the CaM EF3 to a nonpolar amino acid. Five mutations (C156A, C157A, C158V, R159A, and R161A) in the Kv7.4 S2–S3 loop and two mutations (N98A and G99A) in the CaM EF3 led to decreased inhibitory effects of Ca^{2+}/CaM, facilitating Kv7.4:CaM activation in terms of both the activation rate and the voltage dependence of activation. The double mutation C156A/R159A within the S2–S3 loop completely abolished the inhibitory effects of Ca^{2+}/CaM on Kv7.4 activation and rendered Kv7.4 insensitive to changing intracellular calcium levels, which further emphasizes the importance of the Kv7.4 S2–S3 loop in CaM regulation. We also performed co-immunoprecipitation experiments to probe the effect of C156A/R159A on CaM binding. Compared with WT Kv7.4, the double mutant C156A/R159A showed weaker association with Ca^{2+}/CaM but unchanged association with CaM_3 and Apo/CaM, suggesting that the Kv7.4 S2–S3 loop interacts with the Ca^{2+}/EF3 but has no association with the Apo/EF3. The co-immunoprecipitation results coincide with our electrophysiological results. Mutations in the Kv7.4 S2–S3 loop decreased Ca^{2+}/CaM binding as well as Ca^{2+}/CaM inhibition on channel activation, while these mutations had no effect on CaM_3 binding as well as activation of Kv7.4 co-expressed with CaM_3, suggesting that Ca^{2+}/CaM inhibited Kv7.4 activation through an interaction with the Kv7.4 S2–S3 loop.

We also probed CaM regulation of Kv7.4 isoform b, activation of which was reported by Sihn et al. (2016) to be not regulated by CaM. Our results are strikingly different from Sihn et al. (2016) and show that CaM regulates Kv7.4b activation in a calcium-dependent manner similarly to the regulation of Kv7.4 isoform a. CaM_{1234} facilitated Kv7.4b activation in terms of both activation kinetics and the voltage dependence of activation, and CaM_3 phenocopied the facilitating effects of CaM_{1234}. The double mutation C156A/R159A abolished CaM regulation of Kv7.4b activation. These results emphasized the crucial roles of the EF3 and the S2–S3 loop in CaM regulating activation of Kv7.4b. There are cases where the earlier studies failed to find CaM regulation of Kv7.1 and Kv7.3 (Gamper et al., 2005), both of which were later shown to be regulated by CaM (Sachyani et al., 2014; Gomis-Perez et al., 2017; Tobelaim et al., 2017; Chang et al., 2018). Our work proved a unified rather than isoform-dependent mechanism for CaM regulation of Kv7.4 channels.

To the best of our knowledge, the mechanism for CaM-mediated calcium-dependent regulation of voltage-gated channels has remained puzzling since the CaM binding sites were initially found. Heretofore, the most-studied structural presentation accounting for the mechanism for CaM regulation of channel activation comes from SK4 channels (Lee and MacKinnon, 2018). It was proposed that Apo/CaM binds to SK4 channels through the interaction of Apo/C-lobe with the SK4 A and B helices, and calcium loading allows the Ca^{2+}/N-lobe to remain anchored on the A and B helices and enables the Ca^{2+}/N-lobe to contact the S4–S5 linker of SK4 channels and further affect pore opening. In Kv7 channels, it has been widely assumed that the Ca^{2+}-dependent CaM regulation is also driven by conformational changes derived from calcium loading, but detailed interpretation remained unresolved. Apo/CaM binds to Kv7 channels in a clamped form, in which the C-lobe interacts with the A helix of Kv7 channels and the N-lobe interacts with the B helix (Bernardo-Seisdedos et al., 2018; Chang et al., 2018). Calcium binding allow the Ca^{2+}/N-lobe to stay anchored on the Kv7 B helix in a similar configuration to the apo/N-lobe (Sachyani et al., 2014; Strulovich et al., 2016; Sun and MacKinnon, 2017; Bernardo-Seisdedos et al., 2018; Chang et al., 2018), while there are striking differences between the Ca^{2+}/C-lobe and Apo/C-lobe conformations. Structural studies of the interaction between CaM and the Kv7.4 A and B helices showed that calcium binding makes the C-lobe lose interaction with the A helix and bind to the B helix weakly through a much smaller interaction surface (Xu et al., 2013; Chang et al., 2018). Xu et al. (2013) proposed that the interaction of apo/CaM with the Kv7.4 A helix may affect the neighboring S6 in some way to favor channel opening and, in contrast, when CaM switches to Ca^{2+}/CaM and binds to the helix B, loss of the interaction with the A helix causes inhibition of

the currents. Our data demonstrate that the third EF hand of CaM and the S2–S3 loop of Kv7.4 channels play crucial roles in CaM-mediated calcium-dependent regulation of Kv7.4 activation, and lead us to propose a new regulation model (**Figure 9**). Apo/CaM binds only the C-terminal domain of Kv7.4 channels through the interaction of the Ca^{2+}/C-lobe with the A helix and the interaction of the Ca^{2+}/N-lobe with the B helix, and has no association with the voltage sensor domain of Kv7.4 channels. Thus, the voltage sensor could easily move in response to depolarized membrane potentials, which is coupled to pore opening. Upon calcium loading, the CaM C-lobe releases its interaction with the Kv7.4 A helix and binds to the B helix weakly with a much smaller interaction surface (Xu et al., 2013; Chang et al., 2018), making it possible for the Ca^{2+}/EF3 to contact the Kv7.4 S2–S3 loop. This interaction between the Ca^{2+}/EF3 and the Kv7.4 S2–S3 loop makes it possible for Ca^{2+}/CaM to "pull" the voltage sensor of Kv7.4 channels, and thus offers a force opposing the movement of the voltage sensor in response to depolarized potentials, affecting voltage-dependent pore opening. We could not deny the model proposed by Xu et al. (2013), although our model could better explain the shift in the voltage dependence of activation caused by CaM regulation. Probably, the inhibitory effect of Ca^{2+}/CaM on Kv7.4 activation might be a combined effect of the "pulled" voltage sensor and the released helix A. In our model, the interaction of the S2–S3 loop with the Ca^{2+}/EF3 rather than the Apo/EF3 is more likely to be driven by calcium-dependent changes of the constitutive interactions between CaM and the Kv7.4 C-terminal domain. However, the residues in the Kv7.4 A and B helices interacting with Apo/CaM and the residues in the Kv7.4 B helix interacting with Ca^{2+}/CaM are different from the residues in Kv7.1 to a certain degree, so there might be some differences between Kv7.4 and Kv7.1 in the calcium-dependent interaction with the CaM EF3, accounting for the different direction of CaM regulation.

Limited previous studies explored the role of the Kv7 S2–S3 loop in channel function. Gamper et al. (2006) found that increasing H_2O_2 concentrations enhanced Kv7.4 currents and facilitated Kv7.4 activation and that currents of the Kv7.4 triple mutant C156A/C157A/C158A remained unchanged after extracellular application of H_2O_2, so they concluded that the triple cysteines in the S2–S3 loop was critical for the oxidative modification. However, their data showed that extracellular application of H_2O_2 still facilitated the activation rate of Kv7.4 C156A/C157A/C158A, which seemed contradictory to the unchanged currents. Additionally, before extracellular application of H_2O_2 and with only endogenous H_2O_2 in cells, Kv7.4 C156A/C157A/C158A showed a faster activation rate and a leftward shift in the half-activation voltage compared with WT Kv7.4, which contrast the facilitating effects of H_2O_2 and suggested that the S2–S3 loop might be involved in other regulations that affect channel function as well. Ooi et al. (2013) reported that extracellular application of SNAP that forms nitric oxide (NO) inhibited Kv7.4 currents with an inhibition of about 30%, and that the NO inhibition of the Kv7.4 triple mutant C156A/C157A/C158A was much smaller and almost abolished. They also tested S-nitrosylation of WT Kv7.4 and Kv7.4 C156A/C157A/C158A treated with SNAP and found that Kv7.4 C156A/C157A/C158A showed decreased S-nitrosylation, so they concluded that NO possibly inhibited Kv7.4 currents through S-nitrosylation of the triple cysteines in the S2–S3 loop. Both NO and Ca^{2+}/CaM inhibit Kv7.4 channels, and the S2–S3 loop is required for both inhibition, implying a potential correlation between the two

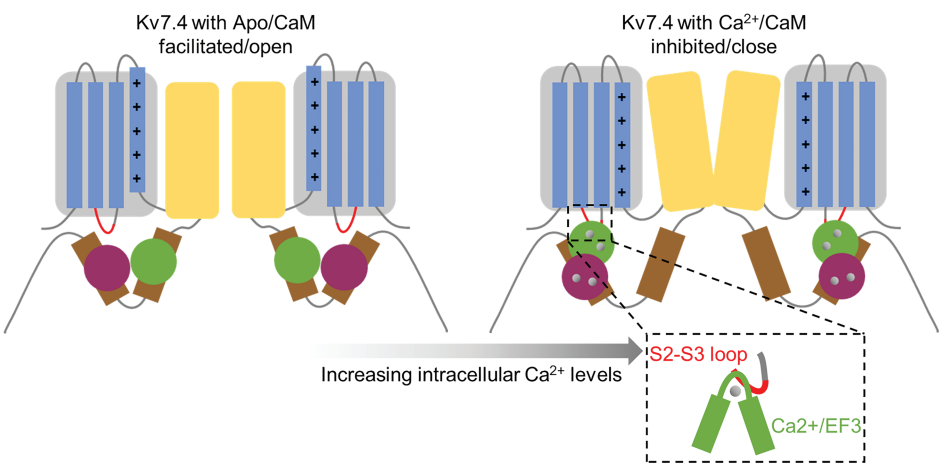

FIGURE 9 | A model for CaM-mediated calcium-dependent regulation of Kv7.4 activation. The gray box represents the voltage sensor domain containing the Kv7.4 transmembrane helixes S1–S4, with positively charged amino acids (shown as plus signs) in the S4 helix. The S2–S3 loop is shown as a red curve. The yellow box represents the pore domain. The brown rectangles represent the A and B helices. The CaM N-lobe is colored in green, and the C-lobe is colored in purple. The gray circles represent calcium bound to CaM. Apo/CaM binds to Kv7.4 channels with the Apo/N-lobe interacting with the B helix and the Apo/C-lobe interacting with the A helix, and Apo/CaM has no association with the Kv7.4 S2–S3 loop. Upon calcium loading, the Ca^{2+}/N-lobe remains anchored on the B helix, while the Ca^{2+}/C-lobe releases interaction with the A helix and binds to the B helix through a much smaller interaction surface, making it possible for the Ca^{2+}/EF3 to contact the Kv7.4 S2–S3 loop and affect motivation of the voltage sensor and opening of the coupled pore.

regulations. For example, possibly S-nitrosylation of the triple cysteines could favor the interaction between Ca^{2+}/CaM and the S2–S3 loop of Kv7.4 channels. Further studies are required to explore the role of the S2-S3 loop in coordinating the process of H_2O_2 regulation, NO regulation, and Ca^{2+}/CaM regulation.

Overall, our results highlight the importance of the Kv7.4 S2–S3 linker in CaM regulation of channel activation. This is the first study to indicate another site in Kv7.4 channels required for CaM regulation in addition to the C-terminal domain. Furthermore, given that the S2–S3 loop sequence is highly conserved among Kv7.2–7.5, this loop might play a similar role in CaM regulation of all these isoforms. More studies about the S2–S3 loop of the other Kv7 isoforms including Kv7.1 may further our understanding of a unified mechanism for CaM regulation of Kv7 channels.

DATA AVAILABILITY STATEMENT

The original contributions presented in the study are included in the article/**Supplementary Material**, further inquiries can be directed to the corresponding author.

AUTHOR CONTRIBUTIONS

WZ designed and implemented the experiments, collected and analyzed data, and wrote the paper. ZY supervised the project and provided guidance. Both the authors contributed to the article and approved the submitted version.

FUNDING

This research was funded by the National Key R&D Program of China Project (2017YFA0103900), the National Natural Science Foundation of China (31571083 and 31970931), the Program for Professor of Special Appointment (Eastern Scholar of Shanghai, TP2014008), the Shanghai Municipal Science and Technology Major Project (No.2017SHZDZX01 and No.2018SHZDZX01), and the Shanghai Rising-Star Program (14QA1400800).

ACKNOWLEDGMENTS

We are grateful to Jiahuai Han at Xiamen University and Lan Bao at the Chinese Academy of Sciences for providing the plasmids. We also appreciate Yanai Mei, Wenyong Fan, Honglan Zheng, and Zhaoyang Li for useful discussion.

SUPPLEMENTARY MATERIAL

The Supplementary Material for this article can be found online at: https://www.frontiersin.org/articles/10.3389/fphys.2020.604134/full#supplementary-material

REFERENCES

Alaimo, A., Etxeberria, A., Gómez-Posada, J. C., Gomis-Perez, C., Fernández-Orth, J., Malo, C., et al. (2018). Lack of correlation between surface expression and currents in epileptogenic AB-calmodulin binding domain Kv72 potassium channel mutants. *Channels* 12, 299–310. doi: 10.1080/19336950.2018.1511512

Alaimo, A., Gómez-Posada, J. C., Aivar, P., Etxeberría, A., Rodriguez-Alfaro, J. A., Areso, P., et al. (2009). Calmodulin activation limits the rate of KCNQ2 K^+ channel exit from the endoplasmic reticulum. *J. Biol. Chem.* 284, 20668–20675. doi: 10.1074/jbc.M109.019539

Bal, M., Zaika, O., Martin, P., and Shapiro, M. S. (2008). Calmodulin binding to M-type K^+ channels assayed by TIRF/FRET in living cells. *J. Physiol.* 586, 2307–2320. doi: 10.1113/jphysiol.2008.152777

Barhanin, J., Lesage, F., Guillemare, E., Fink, M., Lazdunski, M., and Romey, G. (1996). K(V)LQT1 and lsK (minK) proteins associate to form the I(Ks) cardiac potassium current. *Nature* 384, 78–80. doi: 10.1038/384078a0

Beisel, K. W., Nelson, N. C., Delimont, D. C., and Fritzsch, B. (2000). Longitudinal gradients of KCNQ4 expression in spiral ganglion and cochlear hair cells correlate with progressive hearing loss in DFNA2. *Brain Res. Mol. Brain Res.* 82, 137–149. doi: 10.1016/S0169-328X(00)00204-7

Beisel, K. W., Rocha-Sanchez, S. M., Morris, K. A., Nie, L., Feng, F., Kachar, B., et al. (2005). Differential expression of KCNQ4 in inner hair cells and sensory neurons is the basis of progressive high-frequency hearing loss. *J. Neurosci.* 25, 9285–9293. doi: 10.1523/JNEUROSCI.2110-05.2005

Bernardo-Seisdedos, G., Nunez, E., Gomis-Perez, C., Malo, C., Villarroel, A., and Millet, O. (2018). Structural basis and energy landscape for the Ca^{2+} gating and calmodulation of the Kv7.2 K(+) channel. *Proc. Natl. Acad. Sci. U. S. A.* 115, 2395–2400. doi: 10.1073/pnas.1800235115

Black, D. J., Halling, D. B., Mandich, D. V., Pedersen, S. E., Altschuld, R. A., and Hamilton, S. L. (2005). Calmodulin interactions with IQ peptides from voltage-dependent calcium channels. *Am. J. Phys. Cell Physiol.* 288, C669–C676. doi: 10.1152/ajpcell.00191.2004

Brown, D. A., and Passmore, G. M. (2009). Neural KCNQ (Kv7) channels. *Br. J. Pharmacol.* 156, 1185–1195. doi: 10.1111/j.1476-5381.2009.00111.x

Chang, A., Abderemane-Ali, F., Hura, G. L., Rossen, N. D., Gate, R. E., and Minor, D. L. Jr. (2018). A Calmodulin C-lobe Ca^{2+}/-dependent switch governs Kv7 channel function. *Neuron* 97, 836.e836–852.e836. doi: 10.1016/j.neuron.2018.01.035

Delmas, P., and Brown, D. A. (2005). Pathways modulating neural KCNQ/M (Kv7) potassium channels. *Nat. Rev. Neurosci.* 6, 850–862. doi: 10.1038/nrn1785

Etxeberria, A., Aivar, P., Rodriguez-Alfaro, J. A., Alaimo, A., Villacé, P., Gómez-Posada, J. C., et al. (2008). Calmodulin regulates the trafficking of KCNQ2 potassium channels. *FASEB J.* 22, 1135–1143. doi: 10.1096/fj.07-9712com

Evans, T. I., and Shea, M. A. (2009). Energetics of calmodulin domain interactions with the calmodulin binding domain of CaMKII. *Proteins* 76, 47–61. doi: 10.1002/prot.22317

Findeisen, F., Rumpf, C. H., and Minor, D. L. Jr. (2013). Apo states of calmodulin and CaBP1 control CaV1 voltage-gated calcium channel function through direct competition for the IQ domain. *J. Mol. Biol.* 425, 3217–3234. doi: 10.1016/j.jmb.2013.06.024

Gamper, N., Li, Y., and Shapiro, M. S. (2005). Structural requirements for differential sensitivity of KCNQ K^+ channels to modulation by Ca^{2+}/calmodulin. *Mol. Biol. Cell* 16, 3538–3551. doi: 10.1091/mbc.e04-09-0849

Gamper, N., and Shapiro, M. S. (2003). Calmodulin mediates Ca^{2+}–dependent modulation of M-type K^+ channels. *J. Gen. Physiol.* 122, 17–31. doi: 10.1085/jgp.200208783

Gamper, N., Zaika, O., Li, Y., Martin, P., Hernandez, C. C., Perez, M. R., et al. (2006). Oxidative modification of M-type K(+) channels as a mechanism of cytoprotective neuronal silencing. *EMBO J.* 25, 4996–5004. doi: 10.1038/sj.emboj.7601374

Geiser, J. R., van Tuinen, D., Brockerhoff, S. E., Neff, M. M., and Davis, T. N. (1991). Can calmodulin function without binding calcium? *Cell* 65, 949–959. doi: 10.1016/0092-8674(91)90547-C

Ghosh, S., Nunziato, D. A., and Pitt, G. S. (2006). KCNQ1 assembly and function is blocked by long-QT syndrome mutations that disrupt interaction with calmodulin. *Circ. Res.* 98, 1048–1054. doi: 10.1161/01.RES.0000218863.44140.f2

Gomis-Perez, C., Soldovieri, M. V., Malo, C., Ambrosino, P., Taglialatela, M., Areso, P., et al. (2017). Differential regulation of $PI(4,5)P_2$ sensitivity of Kv7.2 and Kv7.3 channels by calmodulin. *Front. Mol. Neurosci.* 10:117. doi: 10.3389/fnmol.2017.00117

Gutman, G. A., Chandy, K. G., Adelman, J. P., Aiyar, J., Bayliss, D. A., Clapham, D. E., et al. (2003). International union of pharmacology. XLI. Compendium of voltage-gated ion channels: potassium channels. *Pharmacol. Rev.* 55, 583–586. doi: 10.1124/pr.55.4.9

Hernandez, C. C., Zaika, O., Tolstykh, G. P., and Shapiro, M. S. (2008). Regulation of neural KCNQ channels: signalling pathways, structural motifs and functional implications. *J. Physiol.* 586, 1811–1821. doi: 10.1113/jphysiol.2007.148304

Jentsch, T. J. (2000). Neuronal KCNQ potassium channels: physiology and role in disease. *Nat. Rev. Neurosci.* 1, 21–30. doi: 10.1038/35036198

Kharkovets, T., Hardelin, J. P., Safieddine, S., Schweizer, M., El-Amraoui, A., Petit, C., et al. (2000). KCNQ4, a K^+ channel mutated in a form of dominant deafness, is expressed in the inner ear and the central auditory pathway. *Proc. Natl. Acad. Sci. U. S. A.* 97, 4333–4338. doi: 10.1073/pnas.97.8.4333

Kim, H. J., Lv, P., Sihn, C. R., and Yamoah, E. N. (2011). Cellular and molecular mechanisms of autosomal dominant form of progressive hearing loss, DFNA2. *J. Biol. Chem.* 286, 1517–1527. doi: 10.1074/jbc.M110.179010

Kosenko, A., and Hoshi, N. (2013). A change in configuration of the calmodulin-KCNQ channel complex underlies Ca^{2+}–dependent modulation of KCNQ channel activity. *PLoS One* 8:e82290. doi: 10.1371/journal.pone.0082290

Kubisch, C., Schroeder, B. C., Friedrich, T., Lütjohann, B., El-Amraoui, A., Marlin, S., et al. (1999). KCNQ4, a novel potassium channel expressed in sensory outer hair cells, is mutated in dominant deafness. *Cell* 96, 437–446. doi: 10.1016/s0092-8674(00)80556-5

Lee, C. H., and MacKinnon, R. (2018). Activation mechanism of a human SK-calmodulin channel complex elucidated by cryo-EM structures. *Science* 360, 508–513. doi: 10.1126/science.aas9466

Linse, S., Helmersson, A., and Forsén, S. (1991). Calcium binding to calmodulin and its globular domains. *J. Biol. Chem.* 266, 8050–8054.

Liu, W., and Devaux, J. J. (2014). Calmodulin orchestrates the heteromeric assembly and the trafficking of KCNQ2/3 (Kv7.2/3) channels in neurons. *Mol. Cell. Neurosci.* 58, 40–52. doi: 10.1016/j.mcn.2013.12.005

Olwin, B. B., Edelman, A. M., Krebs, E. G., and Storm, D. R. (1984). Quantitation of energy coupling between Ca^{2+}, calmodulin, skeletal muscle myosin light chain kinase, and kinase substrates. *J. Biol. Chem.* 259, 10949–10955.

Olwin, B. B., and Storm, D. R. (1985). Calcium binding to complexes of calmodulin and calmodulin binding proteins. *Biochemistry* 24, 8081–8086. doi: 10.1021/bi00348a037

Ooi, L., Gigout, S., Pettinger, L., and Gamper, N. (2013). Triple cysteine module within M-type K^+ channels mediates reciprocal channel modulation by nitric oxide and reactive oxygen species. *J. Neurosci.* 33, 6041–6046. doi: 10.1523/JNEUROSCI.4275-12.2013

Peersen, O. B., Madsen, T. S., and Falke, J. J. (1997). Intermolecular tuning of calmodulin by target peptides and proteins: differential effects on Ca^{2+} binding and implications for kinase activation. *Protein Sci.* 6, 794–807. doi: 10.1002/pro.5560060406

Sachyani, D., Dvir, M., Strulovich, R., Tria, G., Tobelaim, W., Peretz, A., et al. (2014). Structural basis of a Kv7.1 potassium channel gating module: studies of the intracellular c-terminal domain in complex with calmodulin. *Structure* 22, 1582–1594. doi: 10.1016/j.str.2014.07.016

Sanguinetti, M. C., Curran, M. E., Zou, A., Shen, J., Spector, P. S., Atkinson, D. L., et al. (1996). Coassembly of K(V)LQT1 and minK (IsK) proteins to form cardiac I(Ks) potassium channel. *Nature* 384, 80–83. doi: 10.1038/384080a0

Shamgar, L., Ma, L., Schmitt, N., Haitin, Y., Peretz, A., Wiener, R., et al. (2006). Calmodulin is essential for cardiac IKS channel gating and assembly: impaired function in long-QT mutations. *Circ. Res.* 98, 1055–1063. doi: 10.1161/01.res.0000218979.40770.69

Sihn, C. R., Kim, H. J., Woltz, R. L., Yarov-Yarovoy, V., Yang, P. C., Xu, J., et al. (2016). Mechanisms of calmodulin regulation of different isoforms of Kv7.4 K^+ channels. *J. Biol. Chem.* 291, 2499–2509. doi: 10.1074/jbc.M115.668236

Strulovich, R., Tobelaim, W. S., Attali, B., and Hirsch, J. A. (2016). Structural insights into the M-channel proximal C-terminus/calmodulin complex. *Biochemistry* 55, 5353–5365. doi: 10.1021/acs.biochem.6b00477

Sun, J., and MacKinnon, R. (2017). Cryo-EM structure of a KCNQ1/CaM complex reveals insights into congenital long QT syndrome. *Cell* 169, 1042.e1049–1050.e1049. doi: 10.1016/j.cell.2017.05.019

Tobelaim, W. S., Dvir, M., Lebel, G., Cui, M., Buki, T., Peretz, A., et al. (2017). Competition of calcified calmodulin N lobe and PIP2 to an LQT mutation site in Kv71 channel. *Proc. Natl. Acad. Sci. U. S. A.* 114, E869–e878. doi: 10.1073/pnas.1612622114

Wang, Q., Curran, M. E., Splawski, I., Burn, T. C., Millholland, J. M., VanRaay, T. J., et al. (1996). Positional cloning of a novel potassium channel gene: KVLQT1 mutations cause cardiac arrhythmias. *Nat. Genet.* 12, 17–23. doi: 10.1038/ng0196-17

Wang, H. S., Pan, Z., Shi, W., Brown, B. S., Wymore, R. S., Cohen, I. S., et al. (1998). KCNQ2 and KCNQ3 potassium channel subunits: molecular correlates of the M-channel. *Science* 282, 1890–1893. doi: 10.1126/science.282.5395.1890

Wen, H., and Levitan, I. B. (2002). Calmodulin is an auxiliary subunit of KCNQ2/3 potassium channels. *J. Neurosci.* 22, 7991–8001. doi: 10.1523/JNEUROSCI.22-18-07991.2002

Xia, X. M., Fakler, B., Rivard, A., Wayman, G., Johnson-Pais, T., Keen, J. E., et al. (1998). Mechanism of calcium gating in small-conductance calcium-activated potassium channels. *Nature* 395, 503–507. doi: 10.1038/26758

Xu, Q., Chang, A., Tolia, A., and Minor, D. L. Jr. (2013). Structure of a Ca^{2+}/CaM:Kv7.4 (KCNQ4) B-helix complex provides insight into M current modulation. *J. Mol. Biol.* 425, 378–394. doi: 10.1016/j.jmb.2012.11.023

Xu, T., Nie, L., Zhang, Y., Mo, J., Feng, W., Wei, D., et al. (2007). Roles of alternative splicing in the functional properties of inner ear-specific KCNQ4 channels. *J. Biol. Chem.* 282, 23899–23909. doi: 10.1074/jbc.M702108200

Yus-Najera, E., Santana-Castro, I., and Villarroel, A. (2002). The identification and characterization of a noncontinuous calmodulin-binding site in noninactivating voltage-dependent KCNQ potassium channels. *J. Biol. Chem.* 277, 28545–28553. doi: 10.1074/jbc.M204130200

Zhang, Z. N., Li, Q., Liu, C., Wang, H. B., Wang, Q., and Bao, L. (2008). The voltage-gated Na^+ channel Nav1.8 contains an ER-retention/retrieval signal antagonized by the beta3 subunit. *J. Cell Sci.* 121, 3243–3252. doi: 10.1242/jcs.026856

Conflict of Interest: The authors declare that the research was conducted in the absence of any commercial or financial relationships that could be construed as a potential conflict of interest.

Advantages of publishing in Frontiers

OPEN ACCESS
Articles are free to read for greatest visibility and readership

FAST PUBLICATION
Around 90 days from submission to decision

HIGH QUALITY PEER-REVIEW
Rigorous, collaborative, and constructive peer-review

TRANSPARENT PEER-REVIEW
Editors and reviewers acknowledged by name on published articles

Frontiers
Avenue du Tribunal-Fédéral 34
1005 Lausanne | Switzerland

Visit us: www.frontiersin.org
Contact us: frontiersin.org/about/contact

REPRODUCIBILITY OF RESEARCH
Support open data and methods to enhance research reproducibility

DIGITAL PUBLISHING
Articles designed for optimal readership across devices

FOLLOW US
@frontiersin

IMPACT METRICS
Advanced article metrics track visibility across digital media

EXTENSIVE PROMOTION
Marketing and promotion of impactful research

LOOP RESEARCH NETWORK
Our network increases your article's readership